

Advances in
**ORGANOMETALLIC
CHEMISTRY**

VOLUME 18

Advances in
ORGANOMETALLIC CHEMISTRY

VOLUME 18

CONTRIBUTORS TO THIS VOLUME

H. Behrens

Henri Brunner

Joan S. Fessenden

Ralph J. Fessenden

Gregory L. Geoffroy

Wayne L. Gladfelter

A. F. Halasa

Walter Kaminsky

V. D. Mochel

D. N. Schulz

Walter Siebert

Hansjörg Sinn

D. P. Tate

Advances in Organometallic Chemistry

EDITED BY

F. G. A. STONE

DEPARTMENT OF INORGANIC CHEMISTRY
THE UNIVERSITY
BRISTOL, ENGLAND

ROBERT WEST

DEPARTMENT OF CHEMISTRY
UNIVERSITY OF WISCONSIN
MADISON, WISCONSIN

VOLUME 18



1980

ACADEMIC PRESS

A Subsidiary of Harcourt Brace Jovanovich, Publishers

New York London Toronto Sydney San Francisco

COPYRIGHT © 1980, BY ACADEMIC PRESS, INC.

ALL RIGHTS RESERVED.

**NO PART OF THIS PUBLICATION MAY BE REPRODUCED OR
TRANSMITTED IN ANY FORM OR BY ANY MEANS, ELECTRONIC
OR MECHANICAL, INCLUDING PHOTOCOPY, RECORDING, OR ANY
INFORMATION STORAGE AND RETRIEVAL SYSTEM, WITHOUT
PERMISSION IN WRITING FROM THE PUBLISHER.**

ACADEMIC PRESS, INC.

111 Fifth Avenue, New York, New York 10003

United Kingdom Edition published by
ACADEMIC PRESS, INC. (LONDON) LTD.
24/28 Oval Road, London NW1 7DX

LIBRARY OF CONGRESS CATALOG CARD NUMBER: 64--16030

ISBN 0-12-031118-6

PRINTED IN THE UNITED STATES OF AMERICA

80 81 82 83 9 8 7 6 5 4 3 2 1

Contents

LIST OF CONTRIBUTORS	ix
--------------------------------	----

Four Decades of Metal Carbonyl Chemistry in Liquid Ammonia: Aspects and Prospects

H. BEHRENS

I. Introduction	2
II. Reduction of Metal Carbonyls with Alkali Metals and Sodium Tetrahydridoborate in Liquid Ammonia	4
III. Reactions of the Pentacarbonyl Metalates(–II) and the Decacarbonyl Dimetalates(–I) of Chromium, Molybdenum, and Tungsten	10
IV. Reactions of Metal Carbonyls and Metal Carbonyl Derivatives with Liquid Ammonia	19
V. Reactions of Metal Carbonyls and Metal Carbonyl Derivatives with the Multidentate Nitrogen Ligands bipy, phen, and terpy	42
VI. High-Pressure Syntheses	46
VII. Conclusions	47
References	48

Organolithium Catalysis of Olefin and Diene Polymerization

A. F. HALASA, D. N. SCHULZ, D. P. TATE, and V. D. MOCHEL

I. Introduction	55
II. Mechanism of Olefin Polymerization with Polar Ligands	61
III. Mechanism of Diene Polymerization with Polar Ligands	65
IV. Mechanism of Diene Polymerization in Nonpolar Media	71
V. Copolymerization of Dienes and Olefins	78
VI. Use of RLi to Prepare Terminally Functional Diene (Olefin) Polymers	89
VII. Unsolved Problems/Future Trends	93
References	93

Ziegler–Natta Catalysis

HANSJÖRG SINN and WALTER KAMINSKY

I. Scope of Ziegler Catalysis	99
II. Process Operation	105
III. Stereoselectivity, Kinetics, and Mechanism	108
IV. Tailoring Heterogeneous Catalysts	118
V. Homogeneous Ziegler–Natta Catalysts	123
VI. Side Reactions in Homogeneous Catalysts	131
VII. Influence of Water on Homogeneous Catalysts	137
References	143

Chiral Metal Atoms in Optically Active Organo-Transition-Metal Compounds

HENRI BRUNNER

I. Introduction	152
II. Optical Resolution—Enantiomers	153
III. Optical Resolution—Diastereoisomers	160
IV. Methods of Diastereoisomer Separation	165
V. Scope of the Concept of Chiral Metal Atoms in Optically Active Organo-Transition-Metal Compounds	166
VI. Optical Purity	166
VII. Configurational Stability	168
VIII. Ligand Transformations	169
IX. Stereochemical Aspects of the Racemization and Ligand Exchange of (+)- and (-)- $C_5H_5Mn(NO)(COR)PAR_3$	172
X. Metal-Centered Rearrangement in Optically Active Square- Pyramidal Compounds	177
XI. The Stereochemistry of Reactions at Fe—C and Fe—Hal Bonds	180
XII. Miscellaneous Reactions	185
XIII. Optical Induction	186
XIV. Diastereoisomerically Related Pairs of Enantiomers	189
XV. Chiroptical Properties	192
XVI. Absolute Configuration	193
XVII. Table of Optically Active Compounds	195
References	201

Mixed-Metal Clusters

WAYNE L. GLADFELTER and GREGORY L. GEOFFROY

I. Introduction	207
II. Synthesis	209
III. Methods of Characterization	242
IV. Reactivity	249
V. Dynamic NMR Studies	257
VI. Almost Mixed-Metal Clusters	265
References	269

Trends in Organosilicon Biological Research

RALPH J. FESSENDEN and JOAN S. FESSENDEN

I. Introduction	275
II. Silicon Derivatives of Known Active Compounds	276
III. Silicon Biological Agents without Carbon Analogy	288
IV. Detoxification and Elimination of Silicon Compounds	294
V. Summary	295
References	296

Boron Heterocycles as Ligands in Transition-Metal Chemistry

WALTER SIEBERT

I. Introduction	301
II. Mononuclear Complexes	307
III. Dinuclear Complexes	324
IV. Trinuclear Complexes	333
V. Conclusion	337
References	337
SUBJECT INDEX	341
CUMULATIVE LIST OF CONTRIBUTORS	350
CUMULATIVE LIST OF TITLES	352

This Page Intentionally Left Blank

List of Contributors

Numbers in parentheses indicate the pages on which the authors' contributions begin.

- H. BEHRENS (1), *Institute of Inorganic Chemistry, University of Erlangen-Nürnberg, 8520 Erlangen, Federal Republic of Germany*
- HENRI BRUNNER (151), *Institut für Chemie, Universität Regensburg, D-8400 Regensburg, Federal Republic of Germany*
- JOAN S. FESSENDEN (275), *Department of Chemistry, University of Montana, Missoula, Montana 59812*
- RALPH J. FESSENDEN (275), *Department of Chemistry, University of Montana, Missoula, Montana 59812*
- GREGORY L. GEOFFROY (207), *Department of Chemistry, The Pennsylvania State University, University Park, Pennsylvania 16802*
- WAYNE L. GLADFELTER (207), *Department of Chemistry, University of Minnesota, Minneapolis, Minnesota 55455*
- A. F. HALASA* (55), *Central Research Laboratories, The Firestone Tire & Rubber Company, Akron, Ohio 44317*
- WALTER KAMINSKY (99), *Institut für Anorganische und Angewandte Chemie, University of Hamburg, 2000 Hamburg, Federal Republic of Germany*
- V. D. MOCHEL (55), *Central Research Laboratories, The Firestone Tire & Rubber Company, Akron, Ohio 44317*
- D. N. SCHULZ (55), *Central Research Laboratories, The Firestone Tire & Rubber Company, Akron, Ohio 44317*
- WALTER SIEBERT (301), *Fachbereich Chemie der Philipps-Universität, Lahnberge, D-3550 Marburg, Federal Republic of Germany*
- HANSJÖRG SINN (99), *Institut für Anorganische und Angewandte Chemie, University of Hamburg, 2000 Hamburg, Federal Republic of Germany*
- D. P. TATE (55), *Central Research Laboratories, The Firestone Tire & Rubber Company, Akron, Ohio 44317*

* Present address: Kuwait Institute of Scientific Research, P.O. Box 12009, Safat, Kuwait.

This Page Intentionally Left Blank

Four Decades of Metal Carbonyl Chemistry in Liquid Ammonia: Aspects and Prospects

H. BEHRENS

*Institute of Inorganic Chemistry
University of Erlangen-Nürnberg
Federal Republic of Germany*

I. Introduction	2
II. Reduction of Metal Carbonyls with Alkali Metals and Sodium Tetrahydridoborate in Liquid Ammonia	4
A. Experimental Results	4
B. Structures of the Carbonyl Metalates $[M(CO)_3]^{2-}$, $[M_2(CO)_{10}]^{2-}$, and $[HM_2(CO)_{10}]^-$ ($M = Cr, Mo, W$)	7
III. Reactions of the Pentacarbonyl Metalates(–II) and the Decacarbonyl Dimetalates(–I) of Chromium, Molybdenum, and Tungsten	10
A. Monosubstituted Derivatives of the Hexacarbonyls	10
B. Mono- and Dinuclear Hexacoordinated Pentacarbonyl Metalates(0)	12
C. Heterometallic and Inserted Anionic Complexes	14
D. Paramagnetic Mono- and Dinuclear Pentacarbonyl Complexes of Chromium	16
E. Complexes with $M-M'$ Bonds ($M = Cr, Mo, W$; $M' = Ge, Sn, In$)	17
IV. Reactions of Metal Carbonyls and Metal Carbonyl Derivatives with Liquid Ammonia	19
A. Substitution of CO by NH_3 and Addition of NH_3	19
B. "Base Reactions" and Disproportionations	20
C. Carbamoyl Complexes of Transition Metals with the Ligand $CONH_2$	22
D. Liquid Ammonia as Solvent for Organometallic Reactions	33
E. Cyanocarbonyl Metalates	36
F. Mixed Cyanocarbonyl Metalates Prepared from Metal Carbonyl Derivatives and $NaN(SiMe_3)_2$	38
V. Reactions of Metal Carbonyls and Metal Carbonyl Derivatives with the Multidentate Nitrogen Ligands bipy, phen, and terpy	42
A. Titanium and Vanadium	43
B. Chromium, Molybdenum, and Tungsten	43
C. Iron and Cobalt	45
VI. High-Pressure Syntheses	46
VII. Conclusions	47
References	48

I

INTRODUCTION

While studying chemistry in the years 1933–1937 at the University of Freiburg and at the Technische Hochschule in Munich, I had the good fortune early in my career to come into contact with many famous and important chemists such as Hans Fischer, Georg von Hevesy, Walter Hieber, Otto Hönigschmidt, Hermann Staudinger, Heinrich Wieland, and Eduard Zintl. The lectures on complex chemistry given by Walter Hieber, who, at the age of 39, was appointed Professor in Munich in 1935, made a lasting impression, both from their content and from the didactical excellence of their presentation. I was unusually fascinated by his first review on metal carbonyls (1), which appeared in 1937, as it treated a class of compounds which, at that time, could not be reconciled at all with the normal concepts of inorganic complexes. In the same year I, as a graduate student, was involved with the reactivity of the recently discovered HCo(CO)_4 , which is gaseous at room temperature. In the course of this work, I made my decision to make metal carbonyl chemistry the subject of my dissertation. This decision led to an almost 25-year-long collaboration with Walter Hieber.

At this time, the chemistry of metal carbonyls was very much in its first stages of development. It is significant that the systematic study of this field, which had hardly begun to be covered in the textbooks, was almost exclusively carried out by Hieber. Other than the mononuclear metal carbonyls of the VIB Group, iron, ruthenium, and nickel, only the polynuclear species $\text{Fe}_2(\text{CO})_9$, $\text{Ru}_2(\text{CO})_9$, $\text{Co}_2(\text{CO})_8$, $\text{Fe}_3(\text{CO})_{12}$, and $\text{Co}_4(\text{CO})_{12}$ were known (1). Of these, only the structures of the hexacarbonyls of the chromium group (2) and of $\text{Fe}_2(\text{CO})_9$ (3) had been determined by X-ray structure analyses.

With respect to the derivatives of metal carbonyls, the substituted metal carbonyls of the VIB Group (e.g., $\text{Mo(CO)}_3\text{py}_3$), the halogenocarbonyls of iron, ruthenium, iridium, and platinum, the hydridocarbonyls $\text{H}_2\text{Fe(CO)}_4$ and HCo(CO)_4 discovered in 1931 and 1934, and the nitrosyl carbonyls $\text{Fe(CO)}_2(\text{NO})_2$ and $\text{Co(CO)}_3\text{NO}$ were the most important (1). The known anionic CO complexes were limited to $[\text{HFe(CO)}_4]^-$ and $[\text{Co(CO)}_4]^-$. For studies of substitution reactions of metal carbonyls at this time, work was almost totally limited to reactions involving the classical N ligands such as NH_3 , en, py, bipy, and phen.

Thus, it is understandable that at the end of the 1930s research in the area of metal carbonyls was, for the most part, concentrated on new preparative and reaction methods in liquid media and via high-pressure syntheses starting from transition-metal compounds. The objectives were

the discovery of new mono- and polynuclear metal carbonyls as well as further halogeno- and hydridocarbonyls. Furthermore, researchers were also concerned with the search for other ligands that could replace the CO of metal carbonyls and their derivatives. A final area of interest involved the reactions of metal carbonyls with various Lewis bases (4).

One must bear in mind that at this time none of the spectroscopic methods, which are taken for granted nowadays, were available, so that resort had to be made to extremely careful analytical work. However, the so-called "noble gas rule" was an aid to the research at that time, a concept which should not be underestimated since it played a determining role in planning new experiments and contributed to many successes. I still admire the ability of Hieber, who, with the most modest of means, obtained the wonderful scientific results that—40 years later—remain fundamental concepts of organometallic chemistry.

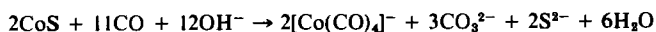
Under these influences, my dissertation was concerned, on the one hand, with the reactions of NiS and CoS with CO in aqueous alkaline suspension (4) and, on the other, with high-pressure syntheses of $\text{Fe}(\text{CO})_5$, $\text{Co}_2(\text{CO})_8$, and $\text{Ni}(\text{CO})_4$ from anhydrous halides and CO in the presence of halogen-absorbing "metal additives" such as Cu and Hg according to (5)



It was observed that the reaction of NiS or $[\text{Ni}(\text{NH}_3)_6][\text{MoS}_4]$ with CO in aqueous alkaline suspension could, in one case, be carried out with an absorption of 4 moles of CO per mole of Ni and, in the other, with only ~ 50% of the total nickel being converted to $\text{Ni}(\text{CO})_4$ (4). The reaction path, which could not at that time be clarified, was later studied by using CO absolutely free of oxygen, and we were able to determine that the quantitative formation of $\text{Ni}(\text{CO})_4$ resulted from a reductive carbonylation (6, 7):



The corresponding reaction of CoS results in the formation of $[\text{Co}(\text{CO})_4]^-$ (6):



The reaction of NiSe with CO in aqueous alkaline suspension is analogous to that of NiS (8).

The structures of the isoelectronic hydridocarbonyls $\text{H}_2\text{Fe}(\text{CO})_4$ and $\text{HCo}(\text{CO})_4$ were the central theme of numerous studies over a period of many years after their discovery by Hieber. Because of their very similar physical characteristics, these complexes were considered to be "pseudo nickel tetracarbonyls" ($\text{H}_2\text{Fe} = \text{HCo} = \text{Ni}$) in which, even then, the

bonding of the hydrogen to the transition metals was intuitively postulated (1). On looking back, it is surprising that it was relatively late that the definite acid character of $\text{HCo}(\text{CO})_4$ in aqueous solution was recognized (9, 10). The reason for this was undoubtedly the fact that, at that time, neither an isolation of the alkali-metal salts from the "base reaction" solution of $\text{Co}_2(\text{CO})_8$ nor an "esterification" of $\text{HCo}(\text{CO})_4$, i.e., the formation of $\text{CH}_3\text{Co}(\text{CO})_4$, had been achieved.

However, in 1941, I was able to show that $\text{HCo}(\text{CO})_4$ is extremely soluble in liquid NH_3 and that $\text{NH}_4[\text{Co}(\text{CO})_4]$ can be isolated at room temperature. This complex can be sublimed at 80°C in vacuum to give long colorless needles (11, 12). With the deep-blue solutions of Li, Na, Ca, or Ba in liquid NH_3 , colorless alkali or alkaline-earth salts of $\text{HCo}(\text{CO})_4$ are formed with evolution of H_2 . Also, by the reaction of $\text{Cd}[\text{Co}(\text{CO})_4]_2$ with sodium in liquid NH_3 , the quantitative formation of $\text{Na}[\text{Co}(\text{CO})_4]$ takes place. Finally, at that time, we were able to prepare $\text{K}[\text{Co}(\text{CO})_4]$ via a reaction analogous to "neutralization" of $\text{NH}_4[\text{Co}(\text{CO})_4]$ with KNH_2 in liquid NH_3 . From these studies, which began in 1941, we showed that liquid NH_3 is an excellent solvent for carbonyl chemistry, and that solutions of the alkali metals in liquid NH_3 function as extremely strong reducing agents (12). These studies represent the basis of "the chemistry of metal carbonyls in liquid NH_3 " which has concerned us continuously now for over 35 years and which has made possible the preparation of numerous new, particularly anionic, carbonyl complexes. Furthermore, these studies in liquid NH_3 have also provided numerous ideas for further experimentation, by both our own and other research groups, which will be presented here.

The following facts concerning the use of liquid NH_3 are of particular importance: (1) its behavior as a solvent similar to water, but with a much lower proton activity; (2) the access to the reaction temperature range of -78 to $+120^\circ\text{C}$ which made possible the preparation and isolation of complexes at low temperatures; and (3) the strong reducing character of the solutions of the alkali metals in liquid NH_3 , which especially allowed for access to the carbonyl metalates having very low oxidation states.

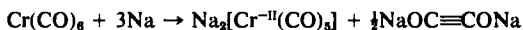
II

REDUCTION OF METAL CARBONYLS WITH ALKALI METALS AND SODIUM TETRAHYDRIDOBORATE IN LIQUID AMMONIA

A. Experimental Results

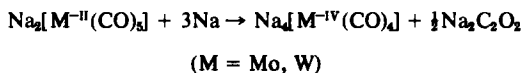
Although the reduction of such mono- and polynuclear metal carbonyls as $\text{Fe}(\text{CO})_5$, $\text{Mn}_2(\text{CO})_{10}$, $\text{Re}_2(\text{CO})_{10}$, $\text{Co}_2(\text{CO})_8$, and $\text{Fe}_3(\text{CO})_{12}$ with finely

divided alkali metals or alkali-metal amalgams in indifferent solvents was first investigated by Hieber's group surprisingly late in the 1950s (13), beginning in 1951 we had success with the quantitative study of such reactions with sodium in liquid NH_3 (14). Short reaction times at -78°C led to the formation of $\text{Na}_2[\text{Fe}(\text{CO})_4]$ or $\text{Na}[\text{Co}(\text{CO})_4]$ from $\text{Fe}(\text{CO})_5$, $\text{Fe}_2(\text{CO})_9$, and $\text{Fe}_3(\text{CO})_{12}$, or $\text{Co}_2(\text{CO})_8$ and $\text{Co}_3(\text{CO})_{12}$. Halogenocarbonyls [e.g., $\text{Fe}(\text{CO})_4\text{I}_2$] were also reduced to the respective *monomeric* carbonyl metalates. The "base reactions" of the Group VIB hexacarbonyls with KOH -methanol led to complicated polynuclear anions whose structures are still not clear. These contain OH^- and CH_3OH ligands as well as CO (13), which means that the preparation of mononuclear pentacarbonyl metalates, such as $[\text{M}(\text{CO})_5]^{2-}$ or $[\text{HM}(\text{CO})_5]^-$ ($\text{M} = \text{Cr}, \text{Mo}, \text{W}$), is not possible by this route because of their extremely strong reducing character. Although it took several years before the first preparation of their isoelectronic counterparts $[\text{Mn}(\text{CO})_5]^-$ and $\text{HMn}(\text{CO})_5$ (13), we had already formed the $[\text{Cr}(\text{CO})_5]^{2-}$ and $[\text{HCr}(\text{CO})_5]^-$ anions by treating $\text{Cr}(\text{CO})_6$ with sodium in liquid NH_3 at -78°C , giving quantitative reduction to the soluble yellow *pentacarbonylchromate*(-II) (15),



whereby most of the evolved CO forms the sparingly soluble disodium acetylenediolate (16).

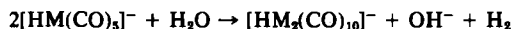
A little later, we were able to obtain the pentacarbonyl metalates(-II) $\text{Na}_2[\text{Mo}^{\text{II}}(\text{CO})_5]$ and $\text{Na}_2[\text{W}^{\text{II}}(\text{CO})_5]$ in low yields (17). The yields were low due to the predominance of further reduction to the sparingly soluble, mononuclear tetracarbonyl metalates(-IV) and formation of $\text{Na}_2\text{C}_2\text{O}_2$:



These complexes have been prepared and spectroscopically characterized by Ellis *et al.* (18) who used the reduction of $(\text{TMEDA})\text{M}(\text{CO})_4$ ($\text{TMEDA} = N,N,N',N'$ -tetramethylethylenediamine) in liquid NH_3 .

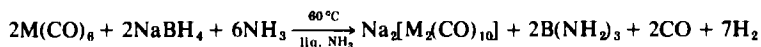
The extremely reactive $[\text{M}^{\text{II}}(\text{CO})_5]^{2-}$ anions ($\text{M} = \text{Cr}, \text{Mo}, \text{W}$) allowed the synthesis of numerous new metal carbonyl complexes of Group VIB, so that what was, until then, rather monotonous chemistry became much more versatile.

In aqueous solution, the intermediate anion $[\text{HM}(\text{CO})_5]^-$ initially formed releases H_2 with complementary oxidation to the dinuclear hydrogen-bridged $[(\text{OC})_5\text{M}-\text{H}-\text{M}(\text{CO})_5]^-$ anions (19), the preparation and structure of which will be discussed in detail.

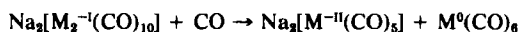


Within the framework of our investigations into the reducing behavior

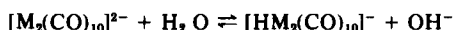
of the hexacarbonyls, we became especially interested in preparative methods leading to the decacarbonyl dimetalates $[M_2(CO)_{10}]^{2-}$ of Group VIB, which are isoelectronic with the dinuclear metal carbonyls of Group VIIB $M_2(CO)_{10}$ ($M = Mn, Tc, Re$). These Group VIB metalates are obtained by closed-system reactions of the hexacarbonyls with $NaBH_4$ in liquid NH_3 (20, 21).



It is interesting that, on the one hand, these yellow decacarbonyl dimetalates disproportionate with CO at $150^\circ C$,



and, on the other, come to a pH-dependent equilibrium in aqueous solution:

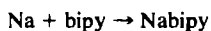
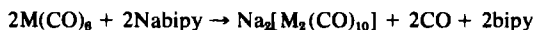


The anions $[M_2(CO)_{10}]^{2-}$ and $[HM_2(CO)_{10}]^-$ can easily be separated via their $[Et_4N]^+$ salts, as a consequence of the different solubilities of these salts in Et_2O (20).

In contrast to the reactions of the hexacarbonyls with $NaBH_4$ in liquid NH_3 , several days of reaction in boiling THF results in reduction to the deeply colored trinuclear carbonyl metalates $Na_2[M_3(CO)_{14}]$ ($M = Cr, Mo, W$), provided the CO evolved is completely removed from the reaction system (22).

Quantitative experiments showed that these anionic cluster-complexes react with bipy and H_2O to give $M(CO)_4bipy$ with evolution of exactly 2 moles of CO and 1 mole of H_2 per mole of $Na_2[M_3(CO)_{14}]$. In this respect, we plan to reinvestigate these complexes, as Churchill and Ni Chang (23) reported that the reaction of $W(CO)_6$ with $[Et_4N]BH_4$ in boiling THF gives red $[Et_4N][W_2(CO)_8H_2]$, the X-ray structure of which leads to the deduction of an anion with two bridging hydrogen ligands (C_{2h} symmetry).

In 1968, we were able to show that at $25^\circ C$ and in the presence of extremely small (catalytic) quantities of bipy, the hexacarbonyls can be reduced by alkali metals to absolutely pure decacarbonyl dimetalates(-I) (24).



The 12 anions that we first discovered, e.g., $[M(CO)_5]^{2-}$, $[HM(CO)_5]^-$, $[M_2(CO)_{10}]^{2-}$, and $[HM_2(CO)_{10}]^-$ ($M = Cr, Mo, W$), have since been the research object of numerous other groups, and further preparative routes have now been developed (25-30). Besides the alkali metals and alkali

amalgams, sodium-potassium alloys, C_6K , and $[Et_4N]BH_4$ as well as various solvents, e.g., hexamethylphosphoramide (HMPA) and dimethoxyethane, have been used.

B. Structures of the Carbonyl Metalates $[M(CO)_5]^{2-}$, $[M_2(CO)_{10}]^{2-}$, and $[HM_2(CO)_{10}]^-$ ($M = Cr, Mo, W$)

As a result of the unusually strong reductive character of the pentacarbonyl metalates(-II) $[M(CO)_5]^{2-}$ ($M = Cr, Mo, W$), and the consequent ready oxidizability of the dinuclear anions $[M_2(CO)_{10}]^{2-}$ and $[HM_2(CO)_{10}]^-$, only relatively lately have we been able to publish an interpreted IR spectrum of $Na_2[Cr(CO)_5]$ (31). There is no doubt, however, that the $[M(CO)_5]^{2-}$ anions have trigonal bipyramidal structures as the observed intensities and frequency differences of the CO bands are inconsistent with a C_{4v} symmetry of a tetragonal pyramid.

Our suggested assignment of the $\nu(CO)$ valence vibrations is based not only on their positions but more so on the frequency separation of the bands within the isoelectronic series $Fe^0(CO)_5$ (32), $[Mn^{-I}(CO)_5]^-$ (32), and $[Cr^{-II}(CO)_5]^{2-}$. Thus, this series may be compared to the similarly isoelectronic series of tetrahedral complexes $Ni^0(CO)_4$, $[Co^{-I}(CO)_4]^-$, and $[Fe^{-II}(CO)_4]^{2-}$. Ellis *et al.* (29) were later able to confirm that $Na_2[Cr(CO)_5]$ prepared by us and by a different route by Kaska (27) is the same complex. This is also, of course, true for this salt which we prepared in 1959 by the reduction of $Na_2[Cr_2(CO)_{10}]$ with sodium in liquid NH_3 (17).

The structure of the dinuclear complex anions $[M_2(CO)_{10}]^{2-}$ ($M = Cr, Mo, W$) was the subject of much argument for over 10 years. At the end of the 1950s we, in collaboration with Beck *et al.* (13), on the basis of the IR spectra, had postulated a nonbridged metal-metal bond, such as was known to occur in the dinuclear metal carbonyls of Group VIIB. A contrasting CO-bridged structure was put forward by Hayter (33) in 1966 for the complexes formed photochemically from the hexacarbonyls and sodium amalgam and described as isomeric with those obtained by us using liquid NH_3 . The contradictions in the IR spectra were rationalized by newer studies together with Lindner *et al.* (34), Kaska (27), and Edgell and Paaue (35). Solvent effects and the nature of the cations both have a marked influence on the frequencies and forms of the CO bands, as less polar solvents (THF) can cause considerable lowering of symmetry due to incomplete dissociation of the dissolved cations and anions (ion pairs).

The three research groups just mentioned were able to prove inde-

pendently that in more polar solvents, in which complete dissociation occurs, the 3 $\nu(\text{CO})$ absorptions expected for D_{4d} symmetry are observed, in accordance with our findings of 10 years earlier (13). In 1970, Dahl and co-workers (36) carried out X-ray structure analyses on $[\text{PPN}][\text{Cr}_2(\text{CO})_{10}]$ and $[\text{PPN}][\text{Mo}_2(\text{CO})_{10}]$ ($\text{PPN} = \text{N}(\text{PPh}_3)_2$) that conclusively proved that both anions have the same D_{4d} structure as $\text{Mn}_2(\text{CO})_{10}$, thus bringing to a successful conclusion an intensive scientific discussion which had lasted for 10 years (see Fig. 1).

The same authors (36) carried out X-ray studies on $[\text{Et}_4\text{N}][\text{HCr}_2(\text{CO})_{10}]$ for which a linear $\text{Cr}-\text{H}-\text{Cr}$ bond in the sense of 2-electron-3-center bonding was found, with the clearly elongated $\text{Cr}-\text{Cr}$ distance leading to D_{4h} symmetry (see Fig. 2). In contrast, the $[\text{HW}_2(\text{CO})_{10}]^-$ anion exists in linear and bent forms, depending upon the cation. Whereas $[\text{Et}_4\text{N}][\text{HW}_2(\text{CO})_{10}]$ has D_{4h} symmetry with eclipsed equatorial carbonyl groups, $[\text{PPN}][\text{HW}_2(\text{CO})_{10}]$ has a bent backbone and staggered equatorial ligands (37).

With respect to the structures of these H-bridged anions, it is interesting to quote two comments (38-40).

Low temperature with single-crystal neutron diffraction techniques has shown that $[\text{Et}_4\text{N}][\text{HW}_2(\text{CO})_{10}]$ has a nonhydrogen framework which is eclipsed and almost linear (or very slightly bent), but the $\text{W}-\text{H}-\text{W}$ bond is markedly bent and asymmetric with a $\text{W}-\text{H}-\text{W}$ angle of 137.1° . In contrast the structure of $[\text{Ph}_4\text{P}][\text{HW}_2(\text{CO})_{10}]$ is nondisordered; the $\text{W}-\text{H}-\text{W}$ linkage is bent and symmetric. (38) The structure is almost identical to that of the isoelectronic $\text{HW}_2(\text{CO})_9\text{NO}$, which can be prepared from $[\text{HW}_2(\text{CO})_{10}]^-$ and NaNO_2 . (39)

A combined room temperature X-ray and neutron diffraction study of $[\text{PPN}][\text{HCr}_2(\text{CO})_{10}]$ has been performed to investigate the effects of crystal packing on the anion and the $\text{Cr}-\text{H}-\text{Cr}$ geometry. A comparison with the earlier work on the $[\text{Et}_4\text{N}]$ salt has shown that the pseudo- D_{4h} geometry of the anion's nonhydrogen framework is maintained. This result indicates that the $[\text{HCr}_2(\text{CO})_{10}]^-$ anion is considerably less susceptible than the tungsten analogue to a twisting deformation from a linear-eclipsed to a bent-staggered configuration. (40)

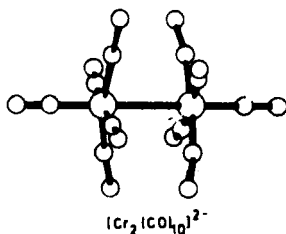


FIG. 1

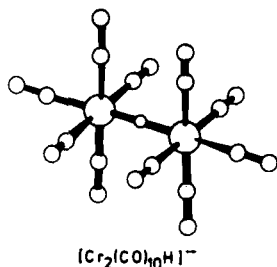


FIG. 2

It is fascinating to the author of this historical review that the $[\text{HM}_2(\text{CO})_{10}]^-$ anions prepared by us in liquid NH_3 over 25 years ago are still the subject of interesting and exciting structural chemical investigations.

Tangential to this theme, I should mention that we have also prepared and characterized by IR spectroscopy nonbridged decacarbonyl dimetalates(-I) having *two different* Group VIB metals, namely, $\text{Na}_2[\text{CrMo}(\text{CO})_{10}]$ and $\text{Na}_2[\text{CrW}(\text{CO})_{10}]$, from $\text{Na}_2[\text{Cr}(\text{CO})_5]$ and $\text{M}(\text{CO})_5 \cdot \text{THF}$ ($\text{M} = \text{Mo}, \text{W}$) (31).

Anders, a former student of mine, together with Graham (41) was earlier able to obtain decacarbonyl dimetalates with one metal of each of Groups VIB and VIIB, namely, $[\text{MnCr}(\text{CO})_{10}]^-$, $[\text{MnMo}(\text{CO})_{10}]^-$, $[\text{MnW}(\text{CO})_{10}]^-$, $[\text{ReCr}(\text{CO})_{10}]^-$, $[\text{ReMo}(\text{CO})_{10}]^-$, and $[\text{ReW}(\text{CO})_{10}]^-$, by reaction of $\text{Na}[\text{M}(\text{CO})_5]$ ($\text{M} = \text{Mn}, \text{Re}$) with $\text{M}(\text{CO})_6$ ($\text{M} = \text{Cr}, \text{Mo}, \text{W}$).

These mixed metalates also have nonbridged structures and may be classified as intermediate between $\text{Mn}_2(\text{CO})_{10}$ and $\text{Re}_2(\text{CO})_{10}$ on the one hand and the isoelectronic anions $[\text{M}_2(\text{CO})_{10}]^{2-}$ ($\text{M} = \text{Cr}, \text{Mo}, \text{W}$) and $[\text{MM}'(\text{CO})_{10}]^{2-}$ ($\text{M} = \text{Cr}; \text{M}' = \text{Mo}, \text{W}$), prepared by us, on the other. The protonation of $[\text{Et}_4\text{N}][\text{ReCr}(\text{CO})_{10}]$ leads to the neutral complex $\text{HReCr}(\text{CO})_{10}$, which has been shown by the X-ray studies of Graham *et al.* to have the same structure as $[\text{HCr}_2(\text{CO})_{10}]^-$ (42).

The reduction of metal carbonyls or their derivatives with sodium in liquid NH_3 , begun by us 35 years ago, has become a method often used successfully by numerous other research groups throughout the world. A few examples are the preparation of $\text{Na}_2[\eta^5\text{-C}_5\text{H}_5\text{V}(\text{CO})_3]$ from $\eta^5\text{-C}_5\text{H}_5\text{V}(\text{CO})_4$ (43) and $[\text{V}^{-\text{III}}(\text{CO})_5]^{3-}$ and $[\text{M}^{-\text{III}}(\text{CO})_3]^{3-}$ ($\text{M} = \text{Co}, \text{Rh}, \text{Ir}$). According to Ellis *et al.* (44), these carbonyl metalates are obtained in the extremely low oxidation state of -III from the anions $[\text{V}^{-\text{I}}(\text{CO})_6]^-$ and $[\text{Co}^{-\text{I}}(\text{CO})_4]^-$ and also from the neutral complexes $\text{M}_3(\text{CO})_{12}$ ($\text{M} = \text{Rh}, \text{Ir}$).

During the 1950s, at the Institute of Inorganic Chemistry at the Tech-

nische Hochschule in Munich, there took place an extremely interesting and stimulating scientific competition between the research groups of my most respected teacher Walter Hieber and myself. Whereas Hieber concentrated his efforts, which were extremely successful, on the polynuclear carbonylferrates (13, 45) having 2, 3, and 4 iron atoms, we concerned ourselves with the various carbonyl metalates of Group VIB.

III

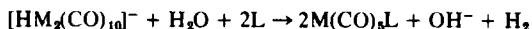
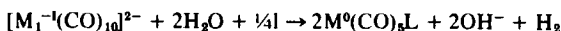
REACTIONS OF THE PENTACARBONYL METALATES(−II) AND THE DECACARBONYL DIMETALATES(−I) OF CHROMIUM, MOLYBDENUM, AND TUNGSTEN

A. Monosubstituted Derivatives of the Hexacarbonyls

Their strong reducing nature is a special characteristic of the pentacarbonyl metalates(−II) and decacarbonyl dimetalates(−I) of chromium, molybdenum, and tungsten that distinguishes them from the other carbonyl metalate anions of the 3d metals, e.g., $[\text{Co}(\text{CO})_4]^-$. The oxidation of the mononuclear species with water



has already been mentioned. In the presence of a monodentate ligand (L), however, $\text{Na}_2[\text{M}(\text{CO})_5]$, $\text{Na}_2[\text{M}_2(\text{CO})_{10}]$, or $\text{Na}[\text{HM}_2(\text{CO})_{10}]$ form with H_2O monosubstituted hexacarbonyls with evolution of H_2 (17, 19–21, 46, 47).

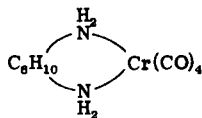


These reactions led to the first preparation of pentacarbonyl complexes of Group VIB, namely, $\text{M}(\text{CO})_5\text{NH}_3$, $\text{M}(\text{CO})_5\text{py}$, and $\text{M}(\text{CO})_5(\text{NH}_2\text{Ph})$ ($\text{M} = \text{Cr}, \text{Mo}, \text{W}$).

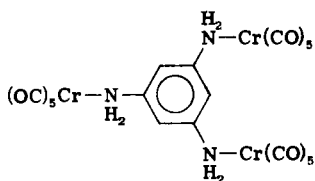
At higher temperatures, the formation of tetracarbonyl derivatives is also possible (e.g., with py) (48).

The analogous reactions using such bidentate ligands as en or phen lead (also via evolution of H_2 and CO) to quantitative formation of the tetracarbonyl derivatives $\text{M}(\text{CO})_4\text{en}$ and $\text{M}(\text{CO})_4\text{phen}$ ($\text{M} = \text{Cr}, \text{Mo}, \text{W}$) (48). Whereas $\text{Na}_2[\text{M}(\text{CO})_5]$ and $\text{Na}_2[\text{M}_2(\text{CO})_{10}]$ react with *o*-phenylenediamine and water to give mononuclear $(\text{H}_2\text{NC}_6\text{H}_4\text{NH}_2)\text{Cr}(\text{CO})_5$, with *m*- and *p*-phenylenediamine, the dinuclear complexes $[(\text{OC})_5\text{M}]\text{H}_2\text{NC}_6\text{H}_4\text{NH}_2[\text{M}(\text{CO})_5]$ are formed, in which two $\text{M}(\text{CO})_5$

groups are linked through aromatic diamine bridges (47). Thus, *o*-phenylenediamine acts exclusively as a monodentate ligand. In contrast, the strongly basic 1,2-cyclohexadienediamine forms the chelate complex (47)



In this series of reactions we were also able to isolate a trinuclear complex for the first time, namely



from $\text{Na}_2=[\text{Cr}(\text{CO})_5]$, 1,3,5-triaminobenzene, and water (47).

Considerable attention has been given to the reactions of the mono- and dinuclear pentacarbonylchromates, -molybdates, and -tungstates with various N ligands, as they were of principal significance to the chemistry of the substituted hexacarbonyls of Group VIB metals. Until then, the mononuclear pentacarbonyl derivatives of the type $\text{M}^0(\text{CO})_5\text{L}$, and the di- or trinuclear, ligand-bridged carbonyl complexes of Group VIB were unknown. The complex $\text{Cr}(\text{CO})_4(\text{PPh}_3)_2$ which we synthesized at that time from $\text{Cr}(\text{CO})_5\text{NH}_3$ and PPh_3 was the first phosphine-substituted derivative of a Group VIB hexacarbonyl (19).

This is understandable when it is considered that the direct substitution of CO in the relatively stable hexacarbonyls by the stronger donor ligands such as py is not possible at low temperatures and that thermal treatment between 160 and 200°C normally causes the mono compound step to be overshoot. It is most impressive how the situation has changed dramatically as a result of the pioneering photochemical studies of Strohmeier *et al.* (49) and how, since 1960, a really hectic development in the area of substituted hexacarbonyls of Group VIB has occurred. In this respect, the derivatives $\text{M}(\text{CO})_5\text{THF}$ have proved to be especially reactive and to constitute a preferred starting material for numerous other pentacarbonyl complexes of chromium, molybdenum, and tungsten.

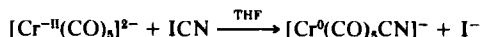
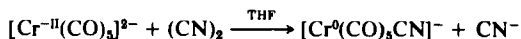
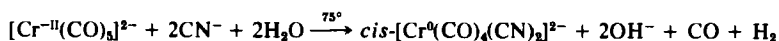
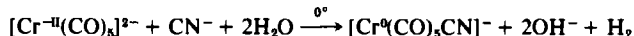
Studies by Guttenberger (50) and Bertrand *et al.* (51) have shown that the ligand-bridged bis(pentacarbonyl metal) complexes, e.g., $(\text{OC})_5\text{M}(\text{NC}-\text{CN})\text{M}(\text{CO})_5$ or $(\text{OC})_5\text{M}-\text{P}(\text{OCH}_2)_3\text{P}-\text{M}(\text{CO})_5$ ($\text{M} = \text{Cr}$,

Mo, W), may also be easily obtained photochemically from the hexacarbonyls and $(\text{CN})_2$ or $\text{P}(\text{OCH}_2)_3\text{P}$ in suitable solvents.

This type of compound was later shown by other authors (52, 53) to be accessible by heating $\text{M}(\text{CO})_6$ with suitable ligands in high-boiling solvents (190–210°C). Examples are $(\text{OC})_5\text{M}-\text{PMe}_2-\text{PMe}_2-\text{M}(\text{CO})_5$ and $(\text{OC})_5\text{M}-\text{AsMe}_2-\text{AsMe}_2-\text{M}(\text{CO})_5$ (52, 53). The synthesis of the series $\text{Cr}(\text{CO})_5\text{NH}_3$, $[(\text{OC})_5\text{Cr}]_2\text{N}_2\text{H}_4$, $[(\text{OC})_5\text{Cr}]_2\text{N}_2\text{H}_2$, and $[(\text{OC})_5\text{Cr}]_2\text{N}_2$ by Sellmann *et al.* (54) in the course of their work on N_2 fixation is especially impressive.

B. Mono- and Dinuclear Hexacoordinated Pentacarbonyl Metalates(0)

Further to the foregoing reactions, my group and others were able to synthesize numerous new anionic and neutral complexes by various reactions of $[\text{M}(\text{CO})_5]^{2-}$ and $[\text{M}_2(\text{CO})_{10}]^{2-}$. Thus, we were able to prepare the cyanocarbonylchromates(0) $[\text{Cr}(\text{CO})_5\text{CN}]^-$ and *cis*- $[\text{Cr}(\text{CO})_4(\text{CN})_2]^{2-}$ by oxidation of $\text{Na}_2[\text{Cr}(\text{CO})_5]$ with aqueous NaCN solution or with $(\text{CN})_2$ or ICN in THF (55, 56):

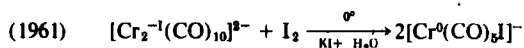


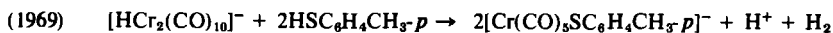
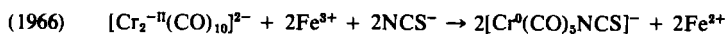
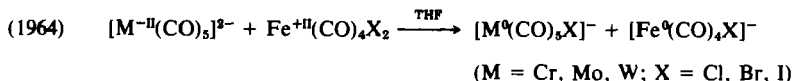
For the analogous reactions of $\text{Na}[\text{M}(\text{CO})_5]$ ($\text{M} = \text{Mn, Re}$) with ICN, we observed a different reaction, namely, that of oxidative elimination, leading to the *cis* configured $[\text{M}(\text{CO})_4(\text{CN})\text{I}]^-$ anions (152):



With the preparation of $\text{Na}[\text{Cr}(\text{CO})_5\text{CN}]$, we not only obtained the first anionic hexacoordinated, pentacarbonyl metalate(0) of Group VIB, but also initiated the extremely extensive chemistry of the $[\text{M}(\text{CO})_5\text{X}]^-$ anions.

Of the many typical redox reactions that we used for the formation of $[\text{M}(\text{CO})_5\text{X}]^-$ anions, the following are given as examples (57–60):





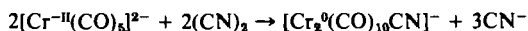
The anions $[\text{Cr}(\text{CO})_5\text{I}]^-$ and $[\text{M}(\text{CO})_5\text{NCS}]^-$ (M = Cr, Mo, W) were prepared by Fischer and Öfele (61) and Wojcicki and Farena (62), respectively, shortly before our own studies.

Considerably later, other research groups described further redox reactions of a similar nature, leading to the anions $[\text{M}(\text{CO})_5\text{C}_4\text{F}_7]^-$ (63), $[\text{M}(\text{CO})_5(\text{C}\equiv\text{CPh})]^-$ (64), $[\text{M}(\text{CO})_5\text{SR}]^-$ (65), or $[\text{M}(\text{CO})_5\text{R}]^-$ (R = Me, Et, NCCCH_3 , PhNH_2) (66).

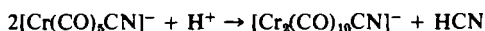
For the sake of completeness, reference should also be made to the work of W. Beck, J. K. Ruff, E. W. Abel, and R. B. King, by whose research groups, between 1963 and 1975, a large number of other $[\text{M}(\text{CO})_5\text{X}]^-$ complexes were synthesized, especially with halide and *pseudo*-halide anions, by thermal or photochemical reactions of $\text{M}(\text{CO})_6$ or $\text{M}(\text{CO})_5\text{THF}$.

Again starting from the decacarbonyl dimetalate(−I) anions, besides the mononuclear $[\text{M}(\text{CO})_5\text{X}]^-$ anions, we were the first to prepare the dinuclear $[\text{M}_2(\text{CO})_{10}\text{X}]^-$ species (M = Cr, Mo, W) with the respective metal having the oxidation state 0. These anions can be formally derived from the unknown dinuclear carbonyls $\text{M}_2(\text{CO})_{11}$ by substituting a CO ligand by X[−] (X = CN, I, NCS, SH, SMe, SEt, SPh).

We obtained the first complex of this type, namely, the $[\text{Cr}_2(\text{CO})_{10}\text{CN}]^-$ anion, as early as 1959, as a by-product of the oxidation of $[\text{Cr}(\text{CO})_5]^{2-}$ with $(\text{CN})_2$ (55, 67):



The monoanion $[\text{Cr}^0(\text{CO})_5\text{CN}]^-$ also gives this dinuclear anion, however, in acid pH regions (55):



The dinuclear species $[\text{Cr}_2(\text{CO})_{10}\text{I}]^-$ (67), $[\text{Cr}_2(\text{CO})_{10}\text{NCS}]^-$ (67), and $[\text{Cr}_2(\text{CO})_{10}\text{SH}]^-$ (60), however, were prepared by reduction of the paramagnetic neutral complexes $\text{Cr}_2(\text{CO})_{10}\text{I}$ (57, 58, 68) and $\text{Cr}_2(\text{CO})_{10}\text{NCS}$ (59), which will be discussed later, as well as from the mononuclear and also paramagnetic $\text{Cr}(\text{CO})_5\text{SH}$ (60) with sodium amalgam in THF:

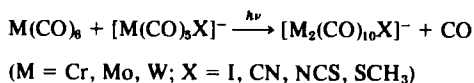


The anions $[\text{Cr}_2(\text{CO})_{10}\text{SH}]^-$ and $[\text{Cr}_2(\text{CO})_{10}\text{SR}]^-$ (R = Me, Et, Ph) are

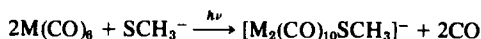
also formed by oxidation and H_2 elimination from $[HCr_2(CO)_{10}]^-$ with water in the presence of SH^- or mercaptans (RSH) (60).

The IR spectra of these anions show that in all cases the complexes are X-bridged with bent or linear $Cr-X-Cr$ bonds ($X = CN, I, NCS, SH, SMe, SEt, SPh$) (60, 69). Dahl and co-workers (70) found by X-ray structure analysis that the $Cr-I-Cr$ angle in $[PPN][Cr_2(CO)_{10}I]$ is $\sim 118^\circ$ (see Fig. 3).

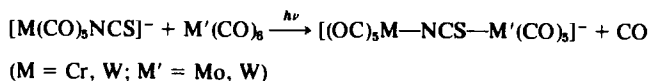
It was somewhat later that Ruff *et al.* (71) turned their attention to the synthesis and structure determination of these dinuclear anions, which they prepared photochemically from $M(CO)_6$ and $[M(CO)_5X]^-$ according to the following process:



or from $M(CO)_6$ and SCH_3^- :



Ruff (71a) was also able to obtain halogen-bridged anionic complexes with different Group VIB metals, namely, $[CrW(CO)_{10}Br]^-$ and $[CrMo(CO)_{10}I]^-$. A little later, we used the same method to gain access to dinuclear NCS-bridged anions with heterometals and bent $M-NCS-M'$ bonds (72):



C. Heterometallic and Inserted Anionic Complexes

Ruff (73) and our group in Erlangen (31) were successful in preparing dinuclear anionic complexes with metals of Groups VIB, VIIB, and

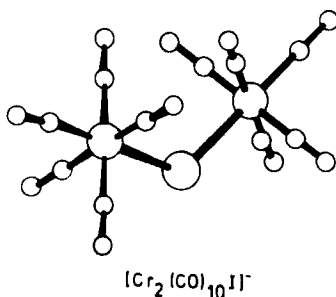
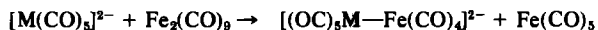
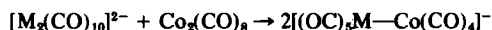


FIG. 3

VIIIB, which are characterized by metal-metal bonding (73 and 31, respectively):



(M = Cr, Mo, W)

Our suggested structure for the $[MFe(CO)_9]^{2-}$ anions, based on IR data, is given in Fig. 4.

With this work, we were able to complete the isoelectronic series based on chromium: $[Cr_2(CO)_{10}]^{2-}$, $[CrMn(CO)_{10}]^-$, $[CrFe(CO)_9]^{2-}$, and $[CrCo(CO)_9]^-$. However, the series cannot be extended to include nickel.

Of particular interest are the insertion reactions carried out by Ruff (74) in which SnI_2 , GeI_2 , or SO_2 is inserted into the metal-metal bonds of $[M_2(CO)_{10}]^{2-}$ anions to give bridged species of the type $[(OC)_5M(EI_2)M(CO)_5]^{2-}$ (E = Ge, Sn) or $[(OC)_5M(SO_2)M(CO)_5]^{2-}$. The insertion of Hg was, however, only successful into $[Cr_2(CO)_{10}]^{2-}$, a result that our own experiments have confirmed. The product is the $[(OC)_5Cr-Hg-Cr(CO)_5]^{2-}$ anion, which is isoelectronic with $(OC)_5Mn-Hg-Mn(CO)_5$ and has linear Cr-Hg-Cr bonds (75). In the case of $K_2[Fe_2(CO)_8]$, the insertion of all the Group IIB metals into the Fe-Fe bond of the nonbridged $[Fe_2(CO)_8]^{2-}$ anion is also possible (75). The anionic complexes $[(OC)_4Fe-M-Fe(CO)_4]^{2-}$ (M = Zn, Cd, Hg) so formed are isoelectronic with the neutral complexes $(OC)_4Co-M-Co(CO)_4$, described by Hieber and Teller (76) over 35 years ago.

A contrasting reaction is that of $Ni(CO)_4$ with $[PPN]_2[W_2(CO)_{10}]$, which gives the anionic cluster compound $[PPN]_2[W_2Ni_3(CO)_{18}]$, whose X-ray structure has been determined by Ruff and co-workers (77):

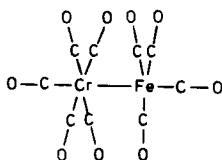
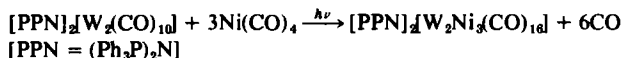
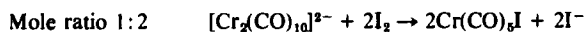
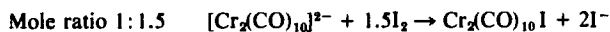


FIG. 4

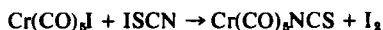
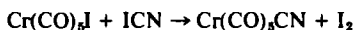
D. Paramagnetic Mono- and Dinuclear Pentacarbonyl Complexes of Chromium

The mono- and dinuclear carbonyl metalates of Cr, Mo, and W, first prepared by us using liquid NH_3 , have also been of great importance for the synthesis of numerous neutral complexes not accessible by other routes. Special attention is drawn to the deeply colored and very unstable mono- and dinuclear paramagnetic complexes $\text{Cr}(\text{CO})_5\text{I}$, $\text{Cr}_2(\text{CO})_{10}\text{I}$, $\text{Cr}(\text{CO})_5\text{CN}$, $\text{Cr}(\text{CO})_5\text{NCS}$, $\text{Cr}_2(\text{CO})_{10}\text{NCS}$, and $\text{Cr}(\text{CO})_5\text{SH}$.

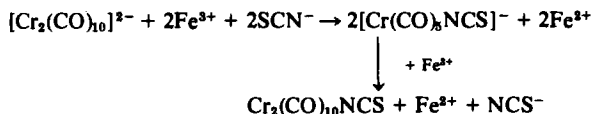
We had already seen that oxidation of $[\text{Cr}_2^{-1}(\text{CO})_{10}]^{2-}$ with I_2 leads to yellow $[\text{Cr}^0(\text{CO})_5\text{I}]^-$ (57). With excess iodine, however, the oxidation goes further, to the deep-blue, hexacoordinated, thermally very unstable $\text{Cr}^{+1}(\text{CO})_6\text{I}$, by which reaction the dinuclear, deep red, paramagnetic, neutral complex of $\text{Cr}_2(\text{CO})_{10}\text{I}$ may be isolated as the intermediate. The actual compound formed is solely dependent upon the mole ratio of $[\text{Cr}_2(\text{CO})_{10}]^{2-} : \text{I}_2$ (57, 58, 68):



Deep-green $\text{Cr}(\text{CO})_5\text{CN}$ and deep-red $\text{Cr}(\text{CO})_5\text{NCS}$, which are stable up to -25°C and, like $\text{Cr}(\text{CO})_5\text{I}$, show the paramagnetism of a single unpaired electron, are formed from the reaction of $\text{Cr}(\text{CO})_5\text{I}$ with ICN or ISCN (78):



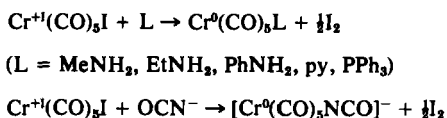
The dinuclear NCS-bridged neutral complex $\text{Cr}_2(\text{CO})_{10}\text{NCS}$ (59) is obtained by oxidation of $[\text{Cr}_2(\text{CO})_{10}]^{2-}$ with excess Fe^{3+} cations in the presence of NCS^- :



All the mono- and dinuclear anionic and neutral complexes of the types $[\text{Cr}(\text{CO})_5\text{X}]^-$, $[\text{Cr}_2(\text{CO})_{10}\text{X}]^-$, $\text{Cr}(\text{CO})_5\text{X}$, and $\text{Cr}_2(\text{CO})_{10}\text{X}$ ($\text{X} = \text{I}, \text{CN}, \text{NCS}$) have been studied in detail by us by IR spectroscopy (69). The neutral dinuclear complex $\text{Cr}_2(\text{CO})_{10}\text{CN}$ has, however, to date eluded isolation (69). Especially characteristic is the mode of formation of the deep-green monomeric and paramagnetic complex $\text{Cr}(\text{CO})_5\text{SH}$ from $[\text{Cr}_2(\text{CO})_{10}]^{2-}$ and SO_2 in aqueous solution (60). Although in organic sol-

vents SO_2 is inserted into the Cr—Cr bond of $[\text{Cr}_2(\text{CO})_{10}]^{2-}$ (74), in H_2O oxidation of Cr^{-1} to Cr^{+1} occurs with simultaneous reduction of SO_2 to SH^- anion. The latter functions as a complex ligand and thus allows formation of $\text{Cr}(\text{CO})_5\text{SH}$ with its bent Cr—S—H grouping. This reductive behavior of $\text{Na}_2[\text{Cr}_2(\text{CO})_{10}]$ may be compared with its reaction with 2-bromo-2-nitrosopropane $\text{Me}_2\text{C}(\text{NO})\text{Br}$ which King and Douglas (79) have shown to lead to (dimethylketimino) pentacarbonylchromium $\text{Me}_2\text{C}=\text{N}(\text{H})\text{Cr}(\text{CO})_5$.

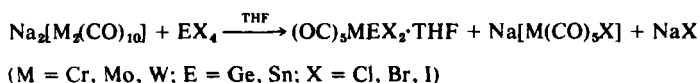
The mono- and dinuclear paramagnetic complexes are of course extremely reactive. We have shown that the reactions of $\text{Cr}(\text{CO})_5\text{I}$ and $\text{Cr}_2(\text{CO})_{10}\text{I}$ with various mono- and bidentate ligands lead to the formation of the respective substitution products of $\text{Cr}(\text{CO})_6$ with simultaneous oxidation to elemental I_2 (80):



The mechanism of the reaction of $\text{Cr}(\text{CO})_5\text{I}$ with NO in Et_2O at low temperature is not yet known. All five CO ligands are eliminated, to give a red solution from which we have precipitated violet $\text{Cr}(\text{NO})_2(\text{PPh}_3)_2\text{I}_2$ on addition of PPh_3 . The NO groups are cis-oriented (81).

E. Complexes with M—M' Bonds ($M = \text{Cr}, \text{Mo}, \text{W}$; $M' = \text{Ge}, \text{Sn}, \text{In}$)

We have also reacted $\text{Na}_2[\text{M}_2(\text{CO})_{10}]$ with the tetrahalides of germanium and tin (EX_4) in THF. Monomeric complexes of the type $(\text{OC})_5\text{MEX}_2\cdot\text{THF}$ are formed, according to (82):

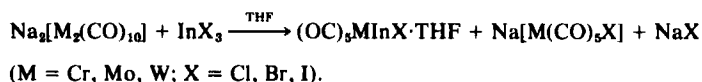


The Group VIB metals are pseudo-octahedrally coordinated, whereas germanium and tin have a pseudo-tetrahedral environment (82).

We obtained the compounds $(\text{OC})_5\text{MGeCl}_2\cdot\text{THF}$ and $(\text{OC})_5\text{MSnX}_2\cdot\text{THF}$ niium and tin (EX_4) in THF. Monomeric complexes of the type reaction of $\text{M}(\text{CO})_6$ with CsGeCl_3 or SnX_2 (83). With $[\text{Et}_4\text{N}]\text{X}$, these compounds give the anions $[\text{M}(\text{CO})_5\text{GeCl}_3]^-$ and $[\text{M}(\text{CO})_5\text{SnX}_3]^-$ (83). We were also able to obtain such anions by the insertion of SnCl_2 into the M—Cl bonds of $[\text{M}^0(\text{CO})_5\text{Cl}]^-$ anions (83). These anions with GeCl_3 and SnCl_3 ligands had been prepared earlier by Ruff (84) by the photochemical

reaction of $M(CO)_6$ with $[Ph_4As][GeCl_3]$ or $[Ph_4As][SnCl_3]$. In 1971, Marks (85) obtained the methyl and butyl derivatives $(OC)_5CrER_2 \cdot THF$ ($E = Ge, Sn$) from $Na_2[Cr_2(CO)_{10}]$ and R_2ECl_2 .

New studies by our group have shown that the indium trihalides InX_3 ($X = Cl, Br, I$) also react with $Na_2[M_2(CO)_{10}]$ according to (86):

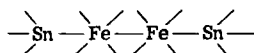


The structure of $Cr(CO)_5InBr \cdot THF$ established by X-ray diffraction shows that in this molecule the Cr, In, and Br atoms and the THF ring form an almost planar structural unit in which the In atom is tricoordinated (86). In the crystals, two additional coordinative bonds to two bromine atoms of neighboring molecules are present, so that the indium is pentacoordinated (see Fig. 5). The molecules are stacked in the c axis, whereby the InBr groups so lie that a double chain having alternating In and Br atoms is formed.

In this context, it is relevant that nonbridged $K_2[Fe_2(CO)_8]$ with Ph_3SnCl or Ph_2SnCl_2 forms neutral complexes in which, in contrast to the corresponding reaction of $Na_2[M_2(CO)_{10}]$ ($M = Cr, Mo, W$), the Fe—Fe bond remains intact (87):

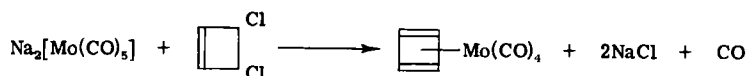


Both complexes unequivocally occur as trans-trans isomers (87):



To complete this section, I should like to mention the following remarkable reactions of $Na_2[M^{-II}(CO)_5]$ and $Na_2[M_2^{-I}(CO)_{10}]$:

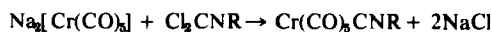
(1) the formation of cyclobutadiene-metal carbonyl complexes (88)



(2) the formation of thiocarbonyl complexes (89)



(3) the formation of isonitrile complexes (90)



(4) the formation of $Cr(CO)_4P_2I_3$ from $Na_2[Cr(CO)_5]$ and P_2I_4 (91).

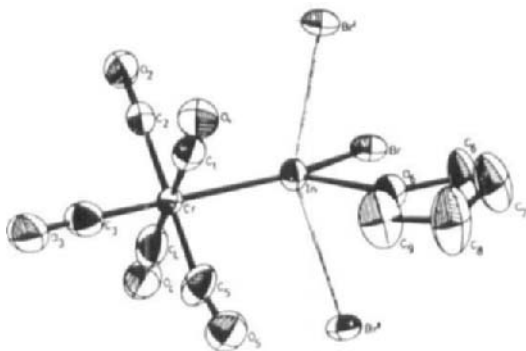


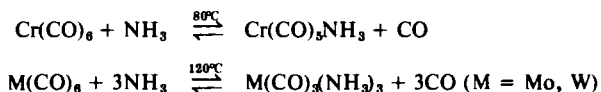
FIG. 5

IV

REACTIONS OF METAL CARBONYLS AND METAL CARBONYL DERIVATIVES WITH LIQUID AMMONIA

A. Substitution of CO by NH₃ and Addition of NH₃

In numerous experiments we have found that liquid NH₃ can replace CO or other ligands in metal carbonyls or their derivatives and also that NH₃ can become an additional ligand bonded to a transition metal. Thus, the hexacarbonyls of Group VIB can form pentacarbonylamine or tricarbonylamine derivatives, depending upon the temperature conditions (92):

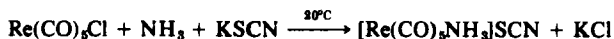


In liquid NH₃, one CO group can also be replaced by NH₃ in the case of the tetracarbonyl complexes M(CO)₄bipy and M(CO)₄phen. "Mixed" species M(CO)₃bipy(NH₃) or M(CO)₃phen(NH₃) (M = Cr, Mo, W) are formed with the remaining CO ligands being in cis positions (92). Mixed complexes of the type M(CO)₃(NN)L (NN = bipy, phen; L = monodentate N, P, or S ligand) have been known since 1935 from the work of Hieber *et al.* (93); and a large number, described by other authors, have been known for a long time. Our own work in liquid NH₃ allowed the first preparation of the respective NH₃ derivatives.

Although Ni(CO)₄ does not enter into reaction with liquid NH₃ up to -33°C, between -25 and 110°C, CO is substituted by NH₃ to give an

inseparable mixture of pale-yellow $\text{Ni}(\text{CO})_3\text{NH}_3$ and $\text{Ni}(\text{CO})_2(\text{NH}_3)_2$ which are only stable as solids up to -60°C (94).

Fischer and Jira (95) treated $[\text{Ni}(\text{NH}_3)_6](\text{SCN})_2$ with $\text{C}_5\text{H}_5\text{K}$ in liquid NH_3 to obtain $[\text{Ni}(\text{NH}_3)_4](\text{C}_5\text{H}_5)_2$. We obtained the same ionic complex directly from $\text{Ni}(\eta^5\text{-C}_5\text{H}_5)_2$ in liquid NH_3 (96). We were also able to show similar behavior for $\text{Re}(\text{CO})_5\text{X}$ ($\text{X} = \text{Cl}, \text{Br}, \text{I}$) which, on treatment with liquid NH_3 at 60 or 120°C for at least 40 h, gives the ionic complexes *cis*- $[\text{Re}(\text{CO})_4(\text{NH}_3)_2]\text{X}$ or $[\text{Re}(\text{CO})_3(\text{NH}_3)_3]\text{X}$ (97). We similarly obtained an ionic pentacarbonylamine complex from $\text{Re}(\text{CO})_5\text{Cl}$ and KSCN in liquid NH_3 (97):

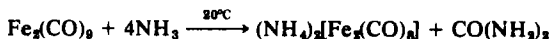


B. "Base Reactions" and Disproportionations

Completely different behavior toward liquid NH_3 is shown by the three iron carbonyls $\text{Fe}(\text{CO})_5$, $\text{Fe}_2(\text{CO})_9$, and $\text{Fe}_3(\text{CO})_{12}$ (98, 99) and the two cobalt carbonyls $\text{Co}_2(\text{CO})_8$ and $\text{Co}_4(\text{CO})_{12}$ (100). Between -21 and 0°C , $\text{Fe}(\text{CO})_5$ and liquid NH_3 give a homogeneous, pale-yellow solution from which $\text{Fe}(\text{CO})_5$ may be recovered on evaporating off the NH_3 . The solution contains the carbamoyl complex $\text{NH}_4[(\text{OC})_4\text{Fe}-\text{CONH}_2]$ which cannot be isolated and which is formed by nucleophilic attack of an NH_3 molecule on a CO ligand, followed by proton release (101). At 20°C after 14 days of reaction, $(\text{NH}_4)_2[\text{Fe}(\text{CO})_4]$ and $\text{CO}(\text{NH}_2)_2$ are obtained (99):



In contrast to the reactions of $\text{M}(\text{CO})_6$ ($\text{M} = \text{Cr}, \text{Mo}, \text{W}$), a redox system operates here which is comparable, also in terms of the reaction mechanism, with the so-called "base reaction" of $\text{Fe}(\text{CO})_5$ (13). The reaction of $\text{Fe}_2(\text{CO})_9$ in liquid NH_3 is similar:



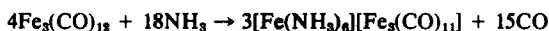
This corresponds to the base reaction of $\text{Fe}_2(\text{CO})_9$ with alcoholic alkali according to the following equation:



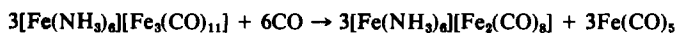
This also leads to the formation of the octacarbonyldiferrate anion $[\text{Fe}_2(\text{CO})_8]^{2-}$ having a nonbridged $\text{Fe}-\text{Fe}$ bond (13).

In contrast, the reaction of $\text{Fe}_3(\text{CO})_{12}$ in liquid NH_3 is comparatively complicated, especially as the time allowed for reaction is of decided

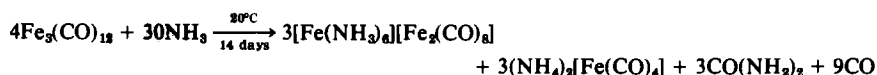
importance (99). The primary reaction is disproportionation:



After about 14 days, the trinuclear carbonylferrate undergoes further reaction with the free CO to form the dinuclear carbonylferrate and $\text{Fe}(\text{CO})_5$.

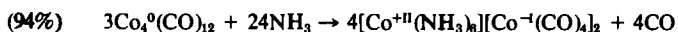
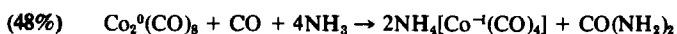
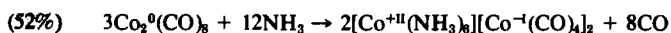


Since, as already described, $\text{Fe}(\text{CO})_5$ reacts to give $(\text{NH}_4)_2[\text{Fe}(\text{CO})_4]$ and $\text{CO}(\text{NH}_2)_2$, the complete reaction equation for $\text{Fe}_3(\text{CO})_{12}$ and liquid NH_3 after 14 days of reaction can be described by the following:



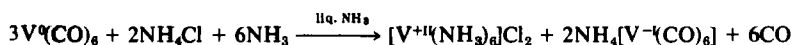
The polynuclear carbonylferrates and their structure determinations by L. F. Dahl have been dealt with in some detail in my lecture *The Chemistry of Metal Carbonyls: The Life Work of Walter Hieber* given at the Symposium on Metal Carbonyls in 1974 in Ettal (102).

The reactions of $\text{Co}_2(\text{CO})_8$ and $\text{Co}_4(\text{CO})_{12}$ in liquid NH_3 have also been the subject of our investigations, and in both cases at 20°C disproportionation of the cobalt occurs with CO elimination. The CO then undergoes a secondary reaction with still unreacted carbonyl to give sublimable $\text{NH}_4[\text{Co}(\text{CO})_4]$ and $\text{CO}(\text{NH}_2)_2$ (100):



Paramagnetic $\text{V}(\text{CO})_6$ behaves analogously in liquid NH_3 , i.e., disproportionation of vanadium occurs, to give $[\text{V}^{+II}(\text{NH}_3)_6][\text{V}^{-I}(\text{CO})_6]_2$ with formation of $\text{NH}_4[\text{V}(\text{CO})_6]$ and urea (103).

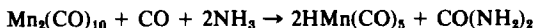
We have also observed the disproportionation of vanadium in the reaction of $\text{V}(\text{CO})_6$ with the ammonio acid NH_4Cl (103):



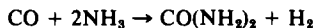
The reaction of $\text{Mn}_2(\text{CO})_{10}$ with liquid NH_3 at 20°C differs from those of the two cobalt carbonyls in that the disproportionation involves the formation of the cation *fac*- $[\text{Mn}(\text{CO})_3(\text{NH}_3)_3]^+$ (104):



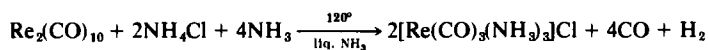
Here, as in isoelectronic $\text{Cr}(\text{CO})_3(\text{NH}_3)_3$, the three CO and the three NH_3 ligands are in *fac* positions. Some of the free CO reduces unchanged $\text{Mn}_2(\text{CO})_{10}$,



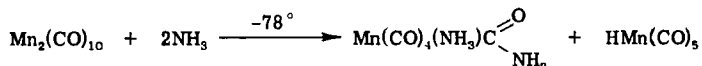
and some of it carbonylates NH_3 :



The reaction of $\text{Re}_2(\text{CO})_{10}$ with NH_4Cl in liquid NH_3 at 120°C occurs without side reactions, giving quantitative oxidation to *fac*- $[\text{Re}(\text{CO})_3(\text{NH}_3)_3]\text{Cl}$ with elimination of H_2 (97):



There is no doubt that most of the mono- and polynuclear metal carbonyls react with liquid NH_3 via nonisolable carbonyl carbamoyl intermediate complexes in which the acid amide group $-\text{CONH}_2$ is directly bound to the transition metal. For the reaction of $\text{Mn}_2(\text{CO})_{10}$ with liquid NH_3 , we have been able to show that, at -78°C , quantitative formation of *cis*- $\text{Mn}(\text{CO})_4(\text{NH}_3)-\text{CONH}_2$ and $\text{HMn}(\text{CO})_5$ occurs (105) according to the following reaction:



At room temperature, the secondary reactions already described play a part and cause the parallel formation of $[\text{Mn}(\text{CO})_3(\text{NH}_3)_3][\text{Mn}(\text{CO})_5]$, $\text{HMn}(\text{CO})_5$, $\text{CO}(\text{NH}_2)_2$, H_2 , and CO (104).

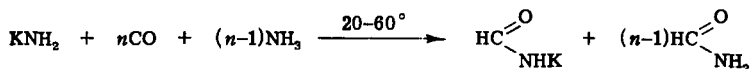
C. Carbamoyl Complexes of Transition Metals with the Ligand CONH_2

Two observations that we made in 1966 have been important in molding the history of the development of this interesting class of compounds. The first involves the reaction of $[\text{Mn}(\text{CO})_6]\text{Cl} \cdot \text{HCl}$ with liquid NH_3 at 20°C (104):

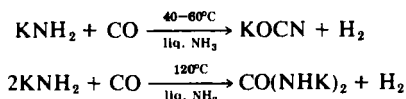


For this reaction, we proposed a mechanism involving a nonisolable intermediate of pentacarbonylcarbamoylmanganese(+I) $\text{Mn}(\text{CO})_5\text{CONH}_2$ (104). The second involves the reactions of CO with solutions of KNH_2 in liquid NH_3 (106). In the presence of a large excess of CO, formamide

and potassium formamide are formed together, viz:

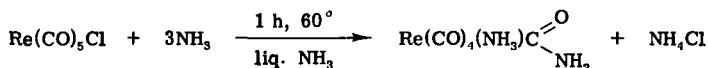


In contrast an excess of KNH_2 , depending on the temperature, causes formation of hydrogen together with potassium cyanate or dipotassium urea:

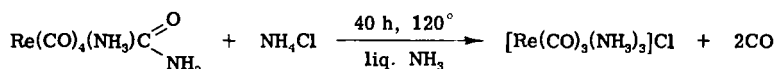
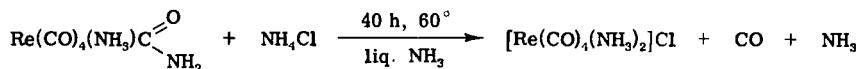


If this reaction of KNH_2 and CO in liquid NH_3 is extended to coordinatively bonded CO in cationic carbonyl complexes, instead of the formation of formamide, carbonylcarbamoyl compounds of the type $\text{M}(\text{CO})_n\text{—CONH}_2$ result, and instead of H_2 and KOCN (or $\text{CO}(\text{NHK})_2$), hydridocarbonyls and NH_4OCN [or $\text{CO}(\text{NH}_2)_2$] are formed.

The first carbonylcarbamoyl complex that we described, *cis*- $\text{Re}(\text{CO})_4(\text{NH}_3)\text{CONH}_2$, was obtained by the reaction of $\text{Re}(\text{CO})_5\text{Cl}$ with liquid NH_3 at 60°C , after a reaction time of only 1 hour, and without CO evolution (107):



The salt $[\text{Re}(\text{CO})_5\text{NH}_3]\text{Cl}$ certainly occurs as an intermediate in this reaction. As the ammonio acid NH_4Cl is formed, depending on the temperature, a prolonged reaction time causes *cis*- $\text{Re}(\text{CO})_4(\text{NH}_3)\text{CONH}_2$ to give the ionic complexes $[\text{Re}(\text{CO})_4(\text{NH}_3)_2]\text{Cl}$ or $[\text{Re}(\text{CO})_3(\text{NH}_3)_3]\text{Cl}$ with CO elimination:



As early as 1965, Angelici (108) was concerned with the reaction of $\text{Mn}(\text{CO})_5\text{Cl}$ with primary and secondary aliphatic amines. He initially considered the product with MeNH_2 , namely, $\text{Mn}(\text{CO})_5(\text{NH}_2\text{Me})(\text{NHMe})$, to be a complex of heptacoordinated manganese. A subsequent X-ray structure analysis showed, however, that it is in fact a hexacoordinated carbamoyl complex, $\text{Mn}(\text{CO})_4(\text{NH}_2\text{Me})\text{CONHMe}$ (109). In continuation of these studies, the reaction of cationic CO complexes of various tran-

sition metals with primary and secondary amines was investigated by Angelici (110); and, in parallel, independent work, our own Erlanger group looked systematically at the reactions in liquid NH_3 between -78 and 120°C . The stabilities and reactivities of the resulting carbamoyl complexes with $-\text{CONHR}$ and $-\text{CONR}_2$ groups are remarkably different from those with the unsubstituted $-\text{CONH}_2$ ligand.

Following our experiments with $\text{Re}(\text{CO})_5\text{Cl}$, we investigated the behavior of $\text{Mn}(\text{CO})_5\text{Cl}$, $\text{Mn}(\text{CO})_4(\text{PPh}_3)\text{Cl}$, and $[\text{Mn}(\text{CO})_4(\text{PPh}_3)_2]\text{Cl}$ with liquid NH_3 ; and, after very short reaction times (max. 10 min), we were able to isolate the three carbamoyl complexes *cis*- $\text{Mn}(\text{CO})_4(\text{NH}_3)\text{CONH}_2$, *fac*- $\text{Mn}(\text{CO})_3(\text{PPh}_3)(\text{NH}_3)\text{CONH}_2$, and *fac*- $\text{Mn}(\text{CO})_3(\text{PPh}_3)_2\text{CONH}_2$. The stabilities of these complexes increase markedly in this order (111). All of them react at 60 – 120°C with NH_4Cl in liquid NH_3 via CO , or CO and PPh_3 , substitution to give ionic $[\text{Mn}(\text{CO})_3(\text{NH}_3)_3]\text{Cl}$.

The ionic species $[\text{Mn}(\text{CO})_5\text{NH}_3]\text{Cl}$, $[\text{Mn}(\text{CO})_4(\text{PPh}_3)\text{NH}_3]\text{Cl}$, and $[\text{Mn}(\text{CO})_4(\text{PPh}_3)_2]\text{Cl}$ are formed from these carbamoyl complex series by reaction with HCl in C_6H_6 , according to the following type of reaction.

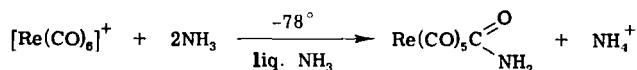


As a general rule, the carbonylcarbamoyl complexes of rhenium are considerably more stable than those of manganese.

In an attempt to isolate the carbamoyl compound $\text{Mn}(\text{CO})_5\text{CONH}_2$, which had earlier been postulated by us as an intermediate in the reaction of $[\text{Mn}(\text{CO})_6]^+$ with liquid NH_3 , we carried out the reaction at -78°C . However, even under these conditions, the only products were $\text{HMn}(\text{CO})_5$ and NH_4NCO (112).

Thus, it may be assumed that, in analogy with the Hofmann acid amide degradation, the $-\text{CONH}_2$ group of the carbamoyl complex is oxidized to NCO^- .

Although, between 20 and 60°C , $[\text{Re}(\text{CO})_6]^+$ behaves similarly to the manganese compound, giving the hydridocarbonyl complex $\text{HRe}(\text{CO})_5$, at -78°C , we were able to isolate and characterize, the extremely unstable $\text{Re}(\text{CO})_5\text{CONH}_2$ (112):

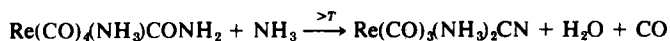


The behavior of cationic penta- and tetracarbonyl complexes of manganese and rhenium toward liquid NH_3 at various temperatures is summarized in Table I (112).

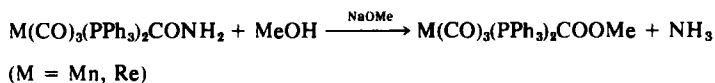
TABLE I

Cationic starting compounds	Temperature (°C)	Reaction products
$[\text{Mn}(\text{CO})_5\text{PPh}_3]^+$	-70	<i>cis</i> - $\text{Mn}(\text{CO})_4(\text{PPh}_3)\text{CONH}_2$
$[\text{Mn}(\text{CO})_5\text{PPh}_3]^+$	30	$\text{HMn}(\text{CO})_4\text{PPh}_3 + \text{NH}_4\text{NCO}$
$[\text{Mn}(\text{CO})_5\text{PEt}_3]^+$	-70	$\text{HMn}(\text{CO})_4\text{PEt}_3 + \text{NH}_4\text{NCO}$
$[\text{Re}(\text{CO})_5\text{PPh}_3]^+$	-33	<i>cis</i> - $\text{Re}(\text{CO})_4(\text{PPh}_3)\text{CONH}_2$
$[\text{Re}(\text{CO})_5\text{PEt}_3]^+$	-78	<i>cis</i> - $\text{Re}(\text{CO})_4(\text{PEt}_3)\text{CONH}_2$
<i>trans</i> - $[\text{Mn}(\text{CO})_4(\text{PEt}_3)_2]^+$	-33	<i>mer-cis</i> - $\text{Mn}(\text{CO})_3(\text{PEt}_3)_2\text{CONH}_2$
<i>trans</i> - $[\text{Re}(\text{CO})_4(\text{PPh}_3)_2]^+$	60	<i>mer</i> - $\text{Re}(\text{CO})_3(\text{PPh}_3)_2\text{CONH}_2$
<i>cis</i> - $[\text{Re}(\text{CO})_4(\text{PEt}_3)_2]^+$	60	<i>fac</i> - $\text{Re}(\text{CO})_3(\text{PEt}_3)_2\text{CONH}_2$
<i>cis</i> - $[\text{Mn}(\text{CO})_4\text{bipy}]^+$	-33	<i>fac</i> - $\text{Mn}(\text{CO})_3(\text{bipy})\text{CONH}_2$
<i>cis</i> - $[\text{Re}(\text{CO})_4\text{bipy}]^+$	60	<i>fac</i> - $\text{Re}(\text{CO})_3(\text{bipy})\text{CONH}_2$
<i>cis</i> - $[\text{Mn}(\text{CO})_4\text{phen}]^+$	-33	<i>fac</i> - $\text{Mn}(\text{CO})_3(\text{phen})\text{CONH}_2$

From these results, it may be concluded that the stabilities increase markedly on going from the penta-, through the tetra- to the tricarbonylcarbamoyl derivatives. As the examples of $\text{Re}(\text{CO})_5\text{CONH}_2$ and $\text{Re}(\text{CO})_5\text{CONHMe}$ (113) show, the complexes with $-\text{CONHR}$ and $-\text{CONR}_2$ ligands are considerably more stable than the comparable $-\text{CONH}_2$ compounds. With gaseous HCl , $\text{Re}(\text{CO})_5\text{CONH}_2$ and the carbonylcarbamoyl complexes listed in Table I revert to the cationic starting compounds. In the case of $\text{Re}(\text{CO})_4(\text{NH}_3)\text{CONH}_2$ in liquid NH_3 , one can observe the elimination of H_2O from the $-\text{CONH}_2$ group,



leading to cyanodiamminetricarbonylrhenium(+I) (112). With CH_3OH , the carbamoyl complexes give the respective carboalkoxo derivatives (114):



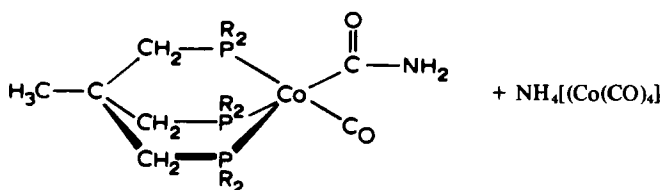
When these results are considered, it is understandable that the pentacoordinated $[\text{Co}(\text{CO})_4\text{PPh}_3]^+$ cation with NHMe_2 forms the very stable *N,N'*-dimethylcarbamoyltriphenylphosphinetricarbonylcobalt(+I) species $\text{Co}(\text{CO})_3(\text{PPh}_3)\text{CONMe}_2$, but, with liquid NH_3 at -50°C the products are $\text{HCo}(\text{CO})_3(\text{PPh}_3)$ and NH_4NCO (115).

The initial step in all of these reactions is nucleophilic attack of an NH_3 molecule on a CO ligand of the cation, with formation of a carbamoyl

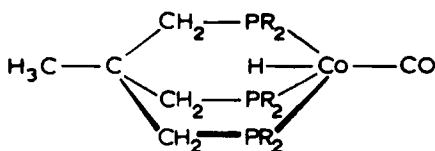
$$\begin{array}{ccc}
 [\text{O}=\text{C}=\text{Co}(\text{CO})_3(\text{PPh}_3)]^+ & \longleftrightarrow & [\text{O}=\text{C}-\text{Co}(\text{CO})_3(\text{PPh}_3)]^+ \\
 & & \downarrow \text{NH}_3 \\
 \text{H}_2\text{N}-\overset{\text{O}}{\parallel}{\text{C}}-\text{Co}(\text{CO})_3(\text{PPh}_3) & \xleftarrow{+\text{NH}_3} & \left[\text{O}=\underset{\text{NH}_3}{\underset{+}{\text{C}}}-\text{Co}(\text{CO})_3(\text{PPh}_3) \right]^+
 \end{array}$$
$$\text{H}_2\text{N}-\overset{\text{O}}{\parallel}\text{C}-\text{Co}(\text{CO})_3(\text{PPh}_3) + \text{NH}_3 \xrightarrow{\text{liq. NH}_3} \left[\text{HN}^{\ominus}-\overset{\text{O}}{\parallel}\text{C}-\text{Co}(\text{CO})_3(\text{PPh}_3) \right]^{-} + \text{NH}_4^{+}$$
$$\left[\begin{array}{c} \text{O} \\ \parallel \\ \text{HN}^{\ominus} - \text{C} - \text{Co}(\text{CO})_3(\text{PPh}_3) \end{array} \right]^{-}$$
$$\left[\begin{array}{c} \text{O} \\ \parallel \\ \text{HN} - \text{C} - \text{Co}(\text{CO})_3(\text{PPh}_3) \\ | \\ \ominus \end{array} \right]^- \xrightarrow{\text{liq. NH}_3} \text{HCo}(\text{CO})_3\text{PPh}_3 + [\text{N}=\text{C}=\text{O}]^- \longleftrightarrow [\text{N}\equiv\text{C}-\text{O}]^-$$
$$\text{Co}(\text{CO})_3(\text{PPh}_3)\text{I} + 3\text{NH}_3 \longrightarrow \text{Co}(\text{CO})_2(\text{PPh}_3)(\text{NH}_3)\text{C} \begin{array}{c} \text{O} \\ \parallel \\ \text{NH}_2 \end{array} + \text{NH}_4\text{I}$$

Many different examples have shown that the Hofmann acid amide

degradation of carbonylcarbamoyl compounds gives hydridocarbonyl complexes [together with NH_4NCO or $\text{CO}(\text{NH}_2)_2$]. Thus, this represents a new and interesting synthetic route to this class of compound. If $[\text{Co}(\text{CO})_2(\text{Ph}_2\text{PCH}_2)_3\text{CMe}][\text{Co}(\text{CO})_4]$, $[(\text{Ph}_2\text{PCH}_2)_3\text{CMe} = 1,1,1\text{-tris}(\text{diphenylphosphinomethyl})\text{ethane}]$ is allowed to react with liquid NH_3 for 12 h at 20°C , $\text{NH}_4[\text{Co}(\text{CO})_4]$ is obtained, together with the monocarbonylcarbamoyl complex $\text{Co}(\text{CO})[(\text{Ph}_2\text{PCH}_2)_3\text{CMe}]\text{CONH}_2$ (116):



If this is heated in liquid NH_3 to 60°C , the hydrido complex $\text{HCo}(\text{CO})(\text{Ph}_2\text{PCH}_2)_3\text{CMe}$ is formed, together with NH_4NCO . On the basis of IR, $^1\text{H-NMR}$, and $^{31}\text{P-NMR}$ spectra, the hydrido complex has the following structure:



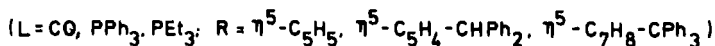
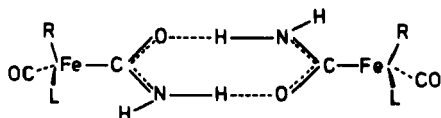
We also investigated the reactions of cationic η^5 -cyclopentadienylcarbonyl complexes of molybdenum, iron, ruthenium, and osmium with liquid NH_3 .

The reactions of $[\eta^5\text{-C}_5\text{H}_5\text{Mo}(\text{CO})_3\text{NH}_3]^+$ or $[\eta^5\text{-C}_5\text{H}_5\text{Mo}(\text{CO})_3\text{PPh}_3]^+$ at 20 or 60°C lead to the carbamoyl compounds *cis*- $\eta^5\text{-C}_5\text{H}_5\text{Mo}(\text{CO})_2(\text{NH}_3)\text{CONH}_2$ and *trans*- $\eta^5\text{-C}_5\text{H}_5\text{Mo}(\text{CO})_2(\text{PPh}_3)\text{CONH}_2$, respectively (117). Here is further evidence that the tendency to form carbamoyl complexes from cationic carbonyl compounds decreases with increasing substitution of the CO groups by ligands with lower π -acceptor character. This is in keeping with the increasing electron density at the carbon atoms of the remaining CO molecules, which is characteristically manifest in the different reaction temperatures. Thus, this allows for a rationalization of the formation of $\eta^5\text{-C}_5\text{H}_5\text{Mo}(\text{CO})_3\text{H}$ from $[\eta^5\text{-C}_5\text{H}_5\text{Mo}(\text{CO})_4]^+$ in liquid NH_3 , even at -60°C , whereas $\eta^5\text{-}$

$\text{C}_5\text{H}_5\text{Mo}(\text{CO})_2(\text{PPh}_3)\text{H}$ only is formed from $[\eta^5\text{-C}_5\text{H}_5\text{Mo}(\text{CO})_3(\text{PPh}_3)]^+$ at 20°C (117).

Table II shows a list of neutral carbamoyl complexes that we have synthesized from $[\eta^5\text{-C}_5\text{H}_5\text{Fe}(\text{CO})_2\text{L}]^+$ ($\text{L} = \text{CO}, \text{PPh}_3, \text{PEt}_3$), $[(\eta^5\text{-C}_5\text{H}_4\text{CHPh}_2)\text{Fe}(\text{CO})_2\text{L}]^+$ ($\text{C}_5\text{H}_4\text{—CHPh}_2 =$ diphenylmethylcyclopentadienyl; $\text{L} = \text{CO}, \text{PPh}_3$), and $[(\eta^5\text{-C}_7\text{H}_8\text{—CPh}_3)\text{Fe}(\text{CO})_3]^+$ ($\text{C}_7\text{H}_8\text{—CPh}_3 =$ triphenylmethylcycloheptadienyl) with liquid NH_3 (118).

On the basis of solid-state, IR-spectroscopic data for these carbamoyl complexes, we had earlier postulated a dimerization of two complex units via hydrogen bridges. This was later confirmed by X-ray structure analyses on other carbamoyl compounds (119, 122). The dicarbonylcarbamoyl complexes always show cis-orientation of the CO ligands.



The oxidation of these carbamoyl complexes with iodine is interesting, as they are converted to the respective isocyanato compounds in accordance with the Hofmann degradation of primary acid amides (118):

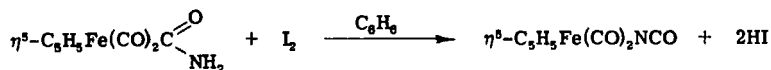
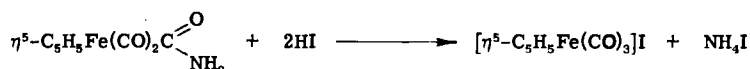


TABLE II

Cationic starting compounds	Carbamoyl compounds
$[\eta^5\text{-C}_5\text{H}_5\text{Fe}(\text{CO})_3]\text{PF}_6$	$\eta^5\text{-C}_5\text{H}_5\text{Fe}(\text{CO})_2\text{CONH}_2$
$[\eta^5\text{-C}_5\text{H}_5\text{Fe}(\text{CO})_2(\text{PPh}_3)]\text{I}$	$\eta^5\text{-C}_5\text{H}_5\text{Fe}(\text{CO})(\text{PPh}_3)\text{CONH}_2$
$[\eta^5\text{-C}_5\text{H}_5\text{Fe}(\text{CO})_2(\text{PEt}_3)]\text{I}$	$\eta^5\text{-C}_5\text{H}_5\text{Fe}(\text{CO})(\text{PEt}_3)\text{CONH}_2$
$[\eta^5\text{-C}_5\text{H}_5\text{Fe}(\text{CO})_2(\text{PEt}_3)]\text{BPh}_4$	No reaction
$[\eta^5\text{-C}_5\text{H}_5\text{Fe}(\text{CO})_2(\text{NH}_3)]\text{I}$	No reaction
$[(\eta^5\text{-C}_5\text{H}_4\text{—CHPh}_2)\text{Fe}(\text{CO})_3]\text{PF}_6$	$(\eta^5\text{-C}_5\text{H}_4\text{—CHPh}_2)\text{Fe}(\text{CO})_2\text{CONH}_2$
$[(\eta^5\text{-C}_5\text{H}_4\text{—CHPh}_2)\text{Fe}(\text{CO})_2(\text{PPh}_3)]\text{Cl}$	$(\eta^5\text{-C}_5\text{H}_4\text{—CHPh}_2)\text{Fe}(\text{CO})(\text{PPh}_3)\text{CONH}_2$
$[(\eta^5\text{-C}_5\text{H}_4\text{—CHPh}_2)\text{Fe}(\text{CO})_2(\text{PPh}_3)]\text{BPh}_4$	No reaction
$[\eta^5\text{-C}_7\text{H}_8\text{Fe}(\text{CO})_3]\text{BF}_4$	No reaction products could be isolated
($\eta^5\text{-C}_7\text{H}_8 =$ cycloheptadienyl)	
$[(\eta^5\text{-C}_7\text{H}_8\text{—CPh}_3)\text{Fe}(\text{CO})_3]\text{BF}_4$	$(\eta^5\text{-C}_7\text{H}_8\text{—CPh}_3)\text{Fe}(\text{CO})_2\text{CONH}_2$

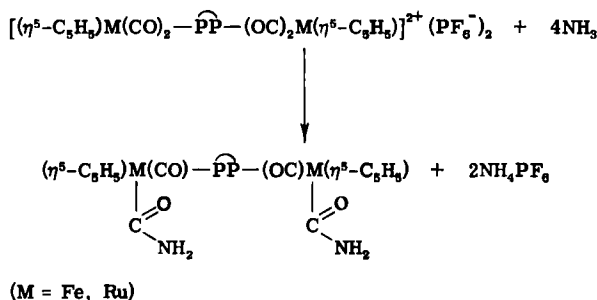
The liberated HI reacts with part of the still-unoxidized carbamoyl complex to give the ionic starting material $[\eta^5\text{-C}_5\text{H}_5\text{Fe}(\text{CO})_3]\text{I}$:



We have also been able to prepare new carbamoyl derivatives of ruthenium and osmium from their cationic cyclopentadienylcarbonyl complexes and liquid NH_3 (119). For these experiments, it was first necessary to synthesize the required cationic starting compounds (120), as only $[\eta^5\text{-C}_5\text{H}_5\text{Ru}(\text{CO})_3]\text{PF}_6$, $[\eta^5\text{-C}_5\text{H}_5\text{Ru}(\text{CO})_2\text{PPh}_3]^+$, and $[\eta^5\text{-C}_5\text{H}_5\text{Ru}(\text{CO})_2\text{C}_2\text{H}_4]\text{PF}_6$ had been described in the literature. The carbamoyl derivatives obtained and the respective starting compounds are summarized in Table III.

A contrasting reaction is that of $[\eta^5\text{-C}_5\text{H}_5\text{Ru}(\text{CO})_2(\text{C}_2\text{H}_4)]\text{PF}_6$ with liquid NH_3 , in which addition of an NH_3 molecule occurs with a change of the π -bonding of C_2H_4 into the σ -C-bonded compound $[\eta^5\text{-C}_5\text{H}_5\text{Ru}(\text{CO})_2\text{-CH}_2\text{-CH}_2\text{-}\ddot{\text{N}}\text{H}_3]\text{PF}_6$ (119).

In the case of iron and ruthenium, we were successful in obtaining the first dinuclear carbamoyl complexes having $\widehat{\text{P}}\text{P}$ ($\widehat{\text{P}}\text{P} = \text{Ph}_2\text{PCH}_2\text{CH}_2\text{PPh}_2$) bridges and a -CONH_2 ligand at both metal atoms (119).



At higher temperatures, all of the cyclopentadienylcarbamoyl compounds of these Group VIIIB metals in liquid ammonia give the respective hydrido complexes $\eta^5\text{-C}_5\text{H}_5\text{M}(\text{CO})_2\text{H}$ ($\text{M} = \text{Fe, Ru, Os}$), $\eta^5\text{-C}_5\text{H}_5\text{Ru}(\text{CO})(\text{L})\text{H}$ ($\text{L} = \text{PPh}_3, \text{PEt}_3$), and $(\eta^5\text{-C}_5\text{H}_5)\text{Ru}(\text{CO})(\text{H})\text{-}\widehat{\text{P}}\text{P}\text{-(H)(OC)Ru}(\eta^5\text{-C}_5\text{H}_5)$ (119).

It should be mentioned that the already known cationic complexes $[\text{M}(\text{CO})_3(\text{PPh}_3)_2\text{Cl}]\text{PF}_6$ ($\text{M} = \text{Fe, Ru, Os}$) also react with liquid NH_3 to give the "noble gas" configured carbamoyl compounds $\text{M}(\text{CO})_4(\text{PPh}_3)_2(\text{Cl})\text{CONH}_2$ ($\text{M} = \text{Fe, Ru, Os}$). With these compounds, we had made the

TABLE III

Cationic starting compounds	Reaction products
$[\eta^5\text{-C}_5\text{H}_5\text{Ru}(\text{CO})_3\text{PF}_6]$	$\eta^5\text{-C}_5\text{H}_5\text{Ru}(\text{CO})_2\text{CONH}_2$
$[\eta^5\text{-C}_5\text{H}_5\text{Ru}(\text{CO})_2\text{CNCH}_3]\text{PF}_6$	$\eta^5\text{-C}_5\text{H}_5\text{Ru}(\text{CO})(\text{CNCH}_3)\text{CONH}_2$
$[\eta^5\text{-C}_5\text{H}_5\text{Ru}(\text{CO})_2\text{C}_6\text{H}_{10}]\text{PF}_6$ (C_6H_{10} = cyclohexene)	$([\eta^5\text{-C}_5\text{H}_5\text{-Ru}(\text{CO})_2\text{NH}_3]\text{PF}_6)$
$[\eta^5\text{-C}_5\text{H}_5\text{Ru}(\text{CO})_2\text{NH}_3]\text{PF}_6$	No reaction
$[\eta^5\text{-C}_5\text{H}_5\text{Ru}(\text{CO})_2\text{NCCH}_3]\text{PF}_6$	$\eta^5\text{-C}_5\text{H}_5\text{Ru}(\text{CO})(\text{NCCH}_3)\text{CONH}_2$
$[\eta^5\text{-C}_5\text{H}_5\text{Ru}(\text{CO})_2\text{PPh}_3]\text{PF}_6$	$\eta^5\text{-C}_5\text{H}_5\text{Ru}(\text{CO})(\text{PPh}_3)\text{CONH}_2$
$[\eta^5\text{-C}_5\text{H}_5\text{Ru}(\text{CO})_2\text{PEt}_3]\text{Cl}$	$\eta^5\text{-C}_5\text{H}_5\text{Ru}(\text{CO})(\text{PEt}_3)\text{CONH}_2$
$[\eta^5\text{-C}_5\text{H}_5\text{Ru}(\text{CO})(\text{P}^i\text{P})]\text{PF}_6$ (P^iP = $\text{Ph}_2\text{P-CH}_2\text{-CH}_2\text{-PPh}_2$)	No reaction
$[\eta^5\text{-C}_5\text{H}_5\text{Os}(\text{CO})_3\text{PF}_6]$ (120)	$\eta^5\text{-C}_5\text{H}_5\text{Os}(\text{CO})_2\text{CONH}_2$

first carbamoyl complexes having a halogen ligand and the metals in the oxidation state +II (119).

Understandably, these compounds having cis CO groups do not undergo a Hofmann acid amide degradation to give the respective hydrido complexes. The stability of these Group VIIIB carbamoyl complexes increases in the order Fe, Ru, Os.

The last class of carbamoyl complexes with which we have been concerned has been that with NO^+ ligands. For preparative and structural studies in this area, besides the cationic cyclopentadienyl nitrosylcarbonyl complexes of Group VIIIB (121), the nitrosylcarbonyl metal cations of Mo and W offer interesting starting materials (121).

The results of our work with Mn and Re are summarized in Table IV.

TABLE IV

Cationic starting compounds	Carbamoyl compounds
$[\eta^5\text{-C}_5\text{H}_5\text{Mn}(\text{CO})_2(\text{NO})]\text{PF}_6$	$\eta^5\text{-C}_5\text{H}_5\text{Mn}(\text{CO})(\text{NO})\text{CONH}_2$
$[\eta^5\text{-C}_5\text{H}_5\text{Re}(\text{CO})_2(\text{NO})]\text{PF}_6$	$\eta^5\text{-C}_5\text{H}_5\text{Re}(\text{CO})(\text{NO})\text{CONH}_2$
$[\eta^5\text{-MeC}_5\text{H}_4\text{Mn}(\text{CO})_2(\text{NO})]\text{PF}_6$	$\eta^5\text{-MeC}_5\text{H}_4\text{Mn}(\text{CO})(\text{NO})\text{CONH}_2$
$[\eta^5\text{-C}_5\text{H}_5\text{Mn}(\text{CO})(\text{CNMe})(\text{NO})]\text{PF}_6^a$	$\eta^5\text{-C}_5\text{H}_5\text{Mn}(\text{CNMe})(\text{NO})\text{CONH}_2$
$[\eta^5\text{-C}_5\text{H}_5\text{Mn}(\text{CO})(\text{CNEt})(\text{NO})]\text{PF}_6^a$	$\eta^5\text{-C}_5\text{H}_5\text{Mn}(\text{CNEt})(\text{NO})\text{CONH}_2$
$[\eta^5\text{-C}_5\text{H}_5\text{Mn}(\text{CO})(\text{PPh}_3)(\text{NO})]\text{PF}_6$	$\eta^5\text{-C}_5\text{H}_5\text{Mn}(\text{PPh}_3)(\text{NO})\text{CONH}_2$
$[\eta^5\text{-C}_5\text{H}_5\text{Mn}(\text{CO})(\text{PEt}_2\text{Ph})(\text{NO})]\text{PF}_6^a$	$\eta^5\text{-C}_5\text{H}_5\text{Mn}(\text{PEt}_2\text{Ph})(\text{NO})\text{CONH}_2$
$[\eta^5\text{-C}_5\text{H}_5\text{Mn}(\text{CO})(\text{AsPh}_3)(\text{NO})]\text{PF}_6$	$\eta^5\text{-C}_5\text{H}_5\text{Mn}(\text{AsPh}_3)(\text{NO})\text{CONH}_2$
$[(\eta^5\text{-C}_5\text{H}_5\text{Mn}(\text{CO})(\text{NO}))_2\text{P}^i\text{P}](\text{PF}_6)_2^b$	$[\eta^5\text{-C}_5\text{H}_5\text{Mn}(\text{NO})\text{CONH}_2]_2\text{P}^i\text{P}$

^a First time prepared.

^b P^iP = $\text{Me}_2\text{PCH}_2\text{CH}_2\text{PMe}_2$, $\text{Ph}_2\text{PCH}_2\text{CH}_2\text{PPh}_2$.

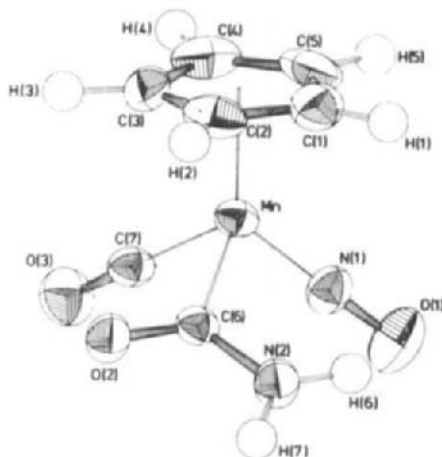


FIG. 6

The crystal structure of $\eta^5\text{-C}_5\text{H}_5\text{Mn(CO)(NO)CONH}_2$, given in Fig. 6, shows that the Mn atom is octahedrally coordinated by the C_5H_5 , CO, NO, and CONH_2 ligands and that the planar carbamoyl group lies in the same plane as the Mn atom. Hydrogen-bridge bonds between the carbamoyl ligands cause the coupling of two molecules to give dimers (122).

In the course of this work, we were also able to convert $\eta^5\text{-C}_5\text{H}_5\text{Mn(L)(NO)CONH}_2$ ($\text{L} = \text{CNEt}$, PET_2Ph) with MeOH into the corresponding carboalkoxonitrosyl complexes $\eta^5\text{-C}_5\text{H}_5\text{Mn(L)(NO)COOMe}$.

The nitrosyl ligand containing carbamoyl complexes of Mo and W are given in Table V (121). These compounds could also be converted into their carboalkoxo derivatives with MeOH.

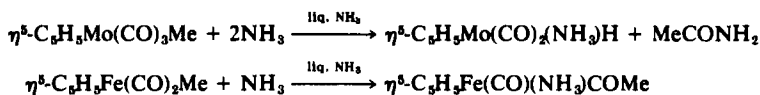
Finally, a comparison of the behavior of the three alkyl carbonyl complexes $\eta^5\text{-C}_5\text{H}_5\text{Mo(CO)}_3\text{Me}$ (123), $\eta^5\text{-C}_5\text{H}_5\text{Fe(CO)}_2\text{Me}$ (123), and $\text{C}_3\text{F}_7\text{Fe(CO)}_3(\text{PPh}_3)\text{I}$ (124) toward liquid NH_3 shows completely different reaction character.

Whereas $\eta^5\text{-C}_5\text{H}_5\text{Mo(CO)}_3\text{Me}$ with liquid NH_3 leads to $\eta^5\text{-C}_5\text{H}_5\text{Mo(CO)}_2$

TABLE V

Cationic starting compounds	Carbamoyl compounds
$[\text{Mo(CO)}_3(\text{PP})(\text{NO})]\text{PF}_6$	$\text{Mo(CO)}_3(\text{PP})(\text{NO})\text{CONH}_2$
$[\text{W(CO)}_3(\text{PP})(\text{NO})]\text{PF}_6$	$\text{W(CO)}_3(\text{PP})(\text{NO})\text{CONH}_2$
$[\text{W(CO)}_3(\text{phen})(\text{NO})]\text{PF}_6$	$\text{W(CO)}_3(\text{phen})(\text{NO})\text{CONH}_2$

(NH₃)H (as the *trans* isomer) and acetamide, $\eta^5\text{-C}_5\text{H}_5\text{Fe}(\text{CO})_2\text{Me}$ gives the acetyl complex $\eta^5\text{-C}_5\text{H}_5\text{Fe}(\text{CO})(\text{NH}_3)\text{COMe}$ via an insertion type reaction (123).



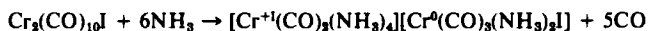
Our preparation of $\eta^5\text{-C}_5\text{H}_5\text{Mo}(\text{CO})_2(\text{NH}_3)\text{H}$ constituted the first isolation of a mixed hydridoammine complex, which cannot be obtained from $\eta^5\text{-C}_5\text{H}_5\text{Mo}(\text{CO})_3\text{H}$ and NH₃. The NH₃ can be replaced by py to give $\eta^5\text{-C}_5\text{H}_5\text{Mo}(\text{CO})_2(\text{py})\text{H}$. The complex $\eta^5\text{-C}_5\text{H}_5\text{Fe}(\text{CO})(\text{NH}_3)\text{COMe}$ is also interesting in being the first solvent-substituted acetyl complex of iron ever prepared.

In the case of $\text{C}_3\text{F}_7\text{Fe}(\text{CO})_3(\text{PPh}_3)\text{I}$, even after only a very short reaction time, no carbamoyl derivative is formed; but, instead, depending upon the reaction time, either CO and PPh₃ substitution to $\text{C}_3\text{F}_7\text{Fe}(\text{CO})_2(\text{NH}_3)_2\text{I}$ or formation of the ionic complex $[\text{C}_3\text{F}_7\text{Fe}(\text{CO})_2(\text{NH}_3)_3]\text{I}$ by addition of a further NH₃ molecule occurs. Both compounds have the CO groups in *cis* positions (124).

To complete this treatment of the manifold types of reactions of the paramagnetic chromium complexes $\text{Cr}(\text{CO})_5\text{I}$ and $\text{Cr}_2(\text{CO})_{10}\text{I}$ (cf. Section III,D), it remains to discuss their behavior toward liquid NH₃ (80). With $\text{Cr}(\text{CO})_5\text{I}$, substitution of three CO ligands by NH₃ and addition of another NH₃ molecule gives *trans*- $[\text{Cr}(\text{CO})_2(\text{NH}_3)_4]\text{I}$, which constitutes the first preparation of a cationic CO complex of chromium:



Based on the mesomerism of dinuclear $\text{Cr}_2(\text{CO})_{10}\text{I}$, $[(\text{OC})_5\text{Cr}^0\text{—I—Cr}^+(\text{CO})_5] \leftrightarrow (\text{OC})_5\text{Cr}^+\text{—I—Cr}^0(\text{CO})_5$, its reaction with liquid NH₃ gives both the *trans*- $[\text{Cr}^+(\text{CO})_2(\text{NH}_3)_4]^+$ cation and the iodo-diamminetricarbonylchromate (0) anion, which is derived from the $[\text{Cr}^0(\text{CO})_5\text{I}]^-$ anion by exchange of two CO with two NH₃ molecules.



Based on the foregoing experimental results, the versatility of metal carbonyls and their derivatives in their reactions with liquid NH₃ may be summarized as follows: (1) substitution of CO or other ligands by NH₃ without change in the oxidation number of the transition metal in question; (2) conversion of covalent carbonyl complexes into ionic compounds by addition of NH₃ molecules; (3) "base reactions" in which the transition metal is reduced to a carbonyl metalate with complementary oxidation of a CO ligand to CO(NH₂)₂; (4) valence disproportionations with

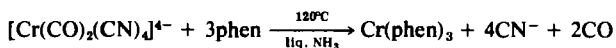
formation of carbonyl metalate anions and hexammine metal cations or carbonyl ammine cations; (5) simultaneous valence disproportionation and "base reaction"; (6) formation of carbamoyl complexes from cationic carbonyl complexes, whereby the former may undergo Hofmann acid amide degradation; and (7) insertion of NH_3 in metal carbonyl complexes.

D. Liquid Ammonia as Solvent for Organometallic Reactions

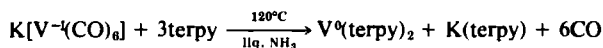
Liquid NH_3 is an excellent solvent for a variety of reactions of metal carbonyls. Of particular importance are the reactions with the N-heterocyclic ligands bipy, phen, and terpy, and with CN^- .

Thus, in liquid NH_3 at 60°C , we were able to react *cis*- $\text{Cr}(\text{CO})_2[(\text{Ph}_2\text{P})_2\text{CH}_2]_2$ (125) with bipy and phen to obtain *cis*- $\text{Cr}(\text{CO})_2(\text{bipy})_2$ and *cis*- $\text{Cr}(\text{CO})_2(\text{phen})_2$ (126). These complexes cannot be obtained from $\text{Cr}(\text{CO})_6$ and the bidentate N ligands directly, as complete substitution of all six CO groups occurs to give $\text{Cr}(\text{bipy})_3$ and $\text{Cr}(\text{phen})_3$ (127), respectively. These reactions are, however, remarkable in that the main products are the mixed species *cis*- $\text{Cr}(\text{CO})_2[(\text{Ph}_2\text{P})_2\text{CH}_2]\text{bipy}$ and *cis*- $\text{Cr}(\text{CO})_2[(\text{Ph}_2\text{P})_2\text{CH}_2]\text{phen}$ (126). We further found that, in liquid NH_3 at 60°C , *trans*- $\text{Cr}(\text{CO})_2[(\text{Ph}_2\text{P})_2\text{CH}_2]_2$ isomerizes to the *cis* compound (126).

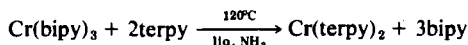
In the case of *cis*- $\text{K}_4[\text{Cr}(\text{CO})_2(\text{CN})_4]$, with phen a ligand exchange also occurs (126):



$\text{K}[\text{V}(\text{CO})_6]$ reacts with 2,2',2''-terpyridyl (terpy) in liquid NH_3 to give complete ligand exchange with simultaneous oxidation of the metal (128), whereby $\text{V}(\text{terpy})_2$ could be prepared for the first time.



We had earlier observed a similar exchange of bipy with terpy in the case of chromium (129):



With bipy or phen, the complex $(\eta^5\text{-C}_5\text{H}_5)_2\text{Ni}$ in liquid NH_3 at 120°C gives, quantitatively, $\text{Ni}(\text{bipy})_2$ or $\text{Ni}(\text{phen})_2$ (96).

We were also able to show that $\text{K}_6[\text{Cr}(\text{CN})_6]$ or $\text{K}_4[\text{Ni}(\text{CN})_4]$ in liquid NH_3 more easily undergoes substitution reactions than the corresponding isoelectronic $\text{Cr}(\text{CO})_6$ and $\text{Ni}(\text{CO})_4$ (130, 131). Thus, even above -60°C , all six CN ligands of $\text{K}_6[\text{Cr}(\text{CN})_6]$ can be replaced by bipy, phen, terpy,

$(\text{Ph}_2\text{P})_2\text{CH}_2$, $(\text{Ph}_2\text{P})_2\text{C}_2\text{H}_4$, or $(\text{Ph}_2\text{As})_2\text{C}_2\text{H}_4$ to give the complexes $\text{Cr}(\text{bipy})_3$ and $\text{Cr}(\text{phen})_3$, first prepared by reductive methods by Herzog and Taube (132), as well as $\text{Cr}(\text{terpy})_2$ (129), $\text{Cr}[(\text{Ph}_2\text{P})_2\text{CH}_2]_3$, $\text{Cr}[(\text{Ph}_2\text{P})_2\text{C}_2\text{H}_4]_3$, and $\text{Cr}[(\text{Ph}_2\text{As})_2\text{C}_2\text{H}_4]_3$. In these reactions, neither the formation of such mixed complexes as $\text{K}_4[\text{Cr}(\text{CN})_4(\text{N}\text{N})]$, $\text{K}_2[\text{Cr}(\text{CN})_2(\text{N}\text{N})_2]$ (NN = bipy, phen) or $\text{K}_3[\text{Cr}(\text{CN})_3\text{terpy}]$, nor the occurrence of the analogous salts with PP [PP = $(\text{Ph}_2\text{P})_2\text{CH}_2$], can be observed. It is significant that, even under the most extreme conditions, it is impossible to replace more than four of the CO ligands in $\text{Cr}(\text{CO})_6$ by the aforementioned ditertiary phosphines or arsines (125).

The isoelectronic counterpart of $\text{Ni}(\text{CO})_4$, the complex $\text{K}_4[\text{Ni}(\text{CN})_4]$, undergoes reactions similar to those of $\text{K}_6[\text{Cr}(\text{CN})_6]$ in liquid NH_3 (131). At room temperature, the complexes $\text{Ni}(\text{PPh}_3)_4$, $\text{Ni}(\text{AsPh}_3)_4$, and $\text{Ni}(\text{SbPh}_3)_4$, first prepared by Wilke *et al.* (133) by other methods, can be obtained. The tendency to complex formation falls markedly along the series as the dipole character of the incoming ligands decreases (131).

Although $\text{Ni}(\text{CO})_4$ first reacts with $(\text{Ph}_2\text{P})_2\text{C}_2\text{H}_4$ at 200°C to give not quite pure $\text{Ni}[(\text{Ph}_2\text{P})_2\text{C}_2\text{H}_4]_2$ (134), the same compound can be obtained analytically pure from $\text{K}_4[\text{Ni}(\text{CN})_4]$ in liquid NH_3 even at $> -33^\circ\text{C}$. With $(\text{Ph}_2\text{As})_2\text{C}_2\text{H}_4$, the corresponding complex $\text{Ni}[(\text{Ph}_2\text{As})_2\text{C}_2\text{H}_4]_2$ is formed (131).

Whereas in $\text{Ni}(\text{CO})_4$ only two CO groups can be replaced by bipy or phen, in $[\text{Ni}(\text{CN})_4]^{4-}$, all of the CN^- ligands can be eliminated to give $\text{Ni}(\text{bipy})_2$ and $\text{Ni}(\text{phen})_2$, which were prepared for the first time by this route (131).

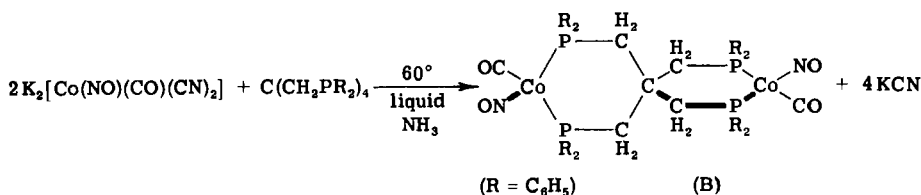
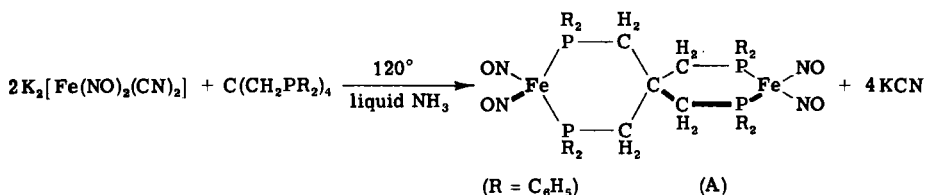
An area that we have examined in some detail is that of the behavior of three isoelectronic nitrosylcarbonyls $\text{Mn}(\text{NO})_3\text{CO}$, $\text{Fe}(\text{NO})_2(\text{CO})_2$, and $\text{Co}(\text{NO})(\text{CO})_3$ in solutions of KCN in liquid NH_3 . With $\text{Mn}(\text{NO})_3\text{CO}$, the diamagnetic, dimeric anion $[\text{Mn}(\text{NO})_2(\text{CN})_2]_2^{4-}$ with cis NO ligands and a Mn—Mn bond is obtained; heating in ethanol causes isomerization to the trans form (135). Reduction with potassium in liquid NH_3 causes rupture of the Mn—Mn bond to give the extremely unstable monomeric $[\text{Mn}(\text{NO})_2(\text{CN})_2]^{3-}$ which is tetrahedral and isoelectronic with the $[\text{Fe}(\text{NO})_2(\text{CN})_2]^{2-}$ anion (135). We isolated the latter from $\text{Fe}(\text{NO})_2(\text{CO})_2$ with KCN in liquid NH_3 at 60°C , although the singly negatively charged anion $[\text{Fe}(\text{NO})_2(\text{CO})\text{CN}]^-$ could not be obtained (136).

We have also used KCN in liquid NH_3 to prepare the compounds $[\text{Co}(\text{NO})(\text{CO})_{3-x}(\text{CN})_x]^{x-}$ ($x = 1, 2, 3$) from $\text{Co}(\text{NO})(\text{CO})_3$ by control of the respective molar ratios (136). An excess of KCN leads to the red-brown $\text{K}_3[\text{Co}(\text{NO})(\text{CN})_3]$, whereas a molar ratio of nitrosylcarbonyl:KCN of 1:1 gives $\text{K}[\text{Co}(\text{NO})(\text{CO})_2(\text{CN})]$. This monocyano complex is very

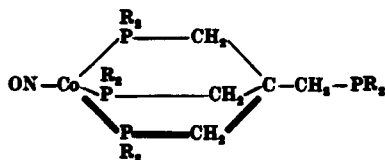
unstable and readily disproportionates into the dicyano complex $K_2[Co(NO)(CO)(CN)_2]$ and $Co(NO)(CO)_3$ (136).

The $\nu(NO)$ frequencies for these three anions decrease with increasing CN^- substitution so that the $[Co(NO)(CN)_3]^{3-}$ anion shows the very low value of 1485 cm^{-1} . This anion is isoelectronic with $[Ni(NO)(CN)_3]^{2-}$ prepared by Hieber and Führling (137).

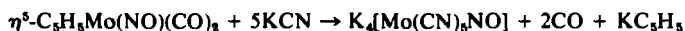
The nitrosylcyano metalates $K_2[Fe(NO)_2(CN)_2]$ and $K_2[Co(NO)(CO)(CN)_2]$ react with tetrakis(diphenylphosphinomethyl)methane in liquid NH_3 at 120° or $60^\circ C$, to give spiroheterocyclic compounds (138):



Fundamentally, optical isomers of the spiroheterocyclic cobalt complex must exist. Since these compounds could not be separated, we tried to synthesize the dicyano derivative under CO substitution by reaction with KCN in liquid NH_3 in the hope that a separation into the optical antipodes might be possible. At $120^\circ C$, however, the reaction gave, besides $K_2[Co(NO)(CO)(CN)_2]$, a complex in which the $C(CH_2PPh_2)_4$ ligand is tridentate (139):



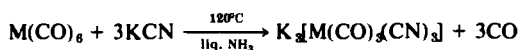
The complex $\eta^5-C_5H_5Mo(NO)(CO)_2$ reacts with KCN in liquid NH_3 at $120^\circ C$ to give the pentacyanonitrosyl complex $K_4[Mo(CN)_5NO]$ by elimination of the C_5H_5 ligand and the two CO groups (140).



The structure of the $[\text{Mo(CN)}_5\text{NO}]^{4-}$ anion has been the subject of attention of many authors (141).

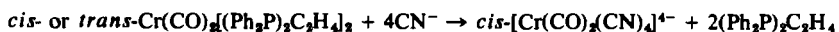
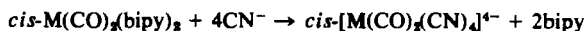
E. Cyanocarbonyl Metalates

The cyanocarbonylchromates(0) $[\text{Cr(CO)}_5\text{CN}]^-$ and *cis*- $[\text{Cr(CO)}_4(\text{CN})_2]^{2-}$, which are formed by the oxidation of $[\text{Cr}^{-\text{II}}(\text{CO})_5]^{2-}$ with aqueous solutions of KCN or with $(\text{CN})_2$ or ICN have been discussed earlier (55, 56). Further studies have shown that the reaction of metal carbonyls or their derivatives with solutions of KCN in liquid NH_3 is a most advantageous method for the synthesis of new cyanocarbonyl metalates of transition metals, since, in liquid NH_3 , alkali cyanides are not subject to solvolysis, and also since the broad temperature range of -78 to $+120^\circ\text{C}$ may be employed. Thus, we have been able to obtain quantitative yields of the tricyano-tricarbonyl metalates (0) *fac*- $[\text{M(CO)}_3(\text{CN})_3]^{3-}$ ($\text{M} = \text{Cr}, \text{Mo}, \text{W}$) by direct reaction of the hexacarbonyls (21):



The bipy-substituted tetracarbonyl complexes $\text{M(CO)}_4\text{bipy}$ ($\text{M} = \text{Cr}, \text{Mo}, \text{W}$) also give the cyanocarbonyl metalates(0) $\text{K}_2[\text{Cr(CO)}_4(\text{CN})_2]$ and $\text{K}_3[\text{M(CO)}_3(\text{CN})_3]$ ($\text{M} = \text{Mo}, \text{W}$) when treated similarly with KCN in liquid NH_3 at 60°C (92).

It is, however, impossible to use this route to obtain cyanocarbonyl metalates having more than three CN^- ligands. The *tetracyanodicarbonyl* metalates(0) of chromium, molybdenum, and tungsten (126) are readily accessible from the dicarbonyl complexes $\text{M(CO)}_2\text{bipy}_2$ ($\text{M} = \text{Cr}, \text{Mo}, \text{W}$), $\text{Cr(CO)}_2[(\text{Ph}_2\text{P})_2\text{CH}_2]_2$, or $\text{Cr(CO)}_2[(\text{Ph}_2\text{P})_2\text{C}_2\text{H}_4]_2$ (125) with KCN in liquid NH_3 at 120°C .



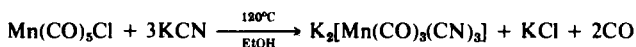
The starting materials $\text{M(CO)}_2\text{bipy}_2$ ($\text{M} = \text{Mo}, \text{W}$) are obtained in quantitative yield when M(CO)_6 ($\text{M} = \text{Mo}, \text{W}$) reacts with bipy in such high-boiling solvents as decalin or tetralin at 190°C (127). The synthesis of $\text{Cr(CO)}_2\text{bipy}_2$ in liquid NH_3 was mentioned earlier (Section IV, D).

With these studies, and with the exception of the $[\text{M(CO)(CN)}_5]^{5-}$ anions, we have achieved access to all of the cyanocarbonyl metalates(0) and can thus present the following isoelectronic series: M(CO)_6 , $[\text{M(CO)}_5\text{CN}]^-$, $[\text{M(CO)}_4(\text{CN})_2]^{2-}$, $[\text{M(CO)}_3(\text{CN})_3]^{3-}$, $[\text{M(CO)}_2(\text{CN})_4]^{4-}$, $[\text{M(CO)(CN)}_5]^{5-}$, and $[\text{M(CN)}_6]^{6-}$ ($\text{M} = \text{Cr}, \text{Mo}, \text{W}$).

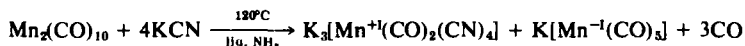
The $[\text{M}(\text{CN})_6]^{6-}$ ions cannot, however, be prepared from carbonyl complexes, and only the deep-green chromium compound $\text{K}_6[\text{Cr}^0(\text{CN})_6]$ can be obtained by reduction of $\text{K}_3[\text{Cr}^{+III}(\text{CN})_6]$ with potassium in liquid NH_3 (142).

The foregoing series of metal(0) complexes of Group VIB corresponds to that of the isoelectronic metal(+I) compounds of Group VIIB: $[\text{M}(\text{CO})_6]^+$, $\text{M}(\text{CO})_5\text{CN}$, $[\text{M}(\text{CO})_4(\text{CN})_2]^-$, $[\text{M}(\text{CO})_3(\text{CN})_3]^{2-}$, $[\text{M}(\text{CO})_2(\text{CN})_4]^{3-}$, $[\text{M}(\text{CO})(\text{CN})_5]^{4-}$, and $[\text{M}(\text{CN})_6]^{5-}$ ($\text{M} = \text{Mn}, \text{Re}$).

Before we began our own studies, the only known cyanocarbonyl complexes of manganese were $\text{Mn}(\text{CO})_5\text{CN}$ (143) and $\text{K}[\text{Mn}(\text{CO})_4(\text{CN})_2]$ (144). We obtained the colorless tricyanotricarbonylmanganate(+I) from $\text{Mn}(\text{CO})_5\text{Cl}$ and KCN in EtOH at 120°C (145).



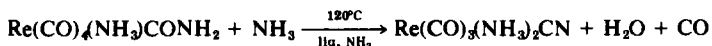
This complex is readily prepared in pure form since, in contrast to $\text{K}_3[\text{Mn}(\text{CO})_2(\text{CN})_4]$ and KCl which are also formed in the reaction, it is extremely soluble in liquid NH_3 . Tetracyanodicarbonylmanganate(+I) is easily isolated if $\text{Mn}_2(\text{CO})_{10}$ reacts with KCN in liquid NH_3 at 120°C (145),



whereby the slightly soluble cyano complex is precipitated. This reaction is comparable to the disproportionation of $\text{Mn}_2(\text{CO})_{10}$ in pure, liquid NH_3 , the complex $[\text{Mn}^{+I}(\text{CO})_3(\text{NH}_3)_3][\text{Mn}^{-I}(\text{CO})_5]$ being formed instead of $\text{K}_3[\text{Mn}^{+I}(\text{CO})_2(\text{CN})_4]$ and $\text{K}[\text{Mn}^{-I}(\text{CO})_5]$ (104).

As with the pentacyanomonomocarbonyl metalates(0) of Group VIB, all attempts to prepare $[\text{Mn}(\text{CO})(\text{CN})_5]^{4-}$ were unsuccessful.

With the exception of $[\text{Re}(\text{CO})(\text{CN})_5]^{4-}$, we have also been able to use new reactions in liquid NH_3 to complete the series of possible cyanocarbonylrhenates(+I) (146). Despite numerous attempts by many research groups, preparation of $\text{Re}(\text{CO})_5\text{CN}$, isoelectronic with $[\text{W}(\text{CO})_5\text{CN}]^-$, has remained elusive. In contrast, we were able to prepare the NH_3 -substituted derivative *fac*- $\text{Re}(\text{CO})_3(\text{NH}_3)_2\text{CN}$ from $\text{Re}(\text{CO})_5\text{Cl}$ and KCN (molar ratio 1:1) in liquid NH_3 at 120°C , and by removal of H_2O and CO from the carbamoyl complex *cis*- $\text{Re}(\text{CO})_4(\text{NH}_3)\text{CONH}_2$ in liquid NH_3 at the same temperature (112, 146).

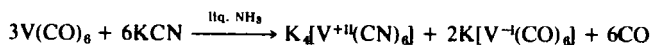


Although $\text{Re}(\text{CO})_5\text{Cl}$ reacts with KCN in methanol at 100°C to give *cis*- $\text{K}[\text{Re}(\text{CO})_4(\text{CN})_2]$ (147), as our experiments have shown, with excess KCN in ethanol the product is *fac*- $\text{K}_2[\text{Re}(\text{CO})_3(\text{CN})_3]$ (146). This tricyano

complex cannot be prepared in liquid NH_3 even with excess KCN and at 120°C . These conditions lead to *fac*- $\text{K}[\text{Re}(\text{CO})_3(\text{CN})_2\text{NH}_3]$, which is also formed from $[\text{Re}(\text{CO})_3(\text{NH}_3)_3]\text{Cl}$ and KCN at 120°C in liquid NH_3 .

For the preparation of *cis*- $\text{K}_3[\text{Re}(\text{CO})_2(\text{CN})_4]$, our starting material was the salt $\{\text{Re}(\text{CO})_2[(\text{Ph}_2\text{P})_2\text{C}_2\text{H}_4]_2\}\text{Cl}$, which we treated with KCN in ethanol at 200°C (146).

All attempts to obtain cyanocarbonylvanadates starting from $\text{V}(\text{CO})_6$ have been unsuccessful, since, with KCN in liquid NH_3 , disproportionation occurs (103).

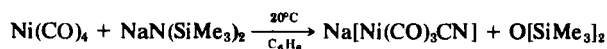
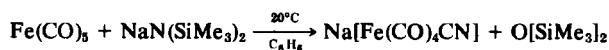


This different behavior of $\text{V}(\text{CO})_6$ toward KCN in liquid NH_3 , compared to $\text{Mn}_2(\text{CO})_{10}$, can be explained in terms of the especially high stability of the $[\text{V}(\text{CO})_6]^-$ anion. However, Rehder (148) has been able to spectroscopically characterize $[\text{Ph}_4\text{P}]_2[\text{V}(\text{CO})_5\text{CN}]$, which he precipitated from the yellow solution formed by UV irradiation of $\text{Na}[\text{V}(\text{CO})_6]$ and NaCN in liquid NH_3 at -50 to -60°C . Thus, the isoelectronic series $[\text{V}^{-1}(\text{CO})_5\text{CN}]^{2-}$, $[\text{Cr}^0(\text{CO})_5\text{CN}]^-$, and $\text{Mn}^{+1}(\text{CO})_5\text{CN}$ can be considered complete.

F. Mixed Cyanocarbonyl Metalates Prepared from Metal Carbonyl Derivatives and $\text{NaN}(\text{SiMe}_3)_2$

In the course of our studies on the preparation of cyanocarbonyl metalates, especially those of Groups VIB and VIIB, encouraged by our successful synthesis of the "mixed" cyanocarbonyl complexes $\text{Re}(\text{CO})_3(\text{NH}_3)_2\text{CN}$ and $[\text{Re}(\text{CO})_3\text{NH}_3(\text{CN})_2]^-$, we extended our work to include the preparation of further complexes containing ligands other than CO and CN^- .

For such experiments, however, liquid ammonia is not suitable. A much more promising reaction offered by that discovered by Wannagat and Seyffert (149) involves treatment of sodium bis(trimethylsilyl)amide with mononuclear metal carbonyls in which nucleophilic attack of the silyl amide on a CO ligand leads to monocyanocarbonyl metalates.



In the first instance we used this method on many different monomeric metal carbonyl derivatives, and thereby obtained numerous new mono-

nuclear monocyancarbonyl metalates not accessible by other routes. These are summarized in Table VI.

Most of these new monocyancarbonyl metalates react with acids, MeI, $[\text{Me}_3\text{O}]\text{BF}_4$, $[\text{Et}_3\text{O}]\text{BF}_4$, R_3EX ($\text{R} = \text{Me, Et, Ph}$; $\text{E} = \text{Si, Ge, Sn}$; $\text{X} = \text{Cl, I}$), and thus are protonated, deuterated, silylated, germylated, or

TABLE VI

Starting compounds	Monocyancarbonyl metalates	Reference
$\text{Cr}(\text{CO})_5\text{py}$	<i>cis</i> - $\text{Na}[\text{Cr}(\text{CO})_4(\text{CN})\text{py}]$	150
$\text{Cr}(\text{CO})_5\text{CNC}_6\text{H}_{11}$ ($\text{CNC}_6\text{H}_{11} = \text{cyclohexyl isonitrile}$)	<i>cis</i> - $\text{Na}[\text{Cr}(\text{CO})_4(\text{CN})\text{CNC}_6\text{H}_{11}]$	150
$\text{Cr}(\text{CO})_5\text{NCCMe}_3$ ($\text{Me}_3\text{CCN} = \text{pivalonitrile}$)	<i>cis</i> - $\text{Na}[\text{Cr}(\text{CO})_4(\text{CN})\text{NCCMe}_3]$	151
$\text{Mn}(\text{CO})_5\text{X}$ ($\text{X} = \text{Cl, Br}$)	<i>cis</i> - $\text{Na}[\text{Mn}(\text{CO})_4(\text{CN})\text{X}]$	152
$\text{Re}(\text{CO})_5\text{X}$ ($\text{X} = \text{Cl, Br}$)	<i>cis</i> - $\text{Na}[\text{Re}(\text{CO})_4(\text{CN})\text{X}]$	152
$\text{C}_4\text{H}_6\text{Fe}(\text{CO})_3$ ($\text{C}_4\text{H}_6 = \text{butadiene}$)	$\text{Na}[(\text{C}_4\text{H}_6)\text{Fe}(\text{CO})_2\text{CN}]$	150
$\text{C}_5\text{H}_8\text{Fe}(\text{CO})_3$ ($\text{C}_5\text{H}_8 = 1,3\text{-pentadiene}$)	$\text{Na}[(\text{C}_5\text{H}_8)\text{Fe}(\text{CO})_2\text{CN}]$	153
$\text{C}_5\text{H}_8\text{Fe}(\text{CO})_3$ ($\text{C}_5\text{H}_8 = \text{isoprene}$)	$\text{Na}[(\text{C}_5\text{H}_8)\text{Fe}(\text{CO})_2\text{CN}]$	154
$\text{C}_6\text{H}_8\text{Fe}(\text{CO})_3$ ($\text{C}_6\text{H}_8 = 1,3\text{-cyclohexadiene}$)	$\text{Na}[(\text{C}_6\text{H}_8)\text{Fe}(\text{CO})_2\text{CN}]$	150
$\text{C}_6\text{H}_{10}\text{Fe}(\text{CO})_3$ ($\text{C}_6\text{H}_{10} = 1,3\text{-hexadiene}$)	$\text{Na}[(\text{C}_6\text{H}_{10})\text{Fe}(\text{CO})_2\text{CN}]$	153
$\text{C}_6\text{H}_{10}\text{Fe}(\text{CO})_3$ ($\text{C}_6\text{H}_{10} = 2,3\text{-dimethylbutadiene}$)	$\text{Na}[(\text{C}_6\text{H}_{10})\text{Fe}(\text{CO})_2\text{CN}]$	153
$\text{C}_7\text{H}_{10}\text{Fe}(\text{CO})_3$ ($\text{C}_7\text{H}_{10} = 1,3\text{-cycloheptadiene}$)	$\text{Na}[(\text{C}_7\text{H}_{10})\text{Fe}(\text{CO})_2\text{CN}]$	154
$\text{C}_8\text{H}_8\text{Fe}(\text{CO})_3$ ($\text{C}_8\text{H}_8 = \text{cyclooctatetraene}$)	$\text{Na}[(\text{C}_8\text{H}_8)\text{Fe}(\text{CO})_2\text{CN}]$	150
$\text{C}_8\text{H}_{14}\text{Fe}(\text{CO})_3$ ($\text{C}_8\text{H}_{14} = 2,5\text{-dimethyl-1,3-hexadiene}$)	$\text{Na}[(\text{C}_8\text{H}_{14})\text{Fe}(\text{CO})_2\text{CN}]$	154
$\text{C}_8\text{H}_8\text{Ru}(\text{CO})_3$ ($\text{C}_8\text{H}_8 = 1,3\text{-cyclohexadiene}$)	$\text{Na}[(\text{C}_8\text{H}_8)\text{Ru}(\text{CO})_2\text{CN}]$	155
$\text{C}_6\text{H}_{10}\text{Ru}(\text{CO})_3$ ($\text{C}_6\text{H}_{10} = 2,3\text{-dimethylbutadiene}$)	$\text{Na}[(\text{C}_6\text{H}_{10})\text{Ru}(\text{CO})_2\text{CN}]$	155
$\text{C}_7\text{H}_{10}\text{Ru}(\text{CO})_3$ ($\text{C}_7\text{H}_{10} = 1,3\text{-cycloheptadiene}$)	$\text{Na}[(\text{C}_7\text{H}_{10})\text{Ru}(\text{CO})_2\text{CN}]$	155
$\text{C}_8\text{H}_8\text{Ru}(\text{CO})_3$ ($\text{C}_8\text{H}_8 = \text{cyclooctatetraene}$)	$\text{Na}[(\text{C}_8\text{H}_8)\text{Ru}(\text{CO})_2\text{CN}]$	155
$\text{C}_3\text{H}_5\text{Mn}(\text{CO})_4$	$\text{Na}[(\text{C}_3\text{H}_5)\text{Mn}(\text{CO})_3\text{CN}]$	157
$\text{C}_3\text{H}_5\text{Re}(\text{CO})_4$	$\text{Na}[(\text{C}_3\text{H}_5)\text{Re}(\text{CO})_3\text{CN}]$	157
$\text{C}_3\text{H}_5\text{Fe}(\text{CO})_2\text{NO}$ ($\text{C}_3\text{H}_5 = \eta^3\text{-allyl}$)	$\text{Na}[(\text{C}_3\text{H}_5)\text{Fe}(\text{CO})(\text{NO})(\text{CN})]$	157

stannylated, giving the corresponding neutral hydrogen isocyanides or isonitrile compounds with CNH(CND) , CNR , or CNER_3 ligands, respectively (152, 155–157).

Spectroscopic data show that the olefin monocyanocarbonylferrates and -ruthenates and their derived isonitrile complexes occur as two isomeric forms, in which the CN^- or isonitrile ligand occupies either an apical or basal position in a square-pyramidal structure.

The X-ray structure of the monoclinic $\text{C}_6\text{H}_8\text{Fe}(\text{CO})_2\text{CNEt}$ (Fig. 7) ($\text{C}_6\text{H}_8 = 1,3\text{-cyclohexadiene}$) shows that the isonitrile ligand CNEt , a CO group, and two C atoms of the diene part of the C_6H_8 ring occupy the basal positions of a square pyramid, with the second CO molecule at the apex (158).

We have also been interested in the behavior of dinuclear metal carbonyls and their derivatives toward $\text{NaN}(\text{SiMe}_3)_2$. With $\text{Mn}_2(\text{CO})_{10}$ and $\text{Re}_2(\text{CO})_{10}$, we obtained the monocyano-enneacarbonyldimetalates(0) $\text{Na}[\text{Mn}_2(\text{CO})_9\text{CN}]$ and $\text{Na}[\text{Re}_2(\text{CO})_9\text{CN}]$ (153). Their structures can be derived from those of the parent carbonyls by replacement of a CO group by the isoelectronic CN^- ligand. The corresponding isonitrile complexes $\text{Mn}_2(\text{CO})_9\text{CNR}$ ($\text{R} = \text{Et}$, SiMe_3 , GeMe_3 , SnMe_3 , PPh_2) also have linear Mn—Mn—CNR units (159).

Thus, it is also characteristic of the dinuclear metal carbonyls that only

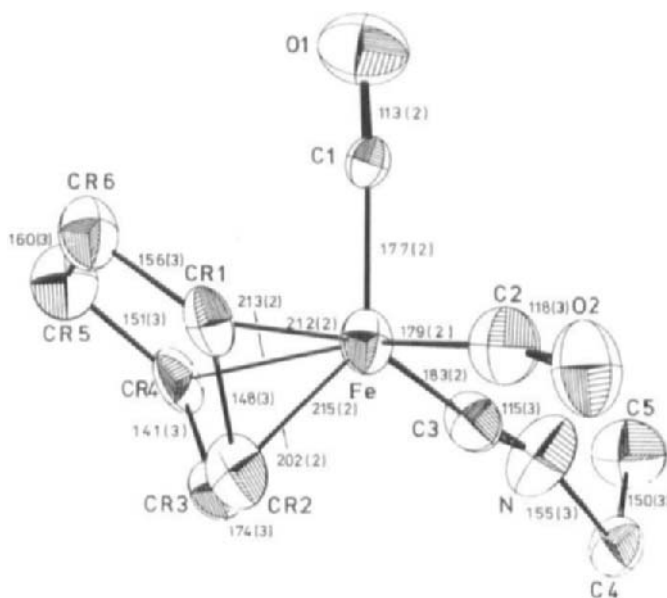


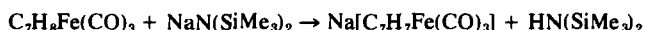
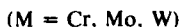
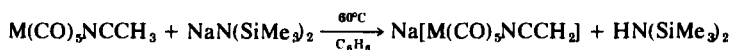
FIG. 7

one CO ligand is replaced by a CN^- anion. The nucleophilic attack of $\text{NaN}(\text{SiMe}_3)_2$ on the mixed carbonyl $\text{MnRe}(\text{CO})_{10}$ occurs only at the equatorial CO of the rhenium, so that the CN^- ligand in the $[\text{MnRe}(\text{CO})_9\text{CN}]^-$ anion is undoubtedly bonded to the rhenium and not to the manganese (160).

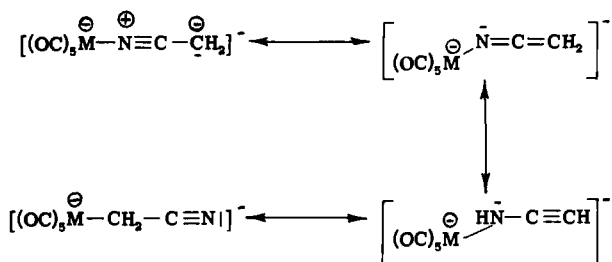
In the cases of the olefin-bridged, iron complexes $(\text{OC})_3\text{Fe}(\text{olen})\text{Fe}(\text{CO})_3$ (olen = cyclooctatetraene, 1,1'-di-2,4-cyclohexadienyl, 1,1'-di-2,4-cycloheptadienyl), we have again shown that reaction with $\text{NaN}(\text{SiMe}_3)_2$ leads exclusively to the corresponding monocyano complexes $[(\text{OC})_5\text{Fe}(\text{olen})\text{Fe}(\text{CO})_2\text{CN}]^-$ (155).

In its reactions with metal carbonyl derivatives having ligands bearing acidic C—H bonds, $\text{NaN}(\text{SiMe}_3)_2$ behaves as a proton acceptor as the silyl amide is a strong base (161).

We have thus been able to show that the acetonitrile-pentacarbonyl complexes $\text{M}(\text{CO})_5\text{NCMe}$ ($\text{M} = \text{Cr}, \text{Mo}, \text{W}$) and cycloheptatriene-iron-tricarbonyl $\text{C}_7\text{H}_8\text{Fe}(\text{CO})_3$ are deprotonated as follows, *without* attack at the CO ligands (151).



On the basis of the ^1H -NMR spectra of the monocyanomethanidopentacarbonyl metalates of Group VIB, we consider that these anions exist as a tautomeric mixture:



The $[\text{C}_7\text{H}_7\text{Fe}(\text{CO})_3]^-$ anion, with its eight π electrons in the C_7H_7 ring was for many years the subject of numerous theoretical treatments and discussions.

Molecular orbital calculations by Hofmann (162) indicated that an η^3 -allyl anion complex with a noncomplexed butadiene group is more stable than an η^4 -butadiene complex, in which the allyl anion portion of the seven-carbon ring is not bonded to the metal. We have now been able to confirm this result by an X-ray structure analysis (see Fig. 8) on $[\text{Ph}_4\text{As}][\text{C}_7\text{H}_7\text{Fe}(\text{CO})_3]$ (163).

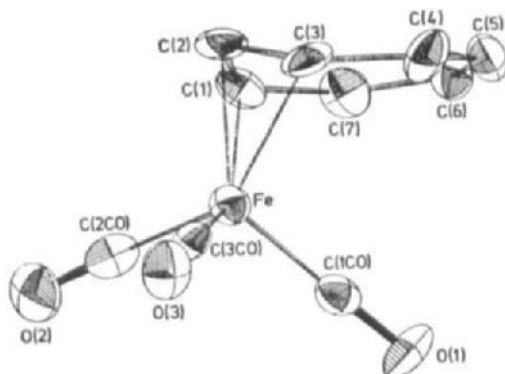
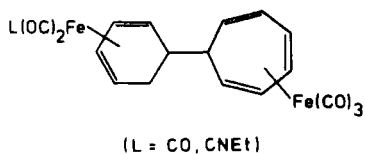


FIG. 8

An ORTEP plot of the $[\text{C}_7\text{H}_7\text{Fe}(\text{CO})_3]^-$ anion shows that the C_7H_7 ring indeed consists of an allyl anion and a diene system. Because only the four π electrons of the allyl anion are involved in bonding to the iron, it has the krypton configuration. Of the numerous reactions of the $[\text{C}_7\text{H}_7\text{Fe}(\text{CO})_3]^-$ anion, those with chloroformic esters are particularly interesting in the present context. These reactions lead to ester-substituted cycloheptatriene-irontricarbonyls, namely, 7- $\text{R}-\text{C}_7\text{H}_7\text{Fe}(\text{CO})_3$ and 1- $\text{R}-\text{C}_7\text{H}_7\text{Fe}(\text{CO})_3$ ($\text{R} = \text{MeOCO}, \text{EtOCO}$) (164).

The 7-isomers are saturated esters, and the 1-isomers are α,β -unsaturated esters. With Et_3ECl ($\text{E} = \text{Si}, \text{Ge}$), *only* the 7-isomers $\text{Et}_3\text{E}-\text{C}_7\text{H}_7\text{Fe}(\text{CO})_3$ are formed with the Et_3E group at the sp^3 -hybridized C atom of the ring (164). The reactions of the extremely nucleophilic $[\text{C}_7\text{H}_7\text{Fe}(\text{CO})_3]^-$ with the electrophilic $[\text{C}_6\text{H}_7\text{Fe}(\text{CO})_3]^+$ or $[\text{C}_6\text{H}_7\text{Fe}(\text{CO})_2\text{CNEt}]^+$ cations led to the first preparation of a dinuclear iron complex having the metal atoms bridged by a cyclohexadienylcycloheptatriene group (165):



V

REACTIONS OF METAL CARBONYLS AND METAL CARBONYL DERIVATIVES WITH THE MULTIDENTATE NITROGEN LIGANDS bipy, phen, AND terpy

Our reactions with liquid NH_3 have repeatedly prompted us to investigate the behavior of metal carbonyl derivatives toward the N-hetero-

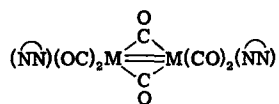
cyclic ligands bipy, phen, and terpy in suitable solvents, which is the subject of the following section.

A. Titanium and Vanadium

Quantitative replacement of the cyclopentadienyl and CO ligands occurs in the reactions of $(\eta^5\text{-C}_5\text{H}_5)_2\text{Ti}(\text{CO})_2$ (166) and $\eta^5\text{-C}_5\text{H}_5\text{V}(\text{CO})_4$ (128) with phen or terpy to give the metal(o) complexes $\text{Ti}(\text{phen})_3$, $\text{Ti}(\text{terpy})_2$, and $\text{V}(\text{terpy})_2$. The complex $\text{V}(\text{terpy})_2$ is also formed by the reaction of terpy with $\text{V}(\text{CO})_4[(\text{Ph}_2\text{P})_2\text{C}_2\text{H}_4]$ or $\text{V}(\text{CO})_2[(\text{Ph}_2\text{P})_2\text{C}_2\text{H}_4]_2$ (167). The latter phosphine-substituted paramagnetic vanadium compounds were first prepared by us from $\text{V}(\text{CO})_6$. In contrast to bipy and phen, below 80°C , the complex $\text{V}(\text{CO})_4[(\text{Ph}_2\text{P})_2\text{C}_2\text{H}_4]$ undergoes disproportionation to give $[\text{V}^{\text{II}}(\text{bipy})_3]\{\text{V}^{\text{I}}(\text{CO})_4[(\text{Ph}_2\text{P})_2\text{C}_2\text{H}_4]\}_2$ or $[\text{V}^{\text{II}}(\text{phen})_3]\{\text{V}^{\text{I}}(\text{CO})_4[(\text{Ph}_2\text{P})_2\text{C}_2\text{H}_4]\}_2$ (167).

B. Chromium, Molybdenum, and Tungsten

Although all six of the CO ligands of $\text{Cr}(\text{CO})_6$ can be replaced by bipy or phen to give $\text{Cr}(\text{bipy})_3$ or $\text{Cr}(\text{phen})_3$, for $\text{Mo}(\text{CO})_6$ and $\text{W}(\text{CO})_6$, even extreme temperature conditions only allow for a maximum substitution of four CO groups (127). With terpy, on the other hand, total replacement occurs with all three hexacarbonyls, giving $\text{M}(\text{terpy})_2$ (129). The reactions of $[\eta^5\text{-C}_5\text{H}_5\text{Mo}(\text{CO})_3]_2$ with bipy, phen, or terpy follow a similar pattern, giving *cis*- $\text{Mo}(\text{CO})_2(\text{bipy})_2$, *cis*- $\text{Mo}(\text{CO})_2(\text{phen})_2$ or $\text{Mo}(\text{terpy})_2$ (166). The reaction of $\eta^3\text{-C}_7\text{H}_8\text{M}(\text{CO})_3$ ($\text{M} = \text{Mo}, \text{W}$; C_7H_8 = cycloheptatriene) with bipy or phen ($\widehat{\text{NN}}$) in nonpolar solvents allowed us to obtain the CO-bridged diamagnetic complexes



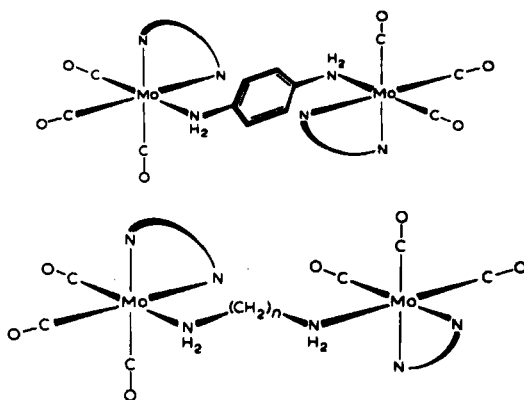
which probably contain metal-metal double bonds (168). Thus, besides the mononuclear types $\text{M}(\text{CO})_4(\widehat{\text{NN}})$ and $\text{M}(\text{CO})_2(\widehat{\text{NN}})_2$ (127), it was also possible to prepare for the first time dinuclear CO-bridged Group VIB carbonyl complexes with bipy and phen (168).

In polar solvents ($\text{L} = \text{MeOH}, \text{Et}_2\text{O}, \text{THF}, \text{MeCOMe}, \text{or MeCN}$), however, the $\eta^6\text{-C}_7\text{H}_8\text{M}(\text{CO})_3$ ($\text{M} = \text{Mo}, \text{W}$) compounds with $\widehat{\text{NN}}$ (bipy, phen) give the mixed mononuclear complexes *fac*- $\text{M}(\text{CO})_3(\widehat{\text{NN}})\text{L}$ (168);

and, in the presence of X^- ($X = \text{Cl}, \text{Br}, \text{I}, \text{CN}, \text{NCS}, \text{N}_3, \text{SH}$), the same reaction leads to the anions $\text{fac}[\text{M}(\text{CO})_3(\text{NN})\text{X}]^-$ (169). These observations opened a route for the synthesis of numerous "mixed" neutral complexes of the type $\text{M}(\text{CO})_3(\text{NN})\text{L}$, where X^- is replaced by NH_3 , py , PPh_3 , PPh_2Cl , or SO_2 , as has already been partially described (170).

The coordinatively unsaturated complexes $[\text{M}(\text{CO})_3(\text{NN})]_2$ are extremely reactive. With polydentate N and P ligands, new mono- or dinuclear bridged mixed-ligand complexes are formed by fission of the CO bridges. Examples are given in Table VII (171, 172).

The CO ligands are in all cases facial to the molybdenum. The complexes $[\text{Mo}(\text{CO})_3(\text{NN})]_2[\text{NH}_2-\text{C}_6\text{H}_4-\text{NH}_2]$ and $[\text{Mo}(\text{CO})_3(\text{NN})]_2[\text{NH}_2(\text{CH}_2)_n\text{NH}_2]$ have the following structures:



Remarkably, $[\text{Mo}(\text{CO})_3\text{bipy}]_2$ is reduced by Nabipy to $[\text{bipy}(\text{OC})_3\text{Mo}-\text{Mo}(\text{CO})_3\text{bipy}]^{2-}$ with a nonbridged metal-metal bond and cis CO ligands (173). With this reaction, we were able to prepare the first example of a derivative of the $[\text{Mo}_2(\text{CO})_{10}]^{2-}$ anion in which four CO groups are replaced by two bipy molecules.

The neutral complex $\text{bipy}(\text{ON})(\text{OC})_2\text{Mo}-\text{Mo}(\text{CO})_2(\text{NO})\text{bipy}$, prepared from $[\text{Mo}(\text{CO})_3\text{bipy}]_2$ and NO, is isosteric with the $[\text{bipy}(\text{OC})_3\text{Mo}-\text{Mo}(\text{CO})_3\text{bipy}]^{2-}$ anion (174). This also has a nonbridged structure having a Mo-Mo bond with the NO ligands occupying the axial positions in the double octahedron.

Further examples of dinuclear CO-bridged compounds of Group VIB are the complexes $[\text{Mo}(\text{CO})_3\text{L}_2]_2$, which we have synthesized from $\text{C}_7\text{H}_8\text{Mo}(\text{CO})_3$ ($\text{C}_7\text{H}_8 = \text{cycloheptatriene}$) and maleic and fumaric esters (L) (175, 176).

TABLE VII

Mononuclear complexes	Dinuclear complexes
$\text{Mo}(\text{CO})_3(\text{N}\ddot{\text{N}})(o\text{-NH}_2\text{-C}_6\text{H}_4\text{-NH}_2)$	$[\text{Mo}(\text{CO})_3(\text{N}\ddot{\text{N}})]_2(p\text{-NH}_2\text{-C}_6\text{H}_4\text{-NH}_2)$
$\text{Mo}(\text{CO})_3(\text{N}\ddot{\text{N}})(m\text{-NH}_2\text{-C}_6\text{H}_4\text{-NH}_2)$	$[\text{Mo}(\text{CO})_3(\text{N}\ddot{\text{N}})]_2[\text{NH}_2(\text{CH}_2)_n\text{NH}_2]$ ($n = 3-7$)
$\text{Mo}(\text{CO})_3(\text{N}\ddot{\text{N}})(p\text{-NH}_2\text{-C}_6\text{H}_4\text{-NH}_2)$	$[\text{Mo}(\text{CO})_3(\text{N}\ddot{\text{N}})]_2[\text{Ph}_2\text{P}(\text{CH}_2)_n\text{PPh}_2]$ ($n = 1-3$)
$\text{Mo}(\text{CO})_3(\text{N}\ddot{\text{N}})(\text{Ph}_2\text{PPPh}_2)$	
$\text{Mo}(\text{CO})_3(\text{N}\ddot{\text{N}})[\text{Ph}_2\text{P}(\text{CH}_2)_n\text{PPh}_2]$ ($n = 1-3$)	

When treated with I_2 (molar ratio 1:1), the CO-bridged species $[\text{M}(\text{CO})_3(\text{N}\ddot{\text{N}})]_2$ is oxidized to the diamagnetic iodine-bridged molybdenum(+I) complexes



which we also obtained (177) from $\text{M}(\text{CO})_4(\text{N}\ddot{\text{N}})$ and I_2 in the molar ratio of 2:1.

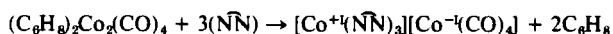
In contrast, the reactions of $\text{M}(\text{CO})_2(\text{N}\ddot{\text{N}})_2$ with iodine lead to the ionic dicarbonyl metal(+II) compounds $[\text{M}(\text{CO})_2(\text{N}\ddot{\text{N}})_2\text{I}]\text{I}$ or $[\text{M}(\text{CO})_2(\text{N}\ddot{\text{N}})_2\text{I}]\text{I}_3$ ($\text{M} = \text{Mo}, \text{W}$) with heptacoordinated metals in the cations (178).

C. Iron and Cobalt

Studies by Hieber and Lipp (179) showed that with bipy $\text{Fe}(\text{CO})_5$ undergoes disproportionation to $[\text{Fe}(\text{bipy})_3][\text{Fe}_3(\text{CO})_{11}]$. Similar reactions occur with other N bases (13), which means that $\text{Fe}(\text{CO})_5$ cannot be used as a starting material to obtain substitution products with N ligands. We have, however, found that $\text{Fe}(\text{CO})_2\text{terpy}$ can be formed from $[\eta^5\text{-C}_5\text{H}_5\text{Fe}(\text{CO})_2]_2$ or $\text{C}_8\text{H}_8\text{Fe}(\text{CO})_3$ (C_8H_8 = cyclooctatetraene) and terpy (180, 181). In the trigonal-bipyramidal complex, both CO molecules are cis-oriented.

It is well known that $\text{Co}_2(\text{CO})_8$ disproportionates on treatment with the N bases NH_3 and $\text{N}\ddot{\text{N}}$ ($\text{N}\ddot{\text{N}}$ = bipy or phen) to give cobalt(+II)bis[tetracarbonylcobaltate(−I)] with the cations $[\text{Co}(\text{NH}_3)_6]^{2+}$ or

$[\text{Co}(\text{N}\ddot{\text{N}})_3]^{2+}$ (13). Using the reaction of $(\text{nor-C}_7\text{H}_8)_2\text{Co}_2(\text{CO})_4$ ($\text{nor-C}_7\text{H}_8$ = norbornadiene) with $\text{N}\ddot{\text{N}}$ in nonpolar solvents, we were able, however, to prepare $\text{Co}_2(\text{CO})_4(\text{N}\ddot{\text{N}})_2$, which are the first real substitution products of $\text{Co}_2(\text{CO})_8$ with N ligands (182); they have the same, CO-bridged structures as $\text{Co}_2(\text{CO})_8$ with each of the metal atoms having two terminal CO ligands replaced by $\text{N}\ddot{\text{N}}$ in cis positions. The same method allowed us to synthesize the diphosphine-substituted complex $\text{Co}_2(\text{CO})_4[(\text{Ph}_2\text{P})_2\text{C}_2\text{H}_4]_2$, which is oxidized by I_2 to $\text{Co}(\text{CO})_2[(\text{Ph}_2\text{P})_2\text{C}_2\text{H}_4]\text{I}$ and reduced by sodium to $\text{Na}\{\text{Co}(\text{CO})_2[(\text{Ph}_2\text{P})_2\text{C}_2\text{H}_4]\}$ (182). In contrast, $(\text{C}_6\text{H}_8)_2\text{Co}_2(\text{CO})_4$ (C_6H_8 = 1,3-cyclohexadiene) with $\text{N}\ddot{\text{N}}$ does not undergo disproportionation into $\text{Co}(+\text{II})$ and $\text{Co}(-\text{I})$, but into $\text{Co}(+\text{I})$ and $\text{Co}(-\text{I})$ (182).



We have also reacted $\text{Co}_2(\text{CO})_8$ with 1-diphenylphosphino-2-diethylaminoethane $[\text{Ph}_2\text{P}-\text{C}_2\text{H}_4-\text{NEt}_2$ ($\text{P}\ddot{\text{N}}$)] and obtained $[\text{Co}(\text{CO})_3(\text{P}\ddot{\text{N}})]$, $[\text{Co}(\text{CO})_4]$ or $\text{Co}_2(\text{CO})_6(\text{P}\ddot{\text{N}})_2$, depending upon the reaction conditions (183). The $\text{P}\ddot{\text{N}}$ ligand is always monodentate, bonding to the cobalt exclusively via the phosphorus. Both ($\text{P}\ddot{\text{N}}$) ligands in the $[\text{Co}(\text{CO})_3(\text{P}\ddot{\text{N}})]^+$ cation are in the axial positions of a trigonal bipyramid and are also in trans positions in the nonbridged $\text{Co}_2(\text{CO})_6(\text{P}\ddot{\text{N}})_2$ (183).

That the $\text{P}\ddot{\text{N}}$ ligands in $\text{Co}_2(\text{CO})_6(\text{P}\ddot{\text{N}})_2$, which can also be obtained from $\text{Co}_2(\text{CO})_4(\text{nor-C}_7\text{H}_8)_2$ ($\text{nor-C}_7\text{H}_8$ = norbornadiene) and $\text{P}\ddot{\text{N}}$ via elimination of metallic cobalt, are monodentate is readily shown by N-methylation with MeI to give the $[\text{Co}_2(\text{CO})_6(\text{Ph}_2\text{P}-\text{CH}_2\text{CH}_2-\text{N}^+\text{Et}_2\text{Me})_2]^{2+}$ cation (183).

VI

HIGH-PRESSURE SYNTHESSES

At the beginning of this review, I mentioned that in my dissertation, over 40 years ago, I was concerned with high-pressure synthesis of metal carbonyls from anhydrous metal halides. As is often the case, the later periods of one's scientific life often see one remembering and returning to the first areas of interest. This has also been true for myself, and in recent times my group has been able to prepare numerous known and unknown derivatives of $\text{Co}_2(\text{CO})_8$ in one step by high-pressure synthesis using cobalt metal, the pertinent ligand, and CO. Several examples are given in Table VIII (184).

TABLE VIII

Starting compounds	Temperature (°C)	CO pressure (bar)	Time (h)	Reaction products
Co + bipy + CO	180	200	24	$[\text{Co}(\text{bipy})_3][\text{Co}(\text{CO})_4]_2$
Co + phen + CO	180	200	24	$[\text{Co}(\text{phen})_3][\text{Co}(\text{CO})_4]_2$
Co + ($\widehat{\text{PP}}$) ^a + CO	150	200	12	$[\text{Co}_2(\widehat{\text{PP}})_2(\text{CO})_4][\text{Co}(\text{CO})_4]_2$
Co + PPh_3 + CO	200	200	72	$\text{Co}_2(\text{CO})_8(\text{PPh}_3)_2$
Co + ($\widehat{\text{PN}}$) ^b + CO	180	350	48	$\text{Co}_2(\text{CO})_8(\widehat{\text{PN}})_2$
Co + SnCl_2 + CO	200	200	72	$[\text{Co}(\text{CO})_4]_2\text{SnCl}_2$ $[\text{Co}(\text{CO})_4]_3\text{SnCl} + \text{CoCl}_2$
Co + InCl + CO	200	200	72	$\{[\text{Co}(\text{CO})_4]_2\text{In}(\mu\text{-Cl})\}_2$
Co + PPh_3 + SnCl_2 + CO	200	200	72	$[\text{Co}(\text{CO})_3\text{PPh}_3]_2\text{SnCl}_2$
Co + ($\widehat{\text{PN}}$) + SnCl_2 + CO	180	300	36	$[\text{Co}(\text{CO})_3(\widehat{\text{PN}})]_2\text{SnCl}_2$
Co + ($\widehat{\text{PN}}$) + Cd + CO	180	300	48	$[\text{Co}(\text{CO})_3(\widehat{\text{PN}})]_2\text{Cd}$
Co + ($\widehat{\text{PN}}$) + HgBr_2 + CO	180	350	48	$[\text{Co}(\text{CO})_3(\widehat{\text{PN}})]_2\text{Hg} + \text{CoBr}_2$

^a $\widehat{\text{PP}}$ = $\text{Ph}_2\text{P}-\text{C}_2\text{H}_4-\text{PPh}_2$.

^b $\widehat{\text{PN}}$ = $\text{Ph}_2\text{P}-\text{C}_2\text{H}_4-\text{NEt}_2$.

VII

CONCLUSIONS

I hope to have shown in this review that our work on reactions in liquid NH_3 has contributed to the development of the preparative chemistry of metal carbonyls, especially in the field of anionic carbonyl metalates, and that it has initiated new impulses and ideas for further advances in this still very active area of organometallic chemistry.

One's own scientific activities are, as a matter of course, always dependent upon and closely bound to the situations of the times. Thus, it is understandable that the fateful developments in Germany in the 1930s and 1940s had grave effects upon my own generation. The beginning of World War II occurred at exactly the time when I began my first independent studies in the area of metal carbonyls. This not only caused numerous plans for the future to be abandoned but also meant that many valuable research years were lost, particularly as a result of the fact that, by the end of the war, the Munich Institute was almost totally destroyed. In this respect, Hieber is to be sincerely thanked, for it was largely through him that his Institute, of which I was a member until 1962, so rapidly regained its international reputation, which could not have been expected in 1945.

Looking back at the tempestuous and fascinating progress in the chemistry of metal carbonyls that has occurred over the past 40 years, and which, at the beginning, were unimaginable, the question automatically arises of how the future might be. In this connection, I can vividly remember the comments of Hieber, particularly at the beginning of the 1950s, as he thought that the chemistry of metal carbonyls would soon be exhausted. This was, of course, during the period prior to the onset of the exciting developments in the organometallic chemistry of the transition metals, beginning in the mid-1950s, which naturally had an enormous influence on the study of metal carbonyls and which allowed this area to break away from its more classical character.

Whether this rate of advancement will increase, or perhaps decrease, is difficult to predict. Based on the experience of the past, however, it seems definite that chemists all over the world will continue to offer new and fundamental ideas for further growth in organometallic chemistry, even though one sometimes thinks that nothing new can possibly develop. If this does occur, it is certain that, as in the past, many other areas of chemistry will be markedly influenced.

In this general context, I am sure that studies of reactions in liquid NH_3 can also play an interesting role in the future, particularly when it is increasingly recognized that experimentation with liquefied gases presents no great difficulty.

Finally, I wish to acknowledge that this research has been primarily the result of the efforts and enthusiasm of very many co-workers and students during both good and bad times.

REFERENCES

1. W. Hieber, *Z. Elektrochem.* **43**, 390 (1937).
2. W. Rüdorff and U. Hofmann, *Z. Phys. Chem. Abt. B* **28**, 351 (1935).
3. R. Brill, *Z. Kristallogr.* **77**, 35 (1934).
4. W. Hieber, *Angew. Chem.* **55**, 1 (1942).
5. W. Hieber, H. Behrens, and U. Teller, *Z. Anorg. Allg. Chem.* **249**, 26 (1942).
6. H. Behrens and E. Eisenmann, *Z. Anorg. Allg. Chem.* **278**, 155, 166 (1955).
7. H. Behrens, *Tagungsber. Chem. Ges. DDR, Hauptjahrestag. 1954*, Akademie-Verlag Berlin, 1955.
8. H. Behrens and G. von Taeuffenbach, *Z. Anorg. Allg. Chem.* **315**, 259 (1962).
9. W. Reppe, "Neue Entwicklungen auf dem Gebiet der Chemie des Acetylens und Kohlenoxids," p. 120, Springer-Verlag, Berlin and New York, 1949.
10. W. Hieber and W. Hübel, *Z. Elektrochem.* **57**, 235 (1953).
11. FIAT Review of German Science, *Naturforsch. Med. Deutschland 1939-1946*, Band 24, "Anorganische Chemie," p. 112.
12. H. Behrens, *Angew. Chem.* **61**, 444 (1949).

13. W. Hieber, W. Beck, and G. Braun, *Angew. Chem.* **72**, 795 (1960), and references cited therein.
14. H. Behrens and R. Weber, *Z. Naturforsch. Teil B* **7**, 321 (1952); *Z. Anorg. Allg. Chem.* **281**, 190 (1955).
15. H. Behrens and R. Weber, *Angew. Chem.* **67**, 521 (1955); *Z. Anorg. Allg. Chem.* **291**, 122 (1957).
16. E. Weiss and W. Büchner, *Helv. Chim. Acta* **46**, 1121 (1963).
17. H. Behrens and W. Haag, *Z. Naturforsch. Teil B* **14**, 600 (1959).
18. J. E. Ellis, C. P. Parnell, and G. P. Hagen, *J. Am. Chem. Soc.* **100**, 3605 (1978).
19. H. Behrens and W. Klek, *Z. Anorg. Allg. Chem.* **292**, 151 (1957).
20. H. Behrens and W. Haag, *Chem. Ber.* **94**, 312 (1961).
21. H. Behrens and J. Vogl, *Chem. Ber.* **96**, 2220 (1963).
22. H. Behrens and W. Haag, *Chem. Ber.* **94**, 320 (1961).
23. M. R. Churchill and S. W.-Y. Ni Chang, *J. Chem. Soc. Chem. Commun.* p. 691 (1973).
24. E. Lindner, H. Behrens, and S. Birkle, *J. Organomet. Chem.* **15**, 165 (1968).
25. H. E. Podall, H. B. Prestridge, and H. Shapiro, *J. Am. Chem. Soc.* **83**, 2057 (1961).
26. U. Anders and W. A. G. Graham, *J. Chem. Soc. Chem. Commun.* p. 499 (1965).
27. W. C. Kaska, *J. Am. Chem. Soc.* **90**, 6340 (1968); **91**, 2411 (1969).
28. R. G. Hayter, *J. Am. Chem. Soc.* **90**, 6340 (1966).
29. J. E. Ellis and G. P. Hagen, *J. Am. Chem. Soc.* **96**, 7825 (1974); J. E. Ellis, S. G. Hentges, D. G. Kalina, and G. P. Hagen, *J. Organomet. Chem.* **97**, 79 (1975); J. E. Ellis and G. P. Hagen, *Inorg. Chem.* **16**, 1357 (1977); J. E. Ellis and E. A. Flom, *J. Organomet. Chem.* **99**, 263 (1975).
30. C. Ungurenasu and M. Palie, *J. Chem. Soc. Chem. Commun.* p. 388 (1975).
31. E. Lindner, H. Behrens, and D. Uhlig, *Z. Naturforsch. Teil B* **28**, 276 (1973).
32. L. H. Jones and R. S. McDowell, *Spectrochim. Acta* **20**, 248 (1964).
33. R. G. Hayter, *J. Am. Chem. Soc.* **88**, 4376 (1966).
34. E. Lindner, H. Behrens, and S. Birkle, *J. Organomet. Chem.* **15**, 165 (1968).
35. W. F. Edgell and N. Pauwe, *J. Chem. Soc. Chem. Commun.* p. 284 (1969).
36. L. B. Handy, J. K. Ruff, and L. F. Dahl, *J. Am. Chem. Soc.* **92**, 7312 (1970).
37. R. D. Wilson, S. A. Graham, and R. Bau, *J. Organomet. Chem.* **91**, C49 (1975).
38. D. W. Hart, R. Bau, and T. F. Koetzle, manuscript in preparation.
39. M. Andrews, D. L. Tipton, S. W. Kirtley, and R. Bau, *J. Chem. Soc. Chem. Commun.* p. 181 (1973); J. P. Olsen, T. F. Koetzle, S. W. Kirtley, M. Andrews, D. L. Tipton, and R. Bau, *J. Am. Chem. Soc.* **96**, 6621 (1974).
40. J. L. Petersen, P. L. Johnson, J. O'Connor, L. F. Dahl, and J. M. Williams, *Inorg. Chem.* **17**, 3460 (1978); R. Bau, R. G. Teller, S. W. Kirtley, and T. F. Koetzle, *Acc. Chem. Res.* **12**, 176 (1979).
41. U. Anders and W. A. G. Graham, *J. Am. Chem. Soc.* **89**, 539 (1967).
42. A. S. Foust, W. A. G. Graham, and R. P. Stewart, Jr., *J. Organomet. Chem.* **54**, C22 (1973).
43. E. O. Fischer and S. Vigoureux, *Chem. Ber.* **91**, 2205 (1958).
44. J. E. Ellis and M. C. Palazzotto, *J. Am. Chem. Soc.* **98**, 8264 (1976); J. E. Ellis, P. T. Barger, and M. L. Winzenburg, *J. Chem. Soc. Chem. Commun.* p. 686 (1977).
45. H. Behrens, *J. Organomet. Chem.* **94**, 139 (1975).
46. H. Behrens, W. Klek, and J. Köhler, *Angew. Chem.* **69**, 716 (1957).
47. H. Behrens and J. Köhler, *Z. Anorg. Allg. Chem.* **300**, 51 (1959).
48. W. Hieber and E. Romberg, *Z. Anorg. Allg. Chem.* **221**, 349 (1935); W. Hieber and F. Mühlbauer, *Z. Anorg. Allg. Chem.* **221**, 337 (1935).

49. W. Strohmeier and K. Gerlach, *Z. Naturforsch. Teil B* **15**, 413 (1960); *Chem. Ber.* **93**, 2087 (1960); W. Strohmeier, K. Gerlach and G. Matthias, *Z. Naturforsch. Teil B* **15**, 621 (1960); W. Strohmeier, K. Gerlach, and D. von Hobe, *Chem. Ber.* **94**, 164 (1961); W. Strohmeier and G. Schönauer, *Chem. Ber.* **95**, 1767 (1962); W. Strohmeier, *Angew. Chem.* **76**, 873 (1964); W. Strohmeier, J. F. Guttenberger, H. Blumenthal, and G. Albert, *Chem. Ber.* **99**, 3419 (1966).
50. J. F. Guttenberger, *Angew. Chem.* **79**, 1071 (1967).
51. R. D. Bertrand, D. A. Allison, and J. G. Verkade, *J. Am. Chem. Soc.* **92**, 71 (1970).
52. R. G. Hayter, *Inorg. Chem.* **3**, 711 (1964).
53. J. Chatt and D. T. Thompson, *J. Chem. Soc.* p. 2713 (1964).
54. D. Sellmann, A. Brandl, and R. Endell, *J. Organomet. Chem.* **111**, 303 (1976).
55. H. Behrens and J. Köhler, *Z. Naturforsch. Teil B* **14**, 463 (1959).
56. H. Behrens and J. Köhler, *Z. Anorg. Allg. Chem.* **306**, 94 (1960).
57. H. Behrens and H. Zizlsperger, *Z. Naturforsch. Teil B* **16**, 349 (1961).
58. H. Behrens and R. Schwab, *Z. Naturforsch. Teil B* **19**, 768 (1964).
59. H. Behrens, R. Schwab, and D. Herrmann, *Z. Naturforsch. Teil B* **21**, 590 (1966).
60. H. Behrens, E. Lindner, and S. Birkle, *Z. Anorg. Allg. Chem.* **369**, 131 (1969).
61. E. O. Fischer and K. Öfele, *Chem. Ber.* **93**, 1156 (1960).
62. A. Wojcicki and M. F. Farona, *J. Inorg. Nucl. Chem.* **26**, 2289 (1964).
63. W. J. Schlientz and J. K. Ruff, *J. Organomet. Chem.* **33**, C64 (1971).
64. W. J. Schlientz and J. K. Ruff, *Synth. Inorg. Met. Org. Chem.* **1**, 215 (1971).
65. W. J. Schlientz and J. K. Ruff, *Inorg. Chem.* **11**, 2264 (1972).
66. J. E. Ellis and G. P. Hagen, *Inorg. Chem.* **16**, 1357 (1977).
67. H. Behrens and D. Herrmann, *Z. Naturforsch. Teil B* **21**, 1234 (1966).
68. H. Behrens, *Angew. Chem.* **80**, 244 (1968).
69. E. Lindner and H. Behrens, *Spectrochim. Acta Part A* **23**, 3025 (1967).
70. L. B. Handy, J. K. Ruff, and L. F. Dahl, *J. Am. Chem. Soc.* **92**, 7327 (1970).
71. J. K. Ruff, *Inorg. Chem.* **7**, 1821 (1968); **8**, 86 (1969); J. K. Ruff and R. B. King, *Inorg. Chem.* **8**, 180 (1969).
72. H. Behrens, D. Uhlig, and E. Lindner, *Z. Anorg. Allg. Chem.* **394**, 8 (1972).
73. J. K. Ruff, *Inorg. Chem.* **7**, 1818 (1968).
74. J. K. Ruff, *Inorg. Chem.* **6**, 2080 (1967).
75. H. Behrens, H.-D. Feilner, E. Lindner, and D. Uhlig, *Z. Naturforsch. Teil B* **26**, 990 (1971).
76. W. Hieber and U. Teller, *Z. Anorg. Allg. Chem.* **249**, 43 (1942).
77. J. K. Ruff, R. P. White, and L. F. Dahl, *J. Am. Chem. Soc.* **93**, 2159 (1971).
78. H. Behrens and D. Herrmann, *Z. Naturforsch. Teil B* **21**, 1236 (1966).
79. R. B. King and W. M. Douglas, *J. Am. Chem. Soc.* **95**, 7528 (1973); R. B. King and C. A. Harmen, *J. Organomet. Chem.* **86**, 139 (1975).
80. H. Behrens and D. Herrmann, *Z. Anorg. Allg. Chem.* **351**, 225 (1967).
81. H. Behrens and H. Schindler, *Z. Naturforsch. Teil B* **23**, 1109 (1968).
82. H. Behrens, M. Moll, and E. Sixtus, *Z. Naturforsch. Teil B* **32**, 1105 (1977).
83. D. Uhlig, H. Behrens, and E. Lindner, *Z. Anorg. Allg. Chem.* **401**, 233 (1973).
84. J. K. Ruff, *Inorg. Chem.* **6**, 1502 (1967).
85. T. J. Marks, *J. Am. Chem. Soc.* **93**, 7080 (1971).
86. H. Behrens, M. Moll, E. Sixtus, and G. Thiele, *Z. Naturforsch. Teil B* **32**, 1109 (1977).
87. H. Behrens, M. Moll, E. Sixtus, and E. Sepp, *Z. Naturforsch. Teil B* **32**, 1114 (1977).
88. R. G. Amiet, P. C. Reeves, and R. Pettit, *J. Chem. Soc. Chem. Commun.* p. 1208 (1967).
89. B. D. Dombeck and R. J. Angelici, *Inorg. Chem.* **15**, 1089 (1976).

90. W. P. Fehlhammer, A. Mayr, and B. Olgemüller, *Angew. Chem.* **87**, 290 (1975).
91. G. Schmid and H.-P. Kempny, *Z. Anorg. Allg. Chem.* **418**, 243 (1975).
92. H. Behrens and N. Harder, *Chem. Ber.* **97**, 433 (1964).
93. W. Hieber and E. Romberg, *Z. Anorg. Allg. Chem.* **221**, 349 (1935); W. Hieber and F. Mühlbauer, *Z. Anorg. Allg. Chem.* **221**, 337 (1935).
94. H. Behrens and H. Zizlsperger, *J. Prakt. Chem.* **14**, 249 (1961).
95. E. O. Fischer and R. Jira, *Z. Naturforsch. Teil B* **8**, 217 (1953).
96. H. Behrens and K. Meyer, *Z. Naturforsch. Teil B* **21**, 489 (1966).
97. H. Behrens and P. Pässler, *Z. Anorg. Allg. Chem.* **365**, 128 (1969).
98. H. Behrens, *Angew. Chem.* **74**, 120 (1962).
99. H. Behrens and H. Wakamatsu, *Z. Anorg. Allg. Chem.* **320**, 30 (1963).
100. H. Behrens and H. Wakamatsu, *Chem. Ber.* **99**, 2753 (1966).
101. H. Behrens, unpublished results.
102. H. Behrens, *J. Organomet. Chem.* **94**, 139 (1975).
103. H. Behrens and K. Lutz, *Z. Anorg. Allg. Chem.* **354**, 184 (1967).
104. H. Behrens, E. Ruyter, and H. Wakamatsu, *Z. Anorg. Allg. Chem.* **349**, 241 (1967).
105. H. Behrens and H. Schlenker, unpublished results.
106. H. Behrens and E. Ruyter, *Z. Anorg. Allg. Chem.* **349**, 258 (1967).
107. H. Behrens, E. Lindner, and P. Pässler, *Z. Anorg. Allg. Chem.* **365**, 137 (1969).
108. R. J. Angelici, *J. Chem. Soc. Chem. Commun.* p. 486 (1965).
109. R. J. Angelici and D. L. Denton, *Inorg. Chim. Acta*, **2**, 3 (1968).
110. R. J. Angelici, *Acc. Chem. Res.* **5**, 335 (1972), and references cited therein.
111. H. Behrens, E. Lindner, D. Maertens, P. Wild, and R.-J. Lampe, *J. Organomet. Chem.* **34**, 367 (1972).
112. H. Behrens, R.-J. Lampe, P. Merbach, and M. Moll, *J. Organomet. Chem.* **159**, 201 (1978).
113. R. W. Brink and R. J. Angelici, *Inorg. Chem.* **12**, 1062 (1973).
114. T. Kruck and M. Noack, *Chem. Ber.* **97**, 1693 (1964).
115. H. Krohberger, H. Behrens, and J. Ellermann, *J. Organomet. Chem.* **46**, 139 (1972).
116. J. Ellermann, J. F. Schindler, H. Behrens, and H. Schlenker, *J. Organomet. Chem.* **108**, 239 (1976).
117. A. Pfister, H. Behrens, and M. Moll, *Z. Anorg. Allg. Chem.* **428**, 53 (1977).
118. J. Ellermann, H. Behrens, and H. Krohberger, *J. Organomet. Chem.* **46**, 119 (1972).
119. H. Behrens and A. Jungbauer, *Z. Naturforsch., Teil B* **34**, 1477 (1979); H. Wagner, A. Jungbauer, G. Thiele, and H. Behrens, *Z. Naturforsch., Teil B* **34**, 1487 (1979) [Crystal structure of $\eta^5\text{-C}_5\text{H}_5\text{Ru}(\text{CO})_2(\text{CONH}_2)_2$]; A. Jungbauer and H. Behrens, *J. Organomet. Chem.*, in press; A. Jungbauer and H. Behrens, *Z. Naturforsch.*, in press.
120. A. Jungbauer and H. Behrens, *Z. Naturforsch. Teil B* **33**, 1083 (1978).
121. H. Behrens, G. Landgraf, P. Merbach, and M. Moll, *J. Organomet. Chem.*, in press; H. Behrens and G. Landgraf, unpublished results.
122. D. Messer, G. Landgraf, and H. Behrens, *J. Organomet. Chem.* **172**, 349 (1979).
123. H. Behrens, A. Pfister, M. Moll, and E. Sepp, *Z. Anorg. Allg. Chem.* **428**, 61 (1977).
124. H. Krohberger, J. Ellermann, and H. Behrens, *Z. Naturforsch. Teil B* **27**, 890 (1972).
125. J. Chatt and H. R. Watson, *J. Chem. Soc.* p. 4980 (1961).
126. H. Behrens, E. Lindner, and J. Rosenfelder, *Chem. Ber.* **99**, 2745 (1966).
127. H. Behrens and N. Harder, *Chem. Ber.* **97**, 426 (1964).
128. H. Behrens, H. Brandl, and K. Lutz, *Z. Naturforsch. Teil B* **22**, 99 (1967).
129. H. Behrens and U. Anders, *Z. Naturforsch. Teil B* **19**, 767 (1964).
130. H. Behrens, K. Meyer, and A. Müller, *Z. Naturforsch. Teil B* **20**, 74 (1965).
131. H. Behrens and A. Müller, *Z. Anorg. Allg. Chem.* **341**, 124 (1965).

132. S. Herzog and R. Taube, *Z. Chem.* **2**, 208 (1962).
133. G. Wilke, E. W. Müller, and M. Körner, *Angew. Chem.* **73**, 33 (1961).
134. J. Chatt and F. A. Hart, *J. Chem. Soc.* p. 1378 (1960).
135. H. Behrens, E. Lindner, and H. Schindler, *Z. Anorg. Allg. Chem.* **365**, 119 (1969).
136. H. Behrens, E. Lindner, and H. Schindler, *Chem. Ber.* **99**, 2399 (1966).
137. W. Hieber and H. Führing, *Z. Anorg. Allg. Chem.* **373**, 48 (1970).
138. J. Ellermann, H. Behrens, H. Dobrzanski, and F. Poersch, *Z. Anorg. Allg. Chem.* **361**, 306 (1968).
139. J. Ellermann, H. Behrens, and H. Dobrzanski, *Z. Naturforsch. Teil B* **23**, 560 (1968).
140. H. Behrens and H. Schindler, *Z. Naturforsch. Teil B* **23**, 1110 (1968).
141. N. G. Conelly, *Inorg. Chim. Acta Rev.* **6**, 47 (1972), and references cited therein (page 65).
142. E. A. Heintz, *J. Inorg. Nucl. Chem.* **21**, 262 (1961).
143. B. Chiswell and L. M. Venanzi, *J. Chem. Soc., A*, p. 417 (1966).
144. W. Hieber and W. Schropp, Jr., *Z. Naturforsch. Teil B* **14**, 460 (1959).
145. H. Behrens, E. Ruyter, and E. Lindner, *Z. Anorg. Allg. Chem.* **349**, 251 (1967).
146. H. Behrens, E. Lindner, and P. Pässler, *Z. Anorg. Allg. Chem.* **361**, 125 (1968).
147. W. Hieber and L. Schuster, *Z. Anorg. Allg. Chem.* **287**, 214 (1956).
148. D. Rehder, *J. Organomet. Chem.* **37**, 303 (1972).
149. U. Wannagat and H. Seyffert, *Angew. Chem.* **77**, 457 (1965).
150. H. Behrens and M. Moll, *Z. Anorg. Allg. Chem.* **416**, 193 (1975).
151. M. Moll, H. Behrens, R. Kellner, H. Knöchel, and P. Würstl, *Z. Naturforsch. Teil B* **31**, 1019 (1976).
152. H. Behrens, H.-J. Ranly, and E. Lindner, *Z. Anorg. Allg. Chem.* **409**, 299 (1974).
153. H. Behrens, M. Moll, W. Popp, and P. Würstl, *Z. Naturforsch. Teil B* **32**, 1227 (1977).
154. M. Moll, H. Behrens, and W. Popp, *Z. Anorg. Allg. Chem.*, **458**, 202 (1979).
155. H. Behrens and W. Popp, unpublished results.
156. H. Behrens, M. Moll, and P. Würstl, *Z. Naturforsch. Teil B* **31**, 1017 (1976).
157. H. Behrens, M. Moll, W. Popp, H.-J. Seibold, E. Sepp, and P. Würstl, *J. Organomet. Chem.*, in press; M. Moll, H.-J. Seibold, and W. Popp, *J. Organomet. Chem.*, in press; P. Merbach, P. Würstl, H.-J. Seibold, and W. Popp, *J. Organomet. Chem.*, in press; H. Behrens and H.-J. Seibold, unpublished results.
158. H. Behrens, G. Thiele, A. Pürzer, P. Würstl, and M. Moll, *J. Organomet. Chem.* **160**, 255 (1978).
159. H. Behrens, P. Würstl, P. Merbach, and M. Moll, *Z. Anorg. Allg. Chem.* **456**, 16 (1979).
160. H. Behrens and V. Schneider, unpublished results.
161. C. Krüger, *J. Organomet. Chem.* **9**, 125 (1967).
162. P. Hofmann, *Z. Naturforsch. Teil B* **33**, 251 (1978), and references cited therein.
163. E. Sepp, A. Pürzer, G. Thiele, and H. Behrens, *Z. Naturforsch. Teil B* **33**, 261 (1978).
164. H. Behrens, K. Geibel, R. Kellner, H. Knöchel, M. Moll, and E. Sepp, *Z. Naturforsch. Teil B* **31**, 1021 (1976).
165. M. Moll, P. Würstl, H. Behrens, and P. Merbach, *Z. Naturforsch. Teil B* **33**, 1304 (1978).
166. H. Behrens and H. Brandl, *Z. Naturforsch. Teil B* **22**, 1216 (1967).
167. H. Behrens and K. Lutz, *Z. Anorg. Allg. Chem.* **356**, 225 (1968).
168. H. Behrens, E. Lindner, and G. Lehnert, *J. Organomet. Chem.* **22**, 439 (1970).
169. H. Behrens, E. Lindner, and G. Lehnert, *J. Organomet. Chem.* **22**, 665 (1970).
170. H. Behrens, G. Lehnert, and H. Sauerborn, *Z. Anorg. Allg. Chem.* **374**, 310 (1970).
171. H. Behrens, W. Topf, and J. Ellermann, *J. Organomet. Chem.* **63**, 349 (1973).
172. H. Behrens, W. Topf, and J. Ellermann, *J. Organomet. Chem.* **63**, 369 (1973).

- 173. G. Lehnert, H. Behrens, and E. Lindner, *Z. Naturforsch. Teil B* **25**, 106 (1970).
- 174. E. Lindner, H. Behrens, and G. Lehnert, *Z. Naturforsch. Teil B* **25**, 104 (1970).
- 175. H. Schaper and H. Behrens, *J. Organomet. Chem.* **113**, 361 (1976).
- 176. H. Schaper and H. Behrens, *J. Organomet. Chem.* **113**, 377 (1976).
- 177. H. Behrens and W. Ziegler, *Z. Anorg. Allg. Chem.* **365**, 269 (1969).
- 178. H. Behrens and J. Rosenfelder, *Z. Anorg. Allg. Chem.* **352**, 61 (1967).
- 179. W. Hieber and A. Lipp, *Chem. Ber.* **92**, 2075 (1959).
- 180. H. Behrens and W. Aquila, *Z. Naturforsch. Teil B* **22**, 454 (1967).
- 181. H. Behrens, H.-D. Feilner, and E. Lindner, *Z. Anorg. Allg. Chem.* **385**, 321 (1971).
- 182. H. Behrens and W. Aquila, *Z. Anorg. Allg. Chem.* **356**, 8 (1967).
- 183. H. Behrens, A. Jungbauer, and M. Moll, *Z. Naturforsch. Teil B* **32**, 1222 (1977).
- 184. H. Behrens, R. Hüller, A. Jungbauer, P. Merbach, and M. Moll, *Z. Naturforsch. Teil B* **32**, 1217 (1977).

This Page Intentionally Left Blank

Organolithium Catalysis of Olefin and Diene Polymerization

A. F. HALASA,* D. N. SCHULZ, D. P. TATE,
and V. D. MOCHEL

Central Research Laboratories
The Firestone Tire & Rubber Company
Akron, Ohio

I. Introduction	55
A. Historical Development	55
B. Scope	58
C. Structure and Reactivity	59
D. Unique Features of RLi-Initiated Polymerizations	60
II. Mechanism of Olefin Polymerization with Polar Ligands	61
III. Mechanism of Diene Polymerization with Polar Ligands	65
IV. Mechanism of Diene Polymerization in Nonpolar Media	71
V. Copolymerization of Dienes and Olefins	78
VI. Use of RLi to Prepare Terminally Functional Diene (Olefin) Polymers	89
VII. Unsolved Problems/Future Trends	93
References	93

I

INTRODUCTION

A. Historical Development

The historical development of alkyllithium-initiated polymerization of olefins and diolefins for the synthesis of elastomeric materials is of interest not only because of its scientific and technological significance but also because of the insight it provides into the thinking and methodology of polymer (elastomer) researchers.

The lithium and alkyllithium initiation of diene polymerization has, from the earliest times, remained in the shadow of other, apparently more important, initiator systems. However, it has now become clear that the alkyllithium catalyst is the most efficient, initiator system at present available for diene polymerization. That organolithium initiators are not used much more widely is due largely to economic considerations,

* Present address: Kuwait Institute of Scientific Research, P.O. Box 12009, Safat, Kuwait.

which favor continued operation of older and less efficient plants utilizing free-radical or coordination-catalyzed processes rather than converting or building new plants based upon alkyllithium initiators.

The earliest mention of lithium initiation of diene polymerization was in 1910–1913 (1–3). It is quite likely that this was conceived in the fertile imagination of a patent lawyer, rather than the scientists involved, as all of the experimentation reported involved sodium and potassium.

A great deal of work was subsequently performed on sodium-initiated formation of polybutadiene involving elemental sodium, as well as with complex mixtures such as the Alfin catalyst. Although polybutadiene rubber of reasonably good quality was obtained, the synthetic processes were inefficient. Basic work done by Ziegler (4–6) during this early period involved alkyllithium addition to dienes in ether and, as will be discussed later, gave polymer structures quite similar to sodium-initiated polymers. Thus, the early work on lithium-initiated diene polymerization was performed in order to supplement the extensive studies on sodium, and only later were the unique differences between sodium and lithium catalysts recognized.

The emulsion SBR (styrene–butadiene rubber) developed in the 1940s, utilizing free-radical initiation, was of enormous benefit to tire technology. The improvement in performance and cost of SBR over natural rubber in tire treads firmly established the utility of synthetic rubber. The success of emulsion SBR led to further research. As a result, the percentage of natural rubber in rubber produced since that time has been steadily declining, and extensive research efforts have been carried along on a continuing basis to develop even better synthetic elastomers.

The development of organometallic initiators, both of the lithium type and of the transition-metal coordination type, occurred rapidly in the decade following the late 1950s. The lithium initiators were developed without the fanfare of coordination-type initiators. This situation developed because of the remarkable ability of the coordination catalysts to induce stereospecific polymerization of α -olefins.

The coordination catalysts were quickly extended to dienes and found to produce the long-sought objective of a "synthetic" natural rubber, i.e., *cis*-1,4-polyisoprene. *cis*-1,4-Polybutadiene was also quickly produced. These were, and still are, erroneously referred to as stereo rubbers. They are actually unique geometric isomers rather than stereoisomers, but the name stereo rubber became established probably because of the relationship in time and catalyst usage to stereo olefin polymerization.

Alkyllithium initiation does not have the specificity of the coordination

catalysts. Thus, polyisoprene made by using alkyllithium, although it has greater than 90% *cis*-1,4 content, does not show the stress-induced crystallization characteristic of natural rubber and of polyisoprene made by use of coordination catalysts. In the case of polybutadiene made by butyllithium initiation in hexane the stereoregularity of geometric isomers is, in fact, close to that of the free-radical-initiated polymers.

At the present time, "synthetic" natural rubber (i.e., *cis*-1,4-polyisoprene) is showing limited growth, with marginal profitability, because of severe competition from natural rubber and difficult availability of isoprene monomer. Thus, the long search for synthetic natural rubber has become more of academic than practical significance. However, for polybutadiene there is no need or desire for specificity as to *cis* or *trans* isomers because a completely amorphous structure is desired for tire treads, by far the largest single application of rubber. In the compounds used for tire treads, either low or high *cis*-content polybutadienes can be used equally well.

Thus, the characteristics that were at first thought to be important in geometrically specific polymerization of dienes turned out to be of relatively little commercial consequence. The irony of this situation is apparent now that the technology of these processes and products has become mature and has settled into a proper role.

It is now apparent that the alkyllithium initiators actually have some very important advantages over both free-radical and coordination catalysts:

- (1) Polybutadiene made by alkyllithium initiators is essentially free of the gel and color sometimes associated with the transition-metal catalysts and thus occupies a large market as an impact modifier in plastics.

- (2) Unlike the coordination catalysts, alkyllithium initiators allow easy formation of styrene-butadiene copolymers, important components of tire treads.

- (3) Alkyllithium initiation can tolerate very high temperatures. As refrigeration is not needed, alkyllithium polymerization can proceed at high reaction rates with low investment and operating costs.

- (4) The 5-7% soap remaining in rubber prepared by the free-radical process results in reduced performance and reduced oil extensibility compared to organometallic-catalyzed polybutadienes.

- (5) The "living" characteristic of lithium initiators is uniquely suited to synthesis of block copolymers. A rapidly growing new type of thermoplastic elastomer market is based on this technology.

- (6) The preparation of functionally terminal "telechelic" polymers is

only possible by the use of organolithium mono- and di-initiators. These telechelic polymers are useful in polyurethane technology.

(7) Microstructure variation in both polybutadiene and polyisoprene polymers has been realized by using alkylolithium initiators in the presence of polar modifiers.

(8) Polybutadienes from alkylolithium initiators are characterized by a high degree of linearity, in contrast to their radical- and coordination-catalyzed counterparts, which are highly branched.

The pioneering work that led to alkylolithium-initiated diene elastomers was conducted at The Firestone Tire & Rubber Company during the 1950s, and this technology was first carried into large-scale commercial practice by Firestone. Subsequently, it has also been commercialized by the Phillips Petroleum Company, Shell Oil Company, and various licensees of the three companies.

The following tabulation illustrates the amounts of diene-type rubber produced in the world by alkylolithium compared to the other types of initiators (7):

	Million metric tons
Emulsion SBR (free-radical initiator)	4.8
Polyisoprene (natural rubber)	3.6
Polybutadiene (transition-metal catalyst)	1.1
Polyisoprene (transition-metal catalyst)	0.6
Polybutadiene and SBR (alkylolithium initiator)	0.8

It is interesting to speculate on the course of events had the early polymerization experiments claimed for Li actually been done, or had ether not been used as the solvent for alkylolithium in Ziegler's early work.

B. Scope

This review is limited to the polymerization of hydrocarbon dienes and olefins by means of organolithium initiators. It is not intended to include activated olefins or dienes that can be polymerized by bases of far lower reactivity or that do not involve direct carbon-lithium bonding.

This review will feature the kinetics and mechanism of RLi-initiated, homo- and copolymerization of hydrocarbon diene and olefin monomers, with and without polar ligands. Hydrocarbon olefin homopolymerization in nonpolar media will not be discussed per se because simple olefins such as ethylene do not polymerize under such conditions, and such reactive, hydrocarbon α -olefins as styrene behave similarly to dienes in

nonpolar media. Also included in this review will be a discussion of the use of alkyllithium compounds for the preparation of functionally terminal diene (olefin) polymers.

C. Structure and Reactivity

The unique feature of the alkyllithium compounds that makes them useful as diene initiators is their character as exceedingly powerful bases; yet they are soluble in organic solvents and quite thermally stable. Alkyllithium compounds are sufficiently basic to add to hydrocarbon monomers. However, lithium salts of stabilized anions, such as acetylide and fluorenyl anions, are too weakly basic to add to such double bonds. Similarly, alkoxides and mercaptides fail to react with hydrocarbon monomers, but lithium alkyl amides react analogously to alkyllithium compounds.

Alkyllithium compounds have solubility and stability because of their ability to associate to form aggregates of definite structure. Such aggregation confers stability but is not extensive enough to cause insolubility. Methyllithium and *n*-butyllithium, for instance, exist in a highly associated form, typical of electron-deficient bonding, e.g., (MeLi)₆ and (BuLi)₄.

A somewhat different form of delocalization occurs in the case of allylic lithium compounds. This phenomenon is particularly appropriate to diene polymerization and will be discussed in detail because the end group of the growing chain is clearly an allylic lithium. In diene polymerization, the conjugated diene complexes with the organolithium initiator to form an associated species that allows addition to occur at the conjugated double bond. Thus, the ability of lithium compounds to add to conjugated dienes may be balanced by two factors—their base strength and their ability to form aggregates.

The addition of amines and ethers to alkyllithium compounds profoundly affects polymerization of such species. Amines and ethers alter the association of RLi compounds and change the course of the polymerization and its kinetics. Also, the presence of small amounts of such impurities as water, alcohols, or α -acetylenes, influences the kinetic chain length. The chain-termination reaction with such acidic protons is almost instantaneous. However, there are certain types of protons, such as α -aromatic, secondary amine, and β -acetylenic, that are not acidic enough to react immediately but will undergo transmetalation during the course of a polymerization reaction. This results in termination or chain transfer of the polymer chain, and limits the realization of polymers of

high molecular weight or high polymerization conversions or both. The presence of polar solvents greatly affects the transmetalation reactions, as will be discussed later, and thus greatly influences the effect that such protons have on the polymerization reaction.

D. Unique Features of RLi-Initiated Polymerizations

A unique feature of alkyllithium initiation is that it takes place in a homogeneous reaction mixture where there is a complete absence of termination or other side reactions, so that "living polymers" are formed. This fact, along with the ability of polar solvents to modify the reactivity and mode of reaction, has enormous implications for the synthesis of polymers.

For example, the formation of living polymers allows the preparation of block polymers by sequential addition of monomers. It also permits the introduction of functional groups on the ends of each chain. From kinetic considerations of live polymer systems, it follows that, in a batch reaction, a fast initiation step relative to the propagation step will result in a very narrow molecular-weight distribution. It also follows that the molecular weight will be directly proportional to the mole ratio of initiator to monomer.

Thus, the use of alkyllithium initiation offers the synthetic chemist a tool of enormous flexibility for "tailor-making" polymers of precise structure. Control of molecular weight, molecular-weight distribution, diene structure, branching, monomer-sequence distribution, and functionality can conveniently be achieved by such techniques as incremental or sequential addition of monomer, initiators, or modifier, programming of temperature, continuous polymerization, or the use of multifunctional reagents.

Typical hydrocarbon monomers polymerizable by using an alkyllithium initiator are

Dienes: butadiene, isoprene, piperylene, and 2,3-dimethylbutadiene.

Olefins: ethylene, styrene, α -methylstyrene, divinylbenzene, and vinyltoluene.

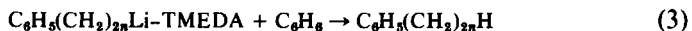
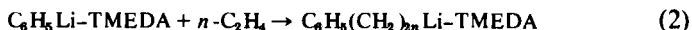
Terminal, functional groups that can conveniently be attached by reactions with the live end are silane, hydroxyl, carboxyl, and mercapto, amino, etc.

II

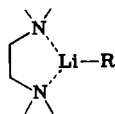
MECHANISM OF OLEFIN POLYMERIZATION WITH POLAR LIGANDS

The insertion of olefins and conjugated dienes between carbon-bound metals has been well documented in the literature (8-10). Hanford and co-workers (11) prepared polyethylenes of molecular weight 1400 by using phenyllithium in ether solvent at high temperatures and under high pressures of ethylene. The propagation reaction was in competition with termination of the active lithium ends.

Eberhardt and co-workers (12, 13) found that lithium alkyls are active toward the telomerization of ethylene and benzene when a *tert*-amine or chelating diamine, such as sparteine or *N,N,N',N'*-tetramethylenethylenediamine (TMEDA), is used [Eqs. (1)-(3)].



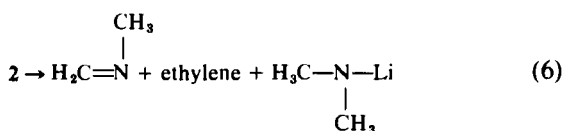
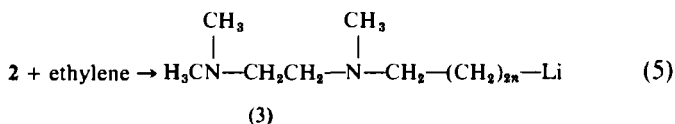
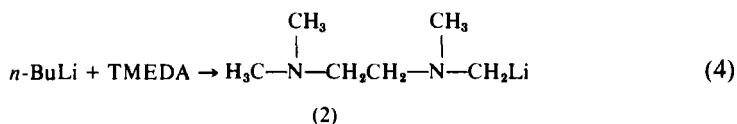
Langer (10) observed that addition of TMEDA to alkyllithium compounds in paraffinic solvents activated the initiation and propagation of ethylene to give polyethylene of high molecular weight without chain transfer to monomer. This work was later confirmed by Kamienski (14) and Smith (15). Bunting and Langer (16) proposed that the activation of the alkyllithium is due to the solvation of the lithium by the two nitrogen atoms of the diamine. A five-membered cyclic structure (1) was proposed as the solvated structure present in paraffinic solvent.



(1)

Langer claimed that structure 1 is monomeric at a concentration of less than 0.1 *M*. The same author stated that aging of the *n*-BuLi-TMEDA enhances the activity of the catalyst and that high-molecular-weight polyethylenes are formed. However, the aged catalyst may in fact be the product obtained by metalation of the diamine TMEDA. The metalated product would be an active site having a kinetics of propagation different from that of alkyllithium. This condition could, in turn, be responsible for the high molecular weight of the polyethylene produced. Confirmation of the involvement of metalated diamine was indicated by the presence

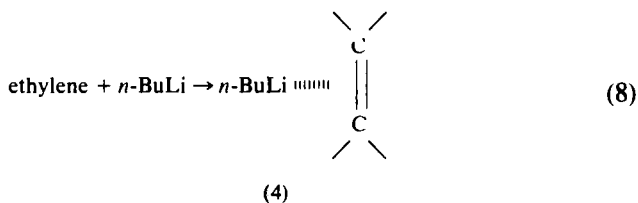
of a substantial proportion of nitrogen present in the polymer [Eqs. (4)–(7)].



Although there are no known reports on the use of $(\text{CH}_3)_2\text{NLi}$ as catalyst for the polymerization of ethylene, there is ample evidence relating to the use of this species as a catalyst for styrene and 1,3-butadiene polymerization in polar solvents (17–19). It is not unreasonable to assume that TMEDA could activate $(\text{CH}_3)_2\text{NLi}$, (2) or both toward ethylene polymerization.

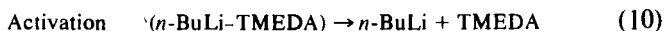
A kinetic study of the oligomerization of ethylene using alkyllithium-TMEDA complexes was carried out by Hay and co-workers (20, 21). These investigators studied the oligomerization of ethylene under conditions involving no chain transfer to monomer. They noted that ethylene oligomerization is initially rapid with $n\text{-BuLi}$ -TMEDA, in hexane as the solvent, between 0 and 60°C under an ethylene pressure of 2 atm. The volume of ethylene consumed in the initial period was found to be independent of the ethylene pressure, as well as the molar ratio of $n\text{-BuLi}$ to TMEDA. However, ethylene uptake increased proportionally with an increase in $n\text{-BuLi}$ concentration. These workers reported that the rate of ethylene consumption was first-order in ethylene pressure and $n\text{-BuLi}$ concentration. Even though TMEDA is essential for the polymerization of ethylene, the rate of ethylene usage was found to be independent of TMEDA concentration. The constant rate of ethylene consumption was expressed as follows: $\text{rate} = -d[\text{E}]/dt = kK_sP[n\text{-BuLi}]$, where K_s is the solubility constant of ethylene in the solvent used, and P is the partial pressure of ethylene over the solvent.

Hay and co-workers (20, 21) suggested that the ethylene initially forms a complex with $n\text{-BuLi}$ according to Eq. (8).



The evidence for **4** was based upon measurements of the uptake of ethylene (after degassing and readmission of ethylene several times to the system.) Hay found that the system absorbed more ethylene (25 times) than the solubility of ethylene in hexane would predict. However, one cannot help but wonder whether or not the solubility of ethylene in *n*-BuLi-hexane or *n*-BuLi-hexane-TMEDA might be different from that of ethylene in hexane alone.

Furthermore, these workers varied the ethylene pressure at a constant consumption rate and concluded that the pressure of ethylene is totally independent of the value of the molar ratio $r = \text{TMEDA}:n\text{-BuLi}$ for a constant alkyllithium concentration. They also reported that the catalyst efficiency (which was based on the observed and calculated molecular weights of polymer, assuming no chain transfer) was on the order of 40–50%. It should be emphasized that without TMEDA the oligomerization of ethylene does not take place, even though the monomer consumption rate and the initiator efficiency are independent of the quantity of TMEDA present in solution. Hay *et al.* (20, 21) suggested that TMEDA causes dissociation of the *n*-BuLi hexamer to give an inactive *n*-BuLi-TMEDA monomer. Further dissociation of this monomeric *n*-BuLi-TMEDA forms the free, *n*-BuLi monomer, which is the active species in the oligomerization reaction [Eqs. (9) and (10)].

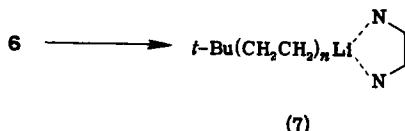
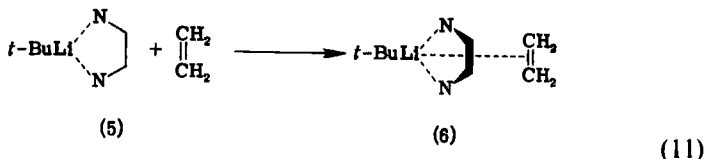


However, the explanation offered by Hay *et al.* (20, 21) appears to be in direct conflict with Langer's suggestion that the five-membered cyclic structure **1** is responsible for the enhanced activities of the complexed *n*-BuLi-TMEDA initiator system (8–10).

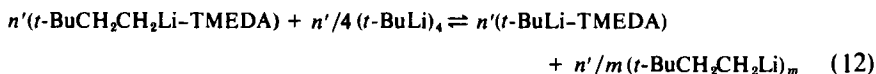
The oligomerization of ethylene using complexed alkyllithium compounds has been further studied by Rodriguez *et al.* (22). However, they used *t*-BuLi-TMEDA as the initiator instead of *n*-BuLi-TMEDA because of the greater reactivity of the former. In contrast to the work of Hay *et al.*, Rodriguez *et al.* observed that r (ratio of TMEDA to *t*-BuLi) affects the propagation reaction. Also, the rate constant varied discontinuously

as the r values passed from 0 to 4.5. In addition, Rodriguez *et al.* reported that the t -BuLi-TMEDA catalyst efficiency was 100%.

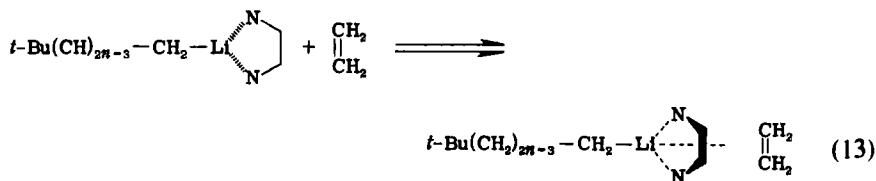
Rodriguez *et al.* (22) concluded from their kinetics studies that the active species initially is a complex (5) between the t -BuLi and the TMEDA and that, in the presence of ethylene, complex 5 takes on a molecule of ethylene to form a *more* active species (6) which, in turn, is responsible for the addition of ethylene to give complex 7 [Eq. (11)].

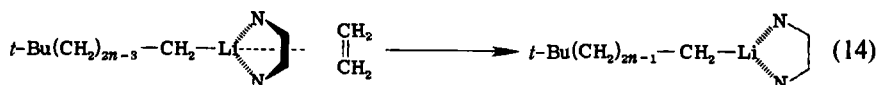


Rodriguez *et al.* (22) proposed that, as the initial uptake of ethylene is fast and the rate decreases progressively until 1 mole of ethylene is consumed per mole of t -BuLi, the following exchange reaction takes place [Eq. (12)]:



However, the decrease in rate was initially explained by the difference in reactivity of the alkyllithiums present, i.e., whether or not a primary or secondary anion was involved. Yet, the propagation reaction was quite different because the structure of the active species did not vary after the addition of the first ethylene unit. The fact that the constant rate (the rate after 1 mole of ethylene is consumed per mole of BuLi) varied linearly with initiator concentration at TMEDA: t -BuLi = 1.0 indicated that a monomeric complex was responsible for the propagation reaction (PELi-TMEDA) [Eqs. (13), (14)].



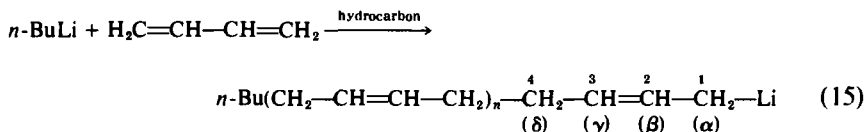


All of the studies published to date fail to identify the active catalyst species present in the RLi-TMEDA polymerization of ethylene. The kinetics data of both Hay and Shué and their co-workers fall short in this respect. A more fundamental approach is needed. It may be appropriate at this time to study the ^{13}C - and ^7Li -NMR of alkyl lithium compounds in the presence of various chelating diamines and polar modifiers such as THF and dimethyl ether.

III

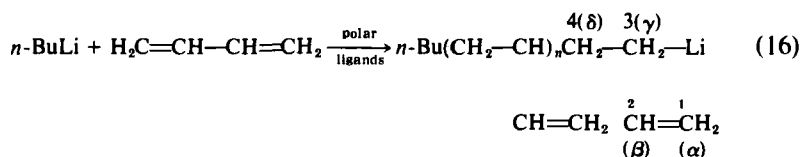
MECHANISM OF DIENE POLYMERIZATION WITH POLAR LIGANDS

When $n\text{-BuLi}$ adds to 1,3-butadiene, lithium-terminated polybutadiene chain ends result. In hydrocarbon media, 1,4-addition is favored.



The structure of the live lithium chain ends is a matter of controversy and will be discussed in a later section. After the lithium-polybutadiene is terminated with protic material, the isolated polybutadiene polymer exhibits a mixed microstructure (~35% *cis*-1,4, ~54% *trans*-1,4, and ~11% 1,2).

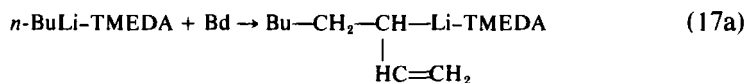
When $n\text{-BuLi}$ polymerizes 1,3-butadiene in the presence of polar ligands (modifiers), 1,2-addition is favored.



The polymer isolated from this type of polymerization shows a high level of 1,2 (vinyl) content.

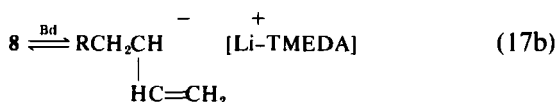
The use of monodentate and bidentate polar ligands such as ethers, amines, chelating diethers, and diamines in RLi diene polymerization has been studied by a number of workers (23-28). For example, the effect of

reaction conditions (e.g., temperature) on the complexed allylic lithium compounds in the presence of polar modifiers has been reported by Uraneck (27), and Antkowiak and co-workers (28). They studied the effect of temperature on the microstructure of polybutadiene prepared from *n*-BuLi in the presence of THF, TMEDA, and diglyme. Their conclusion was that, in the presence of these polar modifiers, the 1,2-addition product decreased with increased temperature. It could be envisaged that such a decrease in the vinyl content (1,2-addition) in favor of 1,4-addition is due to the breaking of the complexed allylic lithium with the polar modifiers to produce a more ionic anion that could isomerize, via allylic rearrangements, to give the 1,4-adduct [Eqs. (17a-c)].

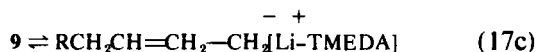


Bd = butadiene

(8)



(9)



(10)

In other words, high temperatures would shift the equilibrium in favor of the dissociated species 10 which would, in turn, favor the 1,4-addition product. ¹H-NMR and UV data for isoprene polymerization by *n*-BuLi-TMEDA also support this notion (28a).

Langer (9, 29) found TMEDA to be the most effective modifier for the RLi polymerizations of dienes, based upon polymerization-rate data and yields of 1,2-addition product. Hay and co-workers (30) studied this reaction in detail and reported both the kinetics and a mechanism for this polymerization. They noted an initial rate enhancement at a *n*-BuLi:TMEDA ratio of 1:2, after which the rate became independent of TMEDA level. The general rate expression appeared to fit Eq. (18). In other words,

$$-(d[\text{M}]/dt)_{t=0} = K_p [\text{M}^2][n\text{-BuLi}] \quad (18)$$

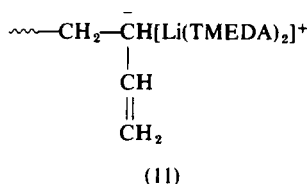
they found that the initial rate was second-order in monomer concentration and first-order with *n*-BuLi and amine concentration. Maximum rate was observed at *n*-BuLi:TMEDA ratios of 1:2. The rate decreased with

conversion, consistent with the polymerization being first-order in converted monomer.

$$-(d[M_0 - x])/dt = k_1[M_0 - x][n\text{-BuLi}] \quad (19)$$

The molecular weight (\bar{M}_n) and molecular-weight distribution (\bar{M}_w/\bar{M}_n) were typical of anionic living end polymerization (e.g., \bar{M}_w/\bar{M}_n approximated a Poisson distribution, 1.06–1.20).

Hay and co-workers reported that the \bar{M}_n increased linearly with conversion at a molar ratio of 1:2. However, at high ratios of *n*-BuLi to TMEDA, the initiator became only 50% efficient. This finding is rather surprising as the addition of TMEDA to alkyl lithium compounds enhanced the rate of the polymerization and without TMEDA, at Hay's polymerization temperature, no polymerization of the 1,3-butadiene took place. The explanation advanced by these authors was that the allylic lithium complex of polybutadiene is complexed with two TMEDA molecules and that complex **11** is the propagating species.



The presence of complex **11**, however, fails to explain the low catalyst efficiency at higher ratios of TMEDA. It appears that at higher ratios of TMEDA self-metalation becomes a competing reaction by producing $\text{R}_2\text{NLi-TMEDA}$ species that have a lower initiation (propagation) rate than *n*-BuLi-TMEDA.

Unpublished work of Halasa and co-workers (31) on the study of live chain ends using ^{13}C -NMR as a probe into their structures has led to some interesting new findings. These workers studied the lithium live ends of polybutadiene in the presence of a new polar modifier, dipiperidylethane (DPE). This modifier forms a complex with *n*-BuLi which initiates the polymerization of 1,3-butadiene to give polymer having 100% 1,2 microstructure.

The ^{13}C -NMR spectrum of polybutadiene polymer made by this initiator shows characteristic resonance peaks at 110–114 ppm assigned to

C-1, the terminal olefinic methylene carbon ($\text{CH}=\overset{1}{\text{CH}_2}$), and at 141–143 ppm assigned to C-2, the internal methine carbon ($\text{CH}=\overset{2}{\text{CH}_2}$). As the

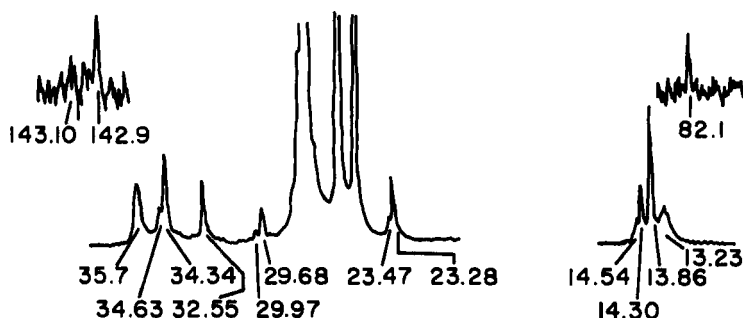
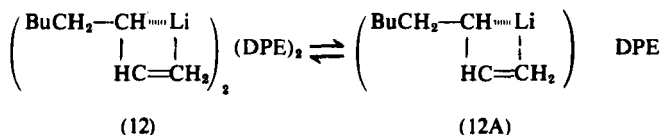


FIG. 1. ^{13}C -NMR spectrum of $n\text{-BuLi} + 1,3$ butadiene (DP 1.0 to 1.5). Note the presence of the peak at 143 ppm, a nonterminal carbon atom of a 1,2 unit without the appearance of its sister, the terminal methylene carbon atom at 110–114 ppm. Instead, a new resonance at 82 ppm associated with complexed methylene units is present. (Bottom is aliphatic region; top is olefin region.)

olefinic region in the ^{13}C -NMR spectrum of this system is the more revealing, these workers examined the resonance in this region at various degrees of polymerization (DP). At low DP, in which 1 unit of 1,3-butadiene added to 1 unit of $n\text{-BuLi}$ in the presence of 2 molecules of DPE, they noted the absence of the resonance for C-1, which normally appears at 110–114 ppm (Fig. 1). Instead, a new resonance at 82 ppm appeared. This new signal at 30 ppm upfield from the expected olefinic resonances may be due to the coordination of the lithium with the olefinic carbons adjacent to it, associated with structures as shown.



The shift position of C-1 is uncertain at this time. If it is indeed the peak at 82 ppm, it has lost a good deal of its olefinic character, as judged by its large upfield shift from its expected position. The complex with DPE would have to provide the additional electronic shielding of the nucleus as shown in structures 12 and 12A. However, more work is needed in this area to clarify these points. It must be pointed out that organolithium interaction with olefins has been noted by others (32).

As the DP increases, the normal signal of the methylene carbon atom (1,2) appears at its usual resonance position, 110–114 ppm, along with three new resonances at 90, 80, and 76 ppm (see Figs. 2 and 3). The latter peaks disappear on neutralization of the allyllithium of polybutadiene with methanol, and the normal absorptions for 1,2-addition at 110–114 and 143 ppm become more pronounced and sharper.

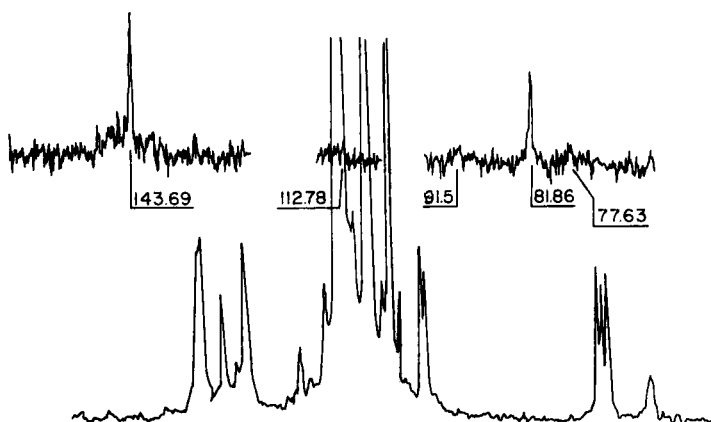


FIG. 2. ^{13}C -NMR spectrum of live poly(Bd)Li (DP = 2, 3, or 4). The signals at 92, 82, and 78 ppm have been assigned to the complexed terminal methylene carbon atom of various DP values. Note the absence of a signal at 110–114 ppm for the noncomplexed terminal methylene also absent in Fig. 1. (Bottom is aliphatic region; top is olefin region.)

As may be seen from Fig. 3, there are no resonance peaks at 120–128 ppm characteristic of 1,4-microstructure in polybutadiene polymer. However, on addition of methanol to the chain live ends, resonance peaks at 120–128 ppm appear in ratios of 60% *trans*-1,4, 14% *cis*-1,4, and 26% 1,2. This suggests that the protonation of the chain live ends with methanol is an independent reaction and does not relate to the actual structure of the propagating species. It may be said that the structure of the allylic lithium of polybutadiene (DP > 1) is postulated to exist in the 1,2-form (13). Yet hydrolysis of 13 gives mixed 1,4- and 1,2-microstructures.

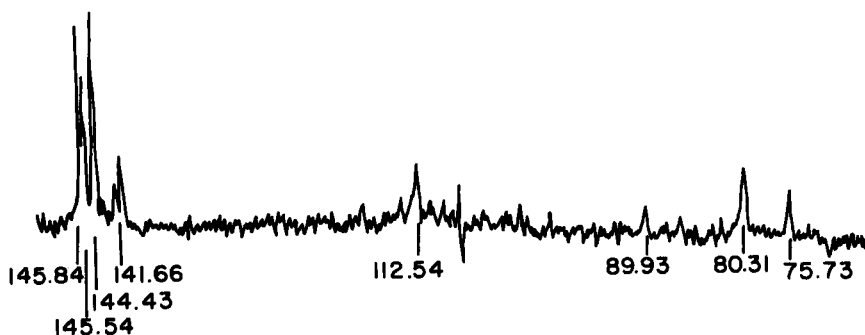
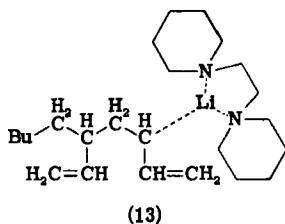


FIG. 3. ^{13}C -NMR spectrum, olefinic region only. Note the peak at 89.93, 80.31, and 75.73 ppm assigned to structure 13 of DP = 1, 2, and 3, and the appearance of a peak at 112 ppm assigned to the terminal methylene in 1,2-poly(Bd).



Several experiments with the RLi-DPE catalyst were repeated; in these, a second polar modifier was added to the *n*-BuLi-DPE initiator, and the microstructure was reexamined after further monomer addition had taken place. We found that the microstructure of essentially 100% 1,2 with *n*-BuLi-DPE decreased to 86% 1,2 on addition of THF, to 90% 1,2 with TMEDA, and to 87% 1,2 with diglyme. This suggests that in complex **13**, the olefinic ligand was displaced by the second polar modifier, giving rise to monomer addition at either C-1 or C-3. Nevertheless, it should be noted that structure **13** was not favored by Morton and co-workers (33) in either benzene or THF solvent. Instead, they favored the σ -bound 1,4 chain ends.

The ^{13}C -NMR spectrum of the initial stage of the reaction in which small amounts of butadiene are gradually added to a large excess of *n*-BuLi-DPE shows a complex pattern in the olefinic region (145.7, 144.6, 143.5, and 142.4 ppm), as shown in Fig. 4. As more 1,3-butadiene is added, these signals first increase in intensity and, except for the peak

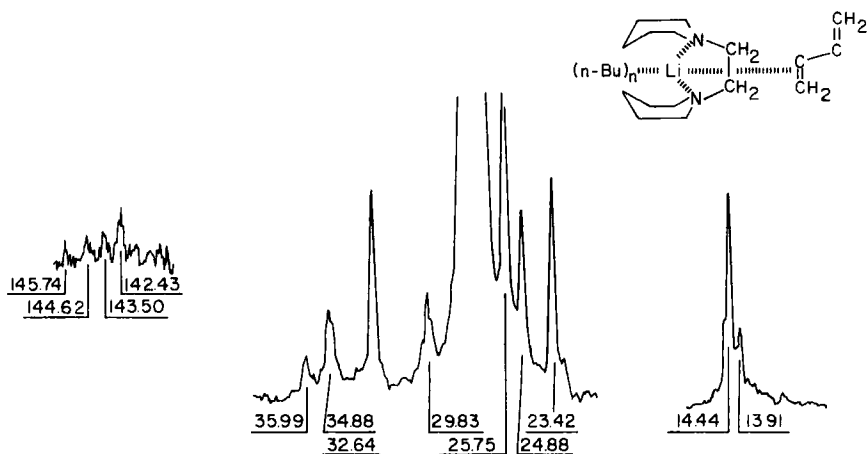
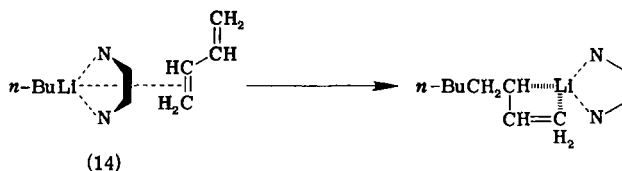


FIG. 4. ^{13}C -NMR spectrum of complex, *n*-BuLi-DPE and 1,3 butadiene. Note absorption peaks between 140 and 146 ppm assigned to π -complexes of Bd and *n*-BuLi-DPE.

at 143.5 ppm, then tend to disappear as the DP increases. The strongest peak remaining, at 143.5 ppm, is due to the C—2 (nonterminal) olefinic carbon of the 1,2-microstructure. The three minor peaks shift to higher field as the sample is heated. It is believed that these signals are due to various associated complexes of initiators and chelating diamines with monomer. These complexes are the precursors to chain growth. A suggested structure is shown here:



IV

MECHANISM OF DIENE POLYMERIZATION IN NONPOLAR MEDIA

The polymerization of 1,4-butadiene and related conjugated dienes in polar media was discussed earlier. The major focus of this part of the review will be devoted to the polymerization of 1,3-butadiene and isoprene in hydrocarbon media, with emphasis on the allylic lithium structure and reactivity.

The discovery in the Firestone Laboratory in the early 1950s by Foster, Stearns, and Forman that isoprene can be polymerized with lithium metal and later with *n*-butyllithium in hydrocarbon media to give stereoregular polyisoprene having 90–93% *cis*-1,4-polyisoprene (having properties similar to those of natural rubber) was a milestone finding (34–38). It gave an impetus to research in the areas of Group I organometallics, and related catalyst fields. A number of investigators (39–43) in several universities started research on the kinetics and other aspects of such polymerization reactions. However, the main aspects that concern us in this section are the structure and reactivity of the alkyllithium catalysts and allylic polymer lithium in nonpolar media.

The structures of alkyllithium compounds have been studied extensively by various investigators, and their findings are given in Table I (44–49). Data in Table I suggest that the alkyllithium compounds in hydrocarbon medium are of either tetrameric or hexameric nature. The highly branched compounds are tetrameric.

There are reports in the literature that the higher molecular-weight alkyllithium compounds such as polystyryl- or polyisopropylolithium may be dimeric (41, 42).

TABLE I
 AGGREGATION STATE OF ALKYL LITHIUM COMPOUNDS

Compound	Solvent	Concentration range	<i>n</i>	Method ^a	Reference
C ₂ H ₅ Li	C ₆ H ₆	0.02–0.23	6.67 ± 0.35	F	44
	C ₆ H ₁₂	0.02–0.10	5.95 ± 0.3	F	45
<i>n</i> -C ₄ H ₉ Li	C ₆ H ₆	0.5–3.4	6.25 ± 0.06	I	46
	C ₆ H ₁₂	0.4–3.3	6.17 ± 0.12	I	46
(CH ₃) ₃ CLi	C ₆ H ₆	0.05–0.18	3.8 ± 0.02	B	47
	C ₆ H ₁₄	0.05–0.123	4.0 ± 0.02	B	47
(CH ₃) ₃ Si—CH ₂ Li	C ₆ H ₆	0.6–2.78	4.0 ± 0.2	B	48
	MP ^b	0.2–0.12	3.9 ± 0.2	B	48
	C ₆ H ₆	0.06–0.49	4.0 ± 0.11	F	49

^a I = Isopiestic; F = freezing-point lowering; B = boiling-point elevation.

^b MP = methylpentane.

It is obvious that alkyllithium compounds in the presence of 1,3-butadiene must lose their structural integrity either before or after addition to the conjugated diene moiety. The published kinetic data (40, 41) suggest that the polymerization rate may depend on the structure of the alkyllithium compounds, even though a fractional kinetic order for catalyst concentration was reported by various investigators (40, 42, 43). The fractional order in catalyst (alkyllithium) should remain when dimers participate in the polymerization. The polymerization of 1,3-butadiene using alkyllithium initiators in various solvents has been studied by Russian workers (50–53). However, the most comprehensive study was made by Sgonnik *et al.* (54) in their investigation of the *sec*-BuLi addition to butadiene. They postulated that mixed alkyllithium-allyllithium species are responsible for the effect on the microstructure of the polybutadiene obtained. These associated species (*sec*-BuLi)_{*m*}–(*sec*-BuM_{*x*}Li)_{*n*} had a mixed reaction order of 0.8 and 0.90. The presence of the associated oligomers was studied by infrared spectroscopy. These workers (54) reported an activation energy of 50 ± 17 kJ/mol (12 ± 4 kcal/mol) and an initiation rate constant at 10°C of 1.5 × 10^{–3} dm³ mol^{–1} sec^{–1}.

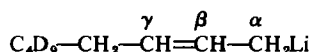
Determination of the absolute rate constant of anionic polymerization has been complicated by the existence of an equilibrium of various associated species. Work on the rate of initiation *K*_i has been reviewed by Bywater (55). Investigation of the rate of propagation *K*_p has involved two kinetic approaches.

The method of Sinn and Onsager (55*a*) made use of low concentrations of initiator and assumed that only the unassociated forms of the growing end were present during chain growth. In contrast, Morton *et al.* (56, 57)

attempted to determine the equilibrium constant K of $\text{Bu(M)}_x\text{Li}_n \cdot n\text{-BuLi(M)}_x\text{Li}$ by viscosity measurements by the addition of a monomeric alkyllithium of lower molecular weight to the growing polymeric chain. Despite these investigations, Bywater (55) concluded in his review that no accurate values for K_p (the propagation rate) of 1,3-butadiene with polymeric lithium had been determined. We consider that the differences in the interpretation of the kinetic results arose from the association of the polymeric lithium with itself and with unconsumed initiator molecules.

Subsequently, several nonkinetic approaches (32) were directed toward determining the structure of the live chain ends (e.g., $^1\text{H-NMR}$ and $^{13}\text{C-NMR}$). For example, Bywater and co-workers (58) studied the addition of *t*-butyllithium to 1,3-butadiene and obtained a complex PMR spectrum for the addition product. They examined the effect of catalyst concentration on the microstructure of the polybutadiene and found that at high catalyst levels, the vinyl content increased as shown in Table II.

The $^1\text{H-NMR}$ spectrum of the 1:1 adduct of *t*-butyllithium- d_9 and normal butadiene ($\text{DP} = 1$) in benzene was characterized by complex resonances; this spectrum was interpreted by these authors as being a mixture of *cis*- and *trans*-1,4-addition products.



The γ -proton resonance showed a complex splitting in both benzene and THF. This splitting of the γ -proton was further simplified by using 1,1,3,4-tetradeuterobutadiene. The resonance of the γ -proton showed only two major signals in the ratio of 2.6:1 separated by only 16 Hz. This situation was interpreted by Bywater and co-workers (58) as being due to restricted rotation of the γ,β -isomerized carbon bond, resulting in *cis*- and *trans*-1,4-isomerization (see Fig. 5). Continuing their study, Bywater and co-workers examined the addition of *t*-butyllithium- d_9 to undeuterated butadiene, to give a polymer having $\text{DP} = 6$. The spectrum of the

TABLE II
CATALYST CONCENTRATION VS VINYL

<i>t</i> -BuLi	DP	1,2 (%)
0.005	8.2	3.0
0.05	9.5	10.3
0.50	9.2	47

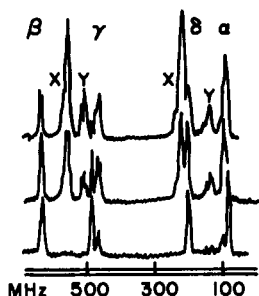


FIG. 5. ^1H -NMR spectra of oligomers $\text{C}_4\text{D}_8(\text{C}_4\text{H}_8\text{D}_4)_n\text{Li}$ formed from 1,1,3,4-tetradeuterobutadiene in benzene at room temperature; DP in ascending order, 1, 2.1, and 3.2. (X,Y) Signals from (predominantly) 1,4- and 1,2-units in nonterminal monomer; (α , β , γ , δ) those from terminal (Li) units. Reprinted with permission from S. Bywater, D. J. Worsfold, and G. Hollingsworth, *Macromolecules* 5, 389 (1972). Copyright by the American Chemical Society.

polymer having DP = 6 (see Fig. 6) showed a complex γ -proton splitting while the α -proton signal became a singlet and the β -proton a doublet. The conclusion reached by these authors was that the adduct of *t*-butyllithium with 1,3-butadiene (regardless of its DP) showed no separate 1,2-structure in the NMR spectra, even though some of the polymers isolated contained as much as 47% 1,2-structures. The definitive experiment claimed by these investigators was the polymerization of 2,3-dideuterobutadiene to provide a polymer having DP = 6, for which the complex γ -signals had disappeared. This suggested that no 1,2-addition was involved since the 2,3-dideuterobutadiene should have eliminated all 1,4-adduct olefin resonance and retained all signals from the $=\text{CH}_2$. Regret-

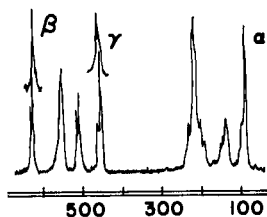
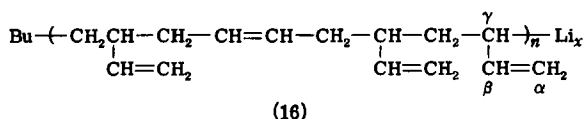
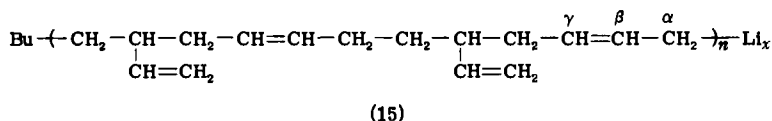


FIG. 6. ^1H -NMR spectra of an oligomer of DP = 6 formed in benzene with 0.5 *M* initiator. The β and γ signals of a similar product were formed in dilute solution, and then this was concentrated to about the same final concentration as used in Fig. 3. The scale is the same as in Fig. 3. Reprinted with permission from S. Bywater, D. J. Worsfold, and G. Hollingsworth, *Macromolecules* 5, 389 (1972). Copyright by the American Chemical Society.

tably, these authors did not show the NMR spectrum supporting this important finding.

The most comprehensive work to date involving PMR spectroscopy to study the propagation step in the alkyllithium polymerization was done by Morton and co-workers. They examined the addition of C_2D_5Li to 1,3-butadiene (59), isoprene (60), 2,3-dimethylbutadiene (60), *cis*- and *trans*-pentadiene (61), and hexadiene (61). These reactions were examined at 1 *M* concentration with DP of 10–40. The chain ends were pseudo-terminated using butadiene- d_8 in order to separate the signals due to the live ends from those of the penultimate units. Examining the data carefully, Morton and co-workers reached the following conclusions: (a) The chain ends were essentially in the 1,4-structure, and no 1,2-structures were noted (even though the polymers isolated usually contain 9% 1,2). However, several workers (58, 62) reported that at concentrations of initiator even lower than that used by Morton *et al.*, the structure showed 47% 1,2 (see Table II). (b) The carbon-bound lithium was postulated to be σ -bonded because of the magnetic equivalence of the α -protons. This implies the absence of π -allyl delocalization bonding at the γ -proton appearing at 4.6 to 4.4 ppm. However, this rather unusual upfield shift of the γ -proton at 4.6–4.4 ppm should have caused some concern to these workers. This large upfield shift of the γ -proton may not be due to partial π -allyl bonding, yet it must certainly indicate a degree of delocalization or interaction between the γ -carbon and the positive nucleus of the lithium.

In a recent ^{13}C -NMR study by Halasa *et al.* (31), the addition of *n*-BuLi to 1,3-butadiene at DP = 10–12 (Fig. 7) was studied in the absence of polar modifiers. The vinyl carbon at DP 12 showed the usual ($=CH_2$) olefinic position at 110–114 ppm, structure 16, and a new and unusual absorption at 90–100 ppm appeared. The latter resonance was shown by a gated decoupling technique to be split into a doublet. This observation indicates that this carbon is a methine carbon and could be the γ -carbon in structure 15 or the γ -carbon in structure 16. Since the methine γ -carbon atom in structure 15 is an olefinic carbon, the assignment of the



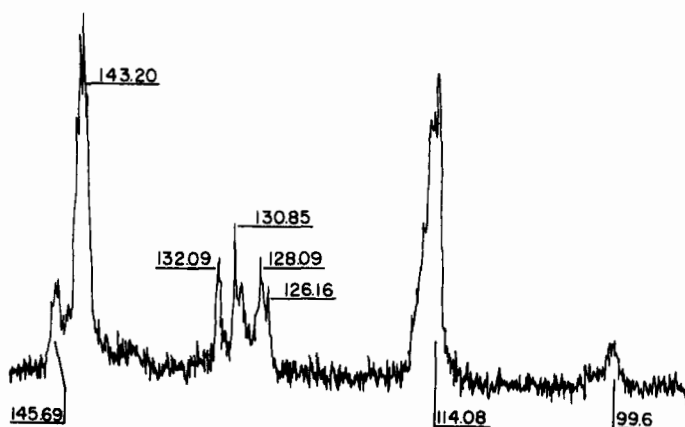


FIG. 7. ^{13}C -NMR spectrum of 1,3-Bd and $n\text{-BuLi}$, $\text{DP} \approx 10\text{--}12$. The signal at 99.6 ppm in curve A was split into a doublet upon coupling with proton nucleus. This suggests that this absorption is that of a methine carbon atom.

signal at 90–100 ppm appears to be due to this carbon. It would be unusual for an sp^2 carbon-bound lithium to have approximately the same chemical shift as the sp^3 carbon in the ^{13}C -NMR spectrum.

Addition of DPE to preformed live lithium in a hydrocarbon solvent showed a shift of the peaks at $\sim 90\text{--}100$ ppm to new signals at 80–85 ppm (see Fig. 8). These new peaks appeared at the same position as shown

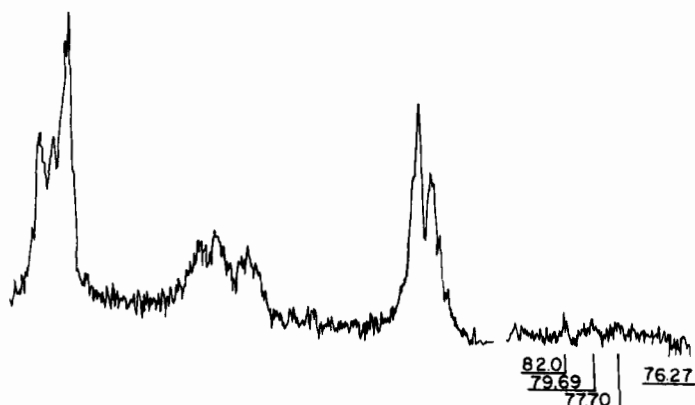
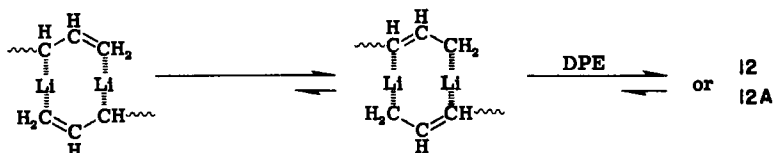


FIG. 8. ^{13}C -NMR spectrum of 1,3-Bd and $n\text{-BuLi}$, $\text{DP} \approx 10\text{--}12$. DPE has been added to premade polymer lithium. Note the shift to upfield of the signal at 99.6, seen in Fig. 7, and the splitting into multiple peaks between 75 and 80 ppm. This suggests that the peak at 99.6 in Fig. 7 is a composite of associated live lithium species.

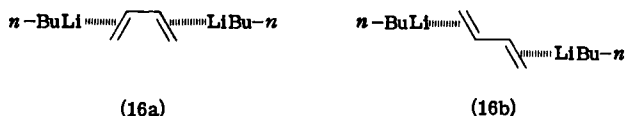
for structure **12** (see Figs. 1 and 2). This shift, observed for both poly(Bd)Li made in the presence of DPE and for preformed live lithium made in hydrocarbon as it is complexed with DPE, suggest that the polybutadienyllithium exists in the following isomeric structures.



Therefore, the conclusion can be drawn from the ^{13}C -NMR spectrum of the system in hydrocarbon media that the live ends may be in the 1,4-structure; this is in agreement with Morton's PMR results. However, the 1,4-structure may contain other structures in an aggregated species, such as dimers or the like.

Because the structure of the live ends in polar and nonpolar media appears to be of two different forms, each with its unique resonance associated with the methine and methylene carbon atoms, it is reasonable to expect that such structures should lead to different microstructures. Furthermore, these species may exist in equilibrium with each other; if so, the detection of these species would be dependent upon their concentrations in the respective solvent media.

A most interesting feature of the ^{13}C -NMR data for 1,3-butadiene polymerization in hydrocarbon solvent is the appearance of resonance peaks at ~ 146 ppm (see Fig. 7). These signals seem to decrease in intensity as the live-end signals appear. These resonances are present in the spectra of both polar and nonpolar live ends. We consider that these signals are a response to a perturbation arising in the initial complex formed between the butadiene and the organolithium initiator and that these complexes dissociate and react as the temperature is raised. It is presumed that these complexes are the starting point for chain growth (see formulas **16a** and **16b**).



The ^{13}C -NMR spectrum of the adduct of *t*-butyllithium and isoprene was studied by Brownstein *et al.* (63), who concluded that this adduct has the 4,1-structure and that the *trans*-1,4-structure is the only isomer present, even though the isolated polymer shows mainly the *cis*-1,4-structure. Examination of the data of these workers suggests that the γ -

carbon of the live ends, which appeared 22.1 ppm upfield from the γ -proton of the dead ends, is an indication that some perturbation of the —C=C— system occurs. Such spectral perturbation (65) has been noted before, even though there was no π -delocalization present. Yuki and co-workers (66) studied the PMR spectra of the adduct of *n*-BuLi and diphenylethylene to isoprene. They concluded that only *cis*-1,4- and *cis*-4,1-anions exist (no evidence of any *trans*-1,4-anion.) However, Yuki *et al.* did point out that signals of some unknown anions appeared in the NMR spectra in both C_6D_6 and $\text{THF-}d_8$. Moreover, some of the signals in their NMR spectra did not show the proper ratios.

Thus, it appears that there is no unambiguous mechanistic interpretation for RLi diene polymerization in nonpolar media and more work is needed. Nevertheless, some ^{13}C -NMR data have been obtained that strongly favor some type of interaction between the positive lithium center and the π -electrons of the double bond, e.g., the stronger shift centered on the methine ($\text{CH}_2=\text{C}$) carbon atom. It also appears that the live-end 1,4-structures in hydrocarbon media are in equilibrium with live ends that give rise to 1,2-structures, as alluded to in the earlier discussion.

V

COPOLYMERIZATION OF DIENES AND OLEFINS

Organolithium reagents have been used to prepare random, block, and graft copolymers. Much work has been done on the copolymerization of diene and olefin monomers, especially 1,3-butadiene and styrene. In this review, we shall emphasize the copolymerization of these two monomers.

When butadiene and styrene are mixed in the presence of an organolithium initiator, the resulting copolymerization process and product will be governed by the reaction conditions. The rate of copolymerization, the relative composition of the copolymer, and the distribution of monomer units (i.e., block, random, etc.) will be determined by such factors as solvent, temperature, and monomer:feed ratio.

As in the case of olefin or diene homopolymerization by RLi, copolymerization is particularly sensitive to solvent effects. Initial-charge (all monomers added together) copolymerization of butadiene and styrene tends to result in a *tapered block* copolymer (a block of butadiene with increasing levels of styrene, followed by a block of styrene) in hydrocarbon solvents and a *random* copolymer (a uniform distribution of butadiene and styrene) in polar media.

In hydrocarbon solvents, butadiene is preferentially polymerized until

it is almost consumed, and then the styrene polymerizes. The styrene uptake starts lower than the monomer charge, gradually increases until the butadiene supply is depleted, and then increases rapidly. Temperature has little effect on the distribution of styrene in such copolymerizations (see Fig. 9).

Two explanations have been advanced for such copolymerization behavior in hydrocarbon solvents. Korotkov (67) suggested that selective complexation or solvation of the lithium chain ends by butadiene causes an increase in the concentration of butadiene about the growing chain ends. In turn, this monomer dominates the early phases of the copolymerization. Consistent with this notion are the high entropies of activation for this copolymerization noted by Morton (68). The work of Oliver and co-workers (64, 65) adds further suggestive support to the concept of preferential solvation. They observed the interaction between the lithium and the double bond of the model compound 3-butenyllithium by ^7Li -NMR, UV, and IR spectroscopy. Similar observations were made by Glaze *et al.* (32) and Halasa *et al.* (31).

However, contrary evidence also exists. Evans and Worsfold (70) measured the reaction rate of styrene with polybutadienyllithium with and without added butadiene. Surprisingly, they found that the rates are similar. Their observation argues against the involvement of butadiene in solvation.

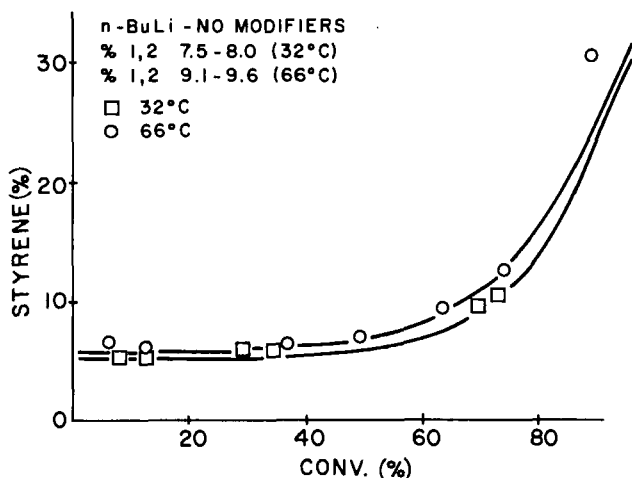


FIG. 9. Styrene uptake in unmodified RLi butadiene-styrene copolymerizations. Reprinted with permission from T. A. Antkowiak, A. E. Oberster, A. F. Halasa, and D. P. Tate, *J. Polym. Sci. Part A-1*, 10, 1319 (1972).

Furthermore, Morton and co-workers (59, 69) examined the PMR spectra of 1,3-butadiene monomers both in the presence and absence of polybutadienyllithium in order to determine whether the diene protons of the monomer are shifted by interaction with the polymer lithium. No shifts were observed. Their finding indicates that if any complex between monomer and C—Li exists, it must be of a shorter lifetime than the NMR time scale. However, such a complex has been observed in the presence of a modifier such as DPE (31).

An alternative rationale for the unusual RLi (hydrocarbon) copolymerization of butadiene and styrene has been presented by O'Driscoll and Kuntz (71). Rather than invoking selective solvation, these workers stated that classical copolymerization kinetics is sufficient to explain this copolymerization. They adapted the copolymer-composition equation, originally derived from steady-state assumptions for free-radical copolymerizations, to the anionic copolymerization of butadiene and styrene. Equation (20) describes the relationship between the instantaneous copolymer composition $d[M_1]/d[M_2]$ with the concentrations of the two monomers in the feed, M_1 and M_2 , and the reactivity ratios, r_1 , r_2 , of the monomers. The r_1 and r_2 values are measures of the preference of the growing chain ends for like or unlike monomers.

$$\frac{d[M_1]}{d[M_2]} = \frac{[M_1]}{[M_2]} \cdot \frac{r_1[M_1] + [M_2]}{r_2[M_2] + [M_1]} \quad (20)$$

$$r_1 = \frac{k_{11}}{k_{12}} \text{ or } \frac{k_{BB}}{k_{BS}}, \quad r_2 = \frac{k_{22}}{k_{21}} \text{ or } \frac{k_{SS}}{k_{SB}}$$

where B = butadiene and S = styrene.

These workers obtained a good correlation between theory and experiment by assuming that

$$k_{BB} = xk_{SB} \quad (\text{or } k_{BB} > k_{BS}) \quad (21)$$

$$k_{BS} = xk_{SS} \quad (\text{or } k_{SB} > k_{SS}) \quad (22)$$

These assumptions were confirmed by several investigators (72–75) who, indeed, found that

$$k_{SB} \gg k_{SS} > k_{BB} > k_{BS}$$

In other words,



It should be noted that anionic copolymerizations, unlike their free-

radical counterparts, involve no actual steady state; however, only a pseudo-steady state may be required. Also, in some instances, initiation by alkylolithium compounds continues during the polymerization and may affect r_1 and r_2 (76) due to the cross-association between the butadienyllithium and the polystyrenyllithium during copolymerization.

Thus, both explanations for the unusual reactivity of B and S to RLi copolymerizations in hydrocarbons are useful together, but are not persuasive by themselves.

Initial-charge RLi copolymerization of butadiene and styrene in hydrocarbons tends toward a tapered-block placement of monomer units. However, it is possible to generate a random copolymer in such solvents if the B:S monomer ratio is kept constant by programmed monomer addition or continuous copolymerization (77-78a).

Random copolymers can also be obtained by RLi copolymerizations in polar media or in the presence of polar ligands. Various polar ligands (e.g., THF, $(C_2H_5)_2O$, TMEDA, or diglyme) have been used as "randomizing agents." Unfortunately, such polar modifiers also tend to raise the vinyl content and reduce the elastomeric behavior of polybutadienes (28, 76). Various organometallic compounds of Cs, Rb, K, and Na have also been employed with RLi in order to prepare random copolymers having low to high vinyl content (79).

Polar modifiers tend to increase the reactivity and uptake of styrene. Figure 10 shows a diglyme-modified copolymerization of butadiene and styrene and should be compared with the unmodified reaction shown in Fig. 9. It can also be seen that the modified copolymerization is sensitive to temperature. The higher uptake of styrene occurs at the lower copolymerization temperature (28).

The living character of organolithium polymerizations makes such processes ideally suited for the preparation of pure as well as tapered-block copolymers. Diene-olefin pure-block copolymers have become important commodities because of their unique structure-property relationships. When such copolymers have an ABA or $(AB)_nX$ [A = polyolefin, e.g., polystyrene or poly(α -methylstyrene); B = polydiene, e.g., polybutadiene or polyisoprene; and X = coupling-agent residue] arrangement of the blocks, the copolymers have found use as thermoplastic elastomers (i.e., elastomers that can be processed as thermoplastics).

There are several different organolithium routes (80) for synthesizing essentially pure ABA or $(AB)_nX$ copolymers:

1. The use of a monolithium initiator and a three-stage sequential copolymerization, Eqs. (25)-(27).
2. The use of a dilithio initiator and a two-step copolymerization, Eqs. (28) and (29).

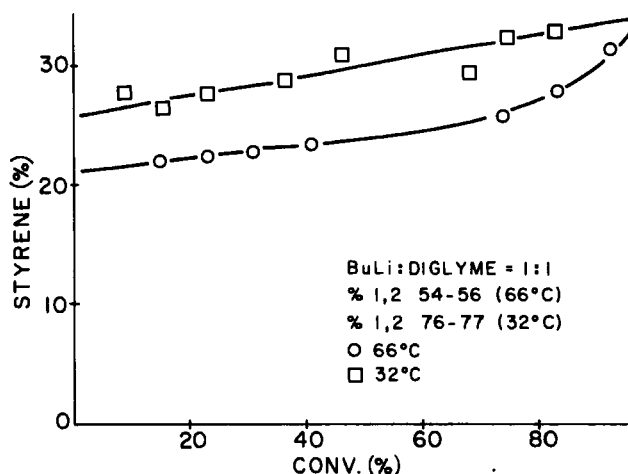
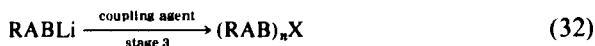
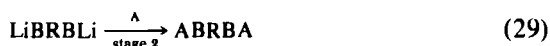


FIG. 10. Styrene uptake in diglyme-modified RLi butadiene-styrene copolymerizations. Reprinted with permission from T. A. Antkowiak, A. E. Oberster, A. F. Halasa, and D. P. Tate, *J. Polym. Sci. Part A-1*, **10**, 1319 (1972).

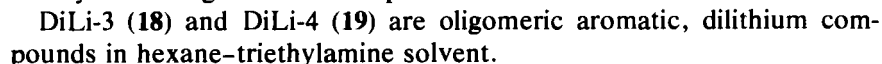
3. The use of a monolithium initiator and a coupling process, Eqs. (30)–(32).

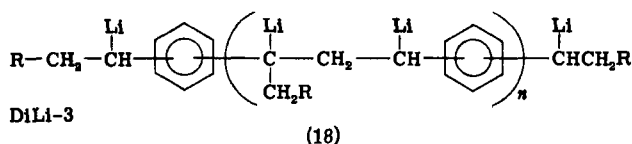


where $n \geq 2$, and X = coupling-agent residue.

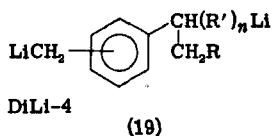
The use of a monolithium initiator and a three-stage sequential copolymerization, Eqs. (25)–(27), is straightforward and requires no further elaboration. However, for success, the dilithium, Eqs. (28) and (29), and coupling, Eqs. (30)–(32), approaches depend upon the proper choice of reagents.

The Lithcoa Co. has commercialized a series of dilithium reagents, DiLi-1 (1A) (17), DiLi-3 (18), and DiLi-4 (19) (86) that also depend upon dimerization or oligomerization of hydrocarbon monomers for increased solubility. These materials have been applied to the synthesis of ABA copolymers. DiLi-1 and DiLi-1A have the following structures (17).





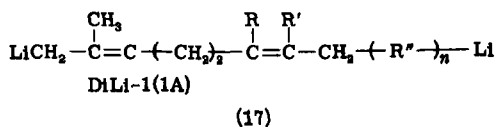
R = *s*-butyl
 $n = 0(\sim 90\%)$; $n = 1(\sim 10\%)$; $n = 2(\text{trace})$



R = *s*-butyl
 $n = 0(\sim 90\%)$; $n = 1(\sim 10\%)$; $n = 2(\text{trace})$

The claimed distribution of mono-, di-, and trilithium compounds in DiLi-3 is 90:10:trace (86). However, other workers (87) have found it to be 22:64:13 by GC/MS analysis; erratic results for this initiator have also been observed by other investigators (88). DiLi-4 is alleged to be more stable in storage than the other DiLi compounds, but confirming tests by independent laboratories are lacking.

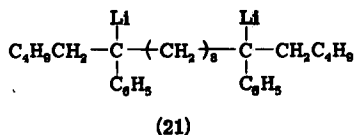
Fetters and co-workers (89, 90) reported a difunctional initiator (20) from lithium and 2,4-hexadiene which, presumably, could be used for the synthesis of ABA copolymers. This initiator is not only oligomeric but also has bulky chain ends for reduced Li association and increased solubility. Although a purely hydrocarbon-soluble initiator was claimed, most of the data were based upon catalysts in benzene-amine solvents. Also, the authors mentioned that this initiator is stable at room temperature, but no detailed aging data were given.



Foss and co-workers (88) reported ABA copolymers obtained from a new dilithium reagent; this organolithium initiator was formed by the addition of *sec*-butyllithium to *m*-diisopropenylbenzene in the presence of a small proportion of triethylamine, followed by reaction with isoprene to improve the hydrocarbon solubility. Unfortunately, the starting ma-

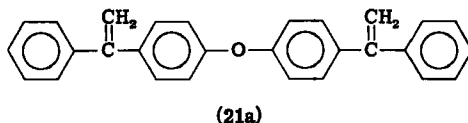
terial, *m*-diisopropenylbenzene, is no longer available in commercial quantities.

Sigwalt and co-workers (91, 92), also, have described a dilithium initiator (21) for use in the preparation of block copolymers. However, a multistep synthesis of this initiator is required.



In addition, compound 21 precipitates from hexane solution after 3 days at room temperature. Oligomerization with isoprene furnishes a more soluble dilithium reagent from which ABA copolymers having good molecular-weight control have been made.

Similarly, Tung and co-workers (92a) reported dilithium anionic initiators based upon double 1,1-diphenylethylene compounds, such as bis-[4-(1-phenylethenyl)phenyl] ether (21a).



Addition of *sec*-BuLi to 21a resulted in a hexane-insoluble dilithium initiator that could be solubilized with 1,3-butadiene, and subsequently used for block-copolymer synthesis. Once again, the starting material for the initiator based upon 21a is available only via special syntheses.

Obviously, the search for the perfect dilithium reagent for use in ABA synthesis has attracted many workers, and yet, no clear (especially commercial) choice has emerged. Further work in this area is to be encouraged.

The synthesis of (AB)_nX block copolymers by the coupling of ABLi, Eqs. (30)–(32), has been accomplished by use of various coupling agents (93). Linear (AB)_nX (*n* = 2) copolymers are formed from reactions involving coupling agents such as bis(chloromethyl) ether, dibromobutane, and α,α' -dichloro-*p*-xylene. Branched or "star" (AB)_nX, *n* > 2, copolymers can be prepared by use of multifunctional joining agents such as silicon tetrachloride, 1,2,4-tris(chloromethyl)benzene, and chloromethylated polystyrene. All of these coupling agents lead to copolymers having a number of branches equal to or less than the functionality of the coupling agent. However, the use of divinylbenzene (DVB) as the joining

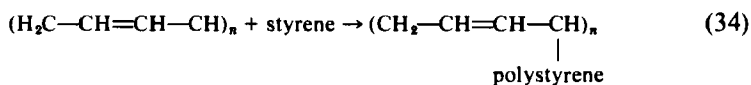
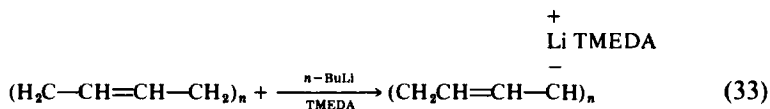
agent can result in star block copolymers having as many as 29 branches, depending upon the RLi:DVB ratio (94).

Anionic metalation and grafting of polymers using alkyllithium compounds has become an important field of activity. The goal of anionic metalation is to generate on the polymer backbone an anion that can be used as a site for further growth of like or unlike monomers. It is only via metalation with alkyllithium compounds that such an operation has become feasible. The discovery (95-97) that chelating diamines enhance the activity of alkyllithium toward abstraction of aromatic, benzylic, and allylic protons, thereby producing the desired anion, has opened up a new area of anionic metalation and grafting.

Several workers have used this approach to metalate hydrocarbon polymers. Plate and co-workers (98), for example, metalated polystyrene and monitored the butane evolution by gas chromatography. They reported a 40% catalyst efficiency. However, they did not report the grafting efficiency or the overall effectiveness of this metalating reagent.

Chalk and co-workers (99, 100), using the same complex, reported the lithiation of poly(2,6-dimethyl-1,4-phenylene) ether and poly(2,6-diphenyl-1,4-phenylene) ether under various metalation conditions. They achieved a catalyst efficiency of only 17%, as determined by the lithium content in the polymers.

Members of a Japanese group (101, 102), using polybutadiene as their base polymer, were able to metalate the allylic position of the polybutadiene chain. The allylic anion was then allowed to react with additional monomer to produce a grafted polybutadiene copolymer, Eqs. (33) and (34).



These workers found that the overall rate of metalation is proportional to the polybutadiene concentration and to the square root of the *n*-butyllithium concentration; the overall activation energy of metalation was 6.6 and 8.4 kcal/mol for polybutadiene and polyisoprene, respectively. They showed that 9%, and as high as 27%, monomer units were metalated.

Independent investigations were conducted on the same substrates (polybutadiene and polyisoprene) in the United States by a group at the Central Research Laboratories of the Firestone Tire & Rubber Company

(103). These workers were interested in preparing useful products (e.g., thermoplastic elastomers) by the use of metalation and grafting. (Thermoplastic elastomers behave like vulcanized materials without the need of sulfur vulcanization.)

Several aspects of the grafting reaction were studied (e.g., grafting efficiency, catalyst efficiency, and catalyst effectiveness). The grafting efficiency was determined by acetone extraction of the ungrafted or homopolystyrene. The grafting efficiency was determined from Eq. (34a).

% Grafted efficiency

$$= \frac{\text{styrene grafted}}{\text{styrene grafted} + \text{homopolystyrene}} \times 100 \quad (34a)$$

On the other hand, catalyst efficiency was defined as the ratio of the calculated \bar{M}_n to the experimental \bar{M}_n [Eq. (34b)]. The calculated \bar{M}_n was determined from the ratio of grams of monomer per mole of metalating agent; the experimental \bar{M}_n was determined by measuring the \bar{M}_n of the styrene block after oxidative degradation of the polybutadiene backbone.

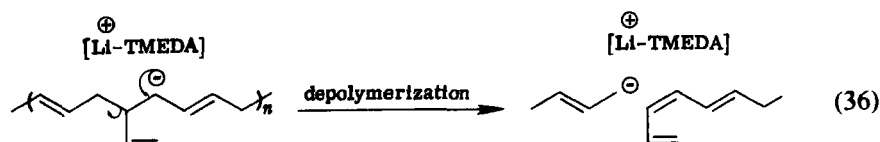
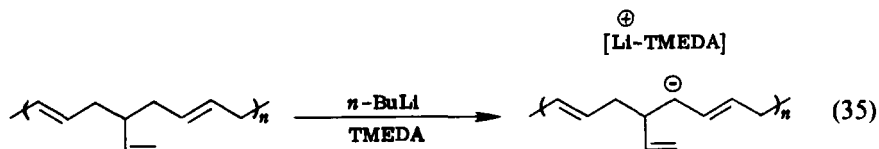
$$\% \text{ Catalyst efficiency} = \frac{M_n \text{ calculated}}{M_n \text{ found}} \times 100 \quad (34b)$$

The overall effectiveness of the method was therefore defined as the product of grafting efficiency and catalyst efficiency. In turn, the structure and properties of the graft copolymer depended directly upon the overall effectiveness of the process.

For example, these workers (103) found that polybutadiene can be successfully metalated by *n*-BuLi-TMEDA, and the product subsequently used to graft styrene monomer to form poly(butadiene-*g*-styrene). This result showed that the grafting-efficiency was 100%. Catalyst efficiency was found to be 75–95%. Thus, the *n*-BuLi-TMEDA metalating and grafting system is particularly effective for polydiene backbones. In fact, Falk and Schlatt (104) showed that poly(butadiene-*g*-styrene) has excellent tensile strength.

Although the use of *n*-BuLi-TMEDA is an effective method for preparing graft copolymers, undesirable side reactions can occur, especially at high temperatures and concentrations of metalating agent (103). For example, a chain depolymerization reaction has been observed during the metalation of polybutadiene with the reagent at 50 and 70°C. This carbon-carbon scission reaction is considered to proceed via the pendant vinyl groups [Eqs. (35) and (36)].

Another method for generating anions on the backbone chain is to have replaceable functional groups that exchange with organolithium

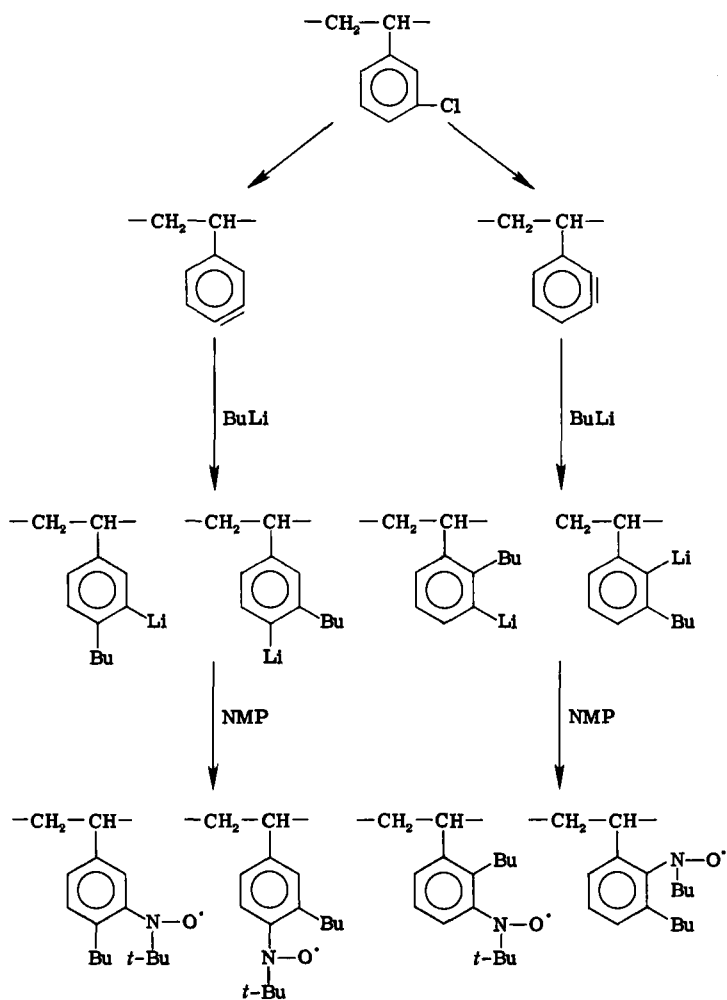


compounds at moderate temperatures without modifying or cross-linking the resulting polymer. Metal-halogen exchange is well known in simple organic compounds (105, 106). The reaction of organolithium compounds with halogenated polyethylene has been disclosed (107), but the reaction products were not well characterized.

Excellent substrates for metal-halogen exchange grafting were found to be copolymers of butadiene and *o*- or *p*-chlorostyrenes (108). When *n*-BuLi-TMEDA was used as the catalyst, no homopolystyrene was found by acetone extraction of the graft polymer, which suggested that the catalyst efficiency (exchange efficiency) was very high. However, when triethylamine was used instead of TMEDA, analysis of the grafted copolymer showed 90% homopolystyrene.

The work of Cameron and co-workers (109, 110) confirmed the position of the lithium in such exchange reactions. These workers studied the metal-halogen exchange of chloro- and bromostyrene copolymers with *n*-BuLi-TMEDA and identified the lithiated sites with 2-methyl-2-nitrosopropane. The samples were studied by ESR, and the signal obtained from the nitroxide-labeled polymer suggested that *n*-BuLi-TMEDA exchanges with bromostyrene via direct metal-halogen exchange whereas reactions of chlorostyrene produce *n*-alkyllithiated styrenes. The results of Cameron and co-workers are consistent with the involvement of benzyne intermediates, shown here for the chlorostyrene case.

These findings suggest that a well defined graft copolymer can be prepared from the lithium-halogen exchange. Also, the use of nitroso labeling has been demonstrated to be a powerful tool for characterizing anionic graft copolymers. In the same work, Cameron *et al.* showed that the ease of lithium-halogen exchange is in the sequence $\text{Cl} < \text{Br} < \text{I}$.



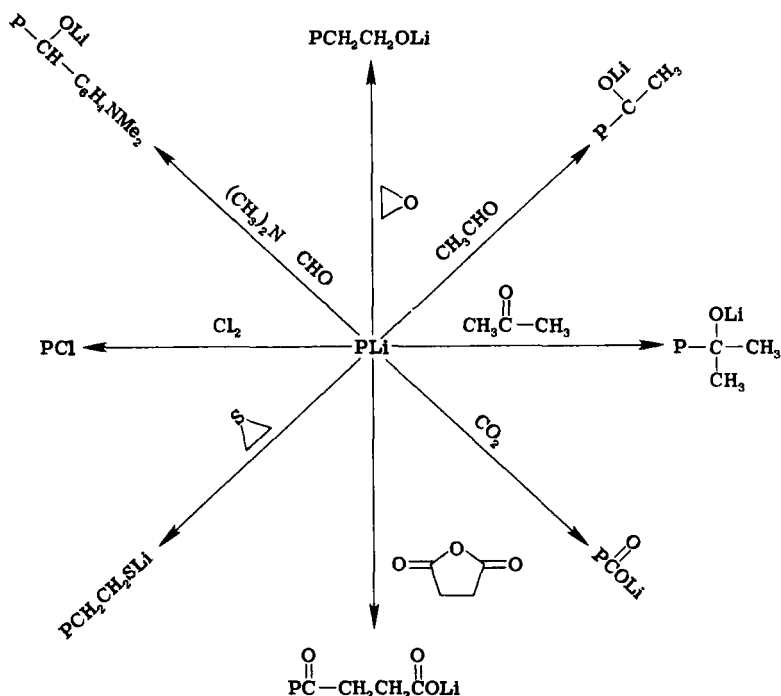
VI

USE OF RLi TO PREPARE TERMINALLY FUNCTIONAL DIENE (OLEFIN) POLYMERS

The utility of functionally terminated ("telechelic") polymers, particularly difunctional materials, rests with the ability of such materials to be chain-extended to afford a high molecular weight and useful physical properties. In general, there are two organolithium-based methods for

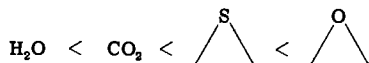
introducing terminal functionality into diene and olefin polymers. One way is to terminate living lithium polymers with appropriate electrophilic reagents; the other is to polymerize dienes or olefins with functionally substituted initiators.

Reaction of live polymers with protic agents (e.g., H_2O , ROH , and RNH_2) results in simple protonation of the live ends and cessation of formation of the kinetic polymer chain. On the other hand, reaction of live polymers with some electrophiles can produce end-group substitution, as well as chain termination, as shown.



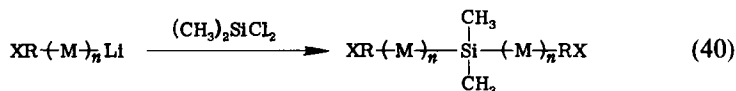
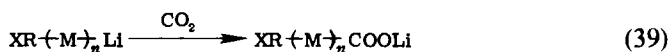
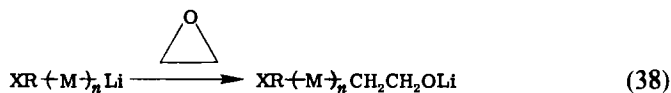
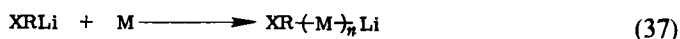
For example, polymers having hydroxyl end groups can be prepared by reaction of polymer lithium with epoxides, aldehydes, and ketones (111-113). Carboxylated polymers result when living polymers are treated with carbon dioxide (111) or anhydrides (114). When sulfur (115, 116), cyclic sulfides (117), or disulfides (118) are added to lithium macromolecules, thiol-substituted polymers are produced. Chlorine-terminus polymers have reportedly been prepared from polymer lithium and chlorine (119). Although lithium polymers react with primary and secondary amines to produce unsubstituted polymers (120), tertiary amines can be introduced by use of *p*-(dimethylamino)benzaldehyde (121).

One drawback to the treatment of dilithium polymers with certain electrophilic agents is the formation of an intractable anionic association or gel. The degree of association is related to the charge density of the electrophile and increases in the following order:



Of course, the practical result of gel formation is an inability to mix the reagents (111, 117, 121a). However, it has been reported that this tendency to form a gel can be greatly reduced by use of solvents having a solubility parameter of ≤ 7.2 (121b).

Functional organolithium reagents have only recently been employed to prepare functionally terminal, polydienes and polyolefins. Of course, the functional groups must be stable to, or protected from, organolithium reagents. Hydroxyl and amino groups have been introduced directly or indirectly in this manner. It is possible to prepare polymers having the same or different end groups by use of functional organolithium initiators [Eqs. (37)–(40), where X = functional group, R = alkyl or aryl group, M = monomer, and (M)_n = polymer].



An example of a functional organolithium initiator is *p*-lithiophenoxide. It acts both as a carrier of hydroxyl functionality and as an initiator for polymerization (122). Unfortunately, *p*-lithiophenoxide has a low solubility, even in such polar solvents as THF, and up to 30% of the initiator is initially inactive toward polymerization. It is difficult to control polymer molecular weights when such initiators are used (123). Trepka (124) improved the solubility of *p*-lithiophenoxide by the introduction of alkyl

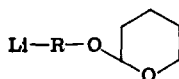
substituents on the ring. However, only moderate yields of the alkylated initiator were reported. Fletcher and Hirshfield (123) described a similar catalyst, $\text{Bu}_4\text{NOC}_6\text{H}_4\text{Li}$, which is soluble in THF. However, no yields for its preparation were given.

Uraneck and Smith [125] reported that the product of 2,4-pentadien-1-ol and *sec*-butyllithium [Eq. (41)] can be used to prepare polymers with terminal hydroxyl groups.

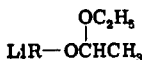


Unfortunately, some of the *sec*-butyllithium (~13%) remains unreacted.

To circumvent the problems of low reactivity, low solubility, and/or low yield associated with the previously mentioned hydroxyl functional initiators, Schulz and co-workers (126) built protected-hydroxyl functionality into organolithium molecules. Specifically, alkyl lithium initiators containing hydroxyl-protecting groups [mixed acetal, e.g., tetrahydropyranyl (22) and α -ethanoxyethyl ether (23)] have been prepared.



(22)



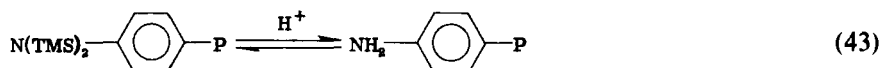
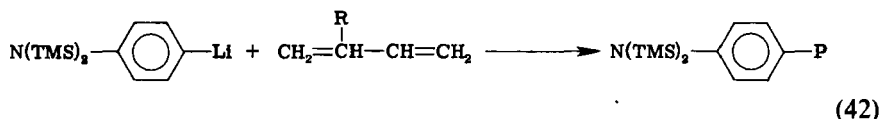
(23)

The mixed-acetal groups are stable both to organolithium reagents and living lithium polymers. Such initiators are preparable in high yield and are soluble in diethyl ether or benzene but insoluble in hexane (126, 127). Hydrolysis procedures have been developed for the removal of these protecting groups (the regeneration of hydroxyl functionality) without concomitant cross-linking of polydiene backbones. Dilute solution hydrolysis is preferred over bulk methods (127a). Hydroxyl polymers prepared via the intermediacy of lithiumalkyl acetal initiators have shown a high degree of functional purity. Furthermore, dihydroxyl-terminated polymers can be prepared gel (association)-free by this method (126). This synthetic method has now been successfully extended to the preparation of telechelic polysiloxanes (127).

Similarly, 3-(dimethylamino)propyllithium has been used by Eisenbach and co-workers (128, 129) to prepare tertiary amine-terminated poly(α -methylstyrene) polymers. However, primary amine-ended polymers have tended to elude synthesis by organolithium methods because primary amine hydrogens "kill" living lithio macromolecules (120).

To avoid this difficulty, Schulz and Halasa (130) found that the primary amine group can be protected from organolithium reagents and lithium polymers by use of the *N,N*-bis(trimethylsilyl)amino, $-\text{N}(\text{TMS})_2$, protecting group. In turn, the $-\text{N}(\text{TMS})_2$ -substituted polymers can be con-

verted to primary amine polymers by simple hydrolysis [Eqs. (42) and (43), where $R = H, CH_3$; $P =$ polydiene polymer]. Furthermore, such preparative procedures are gel (association)-free.



VII

UNSOLVED PROBLEMS/FUTURE TRENDS

Throughout the course of this review, various needs and unsolved problems in the area of organolithium catalysis of olefin and diene polymerization have been identified. The following research objectives merit further investigation by organometallic and/or polymer chemists.

- (1) Use of 7Li -NMR to study the "live" lithium chain ends.
- (2) Use of 6Li - with ^{13}C -NMR to examine the bonding of chain ends.
- (3) Use of tagged ^{13}C monomers to study π - σ perturbations. Will this provide a means of measuring the elusive complex of butadiene with lithium chain ends in the copolymerization of butadiene and styrene in hydrocarbons?
- (4) Determination of the thermodynamics of the interaction of organolithium compounds with polar ligands.
- (5) Examination of polymers prepared in polar media for tacticity. Can tacticity be controlled?
- (6) Synthesis of hydrocarbon-soluble, solely difunctional dilithio reagents for use in preparing ABA copolymers.

REFERENCES

1. F. E. Matthews and E. H. Strange, British Patent 24,790 (1910).
2. C. H. Harries, *Ann.* **383**, 157 (1911).
3. C. H. Harries, U.S. Patent 1,058,056 (April 8, 1913).
4. K. Ziegler, F. Dersch, and H. Wollthan, *Ann.* **511**, 13 (1934).
5. K. Ziegler and L. Jakob, *Ann.* **511**, 45 (1934).
6. K. Ziegler, *Angew. Chem.* **49**, 499 (1936).
7. C. F. Ruebensaal, "The Rubber Industry Statistical Report." International Institute of Synthetic Rubber Producers, Inc., New York, 1977.
8. A. W. Langer, Jr., *Trans. N.Y. Acad. Sci.* **27**, 741 (1965).
9. A. W. Langer, Jr., *Polym. Prepr. Am. Chem. Soc.* **7**, 132 (1966).

10. A. W. Langer, Jr., in "Polyamine Chelated Alkali Metal Compounds" (A. W. Langer, Jr., ed.), *Adv. Chem. Ser.*, **130**, Chapter 1. Am. Chem. Soc., Washington, D.C., 1974.
11. W. E. Hanford, J. R. Poland, and H. S. Young, U.S. Patent 2,377,779 (1945).
12. G. G. Eberhardt and W. A. Butte, *J. Org. Chem.* **29**, 2928 (1964).
13. G. G. Eberhardt and W. R. Davis, *J. Polym. Sci., Part A* **3**, 3753 (1965).
14. C. W. Kamienski, Ref. 10, Chapter 7.
15. W. N. Smith, Jr., U.S. Patent 3,579,492 (1971).
16. W. Bunting and A. W. Langer, Jr., Ref. 10, Chapter 10.
17. A. C. Angood, S. A. Hurley, and P. J. T. Tait, *J. Polym. Sci., Part A-1*, **11**, 2777 (1973).
18. A. C. Angood, S. A. Hurley, and P. J. T. Tait, *J. Polym. Sci., Part A-1*, **13**, 2437 (1975).
19. S. A. Hurley and P. J. T. Tait, *J. Polym. Sci., Part A-1*, **14**, 1565 (1976).
20. J. N. Hay, J. F. McCabe, and J. C. Robb, *J. Chem. Soc. Faraday Trans. 1* p. 1227 (1972).
21. J. N. Hay, D. S. Harris, and M. Wiles, *Polymer* **17**, 613 (1976).
22. F. Rodriguez, M. Abadie, and F. Shué, *Eur. Polym. J.* **12**, 17 (1976).
23. A. Kh. Bagadasaryan, V. M. Frolov, E. I. Tinyakove, and A. B. Dolgoplosk, *Proc. Acad. Sci. USSR* **162**, 582 (1965).
24. A. Sione, P. Sigwalt, and M. Fontanille, *Polymer*, **16**, 605 (1975).
25. F. R. Rembaum, F. R. Ellis, R. C. Morrow, and A. V. Tobolsky, *J. Polym. Sci.*, **61**, 155 (1962).
26. F. C. Foster and J. L. Binder, in "Handling and Uses of the Alkali Metals" (M. Sittig, ed.) *Adv. Chem. Ser.* **19**, Chapter 26. Am. Chem. Soc., Washington, D.C., 1957.
27. C. A. Uraneck, *J. Polym. Sci., Part A-1*, **9**, 2273 (1971).
28. T. A. Antkowiak, A. E. Oberster, A. F. Halasa, and D. P. Tate, *J. Polym. Sci., Part A-1*, **10**, 1319 (1972).
- 28a. S. Dumas, V. Marti, J. Sledz, and F. Shué, *J. Polym. Sci. Polym. Lett. Ed.* **16**, 81 (1978).
29. A. W. Langer, Jr., paper presented at the First Akron Summit Polymer Conference, Akron, Ohio, June 18-19 (1970).
30. J. N. Hay, J. F. McCabe, and J. C. Robb, *J. Chem. Soc. Faraday Trans. 1*, **68**, 1 (1972).
31. A. F. Halasa, V. D. Mochel, and D. W. Carlson, unpublished results.
32. W. H. Glaze, J. E. Hanicak, M. L. Moore, and J. Chandhuri, *J. Organomet. Chem.* **44**, 39 (1972).
33. M. Morton and L. J. Fetters, in "The Stereo Rubbers" (W. M. Saltman, ed.), Chapter 5. Wiley, New York, 1977.
34. L. E. Forman, in "Polymer Chemistry of Synthetic Elastomers, Part II" (J. P. Kennedy and E. G. M. Tornquist, eds.), Chapter 6. Wiley (Interscience), New York, 1969.
35. F. W. Stavely, paper presented before Rubber Div. Am. Chem. Soc., Philadelphia, Pa., November, 1955.
36. F. W. Stavely, *Ind. Eng. Chem.* **48**, 778 (1956).
37. E. G. M. Tornquist, in "Polymer Chemistry of Synthetic Elastomers, Part I" (J. P. Kennedy and E. G. M. Tornquist, eds.), Chapter 2. Wiley (Interscience), New York, 1968.
38. R. S. Stearns and L. E. Forman, *J. Polym. Sci.* **41**, 381 (1959).
39. H. Hsieh, *J. Polym. Sci., Part A*, **3**, 153, 163, 173 (1965).

40. S. Bywater, A. F. Johnson, and D. J. Worsfold, *Can. J. Chem.* **42**, 1255 (1964).
41. M. Morton, E. E. Bostick, and R. Livigni, *Rubber Plast. Age* **42**, 397 (1961).
42. M. Morton and L. J. Fetters, *J. Polym. Sci., Part A*, **2**, 3311 (1964).
43. M. Morton and R. A. Pett, *Polym. Prepr. Am. Chem. Soc. Div. Polym. Chem.* **7**, 151 (1966).
44. T. L. Brown, R. L. Gerteis, D. A. Bafus, and J. A. Ladd, *J. Am. Chem. Soc.* **86**, 2135 (1964).
45. T. L. Brown, J. A. Ladd, and G. N. Newman, *J. Organomet. Chem.* **3**, 1 (1965).
46. D. Margerison and J. P. Newport, *Trans. Faraday Soc.* **59**, 2058 (1963).
47. M. Weiner, C. Vogel, and R. West, *Inorg. Chem.* **1**, 654 (1962).
48. R. H. Baney and R. J. Krager, *Inorg. Chem.* **3**, 1657 (1964).
49. G. E. Hartwell and T. L. Brown, *Inorg. Chem.* **3**, 1656 (1964).
50. V. N. Sgonnik, K. K. Kalninsch, E. Y. Shadrina, N. V. Smirnova, and N. I. Nikolaev, *Vysokomol. Soedin. Ser. A* **16**, 1867 (1974).
51. Kh. B. Tsvetanov, V. N. Sgonnik, B. L. Yerusalimskii, I. M. Panaiotov, and N. I. Nikolaev, *Vysokomol. Soedin. Ser. A* **15**, 2116 (1973).
52. V. N. Sgonnik, K. K. Kalninsch, K. B. Tsvetanov, and N. I. Nikolaev, *Vysokomol. Soedin. Ser. A* **15**, 900 (1975).
53. K. K. Kalninsch, V. N. Sgonnik, N. I. Nikolaev, and I. L. Artamonova, *Vysokomol. Soedin. Ser. A* **13**, 2121 (1971).
54. V. N. Sgonnik, E. Y. Schadrina, K. K. Kalninsch, and B. Erussalimsky, *Makromol. Chem.* **174**, 81 (1973).
55. S. Bywater, *Adv. Polym. Sci.* **4**, 66 (1965).
- 55a. H. Sinn and O. T. Onsager, *Makromol. Chem.* **55**, 167 (1962).
56. M. Morton, L. J. Fetters, and E. E. Bostick, *J. Polym. Sci. C1*, 311 (1963).
57. M. Morton and L. J. Fetters, *J. Polym. Sci., Part A*, **2**, 3311 (1964).
58. S. Bywater, D. J. Worsfold, and G. Hollingsworth, *Macromolecules* **5**, 389 (1972).
59. M. Morton, R. D. Sanderson, and R. Sakata, *Macromolecules* **6**, 181 (1973).
60. M. Morton, R. D. Sanderson, R. Sakata, and L. A. Falvo, *Macromolecules* **6**, 186 (1973).
61. M. Morton and L. A. Falvo, *Macromolecules* **6**, 190 (1973).
62. H. S. Makowski and M. Lynn, *J. Macromol. Chem.* **1**, 443 (1966).
63. S. Brownstein, S. Bywater, and D. J. Worsfold, *Macromolecules* **6**, 715 (1973).
64. J. P. Oliver, J. B. Smart, and M. T. Emerson, *J. Am. Chem. Soc.* **88**, 4101 (1966).
65. J. P. Smart, R. Hogan, P. A. Scherr, M. T. Emerson, and J. P. Oliver, *J. Organomet. Chem.* **64**, 1 (1974).
66. H. Yuki and Y. Okamoto, *J. Polym. Sci., Part A-1* **9**, 1247 (1971).
67. A. A. Korotkov, *Angew. Chem.* **70**, 85 (1958).
68. M. Morton, in "Elastomer Stereospecific Polymerization" (B. L. Johnson and M. Goodman, eds.), *Adv. Chem. Ser.* **52**, Chapter 1, Am. Chem. Soc., Washington, D. C., 1966.
69. M. Morton, R. D. Sanderson, and R. Sakata, *J. Polym. Sci., Part B-9* **61** (1971).
70. A. F. Johnson and D. J. Worsfold, *Makromol. Chem.* **85**, 273 (1965).
71. K. F. O'Driscoll and I. Kuntz, *J. Polym. Sci.* **61**, 19 (1962).
72. M. Morton, in "Copolymerization" (G. Ham, ed.), High Polymer Series, Vol. XVIII, p. 421. Wiley (Interscience), New York, 1964.
73. A. A. Korotkov, *Int. Symp. Macromol. Chem., Prague*, Sept. 1957, Paper No. 66.
74. M. Morton and F. R. Ells, *J. Polym. Sci.* **61**, 25 (1962).
75. A. F. Johnson and D. J. Worsfold, *Makromol. Chem.* **85**, 273 (1965).

76. H. L. Hsieh and W. H. Glaze, *Rubber Chem. Technol.* **43**, 22 (1970).
77. British Patent 994,726 (June 10, 1965).
78. British Patent 903,331 (August 15, 1962).
- 78a. T. C. Bouton and S. Futamura, *Rubber Age N.Y.* **106** (3), 33 (1974).
79. C. F. Wofford, U.S. Patent 3,294,768 (Dec. 27, 1966).
80. A. Noshay and J. E. McGrath, "Block Copolymers—Overview and Critical Survey," Chapter 6. Academic Press, New York, 1973.
81. K. C. Eberly, U.S. Patent 2,947,793 (August 2, 1960).
82. R. P. Zelinski and C. W. Strobel, U.S. Patent 3,108,994 (1963).
83. R. P. Zelinski and H. L. Hsieh, U.S. Patent 3,078,254 (1963).
84. L. J. Fetters and M. Morton, *Macromolecules* **2**, 453 (1969).
85. G. Karoly, *Polym. Prepr. Am. Chem. Soc. Div. Polym. Chem.* **10**, 837 (1969).
86. Lithium Corporation of American, Product Bulletins, Nos. 190–194.
87. G. Jalics, paper presented at the 7th Akron Chemists—Chemical Engineers—Technical Affiliate Symposium, Akron, Ohio, October 20, 1977.
88. R. P. Foss, H. W. Jacobson, and W. H. Sharkey, *Macromolecules* **10**, 287 (1977).
89. L. J. Fetters, U.S. Patent 3,848,008 (Nov. 12, 1974).
90. M. Morton, L. J. Fetters, J. Inomata, D. C. Rubio, and R. N. Young, *Rubber Chem. Technol.* **49**, 303 (1976).
91. P. Sigwalt, P. Guyot, M. Fontaville, and J. P. Vaison, Ger. Offen. 2,623,344 (Dec. 16, 1976).
92. P. Sigwalt and M. Fontaville, French Patent 75 17,716 (Appl. 6/675).
- 92a. L. H. Tung, G. Y. S. Lo, and D. E. Beyer, *Macromolecules* **11**, 616 (1978).
93. L. J. Fetters, *J. Polym. Sci., Part C* **26**, 1 (1969).
94. L. K. Bi and L. J. Fetters, *Macromolecules* **9**, 732 (1976).
95. M. D. Rausch, and D. J. Ciappenelli, *J. Organomet. Chem.* **10**, 127 (1967).
96. A. F. Halasa and D. P. Tate, *J. Organomet. Chem.* **24**, 769 (1970).
97. A. F. Halasa, *J. Organomet. Chem.* **31**, 369 (1971).
98. N. A. Plate, M. A. Jampolskaya, S. L. Davydova, and V. A. Kargin, *J. Polym. Sci., Part C* **22**, 547 (1969).
99. A. S. Hay and A. J. Chalk, French Patent 1,586,729 (1967); U.S. Patent 3,402,144 (1968).
100. A. J. Chalk and I. J. Hoogeboom, *J. Polym. Sci., Part A-1* **9**, 3679 (1971).
101. Y. Minoura, K. Shina, and H. Harada, *J. Polym. Sci., Part A-1* **6**, 559 (1969).
102. Y. Minoura and H. Harada, *J. Polym. Sci., Part A-1* **7**, 3 (1969).
103. D. P. Tate, A. F. Halasa, F. J. Webb, R. W. Koch, and A. E. Oberster, *J. Polym. Sci., Part A-1* **9**, 139 (1971).
104. J. C. Falk and R. J. Schlott, *J. Macromol. Chem. A-7* **8**, 1663 (1973).
105. F. C. Leavitt, U.S. Patent 3,234,193 (1966).
106. E. Husemann, German Patent 1,226,304 (1966).
107. N. A. Plate, S. L. Davydova, M. A. Jampolskaya, M. A. Muktridina, and V. A. Kargin, *Vysokomol. Soedin.* **8**, 1562 (1966).
108. A. F. Halasa, H. E. Adams, and C. J. Hunter, *J. Polym. Sci., Part A-1* **9**, 677 (1971).
109. T. A. Bulloch, G. G. Cameron, and M. J. Elsom, *Polymer* **18**, 930 (1977).
110. T. A. Bulloch, G. G. Cameron, and M. J. Elsom, *Eur. Polym. J.* **13**, 751 (1977).
111. H. Brody, D. H. Richards, and M. Swarc, *Chem. Ind. (London)* p. 1473 (1958).
112. E. J. Goldberg, U.S. Patent 3,055,953 (Sept. 25, 1962).
113. B. F. Goodrich Co., British Patent 964,259 (July 22, 1964).
114. P. Rempp and M. H. Loucheux, *Bull. Soc. Chim. Fr.* 1497 (1958).

115. C. A. Uraneck, J. N. Short, and R. P. Zelinski, U.S. Patent 3,135,716 (June 2, 1964).
116. C. A. Uraneck, J. N. Short, R. P. Zelinski, and H. L. Hsieh (assigned to Phillips), West Germany Patent 1,169,674 (May 6, 1964).
117. D. H. Richards, *J. Polym. Sci. Polym. Lett.* **6**, 417 (1968).
118. J. W. Cleary, U.S. Patent 3,048,568 (Aug. 7, 1962).
119. Phillips Petroleum Co., British Patent 906,315 (Sept. 19, 1962).
120. D. M. French, *Rubber Chem. Technol.* **42**, 90 (1969).
121. R. P. Zelinski, H. L. Hsieh, and C. W. Strobel, U.S. Patent 3,109,871 (Nov. 5, 1963).
- 121a. S. F. Reed, Jr., *J. Polym. Sci., Part A-1* **10**, 1187 (1972).
- 121b. K. Komatsu, A. Nishioka, N. Ohshima, M. Takahashi, and H. Hara, U.S. Patent 4,083,834 (April 11, 1978).
122. S. M. Hirshfield, *NASA Tech. Brief*, 71-10184 (1971); *NASA Tech. Rep.* NPO-10998, 10999 (1967).
123. J. C. Fletcher and S. M. Hirshfield, U.S. Patent 3,755,283 (August 28, 1973).
124. W. J. Trepka, U.S. Patent 3,439,049 (April 15, 1969).
125. C. A. Uraneck and R. L. Smith, U.S. Patent 3,993,854 (November 23, 1976).
126. D. N. Schulz, A. F. Halasa, and A. E. Oberster, *J. Polym. Sci. Part A-1*, **12**, 153 (1974).
127. P. M. Lefebvre, R. Jerome, and P. Teyssie, *Macromolecules* **10**, 871 (1977).
- 127a. D. N. Schulz and J. N. Anderson, U.S. Patent 3,954,885 (May 4, 1976).
128. C. D. Eisenbach, H. Schnecko, and W. Kern, *Eur. Polym. J.* **11**, 699 (1975).
129. C. D. Eisenbach, H. Schnecko, and W. Kern, *Makromol. Chem.* **176**, 1587 (1975).
130. D. N. Schulz and A. F. Halasa, *J. Polym. Sci. Part A-1*, **15**, 2401 (1977).

This Page Intentionally Left Blank

Ziegler-Natta Catalysis

HANSJÖRG SINN and WALTER KAMINSKY

Institut für Anorganische und Angewandte Chemie

University of Hamburg

Hamburg, Federal Republic of Germany

I. Scope of Ziegler Catalysis	99
A. Introduction	99
B. Second-Generation Ziegler Catalysts	102
II. Process Operation	105
III. Stereoselectivity, Kinetics, and Mechanism	108
A. Stereoregulation	108
B. Origin of Activity	114
IV. Tailoring Heterogeneous Catalysts	118
V. Homogeneous Ziegler-Natta Catalysts	123
A. Soluble Systems	123
B. The Titanium System	124
C. Complexation and Alkylation of the Transition Metal	126
D. Nature of the Active Center	128
E. Vanadium, Chromium, and Other Transition-Metal Systems	129
VI. Side Reactions in Homogeneous Catalysts	131
A. Types of Side Reaction	131
B. The Zirconium System	132
C. The Titanium System	135
VII. Influence of Water on Homogeneous Catalysts	137
A. Increase of Activity	137
B. Titanium-Aluminoxane Catalysts	140
References	143

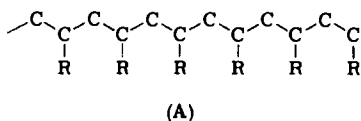
I

SCOPE OF ZIEGLER CATALYSIS

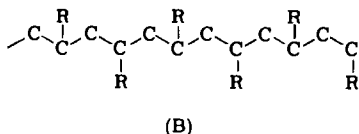
A. Introduction

Ziegler catalysis involves rapid polymerization of ethylene and α -olefins with the aid of catalysts based on transition-element compounds, normally formed by reaction of a transition-element halide or alkoxide or alkyl or aryl derivative with a main-group element alkyl or alkyl halide (1,2). Catalysts of this type operate at low pressures (up to 30 atm), but often at 8–10 atm, and, in special cases, even under reduced pressure, and at temperatures up to 120°C, but often as low as 20–50°C. Approximately 2,200,000 tons of polyethylene and 2,900,000 tons of polypropylene are produced per year with the aid of such catalysts. The polyeth-

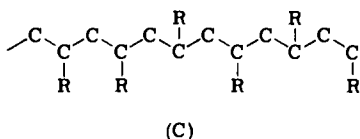
Using such α -olefins as monomers, Natta (4,5) found that most of the product had a stereoregular structure. Thus, under conditions easy to realize, isotactic structures (A)



and syndiotactic structures (B)



are preferred to the statistical atactic structure (C).



The differences between the different forms of polypropylene produced (assuming equal molecular-weight distribution, equal percentage of branching, etc.) are remarkable (Table II).

Using diolefins and carefully selected Ziegler-type catalysts, it has been possible to obtain the 1,4-*cis*-, the 1,4-*trans*-, and the 1,2-polybutadienes more than 98% pure. In the case of polyisoprene, the 3,4-structure is produced. There are thousands of patents involving every combination of pure or mixed main-group alkyls with transition-element compounds, each claiming advantages. However, compositions containing titanium, vanadium, chromium, and, in special cases, molybdenum, cobalt, rhodium, and nickel are primarily used.

Most Ziegler catalyst systems are heterogeneous, but some homogeneous systems are known, and it is not clear at present that stereoregulation and stereoselectivity are the results of heterogeneity.

TABLE I
COMPARISON OF DIFFERENT TYPES OF POLYETHYLENE (3)^a

Polymer type	High pressure		Ziegler	
	HP-HD ^b		Polymethylene	
			Phillips	
Density (g/cm ³)	0.91	0.93	0.95	0.97
Crystallinity (%) at 20°C	65	75	85	95
Optical melting point (°C)	105	120	125	135
Flexural stress at a given strain (kP/cm ²)	~85	~100-140	~300-370	~325-350
Tensile strength (kP/cm ²)	140	200-250	200-450	280-430
Notched impact strength (kP cm/cm ²)	10	5	4	3
Shore hardness	40-45	45-60	~65	~68
CH ₃ groups per 1000 C atoms	20		1-3	1.5

^a Values in the table refer to products having comparable melt index of 0.4-2.0 (ASTM-D 1238-52 T).

^b HP-HD, high-pressure-high-density.

A two-step mechanism for catalysis is widely accepted; (1) adsorption of the monomer, which may be activated, with the configuration established in this step, and (2) insertion of the activated monomer into a metal-carbon bond. This sequence places Ziegler-type polymerization in the context of what Nature accomplishes with enzymes.

Several articles have been published that give detailed information on the subject of this review, covering the literature up to 1975-1979. These include books by Pracejus (6) and Boor (6a) and a chapter by Caunt (7), together with an account of the kinetics of Ziegler-Natta polymerization by Keii (8). In addition, a memorial volume (9) to Ziegler, edited by Chien, summarizes contributions to most fields of study on coordination polymerization. The following areas are reviewed in reference (9); (i)

TABLE II
SOME CHARACTERISTICS OF POLYPROPYLENE

Characteristic	Polypropylene		
	Isotactic	Syndiotactic	Atactic
Melting point (°C)	165-171	125-131	<0
Crystallinity (%)	55-65	50-75	0
Tensile strength (kP/cm ²)	320-350		

considerations concerning stereoregular propylene polymerization (10); (ii) stereoselection and stereoelection in α -olefin polymerization (11); (iii) the number of active sites for the polymerization of ethylene, propylene, and 1-butene by Ziegler-Natta catalysts (12); (iv) the number of propagation centers on solid catalysts for olefin polymerization, and some aspects of the mechanism of their action (13); (v) ethylene polymerization with catalysts of one- or two-component systems based on titanium trichloride complexes (14); (vi) a kinetic model for heterogeneous Ziegler-Natta polymerization (15); (vii) homogeneous complex catalysts for olefin polymerization (16); (viii) transition-metal alkyl polymerization catalysts (17); (ix) a kinetic approach to elucidation of the mechanism of Ziegler-Natta polymerization (18); (x) chain transfer in Ziegler polymerization of ethylene (19); (xi) supported Ziegler-Natta catalysts (20); and (xii) stereospecific polymerization of diolefins by η^3 -allylic coordination complexes (21).

When Ziegler catalysis was first discovered, it was fascinating to see ethylene, a monomer normally difficult to activate, being polymerized under atmospheric pressure at room temperature in a Weck-glass vessel containing gasoline as the solvent, with small amounts of TiCl_4 and $\text{Al}_2\text{Et}_3\text{Cl}_3$, the latter components forming the colloidal suspended catalyst (1,11). However, in practice it was difficult to fabricate the resulting polymer for practical use. In technical processes it is necessary to deactivate the catalyst after polymerization, remove the diluent, and then remove the residues of catalyst with HCl and alcohols. After this treatment, washing the polyethylene with water and drying with steam were necessary. Other complications involved purification of the recovered diluent, feedback of the monomer after a repurification step, and, finally, the necessity of adjusting the molecular weight by oxidative or thermal processes (3). The cost of these steps diminished the advantage of the "low-pressure" polymerization process. One of the main tasks of polyolefin research, therefore, was to develop new catalysts which produce so much polyolefin that the amount of catalyst residue in the final product is below a certain limit and thus does not influence the physical properties of the polymer, thereby avoiding additional removal steps.

B. Second-Generation Ziegler Catalysts

The result of the early work led to development of "second-generation" Ziegler catalysts (23-29). These are discussed in the next section and include (i) nonsupported trivalent titanium compounds, (ii) products of treating magnesium compounds with titanium compounds, and (iii)

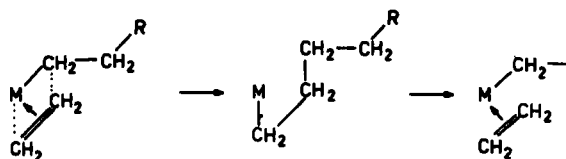
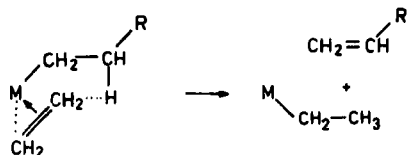
catalysts based on chromium compounds. Thus, later work brought about a remarkable simplification of polymerization and workup processes (see Table III).

Polymers produced with unmodified Ziegler catalysts showed extremely high molecular weight and broad distribution (30), and in some cases there was evidence for "living polymer" (31). In fact, there is no reason for any termination step, except for (i) consecutive reactions which destroy the catalyst; (ii) termination via hydrogenation of the metal-carbon bond, thereby forming saturated polymer and metal hydride; (iii) termination of a growing molecule by β -elimination step, forming a polymer with an olefinic end-group and a metal hydride; and (iv) termination of a growing molecule by the "Verdrngungsreaktion," the monomer forming a polymer having an olefinic end-group and a metal alkyl.

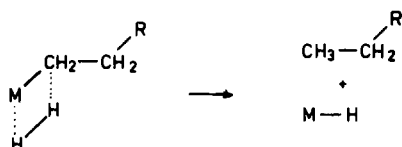
Scheme 1 shows simplified chain propagation and chain-termination steps. Hydrogenation terminates the chains, forming saturated polymers and hydride, the latter adding olefin to reactivate the catalyst centers. As a consequence, the molecular weight of the polymers is decreased.

TABLE III
COMPARISON OF OLD AND NEW ZIEGLER POLYETHYLENE

Conventional process	Second-generation process
Polymerization	Polymerization
Density	Density
Molecular weight (limited influence)	Molecular weight
Molecular-weight distribution (limited influence)	Molecular-weight distribution
Workup	Workup
Catalyst deactivation	Removal and feedback of diluent
Removal of diluent	Drying of polymer
Drying of catalyst residue	
Purification and new drying of diluent	
Waste-water treatment	
Finishing	Finishing
Thermal degradation of molecular weight	
Molecular-weight distribution by blending	
Stabilization	Stabilization

Chain PropagationChain Termination(a) by β -elimination with H-transfer to monomer

(b) by hydrogenation

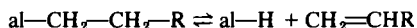
(c) by β -elimination forming hydride

SCHEME 1. Mechanism of ethylene polymerization (M = transition metal).

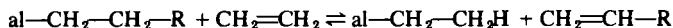
There are difficulties with monomer feedback when the hydrogen pressure is high compared with the partial pressure of ethylene. It is reported that a Phillips Petroleum Company catalyst which operates at ~ 50 atm and 150 – 180°C (27,32) is not influenced by hydrogen in a manner which decreases the molecular weight of the product.

Decrease in molecular weight is also a consequence of labilization of the metal-organic bond brought about by certain ligands and by the nature of the alkyl group (al). Ziegler's early investigations showed that there is an equilibrium which leads to polymers having a vinyl end-group.

The resulting hydride reacts in the same manner as the hydride formed by hydrogenation.



There is evidence of a parallel mechanism which forms polymers with vinyl end-groups without hydride as an intermediate via β -hydrogen abstraction.



This is the "Verdrängungsreaktion" with the monomer, and it is catalyzed by the Ziegler catalyst or its consecutive products. Using aluminum alkyls and ^{14}C -labeled ethylene, under conditions not causing any insertion or hydride formation and in the presence of a "dead" catalyst, an equilibrium distribution of labeled ethylene between the gas phase and the alkyl is reached (33). It has been possible in certain cases to use this effect to reduce molecular weight from over 1 million to some hundreds by increasing the temperature from 25 to 100°C without any loss in efficiency (34).

Consecutive reactions leading to varying of the nature of the catalyst (number and type of active centers) during the polymerization cause broadening of molecular-weight distribution. A multitude of related but different "catalysts" are present during the polymerization, each forming its own polymer. Consequently, the first successful step for "tailoring" catalysts was to avoid the loss of centers and to prevent the uncontrolled formation of new active centers. This was accomplished by using TiCl_3 with lattice distortions, together with exhaustive milling and grinding of the material in the presence of aluminum alkyls, until a particle size of $\sim 60 \text{ \AA}$ was reached. Down to this size, a strong proportionality of activity to surface, determined by X-ray investigation, was found (13) (see p. 143). When milling $\beta\text{-TiCl}_3$ in the presence of α -olefins (ethylene and propylene), polymerization takes place even in the absence of aluminum alkyls (35). The transition-metal catalyst was prepared by treatment with aluminum alkyls, giving network structures in which the aluminum atoms are considered highly active islands in a matrix of hydrocarbons. Such a structure prevents bimolecular reactions of catalyst centers. Similar work has involved polymeric ligands (36,37).

II

PROCESS OPERATION

Process development and process simplification are best understood with flowsheets (ref. 3, p. 59; ref. 38-40). A typical flowsheet involving

a suspension process for ethylene polymerization is given in (38). Aluminum organic compounds [tri(isohexyl)aluminum, isoprenylaluminum] are blended with chloride-containing trivalent titanium compounds [for example, Ti(III) alkoxychlorides or a catalyst based on reaction products of magnesium with titanium] and used with a diluent (normally a hydrogenated naphtha in the boiling range of 130–160°C). The catalyst slurry is fed into the polymerization reactor along with ethylene (99.9% pure) and such comonomers as 1-butene or propylene to adjust the product density to 0.942–0.965 g/cm³. Temperatures are maintained at ~80–90°C and the pressure at 8–10 bar. Catalyst efficiency is doubled if the pressure is increased to 20–25 bar, but even at 8 bar it is high enough to lead to polymerization with 98–99% conversion. No deactivation or washing with an alcohol is necessary. This allows transfer to a centrifuge where 90% of the diluent is withdrawn for immediate recycle to the catalyst preparation stage without purification. After stripping with steam, the polyethylene (free from diluent but wet) is centrifuged to remove water. Final drying takes place in a fluidized-bed air dryer. Because polyethylene is sensitive to oxidative attack (catalyzed by sunlight) (41), antioxidants, substances with phenolic groups, have to be added (42).

In a typical 80,000 tons/year plant, capital costs were about \$220 per metric ton in 1974. To produce 1000 kg of polymer, 1030 kg of monomer is needed, together with 1 kg of hydrogen and 25 kg of diluent. Catalyst and miscellaneous chemicals cost about \$4 per 1000 kg of polyethylene pellets produced. For production, 300 kg of medium-pressure steam, 800 kg of low-pressure steam, 530 kWh of electrical energy, 200 m³ of water, 30 m³ of nitrogen, and ~600 m³ of air are also required. To polymerize propylene in suspension, the same technology can be used. Catalysts now available [based on TiCl₃ (see Table II)] make it unnecessary to separate isotactic from atactic materials.

A further simplification occurred when it was recognized that gas-phase polymerization was possible without any solvent in a fluidized bed. Agitation by fluidization is sometimes assisted by stirring (43). Highly purified gaseous ethylene is fed continuously into a fluidized-bed reactor containing catalysts based on supported chromium (efficiencies up to 600 kg of polyethylene per gram of Cr). The flowsheet of a process developed by Union Carbide is shown in (39). Fluidization is accomplished by circulating the monomer gas which also carries away the heat of polymerization. Temperatures are held at 85–100°C and pressure is held at ~20–25 bar. The polymer particles formed are intermittently removed from the lower part of the vertical polymerization reactor.

Gas-phase polymerization saves 15% on investment compared with liquid-phase processes. To produce 1000 kg of polymer, 1017 kg of mono-

mer is needed, as well as 0.3 kg of hydrogen and 20 kg of butene or propylene as comonomer to adjust the density to $0.94\text{--}0.966\text{ g cm}^{-3}$. Catalyst costs are comparable to those for the liquid-phase process, and 400 kWh of energy is needed.

Wisseroth (43) described the development of gas-phase polymerization of ethylene and propylene. Reference to the original paper is recommended for those interested in large-scale production and technical plants. It is possible to summarize the results of some hundred runs in a nomogram (see Fig. 1). In the same context, the reader may wish to refer to the mathematical modeling of reactors (44). The conclusions drawn by Wisseroth highlight the state of our knowledge and show that a great number of selected parameters can usually be interpreted by use of more than one theory. However, the reported data on solubility (stereospecificity), molecular weight, and valence state, as well as activity of the catalysts, can also be understood on the basis of the widely accepted mechanism summarized by Chien and Hsieh (20, 29).

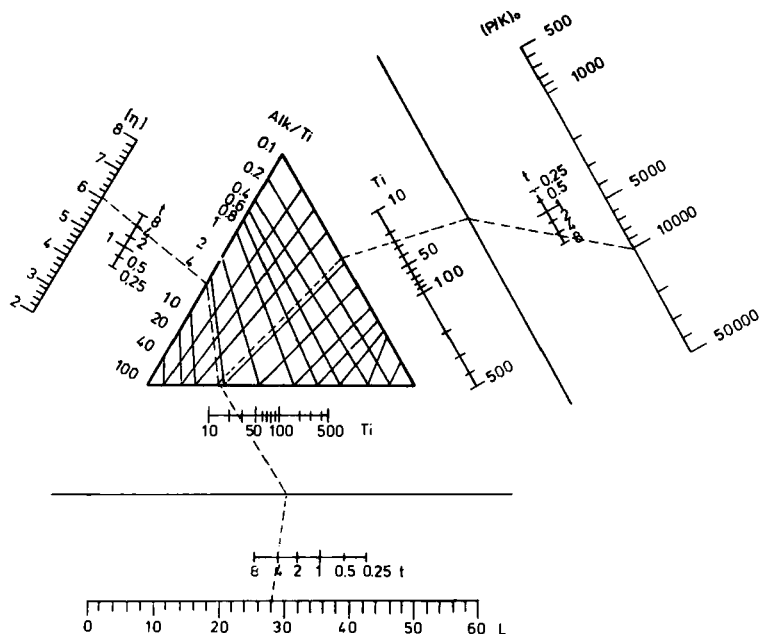


FIG. 1. The reaction-kinetic relationships between the experimental parameters (duration of experiment, quantities, catalyst components, average molecular mass, solubility in *n*-heptane, and catalyst yield) for propylene, gas-phase polymerization. Experiment in a 1-liter autoclave. Catalyst $\text{TiCl}_3\text{--AlEt}_3$, room temperature, 1 bar, time (*t*) in hours. From Wisseroth (43).

The year 1977 marked the start-up of a 75,000 ton/year plant, operating on the gas-phase basis, in which a pretreated catalyst from trialkylaluminum and titanium trichloride is used. The temperature is held at 90°C, and the propylene is recycled by condensation with compression and cooling to serve as a cooling agent during evaporation in the fluidized bed. Yields of 3 g liter⁻¹ min⁻¹ and 15,000 g of polymer per gram of titanium (maximum known 40,000–60,000 g/g) are reported.

III

STEREOREGULATION, KINETICS, AND MECHANISM

A. Stereoregulation

The fact that technical plants produce products on the basis of empirical parameters, but without any certain knowledge as to mechanism and with a lack of kinetic knowledge, is both depressing and stimulating at the same time. Only a few investigators have considered the difficulties that arise from transport phenomena (45–49). The reviewers agree with Reichert (40) that the rate constants and equations reported should be read with skepticism. Well known reviews have been provided by Keii (18) and Cooper (50). It is remarkable that several supported-catalyst systems polymerize propylene and yet have no polymerization activity as homogeneous catalysts (20). All homogeneous-catalyst systems for ethylene polymerization become heterogeneous when the polyethylene is formed. As reported in a later section, there is one homogeneous system based on aluminoxane as the soluble aluminum organic component which polymerizes propylene to an atactic soluble material, and ethylene to insoluble polyethylene. Copolymers are formed (51) as well.

The mechanism of Ziegler-type polymerization has not only to explain rate expressions found by kinetic measurements, but also the structure of the polymer. The structure and the molecular-weight distribution of the polymers are a record of what happened during the polymerization reaction. What is to be explained may be summarized by discussing propylene as a monomer.

On using vanadium-based homogeneous catalysts, polymers consisting of syndiotactic stereo-blocks and stereo-irregular blocks are obtained (52). Interesting changes occur with temperature. It is remarkable that the ratio $M_w:M_n = 2:1$ is reached if the temperature is less than -40°C (53). As Zambelli (10) has summarized, ethylene-propylene copolymers prepared with syndiotactic specific catalysts contain both "meso" and

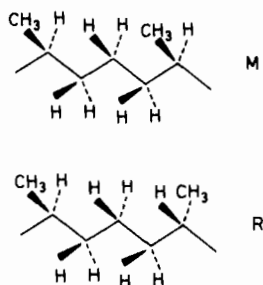


FIG. 2. Isolated ethylene unit in a vinyl chain can be found in a meso (M) or a racemic (R) environment.

"racemic" isolated ethylene units (see Fig. 2). This shows that in this case steric control is due to the chirality of the substituted carbon atom of the last unit of the growing chain (54). Zambelli (55) assumed four-membered rings in the transition state, with "secondary" insertion of the complexed monomer (see Fig. 3).

It must be noted that the approach of the monomer to the reactive metal-carbon bond should occur from the less hindered side. The greater stability of the "trans" complex should arise because the substituted carbon atom of the last unit is involved in the formation of the four-membered ring, so that reaction is hindered. The structure of copolymers of deuteriopropylene from *cis*- and *trans*-(1*d*₁)-propylene proved that, even in syndiotactic polymerization, *cis*-addition to the double bond occurs, because with 1,2-disubstituted monomers, structures of "erythro" and "threo" di-syndiotactic polymers degenerate (see Fig. 4).

If the metal (M) has very bulky substituents, the second insertion step is impossible. With smaller substituents, the monomer always approaches the reactive metal-carbon bond from the same side, the customary situation if M is part of a disturbed crystal lattice, leading to isotactic polymerization (see Fig. 5).

The property of "primary" insertion is demonstrated both by the

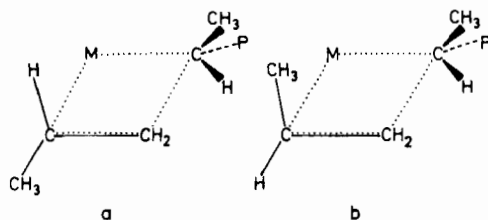


FIG. 3. The active state a (trans) should be more stable than b (cis).

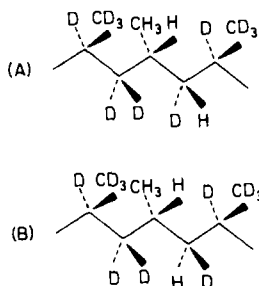


FIG. 4. (A) Threo (or gauche) disyndiotactic copolymer; (B) erythro (or trans) disyndiotactic copolymer. No degeneration of the erythro and threo units takes place in perdeuteropropylene- $1d_1$ -propylene syndiotactic copolymers.

terminal unsaturation of the polymer (56) and by the almost stoichiometric reaction observed between monomer and catalyst (57). The *cis*-addition to the double bond was proved when Miyazawa and Ideguchi (58) established that the polymer of *cis*-($1d_1$)-propylene is erythro-diisotactic, whereas the polymer from *trans*-($1d_1$)-propylene is threo-diisotactic (see Fig. 6). These monomers were initially obtained by Natta *et al.* (59), who first showed that D instead of H is sufficient to cause chirality. Copolymerization of ethylene with propylene shows that isotactic steric control is due to the metal atom only. Chirality of $-\text{C}(\text{CH}_3)\text{H}-\text{P}$, or achirality of $-\text{CH}_2-\text{P}$, the last unit of the growing chain (P), has no influence on isotacticity. All "isolated" CH_2-CH_2 units are in the same steric environment (essentially meso; cf. Fig. 2). Nevertheless, there are disturbances caused by steric and arrangement defects (60). It is believed that stereospecificity is increased proportionally to the M—M and M—Cl distances in the lattices of FeCl_3 , VCl_3 , CrCl_3 , or TiCl_3 (61).

Pino *et al.* (11) summarized the attempts made to produce optically

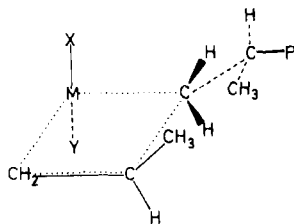


FIG. 5. Steric hindrance above and below M should be determining in order that isotactic propagation shall take place.

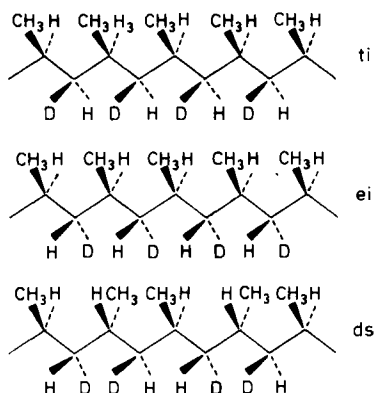


FIG. 6. Three stereoregular polymers have been obtained from *cis*- and *trans*-1*d*₁-propylene: viz., threo-diisotactic (ti), erythro-diisotactic (ei), and disyndiotactic (ds).

active polymers by using racemic monomers. It was found that stereoselectivity is strongly influenced by the distance of the asymmetric carbon atom from the double bond. Very high stereoselectivity is observed for racemic 4-methyl-1-hexene and racemic 3,7-dimethyl-1-octene, where the asymmetric carbon atom is in the α -position relative to the double bond. No stereoselectivity occurs on using 5-methyl-1-heptene; this indicates that, when the chiral center of the monomer is the γ -position, the (chiral) catalytic centers of the catalyst are unable to distinguish between the two monomer antipodes (62).

Stereoselectivity is caused by the chirality of the catalytically active center, and not by chiral atoms in the growing chain. This was strikingly shown by the fact that copolymerization of racemic 4-methyl-1-heptene and 3,7-dimethyl-1-octene with ethylene produces polymers from which the separation of products having optical activity of opposite sign was possible. It may therefore be concluded that insertion of ethylene units into the growing chains neither cancels the stereoselectivity of the polymerization nor decreases it appreciably. On the other hand, using a homogeneous catalyst [formed from $\text{Ti}(\text{CH}_2\text{C}_6\text{H}_5)_4$ and $\text{Al}(\text{CH}_2\text{C}_6\text{H}_5)_3$ (63)] instead of a heterogeneous Ziegler-type catalyst, stereoselectivity with 4-methyl-1-hexene could not be proved. More data are available, and a sophisticated discussion of free-enthalpy values (ΔG) for ground and excited states is presented by Pino *et al.* (11). All of the results are in good agreement with ideas given earlier and may be summarized as shown in Scheme 2 and Fig. 7.

(1) Insoluble Ziegler catalysts contain chiral centers, and these are

type of chirality. Chirality can be induced to a lesser extent by adding polar substances having chiral centers (21).

Many results obtained with diolefins can be explained in essentially the same way as for those with α -olefins. Nevertheless, there are some differences concerning observations made with η^3 -allylnickel complexes and the influence of ligands on the results obtained by using Ziegler-type conditions (64). Some of these systems are far from being true Ziegler-type catalysts. Probably, the structural isomerism of polydienes depends essentially on the specific nature of the metal which forms a complex with the diene involved.

Polymers of 1,4-dienes are obtained in the presence of titanium, and also with Co, Ni, and Rh, where allyl complexes can be isolated. 1,2-Polybutadiene can be produced in the presence of Pd, which is not generally regarded as a Ziegler catalyst. Chromium and molybdenum systems have also been used. Whereas structural isomerism is controlled by the metal in the catalyst center, the geometric isomerism is determined by the ligands and counterions.

For Ziegler-type catalysts based on titanium, we prefer the interpretation proposed by Cossee (65) and Arlman (66); this is based simply on monodentate-trans or bidentate-cis coordination of the diolefin which, respectively, gives a trans or cis configuration in the polymer produced (see Fig. 8).

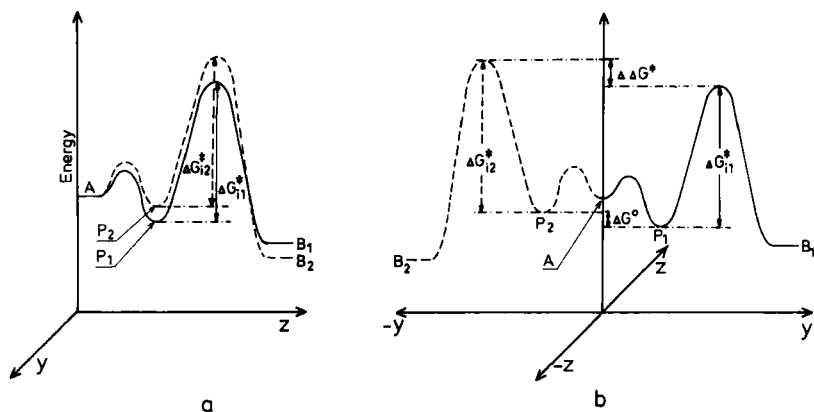


FIG. 7. Reaction path of the two-step addition of a single propylene unit to a growing chain with a completely stereospecific insertion step: (a) (—) formation of an isotactic (meso) diad; (---) formation of a syndiotactic (racemic) diad (projection on the xz plane); (b) projection of these reaction paths on the x,y plane. B_1 , isotactic (meso) diad, has been arbitrarily assumed to be less stable than B_2 , syndiotactic (racemic) diad. For the meaning of A, B_1 , B_2 , P_1 , P_2 , see Scheme 2. From Pino *et al.* (11).

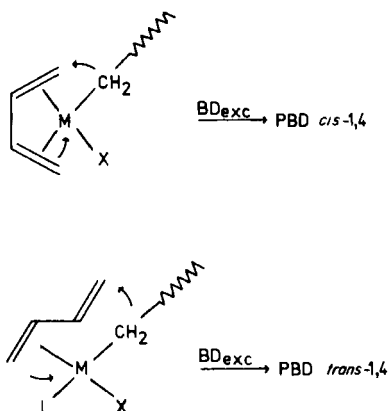


FIG. 8. Control of the cis or trans configurations by the coordinated monomer conformation in 1,4-diolefin polymerizations.

The halide γ -TiCl₃, which offers only one coordination site at the active center, promotes the formation of trans-1,4-polymers, whereas β -TiCl₃, which provides more sites, favors the formation of a mixture of homo-cis- and homo-trans-polymers. Questions about the nature of TiCl₃ structures may be answered by referring to references (6, 67) and (68); for polymerization on catalyst surfaces, refer especially to (69) and (70).

This mechanism can also explain the influence of strongly basic ligands which convert the cis-forming catalyst into a transforming catalyst; for publications in the field of kinetics and mechanism in heterogeneous systems, references (50 and 71-80) should be consulted.

B. Origin of Activity

As already mentioned, nearly all experiments and theories agree that polymerization occurs by addition of an olefin to a catalyst center, followed by insertion of the (stereoregulated, sometimes stereospecific) complexed olefin into a metal-carbon bond at the catalyst center. Figure 9 shows how such an active center can be situated at the edge of a crystal-lattice. It will be seen that the environment of the coordinatively unsaturated, but alkylated, Ti atom demands the stereospecific coordination of the propylene (81).

It is not surprising that much work has been done to determine the number of active sites. Many different structures can be reproducibly obtained (82-84); this is a consequence of the heterogeneous nature of

the catalyst surface, which varies with the mode of catalyst preparation, the temperature and pressure, the duration and intensity of stirring, the milling and grinding, and ultimately with the olefin used in the polymerization. Schnecko *et al.* (12) convincingly showed that the catalyst system is initially sensitive toward the individual monomer during the polymerization (see Figs. 10 and 11).

It must be concluded from the results that reactions take place which change the number of active sites present, due to the different behavior of the polymers in solution. With polyethylene, crystalline insoluble globules cause break-up of the catalyst aggregates, and even crystal scission; with poly(1-butene) the chains are highly solubilized.

Yermakov and Zakharov (13) reported comprehensive work on the difficulties associated with specific quenching techniques which make sure that only the "active" metal-carbon bond is quenched. There is evidence that surface determinations by the BET method can give incorrect results, but a strong correlation of polymerization rate to crystallite surface (determined by X-ray techniques) was found (see Fig. 12). The authors conclude that the formation of propagation centers in the case of unsupported TiCl_3 proceeds with participation of only those surface titanium ions that are situated in special surface regions as outcrops of growth spirals, or on lateral faces (65-69, 85, 86).

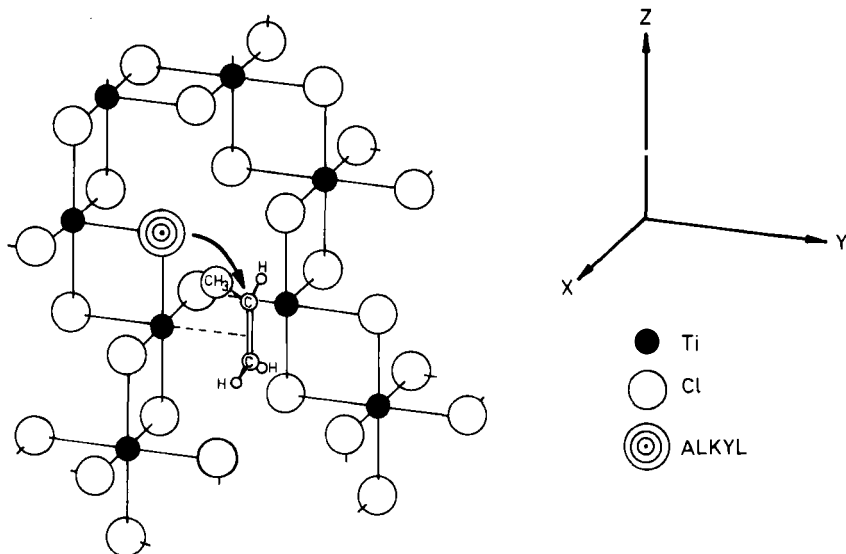


FIG. 9. The active center of polymerization of propylene at the edge of a crystal lattice.

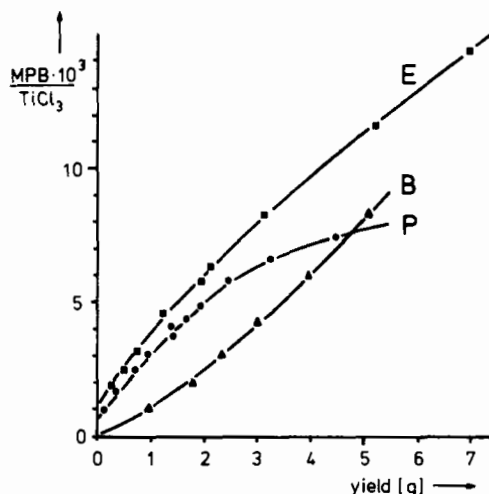


FIG. 10. Normalized metal-polymer bond concentration (MPB) as function of yield of polyethylene in grams (curve E), polypropylene (curve P), and poly(1-butene) (curve B). From Schnecko *et al.* (12).

The surface heterogeneity can easily explain the broad molecular-weight distribution that is observed experimentally, as shown earlier by Clark and Bailey (32). Besides the monomers that cover, or even disturb, the catalyst surface, side reactions occur. Aluminum alkyls in the surrounding solution act as alkylating agents and, depending on the degree

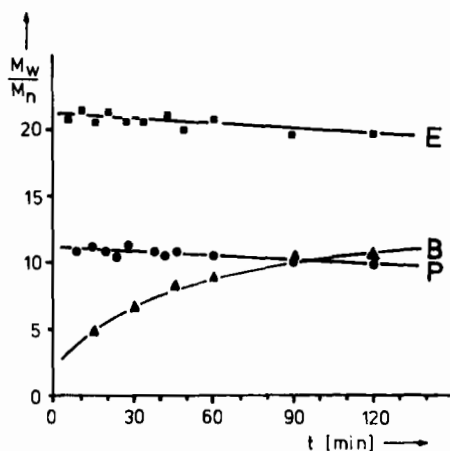


FIG. 11. Polydispersity (M_w/W_n) as a function of time for ethylene (curve E), propylene (curve P), and 1-butene (curve B) polymerizations. From Schnecko *et al.* (12).

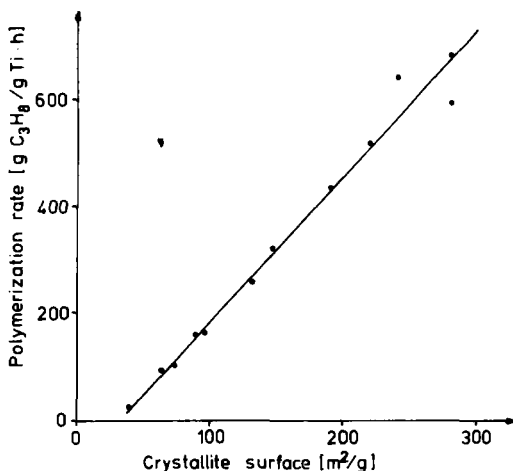


FIG. 12. The ratio between the activity of propylene polymerization catalysts and their specific surface. The specific surface of the samples was calculated from the average sizes of primary crystallites, determined by using X-ray techniques, on the assumption that the crystallites have the form of hexagonal prisms (001 axis). Polymerization at 70°C, cocatalyst AlEt_2Cl , monomer concentration 1 *M*. From Yermakov *et al.* (13).

of chlorination, the donor-acceptor properties are enhanced. With a "mono"-metallic catalyst such as TiCl_2 (where, in an unknown mechanism, alkyltitanium is formed on the surface) polymerization is strongly inhibited when AlEtCl_2 is added (87). Furthermore, there is evidence that titanium alkyls react not only with aluminum alkyls but also with other titanium alkyls thus forming structures $\text{Ti}-\text{CH}_2-\text{CH}_2-\text{Ti}$, or more slowly $\text{Ti}-\text{CH}_2-\text{Ti}$.

If it is borne in mind that usually less than 1% of the titanium atoms are part of a catalyst center, the weak basis of all of the mechanistic and kinetic approaches can be understood. It is still quite unknown how the propagation centers are formed. Whatever is measured, the result is obtained with a substance that contains only a small concentration of the moiety of interest. Nevertheless, the kinetic results summarized by Keii (8), Cooper (50), and Chien and Hsieh (20) are of great value and have been extended with new and more precise results (76-78, 88, 89).

It is now clear that, when propagation centers are formed, olefin polymerization by all solid catalysts (including the Phillips Petroleum catalyst from chromium deposited on oxides, and the Standard Oil catalyst of molybdenum oxide on aluminum oxide) essentially follows the same mechanism: chain growth through monomer insertion into the transition-metal-carbon bond, with precoordination of the monomer. Interestingly,

as mentioned by Hopff and Balint (90), a typical, Ziegler catalyst was first formed with ethylene, Al, AlCl_3 , and TiCl_4 under conditions used by M. Fischer (91).

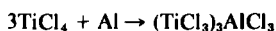
IV

TAILORING HETEROGENEOUS CATALYSTS

To obtain a catalyst for industrial use, the following criteria are important. (1) Formation of catalyst centers should occur before initiating the process. (2) Several catalyst centers should remain stable after initiating polymerization. (3) The environment of the catalyst centers should be stable in view of desired properties of stereoregulation and stereospecificity. (4) Solvating the metal-polymer bond should be possible under defined conditions causing chain transfer by hydride or by monomer. (5) To avoid a final washing, a small proportion of the catalytic material should have a maximum number of active centers. (6) Reactions between catalyst centers should be avoided. It is meaningless to argue whether "trial-and-error" or mechanistic ideas have led to the development of the so-called "Ziegler-type catalyst of the second generation," but it seems evident to the reviewers that the aforementioned criteria are fulfilled in the most efficient catalyst compositions.

The reaction of titanium tetrachloride with organoaluminum compounds leads, after alkylation, complex formation, and reduction, to a variety of titanium compounds that, in the absence as well as the presence of excess aluminum compound, change by aging, thus failing conditions (1)–(3). Better results arise if prolonged reaction, reduction, and aging with an excess of organoaluminum compound occurs, leading to a mixture of partially alkylated titanium- and aluminum halides. Alkylation may be halted with hydrogen chloride, or by adding an excess of titanium tetrachloride. The resulting mixture can be activated with organoaluminum compounds containing large alkyl groups, or even having oligomeric structures, thus fulfilling condition (6).

The first high-activity catalyst for ethylene polymerization which avoided the necessity of washing was derived from titanium(III)alkoxy chloride and triisohexylaluminum (92) [for the patent literature, see (25)]. Another route starts with titanium trichloride. Thus, excellent results as regards activity are obtained with the so-called Stauffer TiCl_3 which contains ~30 mol% of aluminum, obtained according to the following reaction.



Of great interest for basic research are investigations on single crystals. For example, polymer chains can be grown on slits and edges of α - TiCl_3 crystals treated with gaseous aluminum alkyls (67). At first, the TiCl_3 has an α -structure; this is converted into a γ -structure on reaction with titanium tetrachloride. Catalysts having high activity are usually less stereospecific. Stereospecificity is increased by blocking part of the centers with alkylaluminum mono- or dichloride (instead of trialkylaluminum), or adding co-components during preparation which mainly consists of a heat-treatment and a grinding process to fulfill conditions (1)–(4).

Table IV lists the more important combinations for the preparation of highly active and highly stereospecific catalyst systems. As Weissmehl *et al.* (27) pointed out, catalyst efficiencies of higher than 40,000 g of polymer per gram of titanium and isotacticities greater than 97% for propylene polymerization can be obtained.

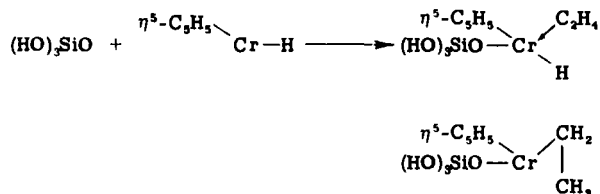
A supported catalyst for ethylene polymerization which requires no alkyl aluminum for activation was first claimed by the Phillips Petroleum Company (32). It consists of chromium oxide on silica, reduced with hydrogen. Krauss and Stach (93) showed that the active sites are Cr(II) centers. The presence of solvent, or even aluminum alkyls, diminishes

TABLE IV
IMPORTANT COMBINATIONS FOR THE DESIGN OF HIGH-ACTIVITY, HIGH-
STEREOSELECTIVITY ZIEGLER CATALYST SYSTEMS FOR PROPYLENE
POLYMERIZATION

TiCl ₃ catalyst components		
Reactants for TiCl ₄ reduction	TiCl ₃ treatment	Possible co-components during TiCl ₃ treatment
Aluminum powder	Grinding	Carboxylic acid chlorides Ethers
Aluminum alkyls	Heating	Tertiary amines Tertiary phosphines Metal chlorides
Cocatalysts		
Aluminum alkyls		Co-components for aluminum alkyls
Aluminumtriethyl Diethylaluminum chloride Ethylaluminum dichloride + Lewis base		Cyclic di- and triolefins Aliphatic ethers Carboxylic acid esters

the activity. In laboratory-scale experiments (43) an unusual upper limit of $\sim 150,000,000$ parts of polyethylene per part of chromium was observed, whereas in production-scale 240,000 parts of polyethylene per part of chromium was reported. Unfortunately, this catalyst is not influenced by hydrogen under polymerization conditions, and there is therefore no possibility of establishing the molecular weight during the reaction.

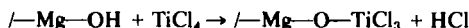
A chromocene catalyst supported on silica has been studied (94), with ethylene adding to a Cr—H bond. It is remarkable that the chromium atom, as well as the migrating hydrogen atom, appears to be essentially neutral. For a discussion, see the original article (94).



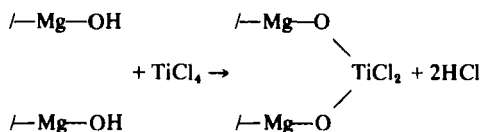
Union Carbide (95, 96) developed chromium catalysts that need activation by aluminum alkyls, but which have the advantage that molecular weight can be controlled with hydrogen, as in the case of the titanium-based catalysts. To prepare the catalysts, organosilanols are combined with chromium trioxide to afford silylchromate. The silylchromate is then deposited on a silica support and activated with an aluminum alkyl (see Fig. 13).

Surprising results were obtained when titanium compounds were chemically attached to the surface of a solid magnesium compound. Eley and co-workers (97) have investigated reactions of partial hydroxylated magnesium oxide and titanium tetrachloride followed by reaction with triethylaluminum. Infrared and gravimetric investigations suggested the following processes.

(a) Complex formation with the surface



or



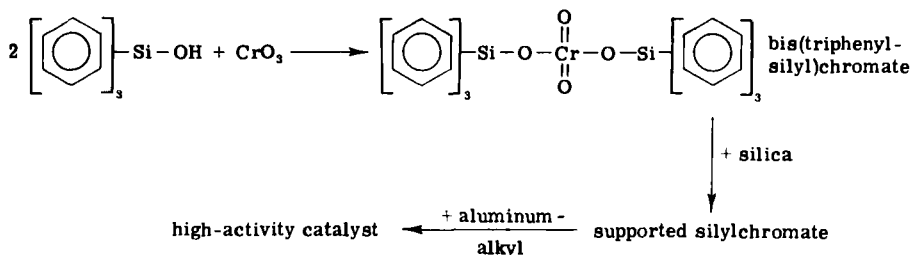
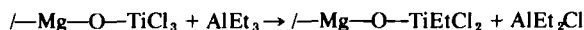
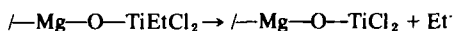


FIG. 13. Preparation of supported alkylaluminum activated chromium catalysts for ethylene polymerization.

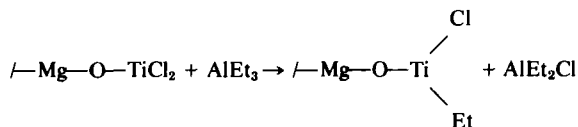
(b) initial alkylation



(c) reduction (simplified)



(d) second alkylation



The titanium(III) alkyl surface compound, formed in the latter reaction, is believed to be the active site. Figure 14 summarizes the results of an investigation of this (98). Yields of ~200,000 g of polyethylene per gram of titanium have been reported. In the presence of certain stereoregulators (e.g., the ethyl ester of benzoic acid), propylene can also be polymerized with a tacticity of 97%. Chien and Hsieh (99), who investigated supported catalysts for stereospecific polymerization of propylene, reported a 100% yield of stereoregular polymers when diethyl ether was added to tribenzyltitanium chloride on $\text{Mg}(\text{OH})\text{Cl}$. Montecatini (28) claimed formation of 150,000 g of polypropylene per gram of titanium. It is perhaps worth mentioning that the structural unit me---O---Ti ($\text{me} = \text{Mg}$ or Si on surface) is assumed to be present. Using soluble oligomeric aluminoxanes $\text{---[Al(Me)OAl(Me)OAl(Me)O]---}_n$ and halogen-free bis(cyclopentadienyl)dimethyltitanium, soluble systems can be formed that polymerize ethylene as well as propylene (see p. 140). Some kinetic data have been summarized by Reichert (40), Caunt (7), Chien and Hsieh (99), and Soga *et al.* (98). Research in this area is continuing intensively.

It should be mentioned that the supported Ziegler-type catalysts have

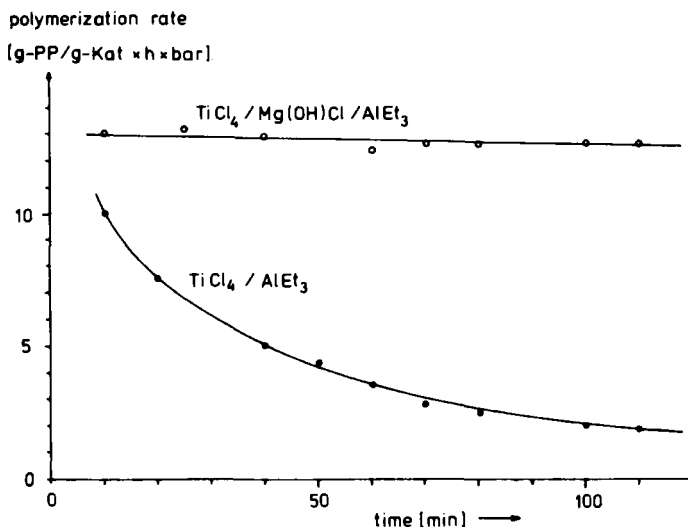


FIG. 14. Variation of the polymerization rate of propylene with the time (at 50°C) in *n*-heptane for two different catalyst systems; catalyst 1 g/100 ml of *n*-heptane in each case. From Soga *et al.* (98).

an increased sensitivity to molecular weights and molecular-weight distribution. The M_w/M_n ratio can be changed from 24 to 4, altering the chemical composition (27). Using the aforementioned soluble system, the value of molecular weight can be changed from several hundred up to more than one million solely by altering the temperature.

For the formation of supported magnesium-titanium catalysts, the preferred reactants are $Mg(OH)Cl$ and $TiCl_4$ (100), $MgCl_2 \cdot 3Mg(OH)_2$ and $Ti(OR)_xCl_y$ (with $x + y = 4$) (101), $MgSO_4 \cdot 3Mg(OH)_2$ and $Ti(OR)_xCl_y$ (102), or $Mg(OH)_2$ and $TiCl_4$ (103–106).

Highly active catalysts are also obtained by treating magnesium alkoxides with titanium(IV) chlorides. During the course of catalyst preparation, the original crystal structure is completely destroyed as new crystalline species are formed. They are probably a mixture of magnesium chloride, magnesium alkoxide, magnesium(alkoxy) halide and magnesium-titanium complexes of the type $[Mg(TiCl_n)(OR)_m]$ (with $n + m = 6$). The final catalyst particles are too small to allow establishment of their structure by X-ray diffraction, and they have a much higher specific area than the original magnesium alkoxide. Other highly active catalysts are formed by reacting pure $MgCl_2$ or $MgCl_2$ -electron-donor adducts [e.g., $MgCl_2 \cdot 6EtOH$] with tetravalent titanium compounds followed by activation with organoaluminum compounds. Table V summarizes some

TABLE V
IMPORTANT NONSUPPORTED MAGNESIUM-TITANIUM CATALYST COMPONENTS
FOR ETHYLENE POLYMERIZATION

Reactants		Probable catalyst species	References
$\text{Mg}(\text{OR})_2 + \text{TiCl}_4$	————→	$(\text{MgCl}_2 \cdot \text{Mg}(\text{OR})_2 \cdot \text{Mg}[\text{TiX}_6])$ (X = Cl, OR)	107-109
$\text{MgCl}_2 + \text{TiCl}_4$	————→	$(\text{MgCl}_2 \cdot \text{Mg}[\text{TiX}_6])$ (X = Cl)	110
$\text{MgCl}_2 \cdot \text{donor} + \text{TiCl}_4$	————→	$(\text{MgCl}_2 \cdot \text{Mg}[\text{TiX}_6])$ (X = Cl, donor)	111

of the more efficient nonsupported magnesium-titanium catalyst components.

Study of these new catalysts is intensive. Small molecular-weight distribution was demonstrated by Petrova (112) and by Baulin *et al.* (113). In addition, polymer substrates have been used (114-116) in order to increase lifetime and activity. As shown by Suzuki (36), stabilization is caused by inhibition of reduction by polymeric ligands. Karol (117, 118) described the reaction of chromocene with silica to form highly active catalysts sensitive to hydrogen. An unknown role is played by the structure $\text{mt}-\text{CH}_2-\text{CH}_2-\text{mt}$ which is formed with ethylene and reduced forms of titanium (119). For soluble systems, it has been shown that the $\text{mt}-\text{CH}_2-\text{CH}_2-\text{mt}$ structure is formed in a bimolecular reaction with β -hydrogen transfer (120). It was considered that this slow, but unavoidable, reaction is the reason for changes in activity during reaction and that the only way to avoid it is to prevent bimolecular reaction of two alkylated species.

V

HOMOGENEOUS ZIEGLER-NATTA CATALYSTS

A. Soluble Systems

Among the great number of known Ziegler-type catalysts homogeneous systems have been preferentially investigated in order to understand the elementary steps of the polymerization, which is simplified in soluble than in heterogeneous systems. The mechanism of Ziegler catalysis has long been debatable; however, the most definitive results have been obtained in the course of studying homogeneous systems. Kinetic studies

and applications of various methods have helped to define the nature of the active centers of some homogeneous catalysts, to explain aging effects of heterogeneous Ziegler catalysts, to establish the mechanism of the interaction with olefins, and to obtain quantitative evidence of some elementary steps (7, 8, 16, 120, 121).

It is necessary to differentiate between the soluble catalyst system itself and the homogeneous (or inhomogeneous) polymerization system. Unfortunately, the well defined bis(cyclopentadienyl)titanium system is a soluble one, but it becomes heterogeneous when polyethylene is formed. It is also ineffective toward propylene. Therefore, the results of Reichert and Meyer and others, (122-124) performed within the first few moments before heterogeneity appears, are important.

It seems that soluble catalysts can be fairly easily removed from polymers. As the color, the stability to light, or the general stability of the polymer depends on the degree to which catalysts have been removed, soluble systems have received more technical attention. In addition, in some cases the diene and copolymerization of α -olefins show extremely high stereoselectivity and activity. On the other hand, there are examples known where residues of even the homogeneous bis(cyclopentadienyl) metal systems lead to "coloring" of the product.

Table VI summarizes important homogeneous Ziegler catalysts. The best known are the systems based on bis(cyclopentadienyl)titanium(IV), titanium⁺alcoholates, vanadium chloride, or chromium acetylacetonate with trialkylaluminum or alkylaluminum halides.

B. The Titanium System

Breslow (139) discovered a homogeneous system well suited for kinetic analysis. He realized that bis(cyclopentadienyl)titanium(IV) compounds, which are very soluble in aromatic hydrocarbons, could be used instead of titanium tetrachloride as the transition-metal compound together with aluminum alkyls to give Ziegler catalysts. Subsequent research on this and other systems with various alkyl groups has been conducted by Natta *et al.* (140, 141), Belov *et al.* (142-144), Patat (145), Patat and Sinn (146) Sinn *et al.* (119, 147), Shilov and co-workers (148-150), Chien and Hsieh (20), Adema (151), Clauss and Bestian (152), Henrici-Olivé and Olivé (153), and Reichert and Schoetter (154) and Fink (155).

With respect to the kinetics of polymerization and the side reactions of the catalyst components, this soluble system is probably the one best understood. It has not been used as yet in a technical process because

TABLE VI
HOMOGENEOUS ZIEGLER CATALYST SYSTEMS

System	Transition metal (M): aluminum compound	Monomer	Temperature [°C]	Normalized activity ($\frac{\text{kg polymer}}{\text{mol M} \cdot \text{h} \cdot \text{bar}}$)	Catalyst yield ($\frac{\text{kg polymer}}{\text{mol M}}$)	References
$\text{Cp}_2\text{TiCl}_2/\text{AlMe}_2\text{Cl}^a$	1:2.5-1:6	Ethylene	30	40-200	—	125, 126
$\text{Cp}_2\text{TiCl}_2/\text{AlMe}_2\text{Cl}/\text{H}_2\text{O}$	1:6:3	Ethylene	30	2,000	—	125
$\text{Cp}_2\text{TiCl}_2/\text{AlEt}_2\text{Cl}$	1:2	Ethylene	15	7-45	—	127, 128
$\text{Cp}_2\text{TiMe}_2/\text{AlMe}_3/\text{H}_2\text{O}$	1:10 ⁵ :5·10 ²	Ethylene	20	3,500	>15,000	34
$\text{Cp}_2\text{TiMe}_2/[\text{Al}(\text{Me})\text{O}]_n$	1:100	Ethylene	20	200	> 5,000	129
$\text{Ti}(\text{O}i\text{Bu})_4/\text{AlEt}_3$	1:3	Ethylene	—	—	—	130
$\text{VO}(\text{acac})_3/\text{Et}_2\text{AlCl}/\text{activator}$	1:50	Ethylene	20	180	—	131
$\text{Cp}_2\text{VCl}_2/\text{Me}_2\text{AlCl}$	1:5	Ethylene	50	13	—	132
$\text{VOCl}_2(\text{AlR}_3\text{Cl}_{3-n}/\text{activator})$		Ethylene				132
$\text{V}(\text{acac})_3$						
$\text{Cr}(\text{allyl})_3$	—	Ethylene	80	0.3	—	14, 133
$\text{Cr}(\text{acac})_3/\text{Et}_2\text{AlCl}$	1:300	Ethylene	20	150	—	131
$\text{Ti}(\text{benzyl})_4$	—	Ethylene	20(80)	$8 \cdot 10^{-3}$ (0.2)	—	134
$\text{Ti}(\text{benzyl})_3\text{Cl}$	—	Ethylene	20	0.4	—	134
$\text{Ti}(\text{benzyl})_4/\text{Et}_2\text{AlCl}$	1:10	Ethylene	20	8	—	29
$\text{Zr}(\text{benzyl})_4$	—	Ethylene	20(80)	0.14(0.8)	—	17, 134
$\text{Zr}(\text{benzyl})_4$	—	Propene		10^{-3}	—	129, 135, 136
$\text{Zr}(\text{benzyl})_3\text{Cl}$	—	Ethylene	20	0.3	—	134
$\text{Cp}_2\text{Zr}/\text{AlEt}_3$	1:6	Ethylene	60	2	—	129
$\text{Cp}_3\text{UCl}/\text{AlEt}_3$		Ethylene			—	137
$\text{U}(\text{allyl})_3\text{Cl}$		Butadiene		2.5	—	138
Supported catalysts for comparison						
$\text{TiCl}_4/\text{AlEt}_2\text{Cl}/\text{cabosil}$		Propene	50	20-48	310	20
$\text{CrO}_3/\text{SiO}_2$		Ethylene	80	2,000	>35,000	13, 40
$\text{TiCl}_4/\text{cocatalyst}/\text{support}$		Ethylene	80	10,000	>10,000	13, 40
$\text{Mg}(\text{OH})\text{Cl}$						

^a $\text{Cp} = \eta^5\text{-C}_5\text{H}_5$.

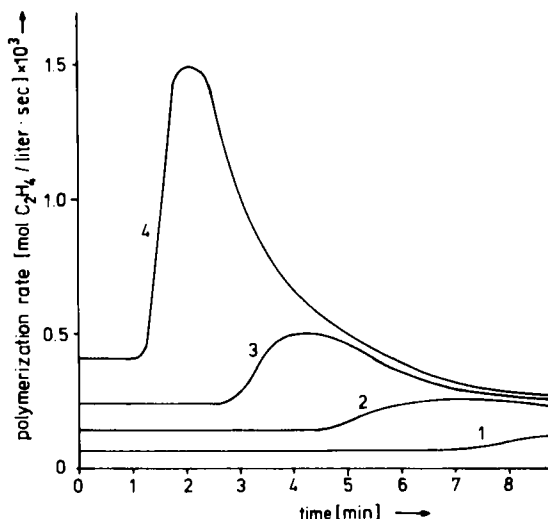


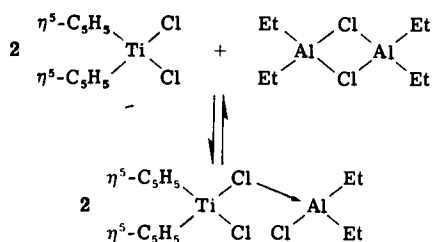
FIG. 15. Polymerization rate as function of time at constant ethylene concentrations; $[\text{Ti(IV)}] = 3 \cdot 10^{-3}$, $[\text{Al}] = 6 \cdot 10^{-3} \text{ M}$. $[\text{C}_2\text{H}_4] = 1.3$ (1), 2.6 (2), 5.2 (3), and 10.4 (4) $\cdot 10^{-2} \text{ M}$. From Reichert and Meyer (122).

of the low activity and short life of systems that contain chloride (see Fig. 15). A halogen-free system has now been found that has a remarkably high activity and long life (see Section VII).

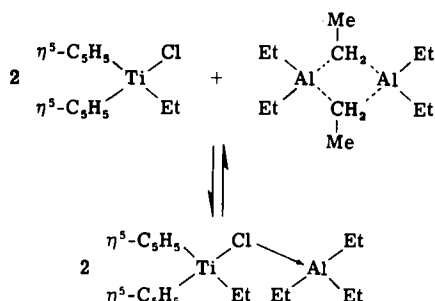
After a short induction period, the activity of polymerization increases as a function of the monomer concentration. After reaching a maximum, a continuous decrease is observed, due to fast aging processes as alkyl exchange, hydrogen transfer, and reduction of the transition-metal species occur in parallel with catalytic polymerization. There exist today a number of different conceptions concerning the nature of the center of polymerization activity. However, the formation of a complex between the titanium and the aluminum components is now accepted by all workers.

C. Complexation and Alkylation of the Transition Metal

In all systems that contain at least one chlorine atom per titanium-aluminum system, there is fast complex formation which can be recognized by color intensification.

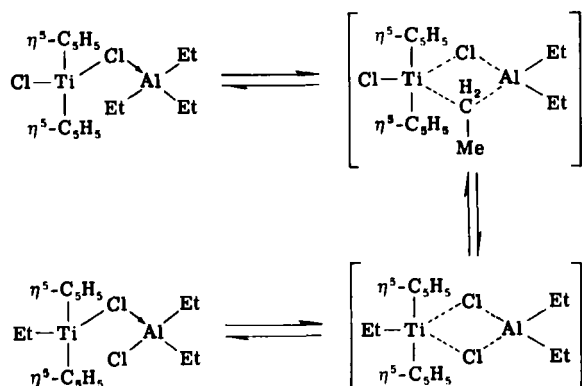


or



These spontaneously formed species cannot be isolated (156); hence they have only been identified spectroscopically (34, 157, 158). Henrici-Olivé and Olivé (159) suggested that soluble titanium-aluminum complexes have an octahedral structure relative to the coordination sphere of the titanium atoms. However, subsequent research (160) showed that, at least for the primarily formed complexes, there is no octahedral structure present. It is most likely that there is a tetrahedral structure for the titanium, in accordance with the 1959 proposal of Breslow and Newburg (127).

If there are at least two atoms of chlorine per titanium atom in the system, then, besides a 1:1 titanium-aluminum complex, a 1:2 complex also exists, as shown by NMR spectroscopy (160). Because, even at low temperatures, a coalescence of the alkyl groups on the aluminum cannot be found, a simple $\text{Ti}-\text{Cl} \rightarrow \text{Al}$ donor bond could be present. In agreement with this idea, no complex formation occurs with the halogen-free system $(\text{C}_5\text{H}_5)_2\text{TiMe}_2\text{-AlMe}_3$. After formation of the complex, alkylation of the titanium component is presumed to take place.

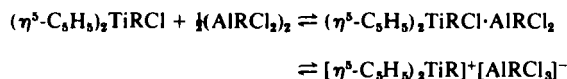


A complex having electron-deficient bonding can be postulated as the transition state. Long (157) showed that alkylation is necessary to form the polymerization-active center. Corresponding results were obtained by Beermann and Bestian (161) for heterogeneous systems obtained from $\text{TiCl}_4\text{-AlR}_3$ or $\text{TiCl}_4\text{-AlR}_n\text{Cl}_{3-n}$.

D. Nature of the Active Center

Breslow and Newburg (162) first pointed out that polymerization takes place mainly if the titanium exists as titanium(IV). A similar deduction was made by Clauss and Bestian (152) and confirmed by Sinn and Patat (163). Breslow and Newburg (127) found that inactive polymerization mixtures, from which Natta *et al.* (156) isolated inactive transition-metal(III) complexes (164, 165), could be reactivated to titanium(IV) compounds by oxidation with oxygen. According to Henrici-Olivé and Olivé (159), the speed of polymerization decreases with increasing intensity of the ESR signals of the developing titanium(III) compound.

The increase in length of the polymer chain occurs by insertion of the monomer in a metal-carbon bond of the active complex. Dyachkovski and co-workers (149) believe, based on kinetic measurements, that the insertion takes place on a titanium cation. An ion of the type $(\text{C}_5\text{H}_5)_2\text{Ti}^+\text{-R}$, derived from complexing and dissociation,



could be the active species of polymerization. In a series of solvents

having increasing polarity (heptane, toluene, CH_2Cl_2), titanium cations could be detected by electrodialysis, with increasing activity of polymerization. Nevertheless, these experiments proved only that, in an electric field, titanium cations can be observed by their migration, and not that these ions are the actual centers of polymerization.

Bier (166) and Gumboldt and Schmidt (167) proposed a model that postulates that polymer chain growth takes place at the alkyl group that is fixed to the aluminum ion, as the original ligands of the aluminum alkyl were found in the polymer. However, if alkyl exchange occurs during polymerization, the final position of the alkyl group is not significant. Rapid exchange of alkyl groups between the titanium and aluminum at room temperature has been proved (132, 163).

Sinn and Patat (163) drew attention to the electron-deficient character of those main-group alkyls that afford complexes with the titanium compound and disputed ionic character for the reaction (146). In agreement with Natta *et al.* (168), they supported the two-step mechanism: "activation" followed by "insertion." The place of insertion has long been the subject of dispute. Henrici-Olivé and Olivé (159) extended the ideas of Cossee (169) for the heterogeneous system to the soluble system. They assumed that main-group alkyls serve as electron-donating groups, thus explaining the different effects of AlR_3 , AlR_2Cl , and AlRCl_2 , respectively. Fink *et al.* (160) showed by ^{13}C -NMR spectroscopy with ^{13}C -enriched ethylene at low temperatures (where no alkyl exchange was observed that, in higher halogenated systems, insertion of the ethylene takes place into a titanium-carbon bond of a titanium-aluminum complex (see Fig. 16). The spectra at 200K showed strong ^{13}C signals belonging to the titanium α - and β -fixed carbon atoms ($\text{Ti}-^{13}\text{C}_\alpha$ 91.3 ppm; $\text{Ti}-^{13}\text{C}_\beta$ 40.1 ppm). Only weak signals of ^{13}C -labeled alkyl groups at the aluminum were observed.

E. Vanadium, Chromium, and Other Transition-Metal Systems

Other well known homogeneous Ziegler catalysts include derivatives of vanadium and organoaluminum compounds (170-172). In contrast to the catalysts containing titanium, which produce polymers with a broad molecular-weight distribution, the compounds containing vanadium produce from the polymerization of ethylene a material with a narrow molecular-weight distribution (173). The vanadium systems are suited to the polymerization of higher α -olefins as well, and are useful for copolymerization, albeit with lower activity (31, 52, 174, 175). Hence, Natta *et al.*

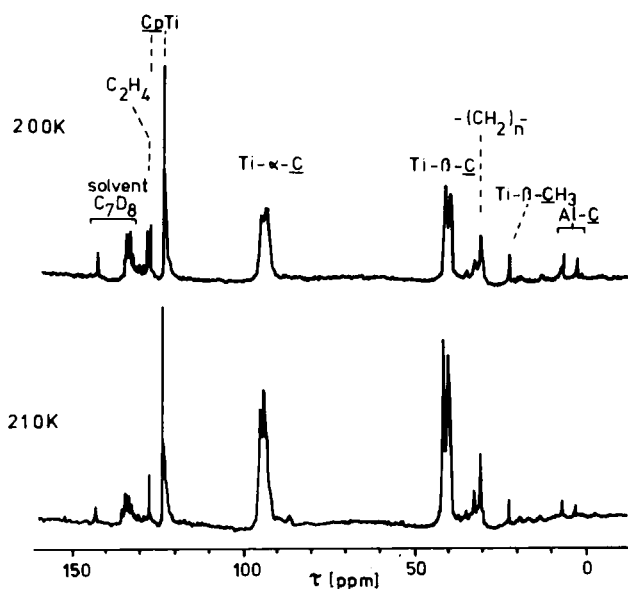


FIG. 16. ^{13}C -FT-NMR spectrum at 200K, and after 15 min at 210K, of the system $(\eta^5\text{-C}_5\text{H}_5)_2\text{Ti}(\text{Et})\text{Cl}-\text{AlEtCl}_2$ with ^{13}C -enriched ethylene. $\text{Al}:\text{Ti}:\text{C}_2\text{H}_4 = 1:1:1$; solvent toluene- d_8 ; strong signals of ^{13}C -enriched atoms are only observed for titanium-carbon bonds and polyethylene. From Fink *et al.* (160).

(176) produced, with $\text{VCl}_4/\text{AlEt}_2\text{Cl}$ at -78°C , syndiotactic polypropylene. These catalysts are initially very active because of the presence of vanadium(III), but they lose a large part of their activity after a short time on production of vanadium(II) and must be reactivated by weak oxidizing agents (173, 177).

Homogeneous systems based on $\text{Cr}(\text{acac})_3/\text{Et}_2\text{AlCl}$ are only very active if $(\text{EtO})_3\text{P}$ is present in the system, or if the $\text{Al}:\text{Cr}$ ratio is greater than 200 (178, 179). Notable also are those soluble catalysts that contain tris(π -allyl)uranium chloride (180, 181). They polymerize butadiene to 1,4-*cis*-polybutadiene with high stereoregulation. The melting point, measured at a heating rate of $16^\circ\text{C}/\text{min}$, is 1.5°C (182), which is higher than that (-2°C) of the same polymer produced by means of a nickel catalyst.

The influence of solvent was especially shown by using nickel-containing catalysts based on nickelporphine complexes. These compounds dissolved in toluene without cocatalysts, oligomerize ethylene to linear α -olefins. Using a suspension in *n*-hexane, high-molecular-weight linear polyethylene is formed (183).

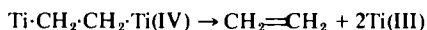
VI

SIDE REACTIONS IN HOMOGENEOUS CATALYSTS

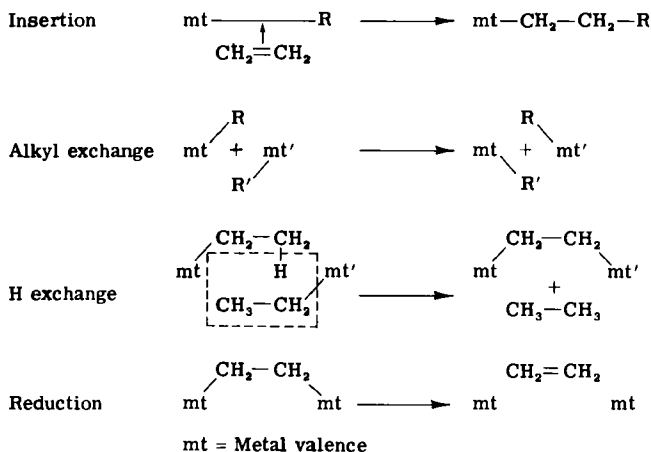
A. Types of Side Reaction

The polymerization of α -olefins, promoted by homogeneous Ziegler-Natta catalysts based on bis(cyclopentadienyl)titanium(IV) or analogous zirconium compounds and aluminum alkyls, occurs simultaneously with a series of other reactions that greatly complicate the kinetic interpretation of the polymerization process (see Scheme 3).

Concomitant with continued olefin insertion into the metal-carbon bond of the titanium-aluminum complex, alkyl exchange and hydrogen-transfer reactions are observed. Whereas the normal reduction mechanism for transition-metal-organic complexes is initiated by release of olefins with formation of hydride followed by hydride transfer (184, 185) to an alkyl group, in the case of some titanium and zirconium compounds a reverse reaction takes place. By the release of ethane, a dimetalloalkane is formed. In a second step, ethylene from the dimetalloalkane is evolved, and two reduced metal atoms remain (119).



Some of the aging process which occurs with homogeneous and hetero-

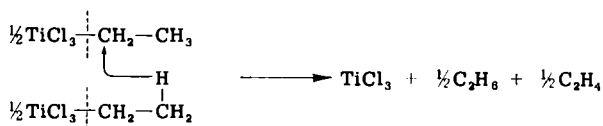
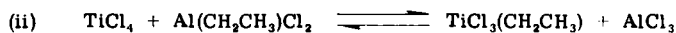
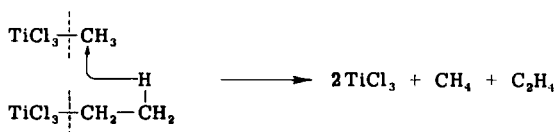
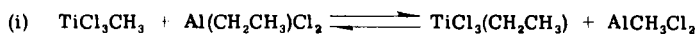


SCHEME 3. Reactions with homogeneous catalysts.

geneous Ziegler catalyst systems can be explained with the aid of these side reactions.

Most titanium(IV) alkyls tend to be reduced by aluminum alkyls in a complicated sequence of reactions accompanied by evolution of alkane and alkene. The catalytic activity of the bis(cyclopentadienyl)titanium-aluminum complexes is associated with the titanium alkyl. Hence, it is very interesting to investigate the mechanism of any reductive reaction. In order to study side reactions in the absence of polymerization, highly alkylated systems completely free of halogen are preferred. Moreover, reduction takes place much faster, the higher the alkyl-group content of the added aluminum alkyl.

Breslow and Newburg (162) suggested for $[\text{TiCl}_2(\eta^5\text{-C}_5\text{H}_5)_2]$ complete alkylation of titanium to give bis(cyclopentadienyl)dialkyltitanium as the first step of the reduction, and that the dialkyl simultaneously decays into a titanium(III) component, with alkane and alkene separation. In contrast, Sinn and Patat (163) established that production of ethylene was slow compared with that of ethane. The first step of the reduction is the transfer of a β -hydrogen atom from one alkyl group to the other with formation of metal— CH_2 — CH_2 —metal structures. Such a β -hydrogen atom-transfer was first proposed by de Vries (186) for the reduction of Ti(IV) compounds by ethylaluminum dichloride.



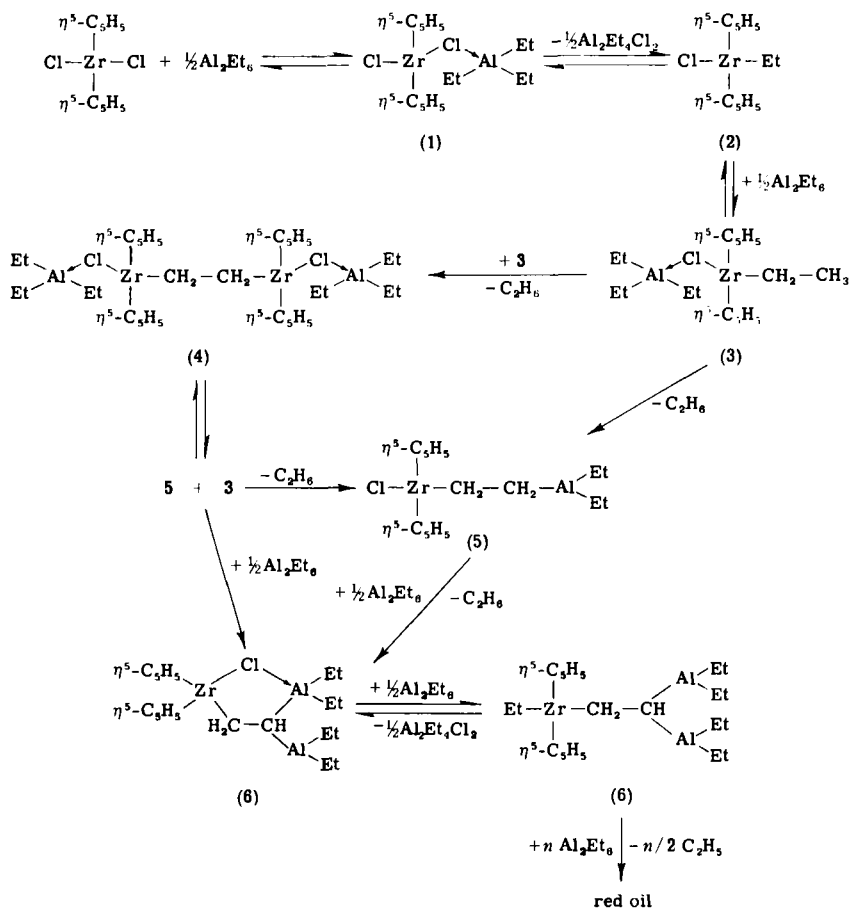
The C_2H_4 was not found, probably because it had polymerized.

Dimetalloalkanes are formed in those systems in which separation of alkanes occurs without polymerization of olefins.

B. The Zirconium System

Numerous intermediate steps have been elucidated for the soluble zirconium system (187). Because of the much greater resistance of zir-

conium to reduction, the study of alkyl exchange and β -hydrogen transfer is more definitive than in the titanium system (see Scheme 4). The reaction pathways of Scheme 4 were proved by using gas-uptake techniques, NMR spectroscopy, mass-balance, and the isolation of intermediate products (188, 189). The first step involves very fast complexation with AlEt_3 accompanied, by alkylation of zirconium. The ethylation step is followed by further complexing by condensation, with subsequent β -hydrogen transfer leading to compounds 4, 5, and 6. The reactions affording 6 are very slow and can only be observed at temperatures above 40°C . Time-concentration curves could be simulated on the basis of reaction rates by analog computer within a very narrow range. However, this is not a mechanistic proof having the stringency of the kinetic studies.



SCHEME 4. Side reactions in the zirconium system.

There is as yet no satisfactory explanation for alkane evolution other than β -hydrogen transfer. Studies with partially labeled compounds, as well as on the kinetics of the isotope ratio, prove this transfer. The species $\text{CH}_2\text{D}\cdot\text{CD}_3$ is generated by using $\text{Al}(\text{CH}_2\text{CD}_3)_3$, and $\text{CH}_3\cdot\text{CD}_2\text{H}$ by using $\text{Al}(\text{CD}_2\text{CH}_3)_3$ (187). The kinetic isotopic effects of the reactions are between 2 and 7, in agreement with the values found in the titanium system (151, 190). The intermediate steps with $\text{Zr}\cdot\text{CH}_2\cdot\text{CH}\cdot\text{Al}_2$ structures have been confirmed not only through characteristic shifts in the PMR spectra (191), but also by the abnormal bond angles and lengths obtained from X-ray studies (see Fig. 17). The carbon-carbon angle of the σ -bonded $\text{CH}_2\text{—CH}_2$ bridge between the zirconium atoms (compound 4 in Scheme 4) is only 76° (192). Compound 6 shows a similarly narrow carbon-carbon angle of 75° for the $\text{Zr}\cdot\text{CH}_2\cdot\text{CH}\cdot\text{Al}$ structure also, but the carbon-aluminum angle is greatly expanded (193). The unusual angle for this compound can be explained in terms of a stretched five-membered heteroring type. The β -C atom distance to zirconium is only slightly longer than that of the α -C atom; this is possibly a reason for the easy

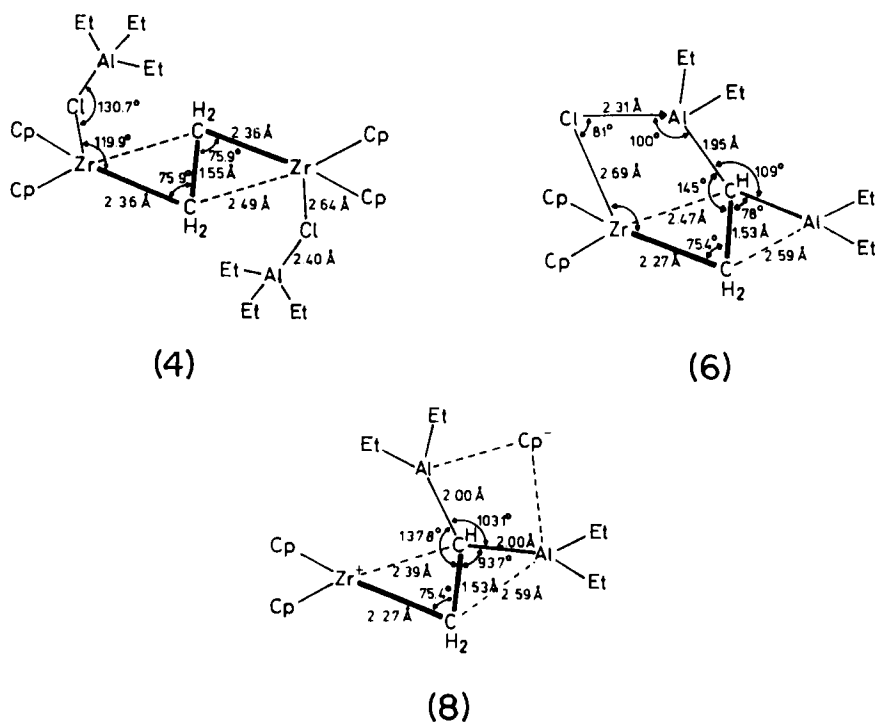


FIG. 17. Comparison of corresponding structural elements of compounds 3, 6, and 8.

release of hydrogen bonded at a β -C atom. In compound **6**, the bridge-building chlorine ligand with its donor function is replaced by a cyclopentadienyl ligand to form compound **8**. In addition to the similarly narrow angle at the zirconium, compound **8** shows a remarkable arrangement for the third cyclopentadienyl ring, completely deviating from the σ - or π -bonding cyclopentadienyl rings in bis(η^5 -cyclopentadienyl)bis-(η^1 -cyclopentadienyl)titanium(IV) (194), and (η^1 -cyclopenta-2,4-dien-1-yl)tris(η^5 -cyclopentadienyl)zirconium(IV) (195). It is removed from Zr(IV)^+ as an anion, and arranged symmetrically in the lattice between two neighboring zirconium centers.

Besides compound **8**, a further remarkable zirconium-aluminum compound (**9**) can be isolated, which is derived from tetra(cyclopentadienyl)-zirconium. The tris(cyclopentadienyl)zirconium(IV) is linked with the trialkylaluminum by a hydrogen atom (see Fig. 18).

Compounds **4** and **6** react with α -olefins and 1,3-dienes on addition of excess trimethylaluminum, and especially on addition of triethylaluminum and water. Dehalogenation takes place, presumably with formation of aluminoxanes (129), to give very active halogen-free homogeneous catalysts for the polymerization of α -olefins, particularly ethylene (see Section VII).

C. The Titanium System

Based on these findings with the zirconium system, mechanisms of reaction in the analogous titanium system (Scheme 5) can be deduced.

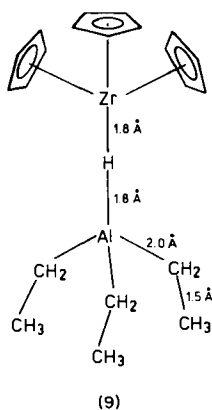
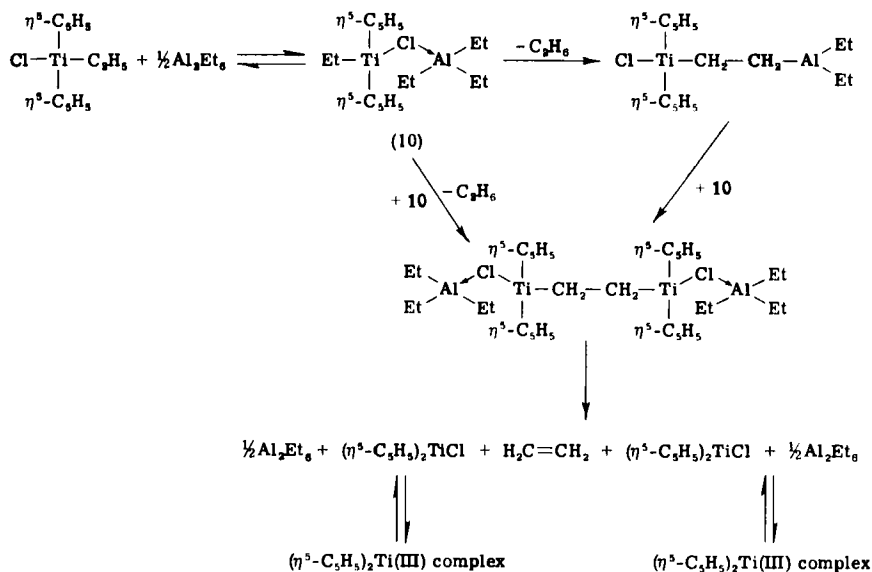


FIG. 18. Structural unit of compound **9**.



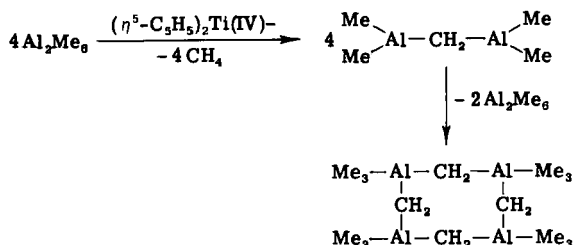
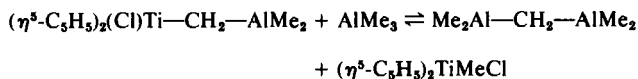
SCHEME 5. Reactions in the titanium systems.

The rate of reaction of the titanium system is ~ 100 times that of the zirconium. The titanium components instantaneously form a complex with AlEt_3 , even at -100°C . After complex formation, the dititanium-ethylene structure is formed by alkane splitting; this compound is very unstable and decomposes with ethylene generation and reduction of the central atom. At room temperature, the titanium(IV) compounds are reduced to the trivalent state within seconds. The rate decreases with increasing number of carbon atoms of the alkyl substituents (119). The prediction that the evolution of ethane starts earlier than that of ethylene is fulfilled (164). In a parallel reaction, an intermediate $\text{Ti-CH}_2\text{-CH}_2\text{-Al}$ structure is also formed from the complex. Through alkyl exchange, a dititanium structure appears; this decomposes along the reaction path by renewed ethylene splitting into trivalent components, as already mentioned.

It is remarkable that a reduced Ziegler type of catalyst that is no longer reactive for ethylene polymerization causes the exchange between ^{14}C -labeled ethylene and the alkyl groups of the triethylaluminum until the equilibrium point is reached. The intermediate structures mentioned were only detected spectroscopically; because of their low stability, they were not isolated.

The α -hydrogen transfer in the analogous titanium-methyl system is

$\sim 10,000$ times slower than the β -hydrogen transfer. Therefore, bis(cyclopentadienyl)dimethyltitanium can be isolated from the starting materials. $\text{Ti}-\text{CH}_2-\text{Al}$ structures, which are relatively stable, are formed with methane evolution. The condensation, however, does not stop at this point. Thus $\text{Al}-\text{CH}_2-\text{Al}$ structures form because of the alkyl exchange (142, 119, 196). These structures again condense under the catalytic influence of $(\text{C}_5\text{H}_5)_2\text{Ti(IV)}$ compounds to yield cyclic oligomer aggregations by separation of trimethylaluminum. Similar results were obtained by Wilke and Schneider (197) when aluminoadamantane was formed.



These compounds are insoluble in hydrocarbons, but soluble in tetrahydrofuran.

VII

INFLUENCE OF WATER ON HOMOGENEOUS CATALYSTS

A. Increase of Activity

Water was considered to be a catalyst poison for many Ziegler-type systems such as TiCl_3 and $(\text{C}_2\text{H}_5)_3\text{Al}$ (192). On the other hand, some patents have been granted for adding water in order to lower the molecular weights and to improve the molecular-mass distribution (199-201). Reichert and Meyer (202) observed a remarkable rise of activity on addition of water to an $\text{Al}:\text{H}_2\text{O}$ ratio of 20 and 100, when polymerizing ethylene with the soluble-catalyst system $(\eta^5\text{-C}_5\text{H}_5)_2\text{Ti}(\text{C}_2\text{H}_5)\text{Cl}-(\text{C}_2\text{H}_5)_3\text{AlCl}_2$. By addition of water in the $\text{Al}:\text{H}_2\text{O}$ ratio of 3:1, Long and Breslow (125) obtained considerable increases in activity for ethylene

polymerization with the catalyst $(\eta^5\text{-C}_5\text{H}_5)_2\text{TiCl}_2\text{-AlMe}_2\text{Cl}$. These workers proposed a stabilized catalyst complex resulting from increase of the Lewis acidity (see Fig. 19).

In systems completely free of chloride, complex formation between the titanium or zirconium compound and the trialkylaluminum was not detected by either NMR or UV spectroscopy (191), or by cryoscopy (189). Such systems were thus assumed to be inactive for polymerization. However, NMR-spectroscopic studies in the presence of ethylene revealed a weak but lasting insertion of ethylene, with formation of polyethylene.

Addition of traces of chloride in the form of bis(cyclopentadienyl)-titanium dichloride lowered the yield of polyethylene and initiated the known reduction reaction (129). Finally, it was found that polyethylene formation was caused by traces of water ($\sim 10^{-6}$ mol%). Consequently, the yield increased to 500,000 g polyethylene per gram of titanium when two equivalents of trimethyl- or triethylaluminum previously treated with one equivalent of water was added to dimethylbis(cyclopentadienyl)titanium (Table VII).

Simple control of molecular weight by choice of temperature proved to be another advantage of this soluble, halogen-free system (203). Polymers can be produced having molecular masses up to about 4 million, with high melting points ($136\text{--}137^\circ\text{C}$), down to linear even-numbered α -olefins, starting with C_{10} . Interestingly, compounds formed from bis(cyclopentadienyl)zirconium(IV) and exhibiting no polymerization activity, even in the case of completely dehalogenated secondary products (34), can also become very active polymerization catalysts by addition of trialkylaluminum previously treated with water. These systems additionally excel in that products having relative masses between a few million and a few hundred can be generated, with almost constant activity, by suitable choice of reaction temperature (see Table VIII).

Mejzlik *et al.* (204) reported an increase of activity on adding water to other well-known catalytic systems based on bis(cyclopentadienyl)-titanium(IV) containing chloride $[(\eta^5\text{-C}_5\text{H}_5)_2\text{TiEtCl-AlEtCl}_2]$.

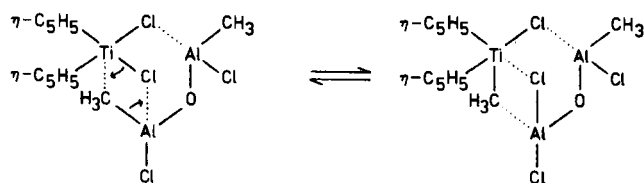


FIG. 19. Stabilized catalyst complex. From Mejzlik and co-workers (204).

TABLE VII
ETHYLENE POLYMERIZATION WITH THE SYSTEM BIS(η^5 -CYCLOPENTADIENYL)DIMETHYLTITANIUM(IV), TRIMETHYLALUMINUM, AND
WATER IN TOLUENE

Yield of polyethylene (g/liter)	Catalyst yield (kg PE/mol Ti)	Activity $\left(\frac{\text{kg PE}}{\text{mol Ti} \cdot \text{h} \cdot \text{bar}}\right)$	Time (h)	Temperature (°C)	Pressure (bar)	Relative molecular weight (viscometric)	[Ti] (M)	[Al] (M)	[H ₂ O] (M)
12.9	>6.5	1.1	2	-10	3	—	$2.0 \cdot 10^{-3}$	$1.5 \cdot 10^{-2}$	—
11.7	>5.9	1.0	2	-10	3	—	$2.0 \cdot 10^{-3}$	$1.5 \cdot 10^{-2}$	^a
7.8	>3.9	0.7	2	-10	3	—	$2.0 \cdot 10^{-3}$	$1.5 \cdot 10^{-2}$	^b
33.6	>47.3	0.06	112	21	7	3,800,000	$7.1 \cdot 10^{-4}$	$1.5 \cdot 10^{-2}$	$<2.5 \cdot 10^{-4}$
36.0	>510	48.0	1.5	21	7	235,000	$7.1 \cdot 10^{-5}$	$1.5 \cdot 10^{-2}$	$7.4 \cdot 10^{-3}$
57.9	>160	15.3	1.5	50	7	90,000	$3.6 \cdot 10^{-4}$	$1.5 \cdot 10^{-2}$	$7.4 \cdot 10^{-3}$
62.7	>170	16.0	1.5	70	7	30,000	$3.6 \cdot 10^{-4}$	$1.5 \cdot 10^{-2}$	$7.4 \cdot 10^{-3}$
48.6	>46,000	3,000	2	12	8	—	$1.5 \cdot 10^{-6}$	$1.2 \cdot 10^{-2}$	$7.4 \cdot 10^{-3}$

^a Addition at $2.0 \cdot 10^{-5}$ M chloride.

^b Addition at $4.0 \cdot 10^{-5}$ M chloride.

TABLE VIII
CONTROL OF MOLECULAR WEIGHT BY REGULATION OF TEMPERATURE IN THE
POLYMERIZATION OF ETHYLENE WITH TRI(CYCLOPENTADIENYL)ZIRCONIUM-
ALUMINUM COMPOUNDS

Yield of polyethylene (g/liter)	Time (h)	Temperature (°C)	Zirconium concentration (M)	Relative molecular weight (viscometric)
81	64	50	$2.2 \cdot 10^{-3}$	1,500,000
45	48	60	$2.2 \cdot 10^{-3}$	363,000
45	64	70	$2.2 \cdot 10^{-3}$	225,000
90	88	80	$2.2 \cdot 10^{-3}$	40,000
80	64	90	$2.2 \cdot 10^{-3}$	Oils and waxes ^a

^a Predominantly α -olefins of empirical formula $C_{2n}H_{4n}$ ($n = 2, 3, 4, \dots$).

B. Titanium-Aluminoxane Catalysts

Preliminary experiments showed a maximum activity at an Al:H₂O ratio of between 2:1 and 5:1. Water and trialkylaluminum react with each other, because the activity disappears if the Al:H₂O ratio drops below 1:3, i.e., all alkyl groups are hydrolyzed (34).

Detailed investigations on the influence of water, and on the reactions between water and organoaluminum species showed that an oligomeric aluminoxane formed from water and trimethylaluminum contains the structure $[-O-Al(Me)-]_n$ (190). The first links of the oligomeric aluminoxanes condense, with the elimination of trialkylaluminum and the build-up of oligomers probably having cyclic structures. These are soluble in hydrocarbons and contain 5–12 aluminum atoms. Essentially uniform glassy or crystalline aluminoxanes can be isolated by fractional precipitation, and characterized by mass spectroscopy and cryoscopy (see Fig. 20). This condensation is comparable to the self-condensation of bis(dialkyl)aluminumalkanes (see Section VI).

Aluminoxanes have long been known to act as catalysts for propene oxide and acetaldehyde polymerization (205–207). Polyakov *et al.* (208) reported an increase of activity after addition of alkylaluminoxanes to a known heterogeneous Ziegler system based on TiCl₃. If these oligomeric aluminoxanes are added, as the organoaluminum component to bis(cyclopentadienyl)dimethyltitanium, very active Ziegler catalysts are obtained. These catalysts are able to polymerize propylene, in contrast to the systems wherein only water is added to the aluminum compound. With this system, the productivity for ethylene was found to be $\sim 1,000,000$ (line 8 in Table VII). Fortunately, similar systems based on well

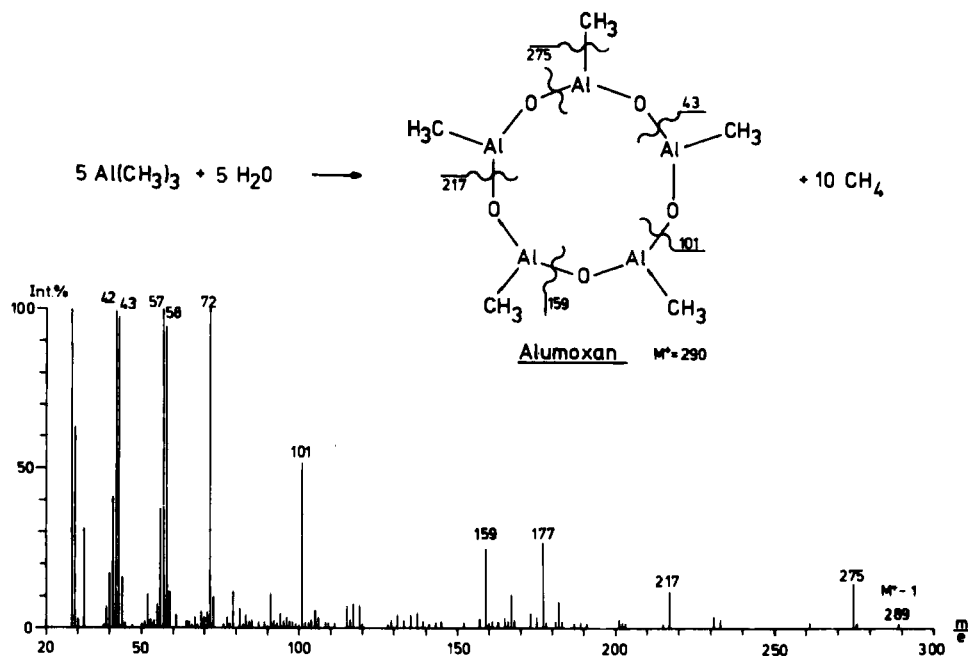


FIG. 20. Cyclic aluminoxane isolated by fractional precipitation, and characterized by mass spectroscopy.

defined oligomeric aluminoxanes (see Table IX) are active for ethylene as well as propylene, thus forming, in the case of propylene a reaction that is homogeneous for at least several hours. Unfortunately, total homogeneity during the whole reaction time could not be proved. Although the activity can differ by a factor of ~ 50 , differences in activity may be compensated for by variation of the concentration of the monomers (e.g., by using liquid propylene and low pressures of ethylene); this allows copolymerization to occur. During several hours, no aging processes were observed, and, in particular, no reduction comparable with those observed in halogen-containing systems was found (see Fig. 21).

After an induction period, the polymerization rate reaches a maximum and then becomes almost constant for over 20 hours. The constant rate of polymerization of the homogeneous system indicates that living polymers are present in this case. Indeed, block copolymers of propylene and ethylene could be obtained with this homogeneous system when ethylene was dissolved in liquid propylene [see also, related experiments with the heterogeneous system (31)].

TABLE IX
POLYMERIZATION OF ETHYLENE, PROPYLENE, AND ETHYLENE-PROPYLENE WITH $(\eta^5\text{-C}_5\text{H}_5)_2\text{Ti}(\text{CH}_3)_2$ -ALUMINOXANE AS CATALYST

Polymer yield (g)	Catalyst yield ^a (kg PE/PP/mol Ti)	Activity $\left(\frac{\text{kg PE}}{\text{mol Ti}\cdot\text{h}\cdot\text{bar}}\right)$	Time (h)	Temperature (°C)	Pressure (bar)	Relative molecular weight (viscometric)	[Ti] (mol)	[Al] (mol)	Remarks
34.7 PE	>1,650	103	2	25	8 E	200,000	$2.1\cdot 10^{-5}$	$3.6\cdot 10^{-3}$	300 ml toluene
36.0 PE	>1,710	107	2	50	8 E	160,000	$2.1\cdot 10^{-5}$	$3.6\cdot 10^{-3}$	300 ml toluene
40.2 PE	>3,350	209	2	20	8 E	980,000	$1.2\cdot 10^{-5}$	$2.1\cdot 10^{-3}$	“Gas-phase polymerization”
40.0 PP	>1,667	—	168	20	8 P	88,000	$2.4\cdot 10^{-5}$	$1.9\cdot 10^{-3}$	50 ml toluene
18.0 PP	>1,500	—	76	10	9.5 P	94,000	$1.2\cdot 10^{-5}$	$1.5\cdot 10^{-3}$	Polymerization in liquid propene
80.0 PE/PP	>6,667	—	48	20	7.5 P + 1.5 E	$[\eta] = 1.19$	$1.2\cdot 10^{-5}$	$1.8\cdot 10^{-3}$	50 ml toluene
35.5 PE/PP	>1,480	—	168	11	8 P + 3 E	$[\eta] = 0.94$	$2.4\cdot 10^{-5}$	$1.8\cdot 10^{-3}$	Polymerization in liquid monomer mixture

^a The yields are markedly increased using aluminoxanes with cryoscopic molecular weights of about 500–800, and an $(\eta^5\text{-C}_5\text{H}_5)_2\text{Zr}(\text{CH}_3)_2$ activity of up to 10^5 (kg PE/mol Zr·h·bar) is found with a productivity of up to 10^7 kg PE/mol Zr.

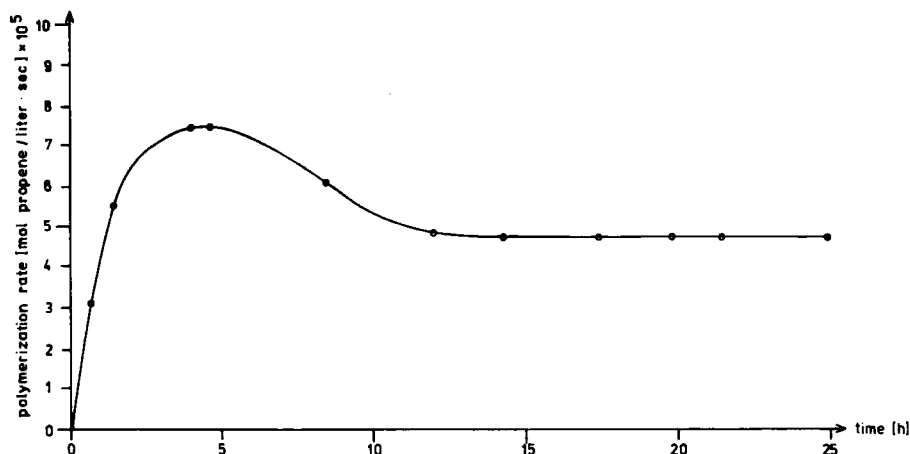


FIG. 21. Polymerization rate versus time at constant propene concentration (4 bar): $[\text{Ti(IV)}]_0 = 2.4 \cdot 10^{-4} \text{ M}$, $[\text{aluminoxane}] = 1.75 \cdot 10^{-2} \text{ M}$, temperature = 294K; solvent = toluene.

If the catalyst solution is mixed with polyethylene and the solvent removed, "gas-phase polymerization" takes place after addition of ethylene (see Table IX).

REFERENCES

1. K. Ziegler, E. Holzkamp, H. Martin, and H. Breil, *Angew. Chem.* **67**, 541 (1955).
2. K. Ziegler, Belgian Patent 533,362 (1954).
3. H. Rudolph, W. Trautvetter, and K. Weirauch, In "Chemische Technologie," (K. Winnacker and L. Küchler, eds.), Vol. 5, p. 60. Carl Hanser, Munich, 1972.
4. G. Natta, *J. Polym. Sci.* **16**, 143 (1955).
5. G. Natta, *Angew. Chem.* **68**, 393 (1956).
6. H. Pracejus, "Koordinationschemische Katalyse Organischer Reaktionen," Verlag Theodor Steinkop, Dresden, 1977.
- 6a. J. Boor, "Ziegler-Natta Catalysts and Polymerizations," Academic Press, New York, 1979.
7. A. D. Caunt, in "Catalysis" (C. Kemball, ed.), Vol. 1, p. 234. Chem. Soc., London, 1977.
8. T. Keii, "Kinetics of Ziegler-Natta Polymerization," Kodansha Ltd., Tokyo, and Chapman & Hall, Ltd., London, 1972.
9. J. C. W. Chien (ed.), "Coordination Polymerization," Academic Press, New York, 1975.
10. A. Zambelli, A Few Considerations on Stereoregular Propylene Polymerization, in Ref. 9, p. 15.
11. P. Pino, A. Oschwald, F. Ciardelli, C. Carlini, and E. Chiellini, Stereoselection and Stereoelection in α -Olefin Polymerization, in Ref. 9, p. 25.
12. H. Schnecko, K. A. Jung, and W. Kern, The Number of Active Sites for the Polymerization of Ethylene, Propylene, and Butene-1 by Ziegler-Natta Catalysts, in Ref. 9, p. 73.

13. Yu. I. Yermakov and V. A. Zakharov, The Number of Propagation Centers in Solid Catalysts for Olefin Polymerization and Some Aspects of Mechanism of Their Action, *in* Ref. 9, p. 91.
14. S. Fuji, Ethylene Polymerization with the Catalysts of One- and Two-Component Systems Based on Titanium Trichloride Complex, *in* Ref. 9, p. 135.
15. P. J. T. Tait, A Kinetic Model for Heterogeneous Ziegler-Natta Polymerization, *in* Ref. 9, p. 155.
16. F. S. Dyachkovskii, Homogeneous Complex Catalysts of Olefin Polymerization, *in* Ref. 9, p. 199.
17. D. G. H. Ballard, Transition Metal Alkyl Polymerization Catalysts, *in* Ref. 9, p. 223.
18. T. Keii, A Kinetic Approach to Elucidate the Mechanism of Ziegler-Natta Polymerization, *in* Ref. 9, p. 263.
19. G. Henrici-Olivé and S. Olivé, Chain Transfer in Ziegler Type Polymerization of Ethylene, *in* Ref. 9, p. 291.
20. J. C. W. Chien and J. T. T. Hsieh, Supported Ziegler-Natta Catalysts, *in* Ref. 9, p. 305.
21. P. Teyssié, M. Julémont, J. M. Thomassin, E. Walckiers, and R. Warin, Stereospecific Polymerization of Diolefins by η^3 -Allylic Coordination Complexes, *in* Ref. 9, p. 327.
22. J. Boor, *Polym. Prepr. Am. Chem. Soc. Div. Polym. Chem.* **15**, 359 (1974).
23. D. G. H. Ballard, E. Jones, R. J. Wyatt, R. T. Murray, and P. A. Robinson, *Polymer* **15**, 169 (1974).
24. A. D. Pomogailo, A. P. Lisitskaya, N. S. Gorkova, and F. S. Dyachkovskii, *Dokl. Akad. Nauk SSSR, Ser. Khim.* **219**, 1375 (1974).
25. B. Diedrich, *Polym. Prepr. Am. Chem. Soc. Div. Polym. Chem.* **16**, 316 (1975).
26. B. Diedrich, *Appl. Polym. Symp.* **26**, 1 (1975).
27. K. Weissmermel, H. Cherdron, J. Berthold, B. Diedrich, K. D. Keil, K. Rust, H. Strametz, and T. Toth, *J. Polym. Sci. Polym. Symp.* **51**, 187 (1975).
28. Anon. *Plastica* **28**, 312 (1975).
29. J. C. W. Chien and J. T. T. Hsieh, *J. Polym. Sci. Polym. Chem. Ed.* **14**, 1915 (1976).
30. H. Wesslau, *Makromol. Chem.* **20**, 111 (1956).
31. G. Bier, *Angew. Chem.* **73**, 186 (1961).
32. A. Clark, *Ind. Eng. Chem.* **59**, 29 (1967).
33. H. W. Ullrich, Ph.D. Thesis, University of Hamburg (1977).
34. A. Andresen, H. G. Cordes, J. Herwig, W. Kaminsky, A. Merck, R. Mottweiler, J. Pein, H. Sinn, and H. Vollmer, *Angew. Chem. Int. Ed. Engl.* **15**, 630 (1976).
35. A. S. Matlack and D. S. Breslow, *J. Polym. Sci. Part A* p. 2853 (1965).
36. T. Suzuki, S. I. Izuka, J. Kondo, and Y. Takegami, *J. Macromol. Sci. Chem.* **11**, 3, 633 (1977).
37. J. G. Lee and C. H. Brubaker, Jr., *J. Organomet. Chem.* **135**, 115 (1977).
38. H. Kreuter and B. Diedrich, *Chem. Eng. (N. Y.)* **81**, 62 (1974).
39. D. M. Rasmussen, *Chem. Eng. (N.Y.)* **79**, 104 (1972).
40. K. H. Reichert, *Chem. Ing. Tech.* **49**, 626 (1977).
41. G. Scott, "Atmospheric Oxidation and Antioxidants." Elsevier, Amsterdam, 1965.
42. J. Voigt, *in* "Chemie, Physik und Technologie der Kunststoffe," (K. A. Wolf, ed.), Vol. 10. Springer Verlag, Berlin and New York, 1966.
43. K. Wisseroth, *Chem. Ztg.* **101**, 271 (1977).
44. J. Fischmann, R. Thiele, K. Lucas, and D. Lehmann, *Plaste Kautsch* **23**, 632 (1976).
45. C. McGreavy, *J. Appl. Chem. Biotechnol.* **22**, 747 (1972).
46. W. R. Schmeal and J. R. Street, *J. Polym. Sci. Polym. Phys. Ed.* **10**, 2173 (1972).
47. B. Boucheron, B. Levresse, and J. P. Machon, *Eur. Polym. J.* **9**, 1095 (1973).

48. B. Boucheron, *Eur. Polym. J.* **11**, 131 (1975).
49. H. Meyer and K. H. Reichert, *Angew. Makromol. Chem.* **57**, 211 (1977).
50. W. Cooper, in "Comprehensive Chemical Kinetics" (C. H. Bamford and C. F. H. Tipper, eds.), Vol. 15. Elsevier, Amsterdam, 1976.
51. J. Herwig, Ph.D. Thesis, University of Hamburg (1979).
52. G. Natta, J. Pasquon, and A. Zambelli, *J. Am. Chem. Soc.* **84**, 1488 (1962).
53. Y. Doi, J. Kinoshita, A. Morinaga, and T. Keii, *J. Polym. Sci. Polym. Chem. Ed.* **13**, 2491 (1975).
54. A. Zambelli, G. Gatti, C. Sacchi, W. O. Crain, Jr., and J. D. Roberts, *Macromolecules* **4**, 475 (1971).
55. A. Zambelli, *Fortschr. Hochpolym. Forsch.* **15**, 31 (1974).
56. P. Longi, G. Mazzanti, A. Roggero, and M. P. Lachi, *Makromol. Chem.* **61**, 63 (1963).
57. Y. Takegami, T. Suzuki, and T. Okazaki, *Bull. Chem. Soc. Jpn.* **42**, 1060 (1969).
58. T. Miyazawa and T. Ideguchi, *J. Polym. Sci., Part B* p. 389 (1963).
59. G. Natta, M. Farina, and M. Peraldo, *Chim. Ind. (Milan)* **42**, 255 (1960).
60. P. Locatelli, A. Immirzi, A. Zambelli, R. Palumbo, and G. Maglio, *Makromol. Chem.* **176**, 1121 (1975).
61. L. A. Rishina, Yu. V. Kissin, and F. S. Dyachkovskii, *Eur. Polym. J.* **12**, 727 (1976).
62. E. Chiellini and M. Marchetti, *Makromol. Chem.* **169**, 59 (1973).
63. A. Oschwald, Dissertation, E. T. H. Zürich (1974).
64. C. Carlini, R. Nocci, and F. Ciardelli, *J. Polym. Sci. Polym. Chem. Ed.* **15**, 767 (1977).
65. P. Cossee, in "Stereochemistry of Macromolecules" (D. Ketley, ed.), Vol. I, p. 145. Dekker, New York, 1967.
66. E. J. Arlman, *J. Catal.* **5**, 178 (1966).
67. G. Henrici-Olivé and S. Olivé, "Polymerisation—Katalyse, Kinetik, Mechanismen." Verlag Chemie, Weinheim, 1969.
68. P. Cossee, *Rec. Trav. Chim. Pays-Bas* **85**, 1151 (1966).
69. L. A. M. Rodriguez and H. M. van Looy, *J. Polym. Sci. Part A-1*, **4**, 1971 (1966).
70. R. T. K. Baker, P. S. Harris, and R. J. Waite, *J. Polym. Sci. Polym. Lett. Ed.* **11**, 45 (1973).
71. I. L. Dubnikova and I. N. Meskova, *Vysokomol. Soedin., Ser. A* **19**, 1101 (1977).
72. M. Nowakowska and H. Maciejewska, *Polimery* **21**, 103 (1976).
73. V. S. Štejnbaek, V. V. Amerik, F. J. Jakobson, Ju. V. Kissin, D. V. Ivanjukov, and B. A. Krencel, *Vysokomol. Soedin. Ser. A* **18**, 111 (1976).
74. J. Mejzlik, L. Vilimová, and M. Lesná, *Chem. Prum.* **27**, 53 (1977).
75. K. Shikata, H. Osawa, and Y. Kida, *J. Polym. Sci. Polym. Chem. Ed.* **14**, 2565 (1976).
76. G. D. Bukatov, N. B. Chumaevskii, V. A. Zakharov, G. I. Kuzentsova, and Yu. I. Yermakov, *Makromol. Chem.* **178**, 953 (1977).
77. V. A. Zakharov, N. B. Chumaevskii, G. D. Bukatov, and Yu. I. Yermakov, *Makromol. Chem.* **177**, 763 (1976).
78. Y. Doi, T. Kohara, H. Koiwa, and T. Keii, *Makromol. Chem.* **176**, 2159 (1975).
79. K. Hashimoto, S. Watanabe, and K. Tarama, *Bull. Chem. Soc. Jpn.* **49**, 12 (1976).
80. O. Novaro, S. Chow, and P. Magnouat, *J. Polym. Sci. Polym. Lett. Ed.* **13**, 761 (1975).
81. P. Cossee, *Tetrahedron Lett.* p. 12 (1960).
82. Yu. I. Yermakov and V. A. Zakharov, *Usp. Khim.* **41**, 377 (1972).
83. J. Mejzlik and M. Lesná, *Vysokomol. Soedin. Ser. B* **15**, 7 (1973).
84. E. W. Duck, D. Grant, A. V. Butcher, and G. D. Timms, *Eur. Polym. J.* **10**, 77 (1974).
85. E. J. Arlman, *J. Catal.* **3**, 89 (1964).
86. E. J. Arlman and P. Cossee, *J. Catal.* **3**, 99 (1964).

87. Yu. I. Yermakov, Monometallic Active Centers, in Ref. 9, especially p. 113.
88. V. A. Zakharov, G. D. Bukatov, N. B. Chumaevskii, and Yu. I. Yermakov, *Makromol. Chem.* **178**, 967 (1977).
89. N. B. Chumaevskii, V. A. Zakharov, G. D. Bukatov, G. I. Kuznetzova, and Yu. I. Yermakov, *Makromol. Chem.* **177**, 747 (1976).
90. H. Hopff and M. Balint, *Polym. Prepr. Am. Chem. Soc. Div. Polym. Chem.* **16**, 324 (1975).
91. M. Fischer (to BASF), West German Patent 874,215 (1963).
92. Hoechst, Belgian Patent 702 472, 702 473 (1966).
93. H. L. Krauss and H. Stach, *Z. Anorg. Allg. Chem.* **366**, 280 (1969).
94. D. R. Armstrong, R. Fortune, and P. G. Perkins, *J. Catal.* **42**, 435 (1976).
95. To Union Carbide, U.S. Patents 3,324,101, 3,324,095 (1963).
96. W. L. Carrick, R. J. Trubett, F. J. Karol, G. L. Karapinka, A. S. Fox, and R. N. Johnson, *J. Polym. Sci. Part A-1*, **10**, 2609 (1972).
97. D. D. Eley, D. A. Keir, and R. Rudham, *J. Chem. Soc. Faraday Trans. 1* **72**, 2, 1685 (1976).
98. K. Soga, S. Katano, Y. Akimoto, and T. Kajiya, *Polym. J.* **5**, 128 (1973).
99. J. C. W. Chien and J. T. T. Hsieh, *J. Polym. Sci.* **14**, 1915 (1976).
100. Solvay, Belgian Patent 650,679 (1963).
101. Hoechst, Belgian Patent 735,290 (1968).
102. Hoechst, Belgian Patent 735,291 (1968).
103. Mitsui Petrochemicals, Japanese Patent 7,040,295 (1967).
104. Solvay, Belgian Patent 726,839 (1968).
105. Montecatini, Belgian Patent 728,002 (1968).
106. Hoechst, Belgian Patent 735,291 (1968).
107. Hoechst, Belgian Patent 743,325 (1969).
108. Hoechst, Belgian Patent 758,994 (1969).
109. Hoechst, Belgian Patent 780,530 (1971).
110. Montecatini, Belgian Patent 747,846 (1969).
111. Hoechst, Belgian Patent 755,185 (1969).
112. T. Petrova, *Eur. Polym. J.* **12**, 571 (1976).
113. A. A. Baulin, L. F. Salaeva, and S. S. Ivančev, *Dokl. Akad. Nauk, SSSR* **231**, 413 (1976).
114. A. D. Pomogajlo, D. A. Krickaja, A. P. Lisickaja, A. N. Ponomarev, and F. S. Dyachkovskii, *Dokl. Akad. Nauk. SSSR* **232**, 391 (1977).
115. A. A. Baulin and S. S. Ivančev, *Plast. Massy* **12**, 22 (1976).
116. F. J. Karol, *Polym. Prepr. Am. Chem. Soc. Div. Polym. Chem.* **18**, 853 (1977).
117. F. J. Karol, *Am. Chem. Soc. Div. Org. Coat. Plast. Chem. Pap.* **37**, 310 (1977).
118. T. S. Dzabiev, F. S. Dyachkovskii, and A. E. Shilov, *Vysokomol. Soedin. Ser. A* **13**, 2474 (1971).
119. E. Heins, H. Hinck, W. Kaminsky, G. Oppermann, P. Raulinat, and H. Sinn, *Makromol. Chem.* **134**, 1 (1970).
120. J. Boor, *Ind. Eng. Chem. Prod. Res. Dev.* **9**, 437 (1970).
121. J. A. Waters and G. A. Mortimer, *J. Polym. Sci. Part A-1*, **10**, 895 (1972).
122. K. H. Reichert and K. R. Meyer, *Kolloid-Z.* **232**, 711 (1969).
123. G. Fink, *Polym. Prepr. Am. Chem. Soc. Div. Polym. Chem.* **16**, 327 (1975).
124. K. R. Meyer and K. H. Reichert, *Angew. Makromol. Chem.* **12**, 175 (1970).
125. W. P. Long and D. S. Breslow, *Justus Liebigs Ann. Chem.* p. 463 (1975).
126. J. C. W. Chien, *J. Am. Chem. Soc.* **81**, 86 (1959).
127. D. S. Breslow and N. R. Newburg, *J. Am. Chem. Soc.* **81**, 81 (1959).

128. K. H. Reichert and K. R. Meyer, *Makromol. Chem.* **169**, 163 (1973).
129. H. Sinn and W. Kaminsky, *Makromol. Kolloid., Freiburg* 1978.
130. C. E. H. Bawn and R. Symcox, *J. Polym. Sci.* **34**, 139 (1959).
131. G. Henrici-Olivé and S. Olivé, *Angew. Chem.* **83**, 782 (1971).
132. G. L. Karapinka and W. L. Carrick, *J. Polym. Sci.* **55**, 145 (1961).
133. G. Wilke, B. Bogdanovic, P. Hardt, P. Heimbach, W. Keim, M. Kröner, W. Oberkirch, K. Tanaka, E. Steinrücke, D. Walter, and H. Zimmermann, *Angew. Chem.* **78**, 157 (1966).
134. U. Gianinni, U. Zuchini, and E. Albizzati, *Polym. Lett.* **8**, 405 (1970).
135. D. G. H. Ballard and P. W. van Lienden, *Makromol. Chem.* **154**, 177 (1972).
136. D. G. H. Ballard, *Adv. Catal.* **23**, 263 (1973).
137. V. K. Vasilev, V. N. Sokolov, and G. P. Kondratenkov, *Dokl. Akad. Nauk SSSR* **238**, 360 (1977).
138. G. Lugli, A. Mazzei, and S. Poggio, *Makromol. Chem.* **175**, 2021 (1974).
139. D. S. Breslow, U.S. Patent 2,827,446 (1958).
140. G. Natta, P. Pino, P. Corradini, F. Danusso, E. Mantica, G. Mazzanti, and G. Moraglio, *J. Am. Chem. Soc.* **77**, 1708 (1955).
141. G. Natta, *J. Nucl. Inorg. Chem.* **49**, 1885 (1955).
142. G. P. Belov, V. I. Kuznetsov, T. I. Solovyeva, N. M. Chirkov, and S. S. Ivanchev, *Makromol. Chem.* **140**, 213 (1970).
143. G. P. Belov, V. N. Belova, L. N. Raspopov, Yu. V. Kissin, A. Brikenshtein, and A. M. Chirkov, *Polym. J.* **3**, 681 (1972).
144. A. B. Agasaryan, G. P. Belov, S. P. Davtyan, and M. L. Eritsyan, *Eur. Polym. J.* **11**, 549 (1975).
145. F. Patat, *Monatsh. Chem.* **88**, 560 (1957).
146. F. Patat and H. Sinn, *Angew. Chem.* **70**, 496 (1958).
147. H. Sinn, H. Hinck, F. Bandermann, and H. F. Grützmacher, *Angew. Chem.* **80**, 190 (1968).
148. A. E. Shilov, *Dokl. Akad. Nauk SSSR* **132**, 599 (1960).
149. F. S. Dyachkovskii, A. K. Shilova, and A. E. Shilov, *J. Polym. Sci.* **16** 2333 (1967).
150. Yu. G. Borodko, E. F. Kyashina, V. B. Panov, and A. E. Shilov, *Kinet. Katal.* **14**, 255 (1973).
151. E. H. Adema, *J. Polym. Sci.* **16**, 3643 (1969).
152. K. Clauss and H. Bestian, *Justus Liebigs Ann. Chem.* **654**, 8 (1962).
153. G. Henrici-Olivé and S. Olivé, *J. Organomet. Chem.* **16**, 339 (1969).
154. K. H. Reichert and E. Schoetter, *Z. Phys. Chem.* **57**, 74 (1968).
155. G. Fink, *Polym. Prepr. Am. Chem. Soc. Div. Polym. Chem.* **13**, 443 (1972).
156. G. Natta, P. Corradini, and I. W. Bassi, *J. Am. Chem. Soc.* **80**, 755 (1958).
157. W. P. Long, *J. Am. Chem. Soc.* **81**, 5312 (1959).
158. W. P. Long and D. S. Breslow, *J. Am. Chem. Soc.* **82**, 1953 (1960).
159. G. Henrici-Olivé and S. Olivé, *Angew. Chem.* **79**, 764 (1967).
160. G. Fink, R. Rottler, D. Schnell, and W. Zoller, *J. Appl. Polym. Sci.* **20**, 2779 (1976).
161. C. Beermann and H. Bestian, *Angew. Chem.* **71**, 618 (1959); D. S. Breslow, *J. Am. Chem. Soc.* **79**, 507 (1957).
162. D. S. Breslow and N. R. Newburg, *J. Am. Chem. Soc.* **79**, 5072 (1957).
163. H. Sinn and F. Patat, *Angew. Chem.* **75**, 805 (1963).
164. F. N. Tebbe and L. J. Guggenberger, *Chem. Commun.* p. 227 (1973).
165. L. J. Guggenberger and F. N. Tebbe, *J. Am. Chem. Soc.* **95**, 7870 (1973).
166. G. Bier, *Kunststoffe* **48**, 354 (1958).
167. A. Gumboldt and H. Schmidt, *Chem. Ztg.* **83**, 636 (1959).

168. G. Natta, P. Pino, E. Mantica, F. Danusso, G. Mazzanti, and M. Peraldo, *Chim. Ind. (Milan)* **38**, 124 (1956).
169. P. Cossee, *J. Catal.* **3**, 80 (1964).
170. W. L. Carrick, *J. Am. Chem. Soc.* **80**, 6455 (1958).
171. W. L. Carrick, R. W. Kluiber, E. F. Bonner, L. H. Wartman, F. M. Rugg, and J. S. Smith, *J. Am. Chem. Soc.* **82**, 3883 (1960).
172. G. Henrici-Olivé and S. Olivé, *Angew. Chem.* **83**, 782 (1971).
173. H. Emde, *Angew., Makromol. Chem.* **60**, 1 (1977).
174. R. J. Kelly, H. K. Garner, H. E. Haxo, Jr., and W. R. Bingham, *Ind. Eng. Chem. Prod. Res. Dev.* **3**, 210 (1962).
175. J. Boor, Jr., and E. A. Youngman, *J. Polym. Sci. Part A* **4**, 1861 (1966).
176. G. Natta, A. Zambelli, G. Lanzi, I. Pasquon, E. R. Mognaschi, A. L. Segre, and P. Centola, *Makromol. Chem.* **81**, 161 (1965).
177. A. Gumboldt, J. Helberg, and G. Schleitzer, *Makromol. Chem.* **101**, 229 (1967).
178. Y. Tajima, K. Tani, and S. Yuguchi, *J. Polym. Sci. Part B* **3**, 529 (1965).
179. G. Natta and L. Porri, Belgian Patent 549,554 (1956).
180. M. Bruzzzone, A. Mazzei, and G. Guilianì, *Rubber Chem. Technol.* **47**, 1175 (1974).
181. G. Lugli, A. Mazzei, and S. Poggio, *Makromol. Chem.* **175**, 2021 (1974).
182. A. D. Chirico, P. C. Lanzani, E. Raggi, and M. Bruzzzone, *Makromol. Chem.* **175**, 2029 (1974).
183. W. Keim, F. H. Kowaldt, R. Goddard, and C. Krüger, *Angew. Chem.* **90**, 493 (1978).
184. J. Chatt and B. L. Shaw, *J. Chem. Soc.* p. 5075 (1962).
185. J. Chatt, R. S. Coffey, A. Gough, and D. T. Thompson, *J. Chem. Soc. A*, p. 190 (1968).
186. H. de Vries, *Recil. Trav. Chim. Pays-Bas* **80**, 866 (1961).
187. H. Sinn and E. Kolk, *J. Organomet. Chem.* **6**, 373 (1966).
188. W. Kaminsky, H.-J. Vollmer, E. Heins, and H. Sinn, *Makromol. Chem.* **175**, 443 (1974).
189. W. Kaminsky and H. Sinn, *Justus Liebigs Ann. Chem.* p. 424 (1975).
190. E. A. Grogorjan, F. S. Dyachkovskii, and A. E. Shilov, *Vysokomol. Soedin.* **7**, 145 (1965).
191. W. Kaminsky and H.-J. Vollmer, *Justus Liebigs Ann. Chem.* p. 438 (1975).
192. W. Kaminsky, J. Kopf, H. Sinn, and H.-J. Vollmer, *Angew. Chem. Int. Ed. Engl.* **15**, 629 (1976).
193. W. Kaminsky, J. Kopf, and G. Thirase, *Justus Liebigs Ann. Chem.* p. 1531 (1974).
194. V. I. Kulishov, E. M. Brainina, N. G. Bokiý, and Yu. T. Struchkov, *Chem. Commun.* p. 475 (1970).
195. G. B. Sakharovskaya, N. N. Korneev, A. F. Popov, E. I. Larikov, and A. F. Zhigach, *Zh. Obshch. Khim.* **34**, 3478 (1964).
196. F. N. Tebbe, G. W. Parshall, and G. S. Reddy, *J. Am. Chem. Soc.* **100**, 3611 (1978).
197. G. Wilke and W. Schneider, *Bull. Soc. Chim. Fr.* **30**, 1462 (1963).
198. K. Veselý, J. Ambroz, R. Vilim, and O. Hamrik, *J. Polym. Sci.* **55**, 25 (1961).
199. G. Seydel, C. Beermann, and H. J. Bahr (to Farbwerke Hoechst) West German Patent 1,022,382 (1958).
200. E. H. Mottus, U.S. Patent 3,184,416 (1965); 3,440,237 (1969).
201. I. N. Meskove, T. M. Usakova, Yu. L. Lejluchina, N. N. Korneeva, and F. S. Dyachkovskii, *Vysokomol. Soedin. Ser. B* **19**, 849 (1977).
202. K. H. Reichert and K. R. Meyer, *Makromol. Chem.* **169**, 163 (1973).
203. A. Andresen, H. G. Cordes, J. Herwig, W. Kaminsky, A. Merck, R. Mottweiler, J. Pein, H. Sinn, and H.-J. Vollmer, West German Patents 2,608,863, 2,608,933 (1977).

- 204. J. Cihlav, J. Mejzlik, and O. Hamrik, *Makromol. Chem.* **179**, 2553 (1978).
- 205. N. Ueyama, T. Araki, and H. Tani, *Macromolecules* **7**, 153 (1974).
- 206. T. Araki, T. Aoyagi, N. Veyama, T. Aoyama, and H. Tani, *J. Polym. Sci. Part A* **11**, 699 (1973).
- 207. H. Tani, T. Araki, N. Oguni, and N. Ueyama, *J. Am. Chem. Soc.* **89**, 173 (1967).
- 208. Z. N. Polyakov, A. S. Semenova, E. Y. Paramonkov, Z. V. Ackhipova, A. F. Popov, M. I. Leitmann, N. M. Korobova, L. G. Stefanovich, and N. N. Korneev, USSR Patent 462, 473 (1971); *Otkryt. Izobret. Prom. Obraztsy Tovarnye Znaki* **53**(10), 172 (1976).

This Page Intentionally Left Blank

Chiral Metal Atoms in Optically Active Organo-Transition-Metal Compounds

HENRI BRUNNER

*Institut für Chemie
Universität Regensburg
Federal Republic of Germany*

I. Introduction	152
II. Optical Resolution—Enantiomers	153
A. General Aspects	153
B. The First Example	154
C. Other Representative Approaches	155
III. Optical Resolution—Diastereoisomers	160
A. Pseudotetrahedral Geometry	160
B. Octahedral Geometry	162
C. Square-Pyramidal Geometry	163
IV. Methods of Diastereoisomer Separation	165
V. Scope of the Concept of Chiral Metal Atoms in Optically Active Organo-Transition-Metal Compounds	166
VI. Optical Purity	166
VII. Configurational Stability	168
VIII. Ligand Transformations	169
A. Retention of Configuration at the Metal Atom	169
B. Inversion of Configuration at the Metal Atom	170
IX. Stereochemical Aspects of the Racemization and Ligand Exchange of (+)- and (-)- $C_5H_5Mn(NO)(COR)PAR_3$	172
A. Kinetics of Racemization and Proposed Mechanism	172
B. Retention of Configuration in Ligand Exchange Reactions	174
C. Steric and Electronic Effects	174
D. The Chiral Intermediate $C_5H_5Mn(NO)(COC_6H_5)$	176
X. Metal-Centered Rearrangement in Optically Active Square- Pyramidal Compounds	177
A. Proposed Mechanism	177
B. Optical Stability	179
XI. The Stereochemistry of Reactions at Fe—C and Fe—Hal Bonds	180
A. SO_2 Insertion	180
B. Carbonylation and Decarbonylation	182
C. Cleavage of Fe—C and Fe—Hal Bonds by Electrophiles	183
XII. Miscellaneous Reactions	185
XIII. Optical Induction	186
A. Asymmetric Synthesis	186
B. Epimerization Equilibria	188
XIV. Diastereoisomerically Related Pairs of Enantiomers	189
XV. Chiroptical Properties	192
XVI. Absolute Configuration	193

XVII. Table of Optically Active Compounds	195
References	201

I

INTRODUCTION

Chemistry is stereochemistry. After development of the fundamental synthetic methods and the structural characterization of many important compounds in such an expanding field as organometallic chemistry during the past 25 years, the problems demanding solution become more subtle, so that more elaborate techniques, e.g., kinetic and spectroscopic measurements, as well as stereochemical methods, gain in importance. Stereochemical information can be obtained by a variety of techniques. Hence, the study of such stereochemical aspects as cis-trans isomerism in square-planar and octahedral transition-metal compounds was a consequence of the increasing availability of IR spectrometers, and temperature-dependent NMR spectroscopy proved to be an extremely valuable technique for the study of nonrigid systems.

An important approach to stereochemical problems is to make use of the concept of chirality. Chirality (*I*), namely, the phenomenon that a chiral object and its mirror image cannot be superimposed, has been classified according to different elements of chirality. Chiral molecules may contain chiral centers, axes, and/or planes (2, 3).

The chiral center most frequently encountered is the asymmetric carbon atom, a tetrahedral C atom, bonded to four different substituents. Chiral centers of this type are known for many other elements (4). However, chiral centers are also found in other polyhedra, e.g., the metal atoms in octahedral compounds containing three bidentate chelate ligands. Chirality axes, present in the atrop isomers of ortho-substituted biaryls, occur in coordination chemistry in appropriately substituted aryl, pyridyl, and carbene metal complexes. Well known examples of planar chirality in organometallic chemistry are ferrocenes, cymantrenes, and benchtorenes containing two different substituents in 1,2- or 1,3-positions relative to each other (5-8).

Chiral molecules may be studied by a great many techniques. Without optical resolution, chiral structures can be detected by the magnetic nonequivalence of diastereotopic groups in NMR spectroscopy. Diastereoisomeric pairs of enantiomers, with and without separation, as well as resolved optically active compounds can be used for the investigation of stereochemical problems. Although stereochemical information can be obtained in many ways, the chiroptical properties of optically active compounds constitute an additional "handle" for assignment and correlation of configuration that is not available to optically inactive probes.

Occasionally, optically active ligands have been employed in organo-transition-metal chemistry to demonstrate the stereospecificity of reactions at metal-ligand bonds with respect to the α -carbon atom of the ligand. Thus, with the help of the chiral 1-phenylethyl group, it could be shown that the alkyl migration in the carbonylation and decarbonylation of (+)-(C₆H₅CH₂)(CH₃)HCCOMn(CO)₅ and (+)-(C₆H₅CH₂)(CH₃)-HCMn(CO)₅, respectively, is a stereospecific reaction (9, 10). Whereas, in this and similar reactions at metal-ligand bonds, stereochemical information has been available for the ligands for some time (8-11), the stereochemistry at the metal center has remained an open question, owing to the nonavailability of chiral metal atoms. Although it has sometimes been pointed out in the literature that organometallic compounds that are chiral at the transition-metal atom should be resolvable (12), it was not until 1969 that the first optical resolution was reported (13). This is the more surprising because in other fields the potential of labeling a chiral center by optical activity has been demonstrated. Thus, since the end of the last century, optically active organic compounds have been increasingly used to study the steric course of reactions; and, after the first resolution of an optically active octahedral Co(III) complex in 1911 (14), the optically active label at the coordination center also permitted an approach to stereochemical problems in classical Werner-type compounds (15, 16).

This article is confined to organo-transition-metal compounds having chiral metal atoms whose optical activity has been demonstrated. Only those compounds are discussed in detail for which there is a choice with respect to the metal configuration and for which a separation or at least an enrichment of isomers with opposite metal configuration has been achieved. After the treatment of such topics as optical resolution, optical purity, optical stability, optical induction, stereochemistry of reactions, relative and absolute configurations, Table I (Section XVII) collects the information available for the compounds under consideration.

The demonstration of chirality by NMR spectroscopy is not dealt with extensively in this review.

II

OPTICAL RESOLUTION—ENANTIOMERS

A. General Aspects

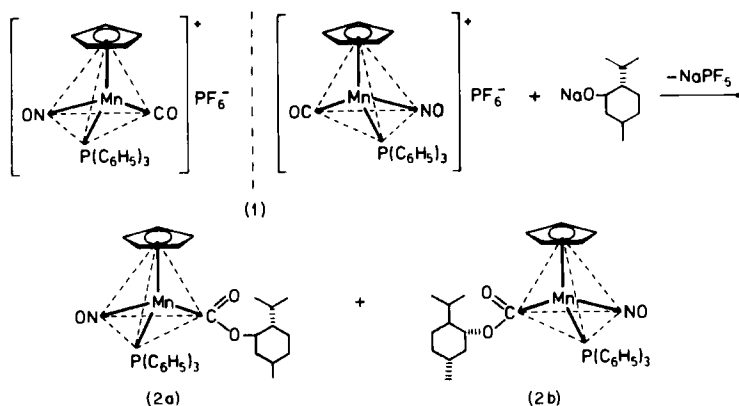
The two mirror-image isomers (*R*) and (*S*) of a chiral molecule are called enantiomers. Racemic mixtures contain the enantiomers (*R*) and

(*S*) in an exact 1:1 ratio. Under achiral conditions enantiomers have identical physical and chemical properties (e.g., solubility), and they exhibit the same spectra. Enantiomers also have identical magnitudes of chiroptical properties, for example, the amount of optical rotation and intensity of circular dichroism at a given wavelength. They differ only in the vectorial parameter, i.e., the sign of the optical rotation and the sign of the circular dichroism; and, most important, they differ under chiral conditions. If the two enantiomers (*R*) and (*S*) of a racemic mixture are combined with an optically active substance (*S*), two diastereoisomers, (*R,S*) and (*S,S*), result. These diastereoisomers are no longer related as image and mirror image, and therefore they differ in all of their physical, chemical, and spectroscopic properties.

The principle of introducing a diastereoisomer relationship into a pair of mirror-image isomers is the basis for each optical resolution. Mostly, the enantiomers of a racemic mixture are combined with an optically active resolving agent, to give a pair of diastereoisomers that are then separated. Hence, for the resolution of an organic acid, optically active amines are generally used, whereas organic amines are normally resolved with optically active acids. In coordination chemistry, chiral ions can be resolved by combination with an optically active counterion. But optical resolutions have also been carried out with other derivatives, e.g., esters for the resolution of racemic alcohols by use of an optically active acid. Increasingly, such methods as kinetic resolution and chromatography with optically active stationary phases are used for optical resolutions.

B. The First Example

The compound $[\text{C}_5\text{H}_5\text{Mn}(\text{CO})(\text{NO})\text{P}(\text{C}_6\text{H}_5)_3]\text{PF}_6$ (**1**), which contains chiral cations in the form of a racemic mixture (see Scheme 1), can be prepared in two steps starting from $\text{C}_5\text{H}_5\text{Mn}(\text{CO})_3$. In the first step, $\text{C}_5\text{H}_5\text{Mn}(\text{CO})_3$ is transformed into $[\text{C}_5\text{H}_5\text{Mn}(\text{CO})_2(\text{NO})]\text{PF}_6$ (**17**, **18**), and in the second step one of the CO ligands is replaced by $\text{P}(\text{C}_6\text{H}_5)_3$ to give $[\text{C}_5\text{H}_5\text{Mn}(\text{CO})(\text{NO})\text{P}(\text{C}_6\text{H}_5)_3]\text{PF}_6$ (**1**) (**19-22**). Metal carbonyl complexes are susceptible to nucleophilic attack at the carbon atom by strong bases such as LiR (**23**). Cationic complexes such as that in Scheme 1 are attacked even by alkoxides OR^- (**24-26**). In this reaction, the alkoxide ion adds to the carbon atom of the carbonyl group, and neutral derivatives having an ester group bonded directly to the metal atom result. By this reaction, an optically active resolving agent such as the menthoxide ion $\text{OC}_{10}\text{H}_{19}^-$ can be introduced into the racemic $[\text{C}_5\text{H}_5\text{Mn}(\text{CO})(\text{NO})\text{P}(\text{C}_6\text{H}_5)_3]\text{PF}_6$. Thus, according to Scheme 1, the enantiomeric



SCHEME 1

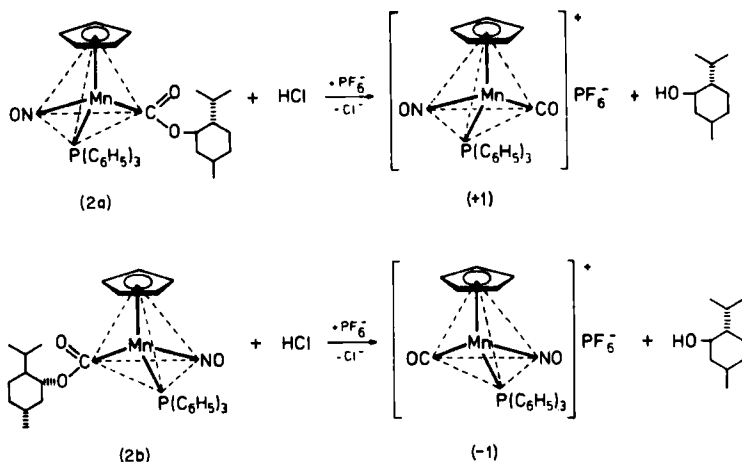
$[C_5H_5Mn(CO)(NO)P(C_6H_5)_3]^+$ cations of **1** are converted into the diastereomeric esters $C_5H_5Mn(COOC_{10}H_{19})(NO)P(C_6H_5)_3$ (**2a**, **2b**) (13, 27). The two diastereoisomers can be easily separated on the basis of their different solubilities. Whereas the (+)-isomer **2a** is soluble in saturated hydrocarbons, the (-)-isomer **2b** is almost insoluble in these solvents.¹

To complete the resolution, after diastereoisomer separation, the optically active resolving agent, the menthoxy ion $OC_{10}H_{19}^-$, must be removed from the diastereoisomers. Alkoxide abstraction from metal-bound ester groups can be easily carried out with acids (24). Dry gaseous HCl in toluene solution immediately converts (+)- and (-)- $C_5H_5Mn(COOC_{10}H_{19})(NO)P(C_6H_5)_3$ (**2a** and **2b**) into (+)- and (-)- $[C_5H_5Mn(CO)(NO)P(C_6H_5)_3]^+Cl^-$, respectively, which are insoluble in toluene (28). In this reaction by elimination of the menthoxy anion, the neutral esters **2a** and **2b** are transformed into the cationic carbonyl complexes shown in Scheme 2. Treatment of the chloride salts in aqueous solution with NH_4PF_6 precipitates the PF_6^- salts (+**1** and -**1**) from the racemic mixture from which the resolution procedure started (28).

C. Other Representative Approaches

The optical resolution shown in Schemes 1 and 2 was carried out by the Regensburg group in 1969–1970. Among other important examples, the following three, described in 1975, are noteworthy. By chance, these

¹ The signs (+) and (-) of the optical rotations given refer to the Na_D line, or to a wavelength of 578 nm, if not indicated otherwise.



SCHEME 2

resolutions were reported by three groups working at Southern California (USC), Dijon, and Rennes, which, together with the Regensburg group, have provided most of the contributions to the new field of optically active organo-transition-metal compounds.

The USC group started its successful optical resolution leading into the important class of optically active iron compounds of the type $\text{C}_5\text{H}_5\text{Fe}(\text{CO})[\text{P}(\text{C}_6\text{H}_5)_3]\text{X}$ with complex **3** prepared by reaction of $\text{Na}[\text{C}_5\text{H}_5\text{Fe}(\text{CO})_2]$ with the chloromethyl menthyl ether (-)- $\text{ClCH}_2\text{OC}_{10}\text{H}_{18}$. A photochemical substitution of a carbonyl ligand by triphenylphosphine in **3** makes the Fe atom an asymmetric center (see Scheme 3). The diastereoisomers **4a** and **4b** can be obtained optically pure in 20% yield by a single recrystallization from hexane. The separated diastereoisomers **4a** and **4b** are converted into the enantiomers (+)- and (-)- $\text{C}_5\text{H}_5\text{Fe}(\text{CO})[\text{P}(\text{C}_6\text{H}_5)_3]\text{CH}_2\text{Cl}$ (+5 and -5) by the action of anhydrous HCl (29, 30).

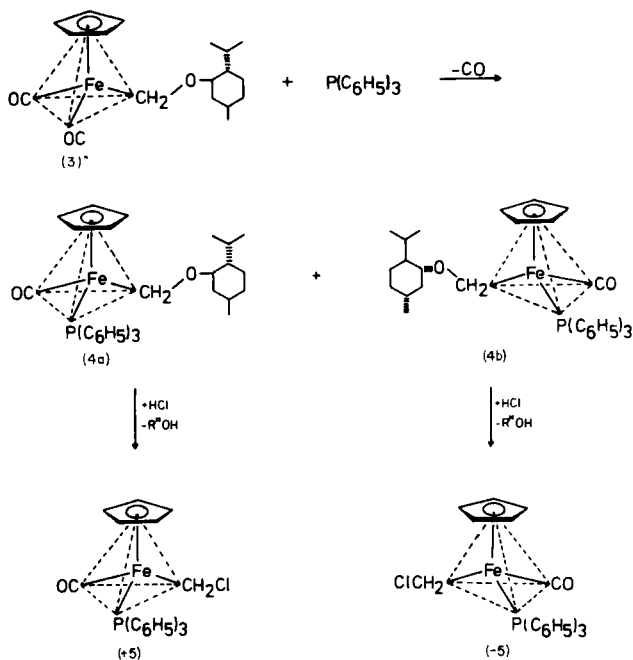
By SO_2 insertion into the Fe—C bonds of +5 and -5, known to be stereospecific with respect to the iron center (see Section XI,A), and interaction with an optically pure chiral shift reagent, it could be shown that the enantiomers (+)- and (-)- $\text{C}_5\text{H}_5\text{Fe}(\text{CO})[\text{P}(\text{C}_6\text{H}_5)_3]\text{CH}_2\text{Cl}$ are optically pure (29, 30).

The separated diastereoisomers **4a** and **4b**, and also the optically active derivatives **5**, with Br instead of Cl, have been used as methylene-transfer reagents for the preparation of cyclopropanes in the reaction with *trans*- β -methylstyrene (30, 31). The optical yields obtained (9–38%) are much

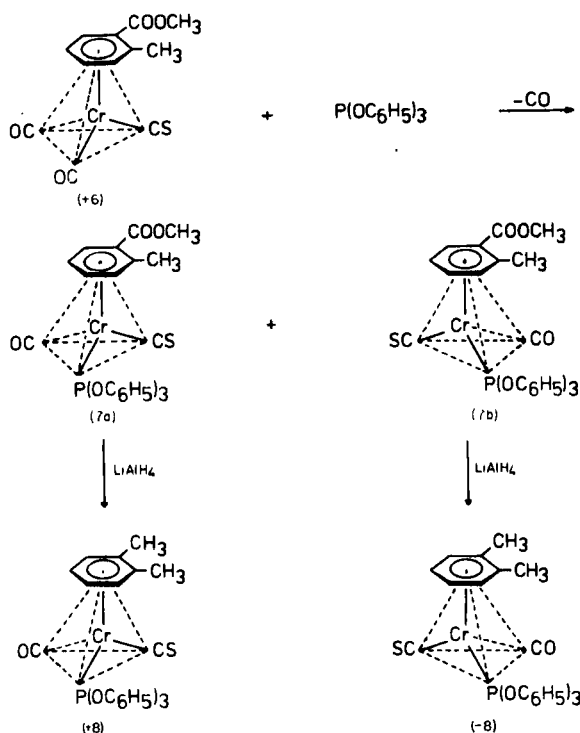
lower than those in the synthesis of cyclopropane derivatives by reaction of Co-dioximato complexes with diazoalkanes (32, 33).

The Rennes group used as the starting material for the first resolution of a chiral chromium atom having four different ligands the $\text{Cr}(\text{CO})_3$ complex of *o*-methylbenzoic acid methyl ester, which can be obtained optically pure (34, 35). The $\text{Cr}(\text{CO})_3$ moiety was converted into a $\text{Cr}(\text{CO})_2(\text{CS})$ group by replacing a CO by a CS ligand. Introduction of the triphenyl phosphite ligand into +6 (see Scheme 4) transformed the Cr atom into a chiral center, and a pair of diastereomers (7a and 7b) having opposite metal configurations was formed. The diastereoisomers, which differ in their ^1H -NMR spectra, could be separated by thin-layer chromatography (36, 37).

The enantiomers +8 and -8 were generated by removal of the planar chirality due to the unsymmetrically substituted arene ring in the separated diastereoisomers (7a and 7b). By treatment with $\text{LiAlH}_4\text{-AlCl}_3$, the ester group was reduced to a methyl group, leaving the asymmetric Cr atom the only element of chirality in the complexes +8 and -8,



SCHEME 3



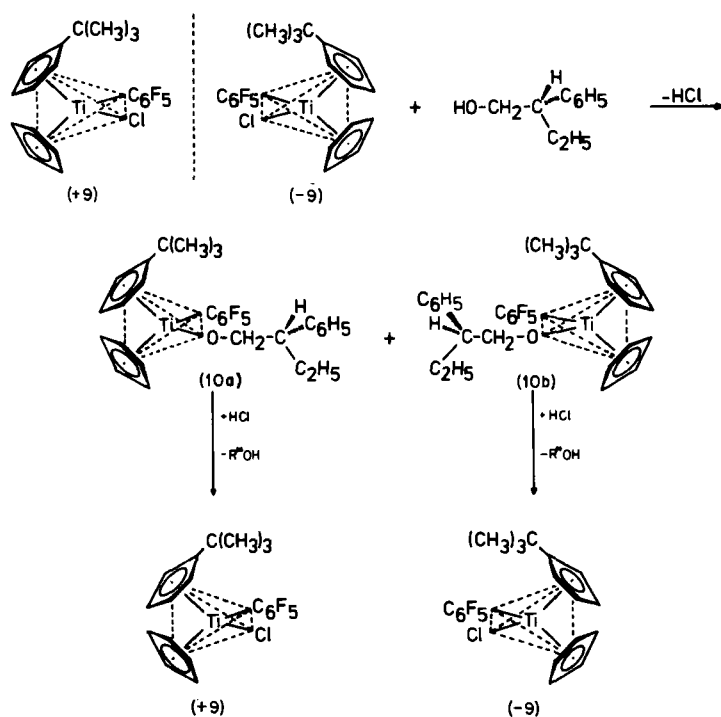
SCHEME 4

the optical purity of which was demonstrated (36, 37). A procedure similar to that outlined in Scheme 4 was used to convert (+)-(1,3-CH₃,COOCH₃)C₅H₃Mn(CO)₃ (38) into (+)-(1,3-CH₃,COOCH₃)C₅H₃Mn(CO)[P(C₆H₅)₃]P(OCH₃)₃ (39, 40).

The approach of the Dijon group for a resolution in the titanocene series started with a compound containing two different five-membered ligands, a C₅H₅ ring and a substituted cyclopentadienyl ring, accessible by reaction of C₅H₅TiCl₃ with Li[C₅H₄C(CH₃)₃], derived from dimethylfulvene and LiCH₃ (41-43). The titanium atom became an asymmetric center by reaction with C₆F₅MgBr, in which only one of the Cl ligands is replaced (see Scheme 5). The racemic mixture (+9/-9) was reacted with the sodium derivative of the alcohol (-)-(S)-phenyl-2-propanol having an optical purity of at least 99%. A pair of diastereoisomers (10a and 10b) was formed; these were separated by preparative thin-layer chromatography into the optically pure components, differing in the chemical shifts in their ¹H NMR spectra (41-43).

Conversion of the separated diastereoisomers **10a** and **10b** into the enantiomers **+9** and **-9** was achieved by treatment with HCl in benzene solution. In the examples given earlier, to accomplish conversion of diastereoisomers into enantiomers, only those bonds were broken that did not involve the chiral metal atom; this was to avoid loss of optical purity through possible change in configuration of the metal atom. In this work, Ti—O bond cleavage had to be used to convert the diastereoisomers (**10**) to the enantiomers (**9**). However, HCl cleavage of the Ti—OR bond in compounds of type **10** was shown to be stereospecific with respect to the chiral Ti atom, and to occur with retention of configuration (44–48). Optically active complexes with a chiral Ti atom could also be obtained by asymmetric decomposition (49, 50).

Other optical resolutions leading to enantiomeric organo-transition-metal complexes have been discussed in previous reviews (51, 52) and are included in Table I (Section XVII).



SCHEME 5

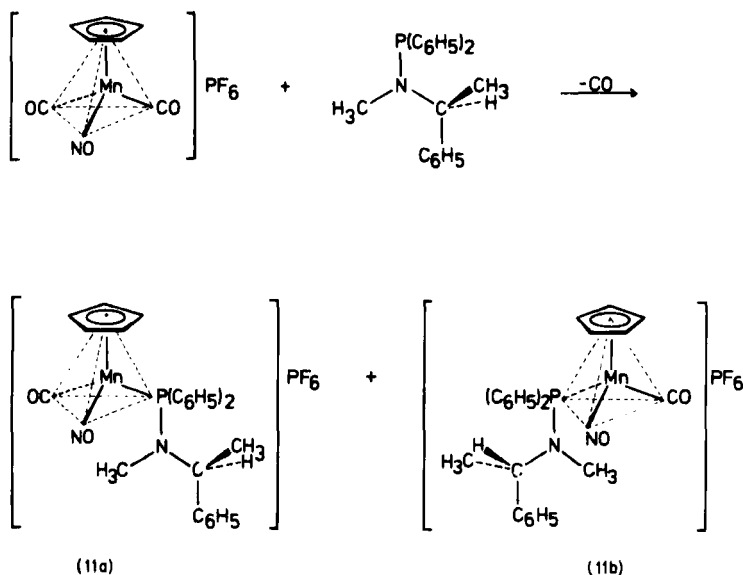
III

OPTICAL RESOLUTION—DIASTEREOISOMERS

A. Pseudotetrahedral Geometry

In the reaction of $[\text{C}_5\text{H}_5\text{Mn}(\text{CO})_2\text{NO}]\text{PF}_6$ with $\text{P}(\text{C}_6\text{H}_5)_3$ a racemic mixture of the enantiomers $[\text{C}_5\text{H}_5\text{Mn}(\text{CO})(\text{NO})\text{P}(\text{C}_6\text{H}_5)_3]\text{PF}_6$ (+/-) is formed, from which the resolution procedure of Scheme 1 commenced. The optically active aminophosphine (*S*)-(+)- $(\text{C}_6\text{H}_5)_2\text{PN}(\text{CH}_3)\text{CH}(\text{CH}_3)(\text{C}_6\text{H}_5)$ (53, 54) can be used instead of triphenylphosphine, and the former was very similar to $\text{P}(\text{C}_6\text{H}_5)_3$ (55) in behavior. Hence it is not surprising that in the reaction with $[\text{C}_5\text{H}_5\text{Mn}(\text{CO})_2\text{NO}]\text{PF}_6$ this ligand also replaces one CO group (see Scheme 6), giving a pair of diastereoisomers (11a and 11b) which differ only in the configuration of the metal. The two diastereoisomers can be separated on the basis of solubility differences (55).

It is generally accepted that the $\eta\text{-C}_5\text{H}_5$ ligand occupies three coordination positions at a metal atom. Therefore, all of the compounds $\text{C}_5\text{H}_5\text{ML}^1\text{L}^2\text{L}^3$ (1-11) discussed so far, with L^1 , L^2 , and L^3 being either two-electron or one-electron ligands, have to be considered as derivatives



SCHEME 6

of the octahedron, with the five-membered ring occupying three coordination positions *cis* to each other. However, in complexes of the type $C_5H_5ML^1L^2L^3$, the transition-metal atom M is surrounded by four different ligands, being an asymmetric center similar to the asymmetric carbon atom in the compounds of type *Cabcd*. As the C_5H_5 ligand, irrespective of its bonding, can only be present or absent, the stereochemistry is that of the tetrahedron. Thus, for a compound of formula $C_5H_5ML^1L^2L^3$, there are only two optical isomers, typical for a tetrahedron (having four different corners) and not the 30 isomers possible for an octahedron. Consequently, as far as stereochemical considerations are concerned, derivatives $C_5H_5ML^1L^2L^3$ can be called *pseudo*-tetrahedral.

The aminophosphine (*S*)-(+)- $(C_6H_5)_2PN(CH_3)CH(CH_3)(C_6H_5)$ in Scheme 6 is a member of the series of optically active phosphines (*S*)- $(C_6H_5)_2PN(R)CH(CH_3)(C_6H_5)$ ($R = H, CH_3, C_2H_5, CH_2C_6H_5$) that are chiral in the 1-phenylethyl group of the amino side chain. These compounds can be prepared by HCl elimination from $(C_6H_5)_2PCl$ and the corresponding optically active amine (*S*)- $HN(R)CH(CH_3)(C_6H_5)$. The primary amine ($R = H$) is commercially available, and the secondary amines (*S*)- $HN(R)CH(CH_3)(C_6H_5)$ ($R = CH_3, C_2H_5, CH_2C_6H_5$) are obtained from it by acylation or Schiff-base formation, followed by $LiAlH_4$ reduction (53, 54). Also, other optically active P ligands, derived from menthol or tartaric acid esters, can be applied to synthesis and separation of diastereoisomers of organo-transition-metal compounds (54).

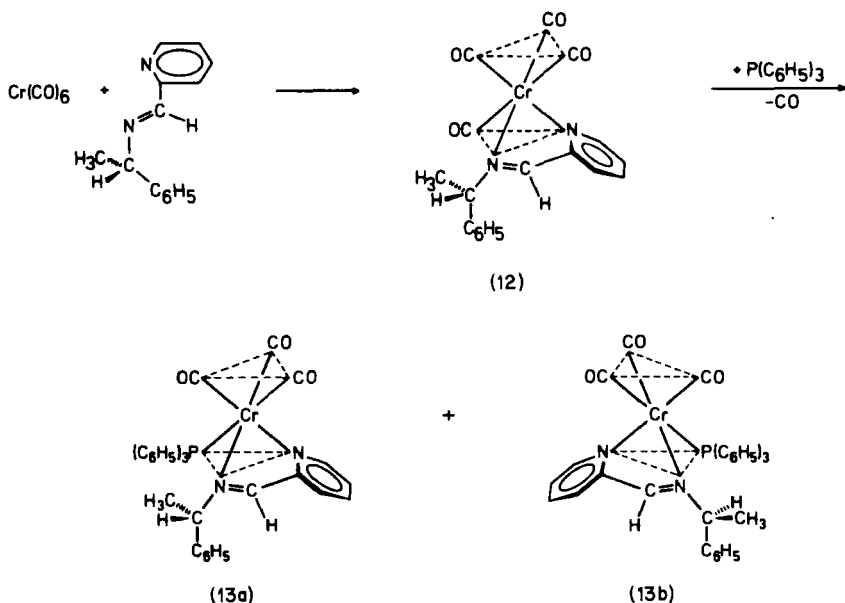
Optically active phosphines, chiral at the phosphorus atom, e.g., $P(CH_3)(C_3H_7)(C_6H_5)$ have been known since 1961 (56). However, their preparation is a lengthy procedure (57), and they racemize by phosphorus inversion at the high temperatures that are frequently necessary for thermal reactions in organometallic chemistry. The aminophosphines described do not suffer from these disadvantages. They do not racemize, and they are readily accessible in large amounts. As phosphines are extremely versatile ligands in organo-transition-metal chemistry, optically active phosphines should be universally applicable as optically active resolving agents; this was demonstrated by the resolution of a large body of aminophosphine-metal complexes (58–67). Furthermore, the aminophosphines exemplify how optically active, but inexpensive, organic compounds (e.g., amines) can be modified, to serve as active chiral resolving agents for organometallic complexes having metal atoms in low oxidation states.

Other examples, such as the conversion of (*R*)-(+)- $H_2NCH(CH_3)(C_6H_5)$ into the corresponding isonitrile (*R*)-(+)- $CNCH(CH_3)(C_6H_5)$ and its organometallic derivatives (68–70) have been discussed in a review (51) and are included in Table I (Section XVII).

B. Octahedral Geometry

Following the first resolution of an octahedral Co^{3+} complex by Alfred Werner (14) in 1911, numerous examples of optically active octahedral transition-metal complexes, mostly of the tris-chelate type with bidentate ligands, have been prepared (15, 16). In organometallic chemistry, optically active octahedral compounds of the type $\text{cis}-(\text{OC})_3\text{ML}^1\text{L}^2\text{L}^3$ have been obtained. As three carbonyl groups in cis position to each other at an octahedron are equivalent to a cyclopentadienyl ligand occupying three coordination positions, the compounds $\text{cis}-(\text{OC})_3\text{ML}^1\text{L}^2\text{L}^3$ correspond to the derivatives $\text{C}_5\text{H}_5\text{ML}^1\text{L}^2\text{L}^3$ just described.

Scheme 7 shows how it is possible, starting with $\text{Cr}(\text{CO})_6$, to introduce three different groups, L^1 , L^2 , and L^3 trans to the $\text{cis}-(\text{CO})_3\text{Cr}$ moiety (71). The Schiff base NN' , derived from 2-pyridinecarbaldehyde and the primary amine (*S*)-(-)- $\text{H}_2\text{NCH}(\text{CH}_3)(\text{C}_6\text{H}_5)$ in a one-step condensation, displaces two CO groups in the hexacarbonyl, necessarily in cis positions. Due to the different ends of the unsymmetrical chelate ligand NN' , the compound $(\text{CO})_4\text{CrNN}'$ (12) already contains two different metal-ligand bonds, ML^1 and ML^2 . In a further reaction step, the ligand $\text{L}^3 = \text{P}(\text{C}_6\text{H}_5)_3$ does not enter the tetracarbonyl $(\text{CO})_4\text{CrNN}'$ (12) trans to N or N', but



SCHEME 7

exclusively *cis* to N and N' (71). The reason for this regiospecificity is the strong *trans* effect of the two carbonyl groups opposite each other. Thus, stereospecifically, the *cis*-trisubstituted complexes chiral at the metal atom are formed. As the Schiff base NN' derives from the optically active amine (*S*)-(-)-1-phenylethylamine, a pair of diastereoisomers (13a and 13b) having opposite metal configuration arises.

For Cr, Mo, and W, these diastereoisomers could be separated by fractional crystallization into the (+)- and (-)-rotating components (71). Similarly, in the reaction of $\text{Mn}(\text{CO})_5\text{Br}$ with the NN' Schiff base (see Scheme 7), the two diastereoisomers of *cis*-(CO)₃Mn(NN')Br, differing only in the manganese configuration, were formed and were resolved (72).

C. Square-Pyramidal Geometry

Compounds of the type $\text{C}_5\text{H}_5\text{ML}^1\text{L}^2\text{L}^3\text{L}^4$, neutral or cationic depending on the nature of the ligands $\text{L}^1\text{--L}^4$, usually have a "four-legged piano-stool" geometry. According to the arguments already given for the compounds $\text{C}_5\text{H}_5\text{ML}^1\text{L}^2\text{L}^3$, the stereochemistry of the complexes $\text{C}_5\text{H}_5\text{ML}^1\text{L}^2\text{L}^3\text{L}^4$ is that of a square pyramid if the C_5H_5 ring is regarded as one ligand.

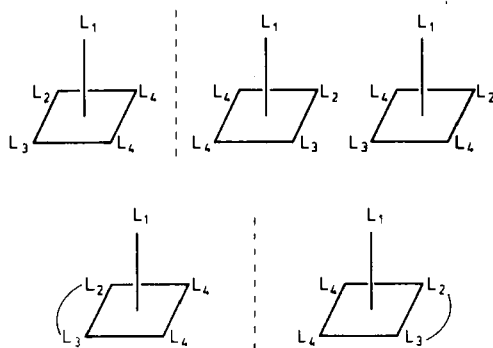
The permutation of five different ligands $\text{L}^1\text{--L}^5$ around the positions of a square pyramid gives rise to a total of 30 different isomers, which may be subdivided into 15 pairs of enantiomers. However, it has been shown how the application of three constraints reduces this large number of isomers to only two, a pair of mirror-image isomers (73).

1. Constraint (a): $\text{L}^1 = \text{C}_5\text{H}_5$. According to the structural evidence available, the C_5H_5 ligand always occupies the top of the pyramid (74).

2. Constraint (b): $\text{L}^5 = \text{L}^4 = \text{CO}$. Two ligands at the basal square become identical; for preparative reasons, carbonyl ligands are used.

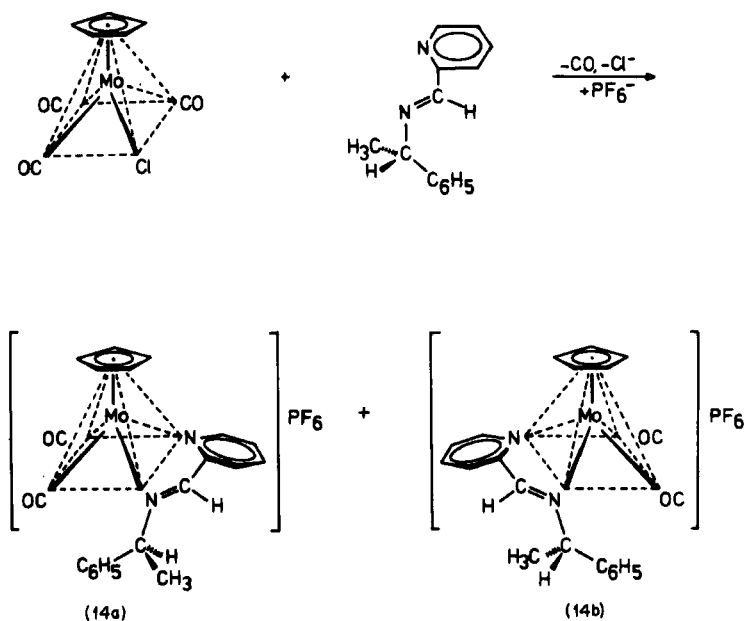
3. Constraint (c): L^2 and L^3 are combined into an unsymmetrical chelate ligand having two different ends $\text{L}^2\text{--L}^3$.

Constraints (a) and (b) decrease the number of possible isomers for $\text{C}_5\text{H}_5\text{M}(\text{CO})_2\text{L}^2\text{L}^3$ derivatives to only three, namely, two enantiomeric isomers having L^2 and L^3 *cis* to each other, and one achiral isomer having L^2 and L^3 *trans* to each other, shown in the first line of Scheme 8. Because of constraint (c), the achiral *trans* isomer is excluded, and the two isomers shown in Scheme 8 (second line), are left as the only possible isomers. Thus, by introducing three constraints, the stereochemistry of a square pyramid can provide a pair of mirror-image isomers (51, 73).



SCHEME 8

Scheme 9 shows how this concept can be realized. The starting material, $C_5H_5Mo(CO)_3Cl$, is a compound having approximately square-pyramidal geometry, with the C_5H_5 ring on top of the pyramid. In its reaction with the Schiff base NN' of 2-pyridinecarbaldehyde and (*S*)-(-)-1-phenylethylamine, a CO ligand and the covalently bonded chloro ligand are displaced from the metal atom by the unsymmetrical chelate ligand. In



SCHEME 9

a subsequent metathetical reaction, Cl^- can be exchanged by PF_6^- which gives more stable compounds. In the cation of **14** the metal atom is an asymmetric center. With the optically active Schiff base NN' , a pair of diastereoisomers is formed that can be separated by fractional crystallization into the (+)- and (-)-rotating components (**14b** and **14a**) for both $\text{M} = \text{Mo}$ and $\text{M} = \text{W}$ (73, 75, 76).

A variety of unsymmetrical optically active chelate ligands LL^* have been used as optically active resolving agents in square-pyramidal complexes of the type $\text{C}_5\text{H}_5\text{M}(\text{CO})_2\text{LL}^*$ ($\text{M} = \text{Mo}, \text{W}$) giving partly cationic species (77–81) and partly neutral complexes (79, 82–91). The field of optically active square-pyramidal complexes has been reviewed (11, 92). All of the known examples are summarized in Table I.

IV

METHODS OF DIASTEREOISOMER SEPARATION

After the preparation of diastereoisomers by introduction of an optically active resolving agent, the next problem in an optical resolution is to separate the diastereoisomers. It should be recalled that the components of a pair of diastereoisomers necessarily have very similar properties. They contain exactly the same ligands and differ only in their arrangement around the metal atom. Several separation techniques have been used, based either on the fact that diastereoisomers differ in solubility, or in retention time during chromatography.

If the solubility difference of two diastereoisomers having opposite metal configuration is large, it is sometimes possible to dissolve the more soluble component, the less soluble component remaining undissolved (13, 93, 94). Also, fractional precipitation of a mixture of diastereoisomers, an operation that can be repeated often in a short time (68), has been successful in some cases. The method most frequently used in the past to separate diastereoisomers having different metal configurations is fractional crystallization. This method gives good results regardless of solubility differences (51); however, each step is very time-consuming. Another disadvantage that fractional crystallization has in common with fractional precipitation is the decrease in the quantities of the fractions enriched in the respective diastereoisomers if the fractionation steps have to be repeated more than once. Chromatographic separation of diastereoisomers, increasingly used in recent years, does not suffer from this disadvantage.

In the purification of organometallic compounds by chromatography

on silica or alumina, an enrichment of each of the two components of a diastereoisomeric pair in the head and tail of a band, respectively, can sometimes be observed. With thin-layer chromatography, much better separations can usually be achieved (37, 42). A big improvement for the separation of diastereoisomeric components of neutral complexes was the development of preparative liquid chromatography (54, 59). For this technique, a very homogeneous silica having small particle size is needed, and a pressure of ~ 1 –2 bar is necessary to force the solvent through the column. Up to a gram of substance can be used. Sometimes the two diastereoisomers separate into two different zones, but generally only an enrichment in the head and the tail of a broad band can be achieved. By zone cutting and repeated chromatography, or by passage through several columns, in many cases both isomers could be obtained optically pure (66).

As described later, diastereoisomers sometimes interconvert at room temperature, or even below. Then, by "milking" the equilibrium by slow crystallization, it is often possible to convert all of the material into a single isomer which is usually configurationally stable in the solid state (51, 63).

V

SCOPE OF THE CONCEPT OF CHIRAL METAL ATOMS IN OPTICALLY ACTIVE ORGANO-TRANSITION-METAL COMPOUNDS

A variety of optically active ligands have been applied to resolve compounds of different geometries and coordination numbers. As is apparent from the examples given and those accumulated in Table I (Section XVII), all of the transition elements of the first triad between Ti and Ni, except V, have served as chiral centers, as well as such second- and third-row elements as Mo, W, and Ru. Many types of ligand usually encountered in organo-transition-metal chemistry have been used. Moreover, efficient methods for the separation of diastereoisomers are available. Thus, labeling a chiral metal center in an organo-transition-metal compound by optical activity as a probe for stereochemical studies is no longer a problem, provided that the metal configuration has the minimum of optical stability required for the resolution procedure.

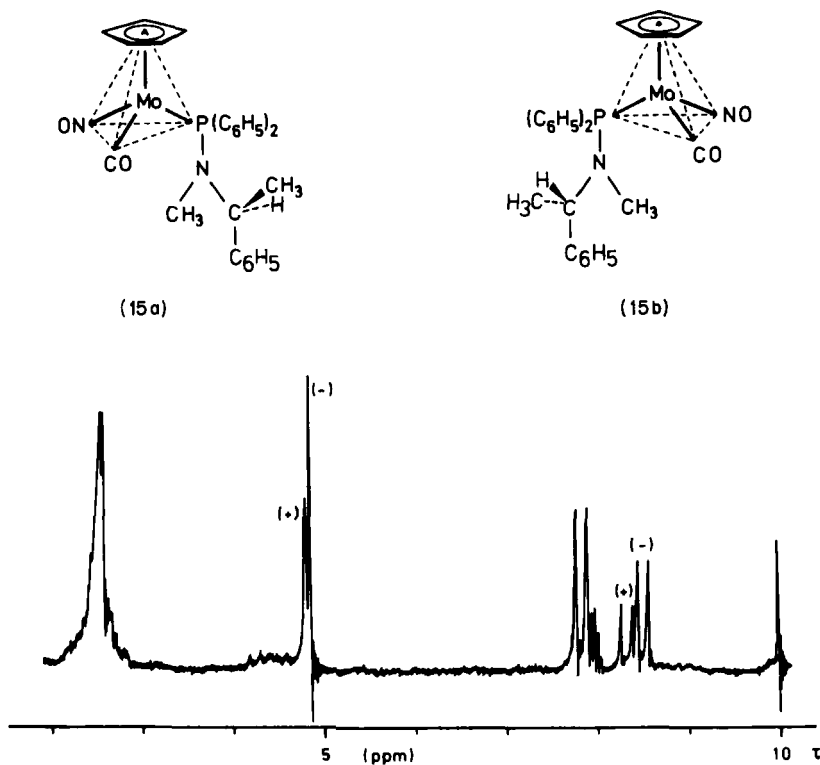
VI

OPTICAL PURITY

As the metal atoms in organo-transition-metal compounds often have 18-electron configurations, the compounds are diamagnetic and give sim-

ple $^1\text{H-NMR}$ spectra containing such diagnostic signals as MC_5H_5 , MCH_3 , MCOCH_3 , sometimes as sharp singlets, sometimes with characteristic couplings to hydrogen or phosphorus (11, 51, 95). This is apparent from the 60-MHz $^1\text{H-NMR}$ spectrum (see Scheme 10) of the mixture of the two diastereoisomers having opposite configuration at the Mo atom (**15a** and **15b**) enriched in the (+)-isomer (acetone- d_6). The diastereoisomers differ a little in the chemical shifts of the C_5H_5 signals, and appreciably in the chemical shifts of the CH-CH_3 doublets, the N-CH_3 signals being isochronous. By integration of the C-CH_3 signals, the diastereoisomer ratio **15a**:**15b** can be determined (54, 59).

Similarly, the optical purity of most of the diastereoisomers described is obvious from their $^1\text{H-NMR}$ spectra. In many cases, the separation of the C_5H_5 signals is much larger than in the $^1\text{H-NMR}$ spectrum shown in Scheme 10. For example, for the $\text{C}_5\text{H}_5\text{M}(\text{CO})_2$ -thioamidato complexes, chemical-shift differences of 0.5–1.0 ppm are found (79, 84–92). As a rule, in compounds containing the 1-phenylethyl group or other substit-



SCHEME 10

uents having aryl groups, the diastereoisomers show big differences in the chemical shifts of their signals. Only in complexes where aromatic rings are absent, are ^1H -NMR differences between diastereoisomers normally small or nonexistent (27, 94). In some of these examples, chemical-shift differences could be induced by the addition of NMR shift-reagents (29, 30, 96). The large chemical-shift differences, therefore, must be attributed to the "beam effect" of aromatic rings (89). Thus, in the ^1H -NMR spectrum of most diastereomeric pairs differing in the metal configuration, there are well separated signals, the integration of which immediately gives the diastereoisomeric purity. Consequently, the diastereoselectivity of an asymmetric synthesis, or the efficiency of different techniques for diastereoisomer separation, can be tested by integrating a ^1H -NMR spectrum. A component of a pair of diastereoisomers is optically pure if only one set of signals in the ^1H -NMR spectrum is left. Also, epimerization at the metal atom on storage, on exposure to light, or in reactions can easily be monitored by ^1H -NMR spectroscopy (11, 92).

The optical purity of enantiomers has been determined by NMR spectroscopy with the help of optically active shift-reagents (29, 30). In other cases, optical purity has been assigned to enantiomeric organo-transition-metal complexes when the conversion to enantiomers started from pure diastereoisomers and when it could be shown that, during reaction, no change in configuration at the metal atom occurred (35, 36). Also, such arguments as constant optical rotation on continued diastereoisomer separation or identical optical rotation with different signs for enantiomers have been used as an indication of optical purity (28).

VII

CONFIGURATIONAL STABILITY

All of the optically active compounds prepared by diastereoisomer separation and/or conversion to enantiomers have proved to be configurationally stable at the metal center as long as they are in the solid state. Concerning their behavior in solution, however, the optically active organo-transition-metal compounds are divided into two groups: (a) compounds configurationally stable at the metal center, which do not racemize or epimerize with respect to the metal atom prior to decomposition and (b) compounds configurationally labile at the metal center which racemize or epimerize with respect to the metal atom prior to decomposition.

Thus, with compounds of type (a), the stereochemistry of substitution, insertion, and cleavage reactions can be studied (8, 11), whereas with compounds of type (b), the mechanism of racemization and epimerization at the chiral metal atom can be investigated (11, 92). In the following sections, representative examples of both types of study will be given, from which it will become evident how optically active labels at metal centers in organo-transition-metal compounds contribute to the elucidation of the stereochemical course of reactions.

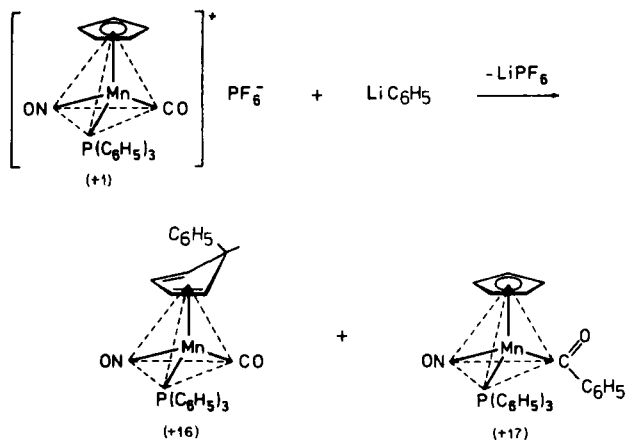
VIII

LIGAND TRANSFORMATIONS

A. Retention of Configuration at the Metal Atom

Optically active compounds obtained by diastereoisomer separation and/or conversion to enantiomers can be used as starting materials for the synthesis of other optically active derivatives, provided that they are optically stable under the reaction conditions. If in these reactions metal-ligand bonds are not involved, the change being restricted to within the ligands, the same relative configurations must be assigned to starting material and product (8, 11). The two most expanded series of this type are discussed in the following sections.

In the reaction of (+)-[C₅H₅Mn(NO)(CO)P(C₆H₅)₃]PF₆ (+1) with LiC₆H₅ (see Scheme 11), two different types of product are obtained



SCHEME 11

because LiC_6H_5 partly attacks the cyclopentadienyl ring and partly the carbonyl group (97–99). In the ring addition reaction, the neutral exocyclopentadiene complex +16 is formed; and in the carbonyl addition reaction, the neutral benzoyl complex +17 is formed. Similarly, (+)- and (–)- $[\text{C}_5\text{H}_5\text{Mn}(\text{NO})(\text{CO})\text{P}(\text{C}_6\text{H}_5)_3]\text{PF}_6$ were reacted with Li methyl and para-substituted Li phenyls (100, 101). The cyclopentadiene complexes are all optically stable, whereas the aroyl compounds are configurationally labile in solution (100) (see Section IX). Other optically active derivatives of this class of compound having the same relative configuration have been prepared by transesterification of (+)- and (–)- $\text{C}_5\text{H}_5\text{Mn}(\text{NO})(\text{COOR})\text{P}(\text{C}_6\text{H}_5)_3$ with $\text{R}'\text{OH}$ to give (+)- and (–)- $\text{C}_5\text{H}_5\text{Mn}(\text{NO})(\text{COOR}')\text{P}(\text{C}_6\text{H}_5)_3$ (11, 27, 102), and, by addition of alkoxide ions OR^- to (+)- and (–)- $[\text{C}_5\text{H}_5\text{Mn}(\text{NO})(\text{CO})\text{P}(\text{C}_6\text{H}_5)_3]\text{PF}_6$, to give (+)- and (–)- $\text{C}_5\text{H}_5\text{Mn}(\text{NO})(\text{COOR})\text{P}(\text{C}_6\text{H}_5)_3$ (11, 27).

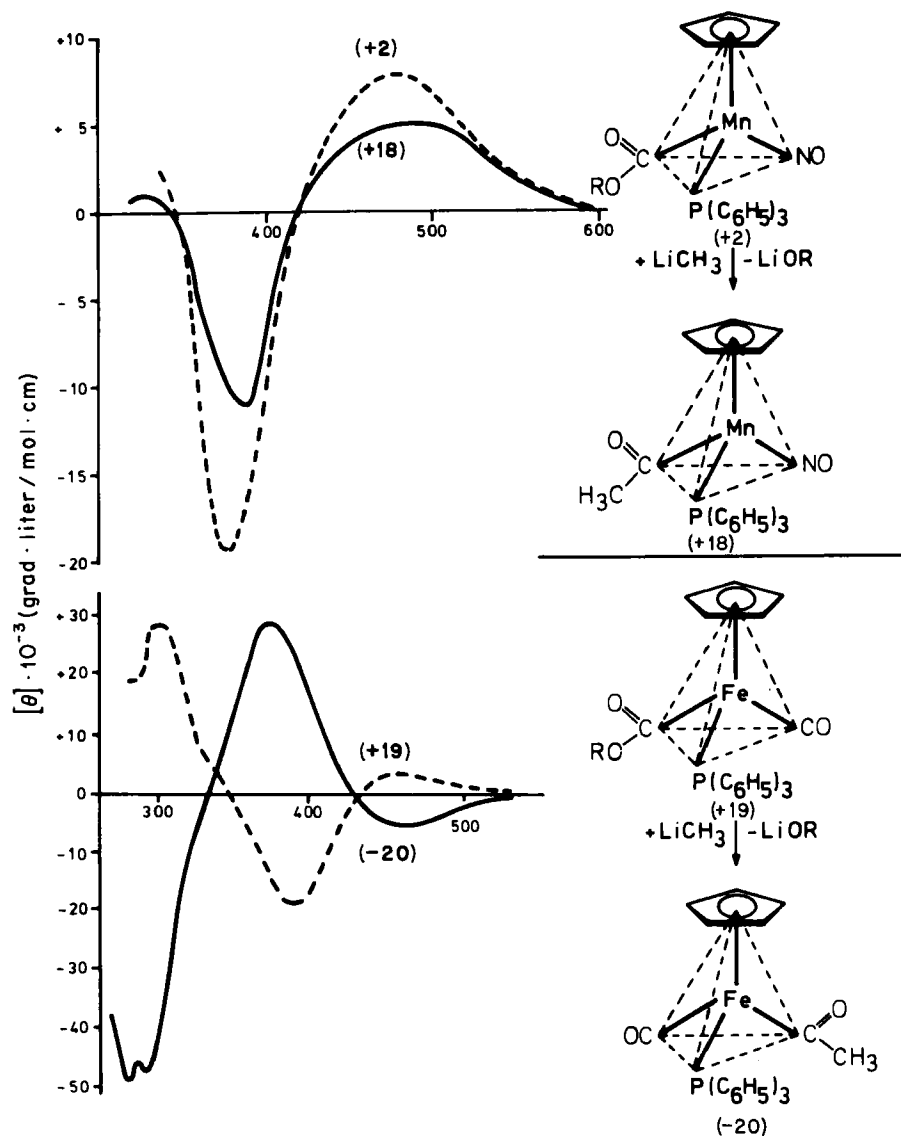
The second class of configurationally related compounds starts with the enantiomers (+)- and (–)- $\text{C}_5\text{H}_5\text{Fe}(\text{CO})[\text{P}(\text{C}_6\text{H}_5)_3]\text{CH}_2\text{Cl}$ (compounds +5 and –5 of Scheme 3), which are powerful alkylating agents. The Cl atom can be replaced by H, CH_3 , C_2H_5 , $i\text{-C}_3\text{H}_7$, C_3H_5 , CN, OCH_3 , Br, or I, leaving the iron configuration unchanged (29–31). The absolute Fe configuration of this series of compounds is known (103).

B. Inversion of Configuration at the Metal Atom

According to Scheme 12 (upper half²), the manganese methyl ester (+)- $\text{C}_5\text{H}_5\text{Mn}(\text{NO})(\text{COOR})\text{P}(\text{C}_6\text{H}_5)_3$ (+2, $\text{R} = \text{C}_{10}\text{H}_{19}$) is, by reaction with LiCH_3 , converted into the acetyl derivative (+18), as discussed in the preceding section. The assignment of the same relative configuration to both complexes +2 and +18 is supported by their chiroptical properties, e.g., the CD spectra shown in Scheme 12 (4, 100).

The iron menthyl esters (+)- and (–)- $\text{C}_5\text{H}_5\text{Fe}(\text{CO})(\text{COOC}_{10}\text{H}_{19})\text{P}(\text{C}_6\text{H}_5)_3$ (93, 94) are completely analogous to the corresponding, manganese compounds (+)- and (–)- $\text{C}_5\text{H}_5\text{Mn}(\text{NO})(\text{COOC}_{10}\text{H}_{19})\text{P}(\text{C}_6\text{H}_5)_3$; only the $\text{Mn}(\text{NO})$ moiety is replaced by the isoelectronic $\text{Fe}(\text{CO})$ group (104). However, if the (+)-iron menthyl ester (+19, $\text{R} = \text{C}_{10}\text{H}_{19}$) is transformed by treatment with LiCH_3 into the acetyl derivative –20 (105), in contrast to the manganese compounds, the chiroptical properties of starting material +19 and reaction product –20 are opposite to each other (see Scheme 12, lower half). This indicates that in the LiCH_3 reaction of +19, the configuration at iron is inverted (105). Obviously, LiCH_3 does not

² Absolute configuration of Mn in +2 and +18 is unknown.



SCHEME 12

attack the ester group, but the carbon atom of the carbonyl ligand; this results in an inversion of the Fe configuration because the former carbonyl group, via CH_3 addition, is transformed into the new functional group, while the former functional group is, by loss of menthoxide,

converted into the new carbonyl group (105). The inversion of configuration at the Fe atom is due to the fact that two ligands change their roles, although the bonds from the iron atom to the ligands do not participate in the reaction. The inversion mechanism shown in Scheme 12 is corroborated by the determination of the absolute configuration of +19 (106, 107), and the correlation of -20 to products of known absolute configuration (103) by reactions not taking place at metal-ligand bonds (108).

Also, the stereochemistry of the transesterification of (+)- and (-)- $\text{C}_5\text{H}_5\text{Fe}(\text{CO})(\text{COOC}_{10}\text{H}_{19})\text{P}(\text{C}_6\text{H}_5)_3$ is in accord with the carbonyl group in compounds of the type $\text{C}_5\text{H}_5\text{Fe}(\text{CO})(\text{COOR})\text{P}(\text{C}_6\text{H}_5)_3$ being more reactive than the ester group toward nucleophilic attack (94, 105). Thus, the assignment of the same relative configuration to compounds that can be transformed into each other by ligand modification is only correct so long as inversions similar to the example $+19 \rightarrow -20$ can be excluded (11).

IX

STEREOCHEMICAL ASPECTS OF THE RACEMIZATION AND LIGAND EXCHANGE OF (+)- AND (-)- $\text{C}_5\text{H}_5\text{Mn}(\text{NO})(\text{COR})\text{PAr}_3$

A. Kinetics of Racemization and Proposed Mechanism

The compounds (+)- and (-)- $\text{C}_5\text{H}_5\text{Mn}(\text{NO})(\text{COC}_6\text{H}_5)\text{P}(\text{C}_6\text{H}_5)_3$ (+17 and -17) represent prototypes of configurationally labile complexes. Solutions of +17 and -17 at room temperature lose their high optical rotations exponentially due to a change in configuration of the Mn atom. By polarimetric kinetics, a half-life (25°C, toluene) of 21 minutes was measured (100, 109).

The racemization of the benzoyl complexes +17 and -17 proved to be dependent on the $\text{P}(\text{C}_6\text{H}_5)_3$ concentration. Increasing the amounts of added $\text{P}(\text{C}_6\text{H}_5)_3$ lengthened the half-lives appreciably (100, 109). To account for this unexpected increase in configurational stability on addition of triphenylphosphine, a dissociation mechanism including chiral intermediates was proposed (see Scheme 13; $\text{R} = \text{C}_6\text{H}_5$).

In the rate-determining step, $\text{P}(\text{C}_6\text{H}_5)_3$ dissociates while the remaining ligands retain their geometry in space, forming a chiral intermediate. The tripod may either invert, a process responsible for the observed racemization, or it may take up triphenylphosphine at the vacant site to give the original compound. As the back-reaction is favored with increasing $\text{P}(\text{C}_6\text{H}_5)_3$ concentration, the decrease in the rate of racemization can be

rationalized. The observed dependence on the $\text{P}(\text{C}_6\text{H}_5)_3$ concentration of the racemization rate is not only qualitatively, but also quantitatively, consistent with the mechanism proposed in Scheme 13 (100, 109).

B. Retention of Configuration in Ligand Exchange Reactions

Besides the kinetic arguments, there is stereochemical evidence for chiral intermediates formed on dissociation of $\text{P}(\text{C}_6\text{H}_5)_3$ from (+)- and (-)- $\text{C}_5\text{H}_5\text{Mn}(\text{NO})(\text{COC}_6\text{H}_5)\text{P}(\text{C}_6\text{H}_5)_3$ (+17 and -17). If the racemization of the benzoyl complex +17 is carried out in the presence of an excess of tri-*p*-anisylphosphine, the chiral intermediate reacts with $\text{P}(4\text{-C}_6\text{H}_4\text{OCH}_3)_3$ to give the corresponding substitution product +21, which is still optically active and which has the same chiroptical properties as the parent $\text{P}(\text{C}_6\text{H}_5)_3$ compound (+17) (109). The $\text{P}(4\text{-C}_6\text{H}_4\text{OCH}_3)_3$ derivative +21 also racemizes in toluene solution, although with a half-life (25°C) of 137 minutes, much more slowly than the $\text{P}(\text{C}_6\text{H}_5)_3$ compound +17; both compounds afford the same chiral intermediate (101). This chiral intermediate can be trapped with CO, giving the optically active compound -22, which turns out to be configurationally stable (110). Thus, Scheme 13 shows that the carbonyl complex -22 can be obtained from the $\text{P}(\text{C}_6\text{H}_5)_3$ derivative +17 in two ways, in a one-step and in a two-step substitution via the $\text{P}(4\text{-C}_6\text{H}_4\text{OCH}_3)_3$ derivative +21. The smaller optical rotations of the carbonyl (-22) obtained in the two-step reaction indicates that the stereoselectivity via +21 is lower than in the one-step reaction, probably because of partial racemization by inversion of the chiral intermediate before it reacts with the *p*-anisylphosphine in the first step. However, the Walden cycle $+17 \rightarrow -22 \leftarrow +21 \leftarrow +17$ (see Scheme 13, lower part) proves that all these reactions proceed with predominant retention of configuration of the Mn atom (even though they are dissociation reactions) because chiral intermediates are formed (110).

Like CO, the ligand $\text{P}(\text{C}_6\text{H}_5)_3$ in +17 can also be replaced by $\text{L} = \text{CNC}_6\text{H}_{11}$, $\text{P}(\text{OC}_2\text{H}_5)_3$, or $\text{P}(n\text{-Bu})_3$, giving optically active substitution products $\text{C}_5\text{H}_5\text{Mn}(\text{NO})(\text{COC}_6\text{H}_5)\text{L}$, which are configurationally stable in solution. With $\text{P}(2\text{-C}_6\text{H}_4\text{CH}_3)_3$, no substitution product could be obtained (110).

C. Steric and Electronic Effects

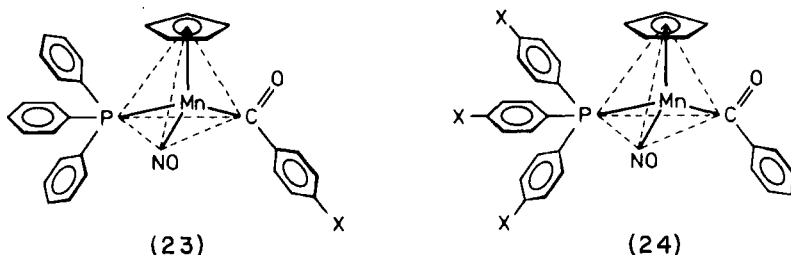
The electronic effect on the rate of racemization of (+)- and (-)- $\text{C}_5\text{H}_5\text{Mn}(\text{NO})(\text{CO-4-C}_6\text{H}_4\text{X})\text{P}(4\text{-C}_6\text{H}_4\text{X})_3$ (23 and 24) has been studied by

using eight different substituents, from $X = \text{CF}_3$ to $X = \text{N}(\text{CH}_3)_2$, in the para positions of the phenyl ring of the benzoyl group in **23** and the triphenylphosphine ligand in **24**, respectively, thus keeping the steric situation at the dissociating Mn—P bond constant (100, 101) (see Scheme 14).

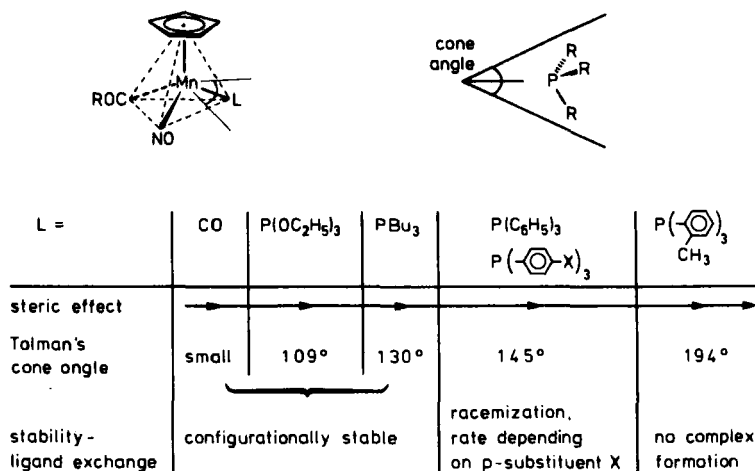
As this topic has already been reviewed, the arguments will not be repeated here (11, 111). It turns out that the half-life of racemization is an extremely sensitive probe for the electron density at the Mn—P bond, being much better than such spectroscopic parameters as shifts of IR stretching vibrations or NMR signals. The result is that the cleavage of the Mn—P bond is fast if electron-donating substituents are attached to the benzoyl group on the metal side and/or electron-attracting substituents are bound to the phenyl rings on the phosphorus side and vice versa (100, 101).

It has been mentioned that in ligand exchange reactions starting with (+)- and (-)- $\text{C}_5\text{H}_5\text{Mn}(\text{NO})(\text{COC}_6\text{H}_5)\text{P}(\text{C}_6\text{H}_5)_3$, the optically active substitution products $\text{C}_5\text{H}_5\text{Mn}(\text{NO})(\text{COC}_6\text{H}_5)\text{L}$ [$\text{L} = \text{CO}$, $\text{CNC}_6\text{H}_{11}$, $\text{P}(\text{OC}_2\text{H}_5)_3$, $\text{P}(\text{4-C}_6\text{H}_4\text{OCH}_3)_3$, $\text{P}(\textit{n}\text{-C}_4\text{H}_9)_3$] can be obtained. With the electronic effect dominating, the electron-attracting ligands CO, $\text{CNC}_6\text{H}_{11}$, and $\text{P}(\text{OC}_2\text{H}_5)_3$ would be expected to give configurationally stable complexes, whereas the configuration of the compound having the electron-donating $\text{P}(\textit{n}\text{-C}_4\text{H}_9)_3$ ligand should be extremely labile. However, all of the products are configurationally stable, indicating that the electronic effect cannot account for the configurational stability observed (100).

With the steric effect, e.g., on the basis of Tolman's cone angles (112–115), this can be rationalized (Scheme 15). The species CO, $\text{CNC}_6\text{H}_{11}$, $\text{P}(\text{OC}_2\text{H}_5)_3$, and $\text{P}(\textit{n}\text{-C}_4\text{H}_9)_3$ are smaller ligands than triaryl phosphines, and obviously small ligands do not dissociate. Dissociation occurs only when a steric borderline situation is attained, as with triarylphosphines. In accordance with this explanation, ortho-substituted triarylphosphines L do not give stable compounds of the type $\text{C}_5\text{H}_5\text{Mn}(\text{NO})(\text{COC}_6\text{H}_5)\text{L}$ at



SCHEME 14



SCHEME 15

all. Thus, for racemization, the steric effect seems to be most important (110). Only in the borderline situation of steric labilization with L = triarylphosphines the electronic effect, as demonstrated, can somehow increase or decrease the rate (100, 101).

The aminophosphine (*S*)-(+)-C₆H₅₂PN(CH₃)CH(CH₃)(C₆H₅) has a size similar to that of P(C₆H₅)₃. Therefore, it is not surprising that the optically active complexes C₅H₅Mn(NO)(COC₆H₅)L of both ligands racemize at almost the same rates, the half-lives for toluene solution at 25°C being 21 minutes for L = P(C₆H₅)₃, and 19 minutes for L = (*S*)-(+)-C₆H₅₂PN(CH₃)CH(CH₃)(C₆H₅) (55).

D. The Chiral Intermediate C₅H₅Mn(NO)(COC₆H₅)

In stereochemical experiments, it cannot be decided whether the planar form, attained via pyramidal inversion of the chiral intermediates (Scheme 13, first line), is a transition state or an intermediate. By calculation (116, 117), however, it can be shown that 16-electron systems of the type C₅H₅Mn(CO)₂, in contrast to the planar structures of such 18-electron systems as C₅H₅Co(CO)₂, are pyramidal, like ammonia, with a barrier to inversion. This barrier should be higher for an acyl substituent than for an ester substituent, in agreement with the experimental results (117).

The manganese esters (+)- and (-)-C₅H₅Mn(NO)(COOR)P(C₆H₅)₃ racemize in solution by change of configuration of the Mn atom in much the same way as the acyl complexes 17 and 18. However, there is no

evidence for the existence of chiral intermediates of the type $C_5H_5Mn(NO)(COOR)$, detectable by the kinetic or stereochemical techniques used for the demonstration of the chirality of the intermediates $C_5H_5Mn(NO)(COR)$ (11).

Such species as $C_5H_5Mn(CO)_2$ with a probable pyramidal structure have also been identified by matrix isolation (118, 119). Thus, matrix isolation, on the one hand, and kinetic and mainly stereochemical investigations on the other, are complementary methods for the study of intermediates having lowered coordination number.

Several complexes with acetyl ligands bonded in a dihapto fashion have now been reported (120–122). It cannot be decided whether the chiral intermediates $C_5H_5Mn(NO)(COC_6H_5)$ contain monohapto or dihapto acyl ligands, because they cannot be observed spectroscopically. However, dihapto bonding would not change the stereochemical outcome of all the results described.

The kinetic and stereochemical results derived from racemization and substitution reactions of the compounds (+)- and (-)- $C_5H_5Mn(NO)(COR)P(C_6H_5)_3$ can also be explained by assuming an intermediate $C_5H_5Mn(NO)(CO)R$, obtained by migration of groups R from the acyl substituent to the metal atom, either in a concerted or a stepwise rearrangement. However, the compounds $C_5H_5Mn(NO)(CO)CH_3$ and $C_5H_5Mn(NO)(CO)C_6H_5$ were prepared, and it could be demonstrated that their reaction with $P(C_6H_5)_3$ is so slow that they can be excluded as intermediates in the racemization and ligand exchange reactions of (+)- and (-)- $C_5H_5Mn(NO)(COR)P(C_6H_5)_3$ (123). On the other hand, in the racemization and epimerization with respect to the Fe atom in (+)- and (-)- $C_5H_5Fe(CO)(COR')PR_3$, the rearrangement products $C_5H_5Fe(CO)(PR_3)R'$ are formed in quantities that increase with temperature (66). Thus, in the iron series, R' obviously migrates to the metal atom (representing a further reaction mode for the chiral intermediate in addition to those outlined in Scheme 13), the stereochemical consequences of which are currently under investigation.

X

METAL-CENTERED REARRANGEMENT IN OPTICALLY ACTIVE SQUARE-PYRAMIDAL COMPOUNDS

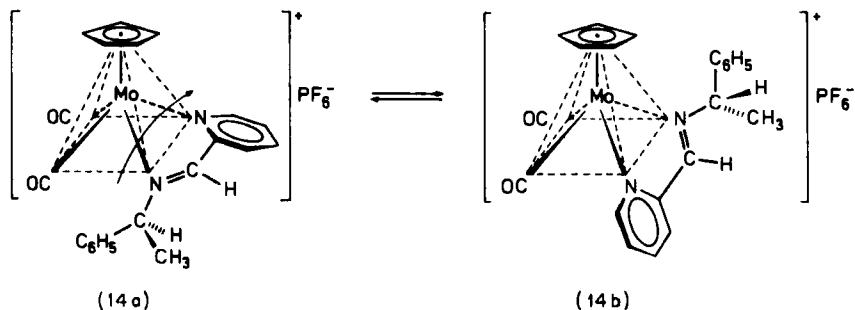
A. Proposed Mechanism

At room temperature, compounds **14a** and **14b** dissolved in acetone or DMF are optically stable. At higher temperatures, however, a clean first-

order decrease of optical rotation is observed (73, 75, 76). During epimerization, the configuration of the Mo atom changes, and an equilibrium $14a \rightleftharpoons 14b$ is established (76) (see Scheme 16).

For the interconversion of the diastereoisomers **14a** and **14b**, as for other compounds having five ligands, an intramolecular mechanism without cleavage of bonds is a very attractive mechanism, but dissociative processes must also be considered (76). Schiff-base exchange could be excluded as an epimerization mechanism; and, if the epimerization is carried out in the presence of triphenylphosphine, the latter does not show up in the reaction product, an argument against free coordination positions during the change of configuration of the Mo atom (76). The rigidity of pseudo-tetrahedral Co complexes $[C_5H_5Co(C_3F_7)NN^*]PF_6$ (124) and the nonrigidity of the pseudo-square-pyramidal Mo complexes $[C_5H_5Mo(CO)_2NN^*]PF_6$, both containing the same unsymmetrical Schiff base NN^* derived from 2-pyridinecarbaldehyde and (*S*)-1-phenylethylamine, also indicate the intramolecular character of the epimerization in the square-pyramidal compounds because an intermolecular mechanism should operate for both of them (11, 92).

Another argument for the intramolecular nature of the metal-centered rearrangement of square-pyramidal compounds consists in the effects of substituents on the rate of epimerization of compounds of the type $C_5H_5M(CO)_2LL'$. Thus, a methyl group in C-6 of the pyridine ring in **14** (Scheme 16) decreases the rate of epimerization by 2 powers of ten compared to the unsubstituted derivative **14** (77). Also, a Schiff base NN^* , derived from 2-quinolinecarbaldehyde, instead of 2-pyridinecarbaldehyde, in the complex $[C_5H_5Mo(CO)_2NN^*]PF_6$ leads to a large decrease in the rate of epimerization (77). Obviously, an annellated benzene ring increases the activation barrier for the pseudo-rotation in much the same way as a 6-methyl group.



SCHEME 16

The drastic drop in the rate of epimerization of ortho-substituted derivatives compared to the unsubstituted or para-substituted complexes is ascribed to the steric effect of the ortho substituents. In an intramolecular isomerization, steric hindrance is expected to increase with the size of the ortho substituents (11, 92). For a dissociation reaction, or for chelate ring opening, a steric acceleration should be observed if the ortho substituents are bulkier. These substituent effects therefore support an intramolecular formulation of the epimerization reaction in Scheme 16.

The simplest possibility for a change in configuration of the metal atom without cleavage of bonds is rotation of the chelate ligand LL' by 180° with respect to the rest of the molecule, as indicated by the arrow in Scheme 16 (11, 76, 92), although several other modes can be envisaged (125–127).

B. Optical Stability

As shown in Section III,C, many different chelate ligands LL' have been used for the synthesis of optically active Mo and W complexes of the type $C_5H_5M(CO)_2LL'$. They have all been investigated with respect to their configurational stability at the metal atom. As a gauge, the rate of epimerization with respect to the metal atom was used, measured both by polarimetric kinetics and by time-dependent 1H -NMR integration (11, 92).

On varying the chelate ligands LL' , large differences in the rate of the metal-centered rearrangement were encountered. The change in configuration of the metal atom in $[C_5H_5Mo(CO)_2LL']PF_6$, in which LL' are neutral four-electron Schiff-base ligands, depending on the substituents, proceeds with half-lives of ~ 30 minutes at temperatures of 75 – $90^\circ C$ (76,77). About the same optical stability was observed for the cations in the complex $[C_5H_5Mo(CO)_2LL']PF_6$ ($LL' =$ propylenediamine) (81), and for the neutral complexes $C_5H_5Mo(CO)_2LL'$, LL' being either the anion of the Schiff base derived from pyrrole-2-carbaldehyde and (*S*)-1-phenylethylamine, or the anion of the 2-pyridine-carboxylic acid thioamide, showing that the charge does not have a large influence on the epimerization rates (82, 88). Much more configurationally labile are the neutral complexes in which LL' is the anion of a thioamide. Depending on the substituents, these complexes epimerize with half-lives of ~ 30 minutes at 30 – $40^\circ C$ (84–87). In the same range are the half-lives for the epimerization of the neutral derivatives with $LL' = o$ -metalated benzaldimines (83). A correlation of corresponding Mo and W compounds reveals that with few exceptions, the W complexes, epimerize a little faster than the

Mo derivatives (76, 77). Further work is needed so that the critical dependence of the rate of isomerization on the nature of the chelate ligand LL' may be understood.

The configurationally most labile optically active square-pyramidal derivative shown to date is compound **25**, simultaneously the first example of an optically active square-pyramidal complex having five independent ligands (67) (see Scheme 17). Starting with **25a** in toluene solution at 0°C , the first-order approach to equilibrium proceeds with a half-life of 27 minutes. The extreme lability of the Mo configuration in **25a** can be used for the following asymmetric transformation. If an equilibrium mixture of **25a** and **25b** that contains both isomers in the ratio $\sim 1:1$ is cooled to -20°C , one isomer (**25a**) starts to crystallize. Because at -20°C , equilibration is still fairly rapid, **25b** is steadily transformed into **25a** until almost all the material is converted into solid **25a** (67). No trace of the corresponding trans isomer can be seen in the ^1H -NMR spectrum on equilibration.

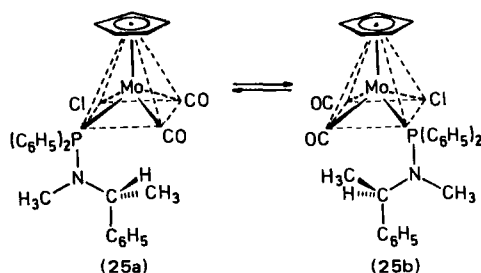
The example of **25** leads to a class of compounds the metal configuration of which is so labile that dynamic NMR spectroscopy is more appropriate than polarimetry for studying inversion of configuration of the metal atom. In this way, the fast interconversion of many square-pyramidal compounds of the type $\text{C}_5\text{H}_5\text{M}(\text{CO})_2\text{LX}$ has been investigated, and the intramolecular character of the metal-centered rearrangement demonstrated, in accord with the mechanism proposed in Section X,A (74, 128-135).

XI

THE STEREOCHEMISTRY OF REACTIONS AT $\text{Fe}-\text{C}$ AND $\text{Fe}-\text{Hal}$ BONDS

A. SO_2 Insertion

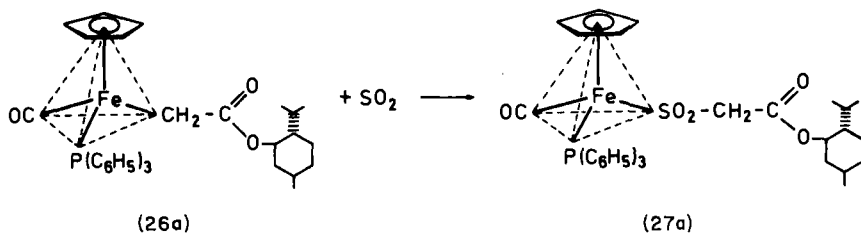
Sulfur dioxide readily inserts into metal-carbon σ bonds (136, 137). The reaction is stereospecific with respect to the configuration at the α -carbon atom of the alkyl group (138) and proceeds with inversion of configuration at the α -carbon atom (139-142). The stereospecificity of the SO_2 insertion with respect to the metal center was demonstrated with diastereoisomeric pairs of enantiomers of Fe compounds (143-146). Also, the stereochemistry of the SO_2 insertion at the iron atom was studied by starting with the optically active iron alkyl derivative **26a** (see Scheme 18). Retention of configuration was concluded from the similarity in the



SCHEME 17

chiroptical properties of the starting material **26a** and the product **27a** (30, 96), and proved by X-ray determination of the absolute configurations (147).

These results are in accord with rear-side attack of SO_2 at the α -carbon atom of the alkyl group, with inversion of configuration of the α -carbon atom, affording a tight ion-pair M^+RSO_2^- , from which first the O- and then the S-bonded products MSO_2R are formed with retention of configuration of the metal atom (8, 30, 136, 145, 147). The stereoselectivity of the SO_2 insertion with respect to the metal configuration is dependent on the alkyl substituent, decreasing from isobutyl to methyl (30). In neat SO_2 the stereoselectivity at iron is usually lower than in $\text{CH}_2\text{Cl}_2/\text{SO}_2$ solution, where the reaction is stereospecific (30, 143, 145). This stereospecificity has been used to determine the enantiomeric purity of $\text{C}_5\text{H}_5\text{FeR}(\text{CO})[\text{P}(\text{C}_6\text{H}_5)_3]$ ($\text{R} = \text{alkyl}$) compounds (29, 30). The reduced selectivity at Fe of the SO_2 insertion into Fe-alkyl bonds in neat SO_2 compared to $\text{CH}_2\text{Cl}_2/\text{SO}_2$ was explained by increased dissociation of the tight ion-pair $\text{C}_5\text{H}_5\text{Fe}(\text{CO})[\text{P}(\text{C}_6\text{H}_5)_3]^+\text{O}_2\text{SR}^-$ in neat SO_2 . Trapping of the cation of $\text{C}_5\text{H}_5\text{Fe}(\text{CO})[\text{P}(\text{C}_6\text{H}_5)_3]^+\text{O}_2\text{SR}^-$ by I^- of added KI led to optically active $\text{C}_5\text{H}_5\text{Fe}(\text{CO})[\text{P}(\text{C}_6\text{H}_5)_3]\text{I}$ (30, 145, 147). In the reaction of optically active $\text{C}_5\text{H}_5\text{Fe}(\text{CO})[\text{P}(\text{C}_6\text{H}_5)_3]\text{CH}_2\text{OR}$ with SO_2 , insertion into



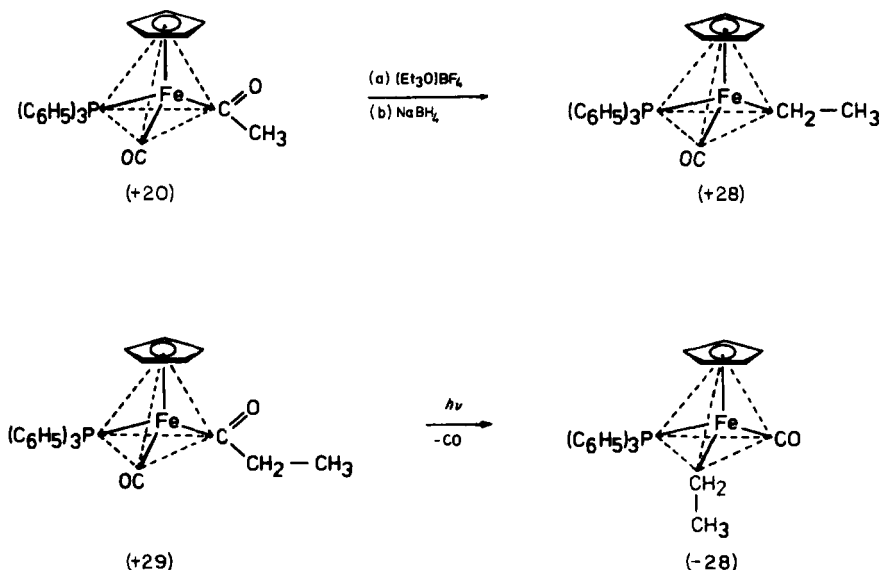
SCHEME 18

C—O before Fe—C was observed, giving the compounds (+)- $\text{C}_5\text{H}_5\text{Fe}(\text{CO})[\text{P}(\text{C}_6\text{H}_5)_3]\text{CH}_2\text{SO}_3\text{R}$ (30).

B. Carbonylation and Decarbonylation

Metal-alkyl bonds can be carbonylated, and metal-acyl bonds can be decarbonylated (10, 137). The carbonylation reaction supposedly proceeds by alkyl migration from the metal to a terminal CO group, ligand L occupying its former position, and vice versa for the decarbonylation process (10, 137). Both reactions have been shown to be stereospecific, with retention of configuration of the carbon atom adjacent to the metal or to the carbonyl group (8-10, 138, 140, 148, 149). With such diastereoisomeric pairs of enantiomers as 1,3-($\text{CH}_3, \text{C}_6\text{H}_5$) $\text{C}_5\text{H}_5\text{Fe}(\text{CO})[\text{P}(\text{C}_6\text{H}_5)_3]\text{COCH}_3$ and $\text{C}_5\text{H}_5\text{Fe}(\text{CO})[\text{P}(\text{C}_6\text{H}_5)_3]\text{COCH}_2\text{CH}(\text{CH}_3)(\text{C}_6\text{H}_5)$, it could be shown that the photochemical decarbonylation is highly stereoselective with respect to the Fe atom, a loss in stereospecificity being due to an epimerization subsequent to CO elimination (144, 150, 151).

In an elegant study, Davison *et al.* (108) demonstrated the alkyl migration step in the decarbonylation of iron acyl derivatives. Starting from (-)- $\text{C}_5\text{H}_5\text{Fe}(\text{CO})(\text{COOC}_{10}\text{H}_{19})\text{P}(\text{C}_6\text{H}_5)_3$ (19b), the (+)-acetyl and (+)-propionyl compounds +20 and +29 (Scheme 19) were prepared by reaction



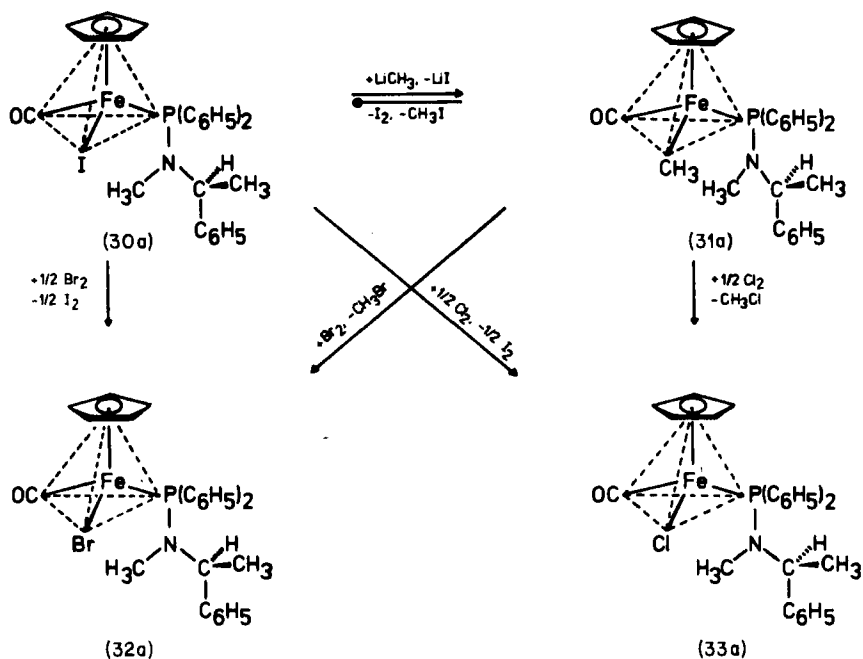
SCHEME 19

with LiCH_3 and LiC_2H_5 , as discussed in Section VIII, B. Although having an inverted configuration compared to the ester **19b** used for their preparation, the two (–)-acyls must have the same relative configuration at the Fe atom (105, 108). Reduction of the (+)-acetyl complex **+20** with NaBH_4 via (–)- $\{\text{C}_5\text{H}_5\text{Fe}(\text{CO})[\text{P}(\text{C}_6\text{H}_5)_3]\text{C}(\text{OC}_2\text{H}_5)\text{CH}_3\}\text{BF}_4$ (95) gives the (+)-ethyl compound **+28** which must necessarily have the same relative configuration of the Fe atom, as the reduction does not involve the asymmetric iron atom (108). Photochemical decarbonylation of the (+)-propionoyl compound **+29** also gives an iron ethyl compound **–28**. The opposite optical rotation shows that compound **–28** has an Fe configuration opposite to that of **+28** formed on reduction, although according to the reduced optical rotations of **–28** compared to **+28**, obviously some racemization has taken place during the photochemical decarbonylation (108), as mentioned before (144, 150, 151). These observations are in agreement with the proposed decarbonylation mechanism with ethyl migration into the site vacated by the leaving terminal CO ligand (10, 137).

C. Cleavage of Fe—C and Fe—Hal Bonds by Electrophiles

The (–)₃₃₅-iron iodo compound **30a** containing the aminophosphine (S)-(+)-(C₆H₅)₂PN(CH₃)CH(CH₃)(C₆H₅), can be easily prepared in large quantities (65). According to Scheme 20, the (–)₃₆₅-iodo complex can be transformed into other optically active compounds: by reaction with LiCH_3 , into the (–)₃₆₅-methyl derivative **31a**, and by interaction with bromine and chlorine, into the corresponding (–)₃₆₅-bromo and (–)₃₆₅-chloro derivatives **32a** and **33a**, respectively (58). Similarly, the Fe—C bond in the (–)₃₆₅-methyl compound **31a** can be cleaved by the halogens I_2 , Br_2 , and Cl_2 to give the corresponding (–)₃₆₅-halo derivatives **30a**, **32a**, and **33a** (58).

The optical rotations of the products show that all of these reactions are stereoselective. By the following reaction cycle, it can be proved that reaction **30a** → **32a** proceeds with retention of configuration of the metal center. Starting with the (–)₃₆₅-methyl compound **31a**, the (–)₃₆₅-bromo complex **32a** can be arrived at in two ways: in a one-step or a two-step reaction. Consequently, the Fe—C bond in **31a** can be directly cleaved by Br_2 , or it can first be cleaved by I_2 , and then, in a second step, the corresponding (–)₃₆₅-iodo derivative **30a** can be converted into the (–)₃₆₅-bromo compound **32a**. If the same stereochemistry for the cleavage of the Fe—C bond in **31a** by the halogens Br_2 and I_2 is assumed, the transformation step (–)₃₆₅-iodo compound **30a** → (–)₃₆₅-bromo compound **32a** must necessarily occur with retention of configuration (58).



SCHEME 20

As the two diastereoisomers of each product have different 1H -NMR spectra, the degree of stereoselectivity for all of the reaction steps in Scheme 20 can be determined by NMR integration. It turned out that, depending on the reaction type and the reaction conditions, different stereoselectivities were found. Hence, the bromination of the $(-)$ ₃₆₅-iodo compound **30a** has a stereoselectivity as high as 80%, whereas the methylation of **30a** and the halogen cleavage of the Fe—C bond in **31a** occur with an optical yield of only ~40% (58).

Interestingly, unreacted starting material in all of the reactions in Scheme 20 was partly epimerized with respect to the iron atom. Similarly, reduced optical purity of reaction product and recovered starting material, compared to the starting material used, was also observed in electrophilic cleavage reactions of other optically active $C_5H_5Fe(CO)[P(C_6H_5)_3]alkyls$ (152) and, earlier, of $(1,3-CH_3, C_6H_5)C_5H_3Fe(CO)[P(C_6H_5)_3]alkyls$, in which the two diastereoisomeric pairs of enantiomers were enriched (143, 145). As an explanation, the formation of a square-pyramidal intermediate by addition of an electrophile to the Fe atom was proposed. Such an intermediate could pseudorotate, like the compounds discussed in Section X. If reversion to the

starting material or conversion to products, for which different pathways including chiral intermediates of reduced coordination number can be envisaged, are not greatly different in rate from that of pseudorotation, all of the stereochemical results obtained can be explained (143, 145, 152, 153).

The cleavage of the Fe—Si bond in $(-)\text{-C}_5\text{H}_5\text{Fe}(\text{CO})[\text{P}(\text{C}_6\text{H}_5)_3]\text{-Si}(\text{CH}_3)(\text{C}_6\text{H}_5)(1\text{-C}_{10}\text{H}_7)$ by Br_2 and I_2 , respectively, proved to be stereoselective with respect to the Si atom, but the Fe compounds $\text{C}_5\text{H}_5\text{Fe}(\text{CO})[\text{P}(\text{C}_6\text{H}_5)_3]\text{Br}$ and $\text{C}_5\text{H}_5\text{Fe}(\text{CO})[\text{P}(\text{C}_6\text{H}_5)_3]\text{I}$ were completely racemized at the Fe atom (154, 155). In the cleavage of the Fe—C bond in optically active $\text{C}_5\text{H}_5\text{Fe}(\text{CO})(\text{COOC}_{10}\text{H}_{19})\text{P}(\text{C}_6\text{H}_5)_3$ and $\text{C}_5\text{H}_5\text{Fe}(\text{CO})[\text{P}(\text{C}_6\text{H}_5)_3]\text{COCH}_3$ by iodine, only optically inactive $\text{C}_5\text{H}_5\text{Fe}(\text{CO})[\text{P}(\text{C}_6\text{H}_5)_3]\text{I}$ is formed (156). As far as the configuration of the α -C atom of the alkyl group is concerned, retention, as well as inversion, has been found for the electrophilic cleavage of Fe—C bonds (8, 139, 140, 157–159). Also, SO_2 -induced epimerization at the α -carbon atom in the alkyl chain of $\text{C}_5\text{H}_5\text{Fe}(\text{CO})[\text{P}(\text{OC}_6\text{H}_5)_3]\text{CH}(\text{C}_6\text{H}_5)\text{Si}(\text{CH}_3)_3$ was reported (160).

XII

MISCELLANEOUS REACTIONS

Whereas the $(-)\text{-}_{385}$ -methyl compound (31a) in Scheme 20 is configurationally stable in solution, even at high temperatures, the corresponding iodo, bromo, and chloro derivatives 30a, 32a, and 33a epimerize in solution by change of configuration at the iron atom (60). The half-life of the Cl compound (33a) at 30°C in benzene is 29 minutes, that of the Br compound (32a) at 45°C is 185 minutes, and that of the I compound (30a) at 70°C is 51 minutes. The epimerization mechanism has been shown to occur by phosphine dissociation. Chiral intermediates could not be demonstrated. If, in the iodo compound $(-)\text{-C}_5\text{H}_5\text{Fe}(\text{CO})[\text{P}(\text{C}_6\text{H}_5)_2\text{N}(\text{R})\text{CH}(\text{CH}_3)(\text{C}_6\text{H}_5)]\text{I}$, the aminophosphine containing an *N*-methyl group ($\text{R} = \text{CH}_3$) is replaced by the aminophosphine carrying an *N*-ethyl group ($\text{R} = \text{C}_2\text{H}_5$), the rate of epimerization at 70°C increases (the half-life decreasing from 51 to 11 minutes) in accordance with the view that an increase in size of the phosphine favors dissociation. It was shown that phosphine exchange and epimerization have the same rates (60).

Another optically active series of configurationally labile compounds has been reported for cobalt. In the complexes $[\text{C}_5\text{H}_5\text{Co}(\text{R}_f)[\text{P}(\text{C}_6\text{H}_5)_2\text{R}^*]\text{I}$, R_f can be CF_3 , C_2F_5 , C_3F_7 ; and the aminophosphines $\text{P}(\text{C}_6\text{H}_5)_2\text{R}^*$ are (*S*)- $(\text{C}_6\text{H}_5)_2\text{PN}(\text{R})\text{CH}(\text{CH}_3)(\text{C}_6\text{H}_5)$ ($\text{R} = \text{H}$, CH_3 , C_2H_5 , $\text{CH}_2\text{C}_6\text{H}_5$) (63). These

compounds epimerize in different solvents with half-lives of ~ 30 minutes near room temperature (the mechanism being unknown), a value similar to that for the epimerization and structural isomerization of $(-)$ - $C_5H_5Co(C_3F_7)(NCS)CNCH(CH_3)(C_6H_5)$ (70).

Other reactions that are stereoselective or stereospecific with respect to the metal configuration are the Ti—O cleavage, discussed in Section II,B, and the Walden inversion at the asymmetric Mo atom discussed in previous reviews (11, 69).

In the preceding paragraphs, different types of compound that are configurationally stable and labile at the metal center, as well as some stereochemical results of their reactions, were discussed. However, this large field has only been lightly plowed, and many important questions remain open. When is a chiral compound optically stable at the metal center, and when is it optically labile? What is the mechanism of the change in the metal configuration in case it is labile? What is the stereochemistry of a reaction at a chiral metal center: retention, inversion, or racemization? Our knowledge of these matters remains rudimentary. Until rationalizations for, and especially predictions regarding, the configurational stability of new compounds and the stereochemical course of their reactions can be made, much detailed information remains to be accumulated. There is still a long way to go before this area of stereochemistry will be as well understood as the stereochemistry of nucleophilic substitution at the asymmetric carbon atom (161) and the asymmetric silicon atom (162).

XIII

OPTICAL INDUCTION

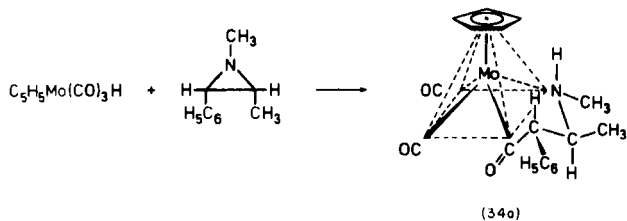
A. Asymmetric Synthesis

Frequently, in the synthesis of optically active organo-transition-metal complexes, the chiral center at the metal atom is built up by starting with a prochiral precursor, as shown for the Mn compounds in Scheme 6. The compound $[C_5H_5Mn(CO)_2NO]PF_6$ contains a symmetry plane bisecting the cyclopentadienyl ring, the manganese atom, the nitrosyl group, and the angle between the two carbonyl groups. If one of the two enantiotopic carbonyl groups is replaced by a monodentate ligand L, the metal atom becomes a chiral center. Under achiral conditions, CO substitution at both sites is equally probable, the enantiomers being formed in a 1:1 ratio (19–22). Toward an optically active ligand L^* , however, the two

Mn—CO sites are no longer equivalent, and two diastereoisomers, differing only in the metal configuration, are formed in a ratio differing from 1:1. When the diastereoisomers are stable toward interconversion, their ratio is a measure of the optical induction of the optically active ligand L^* in the asymmetric synthesis, reflecting the different activation energies for the formation of the two different diastereoisomers from the same prochiral precursor. In the reaction in Scheme 6, the optically active aminophosphine $(C_6H_5)_2PN(CH_3)CH(CH_3)(C_6H_5)$ yields a diastereoisomer ratio of **11a:11b** = 66:34 (55), whereas in the reaction with the prochiral $C_5H_5Mo(CO)_2NO$ the diastereoisomer ratio of **15a:15b** is close to 50:50 (54, 59). As well as the aminophosphine (S) -(+)- $(C_6H_5)_2PN(CH_3)CH(CH_3)(C_6H_5)$, ten other unidentate optically active P ligands were used in the reaction with $C_5H_5Mo(CO)_2NO$, the optical induction ranging between the diastereomer ratios 70:30 and 50:50 (54). Such low optical inductions seem to be representative of asymmetric synthesis in which a chiral center at the metal atom is formed from a prochiral precursor under kinetic control.

Higher optical inductions have been observed in special cases. Thus, in the reaction of $C_5H_5Mo(CO)_3H$ with optically active aziridines (see Scheme 21), the aziridine ring is opened; and, with incorporation of CO, a compound having an unsymmetrical five-membered chelate ring is formed in which the Mo atom is an asymmetric center (90). The two chiral carbon atoms in the aziridine system, mainly because of the tendency of the bulky substituents to stay equatorial in the puckered five-membered chelate ring, control the configuration at the Mo and N atoms, so that only one isomer is formed (**34a**), the absolute configuration of which has been determined (90, 91).

Another example of a reaction leading to exclusive formation of one metal configuration is (+)-bis(π -pinenyl)nickel (163), in which the Ni atom is bonded to two π -allyl systems. The combination of one π -pinenyl system with a Ni atom is a chiral entity, in which the metal is an asymmetric center. The opposite configuration at Ni would result should the



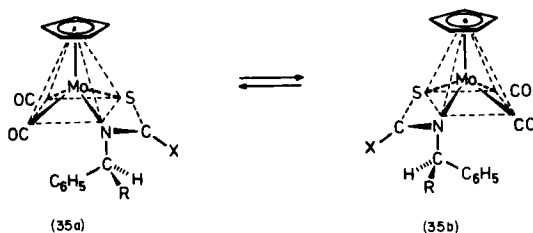
SCHEME 21

Ni be bonded to the other side of the π -pinenyl system, which is sterically severely hindered. Therefore, only one isomer is formed, the X-ray structural characterization of which has been reported (163). Similarly, the diene (+)-carvone favors coordination via one side in the C_8H_8Rh complex, characterized by X-ray crystallography (164–166). In both cases, the metal configuration is coupled to the configuration of the asymmetric carbon atoms in the π -allyl and π -diene ligands, respectively, thus giving rise to the stereochemistry usually encountered in organometallic compounds having planar chirality (5–8).

B. Epimerization Equilibria

As this topic and its relation to asymmetric catalysis has been reviewed (167, 168), only one representative example will be given here. In Section X, it was mentioned that equilibration of the square-pyramidal thioamidato complexes is rapid in toluene solution at ~ 40 – $50^\circ C$ (79, 84–87). It may be recalled that these two diastereoisomers contain exactly the same ligands, differing only in the configuration at the Mo atom. In the equilibration reaction, the labile configuration at the metal center changes under the influence of the stable chirality in the amino side chain of the optically active ligand. Thus, the optically active ligand controls the equilibrium concentration of the two possible metal configurations. A gauge of this optical induction from the ligand to the metal atom is the diastereoisomer ratio at equilibrium, which is identical with the equilibrium constant, reflecting the different energy content of both diastereoisomers, irrespective of the mechanism of the change in configuration at the metal atom (79, 92). For the $C_8H_8Mo(CO)_2$ complexes containing the thioamidato ligand system $SC(X)NCH(R)(C_6H_5)$, the diastereoisomer ratio **35b**:**35a** at equilibrium was studied as a function of the substituents X and R in the thioamidato ligand (see Scheme 22).

The variation of substituent X, the amino component being (*S*)- $NCH(CH_3)(C_6H_5)$, gave the results shown in the first column of the table in Scheme 22. For the formic acid derivative ($X = H$) with a 50:50 equilibrium ratio of both diastereoisomers, there is no optical induction when the labile metal configurations equilibrate under the influence of the stable chirality of the (*S*)- $CH(CH_3)(C_6H_5)$ group in the ligand. On going from the thioamidato system derived from formic acid to those of acetic acid, benzoic acid, and 1-naphthoic acid, the equilibrium ratios in toluene- d_8 at $40^\circ C$ steadily rise, reaching 74% optical purity of the favored diastereoisomer for $X = 1-C_{10}H_7$ (79, 85). Also, a variation of the alkyl substituent R at the inducing asymmetric center was carried out for the



	R = CH ₃	R = CH ₂ -CH ₃	R = CH(CH ₃) ₂
X = H	50 : 50		
X = CH ₃	69 : 31	89 : 11	98 : 2
X = C ₆ H ₅	77 : 23	95 : 5	99 : 1
X = C ₁₀ H ₇	87 : 13		

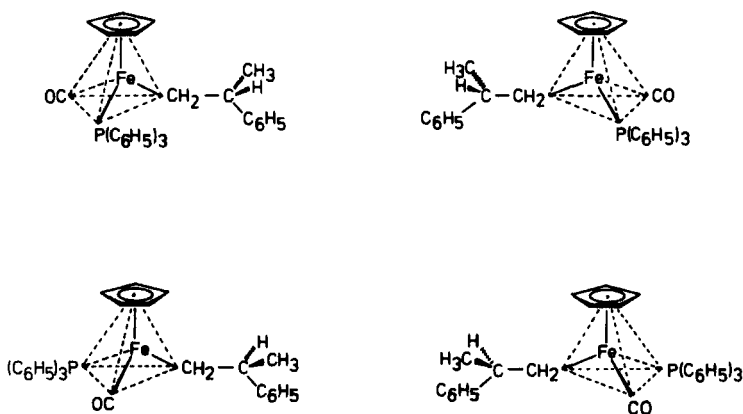
SCHEME 22

acetic acid and benzoic acid series (lines 2 and 3 of the table in Scheme 22). The alkyl substituents $R = \text{CH}_3$, C_2H_5 , and $\text{CH}(\text{CH}_3)_2$ were used. In the acetic acid series, the corresponding equilibrium diastereoisomer ratios were 69:31, 89:11, and 98:2, identical to an asymmetric induction of 38, 78, and 96%. For the benzoic acid series, all ratios were a little larger, that for $R = \text{CH}(\text{CH}_3)_2$ reaching an equilibrium induction of 98% (89). Thus, the metal configuration in labile complexes can be controlled by asymmetric induction from optically active ligands (167). Similar equilibrium studies have been reported for other square-pyramidal complexes of the type $\text{C}_5\text{H}_5\text{M}(\text{CO})_2\text{LL}'$ (88, 92, 169, 170) and for such pseudo-tetrahedral systems as $\text{C}_5\text{H}_5\text{M}(\text{CO})(\text{R})_2(\text{PR}_3)\text{I}$ (63), both containing labile metal configurations.

XIV

DIASTEREOISOMERICALLY RELATED PAIRS OF ENANTIOMERS

In Section III, it was shown that the introduction of an optically active resolving agent (S') into a pair of enantiomers (R)/(S) gives two diastereoisomers (R,S') and (S,S') with different metal configurations. Instead of an optically active resolving agent (S'), a racemic mixture of a chiral ligand (R')/(S') can also be used. Then, not two, but four, isomers are formed: two diastereoisomeric pairs of enantiomers (R,R') and (S,S') as well as (R,S') and (S,R'). An example is presented in Scheme 23,



SCHEME 23

showing the various possible combinations of a chiral center (R')/(S') in the side chain of an alkyl ligand having a chiral Fe configuration (R)/(S) (144, 150).

Similarly, cyclopentadienyl ligands containing the 1-phenylethyl substituent and cyclopentadienyl ligands of planar chirality, e.g., with CH_3 and C_6H_5 substituents in 1,3-position to each other, were used as racemic ligand components (R')/(S'), mainly by the groups of Wojcicki (143–145, 150, 151) and the Dijon group (171–179). Together with an asymmetric metal center of configuration (R)/(S), two diastereomerically related pairs of enantiomers arise. Also, some interesting compounds in which the metal atom is a center of pseudoasymmetry have been described (180, 181).

The separation methods described in Section IV for pairs of optically active diastereoisomers have also been applied to mixtures of diastereoisomeric pairs of enantiomers. By one or other of the following methods, it was possible to separate diastereoisomeric pairs of enantiomers completely or, at least, to obtain enriched fractions. In chromatography under achiral conditions, enantiomers are eluted at identical rates. Therefore, the pairs of enantiomers (RR')/(SS') and (RS')/(SR') can be separated chromatographically in the same way as a pair of optically active diastereoisomers (RS') and (SS'). By application of the methods based on solubility differences for many examples, fractions containing the less soluble pair of enantiomers could be separated from fractions containing the more soluble pair of enantiomers. However, with respect to the separation by solubility differences, the situation with two diastereoisomeric pairs of enantiomers is more complicated than that of a pair of

optically active diastereoisomers, because, besides pairs of enantiomers, pure enantiomers may also crystallize (143–145, 151, 171–179).

As an analytical method for determining the diastereoisomeric purity, thin-layer chromatography is occasionally used, but most frequently ^1H -NMR spectroscopy is employed. Enantiomers give identical spectra. Thus, the ^1H -NMR spectrum of a mixture of diastereoisomeric pairs of enantiomers contains only two sets of signals, one set for each pair of enantiomers; this is analogous to the situation with a pair of optically active diastereoisomers described in Section VI. Hence, by ^1H -NMR spectroscopy, the separation of diastereotopic pairs of enantiomers can be monitored, and the diastereoisomeric purity can be controlled (143–145, 151, 171–179).

With separated pairs of enantiomers (RS')/(SR') and (RR')/(SS'), respectively, optically inactive but chiral at the metal atom, essentially the same stereochemical investigations can be carried out as with optically active compounds. Some of these aspects, including a selection of leading literature references will be given in the following discussion. Labile configurations at the metal center lead to the appearance of new signals in the NMR spectra (142, 145, 151), the stereoselectivity of reactions can be determined (44–48, 142, 145, 151), optical-induction phenomena can be studied (145), and absolute configurations can be assigned to the chiral metal centers (47, 182).

As optically active resolving agents for the preparation of diastereoisomers (Sections II and III) compounds are preferably used that are optically pure and configurationally stable under the reaction conditions employed. As described in Sections VIII–XII, many stereochemical investigations have been performed with optically active diastereoisomers, frequently leading to a partial or complete change in configuration at the metal atom. In these reactions the configuration of the chiral ligand may also change, e.g., by deprotonation of enolizable or benzylic CH bonds. Such a change in the ligand chirality, observable by chiroptical methods, but not observable by such nonchiral methods as NMR spectroscopy, would lead to the four isomers (RS')/(SR')/(SS')/(RR') of two diastereoisomerically related pairs of enantiomers. The same holds true for the preparation of diastereoisomers having different metal configuration on using an optically active compound that is not optically pure. The only difference between the last cases and the general case of diastereoisomeric pairs of enantiomers considered in this chapter, is the quantitative aspect. The ratios of isomers may differ according to the optical purity of the starting materials used, the degree of epimerization at the various chiral centers, and the asymmetric induction between the various chiral centers.

The disadvantage of the use of pairs of enantiomers with respect to optically active compounds is the lack of chiroptical properties. Consequently, such techniques as polarimetric kinetics cannot be used; and the chiroptical methods, a tool (described in the next section) that has proved to be extremely valuable in other areas of stereochemistry for the correlation of configuration of series of compounds or for connecting the configuration of starting materials and products of a chemical reaction in which the chiral center is involved, are not available for the assignment of configurations.

XV

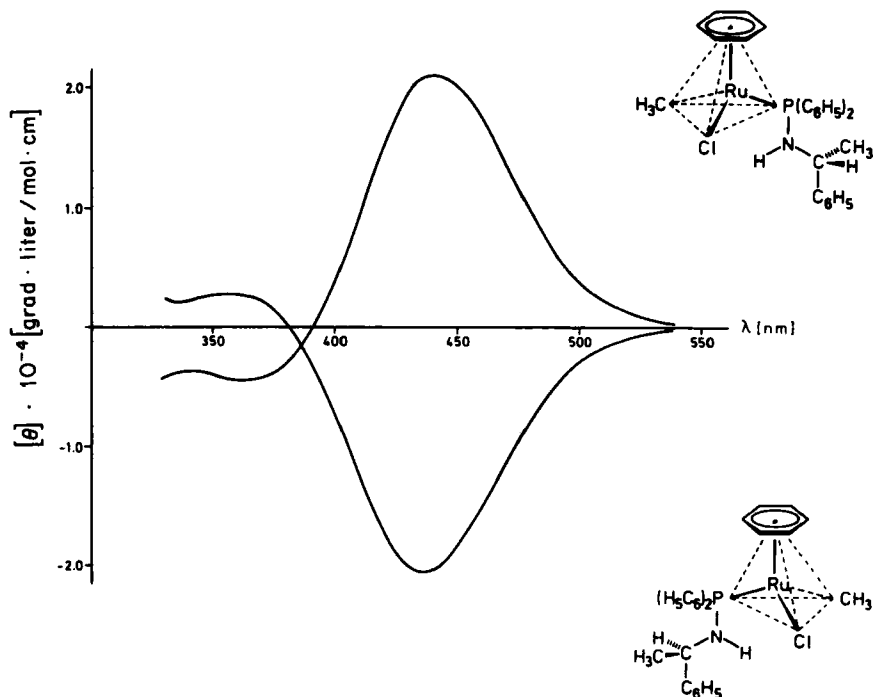
CHIROPTICAL PROPERTIES

Optically active organo-transition-metal compounds exhibit extremely large specific rotations, usually exceeding the specific rotations encountered in organic chemistry by a factor of one or two powers of ten (4). These large rotational values are a consequence of the fact that the compounds are colored, and thus exhibit strong Cotton effects in the visible part of the spectrum.

For some of the compounds, ORD spectra, and for most of them, CD spectra have been reported. The CD spectra of the two diastereoisomers (+)- and (-)- $\text{C}_6\text{H}_5\text{Ru}(\text{Cl})(\text{CH}_3)(\text{C}_6\text{H}_5)_2\text{PN}(\text{H})\text{CH}(\text{CH}_3)(\text{C}_6\text{H}_5)$ (61) in Scheme 24 demonstrate what is representative for most of the diastereoisomers, which differ only in the metal configuration: the two curves are almost mirror images of each other because the CD is mainly determined by the metal chromophore, and the chirality in the ligands usually makes only minor contributions, at least as far as the visible part of the spectrum is concerned. The same also holds for other chiroptical properties. Consequently, the optical rotations of diastereoisomers generally have opposite signs, their values being not far from each other (51). Thus, diastereoisomers differing only in the metal configuration have, in addition to their NMR differentiability, almost opposite chiroptical parameters (4).

In Scheme 25, a series of compounds having different P ligands is shown, all having very similar CD spectra (54). In such cases, the similarity of the CD spectra has been used for the assignment of the same relative configuration to the metal atom, whereas virtually mirror-image morphology of the CD spectra has been taken as an indication of opposite relative configuration at the metal atom (105), arguments that are safe only if the compounds compared are not greatly different from each other (103).

Preliminary attempts have been made to correlate the bands in the CD



SCHEME 24

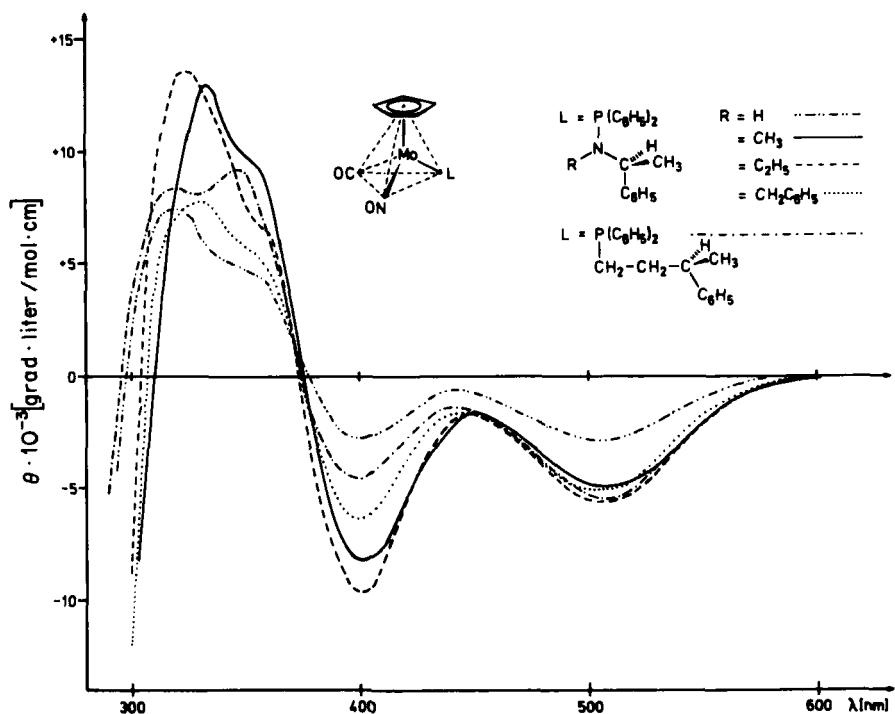
spectra with the metal configuration (42, 103). However, the development of rules for the correlation of configurations in organo-transition-metal chemistry by comparison of chiroptical properties is still an open field of research.

Another open area is the assignment of the various electronic transitions observable in the absorption, CD, and ORD spectra. Owing to the fact that bands in chiroptical spectroscopy have opposite signs, maxima can be more easily identified in CD and ORD spectra than in absorption spectra. Also, such information as the rotatory strength can be used for band assignment, a necessary condition for a widespread use of chiroptical spectroscopy for correlation of configurations.

XVI

ABSOLUTE CONFIGURATION

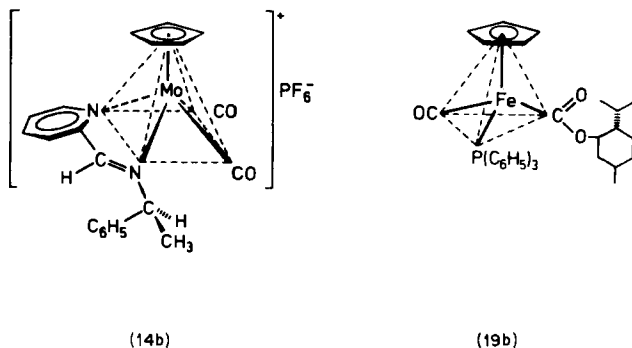
Absolute configurations can be determined by X-ray crystallography, either by the method of anomalous X-ray scattering or by that of internal comparison with a reference of known absolute configuration.



SCHEME 25

With the absolute configuration known, the problem is the assignment of an appropriate configurational symbol to the metal configuration. In the (*R,S*) system of Cahn *et al.* (2, 3), there is no convention as to how ligands that are π -bonded to a metal atom should be treated. According to a proposal by Tirouflet *et al.* (182) and Stanley and Baird (184), polyhapto ligands are considered to be pseudo-atoms of atomic weight equal to the sum of the atomic weights of all of the atoms bonded to the metal atom. By this extension of the (*R,S*) system to polyhapto ligands in organo-transition-metal chemistry, the rank of ligands in the sequence rule can be defined. Hence, $\eta^6\text{-C}_6\text{H}_6$, $\eta^5\text{-C}_5\text{H}_5$, and $\eta^2\text{-C}_2\text{H}_4$ count as pseudo-atoms of atomic weight 72, 60, and 24 (or atomic number 36, 30, and 12), respectively (182, 184).

According to this proposal, and in addition to the rules of Cahn *et al.*, the priority sequence of the four ligands in the Fe complex 19b in Scheme 26 is $\text{C}_5\text{H}_5 > \text{P}(\text{C}_6\text{H}_5)_3 > \text{COOC}_{10}\text{H}_{19} > \text{CO}$, and the configuration at the Fe atom can be specified by use of the sequence rule as (*S*) (106, 107). For the comparison of literature data, it is necessary to note that in some



SCHEME 26

papers a different ligand sequence has been used (108). As with an asymmetric carbon atom, the asymmetric Fe atom in **19b** belongs to chirality class *a*, for which an achiral borderline between (*R*) and (*S*) exists according to Ruch and Schönhofer (185–187).

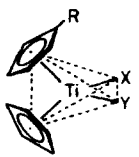
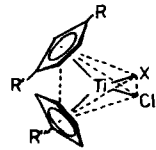
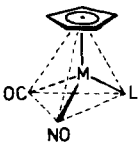
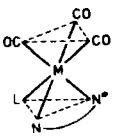
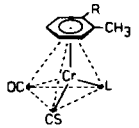
On the other hand, the square-pyramidal and octahedral structures belong to chirality class *b*, for which there is no such achiral separation between (*R*) and (*S*). For the examples known thus far, no ambiguity arises if the metal configuration in square-pyramidal molecules of the type $C_5H_5M(CO)_2L^1L^2$ is specified by using the sequence rule for the three ligands of highest priority (80). Therefore, the symbol for the Mo configuration in compound **14b** is (*R*). The formula and the configurational symbol for **14b** in (78, 80) are not in agreement with the correct absolute configuration of **14b** in the ORTEP of Fig. 1 of (80). If in a complex more chiral centers are present, the metal designation precedes that of carbon, according to a suggestion of Wojcicki (142). Thus, the full specification of configuration for the Mo complex **14b** is (*R,S*) (80).

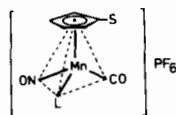
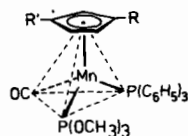
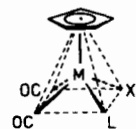
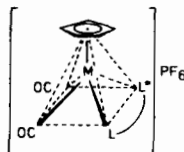
XVII

TABLE OF OPTICALLY ACTIVE COMPOUNDS

Table I collects the information available for optically active organo-transition-metal compounds having chiral metal atoms; a good deal of this material could not be mentioned in the preceding discussion of the more important lines of development. Only examples are included for which opposite configurations for the metal atom are possible, and for which a separation or enrichment of the isomers differing in the metal configuration has been demonstrated. For the sake of brevity, only one

TABLE I

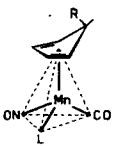
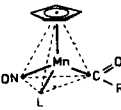
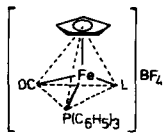
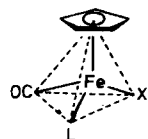
Compound	Remarks	References
	$R = C(CH_3)_3$; $X = C_6F_5$; $Y = OCH_2CH(CH_3)(C_6H_5)$, Cl $R = C(CH_3)_2C_6H_5$; $X = C_6F_5$; $Y = OCH_2CH(C_2H_5)(C_6H_5)$, Cl $R = CH_3$; $X = Cl$; $Y = OC_{10}H_{19}$ $R = CH(CH_3)_2$, $CH(C_6H_5)_2$, $C(CH_3)_2C_6H_5$; $X = Cl$; $Y = OC_6H_5$, $OC_6H_4CH_2-2$, $OC_6H_3CH_2-3-CH(CH_3)_2-6$ $R = CH(CH_3)(C_6H_5)$; $X = Cl$; $Y = C_6F_5$	41, 42 41, 42 188 49 43, 189
	$R = R'' = CH(CH_3)(C_6H_5)$; $R' = H$; $X = C_6F_5$ $R = CH(CH_3)_2$; $R' = CH_3$; $R'' = H$; $X = OC_6H_3(CH_3)_2-2,6$, $OC_6H_3CH_2-3-CH(CH_3)_2-6$ $R', R'' = CH(CH_3)CH_2CH_2$; $X = C_6F_5$, $OC_6H_3(CH_3)_2-2,6$	43 49, 50 50
	$M = Mo$; $L = CNCH(CH_3)(C_6H_5)$, CNC_6H_{11} , $P(C_2H_5)_3$ $M = Mo$; $L = (C_6H_5)_2PN(CH_3)CH(CH_3)(C_6H_5)$ $M = Mo$, W ; $L = (C_6H_5)_2PN(R)CH(CH_3)(C_6H_5)$; $R = H$, CH_3 , C_2H_5 , $CH_2C_6H_5$, $(CH_3)_2PN(CH_3)CH(CH_3)(C_6H_5)$, $(C_6H_5)_2PX$; $X = CH_2CH(CH_3)(C_6H_5)$, $C_{10}H_{19}$, $OC_{10}H_{19}$, $P(OC_{10}H_{19})_3$, $(C_2H_5O)P[OCH(COOC_2H_5)]_2$	69 59, 62 54
	$N-N^* = 2-C_6H_4N-CH=NCH(CH_3)(C_6H_5)$ $M = Cr, Mo, W$; $L = P(C_6H_5)_3$ $M = Mn$; $L = Br$	71 72
	$R = COOCH_3$, CH_3 $L = P(OC_6H_5)_3$, $P(OC_2H_5)_3$, $P(C_6H_5)_3$	36, 37

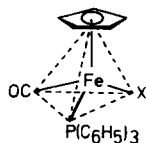


M = Mo, W; X = PF ₆	73, 75, 76
L-L* = 2-C ₅ H ₄ N-CH=NCH(CH ₃)(C ₆ H ₅)	78-80
M = Mo, W; X = PF ₆	
L-L* = (6-CH ₃)-2-C ₅ H ₃ N-CH=NCH(CH ₃)(C ₆ H ₅), (4-CH ₃)-2-C ₅ H ₃ N-CH=NCH(CH ₃)(C ₆ H ₅), [4,6-(CH ₃) ₂]-2-C ₅ H ₂ N-CH=NCH(CH ₃)(C ₆ H ₅), 2-C ₆ H ₄ N-CH=NCH(CH ₃)(C ₆ H ₅)	77, 79
Mo = Mo; X = Cl, PF ₆ ; L-L* = H ₂ NCH(CH ₃)CH ₂ NH ₂	81
M = Mo; L-X = 2-C ₄ H ₉ N-CH=NCH(CH ₃)(C ₆ H ₅)	79, 82
M = Mo, W; L-X = 2-C ₆ H ₄ -CH=NCH(CH ₃)(C ₆ H ₅)	79, 83
M = Mo, W; L-X = SC(R)NCH(R')(C ₆ H ₅); R' = CH ₃ , <i>i</i> -C ₃ H ₇	79, 84-86, 89
R = H, CH ₃ , C ₆ H ₅ , 4-C ₆ H ₄ OCH ₃ , 1-C ₁₀ H ₇ , 2-C ₁₀ H ₇ , NHCH(CH ₃)(C ₆ H ₅)	
M = Mo; L-X = C(2-C ₅ H ₄ N)(C ₆ H ₅)N(H)[CH(CH ₃)(C ₆ H ₅)]	190-192
M = Mo; L-X = 2-C ₅ H ₄ N-C(S)NCH(CH ₃)(C ₆ H ₅)	88
M = Mo; L-X = COCH(R)CH(R')NH(R'')	90, 91
R = H, C ₆ H ₅ ; R' = CH ₃ , C ₂ H ₅ ; R'' = H, CH ₃	
M = Mo; L = (C ₆ H ₅) ₂ PN(CH ₃)CH(CH ₃)(C ₆ H ₅); X = Cl	67
R' = CH ₃	39, 40
R = COOCH ₃ , CH ₃	
S = H, CH ₃	
L = P(C ₆ H ₅) ₃	27, 28, 100
L = (C ₆ H ₅) ₂ PN(CH ₃)CH(CH ₃)(C ₆ H ₅)	53, 55
L = P(4-C ₆ H ₄ X) ₃	101
X = CF ₃ , Cl, F, C ₆ H ₅ , H, CH ₃ , OCH ₃ , N(CH ₃) ₂	

Continued

TABLE I (Continued)

Compound	Remarks	References
	$X = CF_3, Cl, F, C_6H_5, H, CH_3, OCH_3, N(CH_3)_2$ $R = CH_3, 4-C_6H_4X; L = P(C_6H_5)_3$ $R = C_6H_5; L = P(4-C_6H_4X)_3$ $R = C_6H_5; L = (C_6H_5)_2PN(CH_3)CH(CH_3)(C_6H_5)$	100 101 55
	$S = H, CH_3$ $X = CF_3, Cl, F, C_6H_5, H, CH_3, OCH_3, N(CH_3)_2$ $R = OC_{10}H_{19}, OC_2H_5, OCH_3; L = P(C_6H_5)_3$ $R = CH_3, 4-C_6H_4X; L = P(C_6H_5)_3$ $R = C_6H_5; L = P(4-C_6H_4X)_3$ $R = OC_{10}H_{19}; L = P(4-C_6H_4X)_3$ $R = C_6H_5; L = (C_6H_5)_2PN(CH_3)CH(CH_3)(C_6H_5)$ $R = C_6H_5; L = P(C_6H_5)_3, P(4-C_6H_4OCH_3)_3, P(\eta-C_4H_9)_3,$ $P(OC_2H_5)_3, CNC_6H_{11}, CO$	13, 27, 102, 111 100 101, 109 101 55 109, 110
	$L = C(CH_3)N(H)CH(CH_3)(C_6H_5), C(CH_3)OC_2H_5$ $L = C_2H_4$	95, 103, 108 30, 103
	$L = CNCH(CH_3)(C_6H_5), X = I$ $L = (C_6H_5)_2PN(R)CH(CH_3)(C_6H_5), R = CH_3, C_2H_5$ $X = CH_3, COCH_3, Cl, Br, I$	68 58, 60, 65, 66



$X = \text{COOC}_{10}\text{H}_{19}$

93, 94, 103, 106, 107,
156

$X = \text{CH}_2\text{OC}_{10}\text{H}_{19}, \text{CH}_2\text{I}$

29, 30, 31

$X = \text{CH}_2\text{R}, \text{SO}_2\text{CH}_2\text{R}', \text{Cl}, \text{Br}, \text{I}, \text{OCOCF}_3$

29, 30, 103, 147, 152

$\text{R} = \text{R}' = \text{H}, \text{CH}_3, \text{C}_2\text{H}_5, i\text{-C}_3\text{H}_7, \text{C}_3\text{H}_5, \text{C}_6\text{H}_5, \text{COOC}_{10}\text{H}_{19},$

$\text{OC}_{10}\text{H}_{19}$

$\text{R} = \text{CN}, \text{OCH}_3, \text{Cl}, \text{Br}, \text{I}, \text{SO}_3\text{C}_{10}\text{H}_{19}$

96

$X = \text{CH}_2\text{COOC}_{10}\text{H}_{19}, \text{SO}_2\text{CH}_2\text{COOC}_{10}\text{H}_{19}$

103, 105, 108, 156

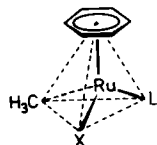
$X = \text{COCH}_3, \text{COC}_2\text{H}_5, \text{CH}_3, \text{C}_2\text{H}_5$

144

$X = \text{R}, \text{COR}, \text{SO}_2\text{R}, \text{R} = \text{CH}_2\text{CH}(\text{CH}_3)(\text{C}_6\text{H}_5)$

154, 155

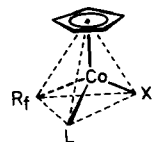
$X = \text{SiCH}_3(\text{C}_6\text{H}_5)(1\text{-C}_{10}\text{H}_7)$



$\text{L} = (\text{C}_6\text{H}_5)_2\text{PN}(\text{H})\text{CH}(\text{CH}_3)(\text{C}_6\text{H}_5)$

61, 64

$\text{X} = \text{Cl}, \text{SnCl}_3$



$\text{L}-\text{X} = 2\text{-C}_4\text{H}_9\text{N}-\text{CH}=\text{NCH}(\text{CH}_3)(\text{C}_6\text{H}_5); \text{R}_f = n\text{-C}_3\text{F}_7$

124

$\text{L} = \text{CNCH}(\text{CH}_3)(\text{C}_6\text{H}_5); \text{X} = \text{NCS}; \text{R}_f = n\text{-C}_3\text{F}_7$

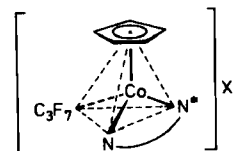
70

$\text{L} = (\text{C}_6\text{H}_5)_2\text{PN}(\text{R})\text{CH}(\text{CH}_3)(\text{C}_6\text{H}_5), \text{R} = \text{H}, \text{CH}_3, \text{C}_2\text{H}_5,$

63

$\text{CH}_2\text{C}_6\text{H}_5$

$\text{R}_f = \text{CF}_3, \text{C}_2\text{F}_5, n\text{-C}_3\text{F}_7; \text{X} = \text{I}$

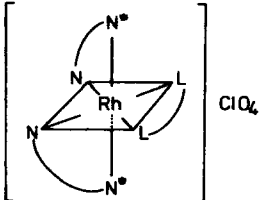
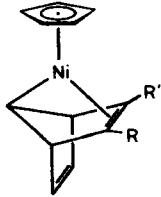


$\text{N}-\text{N}^* = 2\text{-C}_5\text{H}_4\text{N}-\text{CH}=\text{NCH}(\text{CH}_3)(\text{C}_6\text{H}_5)$

124

$\text{X} = \text{PF}_6, \text{I}$

TABLE I (Continued)

Compound	Remarks	References
	$N-N^* = 2-C_5H_4N-CH=NCH(CH_3)(C_6H_5)$ $L-L = [CH(COOCH_3)]_2, (CHCO)_2O$	193
	$R = COOH, R' = COOC_{10}H_{19}$	194

of the two possible configurations at the metal atom in enantiomers or diastereoisomers is shown. The assignment of configuration at the metal atom is arbitrary, except for those compounds, whose absolute configuration has been determined unambiguously. The arrangement of compounds adheres to the Periodic Table from Group IV to Group VIII.

REFERENCES

1. Lord Kelvin, "Baltimore Lectures, 1884 and 1893," pp. 436 and 619. C. J. Clay and Sons, London, 1904.
2. R. S. Cahn, C. K. Ingold, and V. Prelog, *Experientia* **12**, 81 (1956).
3. R. S. Cahn, C. K. Ingold, and V. Prelog, *Angew. Chem.* **78**, 413 (1955); *Angew. Chem. Int. Ed. Engl.* **5**, 385 (1966).
4. H. Brunner, *Angew. Chem.* **83**, 274 (1971); *Angew. Chem. Int. Ed. Engl.* **10**, 249 (1971).
5. K. Schlögl, *Fortschr. Chem. Forsch.* **6**, 479 (1966).
6. K. Schlögl, *Pure Appl. Chem.* **23**, 413 (1970).
7. K. Schlögl, *Top. Stereochem.* **1**, 39 (1967).
8. H. Brunner, "The Organic Chemistry of Iron," Vol. 1, p. 299. Academic Press, New York, 1978.
9. F. Calderazzo and K. Noack, *Coord. Chem. Rev.* **1**, 118 (1966).
10. A. Wojcicki, *Adv. Organomet. Chem.* **11**, 87 (1973).
11. H. Brunner, *Top. Curr. Chem.* **56**, 67 (1975).
12. W. Hieber and J. Ellermann, *Chem. Ber.* **96**, 1643 (1963).
13. H. Brunner, *Angew. Chem.* **81**, 395 (1969); *Angew. Chem. Int. Ed. Engl.* **8**, 382 (1969).
14. A. Werner, *Ber. Dtsch. Chem. Ges.* **44**, 1887 (1911).
15. G. B. Kauffman, *Coord. Chem. Rev.* **12**, 105 (1974).
16. C. J. Hawkins, "Absolute Configuration of Metal Complexes," Wiley (Interscience), New York, 1971.
17. J. J. Eisch and R. B. King, "Organometallic Syntheses," Vol. I, p. 118. Academic Press, New York, 1965.
18. A. N. Nesmeyanov, K. N. Anisov, N. E. Kolobova, and L. L. Krasnoslobodskaya, *Izv. Akad. Nauk SSSR, Ser. Khim.* p. 860 (1970).
19. H. Brunner, *Z. Anorg. Allg. Chem.* **368**, 120 (1969).
20. H. Brunner and H.-D. Schindler, *J. Organomet. Chem.* **19**, 135 (1969).
21. R. B. King and A. Efraty, *Inorg. Chem.* **8**, 2374 (1969).
22. R. A. James and J. A. McCleverty, *J. Chem. Soc., A*, p. 850 (1970).
23. E. O. Fischer, *Angew. Chem.* **86**, 651 (1974).
24. T. Kruck and M. Noack, *Chem. Ber.* **97**, 1693 (1964).
25. R. B. King, M. B. Bisnettè, and A. Fronzaglia, *J. Organomet. Chem.* **4**, 246 (1965).
26. R. B. King, M. B. Bisnettè, and A. Fronzaglia, *J. Organomet. Chem.* **5**, 341 (1966).
27. H. Brunner and H.-D. Schindler, *Z. Naturforsch. Teil B* **26**, 1220 (1971).
28. H. Brunner and H.-D. Schindler, *J. Organomet. Chem.* **24**, c7 (1970).
29. T. C. Flood, F. J. DiSanti, and D. L. Miles, *J. Chem. Soc. Chem. Commun.* p. 336 (1975).
30. T. C. Flood, F. J. DiSanti, and D. L. Miles, *Inorg. Chem.* **15**, 1910 (1976).
31. A. Davison, W. C. Krusell, and R. C. Michaelson, *J. Organomet. Chem.* **72**, c7 (1974).

32. A. Nakamura, A. Konishi, Y. Tatsuno, and S. Otsuka, *J. Am. Chem. Soc.* **100**, 3443 (1978).
33. A. Nakamura, A. Konishi, R. Tsujitani, M.-A. Kudo, and S. Otsuka, *J. Am. Chem. Soc.* **100**, 3449 (1978).
34. R. Dabard, A. Meyer, and G. Jaouen, *C. R. Acad. Sci., Ser. C* **286**, 201 (1969).
35. G. Jaouen and R. Dabard, *J. Organomet. Chem.* **21**, 43 (1970).
36. G. Simonneaux, A. Meyer, and G. Jaouen, *J. Chem. Soc. Chem. Commun.* p. 69 (1975).
37. G. Jaouen, A. Meyer, and G. Simonneaux, *Tetrahedron* **31**, 1889 (1975).
38. R. Riemschneider and W. Herrmann, *Justus Liebigs Ann. Chem.* **648**, 68 (1961).
39. F. le Moigne and R. Dabard, *J. Organomet. Chem.* **60**, c14 (1973).
40. F. le Moigne, R. Dabard, and M. le Plouzennec, *J. Organomet. Chem.* **122**, 365 (1976).
41. C. Moise, J. C. Leblanc, and J. Tirouflet, *J. Am. Chem. Soc.* **97**, 6272 (1975).
42. J. C. Leblanc, C. Moise, and J. Tirouflet, *Nouv. J. Chim.* **1**, 211 (1977).
43. J. C. Leblanc, C. Moise, and J. Tirouflet, *J. Organomet. Chem.* **148**, 171 (1978).
44. A. Dormond, J. P. Letourneux, and J. Tirouflet, *C. R. Acad. Sci., Ser. C* **280**, 477 (1975).
45. T. Bounthakna, J. C. Leblanc, and C. Moise, *C. R. Acad. Sci. Ser. C* **280**, 1431 (1975).
46. J. Besançon, F. Huq, and M. Colette, *J. Organomet. Chem.* **96**, 63 (1975).
47. J. Besançon, S. Top, J. Tirouflet, J. Dusauso, C. Lecomte, and J. Protas, *J. Chem. Soc. Chem. Commun.* p. 325 (1976).
48. J. Besançon, S. Top, J. Tirouflet, Y. Dusauso, C. Lecomte, and J. Protas, *J. Organomet. Chem.* **127**, 153 (1977).
49. A. Dormond, J. Tirouflet, and F. le Moigne, *J. Organomet. Chem.* **69**, c7 (1974).
50. A. Dormond, J. Tirouflet, and F. le Moigne, *J. Organomet. Chem.* **101**, 71 (1975).
51. H. Brunner, *Ann. N.Y. Acad. Sci.* **239**, 213 (1974).
52. J. Tirouflet and G. Jaouen, *Actual. Chim.* **4**, 6 (1975).
53. H. Brunner and W. Rambold, *Angew. Chem.* **85**, 1118 (1973); *Angew. Chem. Int. Ed. Engl.* **12**, 1013 (1973).
54. H. Brunner and J. Doppelberger, *Chem. Ber.* **111**, 673 (1978).
55. H. Brunner and W. Steger, *Z. Naturforsch. Teil B* **31**, 1493 (1976).
56. L. Horner, H. Winkler, A. Rapp, A. Mentrup, H. Hoffmann, and P. Beck, *Tetrahedron Lett.* p. 161 (1961).
57. K. Naumann, G. Zon, and K. Mislow, *J. Am. Chem. Soc.* **91**, 7012 (1969).
58. H. Brunner and G. Wallner, *Chem. Ber.* **109**, 1053 (1976).
59. H. Brunner and J. Doppelberger, *Bull. Soc. Chim. Belg.* **84**, 923 (1975).
60. H. Brunner and F. Rackl, *J. Organomet. Chem.* **118**, c19 (1976).
61. H. Brunner and R. G. Gastinger, *J. Chem. Soc. Chem. Commun.* p. 488 (1977).
62. M. G. Reisner, I. Bernal, H. Brunner, and J. Doppelberger, *J. Chem. Soc. Dalton Trans.* p. 1664 (1978).
63. H. Brunner, J. Doppelberger, P. Dreischl, and T. Möllenberg, *J. Organomet. Chem.* **139**, 223 (1977).
64. H. Brunner and R. G. Gastinger, *J. Organomet. Chem.* **145**, 365 (1978).
65. H. Brunner, M. Muschiol, and W. Nowak, *Z. Naturforsch. Teil B* **33**, 407 (1978).
66. H. Brunner and H. Vogt, *Z. Naturforsch. Teil B* **33**, 1231 (1978).
67. G. M. Reisner, I. Bernal, H. Brunner, M. Muschiol, and B. Siebrecht, *J. Chem. Soc. Chem. Commun.* p. 691 (1978).
68. H. Brunner and M. Vogel, *J. Organomet. Chem.* **35**, 169 (1972).

69. H. Brunner and M. Lappus, *Angew. Chem.* **84**, 955 (1972); *Angew. Chem. Int. Ed. Engl.* **11**, 923 (1972).
70. H. Brunner and W. Rambold, *Z. Naturforsch. Teil B* **29**, 367 (1974).
71. H. Brunner and W. A. Herrmann, *J. Organomet. Chem.* **57**, 183 (1973).
72. H. Brunner and M. Lappus, *Z. Naturforsch. Teil B* **29**, 262 (1974).
73. H. Brunner and W. A. Herrmann, *Chem. Ber.* **105**, 3600 (1972).
74. K. W. Barnett and D. W. Slocum, *J. Organomet. Chem.* **44**, 1 (1972).
75. H. Brunner and W. A. Herrmann, *Angew. Chem.* **84**, 442 (1972); *Angew. Chem. Int. Ed. Engl.* **11**, 418 (1972).
76. H. Brunner and W. A. Herrmann, *Chem. Ber.* **106**, 632 (1973).
77. H. Brunner and W. A. Herrmann, *J. Organomet. Chem.* **74**, 423 (1974).
78. S. J. LaPlaca, I. Bernal, H. Brunner, and W. A. Herrmann, *Angew. Chem.* **87**, 379 (1975); *Angew. Chem. Int. Ed. Engl.* **14**, 353 (1975).
79. H. Brunner, W. A. Herrmann, and J. Wachter, *J. Organomet. Chem.* **107**, c11 (1976).
80. I. Bernal, S. J. LaPlaca, J. Korp, H. Brunner, and W. A. Herrmann, *Inorg. Chem.* **17**, 382 (1978).
81. H. Brunner and M. Muschiol, *Z. Naturforsch. Teil B* **33**, 247 (1978).
82. H. Brunner and W. A. Herrmann, *J. Organomet. Chem.* **63**, 339 (1973).
83. H. Brunner and J. Wachter, *J. Organomet. Chem.* **107**, 307 (1976).
84. H. Brunner and J. Wachter, *Angew. Chem.* **88**, 342 (1976); *Angew. Chem. Int. Ed. Engl.* **15**, 316 (1976).
85. H. Brunner and J. Wachter, *Chem. Ber.* **110**, 721 (1977).
86. M. G. Reisner, I. Bernal, H. Brunner, and J. Wachter, *J. Organomet. Chem.* **137**, 329 (1977).
87. H. Brunner, E. Bauer, and J. Wachter, *Chem. Ber.* **111**, 379 (1978).
88. H. Brunner and G. Spettel, *J. Organomet. Chem.* **160**, 149 (1978).
89. H. Brunner and R. Lukas, *Chem. Ber.*, **112**, 2528 (1979).
90. W. Beck, W. Danzer, A. T. Liu, and G. Huttner, *Angew. Chem.* **88**, 511 (1976); *Angew. Chem. Int. Ed. Engl.* **15**, 495 (1976).
91. A. T. Liu, G. Huttner, H. Lorenz, and W. Beck, *J. Organomet. Chem.* **129**, 91 (1977).
92. H. Brunner, *Chem. Unserer Zeit* **11**, 157 (1977).
93. H. Brunner and E. Schmidt, *J. Organomet. Chem.* **21**, p53 (1970).
94. H. Brunner and E. Schmidt, *J. Organomet. Chem.* **50**, 219 (1973).
95. A. Davison and D. L. Reger, *J. Am. Chem. Soc.* **94**, 9237 (1972).
96. T. C. Flood and D. L. Miles, *J. Am. Chem. Soc.* **95**, 6460 (1973).
97. H. Brunner and M. Langer, *J. Organomet. Chem.* **54**, 221 (1973).
98. P. M. Treichel and R. L. Shubkin, *Inorg. Chem.* **6**, 1328 (1967).
99. M. Y. Darensbourg, *J. Organomet. Chem.* **38**, 133 (1972).
100. H. Brunner and M. Langer, *J. Organomet. Chem.* **87**, 223 (1975).
101. H. Brunner and J. A. Aclasis, *J. Organomet. Chem.* **104**, 347 (1976).
102. H. Brunner and H.-D. Schindler, *Chem. Ber.* **104**, 2467 (1971).
103. C. K. Chou, D. L. Miles, R. Bau, and T. Flood, *J. Am. Chem. Soc.* **100**, 7271 (1978).
104. F. Seel, *Z. Anorg. Allg. Chem.* **249**, 308 (1942).
105. H. Brunner and E. Schmidt, *J. Organomet. Chem.* **36**, C18 (1972).
106. M. G. Reisner, I. Bernal, H. Brunner, and M. Muschiol, *Angew. Chem.* **88**, 847 (1976); *Angew. Chem. Int. Ed. Engl.* **15**, 776 (1976).
107. G. M. Reisner, I. Bernal, H. Brunner, and M. Muschiol, *Inorg. Chem.* **17**, 783 (1978).
108. A. Davison and N. Martinez, *J. Organomet. Chem.* **74**, C17 (1974).
109. H. Brunner, J. Aclasis, M. Langer, and W. Steger, *Angew. Chem.* **86**, 864 (1974); *Angew. Chem. Int. Ed. Engl.* **13**, 810 (1974).

110. H. Brunner and W. Steger, *J. Organomet. Chem.* **120**, 239 (1976).
111. H. Brunner, *J. Organomet. Chem.* **94**, 189 (1975).
112. C. A. Tolman, *J. Am. Chem. Soc.* **92**, 2953 (1970).
113. C. A. Tolman, *J. Am. Chem. Soc.* **92**, 2956 (1970).
114. C. A. Tolman, W. C. Seidel, and L. W. Gosser, *J. Am. Chem. Soc.* **96**, 53 (1974).
115. C. A. Tolman, *Chem. Rev.* **77**, 313 (1977).
116. P. Hofmann, *Angew. Chem.* **39**, 551 (1977); *Angew. Chem. Int. Ed. Engl.* **16**, 536 (1977).
117. P. Hofmann, Habilitationsschrift, Universität Erlangen, 1978.
118. P. S. Braterman and J. D. Black, *J. Organomet. Chem.* **39**, c3 (1972).
119. W. Strohmeier, *Fortschr. Chem. Forsch.* **10**, 306 (1968).
120. R. R. Hitch, S. K. Gondal, and C. T. Sears, *J. Chem. Soc. Chem. Commun.* p. 777 (1971).
121. G. Fachinetti, G. Fochi, and C. Floriani, *J. Chem. Soc. Dalton Trans.* p. 1946 (1977).
122. G. Fachinetti, C. Floriani, and H. Stoeckli-Evans, *J. Chem. Soc. Dalton Trans.* p. 2297 (1977).
123. H. Brunner and W. Steger, *Bull. Soc. Chim. Belg.* **85**, 883 (1976).
124. H. Brunner and W. Rambold, *J. Organomet. Chem.* **64**, 373 (1974).
125. M. Gielen and N. Vanlauten, *Bull. Soc. Chim. Belg.* **79**, 679 (1970).
126. W. Hässelbarth and E. Ruch, *Theor. Chim. Acta* **29**, 259 (1973).
127. J. E. Musher and W. C. Agosta, *J. Am. Chem. Soc.* **96**, 1320 (1974).
128. L. M. Jackman and F. A. Cotton, "Dynamic Nuclear Magnetic Resonance Spectroscopy," pp. 494-496. Academic Press, 1975.
129. J. W. Faller and A. S. Anderson, *J. Am. Chem. Soc.* **92**, 5852 (1970).
130. J. W. Faller, A. S. Anderson, and A. Jakubowski, *J. Organomet. Chem.* **27**, c47 (1971).
131. J. W. Faller, A. S. Anderson, and C. Chen, *J. Organomet. Chem.* **17**, F7 (1969).
132. J. W. Faller, A. S. Anderson, and C. Chen, *J. Chem. Soc. Chem. Commun.* p. 719 (1969).
133. G. Wright and R. J. Mawby, *J. Organomet. Chem.* **51**, 281 (1973).
134. E. Pfeiffer, J. Kuypers, and K. Vrieze, *J. Organomet. Chem.* **105**, 371 (1976).
135. T. C. Flood, E. Rosenberg, and A. Sarhangi, *J. Am. Chem. Soc.* **99**, 4334 (1977).
136. A. Wojcicki, *Adv. Organomet. Chem.* **12**, 31 (1974).
137. F. Calderazzo, *Angew. Chem.* **89**, 305 (1977); *Angew. Chem. Int. Ed. Engl.* **16**, 299 (1977).
138. J. J. Alexander and A. Wojcicki, *Inorg. Chim. Acta* **5**, 655 (1971).
139. G. M. Whitesides and D. J. Boschetto, *J. Am. Chem. Soc.* **93**, 1529 (1971).
140. P. L. Bock, D. J. Boschetto, J. R. Rasmussen, J. P. Demers, and G. M. Whitesides, *J. Am. Chem. Soc.* **96**, 2814 (1974).
141. D. Dong, D. A. Slack, and M. C. Baird, *J. Organomet. Chem.* **153**, 219 (1978).
142. K. Stanley and M. C. Baird, *J. Am. Chem. Soc.* **99**, 1808 (1977).
143. T. G. Attig and A. Wojcicki, *J. Am. Chem. Soc.* **96**, 262 (1974).
144. P. Reich-Rohrwig and A. Wojcicki, *Inorg. Chim. Acta* **13**, 2457 (1974).
145. T. G. Attig, R. G. Teller, S. M. Wu, R. Bau, and A. Wojcicki, *J. Am. Chem. Soc.* **101**, 619 (1979).
146. S. R. Su and A. Wojcicki, *J. Organomet. Chem.* **27**, 231 (1971).
147. S. L. Miles, D. L. Miles, R. Bau, and T. C. Flood, *J. Am. Chem. Soc.* **100**, 7278 (1978).
148. G. M. Whitesides and D. J. Boschetto, *J. Am. Chem. Soc.* **91**, 4313 (1969).
149. R. W. Johnson and R. G. Pearson, *J. Chem. Soc. Chem. Commun.* p. 986 (1970).

150. T. G. Attig, P. Reich-Rohrwig, and A. Wojcicki, *J. Organomet. Chem.* **51**, c21 (1973).
151. T. G. Attig and A. Wojcicki, *J. Organomet. Chem.* **82**, 397 (1974).
152. T. C. Flood and D. L. Miles, *J. Organomet. Chem.* **127**, 22 (1977).
153. T. C. Flood and F. J. DiSanti, *J. Chem. Soc. Chem. Commun.* p. 18 (1975).
154. G. Cerveau, E. Colomer, R. Corriu, and W. E. Douglas, *J. Chem. Soc. Chem. Commun.* p. 410 (1975).
155. G. Cerveau, E. Colomer, R. Corriu, and W. E. Douglas, *J. Organomet. Chem.* **135**, 373 (1977).
156. H. Brunner and J. Strutz, *Z. Naturforsch. Teil B* **29**, 446 (1974).
157. P. L. Bock and G. M. Whitesides, *J. Am. Chem. Soc.* **96**, 2826 (1974).
158. D. Slack and M. C. Baird, *J. Chem. Soc. Chem. Commun.* p. 701 (1974).
159. D. A. Slack and M. C. Baird, *J. Am. Chem. Soc.* **98**, 5539 (1976).
160. K. Stanley, D. Groves, and M. C. Baird, *J. Am. Chem. Soc.* **97**, 6599 (1975).
161. L. H. Sommer, "Stereochemistry, Mechanism, and Silicon." McGraw-Hill, New York, 1965.
162. C. K. Ingold, "Structure and Mechanism in Organic Chemistry." Cornell Univ. Press, Ithaca, New York, 1969.
163. B. Henc, H. Pauling, and G. Wilke, *Justus Liebigs Ann. Chem.* p. 1820 (1974).
164. W. Winter, B. Koppenhöfer, and V. Schurig, *J. Organomet. Chem.* **150**, 145 (1978).
165. B. F. G. Johnson, J. Lewis, and D. I. Yarrow, *J. Chem. Soc. Dalton Trans.* p. 1054 (1974).
166. V. Schurig, *J. Organomet. Chem.* **74**, 457 (1974).
167. H. Brunner, *Acc. Chem. Res.*, **12**, 250 (1979).
168. P. Pino and G. Consiglio, in "Fundamental Research in Homogeneous Catalysis," p. 147. Plenum, New York, 1977.
169. W. Beck and W. Petri, *J. Organomet. Chem.* **127**, c40 (1977).
170. W. Beck and U. Nagel, submitted for publication.
171. F. le Moigne, A. Dormond, J. C. Leblanc, C. Moise, and J. Tirouflet, *J. Organomet. Chem.* **54**, c13 (1973).
172. C. Moise, J. C. Leblanc, and J. Tirouflet, *Tetrahedron Lett.* p. 1723 (1974).
173. A. Dormond, T. Kolavudh, and J. Tirouflet, *C. R. Acad. Sci. Ser. C* **282**, 551 (1976).
174. J. C. Leblanc, C. Moise, and T. Bounthakna, *C. R. Acad. Sci. Ser. C* **278**, 973 (1974).
175. J. Besançon, S. Top, and J. Tirouflet, *C. R. Acad. Sci. Ser. C* **281**, 135 (1975).
176. R. Broussier, H. Normand, and B. Gautheron, *Tetrahedron Lett.* p. 4077 (1976).
177. A. Dormond and T. Kolavudh, *J. Organomet. Chem.* **125**, 63 (1977).
178. J. Besançon and S. Top, *J. Organomet. Chem.* **127**, 139 (1977).
179. A. Dormond, T. Kolavudh, and J. Tirouflet, *J. Organomet. Chem.* **164**, 317 (1979).
180. A. Dormond, Ou-Khan, and J. Tirouflet, *C. R. Acad. Sci. Ser. C* **278**, 1207 (1974).
181. J. Leblanc and C. Moise, *J. Organomet. Chem.* **131**, 35 (1977).
182. C. Lecomte, Y. Dusauso, J. Protas, J. Tirouflet, and A. Dormond, *J. Organomet. Chem.* **73**, 67 (1974).
183. S. Brunie, J. Mazan, N. Langlois, and H. B. Kagan, *J. Organomet. Chem.* **114**, 225 (1976).
184. K. Stanley and M. C. Baird, *J. Am. Chem. Soc.* **97**, 6599 (1975).
185. E. Ruch and A. Schönhofer, *Theor. Chim. Acta* **10**, 91 (1968).
186. E. Ruch, *Theor. Chim. Acta* **11**, 183 (1968).
187. E. Ruch, *Angew. Chem.* **89**, 67 (1977); *Angew. Chem. Int. Ed. Engl.* **16**, 65 (1977).
188. H. Brunner and H.-D. Schindler, *J. Organomet. Chem.* **55**, c71 (1973).
189. J. C. Leblanc and C. Moise, *J. Organomet. Chem.* **120**, 65 (1976).
190. H. Brunner and J. Wachter, *J. Organomet. Chem.* **113**, c58 (1976).

191. H. Brunner, H. Schwägerl, J. Wachter, G. M. Reisner, and I. Bernal, *Angew. Chem.* **90**, 478 (1978); *Angew. Chem. Int. Ed. Engl.* **17**, 453 (1978).
192. H. Brunner, H. Schwägerl, and J. Wachter, *Chem. Ber.*, **112**, 2079 (1979).
193. M. A. Haga, H. Yukawa, and T. Tanaka, *J. Organomet. Chem.* **128**, 265 (1977).
194. H. Brunner and W. Pieronczyk, *Bull. Soc. Chim. Belg.* **86**, 725 (1977).

Mixed-Metal Clusters

WAYNE L. GLADFELTER

*Department of Chemistry
University of Minnesota
Minneapolis, Minnesota*

and

GREGORY L. GEOFFROY

*Department of Chemistry
The Pennsylvania State University
University Park, Pennsylvania*

I. Introduction	207
II. Synthesis	209
A. Pyrolysis Reactions	227
B. Addition of Coordinatively Unsaturated Species	230
C. Redox Condensations	233
D. Reaction of Carbonylmetalates with Metal Halides	236
E. Other Methods	237
F. Synthetic Strategies	239
III. Methods of Characterization	242
A. Mass Spectrometry	242
B. Infrared Spectroscopy	244
C. Electronic Absorption Spectroscopy	246
D. Nuclear Magnetic Resonance Spectroscopy	247
E. Mössbauer Spectroscopy	247
F. Structure Determination by X-Ray and Neutron Diffraction	248
G. Chromatographic Properties	248
IV. Reactivity	249
A. Ligand Substitution Reactions	250
B. Acid-Base Reactions	253
C. Reactions with H ₂ and CO	254
D. Reactions with Alkynes	255
E. Catalytic Reactions	256
V. Dynamic NMR Studies	257
A. Trinuclear Clusters	258
B. Tetranuclear Clusters	259
VI. Almost Mixed-Metal Clusters	265
Addendum	268
References	269

I

INTRODUCTION

Transition-metal cluster compounds are currently under intensive scrutiny because of their potential catalytic applications, both as models for

understanding catalytic metal surfaces (123–125, 127) and as catalysts in their own right (129, 141, 145). Numerous reviews (7, 36, 40, 41, 90, 100, 125, 127, 159) on various aspects of the chemistry and properties of clusters have appeared, including reviews of tetranuclear carbonyl clusters (40), high-nuclearity metal carbonyl clusters (41), hydrido transition-metal clusters (90), structural and bonding patterns in cluster chemistry (159), clusters and surfaces (125), very small metallic and bimetallic clusters and their relevance to the cluster-surface analogy (127), and NMR studies of clusters (7). The purpose of this review is to address an increasingly important subset of clusters, those that contain a mixture of different transition metals in their metal framework.

Mixed-metal clusters are of interest from three principal perspectives. First, they should prove valuable as precursors for the preparation of bimetallic and multimetallic *heterogeneous* catalysts (17, 141, 145). Such catalysts could be prepared by allowing clusters to adsorb onto such catalyst supports as SiO_2 and Al_2O_3 , followed by pyrolysis to remove the ligands. This technique could yield multimetallic catalysts having precisely defined compositions and high dispersion, provided that the degree of aggregation which occurs during the pyrolysis step is minimal. Second, mixed-metal clusters may find important applications in *homogeneous* catalysis. In particular, because of the different reactivities of the different metals present in mixed-metal clusters, multimetal homogeneous catalysts may show reactivity patterns significantly different from those of homometallic clusters. Finally, the low symmetry of mixed-metal clusters makes them useful for probing various aspects of the reactivity and molecular dynamics of clusters. For example, the dynamic properties of $\text{H}_2\text{FeRu}_2\text{Os}(\text{CO})_{13}$ were clearly resolved because of its mixed-metal character (77). The consequent low symmetry allowed the carbonyls to become nonequivalent and distinguishable by ^{13}C -NMR spectroscopy. Likewise, the specific sites of substitution in $\text{H}_2\text{FeRu}_3(\text{CO})_{12}(\text{PMe}_2\text{Ph})$ were determined by NMR spectroscopy because of the inherent low symmetries of the isomers of this complex (82).

In this review, we have attempted to compile a comprehensive listing of all of the mixed-metal clusters that have been prepared. It has been necessary to adhere to a specific definition of a mixed-metal cluster, and the following two criteria have been set by us for detailed coverage in this review.

- (1) Only transition metals are considered under the mixed-metal category.
- (2) By definition, a cluster must contain at least three metals, and a portion of the cluster must contain a closed polyhedron.

These criteria have arbitrarily ruled out many compounds that may be of interest. We mention several of these in a noncomprehensive section at the end of this review.

The clusters that we have surveyed are collected in Table I.¹ Clusters in this table are listed under the earliest transition metal contained within their framework. The groups of the periodic table are listed in succession, and within each group the metals are arranged by period. The entries in each metal listing are further categorized according to the size of the clusters, with smaller clusters listed before larger ones. For illustration, $\text{FeCo}_2(\text{CO})_8(\text{C}_2\text{Ph}_2)$ appears before $\text{FeNi}_2(\text{Cp})_2(\text{CO})_5$, but both are listed prior to $\text{FeCo}_3\text{H}(\text{CO})_{12}$.

Some interesting statistics are revealed in Table I. Of the 161 entries, clusters containing four metals dominate, having 83 separate entries. Three-metal clusters are next, with 56. There are 11 five-metal clusters and 10 six-metal clusters, but only 1 cluster containing more than six metals. The largest mixed-metal cluster is the X-ray-characterized $[\text{Fe}_6\text{Pd}_6\text{H}(\text{CO})_{24}]^{3-}$ containing twelve metals (*III*). Forty percent of the mixed-metal clusters shown in Table I contain iron (64 entries). The next largest contributor is cobalt, with 53 entries. The ranking by element with respect to number of entries is as follows: Fe (64) > Co (53) > Os (45) > Ru (32) > Pt (26) > Ni (19) > Rh (16), Re (16) > Mo (12), W (10) > Mn (8) > Ir (7) > Cr (4), Cu (4), Au (4) > Pd (3) > Ta (2) > Ti (1), Zr (1), V (1), Tc (1).

II

SYNTHESIS

It has been said that noticeably few metal clusters have been prepared by designed or rational synthetic procedures (52, 55). Indeed, most clusters have been prepared by placing together a variety of reagents, allowing them to react, and then examining the reaction mixtures to find out what compounds have been prepared. This is particularly true of mixed-metal clusters, and a real need exists for the development of synthetic procedures that can be used for the designed synthesis of particular compounds.

Examination of the methods that have been used in preparing the mixed-metal clusters listed in Table I reveals that the majority have been synthesized via four general types of reaction: (1) pyrolysis, (2) addition

¹ For more recent listings, see Addendum, p. 268.

TABLE I
MIXED-METAL CLUSTERS

Index No.	Cluster ^a	Color	ν_{CO} ^b	Other available spectral data ^c	Crystal structure	References
Titanium						
1	$\text{TiCo}_2(\text{Cp})_2(\text{CO})_8$	—	—	—	No	140
Zirconium						
2	$\text{Zr}_2\text{Co}_2(\text{Cp})_4(\text{CO})_5$	—	—	—	No	140
Vanadium						
3	$\text{VCo}_3(\text{Cp})(\text{CO})_9$	Black-brown	Pentane: 2086 w, 2063 s, 2054 s, 2025 m, 1864 m	Mass	No	85
Tantalum						
4	$[(\text{Ta}_4\text{Mo}_2\text{Cl}_{12})\text{Cl}_6]^{2-}$	Dark green	—	UV-vis, far-IR, mag, ESR	No	117
5	$[(\text{Ta}_5\text{MoCl}_{12})\text{Cl}_6]^{2- \rightarrow 3-}$	Dark red	—	UV-vis, far-IR, mag	No	117
Chromium						
6	$\text{CrPt}_2(\mu\text{-C(OMe)Ph})(\text{CO})_6\text{L}_2$ L = $\text{PMe}(t\text{-Bu})_3$, PCy_3	Red	L = $\text{PMe}(t\text{-Bu})_3$: 2019 vs, 1936 vs, 1908 vs, br, 1876 m	^1H , ^{31}P	No	18
7	$\text{CrFe}_2(\text{CO})_{11}(\text{PPh})$	Deep red	Hexane: 2083 w, 2057 w, 2036 vs, 2024 vs, 2016 s, 2004 s, 1982 m, 1968 w, 1945 w, 1938 m,	Mass, ^1H	Yes	93
8	$\text{CrFeCo}_2(\text{CO})_{14}\text{S}$	Black	Cyclohexane: 2108 w, 2071 m, 2059 s, 2040 m, 2033 w, 1989 m, 1963 s	—	Yes	132

9	$[\text{Cr}_2\text{Ni}_3(\text{CO})_{18}]^{2-}$	Dark red	CH_2Cl_2 : 2040 w, 1982 s, 1925 w, 1890 m, 1842 mw, 1795 w	—	Yes	134
Molybdenum (see also entries 4 and 5)						
10	$\text{Mo}_2\text{Fe}(\text{Cp})_2(\text{CO})_8$	Red	Pentane: 2050, 2020, 2000, 1900, 1875	^1H	No	57
11	$\text{Mo}_2\text{Pt}(\text{Cp})_2(\text{CO})_4(\text{PPh}_3)_2$	Red	Pentane: 1980, 1800	^1H	No	57
12	$\text{MoOs}_3\text{H}(\text{Cp})(\text{CO})_{12}$	—	—	—	No	48
13	$\text{MoOs}_3\text{H}_3(\text{Cp})(\text{CO})_{11}$	—	—	—	No	48
14	$\text{MoCo}_3(\text{Cp})(\text{CO})_{11}$	Black	CCl_4 : 2092 s, 2052 vs, 2045 vs, 2034 s, 1996 s, 1982 m, 1956 s, 1887 w, 1861 m, 1835 sh	^1H , Mass	Yes	137
15	$[\text{Mo}_2\text{Fe}_2(\text{Cp})_2(\text{CO})_{10}]^{2-}$	Maroon	CH_2Cl_2 : 1998 ms, 1932 vs, 1884 vs, 1868 ms (sh)	^1H	No	88
16	$[\text{Mo}_2\text{Ni}_4(\text{CO})_{14}]^{2-}$	—	—	—	Yes	134
17	$\text{Mo}_2\text{Pd}_2(\text{Cp})_2(\text{CO})_6\text{L}_2$ L = PPh_3 , PEt_3	Violet	KBr: 1842 vs, 1801 m, 1772 vs	^1H	Yes	21,60
18	$\text{Mo}_2\text{Pt}_2(\text{Cp})_2(\text{CO})_6(\text{PPh}_3)_2$	Black	KBr: 1831 vs, 1805 w (sh), 1741 vs	—	No	26
19	$[\text{Mo}_2\text{Ni}_5(\text{CO})_{16}]^{2-}$	Red-orange	CH_2Cl_2 : 2039 w, 1994 s, 1933 m, 1901 s, 1838 w, 1786 w		Yes	134
Tungsten						
20	$\text{WPt}_2\{\mu\text{-C}(\text{OMe})\text{Ph}\}(\text{CO})_6\text{L}_2$ L = $\text{PMe}(\text{i-Bu})_2$, PCy_3	Red	Cyclohexane, L = $\text{PMe}(\text{i-Bu})_2$: 2032 s, 1940 m, 1922 s, 1914 (sh)	^1H , ^{31}P , ^{13}C	Yes	18
21	$\text{W}_2\text{Ni}(\mu\text{-CC}_6\text{H}_4\text{CH}_3)_2(\text{Cp})_2(\text{CO})_4$	Purple	—	—	No	19
22	$\text{W}_2\text{Pd}(\mu\text{-CC}_6\text{H}_4\text{CH}_3)_2(\text{Cp})_2(\text{CO})_4$	Purple	—	—	No	19

Continued

TABLE I (Continued)

Index No.	Cluster ^a	Color	ν_{CO} ^b	Other available spectral data ^c	Crystal structure	References
23	$\text{W}_2\text{Pt}(\mu\text{-CC}_6\text{H}_4\text{CH}_3)_2(\text{Cp})_2(\text{CO})_4$	Purple	—	—	No	19
24	$\text{WRu}_3\text{H}(\text{Cp})(\text{CO})_{12}$	—	—	—	No	48
25	$\text{WOs}_3\text{H}(\text{Cp})(\text{CO})_{12}$	Red	—	^1H	Yes	48
26	$\text{WOs}_3\text{H}_2(\text{Cp})(\text{CO})_{11}$	Orange	—	^1H	Yes	48
27	$\text{WCo}_3(\text{Cp})(\text{CO})_{11}$	Black	CCl_4 : 2090 s, 2052 vs, 2045 vs, 2034 s, 1994 s, 1976 m, 1944 s, 1885 w, 1859 m, 1832 s	^1H	No	137
28	$[\text{W}_2\text{Fe}_2(\text{Cp})_2(\text{CO})_{10}]^{2-}$	Red-violet	CH_2Cl_2 : 1997 w, 1930 ms, 1880 m (br)	^1H	No	88
29	$[\text{W}_2\text{Ni}_2(\text{CO})_{16}]^{2-}$	Orange	CH_2Cl_2 : 2036 w, 1998 s, 1930 mw, 1896 s, 1835 m, 1791 w	—	Yes	134
Manganese						
30	$[\text{MnFe}_2(\text{CO})_{12}]^-$	Blue-black	THF: 2063, 1999, 1990, 1972, 1944, 1903, 1827, 1785	UV, ^{13}C	No	15,73
31	$[\text{MnFe}_2(\text{CO})_{11}\text{L}]^-$ L = PPh_3 , PMePh_2 , $\text{P}(\text{O}-i\text{-Pr})_3$	Dark green	THF, L = PPh_3 : 2040 m, 1997 w (sh), 1974 s, 1953 s, 1927 m, 1887 w, 1785 w, 1750 w	Möss, ^1H	No	53
32	$\text{MnFe}_2(\text{Cp})(\text{CO})_4(\text{PPh})$	Deep red	—	—	Yes	91,92
33	$[\text{MnOs}_2(\text{CO})_{12}]^-$	Red	THF: 2080 w, 2018 s, 1981 vs, 1943 m, 1914 m, 1897 sh, 1887 m	—	No	106

34	$\text{MnOs}_2\text{H}(\text{CO})_{12}$	Orange	Hexane: 2136 w, 2081 s, 2051 vs, 2038 vs, 2016 m, 2001 m, 1993 m, 1975 m, 1957 m, 1951 m	Mass	No	106
35	$[\text{MnNi}_2(\text{Cp})_2(\text{CO})_3]^-$	Green-black	THF: 1971 vs, 1896 s, 1878 s (sh), 1744 w, 1688 m, 1647 w (sh)	^1H	No	87
36	$\text{MnOs}_3\text{H}(\text{CO})_{16}$	Yellow	Hexane: 2136 w, 2093 m, 2069 s, 2056 s, 2031 m, 2022 m, 2015 m, 2006 m, 1996 m, 1988 m (br), 1977 m, 1970 w	Mass	No	106
37	$\text{MnOs}_3\text{H}_3(\text{CO})_{13}$	Scarlet	KBr: 2133 m, 2086 s, 2055 s, 2043 sh, 2020 sh, 2008 s, 1990 sh, 1950 m, 1830 m	—	No	106
Technetium						
38	$[\text{TcFe}_2(\text{CO})_{12}]^-$	Dark red	THF: 2077 w, 2008 w, 1987 s, 1943 m, 1903 w, 1815 w, 1783 w	—	No	109
Rhenium						
39	$[\text{ReFe}_2(\text{CO})_{12}]^-$	Yellow	THF: 2075 w, 2006 m, 1991 s, 1946 m, 1903 w, 1814 w, 1785 w	—	No	66
40	$[\text{ReOs}_2(\text{CO})_{12}]^-$	Orange	THF: 2085 w, 2021 s, 2009 s, 1990 s, 1954 w, 1941 sh, 1925 sh, 1887 m	—	No	106
41	$\text{ReOs}_2\text{H}(\text{CO})_{12}$	Yellow	Hexane: 2136 w, 2086 s, 2058 sh, 2053 vs, 2029 m, 2014 m, 2000 s, 1992 m, 1982 m, 1967 m, 1953 m	Mass	No	106

Continued

TABLE I (Continued)

Index No.	Cluster ^a	Color	ν_{CO}^b	Other available spectral data ^c	Crystal structure	References
42	$\text{Re}_2\text{RuH}_2(\text{CO})_{12}$	Yellow	Hexane: 2095 m, 2091 sh, 2070 m, 2042 s, 2034 sh, 2009 m, 2001 m, 1987 m, 1978 m, 1956 m	—	No	106
43	$\text{Re}_2\text{PtH}_2(\text{CO})_8(\text{PPh}_3)$	—	—	—	Yes	149
44	$\text{Re}_2\text{AuH}(\text{CO})_8(\text{PPh}_3)$	—	—	—	No	149
45	$[\text{ReRu}_3(\text{CO})_{16}]^-$	Orange-red	THF: 2009 vs, 1982 s, 1960 (br) sh, 1932 sh, 1891 m	—	No	106
46	$\text{ReOs}_3\text{H}(\text{CO})_{15}$	Orange	KBr: 2131 w, 2091 s, 2070 sh, 2057 sh, 2051 s, 2018 s, 1991 sh, 1971 sh, 1950 m, 1933 m	Mass	Yes	47, 106 144
47	$\text{ReOs}_3\text{H}(\text{CO})_{15}(\text{NCCH}_3)$	—	C_6H_{12} : 2114 vw, 2084 m, 2058 m, 2029 m, 2015 sh, 2002 s, 1991 m, 1981 w, 1971 m, 1965 sh, 1932 w	Mass	No	142, 143
48	$\text{ReOs}_3\text{H}_3(\text{CO})_{13}$	Orange	KBr: 2138 s, 2090 s, 2063 sh, 2030 br, 1983 s, 1968 sh, 1900 m	—	No	106
49	$\text{ReOs}_3\text{H}(\text{CO})_{16}$	Yellow	—	^1H , Mass	No	144
50	$\text{ReOs}_3\text{H}_3(\text{CO})_{12}$	—	—	—	No	142, 143
51	$\text{Re}_2\text{Ru}_2\text{H}_2(\text{CO})_{16}$	Yellow	—	—	No	106
52	$\text{Re}_2\text{Os}_3\text{H}_2(\text{CO})_{10}$	—	—	—	No	143
53	$\text{Re}_2\text{Os}_3\text{H}_2(\text{CO})_{19}$	—	C_6H_{12} : 2107 m, 2078 m, 2062 m, 2051 m, 2015 s, 2004 s, 2000 s, 1994 s, 1986 m, 1976 s, 1964 s, 1950 vw, 1930 w	^1H , Mass	No	144
54	$\text{Re}_2\text{Os}_3\text{H}_2(\text{CO})_{20}$	Yellow	—	^1H , ^{13}C , Mass	Yes	144

Iron (*see also* entries 7, 8, 10, 15, 28, 30–32, 38, and 39)

55	$\text{FeRu}_2(\text{CO})_{12}$	Orange-red	Cyclohexane: 2067 s, 2042 vs, 2034 s, 2012 w, 1988 w	UV-vis, Mass	No	161
56	$\text{FeOs}_2(\text{CO})_{12}$	Orange	Heptane: 2070 s, 2042 vs, 2034 vs, 2022 m, 2008 w, 2003 m, 1988 w	—	No	121
57	$\text{FeCo}_2(\text{CO})_9\text{Y}$ Y = S, Se, Te	Violet	Hexane, Y = S: 2104 vw, 2066 s, 2054 vs, 2042 s, 2029 m, 2000 vw, 1985 m, 1950 vw	^{13}C	Yes	99,148,151
58	$\text{FeCo}_2(\text{CO})_9(\text{PPh})$	Black	Light petroleum: 2101 w, 2059 vs, 2048 vs, 2039 vs, 1981 w, 1969 w	Mass	No	32
59	$\text{FeCo}_2(\text{CO})_8(\text{L})\text{S}$ L = PPh_3 , AsPh_3 , $\text{P}(\text{OEt})_3$, PEt_2Ph , $\text{P}(n\text{-Bu})_3$	Red-brown	Hexane, L = PPh_3 : 2080 m, 2038 s, 2031 (sh), 2027 m, 2017 m, 1986 w, br, 1966 w, br, 1949 vw	Möss, ^1H , ^{13}C	No	31,133
60	$\text{FeCo}_2(\text{CO})_7(\text{L})_2\text{S}$ L = PPh_3 , $\text{P}(n\text{-Bu})_3$, PEt_2Ph , $\text{CNC}(\text{CH}_3)_3$	Dark green or red	Hexane, L = $\text{CNC}(\text{CH}_3)_3$: 2062 sh, 2054 m, 2027 sh, 2020 vs, 2006 s, 1999 m, 1984 m, 1948 m	Möss, ^1H , ^{13}C	No	31,126,133
61	$\text{FeCo}_2(\text{CO})_6(\text{L})_2\text{S}$ L = PPh_3 , $\text{P}(n\text{-Bu})_3$, $\text{CNC}(\text{CH}_3)_3$	Réd	Hexane, L = $\text{CNC}(\text{CH}_3)_3$: 2039 m, 2029 s, 2016 s, 2002 vs, 1996 s, 1983 s, 1970 m, 1931 m, 1864 vw, 1831 w, 1823 w	^1H , ^{13}C	No	126,133
62	$\text{FeCo}_2\text{H}(\text{CO})_4(\text{CR})$ R = CH_3 , C_2H_5 , C_6H_5	Maroon	Hexane, R = CH_3 : 2101 m, 2065 m, 2053 s, 2047 s, 2037 s, 2018 m, 2014 m, 1994 w, 1989 m	UV-vis, Mass, ^1H	No	64
63	$\text{FeCo}_2(\text{CO})_8(\text{PhC}_2\text{Ph})$	—	—	Mass	No	53
64	$\text{FeRh}_2(\text{Cp})_2(\text{CO})_6$	Green	2054 s, 2002 s, 1989 s, 1980 s, 1839 w, 1792 m	^1H , ^{13}C , Möss	No	86,102

Continued

TABLE I (Continued)

Index No.	Cluster ^a	Color	ν_{CO} ^b	Other available spectral data ^c	Crystal structure	References
65	$\text{FeNi}_2(\text{Cp})_2(\text{CO})_5$	Green-black	Hexane: 2050 vs, 2004 s, 1983 s, 1823 vw, 1790 w, 1762 m	Möss	Yes	87,154
66	$\text{FeNi}_2(\text{Cp})_2(\text{CO})_2(\text{PhC}_2\text{R})$ R = H, Ph, C_2Ph	Black	R = Ph: 2043, 1967	^1H	No	155
67	$\text{FePt}_2(\text{CO})_4[\text{P}(\text{OPh})_3]_3$	Orange	Cyclohexane: 2032 sh, 2015 s, 1952 m, 1918 m	—	Yes	11,12,29
68	$\text{Fe}_2\text{Ru}(\text{CO})_{12}$	Purple	Cyclohexane: 2057 s, 2044 vs, 2023 w (sh), 2004 m (br), 1859 vvw, 1834 vvw	Mass, ^{13}C , UV-vis	No	161
69	$\text{Fe}_2\text{Ru}(\text{Cp})(\text{CO})_6(\text{PPh}_3)(\text{C}_2\text{Ph})$	Dark red	2066 s, 2049 s, 2022 w, 2007 sh, 1974 m (br), 1944 vs	Mass	No	1,27
70	$\text{Fe}_2\text{Os}(\text{CO})_{12}$	Purple	Hexane: 2117 w, 2055 s, 2041 s, 2036 s, 2013 m, 2001 m, 1990 sh, 1860 vw, 1827 vw	—	No	104,121
71	$\text{Fe}_2\text{Co}(\text{Cp})(\text{CO})_9$	Brown	2080 s, 2033 s, 2013 s, 2001 sh, 1981 m, 1848 w, 1812 m	^1H , ^{13}C , Möss	No	86,102
72	$\text{Fe}_2\text{CoH}_2(\text{CO})_9\text{CR}$ R = H, CH_3 , C_3H_5 , C_3H_7	Pink	Hexane: 2101 m, 2054 vs, 2047 vs, 2038 s, 2017 m, 1988 m, 1985 m	—	No	64
73	$\text{Fe}_2\text{Rh}(\text{Cp})(\text{CO})_9$	Green	2079 s, 2037 s, 2032 sh, 2015 s, 1999 s, 1982 sh, 1844 w, 1803 m	^1H , ^{13}C , Möss	No	86,102
74	$\text{Fe}_2\text{Ni}(\text{Cp})(\text{CO})_7(\text{CEt})$	Grey-violet	Heptane: 2070 s, 2036 vs, 2012 s, 1986 m, 1974 m, 1954 mw	^1H , Möss	No	118

75	$\text{Fe}_2\text{Ni}(\text{Cp})(\text{CO})_8(\text{C}_2\text{Me})$	Grey-violet	Heptane: 2060 s, 2020 vs, 1990 s, 1982 s (sh), 1968 m	^1H , Möss	No	118
76	$\text{Fe}_2\text{Pt}(\text{CO})_9\text{L}$ L = PPh_3 , PMePh_2 , PMe_2Ph , AsPh_3 , PMe_3	Deep red	Cyclohexane, L = PPh_3 : 2074 s, 2035 s, 2014 s, 2001 m, 1985 s, 1973 (sh), 1924 w, br	^1H	Yes	28,29,115
77	$\text{Fe}_2\text{Pt}(\text{CO})_9\text{L}_2$ L = PMePh_2 , PMe_2Ph , $\text{P}(\text{OMe})_2\text{Ph}$, $\text{P}(\text{OPh})_3$, dppe, diars	Deep red	Cyclohexane, L = PMe_2Ph : 2051 s, 1998 s, 1971 m, 1948 m, 1892 w, br	^1H	No	28,29,43
78	$\text{FeRuOs}_2\text{H}_2(\text{CO})_{13}$	Orange	Hexane: 2121 w, 2086 s, 2073 s, 2041 vs, 2032 m, 2024 m, 2013 w, 1993 m, 1882 w, 1870 w, 1855 m, 1824 m	^1H , ^{13}C , UV-vis, Mass	No	77,78
79	$\text{FeRu}_2\text{OsH}_2(\text{CO})_{13}$	Orange-red	Hexane: 2111 vw, 2085 s, 2073 s, 2041 vs, 2026 m, 2016 w, 1991 m, 1887 w, 1877 w, 1861 m, 1849 m	^1H , UV-vis, Mass	No	78
80	$[\text{FeRu}_2\text{Co}(\text{CO})_{13}]^-$	Red-brown	CH_2Cl_2 : 2072 w, 2028 s, 2008 vs, 1995 s (sh), 1950 m (sh), 1826 w (sh), 1795 m, br	—	No	147
81	$[\text{FeRu}_3\text{H}(\text{CO})_{13}]^-$	Black	CH_2Cl_2 : 2073 w, 2031 s, 2013 s, 1998 s, 1974 m, 1944 m, 1840 w, 1811 m	—	Yes	80
82	$\text{FeRu}_3\text{H}_2(\text{CO})_{13}$	Red	Cyclohexane: 2112 vvw, 2084 vs, 2073 vs, 2063 w, 2041 vs, 2031 m, 2021 w, 1992 m, 1884 w, 1845 m	^1H , ^{13}C , UV-vis	Yes	77-79,101, 119,161
83	$\text{FeRu}_3\text{H}_2(\text{CO})_{12}\text{L}$ L = $\text{P}(\text{OMe})_3$, $\text{P}(\text{OEt})_2\text{Ph}$, PPh_3 , PMePh_2 , PEt_2Ph , PMe_2Ph , PMe_3 , $\text{P}(i\text{-Pr})_3$	Dark red	Hexane, L = PMe_2Ph : 2096 s, 2072 s, 2064 s, 2046 s, 2034 (sh), 2028 s, 2020 s, 2012 m, 1990 m, 1984 m, 1876 w, 1850 m, 1806 m	^1H	No	82

Continued

TABLE I (Continued)

Index No.	Cluster ^a	Color	ν_{CO} ^b	Other available spectral data ^c	Crystal structure	References
84	FeRu ₃ (CO) ₁₂ (RC ₂ R') R,R' = Ph (2 isomers) R,R' = CH ₃ (2 isomers) R = Ph, R' = CH ₃ (3 isomers)	Brown, red-brown	Hexane, R,R' = Ph, isomer I: 2095 m, 2064 s, 2049 s, 2036 s, 2024 m, 2016 m, 1998 m, 1986 w, 1976 w, 1962 vw	¹ H, Mass	Yes	74
85	FeRu ₃ H ₄ (CO) ₁₂	Orange	Cyclohexane: 2085 s, 2070 s, 2054 s, 2044 vw, 2031 m (br), 2012 w, 1998 w, 1990 w	¹ H	No	107
86	FeOs ₃ H ₂ (CO) ₁₃	Orange	Heptane: 2086 s, 2072 s, 2040 vs, 2032 m, 2025 m, 2015 w, 1994 w, 1875 w, 1848 m	—	No	121
87	FeCo ₃ H(CO) ₁₂	Purple	Hexane: 2059 s, 2050 s, 2026 m, 1986 m, 1885 m	UV-vis, Mass, ¹³ C	No	8,35,39,63, 103,116
88	FeCo ₃ H(CO) ₁₁ L L = PMePh ₂ , PEt ₃ , P(OPr) ₃ , P(OPh) ₃ , P(OMe) ₃ , PPh ₃	Purple	Hexane, L = PMePh ₂ : 2076 m, 2040 s, 2031 vs, 2008 s, 1996 m (sh), 1970 m, 1935 vw, 1891 w, 1865 m, 1846 m	¹ H, Mass, Möss, ¹³ C	No	8,54,89
89	FeCo ₃ H(CO) ₁₀ L ₂ L = PMePh ₂ , PPh ₃ , PEt ₃ , P(OPh) ₃ , P(OPr) ₃ , P(OMe) ₃ L ₂ = dppe	Blue-green	CHCl ₃ , L = PMePh ₂ : 2050 vs, 2017 vs, 1991 vs, 1951 m (sh), 1866 w (sh), 1826 m (br)	¹ H, Möss, ¹³ C	No	8,54,89
90	FeCo ₃ H(CO) ₈ L ₃ L = PMePh ₂ , P(OMe) ₃ L ₃ = 3/2 dppe	Green	Cyclohexane, L = P(OMe) ₃ : 2040 s, 2009 m, 1990 s, 1963 w, 1833 m, 1821 m	Möss, ¹³ C	Yes	8,54,89, 153

91	$\text{FeCo}_3\text{H}(\text{CO})_8\text{L}_4$ \ L = $\text{P}(\text{OMe})_3$ L ₃ = dppe	Purple	Cyclohexane, L = $\text{P}(\text{OMe})_3$: 2043 w, 2022 w, 2012 m, 1985 m (br), 1945 m, 1827 w, 1816 m	Mass, Möss	No	54,89
92	$\text{FeCo}_3\text{H}(\text{CO})_9(\text{PhC}_2\text{Ph})_2$	—	—	—	No	63
93	$[\text{FeCo}_3(\text{CO})_{12}]^-$	Purple	CH_3CN : 2066 w, 2008 s, 1974 m, 1932 m, 1815 m	—	No	39
94	$[\text{FeCo}_3(\text{CO})_{11}\text{L}]^-$ L = PPh_3 , PMePh_2 , $\text{P}(\text{OPr})_3$	Dark purple	THF, L = PMePh_2 : 2007 s, 1961 vs, 1941 s, 1934 s, 1905 m (sh), 1815 vw, 1773 m (br)	^1H	No	53
95	$[\text{FeCo}_3(\text{CO})_{10}(\text{dppe})]^-$	Dark purple	THF: 2011 s, 1963 vs, 1944 vs, 1895 m (sh), 1807 w, 1774 m, 1749 m	^1H	No	53
96	$[\text{FeCo}_3(\text{CO})_{10}(\text{PhC}_2\text{Ph})]^-$	Black-violet	THF: 2043 m, 1994 s, 1980 s, (sh), 1973 s (sh), 1969 s (sh), 1935 m, 1850 w, 1815 m	^1H	No	53
97	$[\text{Fe}_2\text{RuCo}(\text{CO})_{13}]^-$	Brown	CH_2Cl_2 : 2074 w, 2030 s, 2008 vs, 1997 s (sh), 1950 m (sh), 1826 w (sh), 1796 m, br	—	No	147
98	$\text{Fe}_2\text{Ru}_2\text{H}_2(\text{CO})_{13}$	Red	2105 vw, 2084 s, 2072 m, 2066m, 2057 s, 2041 vs, 2031 m, 2015 s, 2003 w, 1979 m, 1888 w (br), 1860 w (br)	—	No	78
99	$\text{Fe}_2\text{Rh}_2(\text{Cp})_2(\text{CO})_8$	Purple	2039 s, 2005 s, 1972 m, 1956 m, 1935 m, 1849 w, 1788 w	^1H	Yes	49,51,102

Continued

TABLE I (Continued)

Index No.	Cluster ^a	Color	ν_{CO} ^b	Other available spectral data ^c	Crystal structure	References
100	$\text{Fe}_2\text{Ni}_2(\text{Cp})_2(\text{CO})_6(\text{RC}_2\text{R}')$ R = Ph, R' = H, Ph, C ₂ Ph R, R' = Et	—	R = Ph: 2023, 1980 s, 1961	¹ H	Yes	115
101	$[\text{Fe}_3\text{Co}(\text{CO})_{13}]^-$	Black	CH_2Cl_2 : 2074 w, 2004 vs, 1971 m, 1930 m (sh), 1816 m, br	—	No	40,147
102	$\text{Fe}_3\text{Rh}(\text{Cp})(\text{CO})_{11}$	Red	2069 s, 2033 sh, 2025 s, 1993 s, 1977 m, 1957 m, 1945 sh, 1873 m, 1826 w	¹ H	Yes	50,102
103	$[\text{Fe}_3\text{NiH}(\text{CO})_{12}]^-$	Green-brown	2060 vw, 2020 m, 1990 s, 1965 m, 1935 mw, 1875 w, 1830 w, 1790 w	¹ H	No	34,40,110
104	$[\text{Fe}_3\text{Ni}(\text{CO})_{12}]^{2-}$	Brown	THF: 2010 vw, 1955 ms, 1935 s, 1990 mw, 1810 w, 1790 w	—	No	34,40,110
105	$[\text{Fe}_4\text{Pd}(\text{CO})_{16}]^{2-}$	Brown	THF: 1985 s, 1975 s, 1940 ms, 1920 (sh)	—	Yes	110,111
106	$[\text{Fe}_4\text{Pt}(\text{CO})_{16}]^{2-}$	Brown	THF: 1987 s, 1972 s, 1965 (sh), 1935 ms, 1920 (sh)	—	Yes	110,111
107	$\text{Fe}_2\text{Ir}_2\text{Cu}_4(\text{CO})_8(\text{PPh}_3)_2(\text{C}_2\text{R})_8$ R = Ph, <i>p</i> -C ₆ H ₄ CH ₃	Violet	CHCl_3 : 2048 s, 2008 s, 1982 s, 1970 s	¹ H	No	2
108	$[\text{Fe}_8\text{Pd}_8\text{H}(\text{CO})_{24}]^{3-}$	—	—	—	Yes	111
Ruthenium (see also entries 24, 42, 45, 51, 55, 68, 69, 78–85, 97, and 98)						
109	$\text{RuOs}_2(\text{CO})_{12}$	Yellow	CHCl_3 : 2066 vs, 2032 s, 2014 w, 2004 w	¹ H	No	70,80,96
110	$\text{RuPt}_2(\text{CO})_5\text{L}_3$ L = PPh_3 , PMePh_2 , PMe_2Ph , AsPh_3 , $\text{P}(\text{OMe})_2\text{Ph}$	Yellow	Cyclohexane, L = PMe_2Ph : 2024 s, 1964 (sh), 1952 s, 1848 w, 1784 s	¹ H	No	28,30

111	$\text{RuPt}_2(\text{CO})_4[\text{P}(\text{OMe})_2\text{Ph}]_4$	Yellow	Cyclohexane: 1955 s, 1854 w, 1801 s, 1780 s	^1H	No	30
112	$\text{Ru}_2\text{Os}(\text{CO})_{12}$	Yellow	CHCl_3 : 2062 vs, 2020 s, 2013 w, 2004 w (sh)	^{13}C , Mass	No	70,80,96
113	$\text{Ru}_2\text{Pt}(\text{CO})_8(\text{dppe})$	Red	Cyclohexane: 2073 s, 2027 s, 2001 sh, 1989 s, 1981 sh, 1972 sh, 1963 sh	^1H	No	30
114	$\text{Ru}_2\text{Pt}(\text{CO})_7(\text{PMe}_2\text{Ph})_3$	Yellow	Cyclohexane: 2022 s, 1956 sh, 1944 s, 1853 w, 1816 s, 1768 s	^1H	No	28
115	$\text{RuOs}_2\text{CoH}(\text{CO})_{13}$	Orange	Hexane: 2122 w, 2078 s, 2056 vs, 2035 m, 2030 m, 2018 w, 1996 s, 1903 w, 1858 m	^1H	No	147
116	$\text{RuOs}_3\text{H}_4(\text{CO})_{12}$	Yellow	2081 s, 2063 s, 2022 s, 1994 w	—	No	78
117	$\text{RuCo}_3\text{H}(\text{CO})_{12}$	Red	Hexane: 2064 s, 2057 s, 2023 m, 2015 sh, 1887 m	Mass	No	116,161
118	$\text{Ru}_2\text{OsCoH}(\text{CO})_{13}$	Orange	Hexane: 2111 w, 2076 s, 2056 vs, 2034 m, 2028 m, 2018 m, 1907 w, 1862 m	^1H	No	147
119	$\text{Ru}_2\text{Os}_2\text{H}_4(\text{CO})_{12}$	Yellow	2081 s, 2063 s, 2022 s, 1994 w	—	No	78
120	$\text{Ru}_3\text{OsH}_4(\text{CO})_{12}$	Yellow	2081 s, 2063 s, 2022 s, 1994 w	—	No	78
121	$[\text{Ru}_3\text{Co}(\text{CO})_{13}]^-$	Red	CH_2Cl_2 : 2072 w, 2024 vs, 1992 m, 1823 w (sh), 1794 m, br	—	Yes	147
122	$\text{Ru}_3\text{CoH}(\text{CO})_{13}$	Red	Hexane: 2109 w, 2088 w, 2073 s, 2061 vs, 2054 vs, 2034 m, 2024 m, 2017 m, 1971 vw, 1909 w, 1865 m	^1H	No	147

Continued

TABLE I (Continued)

Index No.	Cluster ^a	Color	ν_{CO} ^b	Other available spectral data ^c	Crystal structure	References
123	$\text{Ru}_3\text{CoH}_3(\text{CO})_{12}$	Red	Hexane: 2111 w, 2088 s, 2080 m, 2068 s, 2052 vs, 2041 m, 2036 m, 2027 m, 2012 w, 2002 w, 1878 w (br)	^1H	Yes	81
Osmium (<i>see also</i> entries 12, 13, 25, 26, 33, 34, 36, 37, 40, 41, 46–50, 53–54, 56, 70, 78, 79, 86, 109, 112, 115, 116, and 118–120)						
124	$\text{OsCo}_2(\text{CO})_{11}$	Red	Heptane: 2127 w, 2069 s, 2049 vs, 2025 m, 1823 m	—	No	121
125	$\text{OsPt}_2(\text{CO})_5\text{L}_3$ L = PPh_3 , PMePh_2	Yellow	Cyclohexane, L = PPh_3 : 2022 s, 1943 s, 1847 w, 1795 s, 1774 s	^1H	No	28,30
126	$\text{Os}_2\text{Pt}(\text{CO})_7(\text{PMe}_2\text{Ph})_3$	Orange	Cyclohexane: 2018 s, 1944 m, 1848 w, 1820 m, 1756 m	^1H	No	28,30
127	$\text{OsCo}_3\text{H}(\text{CO})_{12}$	Red	Hexane: 2064 s, 2056 s, 2018 m, 1890 m	Mass	No	103
128	$\text{Os}_2\text{Co}_2\text{H}_2(\text{CO})_{12}$	Orange	Hexane: 2112 w, 2081 s, 2078 s, 2057 vs, 2046 s, 2028 m, 2015 m	—	No	121
129	$\text{Os}_2\text{Pt}_2\text{H}_2(\text{CO})_8(\text{PPh}_3)_2$	—	Cyclohexane: 2059 s, 2031 vs, 2011 w, 1981 s, 1963 w, 1943 m	^1H , ^{31}P	Yes	30,67
130	$\text{Os}_3\text{CoH}_3(\text{CO})_{12}$	Pale yellow	Cyclohexane: 2076 vs, 2066 ms, 2049 w, 2030 vs, 2025 vs, 2012 w, 2005 s, 2000 sh, 1982 w	^1H , ^{13}C	Yes	23

131	$\text{Os}_3\text{RhH}_2(\text{CO})_{10}(\text{acac})$	Black	—	^1H	No	67
132	$\text{Os}_3\text{NiH}_2(\text{CO})_{10}(\text{PPh}_3)_2$	Orange	2073 s, 2065 m, 2037 vs, 2015 s, 1999 s, 1985 m (sh), 1973 m, 1959 w (sh), 1855 m, 1821 m	^1H , ^{31}P	No	67
133	$\text{Os}_3\text{PtH}_2(\text{CO})_{10}(\text{PPh}_3)\text{L}$ L = PPh_3 , AsPh_3	—	—	^1H , ^{31}P	Yes	67
134	$\text{Os}_3\text{PtH}_2(\text{CO})_{11}(\text{PPh}_3)$	—	—	^{31}P	No	67
135	$\text{Os}_3\text{PtH}_2(\text{CO})_{10}\text{L}$ L = PPh_3 , PCy_3	Dark green	Cyclohexane, L = PPh_3 : 2079 m, 2053 sh, 2045 s, 2029 vw, 2019 s, 1989 s, 1975 m, 1963 w, 1947 w	^1H	Yes	67
136	$\text{Os}_3\text{AuX}(\text{CO})_{10}\text{L}$ L = PPh_3 , X = Cl, Br, I, SCN L = $\text{P}(\text{C}_6\text{H}_4\text{Me})_3$, X = Cl	Red	Cyclohexane, L = PPh_3 , X = Cl: 2096 m, 2045 vs, 2016 s, 2009 s, 1990 sh, 1983 m, 1976 w (sh), 1965 m	Raman, Mass	Yes	24
137	$\text{Os}_3\text{AuH}(\text{CO})_{10}(\text{PPh}_3)$	Green	—	^1H	No	67
138	$\text{Os}_3\text{Au}_2(\text{CO})_{10}(\text{PPh}_3)_2\text{S}_2$	Orange	Cyclohexane: 2060 m, 2032 s, 2020 s, 1988 sh, 1973 m, 1955 s	—	No	24
Cobalt (<i>see also</i> entries 1–3, 8, 14, 27, 57–63, 71, 72, 80, 87–97, 101, 115, 117, 118, 121–124, 127, 128, and 130)						
139	$\text{CoNi}_2(\text{Cp})_3(\text{CO})_2$	—	1723	—	Yes	157
140	$\text{Co}_2\text{Pt}(\text{CO})_7\text{L}_2$ L ₂ = dppe, dpae	Red-brown	KBr: 2049 s, 2010 s, 1975 vs, 1970 sh, 1729 s	—	No	59
141	$\text{Co}_2\text{Rh}_2(\text{CO})_{12}$	Brown	Pentane: 2074 w, 2064 s, 2059 s, 2038 m, 2030 m, 1920 w, 1910 sh, 1885 s, 1871 s, 1855 w	UV	No	113

Continued

TABLE I (Continued)

Index No.	Cluster ^a	Color	ν_{CO}^b	Other available spectral data ^c	Crystal structure	References
142	$\text{Co}_2\text{Rh}_2(\text{CO})_{10}(\text{PF}_3)_2$	Deep brown	Pentane: 2104 vw, 2096 s, 2078 sh, 2070 vs, 2062 sh, 2047 s, 1924 w, 1889 s, 1878 s, 1863 sh	^{19}F , ^{31}P	No	65
143	$\text{Co}_2\text{Rh}_2(\text{CO})_8(\text{PF}_3)_4$	Deep brown	Pentane: 2070 vs, 2062 vw (sh), 2045 s, 2035 vw (sh), 1922 m, 1887 s, 1874 s	^{19}F , ^{31}P	No	65
144	$\text{Co}_2\text{Ir}_2(\text{CO})_{12}$	Dark red	Pentane: 2072 s, 2061 s, 2055 s, 2036 m, 2033 m, 2030 m, 1885 w, 1867 sh, 1865 s	UV, Mass	Yes	14,113
224 145	$\text{Co}_2\text{Ir}_2(\text{CO})_8(\text{PF}_3)_4$	Dark brown	Pentane: 2090 w (sh), 2075 s (sh), 2068 s, 2044 m, 2035 (sh), 2018 m, 1872 s (br), 1865 s (br)	—	No	65
146	$\text{Co}_2\text{Pt}_2(\text{CO})_8\text{L}_2$ L = PPh_3 , PEt_3	Red	Toluene, L = PPh_3 : 2061 s, 2034 vs, 2018 sh, 1992 s, 1937 m, 1871 m, 1825 s, 1820 s	—	Yes	20,26,71
147	$\text{Co}_3\text{Rh}(\text{CO})_{12}$	Brown	Pentane: 2066 m, 2059 s, 2056 sh, 2037 m, 2031 m, 1909 w, 1882 s, 1856 s	UV, Mass, ^{13}C	No	97,113
148	$[\text{Co}_3\text{Ni}(\text{CO})_{11}]^-$	Brown	THF: 2050 vw, 2000 vs, 1960 m, 1950 sh, 1865 m, 1845 m, 1740 m	—	No	38
149	$\text{Co}_3\text{Ni}(\text{Cp})(\text{CO})_8(\text{CNR})$ R = Me, <i>t</i> -Bu	—	Hexane, R = Me: 2065 w, 2057 m, 2029 w, 2013 s, 2006 s, 1845 m, 1838 m, 1830 sh	—	No	126

150	$\text{Co}_3\text{Ni}(\text{Cp})(\text{CO})_9$	Green	Hexane: 2082 s, 2043 vs, 2025 vs, 2013 m, 1850 s	^1H	No	87
151	$\text{Co}_2\text{Pt}_3(\text{CO})_9(\text{PETe})_3$	Dark violet	2016 s, 1988 sh, 1980 s, 1848 w, 1860 w, 1825 s, 1807 s, 1761 m	—	Yes	20
152	$\text{Co}_2\text{Rh}_4(\text{CO})_{16}$	—	—	—	No	113,150
153	$[\text{Co}_2\text{Rh}_4(\text{CO})_{15}\text{C}]^{2-}$	—	—	—	No	10
154	$[\text{Co}_4\text{Ni}_2(\text{CO})_{14}]^{2-}$	Dark red	THF: 2020 w, 1990 sh, 1977 s, 1958 s, 1790 m, 1749 sh	—	Yes	13,38
Rhodium (see also entries 64, 73, 99, 102, 131, 141–143, 147, 152, and 153)						
155	$\text{Rh}_2\text{Ir}_2(\text{CO})_{12}$	Orange	Pentane: 2071 s, 2042 m, 2034 m, 2022 w, 1923 w, 1887 s, 1867 s, 1855 w	UV, Mass	No	113
156	$\text{Rh}_2\text{Cu}_4(\text{PPh}_2\text{R})_2(\text{C}_2\text{Ar})_8$ R = Me, Ph; Ar = Ph, <i>p</i> -C ₆ H ₄ Me, <i>p</i> -C ₆ H ₄ F	Violet	—	IR, ^1H	No	2
157	$\text{Rh}_3\text{Ir}(\text{CO})_{12}$	Orange	Heptane: 2073 m, 2070 s, 2042 s, 2034 w, 2021 m, 1887 s, 1868 m	UV, Mass	No	113
158	$[\text{Rh}_4\text{Pt}(\text{CO})_{14}]^{2-}$	Yellow-brown	THF: 2000 s, 1956 s, 1810 m, 1790 m, 1735 w	^{195}Pt	Yes	34,75
159	$[\text{Rh}_5\text{Pt}(\text{CO})_{15}]^-$	Brown	THF: 2082 vw, 2038 s, 2011 m, 1791 ms	^{195}Pt	Yes	75
Iridium (see also entries 107, 144, 145, 155 and 157)						
160	$\text{IrCu}_3(\text{PPh}_3)_3(\text{C}_2\text{Ph})_2$	Buff	—	IR	No	2
161	$\text{Ir}_2\text{Cu}_4(\text{PPh}_2\text{R})_2(\text{C}_2\text{Ar})_8$ R = Me; Ar = Ph, C ₆ F ₅ R = Ph; Ar = Ph, <i>p</i> -C ₆ H ₄ Me, <i>p</i> -C ₆ H ₄ F	Purple	—	^1H	Yes	2,3,45

Continued

TABLE I (Continued)

Index No.	Cluster ^a	Color	ν_{CO} ^b	Other available spectral data ^c	Crystal structure	References
Nickel (<i>see</i> entries 9, 16, 19, 21, 29, 35, 65, 66, 74, 75, 100, 103, 104, 132, 139, 148–150, and 154)						
Palladium (<i>see</i> entries 17, 22, 105, and 108)						
Platinum (<i>see</i> entries 6, 11, 18, 20, 23, 43, 67, 76, 77, 106, 110, 111, 113, 114, 125, 126, 129, 133–135, 140, 146, 151, 158, and 159)						
Copper (<i>see</i> entries 107, 156, 160, and 161)						
Gold (<i>see</i> entries 44 and 136–138)						

^a Cp = $\eta^5\text{-C}_5\text{H}_5$; dppe = $\text{Ph}_2\text{PCH}_2\text{CH}_2\text{PPh}_2$; diars = $\sigma\text{-(AsPh}_2)_2\text{C}_6\text{H}_4$; acac = $\text{CH}_3\text{C(O)CHC(O)CH}_3$; dpae = $\text{Ph}_2\text{AsCH}_2\text{CH}_2\text{AsPh}_2$; Ph = C_6H_5 ; Bu = C_4H_9 ; Cy = C_6H_{11} ; Me = CH_3 ; Et = C_2H_5 ; Pr = C_3H_7 . ^b THF = tetrahydrofuran. ^c Mass = mass spectral data; Möss = Mössbauer data; IR = infrared data other than ν_{CO} ; UV-vis = electronic absorption spectral data; ^1H = ^1H NMR data; ^{31}P = ^{31}P NMR data; ^{13}C = ^{13}C NMR data; ^{19}F = ^{19}F NMR data; ^{195}Pt = ^{195}Pt NMR data; Raman = Raman spectral data.

to coordinatively unsaturated compounds, (3) redox condensations, and (4) reaction of carbonylmetalates with metal halides. Each of these reaction types will be discussed, and several examples are given in each case. These are followed by sections on miscellaneous synthetic reactions and possible synthetic strategies for future syntheses of mixed-metal clusters.

A. Pyrolysis Reactions

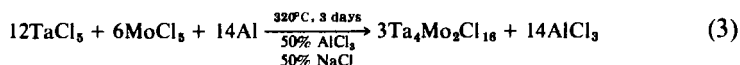
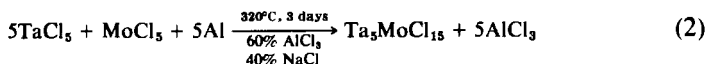
Pyrolysis reactions generally involve heating together two or more stable compounds of different metals, presumably to give fragments that then combine to yield the mixed-metal clusters. The amount of heat necessary to drive these reactions varies considerably, but in some cases simply stirring the reactants at ambient temperature is sufficient. These reactions are not generally adaptable to designed synthesis. They usually yield a variety of products that must be separated by chromatography, to give moderate to very low yields of the mixed-metal clusters.

1. Pyrolysis of Two Monomeric Species

Relatively few clusters have been prepared by the pyrolysis of two monomeric compounds, and only two examples are given. Stone and co-workers (28, 30) allowed $\text{H}_2\text{Os}(\text{CO})_4$ to react with several $\text{Pt}(0)$ complexes, and, although most of the reactions involved an unsaturated starting complex and will accordingly be discussed in Section II,B, $\text{Os}_2\text{Pt}(\text{CO})_7(\text{PPh}_2\text{Me})_3$ resulted from the reaction shown in Eq. (1).



Meyer and McCarley (117) prepared Ta_4Mo_2 and Ta_5Mo clusters by the pyrolysis of TaCl_5 with MoCl_5 according to the stoichiometries shown in Eqs. (2) and (3).

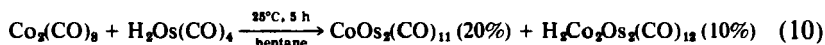
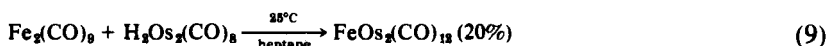
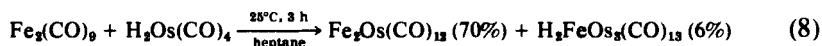
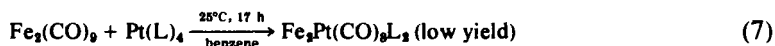
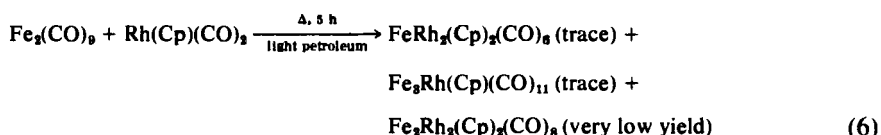
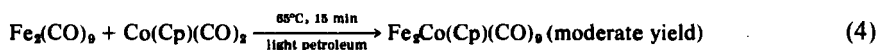


Processing afforded salts of the anions $[(\text{Ta}_4\text{Mo}_2\text{Cl}_{12})\text{Cl}_6]^{2-}$ and $[(\text{Ta}_5\text{MoCl}_{12})\text{Cl}_6]^{2-}$, and these were fully characterized. Although niobium and tantalum had been reported (135) to form mixed-metal cluster

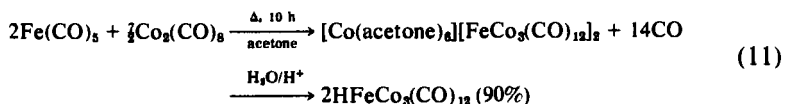
compounds of the type $Ta_{6-x}Nb_xBr_{14}$, discrete species were not isolated and the work of Meyer and McCarley thus represents the first successful characterization of mixed-metal halide clusters.

2. Pyrolysis of Metal Carbonyl Dimers

Metal carbonyl dimers have proved to be useful reagents for the synthesis of mixed-metal clusters. This is particularly true for Fe and Co clusters since $Fe_2(CO)_9$ and $Co_2(CO)_8$ are readily available starting materials. The prediction of the reaction products is usually fruitless. However, examination of the available data indicates that the initial dimeric unit is preserved in approximately half of the reactions. Typical examples are illustrated in Eqs. (4–6) (102), (7) (28), and (8–10) (121).

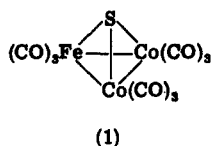


The first mixed-metal cluster $HFeCo_3(CO)_{12}$ was synthesized by Chini and co-workers in 1959 by using a two-step reaction of this type (35).



This particular reaction may proceed via the initial disproportionation of $Co_2(CO)_8$ to give $[Co(CO)_4]^-$ which then undergoes redox condensation with $Fe(CO)_5$.

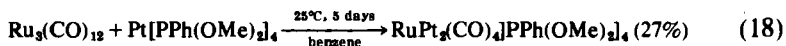
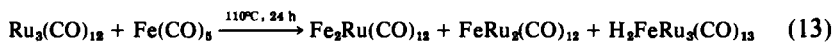
The preferred preparative method for $FeCo_2(CO)_9S$ (1) is condensation of the dimers $Fe_2(CO)_9S_2$ and $Co_2(CO)_8$, Eq. (12) (99).



Interestingly, this cluster was initially discovered by careful analysis of the products from a hydroformylation reaction of thiophene using $\text{Co}_2(\text{CO})_8$ as the catalyst in a steel bomb (99). The sulfur was apparently abstracted from thiophene, and the iron apparently came from the reaction vessel.

3. Pyrolysis of Metal Carbonyl Clusters

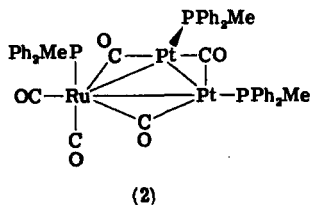
The pyrolysis of clusters in the presence of monomers, dimers, or other clusters usually requires much more severe reaction conditions than those previously discussed. Common starting materials such as $\text{Ru}_3(\text{CO})_{12}$ and $\text{Os}_3(\text{CO})_{12}$ are themselves quite stable compounds. The reaction of $\text{Ru}_3(\text{CO})_{12}$ with a variety of compounds has yielded many mixed-metal clusters, as illustrated by Eqs. (13) (101, 161), (14) (96), (15) (30), (16) (28), (17) (28, 30), and (18) (30).



The higher temperature and longer reaction time for Eq. (14) compared to Eq. (13) reflects the greater difficulty of breaking $\text{Os}_3(\text{CO})_{12}$ into fragments.

The reactions of various platinum derivatives with $\text{Ru}_3(\text{CO})_{12}$, Eqs. (15)–(18), were explored by Stone and co-workers (28, 30). As seen by comparison of Eqs. (14)–(18), the exact product that resulted was very dependent on the particular platinum complex employed. All of the reactions involved phosphine transfer from platinum to ruthenium during

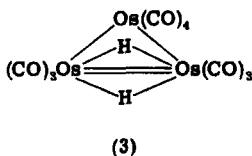
the course of the reaction. X-Ray structural analysis of $\text{RuPt}_2(\text{CO})_5(\text{PPh}_2\text{Me})_3$ (**2**) shows that this cluster has the ruthenium-bound phosphine located in an axial position, unlike the other substituted triangular clusters which possess the substituted ligand in an equatorial position (120).



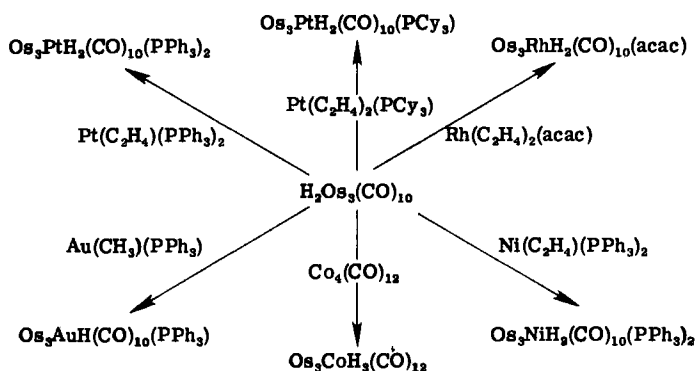
B. Addition of Coordinatively Unsaturated Species

This synthetic method has only recently become important. It is closely related to the pyrolysis technique, as coordinatively unsaturated species are presumably formed during pyrolysis by dissociation of ligands or cleavage of metal-metal bonds. These coordinatively unsaturated species are apparently the key intermediates that condense to give the cluster products. The addition of a metal nucleophile to a *preformed* coordinatively unsaturated compound occurs, in general, under much milder conditions, and these reactions appear quite adaptable to design. They also normally give much higher yields of the cluster products than do the pyrolysis reactions.

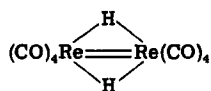
$\text{H}_2\text{Os}_3(\text{CO})_{10}$, whose structure is shown in 3, has been extensively used by Stone and co-workers (67, 68) in synthesizing mixed-metal clusters that contain the Os_3 framework. Several of these reactions, including the adaptation with $\text{Co}_4(\text{CO})_{12}$ of Johnson *et al.* (23), are summarized in Scheme 1. X-Ray structural analyses demonstrated that $\text{Os}_3\text{PtH}_2(\text{CO})_{10}(\text{PCy}_3)$ (67) and $\text{Os}_3\text{CoH}_3(\text{CO})_{12}$ (23) have tetrahedral structures.



Stone and co-workers (68) also employed the unsaturated dimer $\text{H}_2\text{Re}_2(\text{CO})_8$, **4** (22), to prepare the clusters $\text{Re}_2\text{PtH}_2(\text{CO})_9(\text{PPh}_3)$ and $\text{Re}_2\text{AuH}(\text{CO})_9(\text{PPh}_3)$, Eqs. (19) and (20).



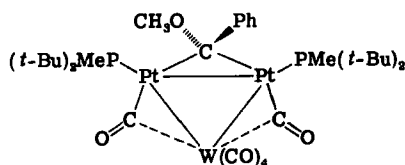
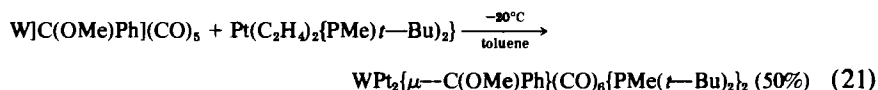
SCHEME 1



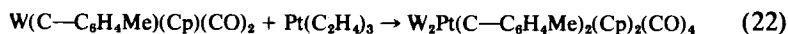
(4)



The reaction of nucleophilic Pt(0), Pd(0), and Ni(0) complexes with unsaturated metal-metal bonds has been extended by Stone and co-workers (18, 19) to include carbene and carbyne derivatives, Eqs. (21) (18) and (22) (19).



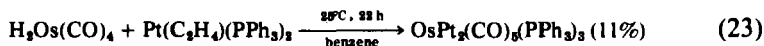
(5)



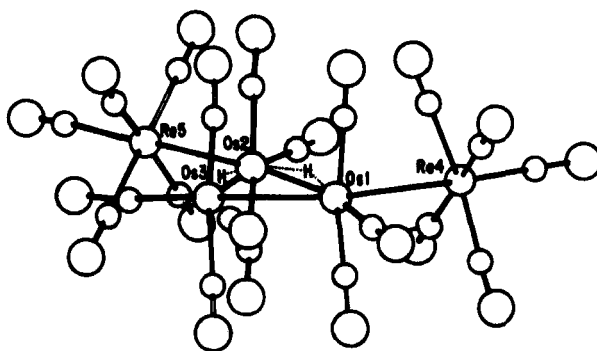
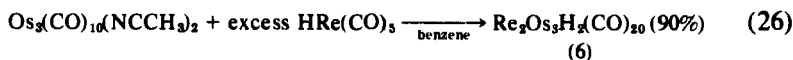
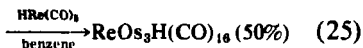
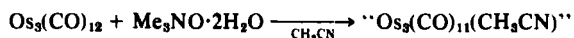
It should be noted that the carbene ligand migrated from W to a position bridging the Pt-Pt bond during the course of reaction (21). On the basis

of these various synthetic studies, Stone *et al.* (19) proposed a formal analogy between the addition of metal nucleophiles to olefins, metal carbenes, and doubly bonded metal-metal compounds and a similar analogy between the addition of metal nucleophiles to alkynes, metal carbynes, and triply bonded metal-metal compounds (see Scheme 2).

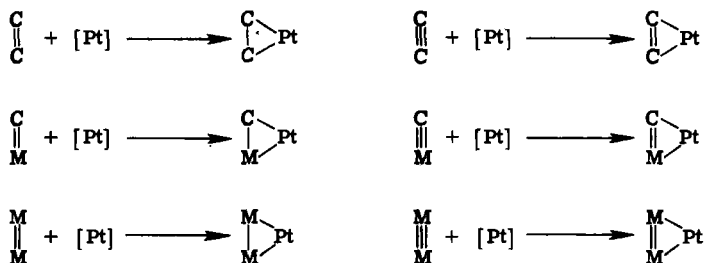
Mixed-metal clusters have also been prepared by the reaction of coordinatively unsaturated monomeric Pt(0) complexes with $\text{H}_2\text{Os}(\text{CO})_4$, Eqs. (23) (28) and (24) (67).



Shapley and co-workers (144) studied the addition of metal hydride complexes to "lightly stabilized" metal clusters such as $\text{Os}_3(\text{CO})_{10}(\text{NCCH}_3)_2$ and $\text{Os}_3(\text{CO})_{10}(\text{COT})_2$. The acetonitrile and cyclooctene ligands are readily displaced, to give an unsaturated species that then appears to add the metal hydride oxidatively. Me_3NO has also been used to oxidize and remove one of the carbonyls of $\text{Os}_3(\text{CO})_{12}$, to generate a similar coordinatively unsaturated species. Owing to the relatively mild conditions that are used in these reactions, the initial products do not react further and hence give an interesting series of open clusters in high yields, Eqs. (25) and (26).

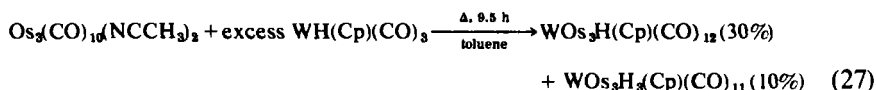


(6)



SCHEME 2

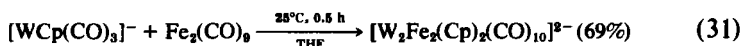
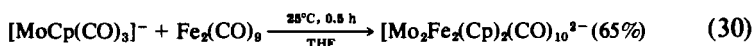
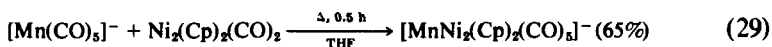
Similar reactions employing $\text{WH}(\text{Cp})(\text{CO})_3$ yielded closed tetranuclear clusters, Eq. (27) (48).



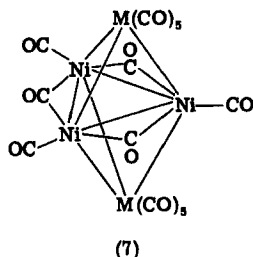
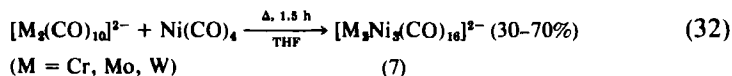
C. Redox Condensations

The reaction of a carbonylmetalate with a neutral metal carbonyl has been labeled a "redox condensation" by Chini *et al.* (40, 41) and has been as widely used as a pyrolysis reaction for synthesizing mixed-metal clusters. Carbonylmetalates usually react rapidly with most neutral carbonyls, even under very mild conditions. A large number of mixed-metal *hydride* clusters have been formed via this type of reaction, primarily because the initial products are anionic clusters that in many cases may be protonated to yield the neutral hydride derivative.

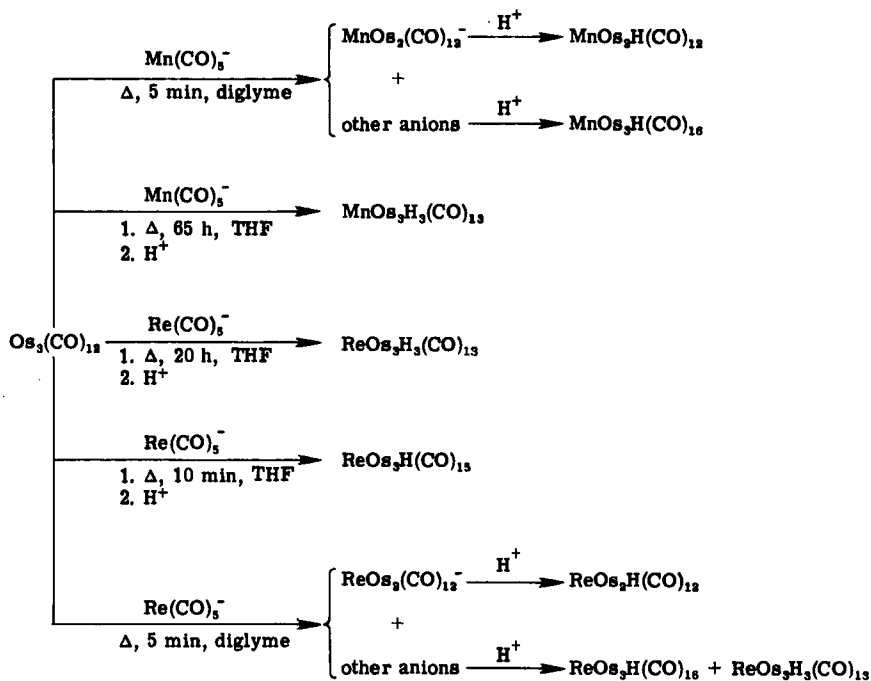
The reaction of carbonylmetalates with monomeric and dimeric carbonyls has yielded many mixed-metal clusters, as illustrated by the reactions shown in Eqs. (28) (15), (29) (87), (30) (88), and (31) (88).



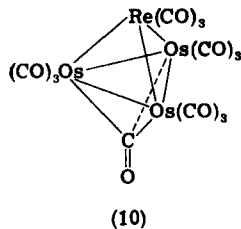
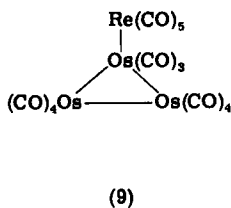
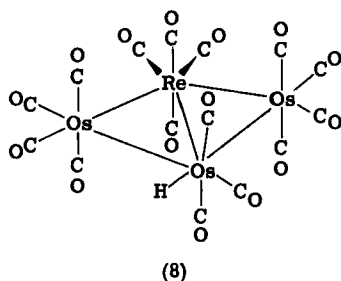
A series of trigonal bipyramidal clusters of the general formula $[\text{M}_2\text{Ni}_3(\text{CO})_{16}]^{2-}$ ($\text{M} = \text{Cr}, \text{Mo}, \text{W}$) were prepared by Dahl and co-workers (134) via the reaction shown in Eq. (32).



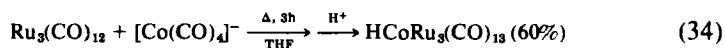
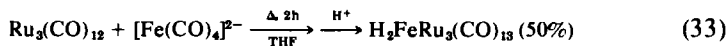
The reaction of carbonylmatalates with trinuclear clusters provides, in many cases, a convenient synthesis of tetranuclear clusters. This reaction was first explored by Knight and Mays (105, 106), who allowed $[Mn(CO)_5]^-$ and $[Re(CO)_5]^-$ to react with trimeric clusters of the iron triad. A summary of the products that they obtained on using $Os_3(CO)_{12}$ as the starting trimer is shown in Scheme 3. Of particular mechanistic



interest are the tetranuclear clusters that were formed. As indicated in Scheme 3, the carbon monoxide:metal ratio in the tetranuclear products decreased as the rigor of the reaction conditions increased. It is reasonable to assume that this also corresponds to an increase in the number of metal-metal bonds. It was suggested that the clusters $\text{ReOs}_3\text{H}(\text{CO})_{16}$ and $\text{ReOs}_3\text{H}(\text{CO})_{15}$ are intermediates along the reaction path to the final tetrahedral cluster $\text{ReOs}_3\text{H}_3(\text{CO})_{13}$. Unfortunately, only the crystal structure of $\text{ReOs}_3\text{H}(\text{CO})_{15}$ (8), has been reported (47), but it was suggested that $\text{ReOs}_3\text{H}(\text{CO})_{16}$ and $\text{ReOs}_3\text{H}(\text{CO})_{13}$ have structures 9 and 10, respectively (106).

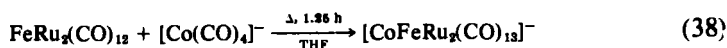
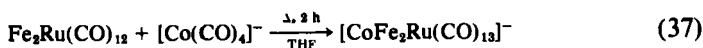
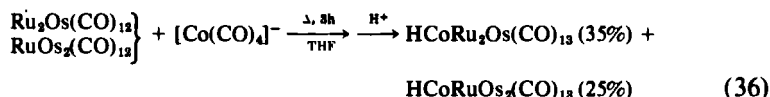
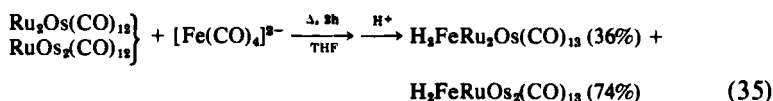


The reaction of $[\text{Fe}(\text{CO})_4]^{2-}$ and $[\text{Co}(\text{CO})_4]^-$ with metal carbonyl trimers has also been shown to be useful for the preparation of mixed-metal clusters, Eqs. (33) (78) and (34) (147).



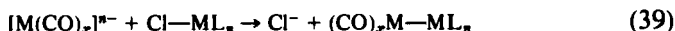
The 50% yield of $\text{H}_2\text{FeRu}_3(\text{CO})_{13}$ from Eq. (33) constitutes a significant improvement over previous pyrolysis methods (101, 161). These particular reactions can be scaled up, to produce several grams of the clusters in a single reaction, and consequently these mixed-metal clusters are readily available for reactivity studies. Clusters that contain three differ-

ent metals within the cluster framework were prepared by similar reactions, Eqs. (35) (78) and (36)–(38) (147).

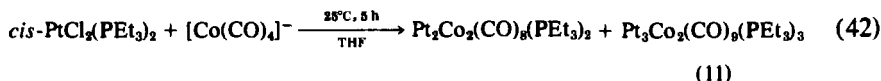
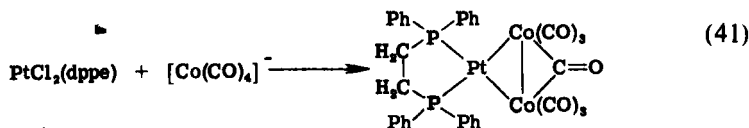
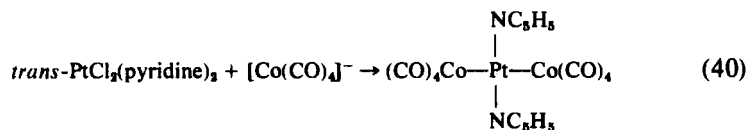


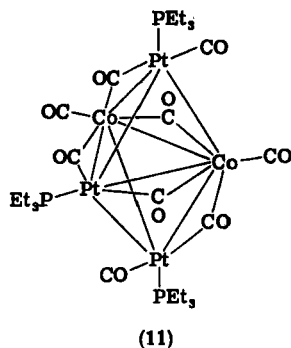
D. Reaction of Carbonylmatalates with Metal Halides

Carbonylmatalates will displace a halide from a metal halide complex to yield a metal-metal bonded species, Eq. (39). With di- and polyhalide

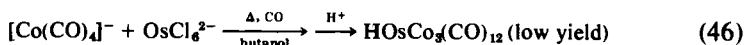
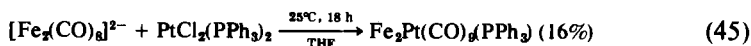
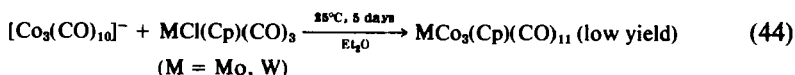
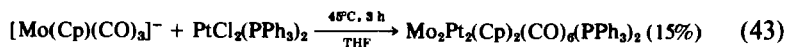


complexes or with dimeric carbonylmatalates, cluster compounds can result. The configuration of the metal-metal bonded product is very dependent upon the nature of the starting complex. For example, reaction of *trans*-PtCl₂(pyridine)₂ with [Co(CO)₄][−] gives a linear Co—Pt—Co species, Eq. (40) (25, 128), whereas a Co₂Pt cluster results from the reaction of PtCl₂(dppe) with [Co(CO)₄][−], Eq. (41) (59). However, reaction of *cis*-PtCl₂(PEt₃)₂ with [Co(CO)₄][−] leads to the formation of the tetra- and pentanuclear products shown in Eq. (42) (20).





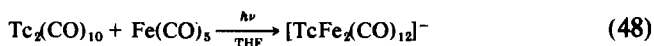
Further examples of this synthetic technique are shown in Eqs. (43) (26), (44) (137), (45) (43), and (46) (103).



The last of these reactions illustrates the use of a pure metal halide complex as a reagent in syntheses of this type.

E. Other Methods

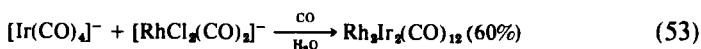
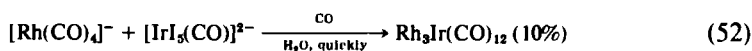
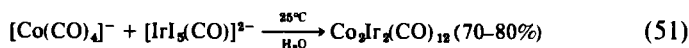
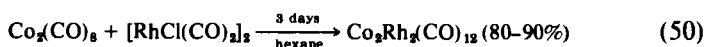
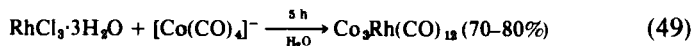
Many metal clusters have been prepared by reactions that do not fall into any of the above categories. Space does not permit a discussion of all of these, but we shall illustrate a few by examples. Somewhat surprisingly, photochemical techniques have only been used to produce two mixed-metal clusters, and these were prepared by Sheline and co-workers (66, 109) by photolysis of mixtures of $\text{M}_2(\text{CO})_{10}$ (M = Tc, Re) and $\text{Fe}(\text{CO})_5$, Eqs. (47) (66) and (48) (109).



The yield of the anionic clusters was reduced when the photochemical

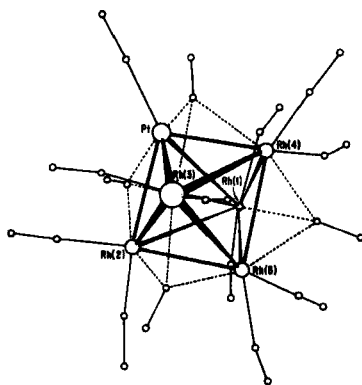
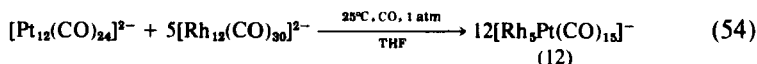
reactions were conducted in hydrocarbon solutions, and in these cases linear triatomic $M_2Fe(CO)_{14}$ species were isolated.

Chini *et al.* synthesized a series of mixed-metal clusters that contain various combinations of the metals within the cobalt triad (113). The reactions shown in Eqs. (49)–(53) are illustrative.



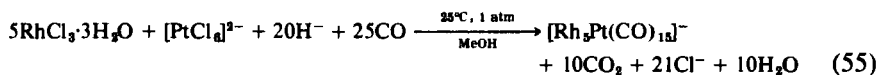
Although these reactions could be classified as the addition of a carbonylmetalate to a metal halide complex, they do not appear to entail simple addition and, instead, are relatively complex.

Chini and co-workers (75) also prepared $[Rh_5Pt(CO)_{15}]^-$ (12; from Ref. 75) by the scrambling of the two anionic clusters shown in Eq. (54).



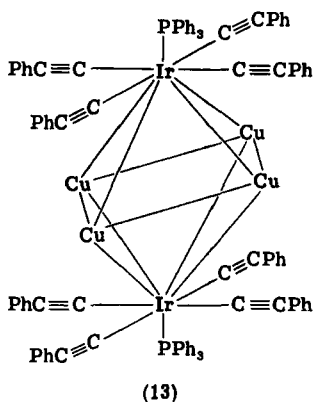
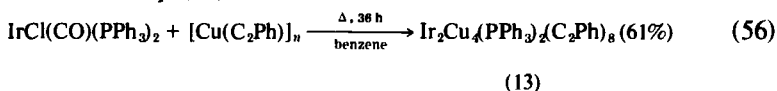
(12)

It is surprising that only one product resulted from this reaction, but $[Rh_5Pt(CO)_{15}]^-$ must be particularly stable as it is also formed from the metal halide salts, Eq. (55) (75).

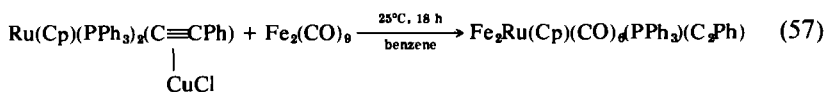


NMR studies showed that $[\text{Rh}_5\text{Pt}(\text{CO})_{15}]^-$ maintains its integrity in solution, but it does react with carbon monoxide in the presence of OH^- or reductants to form $[\text{Rh}_4\text{Pt}(\text{CO})_{14}]^{2-}$ (34, 75).

Bruce and co-workers (2, 3) prepared several mixed-metal clusters that contain copper. Unlike most of the compounds discussed in this review, these particular mixed-metal clusters possess acetylides as ligands instead of carbon monoxide. $\text{Ir}_2\text{Cu}_4(\text{PPh}_3)_2(\text{C}_2\text{Ph})_8$ (13) (3, 45) results from the reaction shown in Eq. (56).



Also isolated from reaction (56) was a small amount (4%) of a complex which analyzed for $\text{IrCu}_3(\text{PPh}_3)_3(\text{C}_2\text{Ph})_2$ but whose structure has not yet been reported. The analogous $\text{Rh}_2\text{Cu}_4(\text{PPh}_3)_2(\text{C}_2\text{Ph})_8$ cluster was prepared by a similar procedure. $\text{Ir}_2\text{Cu}_4(\text{PPh}_3)_2(\text{C}_2\text{Ph})_8$ reacts with $\text{Fe}_2(\text{CO})_9$ to yield purple crystals of $\text{Fe}_2\text{Ir}_2\text{Cu}_4(\text{PPh}_3)_2(\text{C}_2\text{Ph})_8$ (2). Spectral evidence indicates that the Ir_2Cu_4 core is unchanged in the product and that the iron atoms are simply π -bound to the acetylide ligands. A somewhat similar reaction was used to prepare $\text{Fe}_2\text{Ru}(\text{Cp})(\text{CO})_6(\text{PPh}_3)_2(\text{C}_2\text{Ph})$, except that in this case the iron atoms are part of the triangular framework of the cluster, Eq. (57) (1, 27).



F. Synthetic Strategies

Although serendipity still plays an important role in the successful synthesis of a desired cluster, sufficient precedented reactions now exist

to allow derivation of an initial synthetic strategy; this is especially true for triangular and tetranuclear clusters, and may even extend to larger clusters. In this section we have summarized several reactions that may be adaptable to design.

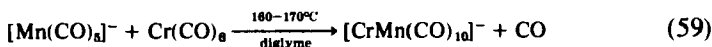
It appears that the most logical way to synthesize any desired triangular or tetranuclear cluster is to begin with monomeric complexes and build the desired cluster by adding one metal at a time. As outlined in Scheme 4, we suggest that to prepare a desired tetrahedral cluster, the reaction should start by allowing two monomeric organometallic complexes to react, to yield a metal-metal dimer. This in turn could react with another monomeric complex, to produce a triangular cluster that could then be capped by the addition of a fourth monomeric complex.

The first step in this synthetic approach is to form a metal-metal dimer. Numerous organometallic dimers have been prepared, and examples of the reaction types that appear most useful are tabulated here [Eqs. (58) (160), (59) (16), (60) (131), (61) (61), and (62) (122)].

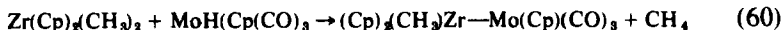
Reaction of a metal halide complex with a carbonylmetalate



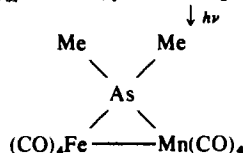
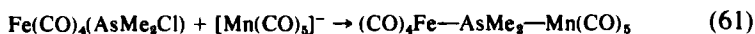
Reaction of a neutral carbonyl with a carbonylmetalate



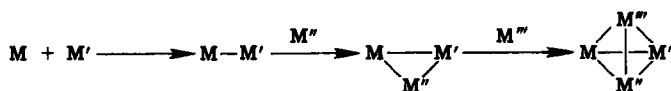
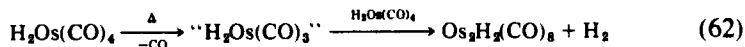
Coupling of metal hydride and metal alkyl complexes



Bridge-assisted reactions



Addition of metal hydrides to coordinatively unsaturated complexes



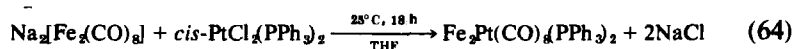
SCHEME 4

Much less effort has been directed toward the rational preparation of triangular clusters than to the synthesis of dimers. A survey of the methods used to prepare existing triangular clusters suggests that the reaction types listed next hold the most promise for the designed synthesis of new triangular species.

Addition of a dimeric carbonylmatalate to a neutral carbonyl [Eq. (63) (43)]:



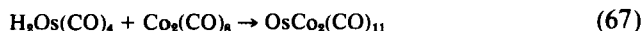
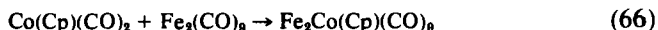
Addition of a dimeric carbonylmatalate to a metal halide complex [Eq. (64) (43)]:



Addition of a monomeric carbonylmatalate to a neutral dimer [Eq. (65) (87)]:



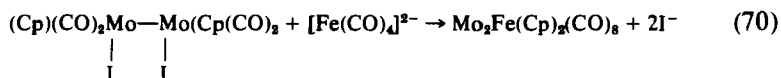
Condensation of monomeric and dimeric neutral carbonyl complexes [Eqs. (66) (102) and (67) (121)]:



Addition across multiple metal-metal bonds [Eqs. (68) (68) and (69) (57)]:

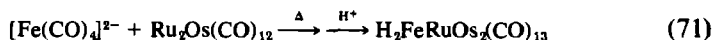


Addition of a carbonylmatalate to a dihalide dimer [Eq. (70) (57)]:

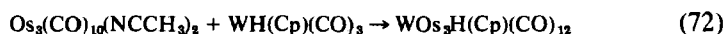


The two types of reactions that appear most useful for the preparation of tetranuclear clusters are those given next.

Addition of a carbonylmatalate to a neutral carbonyl trimer [Eq. (71) (78)]:



Addition of a metal hydride to an unsaturated trimer [Eq. (72) (48)]:



In principle, both of these types of reaction could be employed to build up large clusters by the addition of a carbonylmatalate or a metal hydride

across the triangular faces of tetranuclear clusters. However, these reactions, have yet to be demonstrated.

III

METHODS OF CHARACTERIZATION

The spectroscopic methods chosen to characterize a particular compound will depend on the character of that compound as well as the type of information to be gained. For example, neutral clusters are readily characterized by mass spectrometry, whereas this method has been of little use for characterizing anionic clusters. Likewise, the subject of interest is the location of a hydride ligand or the site of phosphine or phosphite substitution, the most versatile tools are NMR spectroscopy and X-ray diffraction. We cannot discuss all the common characterization techniques in detail, but we shall highlight a few of the more important features.

A. Mass Spectrometry

Mass spectrometry has been an extremely useful tool for the characterization of neutral organometallic clusters, except for those few cases which have extremely high molecular weights or possess such ligands as PPh_3 that reduce the volatility of the compound. Mass spectrometry has not been a useful characterization technique for ionic clusters because these compounds are insufficiently volatile to permit study by conventional electron-impact techniques. However, there is some hope that with the development of field-desorption techniques ionic clusters as well as neutrals will be capable of being analyzed by mass spectrometry (146).

A typical mass spectrum is that of $\text{H}_2\text{FeRu}_2\text{Os}(\text{CO})_{13}$, shown in Fig. 1. In general, the spectrum of a mixed-metal cluster will show the parent ion, as well as ions corresponding to loss of each of the carbonyl and the hydrogen ligands, all the way down to the bare metal core. Three features of the mass spectrum are important for characterizing a compound. First, the position of the parent ion gives an indication of the molecular weight of the compound. Caution, however, must be exercised to ensure that the ion observed is indeed the parent ion. Most clusters will show the parent ion in their mass spectrum, but its intensity is variable.

Second, the carbonyl-loss pattern can indicate the number of carbonyl ligands that a cluster possesses. The number of carbonyls may be readily

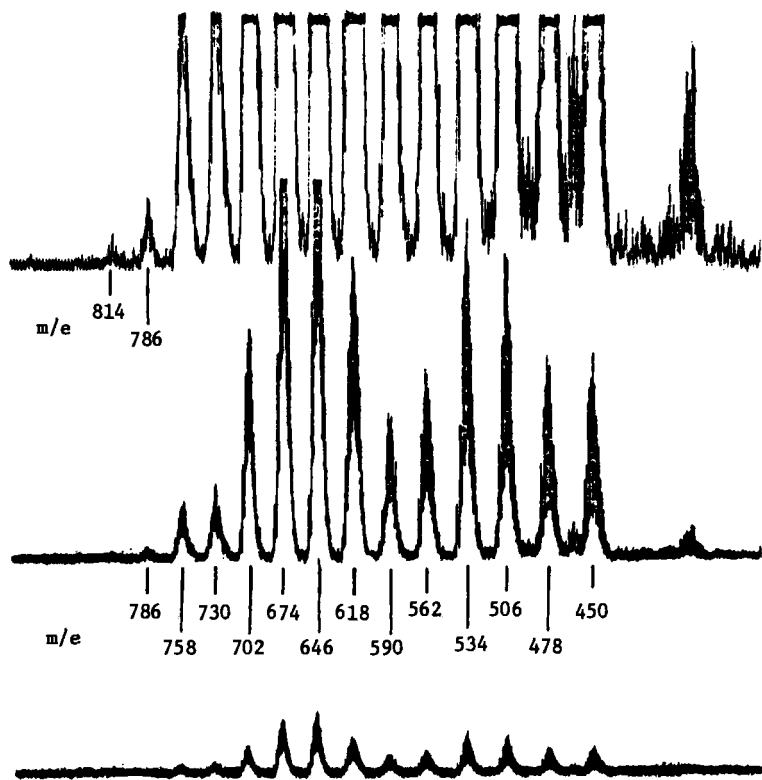


FIG. 1. Low-Resolution electron-impact mass spectrum of $\text{H}_2\text{FeRu}_2\text{Os}(\text{CO})_{13}$.

determined simply by counting the ions that are separated by 28 mass units due to successive loss of each of the carbonyls. For example, in the spectrum of $\text{H}_2\text{FeRu}_2\text{Os}(\text{CO})_{13}$ (Fig. 1), ions corresponding to loss of all 13 carbonyls are observed.

Finally, the isotopic distribution of the parent ion can serve as a fingerprint for a given metal composition. The isotopic distribution of the parent ion of $\text{H}_2\text{FeRuOs}_2(\text{CO})_{13}$ is shown in Fig. 2. The wide isotopic distribution from m/e 911 to m/e 895 arises because iron, ruthenium, and osmium have, respectively, 4, 9, and 7 naturally occurring isotopes of appreciable abundance. The various combinations, taken together with the appropriate weighting factors, give the calculated distribution shown in Fig. 2. If the metal composition of a particular cluster is uncertain, the experimental isotopic distribution may be compared with that calculated for a number of trial compositions, and thus the correct composition can often be uniquely determined.

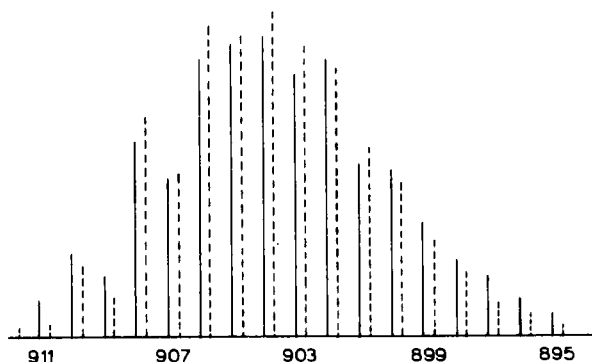


FIG. 2. Comparison of observed (—) and calculated (---) isotopic distribution of the parent ion of $\text{FeRuOs}_3\text{H}_5(\text{CO})_{13}$. Reprinted with permission from Geoffroy and Gladfelter (78). Copyright by the American Chemical Society.

Mixtures of compounds are often difficult to analyze using electron-impact mass spectrometry because of overlapping mass peaks from fragment ions of all the compounds present. However, chemical-ionization mass spectrometry has proved useful for analysis of such mixtures since only the parent ions of each compound present are normally observed. If metal carbonyls are studied and the instrument is operated in the negative-ion mode, only ions corresponding to the parent minus one carbonyl are seen. For example, the mixture of compounds $\text{Ru}_3(\text{CO})_{12}$, $\text{Ru}_2\text{Os}(\text{CO})_{12}$, $\text{RuOs}_2(\text{CO})_{12}$, and $\text{Os}_3(\text{CO})_{12}$ has proved extremely difficult to separate using normal chromatographic or fractional recrystallization techniques. We have found that the electron-impact mass spectrum of this mixture of compounds shows essentially a continuum of mass peaks, beginning with the parent ion of $\text{Os}_3(\text{CO})_{12}$ at m/e 906 (78). However, the chemical-ionization mass spectrum of this mixture showed ions at m/e 878, 789, 700, and 611, corresponding to the parent ions minus one carbonyl for each of the four clusters. From the relative intensities of the peaks, we were able to estimate the relative ratios of the four trimers in the mixture as 1:2:2:1 (78).

B. Infrared Spectroscopy

Infrared spectroscopy is most useful for identifying a known compound via comparison with published infrared data. In general, it is not possible to determine the structure or composition of a cluster by its infrared spectrum alone, although the spectrum can provide several useful indi-

cators. The region that has proved most useful is from 1700 to 2200 cm^{-1} , where carbonyl ligands generally absorb. The rest of the infrared spectrum has so far been useful only for determining the presence or absence of other types of ligands. For example, a cluster that contains PPh_3 will show the characteristic ligand vibrations below 1600 cm^{-1} . In the carbonyl region, carbonyls that are bound to a single metal atom normally appear between 2200 and 1900 cm^{-1} , whereas carbonyls that bridge two or three metals generally give a band in the 1900–1700 cm^{-1} region. Triply bridging carbonyls generally give a band lying in the lowest region. Caution should be exercised in assigning a carbonyl in the 1850–1950 cm^{-1} region to a terminal or bridging position since the charge of the cluster can substantially affect the position of the bands in the infrared spectrum. Anionic clusters, for example, generally show all their carbonyl vibrations at lower energy than the corresponding vibrations of a neutral cluster of similar composition.

For illustration, Fig. 3 shows the infrared spectra of $\text{H}_2\text{FeRu}_3(\text{CO})_{13}$, $\text{H}_2\text{FeRu}_2\text{Os}(\text{CO})_{13}$, $\text{H}_2\text{FeRuOs}_2(\text{CO})_{13}$, and $\text{H}_2\text{FeOs}_3(\text{CO})_{13}$ (78). Only the structure of $\text{H}_2\text{FeRu}_3(\text{CO})_{13}$ has thus far been determined by X-ray diffraction (79), but the remarkable similarity of the infrared spectra shown in Fig. 3 indicates that the other three clusters must have similar structures. In each case, the compounds show a set of bands between 2100 and 1950 cm^{-1} which may be attributed to the 11 terminal carbonyls, and

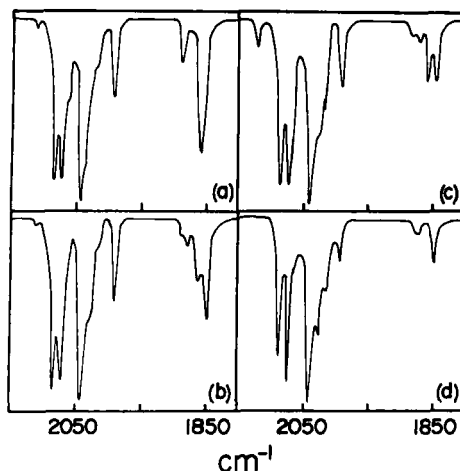


FIG. 3. Carbonyl region of the infrared spectra of (a) $\text{FeRu}_3\text{H}_2(\text{CO})_{13}$, (b) $\text{FeRu}_2\text{OsH}_2(\text{CO})_{13}$, (c) $\text{FeRuOs}_2\text{H}_2(\text{CO})_{13}$, and (d) $\text{FeOs}_3\text{H}_2(\text{CO})_{13}$ measured in cyclohexane solution. Reprinted with permission from Geoffroy and Gladfelter (78). Copyright by the American Chemical Society.

a grouping of bands near 1850 cm^{-1} which were assigned to the bridging carbonyls.

C. Electronic Absorption Spectroscopy

Electronic absorption spectroscopy is generally not very useful for characterizing mixed-metal clusters, although most mixed-metal clusters are highly colored and show rich UV-visible spectra. The bands that are observed may, in most cases, be attributed to transitions between orbitals involved in the metal-metal bonding. A comparison of the electronic absorption spectra of $\text{H}_2\text{FeRu}_3(\text{CO})_{13}$, $\text{H}_2\text{FeRu}_2\text{Os}(\text{CO})_{12}$, and $\text{H}_2\text{FeRuOs}_2(\text{CO})_{13}$ is shown in Fig. 4 (78). The spectra are virtually identical, showing only a spectral blue shift as the osmium content increases. This spectral shift is consistent with the notion that the observed bands are due to metal-metal transitions which increase in energy as the strength of the metal-metal bonds increases as more third-row metal character is incorporated. Similar shifts have been observed in the spectra of $\text{Fe}_3(\text{CO})_{12}$, $\text{Fe}_2\text{Ru}(\text{CO})_{12}$, $\text{FeRu}_2(\text{CO})_{12}$, $\text{Ru}_3(\text{CO})_{12}$, and $\text{Os}_3(\text{CO})_{12}$ (37, 156, 161); and detailed electronic absorption-spectral studies of the latter compounds have conclusively shown that the electronic transitions are between orbitals involved in the metal-metal bonding (156).

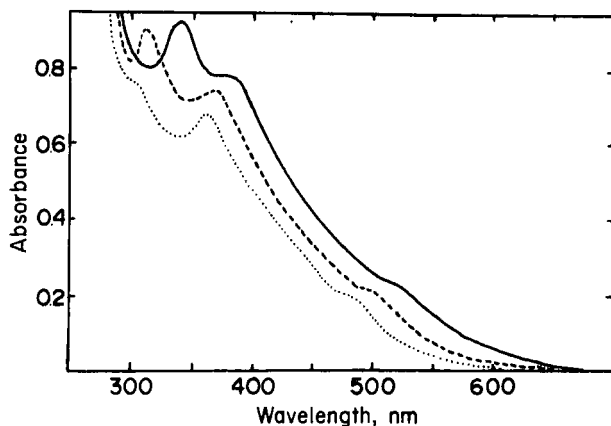


FIG. 4. Electronic absorption spectra of $\text{FeRu}_3\text{H}_2(\text{CO})_{13}$ (—), $\text{FeRu}_2\text{OsH}_2(\text{CO})_{12}$ (---), and $\text{FeRuOs}_2\text{H}_2(\text{CO})_{13}$ (····) measured in hexane solution. Reprinted with permission from Geoffroy and Gladfelter (78). Copyright by the American Chemical Society.

D. Nuclear Magnetic Resonance Spectroscopy

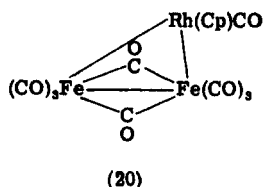
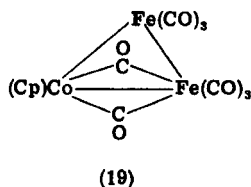
Nuclear magnetic resonance spectroscopy has proved to be quite useful for characterizing metal clusters, particularly clusters that have hydride ligands (7, 90, 95). As with infrared spectroscopy, a complete structure of an unknown cluster cannot be determined by measurement of its NMR spectrum, but some insight into structural features may be obtained. ^1H NMR has been most useful for detecting the presence of hydride ligands and in many cases has led to an accurate assessment of their chemical environment. Although the hydride resonances for clusters generally lie in the chemical-shift range of τ 15–45, for structurally similar clusters the chemical shifts of hydride ligands seldom differ by more than a few parts per million. Thus, by comparing the chemical shift of an unknown compound with those reported for related compounds, the possibilities for the hydride chemical environment can usually be narrowed. ^1H -NMR spectroscopy is extremely useful for determining if the several hydrides that are present in a polyhydride cluster lie in equivalent or nonequivalent positions. However, as discussed in Section V, metal clusters are normally fluxional at room temperature, and care must be taken to ensure that the static spectrum has been obtained when inferring structural information.

^{13}C -NMR spectroscopy has largely been used to study the fluxional properties of metal clusters, but structural information has been obtained in selected cases. It has been amply demonstrated that resonances due to bridging carbonyls lie much farther downfield than those of terminally bound carbonyls in the same cluster. Furthermore, the terminal carbonyls in such mixed-metal clusters as $\text{H}_2\text{FeRuOs}_2(\text{CO})_{13}$ often group together in regions characteristic of carbonyls bound to a given metal (77). For example, in $\text{H}_2\text{FeRuOs}_2(\text{CO})_{13}$ the resonances of the carbonyls bound to osmium occur in the 168–177 ppm region, the resonances of those bound to ruthenium occur in the 184–189 ppm region, and the resonances of those terminally bound to iron occur in the 204–211 ppm region; see Fig. 6 (77).

E. Mössbauer Spectroscopy

Mössbauer spectroscopy has thus far only been used to characterize mixed-metal clusters that contain iron, but it has been useful in deducing structures in several instances. The principal utility of the technique has been in determining whether or not the several iron atoms in a cluster are in equivalent environments. An application to the characterization of

mixed-metal clusters comes from the compounds $\text{Fe}_2\text{Co}(\text{Cp})(\text{CO})_9$ and $\text{Fe}_2\text{Rh}(\text{Cp})(\text{CO})_9$. Two different environments for the iron atoms were observed for the cobalt compound, whereas only a simple doublet was seen in the spectrum of the rhodium derivative, indicating that the two iron atoms are in equivalent positions (102). Structures 19 and 20 were suggested on the basis of these data. Likewise, doublets having broadened lines were observed in the spectra of $\text{Fe}_2\text{Rh}_2(\text{Cp})_2(\text{CO})_8$ and $\text{Fe}_3\text{Rh}(\text{Cp})(\text{CO})_{11}$, indicating nonequivalent iron atoms, as was subsequently confirmed by X-ray analysis (50, 51, 102).



Mössbauer spectroscopy can indeed be a very useful technique for characterizing iron-containing clusters, but it will continue to be of limited use for other metals.

F. Structure Determination by X-Ray and Neutron Diffraction

The best way to ascertain the structure of any compound is to determine its structure by X-ray or neutron diffraction. Indeed, as indicated in Table I, many mixed-metal clusters have had their structures examined by X-ray crystallography, and at least one by neutron diffraction. Space does not permit presentation of the structures of all of these clusters, and the reader is referred to the original articles.

G. Chromatographic Properties

Although liquid chromatography has been extensively used for separating mixed-metal clusters, very little attention has been given to using this technique for identifying compounds. With the advent of analytical high-pressure liquid chromatographs, the capability is available for identifying previously prepared compounds by comparison of retention times, much as gas chromatography has been used in studies of organic compounds. A typical chromatogram that may be obtained for a mixture of

clusters with a commercial high-performance analytical instrument is shown in Fig. 5; it illustrates the kind of separation that can now be achieved. Workers within a group having its own analytical instrument can accumulate a list of retention times of known compounds under a standard set of chromatographic conditions, and then simply compare retention times for compounds resulting from new reactions. Caution must, however, be exercised, as it is not unlikely that several compounds have similar retention times, and this technique can, at best, only complement other identification methods. We have found analytical high-pressure liquid chromatography extremely useful for following the course of reactions and for suggesting the identity of products (62). Columns of microporous silica, such as Waters Associates' μ -Porasil column, appear most useful.

IV REACTIVITY

There have been relatively few studies of the reactivity of mixed-metal clusters, in part because few have been available in sufficient quantity to

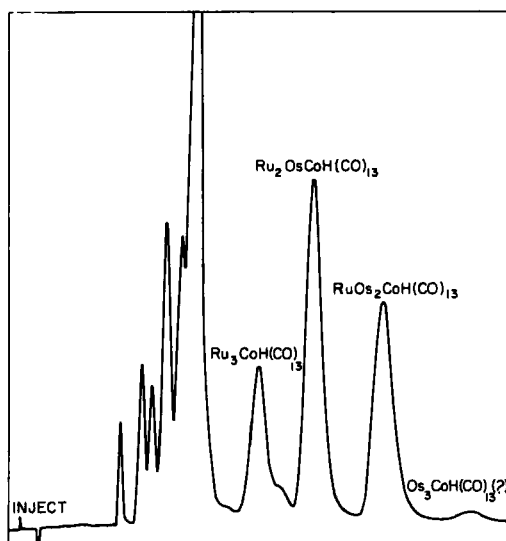
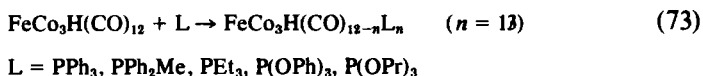


FIG. 5. High-pressure liquid chromatogram of the mixture of clusters obtained from the addition of $[\text{Co}(\text{CO})_4]^-$ to $\text{Ru}_3(\text{CO})_{12}$, followed by protonation with H_3PO_4 . The separation was achieved by using a 25-cm Waters Associates μ -Porasil column with hexane as the eluting solvent at a flow rate of 1.5 ml/min.

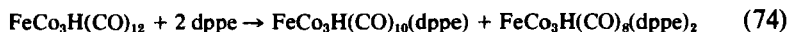
permit study. The majority of investigations have centered on ligand substitution reactions employing Group V donor ligands. These are discussed first, followed by brief discussions of the acid-base chemistry of mixed-metal clusters and their reactions with H_2 , CO, and alkynes. Finally, we present those few studies in which mixed-metal clusters have been employed as catalysts.

A. Ligand Substitution Reactions

Substitution of the neutral cluster $FeCo_3H(CO)_{12}$ with phosphorus donor ligands has been extensively studied by several groups (54, 89, 153). Cooke and Mays (54) noted that mono-, di-, and trisubstituted derivatives could be prepared, depending on the initial reaction conditions and reagent ratios, Eq. (73).



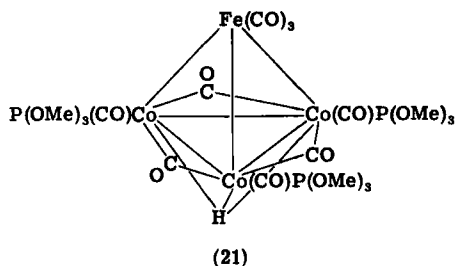
Infrared- and ^{57}Fe -Mössbauer-spectral studies indicated that substitution in these derivatives occurs exclusively at cobalt, with one ligand per cobalt atom in the trisubstituted derivatives (54). Only with the chelating dppe ligand was a tetrasubstituted product formed, Eq. (74).



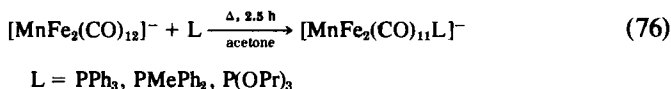
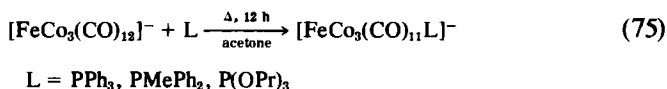
The ^{57}Fe -Mössbauer spectrum of $FeCo_3H(CO)_8(\text{dppe})_2$ indicated the presence of a 1:3 ratio of two isomers. The less abundant isomer was attributed to a cluster having both dppe ligands attached to cobalt atoms, and the second isomer was assigned a structure having one dppe ligand bridging to the iron. It was noted that $FeCo_3H(CO)_{12}$ is considerably more inert to substitution than the isoelectronic $Co_4(CO)_{12}$.

Kaesz and co-workers (89) reported the reaction of $FeCo_3H(CO)_{12}$ with $P(OMe)_3$, and they were able to isolate a tetrasubstituted product in which the fourth $P(OMe)_3$ ligand was bound to iron. The structure of $FeCo_3H(CO)_9\{P(OMe)_3\}_3$ was determined by X-ray diffraction at $-139^\circ C$ and is shown in 21. The hydride ligand was located on the C_3 axis, situated below the Co_3 face. An independent neutron-diffraction study by Bau and co-workers (153) on the same cluster confirmed the position of the hydrogen. These results were particularly significant since the location of the hydride ligand in the parent $FeCo_3H(CO)_{12}$ cluster generated considerable discussion since its initial report. Unfortunately, the quadrupole moment of the cobalt nuclei had prevented observation of a 1H -

NMR signal for the hydride ligand in $\text{FeCo}_3\text{H}(\text{CO})_{12}$ or any of its derivatives (54, 89).

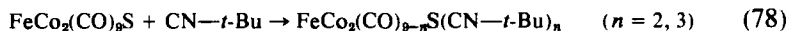
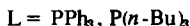


Cooke and Mays (53) also studied the substitution of the anionic clusters $[\text{FeCo}_3(\text{CO})_{12}]^-$ and $[\text{MnFe}_2(\text{CO})_{12}]^-$, Eqs. (75) and (76).



Unlike $\text{FeCo}_3\text{H}(\text{CO})_{12}$, only monosubstituted derivatives could be isolated with $[\text{FeCo}_3(\text{CO})_{12}]^-$. This was attributed to a greater stabilization of the anionic cluster by the π -accepting CO groups (53).

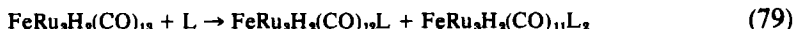
Reaction of $\text{FeCo}_2(\text{CO})_9\text{S}$ with a series of phosphines (31, 133) and isocyanides (126) yielded mono-, di-, and trisubstituted derivatives, Eqs. (77) and (78). ^{57}Fe -Mössbauer spectra of the phosphine-substituted derivatives indicated that substitution at cobalt occurs prior to substitution at iron (31). Unfortunately, no crystallographic evidence has been obtained for any of these derivatives, and the precise stereochemistry has not been resolved, even with the aid of ^{13}C -NMR spectra (9). The problem is compounded with the isocyanide ligands since several isomers of the trisubstituted derivatives are formed.



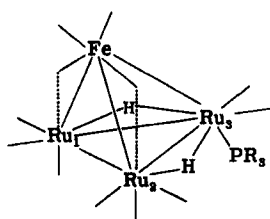
Rossetti and co-workers (133) investigated the kinetics and mechanism of the substitution of $\text{FeCo}_2(\text{CO})_9\text{S}$ and its derivatives. Both associative and dissociative paths were observed in each of the three substitution steps. However, the first and second phosphine ligands substituted predominantly by an associative pathway, although the first substitution was

much faster than the second. It was suggested that initial attack occurs by the phosphine on the triangular face opposite the sulfur atom. Substitution of the third ligand was slow and occurred principally via a dissociative pathway.

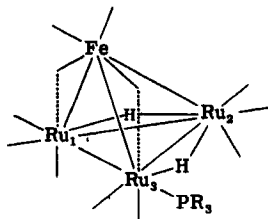
We recently studied the substitution of $\text{FeRu}_3\text{H}_2(\text{CO})_{13}$ with a series of phosphorus donor ligands and prepared several mono- and disubstituted derivatives, Eq. (79) (82).



$^{31}\text{P}\{^1\text{H}\}$ and ^1H -NMR data indicate that the monosubstituted derivatives exist in the two isomeric forms 22 and 23. These isomers were found to interconvert on the NMR time scale, and this process will be discussed in more detail in Section V. The disubstituted derivatives appeared to form at a lower rate than the monosubstituted derivatives, and attempts at further substitution led to break-up of the cluster. When such basic phosphines as PEt_2Ph were employed, deprotonation of the starting cluster occurred, to yield $[\text{FeRu}_3\text{H}(\text{CO})_{13}]^-$. Cooke and Mays (54) observed similar deprotonation in their study of $\text{FeCo}_3\text{H}(\text{CO})_{12}$.



(22)



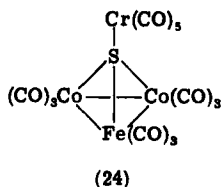
(23)

An investigator would like to be able to predict the metal of a mixed-metal cluster at which substitution would occur. From the limited data available, the only reasonable conclusion that can be drawn is that Co substitutes more readily than Fe in mixed Fe—Co clusters. Clearly, further studies are needed in order to assemble sufficient data to permit a confident approach to this question.

$\text{FeCo}_2(\text{CO})_9\text{S}$ has been shown to undergo a unique reaction in which the cluster itself acts as a donor ligand, Eq. (80) (132).



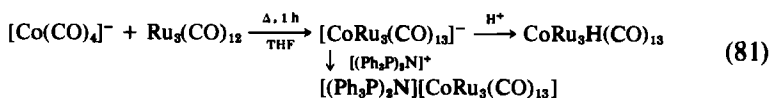
(24)



X-Ray structural data indicate that essentially no change in the geometry of the FeCo_2S cluster occurs upon complexation to $\text{Cr}(\text{CO})_5$.

B. Acid-Base Reactions

In many cases anionic mixed-metal clusters can be protonated to yield neutral hydride clusters, and likewise neutral hydride clusters can be deprotonated to yield anionic species. For example, $[\text{CoRu}_3(\text{CO})_{13}]^-$ is the initial product resulting from the addition of $[\text{Co}(\text{CO})_4]^-$ to $\text{Ru}_2(\text{CO})_{12}$. This cluster can either be isolated as its $[(\text{Ph}_3\text{P})_2\text{N}]^+$ salt or protonated with H_3PO_4 to give $\text{CoRu}_3\text{H}(\text{CO})_{13}$, Eq. (81) (147).

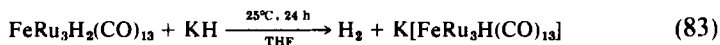


Such protonation reactions as these are usually accomplished by using such noncomplexing, nonoxidizing acids as H_3PO_4 . Care should be taken in protonating anionic clusters as many of the corresponding neutral hydride clusters are thermally unstable and decompose rapidly. For example, attempted protonation of $[\text{FeCo}_3(\text{CO})_{10}(\text{C}_2\text{Ph}_2)]^-$ did not give the expected $\text{FeCo}_3\text{H}(\text{CO})_{10}(\text{C}_2\text{Ph}_2)$, but rather $\text{FeCo}_2(\text{CO})_8(\text{C}_2\text{Ph}_2)$, Eq. (82) (53).



Likewise, we have prepared the anionic clusters $[\text{CoFeRu}_2(\text{CO})_{13}]^-$ and $[\text{CoFe}_2\text{Ru}(\text{CO})_{13}]^-$, but all attempts to isolate the corresponding neutral hydride clusters after protonation have failed, apparently because of their instability (147).

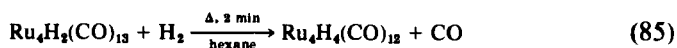
Deprotonation reactions are not so facile. Such bases as OH^- and NR_3 have to be used with caution as they can lead to cluster degradation via attack of the base on the carbonyl ligands. Inkrott and Shore (94) reported a deprotonation method using KH , and we (80) have successfully employed this procedure to deprotonate $\text{FeRu}_3\text{H}_2(\text{CO})_{13}$, Eq. (83).



The only study of the kinetics of a protonation reaction of a mixed-metal cluster was conducted by Cooke and Mays (53) who studied the deuterium isotope effect on the rate of protonation of $[\text{FeCo}_3(\text{CO})_{12}]^-$ and $[\text{FeCo}_3(\text{CO})_{11}\{\text{P}(\text{O}-i\text{-Pr})_3\}]^-$. Large deuterium isotope effects were observed, and for $[\text{FeCo}_3(\text{CO})_{12}]^-$ $k_{\text{H}}/k_{\text{D}} = 17.8 \pm 1$ whereas for $[\text{FeCo}_3(\text{CO})_{11}\{\text{P}(\text{O}-i\text{-Pr})_3\}]^-$, $k_{\text{H}}/k_{\text{D}} = 8.3 \pm 1$. These large values were attributed to "tunneling" of the proton through the ligand barrier to reach its site below the Co_3 face.

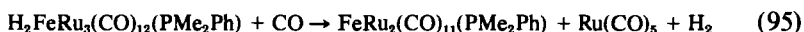
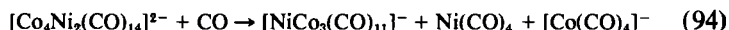
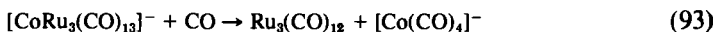
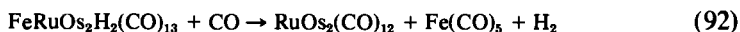
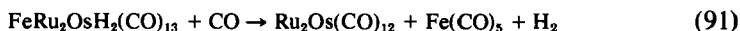
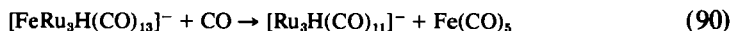
C. Reactions with H_2 and CO

A number of metal clusters have been demonstrated to react with H_2 , often leading to replacement of one CO by two hydride ligands. Kaesz and co-workers (107) first demonstrated this reaction for a mixed-metal cluster when they prepared $\text{FeRu}_3\text{H}_4(\text{CO})_{12}$ from $\text{FeRu}_3\text{H}_2(\text{CO})_{13}$, Eq. (84) (107). Other examples are shown in Eqs. (85) (107), (86) (81), and (87) (48).



This type of reaction appears to have considerable generality, and we suspect that many clusters having one or two hydride ligands can be converted into tri- and tetrahydrides, respectively. Those reactions appear favored because of the loss of steric crowding upon replacing one CO with two hydrogens. We know of no examples in which hydride clusters have been prepared from nonhydride clusters having the same metal framework via a reaction of this type, or of any related reactions that lead to clusters having more than four hydrides. As may be seen by comparing the reaction conditions given in Eqs. (84)–(86), the relative reactivity is greatly dependent upon the specific metals involved, even for isoelectronic clusters.

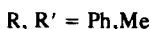
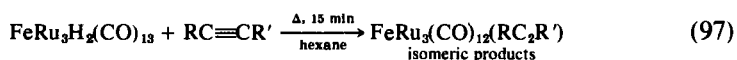
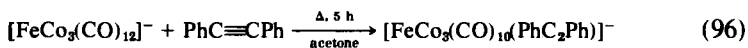
A number of mixed-metal clusters have been demonstrated to react with CO, often under quite mild conditions, Eqs. (88)–(93) (80), (94) (38), and (95) (80).



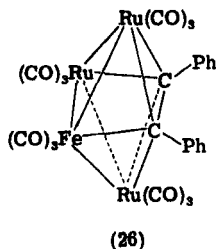
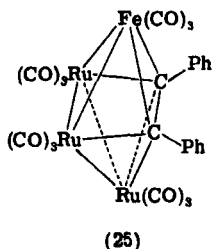
The reaction expressed in Eq. (88) is the reverse of the hydrogen addition [Eq. (84)] and constitutes one of the few demonstrated cases of reductive elimination of H_2 from an intact cluster. The tetranuclear clusters that have been studied appear to fragment consistently in the presence of CO, to produce a metal carbonyl trimer and a monomeric fragment in highly specific fashions.

D. Reactions with Alkynes

The only examples of the reaction of mixed-metal clusters with alkynes are shown in Eqs. (96) (53), (97) (74), and (98) (63).



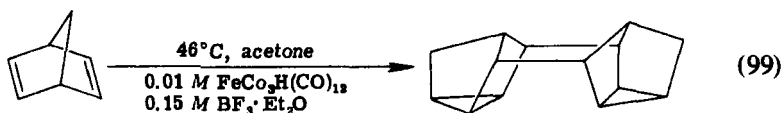
The most extensive study was conducted with $\text{FeRu}_3\text{H}_2(\text{CO})_{13}$ (74). This cluster reacts with diphenylacetylene to produce two isomers of $\text{FeRu}_3(\text{CO})_{12}(\text{PhC}_2\text{Ph})$, and these were characterized by X-ray crystallography as **25** and **26**. These structures are similar to those of $\text{Ru}_4(\text{CO})_{12}(\text{PhC}_2\text{Ph})$ (98) and $\text{Co}_4(\text{CO})_{10}(\text{PhC}_2\text{Ph})$ (58) and appear to result from insertion of the alkyne across one of the metal-metal bonds. Interestingly, the two isomers **25** and **26** slowly interconvert in refluxing hexane, to give an equilibrium mixture containing **26** as the major component. With the unsymmetrical alkyne $\text{PhC}\equiv\text{CMe}$, three isomers of $\text{FeRu}_3(\text{CO})_{12}(\text{PhC}_2\text{Me})$ result.



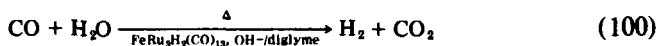
E. Catalytic Reactions

Only a few mixed-metal clusters have been studied as homogeneous catalysts, and in all these studies the exact nature of the catalytically active species is unknown. Labroue and Poilblanc (108) reported the use of $\text{Co}_3\text{Rh}(\text{CO})_{12}$ and $\text{Co}_2\text{Rh}_2(\text{CO})_{12}$ as catalysts for the hydrogenation of styrene to ethylbenzene at 27°C and ~ 2 atm H_2 . No induction period was observed, and the initial rate for $\text{Co}_2\text{Rh}_2(\text{CO})_{12}$ was twice that for $\text{Co}_3\text{Rh}(\text{CO})_{12}$. $\text{Co}_4(\text{CO})_{12}$ was inactive under the same conditions. Addition of $\text{P}(\text{OMe})_3$ to the reaction mixture increased the rate of hydrogenation to the same magnitude as that found for $\text{RhCl}(\text{PPh}_3)_3$. Unfortunately, the reaction mixture contained unidentifiable products that were not, by comparison, simply the substituted $\text{Co}_2\text{Rh}_2(\text{CO})_{12-n}[\text{P}(\text{OMe})_3]_n$ ($n = 1, 2, 3$) clusters. A possible correlation between the catalytic and fluxional properties of these molecules was suggested (108).

Mays and co-workers (33) found that $[\text{FeCo}_3(\text{CO})_{12}]^-$ and $\text{FeCo}_3\text{H}(\text{CO})_{12}$ catalyze the dimerization of norbornadiene, Eq. (99). The results were highly dependent on the solvent and the cocatalysts employed. $\text{FeCo}_3\text{H}(\text{CO})_{12}$ was more effective than $[\text{FeCo}_3(\text{CO})_{12}]^-$, but the nature of the actual catalytic species was not determined.



Ford and co-workers (72) reported that several metal clusters catalyze the water gas shift reaction, Eq. (100).



The most active catalyst studied was $\text{FeRu}_3\text{H}_2(\text{CO})_{13}$, but the actual catalytic mechanism is still not known. In view of the reaction shown in

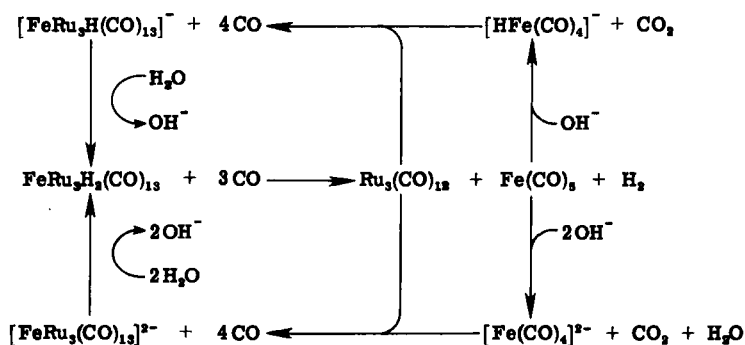
Eq. (89), it is possible that the reaction proceeds via one of the catalytic cycles shown in Scheme 5 (80).

An important application of metal carbonyl clusters may come in their use as precursors for heterogeneous catalysts. In this regard, mixed-metal clusters are ideally suited for the preparation of bimetallic catalyst systems. Anderson and co-workers (17) examined the adsorption of clusters, including $\text{Co}_3\text{Rh}(\text{CO})_{12}$ and $\text{Co}_2\text{Rh}_2(\text{CO})_{12}$, onto alumina and silica. Adsorption of the clusters was more facile on alumina and was assisted by the presence of oxygen. $\text{Co}_2\text{Rh}_2(\text{CO})_{12}$ was found to lose its bridging carbonyls upon adsorption, and further loss of carbonyl occurred at temperatures $>300\text{K}$. These studies also showed that, upon reduction at 650°C under an H_2 atmosphere, $\text{Co}_2\text{Rh}_2(\text{CO})_{12}$ forms a highly dispersed Co—Rh bimetallic catalyst. Importantly, this process gave a much higher degree of dispersion than could be obtained by conventional impregnation techniques using an aqueous solution of $\text{Co}(\text{NO}_3)_2$ and $\text{RhCl}_3 \cdot 3\text{H}_2\text{O}$.

V

DYNAMIC NMR STUDIES

A common feature of metal clusters is their stereochemical nonrigidity, in which carbonyl and hydride ligands exchange their coordination sites. Mixed-metal clusters are ideally suited for studies of the fluxional processes in clusters because of the low symmetry inherent in their metal framework. In such clusters, the majority of the ligands are in chemically nonequivalent positions and should thus be distinguishable by NMR

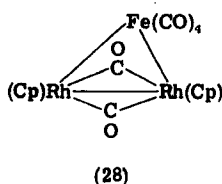
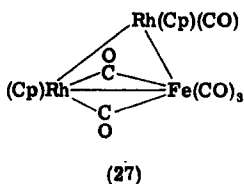


SCHEME 5

spectroscopy. The following discussion briefly describes those studies that have been conducted. The methodology has previously been discussed (7), and will not be repeated here.

A. Trinuclear Clusters

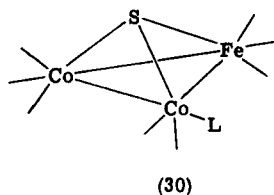
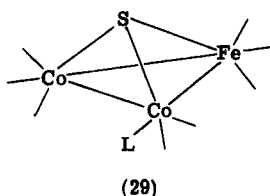
Mays and co-workers (86) found that both $\text{Fe}_2\text{Rh}(\text{Cp})(\text{CO})_9$ and $\text{Fe}_2\text{Co}(\text{Cp})(\text{CO})_9$ are fluxional, but were unable to obtain a low-temperature limiting spectrum. A limiting spectrum was observed, however, with $\text{FeRh}_2(\text{Cp})_2(\text{CO})_6$. ^{57}Fe mössbauer data on solid samples of this cluster had previously led (102) to assignment of the structure as 27, but the ^{13}C -NMR spectrum at -70°C (234.5 ppm, t, 2C; 193.3 ppm, s, 2C; 190.0 ppm, s, 2C) was consistent only with structure 28. The triplet observed at room temperature agreed well with the average chemical shift calculated from the -70°C spectrum, but differed considerably in its ^{103}Rh - ^{13}C coupling constant. It is possible that at higher temperatures isomer 27 is also present; this could account for the increase in the average ^{103}Rh - ^{13}C coupling constant.



Johnson and co-workers (73) examined the ^{13}C -NMR spectra of a series of metal carbonyl trimers, including $\text{Fe}_2\text{Ru}(\text{CO})_{12}$ and $[\text{MnFe}_2(\text{CO})_{12}]^-$. Each of these showed only a singlet at the lowest temperatures examined, indicating rapid exchange of the carbonyls. We have found that, at room temperature, $\text{Ru}_2\text{Os}(\text{CO})_{12}$ shows a 192.0-ppm singlet that broadens upon cooling to -90°C (80). The position of the singlet agrees very well with the chemical shift calculated from a weighted average of the singlets observed in the spectra of $\text{Ru}_3(\text{CO})_{12}$ (198 ppm, 25°C) and $\text{Os}_3(\text{CO})_{12}$ (178.1 ppm, 156°C).

Aime and co-workers (9) studied the ^{13}C -NMR spectra of $\text{FeCo}_2(\text{CO})_9\text{S}$ and several of its phosphine derivatives. At -115°C , $\text{FeCo}_2(\text{CO})_9\text{S}$ exhibits three peaks in a 1:2:6 intensity ratio. The large peak was attributed to the Co—CO which undergo rapid scrambling. At -65°C , the Fe—CO groups undergo localized scrambling on the Fe atom, and, above this

temperature, all of the carbonyls become equivalent. The ^{13}C -NMR spectra of the substituted $\text{FeCo}_2(\text{CO})_{9-n}\text{S}(\text{L})_n$ ($n = 1-3$) derivatives indicated that the first two phosphines bind successively to the Co atoms, and the third phosphine binds to Fe. Although this study indicated that the phosphines all substitute within the equatorial FeCo_2 plane, it was not possible to assign the absolute stereochemistry. For instance, both **29** and **30** are possible structures for the monosubstituted derivative.



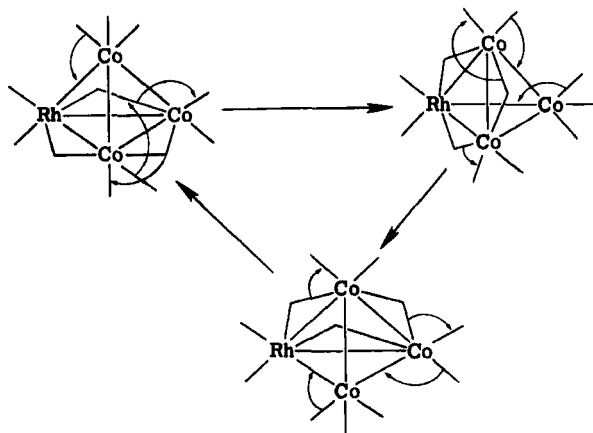
These $\text{FeCo}_2(\text{CO})_{9-n}\text{S}(\text{L})_n$ ($n = 1-3$) clusters are fluxional on the NMR time scale (9). In each case, localized exchange occurs first on the unsubstituted Co atom, and then on Fe. Finally, exchange of all the carbonyls occurs, to yield only a single resonance in the high-temperature spectrum. Line-shape analysis led to the following order of activation energies for exchange of the carbonyls bound to iron.



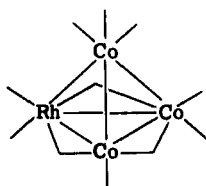
It was suggested that an increase in the electron density on the cluster due to substitution weakens the metal-metal bonds and thereby facilitates scrambling within the $\text{Fe}(\text{CO})_3$ fragment (9). The mechanism of carbonyl exchange between the metals remains unclear.

B. Tetranuclear Clusters

$\text{Co}_3\text{Rh}(\text{CO})_{12}$ exhibits a ^{13}C spectrum at -85°C consistent with structure **31** (97). At this temperature, the carbonyls bound to the unique cobalt give rise to a single resonance, indicating that they rapidly interchange. The next process ($T_c = -45^\circ\text{C}$) involves interchange of the carbonyls on the three RhCo_2 faces. The Rh is always maintained in the basal triangle in this process although the bridging carbonyls exchange positions (see Scheme 6). At temperatures above -30°C , all the carbonyls become equivalent. The mechanism for this last process probably involves a tetrahedral intermediate similar to that proposed by Cotton *et al.* (56) to explain the fluxionality of $\text{Rh}_4(\text{CO})_{12}$.

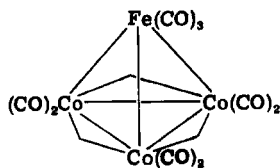


SCHEME 6



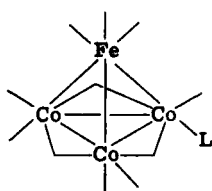
(31)

Milone and co-workers (8) examined the ^{13}C -NMR spectra of $\text{FeCo}_3\text{H}(\text{CO})_{12}$ (32) and some of its substituted derivatives. At -89°C , two resonances in a 1:2 ratio were observed in the spectrum of $\text{FeCo}_3\text{H}(\text{CO})_{12}$. As the temperature was raised, the farthest upfield, and more intense, peak broadened significantly. It was assumed that the cobalt carbonyls rapidly exchange at -85°C , and this peak was attributed to an average cobalt carbonyl resonance that broadens at room temperature due to coupling to ^{59}Co . The second resonance was attributed to rapidly exchanging Fe carbonyls. The observed disparity of intensities (1:2 observed, 1:3 expected) is similar to that found for the isoelectronic $\text{Co}_4(\text{CO})_{12}$.

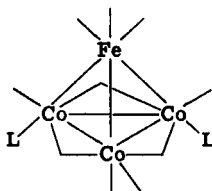


(32)

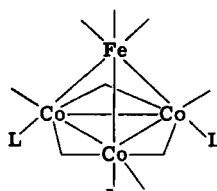
The substituted $\text{FeCo}_3\text{H}(\text{CO})_{12-n}(\text{L})_n$ ($n = 1-3$) derivatives (8) all yielded spectra consistent with the proposed or proved structures 33, 34, and 35. Increasing substitution slowed the exchange processes within the Co_3 triangle. Arguments were advanced to the effect that substitution of a carbonyl with a phosphine ligand increases the electron density on the cluster, and this in turn increases the need for the bridging carbonyls as an effective means of removing the excess electron density. As the transitional state in the fluxional process would involve breaking the carbonyl bridges, the activation barrier should therefore increase.



(33)



(34)



(35)

We have studied the dynamic properties of $\text{FeRu}_3\text{H}_2(\text{CO})_{13}$, $\text{FeRu}_2\text{OsH}_2(\text{CO})_{13}$, and $\text{FeRuOs}_2\text{H}_2(\text{CO})_{13}$ (77). The structure of $\text{FeRu}_3\text{H}_2(\text{CO})_{13}$ was determined by X-ray crystallography (79), and $\text{FeRu}_2\text{OsH}_2(\text{CO})_{13}$ and $\text{FeRuOs}_2\text{H}_2(\text{CO})_{13}$ were assumed to have similar structures on the basis of their infrared, electronic absorption, and NMR spectral data (78). The mechanisms of CO exchange were found by ^{13}C -NMR spectroscopy to be identical for these three clusters, and our further discussion will involve only $\text{FeRuOs}_2\text{H}_2(\text{CO})_{13}$. This cluster exists in the two isomeric forms shown with their C_s and C_1 symmetry labels. The low-temperature limiting ^{13}C -NMR spectrum of the mixture of these isomers is shown in Fig. 6. Nineteen of the 21 chemically nonequivalent carbonyls present in the isomeric mixture are clearly observable in the ^{13}C -NMR spectrum, illustrating the utility of mixed-metal clusters in studies of this type. Three basic exchange processes occur in these clusters as the temperature is raised from -60 to $+100^\circ\text{C}$. The first process involves exchange of the bridging and terminal carbonyls bound to iron (C_1 , $T_c = -40^\circ\text{C}$; C_s , $T_c = -20^\circ\text{C}$). In the second process, eight carbonyls execute a cyclic motion around the Fe-M-M triangle that initially contained the bridging carbonyls (C_1 , $T_c = -20^\circ\text{C}$; C_s , $T_c = 20^\circ\text{C}$). The third process manifests itself in two distinct ways (see Scheme 7). First, the two enantiomers of the C_1 isomer interconvert; this occurs by a shift in the metal framework in which the Fe moves away from Os_A and toward Os_B , concerted with movement of the hydride that bridges

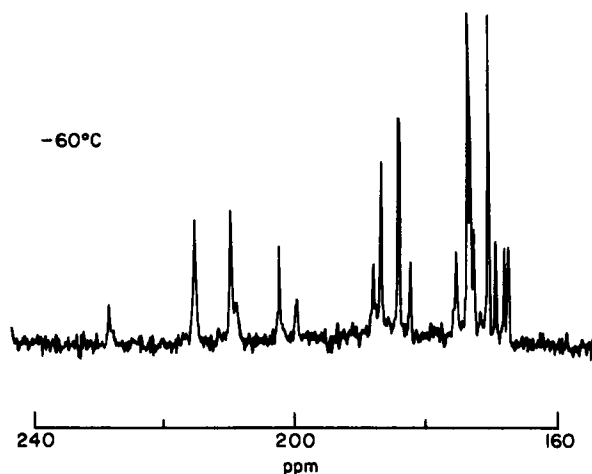
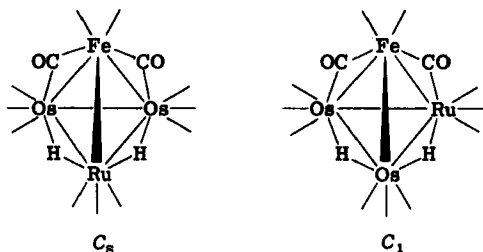
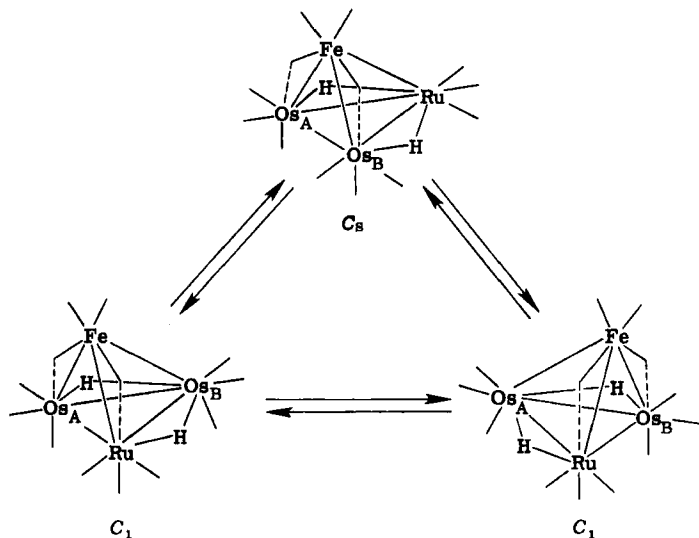


FIG. 6. $^{13}\text{C}\{^1\text{H}\}$ NMR spectrum of $\text{FeRuOs}_3\text{H}_2(\text{CO})_{13}$ at -60°C .

the Os_A —Ru bond to a position bridging the Os_B —Ru bond. Finally, in the last process, the Fe moves away from Ru and toward Os_A , to give the C_s isomer. The interconversion of the three faces of the cluster that possess the bridging carbonyls, coupled with the cyclic exchange process about each of these faces, leads to total exchange of all of the carbonyls in the cluster. The activation barriers for each of the three exchange processes (bridge exchange, cyclic exchange, and metal shift) was observed to increase in the order $\text{FeRu}_3\text{H}_2(\text{CO})_{13} < \text{FeRu}_2\text{OsH}_2(\text{CO})_{13} < \text{FeRuOs}_2\text{H}_2(\text{CO})_{13}$.

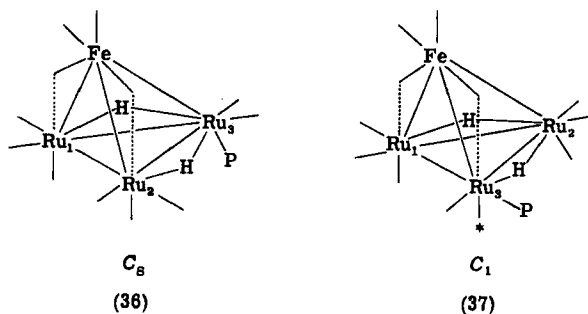


In a separate study, ^1H -, ^{31}P -, and ^{13}C -NMR spectra were used in order to show that $\text{FeRu}_3\text{H}_2(\text{CO})_{12}(\text{PMe}_2\text{Ph})$ exists in the two isomeric forms **36** and **37** (82). An alternative substitution site in the C_1 isomer that was also consistent with the NMR data is indicated by the asterisk. Complete assignment of the ^{13}C -NMR spectrum of the compound was not possible because of overlapping resonances, but much information was extracted



SCHEME 7

from the ^1H -NMR spectrum. These two isomers were found to interconvert, presumably by the same type of intrametallic rearrangement process already discussed.



Perhaps of greater importance was comparison of the series of $\text{FeRu}_3\text{H}_2(\text{CO})_{12}\text{L}$ clusters in which $\text{L} = \text{P}(\text{OMe})_3$, $\text{P}(\text{OEt})_2\text{Ph}$, PPh_3 , PMePh_2 , PEt_2Ph , PMe_2Ph , PMe_3 , and $\text{P}(i\text{-Pr})_3$ (82). A comparison of the $\text{C}_8 \rightleftharpoons \text{C}_1$ equilibrium constants with the cone angle and basicity of the phosphorus ligand for the various derivatives in hexane solution is shown in Table II. No correlation was found on using only size or basicity alone, and both factors affect the position of this equilibrium. With large ligands, the cluster exists totally as the C_8 isomer, regardless of ligand basicity. With smaller ligands, the complex may exist as both isomers, but with

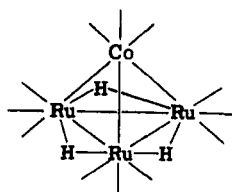
TABLE II
EFFECT OF LIGAND SIZE AND BASICITY ON THE $C_1 \rightleftharpoons C_s$
EQUILIBRIUM OF $\text{FeRu}_3\text{H}_2(\text{CO})_{11}\text{L}$ (82)

Ligand	Cone angle (degrees) ^a	Basicity (cm^{-1}) ^a	<i>K</i>
$\text{P}(i\text{-Pr})_3$	160	2059.2	>100
PPh_3	145	2068.9	>100
PMePh_2	136	2067.0	11
PEt_2Ph	136	2063.7	11
$\text{P}(\text{OMe})_3$	107	2079.5	10
$\text{P}(\text{OEt})_2\text{Ph}$	116	2074.2	5.5
PMe_2Ph	122	2065.3	1.8
PMe_3	118	2064.1	0.4

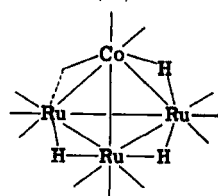
^a Data taken from C. A. Tolman, *Chem. Rev.* 77, 313 (1977).

the C_1 isomer increasing in stability as the basicity of the phosphorus donor ligand increases. The equilibrium was found to be quite solvent-dependent, and more polar solvents favored the C_s isomer.

The solid-state structure of $\text{Ru}_3\text{CoH}_3(\text{CO})_{12}$ was shown by X-ray crystallography to have C_{3v} symmetry (38) (81). However, infrared and ^1H -NMR spectroscopy showed that more than one isomer of this cluster exists in solution. The C_{3v} structure 38 has no bridging carbonyls, but the infrared spectrum of the cluster in hexane solution showed ν_{CO} at 1878 cm^{-1} . ^1H -NMR measurements at -100°C and 360 MHz confirmed the presence of two isomers and showed that the second isomer contains three nonequivalent hydrogens. Structure 39 was suggested for the second isomer. At elevated temperatures, these isomers interconvert ($T_c = -40^\circ\text{C}$).



(38)



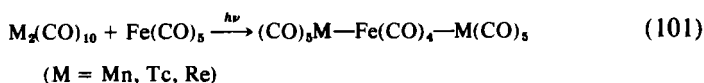
(39)

VI

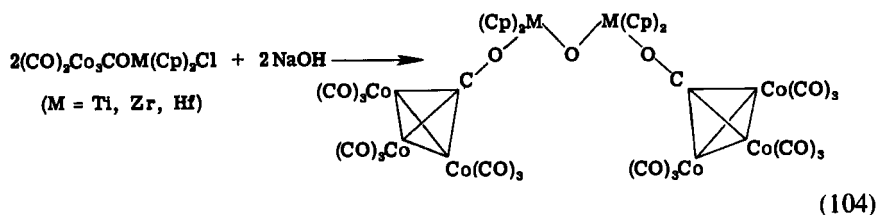
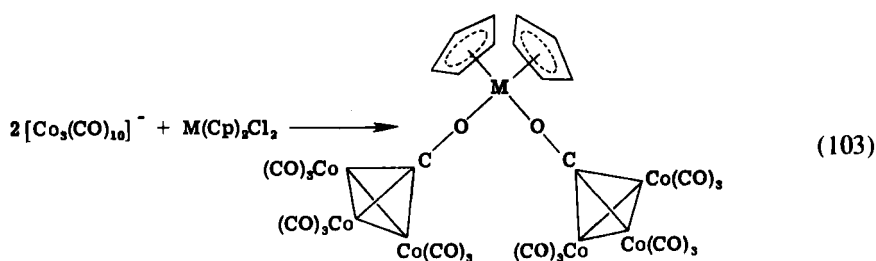
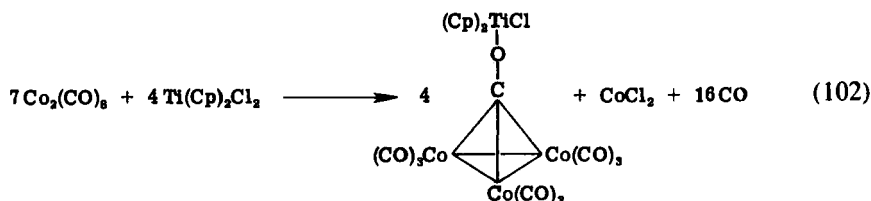
ALMOST MIXED-METAL CLUSTERS

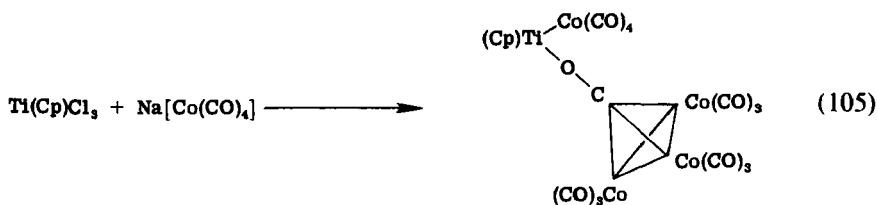
Because of the requirements set at the beginning of this chapter concerning the scope of this review, we have had to exclude several interesting compounds, but, as these may be of interest to some readers, they are briefly mentioned here although this section is not meant to be comprehensive.

A number of linear mixed-metal carbonyls are known. Sheline and co-workers prepared a series of $M-Fe-M$ ($M = Tc, Re$) trimers by photolysis of $Fe(CO)_5$ and the corresponding $M_2(CO)_{10}$, Eq. (101) (66, 109).

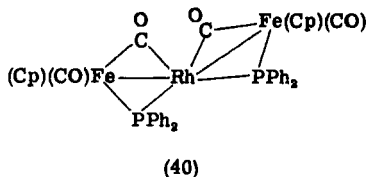
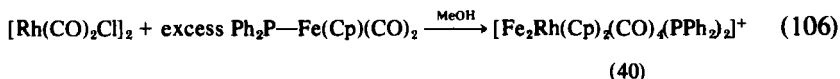


Schmid and co-workers (136) prepared several derivatives that possess the $[Co_3CO_{10}]^-$ unit as an oxygen donor ligand to another metal. Reactions (102) (138), (103) (152), (104) (152), and (105) (139) are illustrative.



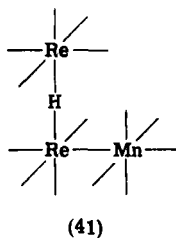


The bridged oligomer $[\text{Fe}_2\text{Rh}(\text{Cp})_2(\text{CO})_2(\text{PPh}_2)_2]^+$ (**40**) is prepared by the reaction shown in Eq. (106) (83, 84, 114).

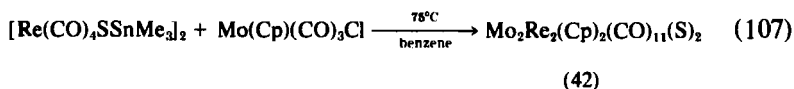


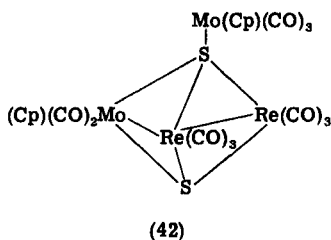
Norton and co-workers (5, 6) developed an improved synthetic method for this trimer, and they prepared the Ru_2Ir and Fe_2Ir analogs. These compounds undergo racemization on the NMR time scale with free energies of activation of 12.6, 17.5, and 17.8 kcal/mol for the Fe_2Rh , Fe_2Ir , and Ru_2Ir complexes, respectively.

$\text{HMnRe}_2(\text{CO})_{14}$ **41** was shown to have a "bent" disposition of metals with the hydride lying between the Re atoms (44, 69).

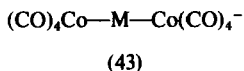


Dahl and co-workers prepared the unusual compound $\text{Mo}_2\text{Re}_2(\text{Cp})_2(\text{CO})_{11}(\text{S})_2$ (**42**) containing both tri- and tetracoordinated sulfur ligands, Eq. (107) (158).

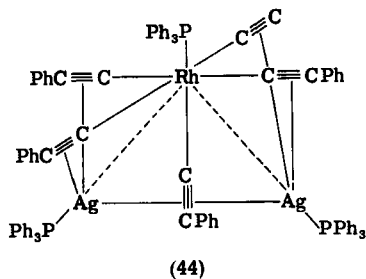




Chini and co-workers (42) found that $[\text{Co}(\text{CO})_4]^-$ reacts with CuI and AgI to give high yields of $[(\text{CO})_4\text{CoCuCo}(\text{CO})_4]^-$ and $[(\text{CO})_4\text{CoAgCo}(\text{CO})_4]^-$ of structure 43. The copper complex is less stable than the silver species and readily dissociates in CH_3CN . Reaction (108), however, is reversible, and the starting material can be recovered after solvent removal.



$\text{Rh}_2\text{Ag}(\text{PPh}_3)_3[\text{C}_2(\text{C}_6\text{F}_5)]_5$ (44) has been prepared by a reaction similar to that which gave $\text{Ir}_2\text{Cu}_4(\text{PPh}_3)_2(\text{C}_2\text{Ph})_8$ (4, 46). The structure shows octahedral Rh coordination and tetrahedral Ag coordination. The 3.1 Å Rh—Ag distances indicate that little metal-metal bonding exists.



ACKNOWLEDGMENTS

We are most grateful to Professors P. Braunstein, P. Chini, L. Milone, J. Shapley, and F. G. A. Stone for providing preprints of their work prior to publication, and to Elizabeth Gladfelter and Carla Hofland for assistance in preparation of the manuscript. Our own research described herein was supported in part by the Office of Naval Research.

ADDENDUM

Tabulated below are all the mixed-metal clusters that have been most recently reported.

$\text{MnFe}_2(\text{Cp})(\text{CO})_8(\text{PPh}_3)(\mu\text{-PPh})$, $\text{MnFe}_2\text{Cp}(\text{CO})_8(\mu\text{-PPh})$ [G. Huttner, J. Schneider, H.-D. Muller, G. Mohr, J. Seyeryl, and L. Wohlfahrt, *Angew. Chem. Int. Ed. Engl.* **18**, 76 (1979)].

$\text{Ru}_3\text{Ni}(\text{Cp})(\text{CO})_8(\text{C}_2\text{C}(\text{H})\text{Bu})$ [E. Sappa, A. Tiripicchio, and M. T. Camellini, *J. Chem. Soc. Chem. Commun.* p. 254 (1979)].

$\text{MoFeCo}_2(\text{Cp})(\text{CO})_{11}(\mu\text{-PPh})(\mu\text{-AsMe}_2)$, $\text{MoCo}_3(\text{Cp})(\text{CO})_{11}(\mu\text{-PPh})(\mu\text{-AsMe}_2)$, $\text{FeCo}_2(\text{CO})_8(\mu\text{-PPh})$, $\text{MoCo}_2(\text{Cp})(\text{CO})_8(\mu\text{-AsMe}_2)(\mu\text{-PPh})$, $\text{MoFeCo}(\text{Cp})(\text{CO})_8(\mu\text{-PPh})$ [F. Richter, H. Beurich, and H. Vahrenkamp, *J. Organomet. Chem.* **166**, C5 (1978)].

$\text{WFeCo}(\text{Cp})(\text{CO})_8(\text{S})$, $\text{MoFeCo}(\text{Cp})(\text{CO})_8(\text{S})$, $\text{MoFeCo}(\text{Cp})(\text{CO})_7(\text{PPhMe}_2)(\text{S})$, $\text{MoFeCo}(\text{Cp})(\text{CO})_8(\text{PPhMe}_2)(\text{S})$, $\text{CrFeCo}(\text{Cp})(\text{CO})_8(\text{S})$ [F. Richter and H. Vahrenkamp, *Angew. Chem. Int. Ed. Engl.* **17**, 864 (1978)].

$\text{MoCo}_2(\text{Cp})(\text{CO})_8(\text{CR})$ ($\text{R} = \text{H}, \text{CH}_3, \text{Ph}$), $\text{WCo}_2(\text{Cp})(\text{CO})_8(\text{CR})$ ($\text{R} = \text{H}, \text{CH}_3, \text{Ph}$), $\text{CrCo}_2(\text{Cp})(\text{CO})_8(\text{CR})$ ($\text{R} = \text{H}, \text{CH}_3, \text{Ph}$) [H. Beurich and H. Vahrenkamp, *Angew. Chem. Int. Ed. Engl.* **17**, 863 (1978)].

$\text{MoFeCo}_2(\text{Cp})(\text{CO})_8(\mu\text{-AsMe}_2)(\mu\text{-S})$, $\text{MoWFeCo}(\text{Cp})_2(\text{CO})_7(\mu\text{-AsMe}_2)(\mu\text{-S})$ [F. Richter and H. Vahrenkamp, *Angew. Chem. Int. Ed. Engl.* **18**, 531 (1979)].

$[\text{Fe}_2\text{Ag}(\text{CO})_8\{\text{CHC}(\text{Ph})\text{NHMe}\}(\mu\text{-PPh}_2)]^+$ [A. J. Carty, G. N. Mott, and N. J. Taylor, *J. Am. Chem. Soc.* **101**, 3131 (1979)].

$\text{W}_2\text{Pd}_2(\text{Cp})_2(\text{CO})_8(\text{PET}_3)_2$, $\text{Mo}_2\text{Pt}_2(\text{Cp})_2(\text{CO})_8(\text{PET}_3)_2$ [R. Bender, P. Braunstein, Y. Dusaosoy, and J. Protos, *J. Organomet. Chem.* **172**, C51 (1979)].

$\text{Ru}_3\text{Ni}(\text{Cp})(\text{CO})_8(\text{C}_6\text{H}_9)$ [D. Osella, E. Sappa, A. Tiripicchio, and M. Camellini, *Inorg. Chim. Acta* **34**, L289 (1979)].

$\text{FeCo}_2(\eta^5\text{-C}_5\text{Me}_5)_2(\text{CO})_8$ [L. M. Cirjak, R. E. Ginsberg, and L. F. Dahl, *J. Chem. Soc. Chem. Commun.* p. 470 (1979)].

$[\text{Rh}_6\text{CuC}(\text{CO})_{15}(\text{MeCN})]^-$, $[\text{Rh}_4\text{Pt}(\text{CO})_{12}]^{2-}$, $[\text{Rh}_6\text{Ni}(\text{CO})_{16}]^{2-}$, $[\text{Rh}_6\text{Pt}(\text{CO})_{14}]^{2-}$, $[\text{Fe}_3\text{Pt}_3(\text{CO})_{15}]^{2-}$, $[\text{Fe}_3\text{Pt}_3\text{H}(\text{CO})_{15}]^-$, $[\text{Fe}_4\text{Pt}_6(\text{CO})_{22}]^{2-}$, $[\text{Fe}_8\text{Pd}_8(\text{CO})_{24}]^{4-}$, $[\text{Ni}_3\text{Pt}_3(\text{CO})_{12}]^{2-}$ (G. Longoni, U.S.-Italy Cooperative Science Seminar on the Chemistry of Cluster Compounds and Its Relationship to Catalysis, Gargnano sur Garda, Italy, August 29-31, 1979).

$\text{Rh}_6\text{CuC}(\text{CO})_{15}(\text{MeCN})_2$ (V. Albano, in U.S.-Italy Cooperative Science Seminar on the Chemistry of Cluster Compounds and Its Relationship to Catalysis, Gargnano sur Garda, Italy, August 29-31, 1979).

$\text{FeCo}_2(\text{Cp})(\text{CO})_8(\text{C}_2\text{R})$, $\text{FeCo}_2(\text{CO})_8(\text{C}_2\text{Et}_2)$ (L. Milone, in U.S.-Italy Cooperative Science Seminar on the Chemistry of Cluster Compounds

and Its Relationship to Catalysis, Gargnano sur Garda, Italy, August 29–31, 1979).

$\text{Co}_2\text{Pt}(\text{CO})_7(\text{Ph}_2\text{PCH}_2\text{CH}_2\text{PPh}_2)$ (P. Braunstein, in U.S.–Italy Cooperative Science Seminar on the Chemistry of Cluster Compounds and Its Relationship to Catalysis, Gargnano sur Garda, Italy, August 29–31, 1979).

$\text{WFePt}(\text{Cp})(\text{CO})_5(\text{PPh}_2\text{Me})_2(\text{CR})$ (T. V. Ashworth, M. Chetcuti, J. Martin-Gil, J. A. K. Howard, M. Laguna, P. Mitrprachachon, R. Navarro, and F. G. A. Stone, *Int. Conf. Organomet. Chem.*, 9th. Dijon, France, September 3–7, 1979).

$\text{MnCo}_2(\text{CO})_{10}(\text{E})$ ($\text{E} = \text{S}, \text{PPh}, \text{AsMe}$), $\text{MoCo}_2(\text{Cp})(\text{CO})_8(\text{E})$ ($\text{E} = \text{S}, \text{PPh}, \text{AsMe}$), $\text{MoCo}_2(\text{Cp})(\text{CO})_7(\mu\text{-AsMe}_2)(\text{E})$ ($\text{E} = \text{S}, \text{PPh}, \text{AsMe}$) (H. Vahrenkamp, *Int. Conf. Organomet. Chem.* 9th. Dijon, France, September 3–7, 1979).

$\text{OsPt}_2(\text{CO})_5(\text{PPh}_3)_2(\text{C}_4\text{H}_8)$, $[\text{Fe}_2\text{Pt}_2\text{H}(\text{CO})_8(\text{PPh}_3)_2]^-$, $\text{Fe}_2\text{Pt}_2\text{H}_2(\text{CO})_8(\text{PPh}_3)_2]^-$, $\text{Fe}_2\text{Pt}(\text{CO})_8(\text{C}_8\text{H}_{12})$ (L. J. Farrugia, J. A. K. Howard, and P. Mitrprachachon, *Int. Conf. Organomet. Chem.* 9th. Dijon, France, September 3–7, 1979).

REFERENCES

1. O. M. Abu Salah, and M. I. Bruce, *J. Chem. Soc. Dalton Trans.* 2311 (1975).
2. O. M. Abu Salah, and M. I. Bruce, *Aust. J. Chem.* **29**, 531 (1976).
3. O. M. Abu Salah, M. I. Bruce, S. A. Beznán, and M. R. Churchill, *J. Chem. Soc. Chem. Commun.* p. 858 (1972).
4. O. M. Abu Salah, M. I. Bruce, M. R. Churchill, and B. G. DeBoer, *J. Chem. Soc. Chem. Commun.* p. 688 (1974).
5. A. Agapiou, R. F. Jordan, L. A. Zyzyck, and J. R. Norton, *J. Organomet. Chem.* **141**, c35 (1977).
6. A. Agapiou, S. E. Pedersen, L. A. Zyzyck, and J. R. Norton, *J. Chem. Soc. Chem. Commun.* 393 (1977).
7. S. Aime and L. Milone, *Prog. Nucl. Magn. Reson. Spectrosc.* **11**, 183 (1977).
8. S. Aime, L. Milone, D. Osella, and A. Poli, *Inorg. Chim. Acta* **30**, 45 (1978).
9. S. Aime, L. Milone, R. Rossetti, and P. L. Stanghellini, *Inorg. Chim. Acta* **25**, 103 (1977).
10. V. G. Albano, P. Chini, S. Martinengo, M. Sansoni, and D. Strumolo, *J. Chem. Soc. Chem. Commun.* p. 299 (1974).
11. V. G. Albano and G. Ciani, *J. Organomet. Chem.* **66**, 311 (1974).
12. V. G. Albano, G. Ciani, M. I. Bruce, G. Shaw, and F. G. A. Stone, *J. Organomet. Chem.* **42**, c99 (1972).
13. V. G. Albano, G. Ciani, and P. Chini, *J. Chem. Soc. Dalton Trans.* p. 432 (1974).
14. V. G. Albano, G. Ciani, and S. Martinengo, *J. Organomet. Chem.* **78**, 265 (1974).
15. U. Anders and W. A. G. Graham, *J. Chem. Soc. Chem. Commun.* p. 291 (1966).
16. A. Anders and W. A. G. Graham, *J. Am. Chem. Soc.* **89**, 539 (1967).
17. J. R. Anderson, P. S. Elmes, R. F. Howe, and D. E. Mainwaring, *J. Catal.* **50**, 508 (1977).

18. T. V. Ashworth, M. Berry, J. A. K. Howard, M. Laguna, and F. G. A. Stone, *J. Chem. Soc. Chem. Commun.* p. 45 (1979).
19. T. V. Ashworth, J. A. K. Howard, and F. G. A. Stone, *J. Chem. Soc. Chem. Commun.* p. 42 (1979).
20. J. P. Barbier, P. Braunstein, J. Fischer, and L. Ricard, *Inorg. Chim. Acta* **31**, L361 (1978).
21. R. Bender, P. Braunstein, Y. Dusauroy, and J. Protas, *Angew. Chem. Int. Ed. Engl.* **17**, 596 (1978).
22. M. J. Bennett, W. A. G. Graham, J. K. Hoyano, and W. L. Hutcheon, *J. Am. Chem. Soc.* **94**, 6232 (1972).
23. S. Bhaduri, B. F. G. Johnson, J. Lewis, P. R. Raithby, and D. J. Watson, *J. Chem. Soc. Chem. Commun.* p. 343 (1978).
24. C. W. Bradford, W. van Bronswijk, R. J. H. Clark, and R. S. Nyholm, *J. Chem. Soc., A* p. 2889 (1970).
25. P. Braunstein and J. Dehand, *Bull. Soc. Chim. Fr.* p. 1997 (1975).
26. P. Braunstein, J. Dehand, and J. F. Nennig, *J. Organomet. Chem.* **92**, 117 (1975).
27. M. I. Bruce, O. M. Abu Salah, R. E. Davis, and N. V. Raghovan, *J. Organomet. Chem.* **64**, c48 (1974).
28. M. I. Bruce, G. Shaw, and F. G. A. Stone, *J. Chem. Soc. Chem. Commun.* p. 1288 (1971).
29. M. I. Bruce, G. Shaw, and F. G. A. Stone, *J. Chem. Soc. Dalton Trans.* p. 1082 (1972).
30. M. I. Bruce, G. Shaw, and F. G. A. Stone, *J. Chem. Soc. Dalton Trans.* p. 1781 (1972).
31. K. Burger, L. Korecz, and G. Bor, *J. Inorg. Nucl. Chem.* **31**, 1527 (1969).
32. J. C. Burt, and G. Schmid, *J. Chem. Soc. Dalton Trans.* p. 1385 (1978).
33. G. A. Catton, G. F. C. Jones, M. J. Mays, and J. A. S. Howell, *Inorg. Chim. Acta* **20**, L41 (1976).
34. P. Chini, personal communication, 1978.
35. P. Chini, *Int. Congr. Pure Appl. Chem.*, 17th, 1959.
36. P. Chini, *Inorg. Chim. Acta Rev.* **2**, 31 (1968).
37. P. Chini, *Pure Appl. Chem.* **23**, 489 (1970).
38. P. Chini, A. Cavalieri, and S. Martinengo, *Coord. Chem. Rev.* **8**, 3 (1972).
39. P. Chini, L. Colli, and M. Peraldo, *Gazz. Chim. Ital.* **90**, 1005 (1960).
40. P. Chini and B. T. Heaton, *Top. Curr. Chem.* **71**, 1 (1977).
41. P. Chini, G. Longoni, and V. G. Albano, *Adv. Organomet. Chem.* **14**, 285 (1976).
42. P. Chini, S. Martinengo, and G. Longoni, *Gazz. Chim. Ital.* **105**, 203 (1975).
43. P. A. Christian, Ph.D. Thesis, Stanford University, 1978.
44. M. R. Churchill and R. Bau, *Inorg. Chem.* **6**, 2086 (1967).
45. M. R. Churchill and S. A. Beznar, *Inorg. Chem.* **13**, 1418 (1974).
46. M. R. Churchill and B. G. DeBoer, *Inorg. Chem.* **14**, 2630 (1975).
47. M. R. Churchill and F. J. Hollander, *Inorg. Chem.* **16**, 2493 (1977).
48. M. R. Churchill, F. J. Hollander, J. R. Shapley, and D. S. Foose, *J. Chem. Soc. Chem. Commun.* p. 534 (1978).
49. M. R. Churchill and M. V. Veidis, *J. Chem. Soc. Chem. Commun.* p. 529 (1970).
50. M. R. Churchill and M. V. Veidis, *J. Chem. Soc. Chem. Commun.* p. 1470 (1970).
51. M. R. Churchill and M. V. Veidis, *J. Chem. Soc., A*, p. 2170 (1971).
52. J. P. Collman, R. G. Finke, P. L. Matlock, R. Wahren, R. G. Komoto, and J. F. Brauman, *J. Am. Chem. Soc.* **100**, 1119 (1978).
53. C. G. Cooke and M. J. Mays, *J. Organomet. Chem.* **74**, 449 (1974).

54. C. G. Cooke, and M. J. Mays, *J. Chem. Soc. Dalton Trans.* p. 455 (1975).
55. F. A. Cotton, *Q. Rev. Chem. Soc.* **20**, 389 (1966).
56. F. A. Cotton, L. Kruczynski, B. L. Shapiro, and L. T. Johnson, *J. Am. Chem. Soc.* **94**, 6191 (1972).
57. M. D. Curtis and R. J. Klinger, *J. Organomet. Chem.* **161**, 23 (1978).
58. L. F. Dahl and D. L. Smith, *J. Am. Chem. Soc.* **84**, 2450 (1962).
59. J. Dehand and J. F. Nennig, *Inorg. Nucl. Chem. Lett.* **10**, 875 (1974).
60. J. Dehand and M. Pfeffer, *J. Organomet. Chem.* **104**, 377 (1976).
61. W. Ehrl and H. Vahrenkamp, *Chem. Ber.* **106**, 2556, 2563 (1973).
62. C. T. Enos, G. L. Geoffroy, and T. H. Risby, *J. Chromatogr. Sci.* **15**, 83 (1977).
63. R. Epstein and G. L. Geoffroy, unpublished observations.
64. R. A. Epstein, H. W. Withers, and G. L. Geoffroy, *Inorg. Chem.* **18**, 942 (1979).
65. H. Eshtiagh-Hosseini and J. F. Nixon, *J. Organomet. Chem.* **150**, 129 (1978).
66. G. O. Evans, J. P. Hargaden, and R. K. Sheline, *J. Chem. Soc. Chem. Commun.* p. 186 (1967).
67. L. J. Farrugia, J. A. K. Howard, P. Mitprachachon, J. L. Spencer, F. G. A. Stone, and P. Woodward, *J. Chem. Soc. Chem. Commun.* p. 260 (1978).
68. L. J. Farrugia, J. A. K. Howard, P. Mitprachachon, J. L. Spencer, F. G. A. Stone, and P. Woodward, to be published (1979).
69. W. Fellmann and H. D. Kaesz, *Inorg. Nucl. Chem. Lett.* **2**, 63 (1966).
70. R. P. Ferrari, G. A. Vaglio, and M. Valle, *J. Chem. Soc. Dalton Trans.* p. 1164 (1978).
71. J. Fischer, A. Mitschler, R. Weiss, J. Dehand, and J. F. Nennig, *J. Organomet. Chem.* **91**, c37 (1975).
72. P. C. Ford, R. G. Rinker, C. Ungermann, R. M. Laine, V. Landis, and S. A. Moya, *J. Am. Chem. Soc.* **100**, 4595 (1978).
73. A. Forster, B. F. G. Johnson, J. Lewis, T. W. Matheson, B. H. Robinson, and W. G. Jackson, *J. Chem. Soc. Chem. Commun.* p. 1042 (1974).
74. J. R. Fox, W. L. Gladfelter, G. L. Geoffroy, V. W. Day, S. Abdel-Meguid, and I. Tavanailpour, *J. Am. Chem. Soc.* to be submitted.
75. A. Fumagalli, S. Martinengo, P. Chini, A. Albinati, S. Bruckner, and B. T. Heaton, *J. Chem. Soc. Chem. Commun.* p. 195 (1978).
76. G. L. Geoffroy and R. A. Epstein, *Inorg. Chem.* **16**, 2795 (1977).
77. G. L. Geoffroy and W. L. Gladfelter, *J. Am. Chem. Soc.* **99**, 6775 (1977).
78. G. L. Geoffroy and W. L. Gladfelter, *J. Am. Chem. Soc.* **99**, 7565 (1977).
79. C. J. Gilmore and P. Woodward, *J. Chem. Soc., A* p. 3453 (1971).
80. W. L. Gladfelter, J. R. Fox, and G. L. Geoffroy, unpublished results.
81. W. L. Gladfelter, G. L. Geoffroy and J. Calabrese, *Inorg. Chem.* to be submitted (1979).
82. W. L. Gladfelter, J. A. Smeqal, T. A. Foreman, and G. L. Geoffroy, *J. Am. Chem. Soc.* to be submitted.
83. R. J. Haines, J. C. Burckett-St. Laurent, and C. R. Nolte, *J. Organomet. Chem.* **104**, c27 (1976).
84. R. J. Haines, R. Mason, J. A. Zubietta, and C. R. Nolte, *J. Chem. Soc. Chem. Commun.* p. 990 (1972).
85. H. J. Hausteine and K. E. Schwarzhans, *Z. Naturforsch. Teil B* **33**, 1108 (1978).
86. J. A. S. Howell, T. W. Matheson, and M. J. Mays, *J. Organomet. Chem.* **88**, 363 (1975).
87. A. T. T. Hsieh and J. Knight, *J. Organomet. Chem.* **26**, 125 (1971).
88. A. T. T. Hsieh and M. J. Mays, *J. Organomet. Chem.* **39**, 157 (1972).

89. B. T. Huie, C. B. Knobler, and H. D. Kaesz, *J. Am. Chem. Soc.* **100**, 3059 (1978).
90. A. P. Humphries and H. D. Kaesz, *Prog. Inorg. Chem.*, **25**, 145 (1979).
91. G. Huttner, A. Frank, and G. Mohr, *Z. Naturforsch. Teil B* **31**, 1161 (1976).
92. G. Huttner, G. Mohr, and A. Frank, *Angew. Chem. Int. Ed. Engl.* **15**, 682 (1976).
93. G. Huttner, G. Mohr, and P. Friedrick, *Z. Naturforsch. Teil B* **33**, 1254 (1978).
94. K. E. Inkrott and S. G. Shore, *J. Am. Chem. Soc.* **100**, 3954 (1978).
95. L. M. Jackman and F. A. Cotton, Eds., "Dynamic Nuclear Magnetic Resonance Spectroscopy," Academic Press, New York, 1975.
96. B. F. G. Johnson, R. D. Johnston, J. Lewis, I. G. Williams, and P. A. Kilty, *J. Chem. Soc. Chem. Commun.* p. 864 (1968).
97. B. F. G. Johnson, J. Lewis, and T. W. Matheson, *J. Chem. Soc. Chem. Commun.* p. 441 (1974).
98. B. F. G. Johnson, J. Lewis, B. Reichert, K. T. Schorpp, and G. M. Sheldrick, *J. Chem. Soc. Dalton Trans.* p. 1417 (1977).
99. S. A. Khattab, L. Marko, G. Bor, and B. Marko, *J. Organomet. Chem.* **1**, 373 (1964).
100. R. B. King *Prog. Inorg. Chem.* **15**, 287 (1972).
101. J. Knight and M. J. Mays, *Chem. Ind. (London)* p. 1159 (1968).
102. J. Knight and M. J. Mays, *J. Chem. Soc., A* p. 654 (1970).
103. J. Knight and M. J. Mays, *J. Chem. Soc., A* p. 711 (1970).
104. J. Knight and M. J. Mays, *J. Chem. Soc. Chem. Commun.* p. 1006 (1970).
105. J. Knight and M. J. Mays, *J. Chem. Soc. Chem. Commun.* p. 62 (1971).
106. J. Knight and M. J. Mays, *J. Chem. Soc. Dalton Trans.* p. 1022 (1972).
107. S. A. R. Knox, J. W. Koepke, M. A. Andrews, and H. D. Kaesz, *J. Am. Chem. Soc.* **97**, 3942 (1975).
108. D. Labroue and R. Poilblanc, *J. Mol. Catal.* **2**, 329 (1977).
109. M. W. Lindauer, G. O. Evans, and R. K. Sheline, *Inorg. Chem.* **7**, 1249 (1968).
110. G. Longoni and M. Manassero, *Eur. Inorg. Chem. Symp.*, 3rd, 1978.
111. G. Longoni and M. Manassero, unpublished results (communicated by P. Chini).
112. S. Martinengo and P. Chini, *Gazz. Chim. Ital.* **102**, 344 (1972).
113. S. Martinengo, P. Chini, V. G. Albano, F. Cariati, and T. Salvatori, *J. Organomet. Chem.* **59**, 379 (1973).
114. R. Mason and J. A. Zubieta, *J. Organomet. Chem.* **66**, 279 (1974).
115. R. Mason, J. Zubieta, A. T. T. Hsieh, J. Knight, and M. J. Mays, *J. Chem. Soc. Chem. Commun.* p. 200 (1972).
116. M. J. Mays and R. N. F. Simpson, *J. Chem. Soc., A* p. 1444 (1968).
117. J. L. Meyer and R. E. McCarley, *Inorg. Chem.* **17**, 1867 (1978).
118. L. Milone, personal communication, 1978.
119. L. Milone, S. Aime, E. W. Randall, and E. Rosenberg, *J. Chem. Soc. Chem. Commun.* p. 452 (1975).
120. A. Modinos and P. Woodward, *J. Chem. Soc. Dalton Trans.* p. 1534 (1975).
121. J. R. Moss and W. A. G. Graham, *J. Organomet. Chem.* **23**, c23 (1970).
122. J. R. Moss and W. A. G. Graham, *Inorg. Chem.* **16**, 75 (1977).
123. E. L. Muetterties, *Bull. Soc. Chim. Belg.* **84**, 959 (1975).
124. E. L. Muetterties, *Science* **196**, 839 (1977).
125. E. L. Muetterties, T. N. Rhodin, E. Band, C. F. Brucker, and W. R. Pretzer, in press.
126. J. Newman and A. R. Manning, *J. Chem. Soc. Dalton Trans.* p. 2549 (1974).
127. G. A. Ozin, *Catal. Rev.-Sci. Eng.* **16**, 191 (1977).
128. R. G. Pearson and J. Dehand, *J. Organomet. Chem.* **16**, 485 (1969).
129. C. U. Pittman, Jr., and R. C. Ryan, *Chem. Tech.* p. 170 (1978).

130. V. Raverdino, S. Aime, L. Milone, and E. Sappa, *Inorg. Chim. Acta* **30**, 9 (1978).
131. P. Renaut, G. Tainturier, and B. Gautheron, *J. Organomet. Chem.* **150**, c9 (1978).
132. F. Richter and H. Vahrenkamp, *Angew. Chem. Int. Ed. Engl.* **17**, 444 (1978).
133. R. Rossetti, G. Gervasio, and P. L. Stanghellini, *J. Chem. Soc. Dalton Trans.* p. 222 (1978).
134. J. K. Ruff, R. P. White, Jr., and L. F. Dahl, *J. Am. Chem. Soc.* **93**, 2159 (1971).
135. H. Schafer and B. Spreckelmeyer, *J. Less-Common Met.* **11**, 73 (1966).
136. G. Schmid, *Angew. Chem. Int. Ed. Engl.* **17**, 392 (1978).
137. G. Schmid, K. Bartl, and R. Boese, *Z. Naturforsch. Teil B* **32**, 1277 (1977).
138. G. Schmid, V. Batzel, and B. Stutte, *J. Organomet. Chem.* **113**, 67 (1976).
139. G. Schmid, B. Stutte, and R. Boese, *Chem. Ber.* **111**, 1239 (1978).
140. K. E. Schwarzahns and H. Steiger, *Angew. Chem. Int. Ed. Engl.* **11**, 535 (1972).
141. J. R. Shapley, *Strem Chem.* **6**, 3 (1978).
142. J. R. Shapley, personal communication, 1978. The compound originally formulated as $\text{HReOs}_3(\text{CO})_{15}$ in ref. (143) was shown to be $\text{HReOs}_3(\text{CO})_{15}(\text{CH}_3\text{CN})$.
143. J. R. Shapley, G. A. Pearson, and D. S. Foose, *Abstr. Pap. Am. Chem. Soc. Meet.* **175**, INORG. 74 (1978).
144. J. R. Shapley, G. A. Pearson, M. Tachikawa, G. Schmidt, M. R. Churchill, and F. J. Hollander, *J. Am. Chem. Soc.* **99**, 8064 (1977).
145. A. K. Smith and J. M. Basset, *J. Mol. Catal.* **2**, 229 (1977).
146. B. Soltmann, C. C. Smeley, and J. F. Holland, *Anal. Chem.* **49**, 1164 (1977).
147. P. C. Steinhardt, W. L. Gladfelter, and G. L. Geoffroy, *Inorg. Chem.*, in press.
148. D. L. Stevenson, C. H. Wei, and L. F. Dahl, *J. Am. Chem. Soc.* **93**, 6027 (1971).
149. F. G. A. Stone, personal communication, 1978.
150. F. G. A. Stone and S. H. H. Chaston, *Int. Coord. Chem. Conf.*, 11th, (1968).
151. C. E. Strouse and L. F. Dahl, *J. Am. Chem. Soc.* **93**, 6032 (1971).
152. B. Stutte, V. Batzel, R. Boese, and G. Schmid, *Chem. Ber.* **111**, 1603 (1978).
153. R. G. Teller, R. D. Wilson, R. K. McMullan, T. Koetzel, and R. Bau, *J. Am. Chem. Soc.* **100**, 3071 (1978).
154. B. K. Teo, Ph.D. Thesis, University of Wisconsin, Madison, Wis., 1974.
155. J. F. Tilney-Bassett, *J. Chem. Soc.* p. 4784 (1963).
156. D. R. Tyler, R. A. Levenson, and H. B. Gray, *J. Am. Chem. Soc.* **100**, 7888 (1978).
157. V. A. Uchtman and L. F. Dahl, *J. Am. Chem. Soc.* **91**, 3763 (1969).
158. P. J. Vergamini, H. Vahrenkamp, and L. F. Dahl, *J. Am. Chem. Soc.* **93**, 6326 (1971).
159. K. Wade, *Adv. Inorg. Chem. Radiochem.* **18**, 1 (1976).
160. I. Wender and P. Pino, "Organic Synthesis via Metal Carbonyls," Vol. 1. Wiley (Interscience), New York, 1968.
161. D. B. W. Yawney and F. G. A. Stone, *J. Chem. Soc., A* p. 502 (1969).

This Page Intentionally Left Blank

Trends in Organosilicon Biological Research

RALPH J. FESSENDEN and JOAN S. FESSENDEN

Department of Chemistry
University of Montana
Missoula, Montana

I. Introduction	275
II. Silicon Derivatives of Known Active Compounds	276
A. Introduction	276
B. Silyl Groups as Space-Filling Groups	281
C. Trimethylsiloxy Derivatives	282
D. Silylated Steroids	283
E. Silyl and Siloxy Alkylamines	285
F. Silylated Benzhydryl Ethers	286
III. Silicon Biological Agents without Carbon Analogy	288
A. Introduction	288
B. Siloxanes	288
C. Silatranes	291
IV. Detoxification and Elimination of Silicon Compounds	294
V. Summary	295
References	296

I

INTRODUCTION

The number of studies of organosilicon compounds as potential medicinal and biological agents has expanded rapidly in recent years. In this article, the trends taken by these investigations are discussed. For more comprehensive coverage, the reader is referred to a number of recent reviews (1-12).

The general pattern of research into the biological effects of organosilicon compounds may be categorized into three major divisions: (a) polymeric material with (or, of more importance, without) biological action, (b) silicon derivatives of known active compounds, and (c) biologically active silicon compounds that do not have known carbon counterparts. This review will deal primarily with (b) and (c), the search for biologically active organosilicon compounds.

Next to oxygen, silicon is the most common element in the earth's crust. Many primitive plants and animals, such as horsetails (*Equisetum*), diatoms, and some sponges, use silicates as part of their skeletal com-

ponents, much as mammals use calcium compounds. Many higher plants, such as certain grains and conifers, also require silicates for normal growth. Until recently, it was thought that silicon compounds play no role in the biochemistry of the higher animals. Recent research, however, indicates that traces of silicates may be of importance in growth and reproduction. It has been reported that the presence of silicon compounds alters calcium metabolism (10).

As far as we know, the incorporation of silicon into organisms involves silicon compounds in which each silicon atom is bonded to four oxygen atoms, as inorganic silicates or as silicate esters of such organic compounds as acid mucopolysaccharides and polyuronides (13). With the possible exception of certain bacteria, organosilicon compounds containing the Si—C bond have not been found in living systems. For this reason, it might be expected that the incorporation of a silicon atom into an organic biological agent would render the agent toxic. This is indeed the case with most metals; for example, organometallics containing mercury or arsenic are poisonous. However, the fact that an organic compound contains a silicon atom does not necessarily result in toxicity; many organosilicon compounds are devoid of all pharmacological activity. On the other hand, some organosilicon compounds are extremely active. It is therefore concluded that the silicon atom per se does not impart biological activity to a compound, but rather the unique shape and polarity of the compound are usually the important factors.

II

SILICON DERIVATIVES OF KNOWN ACTIVE COMPOUNDS

A. Introduction

There is a growing body of literature dealing with the pharmacology of organosilicon derivatives of known active compounds. Table I summarizes the results of many of the synthetic and pharmacological studies of silicon derivatives of biologically active compounds. Unfortunately, many potentially active silicon derivatives have been synthesized, but have never been subjected to extensive pharmacological testing. Some of these compounds have not been tested at all. Even in the reports in which pharmacological data are provided, it is unusual to find direct experimental comparisons of a carbon compound and its silicon analog. Thus, conclusions concerning the biological effects of silicon substitution must often be made on scanty data.

A silicon derivative of a biologically active organic compound usually shows an activity equal to, or (more commonly) less than, that of the parent compound. This is not a surprising observation. Compounds selected for derivatization have been widely used as drugs. Such compounds usually represent an optimization of structure in terms of absorption, biotransport, ability to fit onto an active site, and detoxification. Placement of a silicon atom or a silyl group in such an optimized structure would be very unlikely to increase or even maintain the original activity. One example of an exception to this generalization is ethylmethylbis-(hydroxymethylcarbamoyl)silane (1), which has a greater sedative activity than its carbon counterpart (22). However, the carbon compound does not constitute the most active compound in its class.



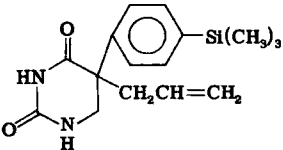
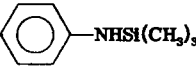
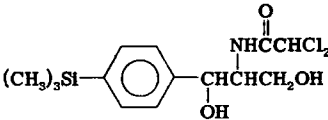
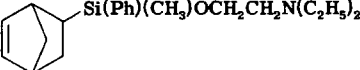
(1)

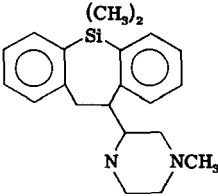
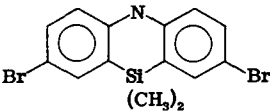
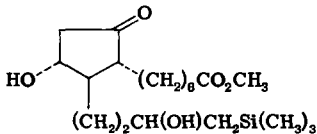
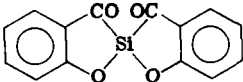
The pharmacological activity of a silicon-containing drug is often short-lived compared to that of the parent drug. This could be due either to a greater ease of metabolism, which appears to be the case with the meprobamates (32), or to a greater ease of hydrolysis, as is reported for the benzhydryl ethers (33). Silicon derivatives of drugs may find practical use in situations where a short duration of drug activity is desired.

Most of the silyl derivatives of biologically active compounds can be classed either as compounds having a silyl moiety substituted *onto* the parent skeleton or as compounds having a silicon atom *instead of* one of the atoms of the parent structure. In either type of derivatization, examples for study must be chosen carefully because Si—H and Si—N bonds are substantially more reactive than C—H and C—N bonds. The Si—C bond and, to a lesser extent, the Si—O bond are biologically stable. For these reasons, a SiH₃ group would not normally be substituted for a CH₃ group or an NH₃⁺ group. Instead, the more bulky Si(CH₃)₃ group would usually be used. To avoid changes in biological activity that arise simply because of the bulk of the trimethylsilyl group, active compounds that contain a carbon or nitrogen atom bonded only to carbon and oxygen atoms are frequently chosen as parent compounds. Examples of compounds in which a silicon atom has been substituted directly for such a carbon or nitrogen atom are shown in Table II.

Substitution of a silicon atom for another atom in a biologically active compound should provide clues to structure-activity relationships. The structural and electronic effects of silicon substitution are, to a reasonable extent, predictable. For example, substitution of a silicon atom for a carbon atom places a slightly larger, more electropositive, atom in the

TABLE I
CLASSES OF BIOLOGICALLY ACTIVE ORGANIC COMPOUNDS AND THEIR ORGANOSILICON DERIVATIVES

Compound or class	General type of activity	Typical organosilicon derivative	Reference
Acetylcholine	Cholinergic	$\text{CH}_3\text{CO}_2\text{CH}_2\text{CH}_2\text{Si}(\text{CH}_3)_3$	14
Barbiturates	Hypnotic		15
Benzhydryl ethers	Anti-Parkinson, antihistamine	$\text{Ph}_2\text{Si}(\text{CH}_3)\text{OCH}_2\text{CH}_2\text{N}(\text{CH}_3)_2$	16
Benzocaine	Local anesthetic	$\text{C}_2\text{H}_5\text{O}_2\text{C}-$ 	17
Carbachol	Cholinergic	$\text{NH}_2\text{C}(=\text{O})\text{CH}_2\text{CH}_2\text{Si}(\text{CH}_3)_3$	18
Chloramphenicol	Antibiotic		19
Ciclonium bromide	Antispasmodic		20

	Curare-like	Ganglion blocker	$(\text{CH}_3)_3\text{N}^+\text{CH}_2\text{CH}_2\text{CH}_2\text{Si}(\text{CH}_3)_2\text{OSi}(\text{CH}_3)_2\text{CH}_2\text{CH}_2\text{CH}_2\text{N}^+(\text{CH}_3)_3$	21
	Meprobamate	Muscle relaxant	$\text{C}_3\text{H}_7\text{Si}(\text{CH}_3)(\text{CH}_2\text{OCONH}_2)_2$	22
	Perathiepin	Psychotropic agent		23
279	Phenothiazine	Psychotropic agent		24
	Prostaglandins	—		25,26
	Salicylic acid	Analgesic		27

Continued

TABLE I (Continued)

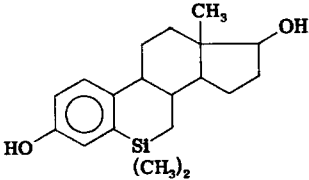
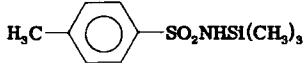
Compound or class	General type of activity	Typical organosilicon derivative	Reference
Steroids	Estrogenic		28,29
Sulfonamides	Bacteriostatic		30,31

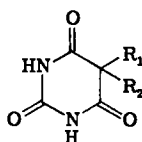
TABLE II
SELECTED DIRECT SILICON ANALOGS OF KNOWN DRUGS

Parent drug	General structure	Z	Reference
Acetylcholine	$\text{CH}_3\text{CO}_2\text{CH}_2\text{CH}_2\text{Z}(\text{CH}_3)_3$	$\text{N}^+, \text{C}, \text{Si}$	14
Carbachol	$\text{H}_2\text{NCO}_2\text{CH}_2\text{CH}_2\text{Z}(\text{CH}_3)_3$	$\text{N}^+, \text{C}, \text{Si}$	18
Meprobamate	$\text{C}_3\text{H}_7\text{Z}(\text{CH}_3)(\text{CH}_2\text{OCONH}_2)_2$	C, Si	22
Benzhydryl ether	$\text{Ph}_2\text{Z}(\text{CH}_3)\text{OCH}_2\text{CH}_2\text{N}(\text{C}_2\text{H}_5)_2$	C, Si	34
Phenylglycine ester	$\begin{array}{c} \text{NH}_3\text{Cl} \\ \\ \text{PhCHCO}_2(\text{CH}_3)_3\text{Z}(\text{CH}_3)_3 \end{array}$	C, Si	35

structure. The result is a compound that usually has similar, but slightly different, physical and chemical properties. Some of these differences can be measured quantitatively (for example, partition coefficients; cf. Section II,B). To date, there have been no reported studies in which a silicon atom was used to help in the determination of the structure-activity relationships of a class of drugs.

B. Silyl Groups as Space-Filling Groups

Biologically active organic compounds contain both functional and space-filling groups. Both are usually necessary in order to impart activity. Much synthetic work in medicinal chemistry revolves around varying the parameters of the space-filling portion of a molecule. The space-filling group is often a straight-chain or branched alkyl group. This group probably provides hydrophobic character as well as a particular shape that allows the molecule to fit onto the active site. A pattern of increasing biological activity with increasing chain length, followed by decreasing activity after a "cut-off" point, is very common. The barbiturates (2) provide a classic example. The parent of the class, barbituric acid (R_1 and $\text{R}_2 = \text{H}$), has no sedative activity. As the sizes of R_1 and R_2 are increased, sedative activity increases to a maximum, then decreases.



Barbiturate
(2)

Silyl groups, which tend to increase lipid solubility, may be used as a substitute for alkyl branching in space-filling groups. Direct substitution of a silicon atom for a carbon atom increases the hydrophobic character of a compound, even without the addition of more alkyl groups. Table III lists the relative partition coefficients of two pairs of carbon and silicon compounds in octanol-water, a system used to approximate the lipid-water system within an organism. As may be seen from the table, the silicon compounds are two to five times more soluble in the octanol phase; this effect falls off with an increasing number of carbon atoms in the parent structure (36).

On considering these data, it would be expected that silyl groups would increase biological activity requiring enhanced lipid solubility. The silyl group should be especially useful when increase in the length of a carbon chain will not impart the desired characteristics. To date, there is no report in which such a case has been specifically identified, although this would appear to be an interesting facet of organosilicon biological agents. Table IV lists a few compounds in which the silyl group appears to act only as a hydrophobic, space-filling group.

C. Trimethylsiloxy Derivatives

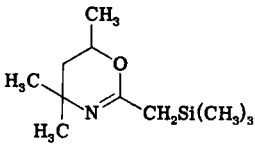
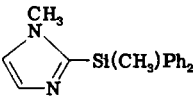
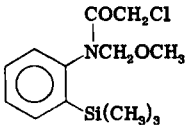
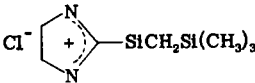
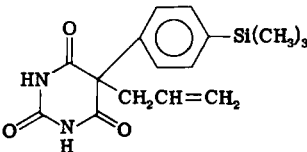
Trimethylsiloxylation is extensively used for analytical purposes; however, only a few siloxy derivatives have been characterized and subjected to pharmacological testing. The inclusion of a trimethylsiloxy group $(\text{CH}_3)_3\text{SiO}-$ would be expected to increase the lipid solubility of a drug and thus to alter its transport and distribution within an organism. The silicon-oxygen bond can be hydrolyzed under physiological conditions; therefore, it would also be expected that the activity of a siloxy compound would arise from the parent drug, which would be released *in vivo*. There

TABLE III
PARTITION COEFFICIENTS OF SOME CARBON AND
SILICON COMPOUNDS IN OCTANOL-WATER^a

Compound	Partition coefficient
$\text{PhC}(\text{CH}_3)_3$	1.0×10^4
$\text{PhSi}(\text{CH}_3)_3$	5.1×10^4
$\text{PhCH}(\text{CH}_3)_2$	4.6×10^3
$\text{PhSiH}(\text{CH}_3)_2$	9.8×10^3

^a See reference (36).

TABLE IV
SELECTED ACTIVE COMPOUNDS CONTAINING SILYL SPACE-FILLING GROUPS

Structure	Activity	References
	Active against peptic ulcers	37
	Sedative-hypnotic	38
	Herbicide	39
	Anti-inflammatory, analgesic	40
	Sedative	15
$(\text{CH}_3)_3\text{SiCH}_2\text{CH}_2\text{CH}_2\text{ONO}_2$	Coronary dilator	41

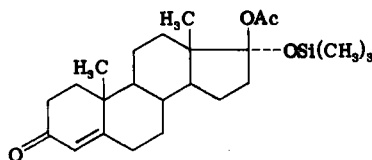
is no indication in the literature that siloxylation alters the principal action of a drug (25-27, 42-48).

D. Silylated Steroids

Silylated steroids, especially steroids having sex-hormone activity, have been the subject of numerous investigations. There has been no comprehensive investigation of the general effects of silylation of steroids. From the activity noted for the sex hormones, such a study is probably warranted.

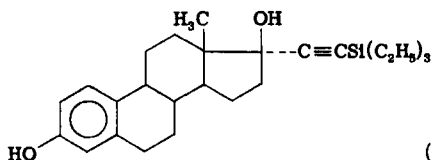
1. Silyl Groups Attached to a Steroid Ring

Steroids having trimethylsiloxy groups attached to one of the rings have been reported. Although silylation of a hydroxyl group enhances lipid solubility, the silylation appears not to alter the activity of the steroid to any great extent. Compound 3, for example, has an activity equal to or less than that of progesterone when injected, but it has the same oral activity as pregnin (46).

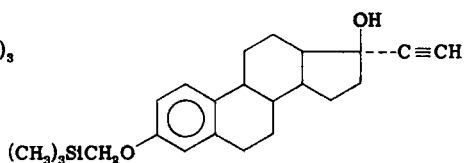


(3)

Although the silicon-oxygen bond is hydrolytically unstable, the silicon-carbon bond is stable toward hydrolysis (but not necessarily stable toward metabolic hydrolysis). It might be anticipated that a carbon-silylated compound would show less activity than the parent compound. However, compound 4 has four times the antifertility activity and 75% of the estrogenic activity of its carbon analog ethynylestradiol (49). Similar results have been reported for a (trimethylsilyl)methyl ether (5) of ethynylestradiol, which is reported to have estrogenic activity (50). These observations suggest that the side-chain space-filling requirements of this steroid have not yet been optimized.



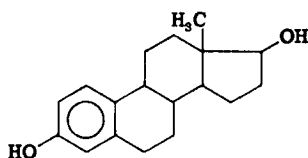
(4)



(5)

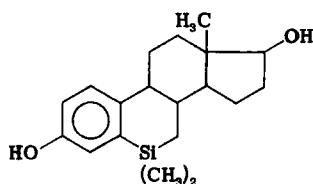
2. Silyl Groups within a Steroid Ring

From a synthetic standpoint, the most interesting silylated steroids are those having silicon substituted for one of the carbon atoms of a ring. Only one such system has been reported, that of the 6-silasteroids. A number of these compounds, for example 7, have been screened for estrogenic, antiestrogenic, and postcoital antifertility effects; but no significant activity was noted (29).



Estradiol

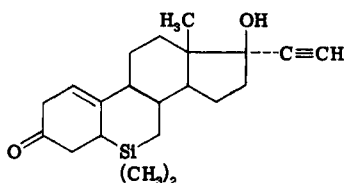
(6)



6-Sila counterpart

(7)

Using X-ray crystallographic techniques, McPhail and Miller determined that the normal conformation of the A/B ring juncture in **8** is significantly altered by the presence of the silicon atom (51). Presumably, this alteration in stereochemistry, along with the bulk of the *gem*-dimethyl grouping (not found in active estrogens), is sufficient to cause loss of hormonal activity.



(8)

E. Silyl and Siloxy Alkylamines

In general, organic amines exhibit pharmacological activity. Organosilicon compounds containing amino groups are no exception. In fact, one of the first organosilicon compounds reported to have an abnormally high toxicity was a δ -silylalkylamine (**9**) (52).

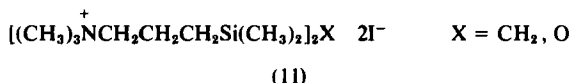


(9)

A variety of silylated alkylamines showing a wide diversity of biological activity have been studied. For example, a series of silylated amines is reported to have long-term insect-repellent activity (up to 30 days); compound **10** is typical of the group (53). Silylalkylamines having quaternary ammonium groups, such as **11**, have been reported to have curare-like activity (54).

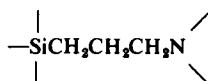


(10)



Other investigators report silylated amines having antimicrobial (55–57), anticoagulant (58), spasmolytic (35), psychotropic (59), anti-inflammatory, analgesic, sedative, and hypnotic activity, as well as utility in the treatment of peptic ulcers (37). Voronkov reviewed many of these studies (2, 4, 10).

Because of the wide spectrum of activity shown by amines, definitive conclusions concerning structure–activity relationships cannot be made at this time. However, studies using single test systems reveal that the most active silylated amines contain the silicon atom in a γ position relative to the nitrogen, as shown in partial structures 12 and 13 (55, 56). Some examples of compounds containing these groupings are found in Tables I and II. The silylated benzhydryl ethers (Section II,F) and silatranes (Section III,C) also contain this type of grouping.

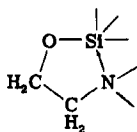


(12)



(13)

The activity of these particular groupings probably arises in part from the distance between the nitrogen atom and the hydrocarbon branch (at the silicon atom). A similar structure–activity relationship has also been noted in carbon systems (60). However, the silicon–nitrogen system may assume a cyclic conformation in which the unshared electrons of the nitrogen are coordinated with the d orbitals of the silicon atom (14). The potential for such a structural feature does not exist in most carbon systems. Silicon-to-nitrogen coordination is an important feature of the silatranes (61, 62), although physical evidence for such coordination in open-chain silylalkylamines is lacking (52).

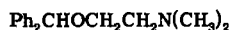


(14)

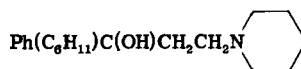
F. Silylated Benzhydryl Ethers

The benzhydryl ethers constitute a class of drugs that exhibit antihistamine activity and also find use in the treatment of tremors characteristic

of Parkinson's syndrome. The parent compound of the class is diphenhydramine (**15**), an antihistamine. The benzhydryl group has been the subject of extensive investigation, and useful activity is found even in such distant congeners as trihexylphenidyl (**16**), an antitremor agent (**63**).



Diphenhydramine
(15)



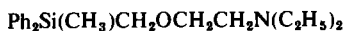
Trihexylphenidyl
(16)

The synthesis and pharmacological testing of the silicon analogs of benzhydryl ethers have been the subject of a number of investigations (**16**, **20**, **33**, **64**). In most cases, the benzyl carbon atom is replaced by a silicon atom. (Because of the relative instability of the Si—H bond, the SiCH₃ group replaces the benzyl CH group.) In general, such silicon compounds as **17** possess the same type of biological activity as their carbon counterparts; however, they are generally less active and shorter-acting. The toxicities of the silylated drugs (LD₅₀ ~ 150 mg/kg) are equivalent to that of **16**, which is used clinically as an antitremor agent in Parkinson's syndrome. However, doses of 32–50 mg/kg of the silicon compounds are required to inhibit tremorine-induced tremors for 1 hour, and almost-toxic doses are required to block the tremors completely (**34**).



(17)

Silicon analogs that are not readily hydrolyzed (that is, that contain no SiO bond), such as **18** and **19**, also show antitremor activity, but to a lesser extent. Doses of 20–40 mg/kg resulted in 0–8% inhibition after 1 hour, compared to 60% inhibition by **16** at a dose of only 10 mg/kg (**65**).



(18)



(19)

Silylated benzhydryl ethers containing a quaternary nitrogen atom, such as **20**, are reported to be anticholinergic agents of short duration (**66**).



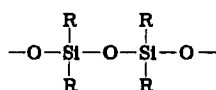
(20)

III

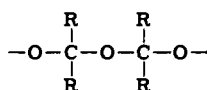
SILICON BIOLOGICAL AGENTS WITHOUT CARBON ANALOGY

A. Introduction

One of the most exciting areas of organometallic research today is that of organosilicon biological agents that do not have carbon analogs. Because of the unique characteristics of the silicon atom, it is possible to synthesize organosilicon compounds whose carbon counterparts are chemically unstable. The classical case is that of the polysiloxanes and cyclosiloxanes. The carbon analogs of this class of compounds would be polymeric or oligomeric ketals. Polysiloxanes (21) are stable, whereas polyketals (22) are quite fragile.

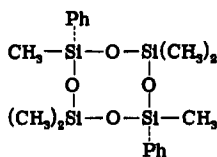


Polysiloxane
(21)

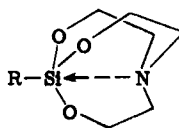


Polyketal
(22)

Two major classes of organosilicon compounds having unique biological activity have been discovered in recent years: phenylsiloxanes, such as *cis*-2,6-diphenylhexamethylcyclotetrasiloxane (23), which shows estrogenic activity; and the silatrane (24), which exhibit wide-ranging biological effects, depending on the structure of the R group.



Phenylcyclotetrasiloxane
(23)



Silatrane
(24)

B. Siloxanes

Most polysiloxanes and cyclosiloxanes possess no biological activity. Up into the late 1960s, it was assumed that *all* polysiloxane fluids were biologically inert. At that time, the totally unanticipated discovery at Dow Corning Corporation in the United States that some phenyl-con-

taining polysiloxanes possess potent estrogenic activity totally altered that view. Because silicone fluids are used extensively in industry, as well as in cosmetics and food processing, this observation caused great concern within the industry. Many silicone fluids were investigated by workers within and outside of those firms most affected by the discovery. The conclusions of these investigators are that a phenyl group is needed for activity, and that the dimethylpolysiloxane fluids are bland (67-69); however, the search for potentially detrimental (or useful) effects of polysiloxanes continues.

1. *Biological Effects of cis-2,6-Diphenylhexamethylcyclotetrasiloxane (23)*

Of all the siloxanes studied, compound **23** has the greatest biological activity. Although its toxicity is low ($LD_{50} > 5000$ mg/kg), **23** has potent hormone-like activity similar to that of such known estrogens as estradiol benzoate. Administration of **23** to rats, mice, rabbits, rhesus monkeys, and dogs results in marked changes in the genital organs. This action is species-dependent. Guinea pigs do not show the same response.

When 0.1-10 mg/kg of **23** is administered to a male animal, either as a single oral dose or over a period of time (2-20 days), blood testosterone levels drop, and atrophy of the testes, prostate, and epididymis is observed. Sperm death also occurs (70-73). In beagle dogs, the ability to ejaculate is also impaired (73). In the female, compound **23** causes hypertrophy of the uterus lining and dilation of the uterine glands, as well as disruption of the estral cycle. When given to pregnant females, **23** causes loss of the fetus, especially if administered prior to implantation of the fertilized ovum (74-76). This compound has been patented as an antifertility agent (77, 78).

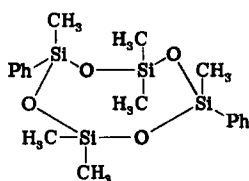
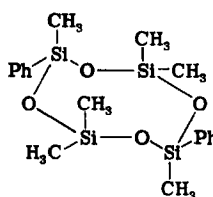
Bennett and Le Vier reported that **23** also increases the dopamine content of the brain; thus it has possible use in the treatment of Parkinson's syndrome (79). Because of its effect in decreasing the size of the prostate gland, the compound also may have value in the treatment of prostate cancer (80).

2. *Structure and Biological Activity*

The unique hormonal activity of siloxanes is limited to methylaryl-substituted, linear di- and trisiloxanes and cyclic tri- and tetrasiloxanes (67, 75, 76, 81). In general, at least one arylsilicon grouping is necessary for activity. The substitution of an alkyl group for a phenyl group either decreases the activity markedly or eliminates it entirely. Cyclosiloxanes

are more active than linear siloxanes, and cyclotetrasiloxanes are more active than cyclotrisiloxanes. Of the cyclotrisiloxanes, only the *trans*-2,4-diphenyl isomer is active; the *cis* isomer is devoid of activity. Cyclopentasiloxanes are inactive. Figure 1 lists some siloxanes and cyclosiloxanes that exhibit estrogenic activity.

The conformations of both *cis*- and *trans*-**23** have been studied. The eight-membered ring of the more active *cis* isomer is in a boat conformation, whereas the *trans* isomer has a chair conformation (82) (see Fig. 2). In both conformations, the phenyl groups are projected in equatorial positions.

*cis*-(23)*trans*-(23)

Why *cis*-**23** elicits a biological response similar to that of a steroid is not known, although some preliminary studies indicated that the response

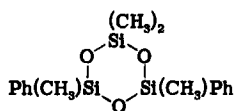
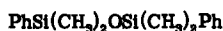
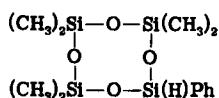
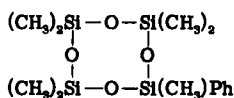
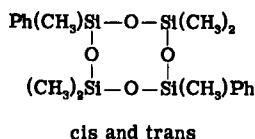
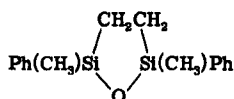
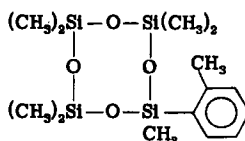
*cis* and *trans*

FIG. 1. Some siloxanes having estrogenic activity. For more complete listings, including inactive siloxanes, see Refs. (76) and (81).

arises from antigonadotropic activity of the siloxane (which is partly concentrated in the pituitary gland) and also to direct antiandrogenic activity (70, 83).

Besides the estrogenic activity of some phenylsiloxanes, otherwise-inert siloxane polymers can act as "holders" for other active groups. For example, a polymer containing quaternary ammonium groups and sulfonate or sulfate surfactant groups can be applied to a glass surface; the treated surface is rendered permanently bacteriostatic and fungistatic. Aquarium systems with filters containing a similar polymer remain free of algae (84). A more recent report deals with anticoagulant activity of heparin-containing silicone polymers (85). These effects probably have little to do with the siloxane structure, but are due to the attached active groups.

C. Silatranes

Another promising area of research in organosilicon biological chemistry is that of the silatranes (24), which are siloxyalkylamines having the structure of a three-winged cage. These compounds show a wide range of toxicity in mammals and a variety of biological activities. Arylsilatranes ($R = \text{aryl}$), for example, are extremely toxic substances, with LD_{50} values of 0.1–10 mg/kg, whereas alkoxysilatranes ($R = \text{alkoxy}$) are reported to be virtually nontoxic (2).

1. Toxicity

Silatrane itself ($R = H$) has an LD_{50} of ~ 100 mg/kg. In general, the aryl- and thienylsilatranes are more toxic, and the alkyl-, alkenyl-, and alkoxysilatranes are less toxic. It was reported that there is a direct relationship between the toxicity and the rate of hydrolysis of the silicon-oxygen bonds, a more rapidly hydrolyzed silatrane being less toxic (86).

The extreme toxicity of the arylsilatranes has found practical application. (*p*-Chlorophenyl)silatrane has been marketed in the United States as a rat poison. This compound has the dual advantages of not being dermally absorbed by humans and of being rapidly deactivated *in vivo*, so that the dead rats are not toxic (7, 87).

2. Sublethal Activity

Toxicity is an important biological test and is also a signpost that other types of activity will be noted for the toxic compound at sublethal levels.

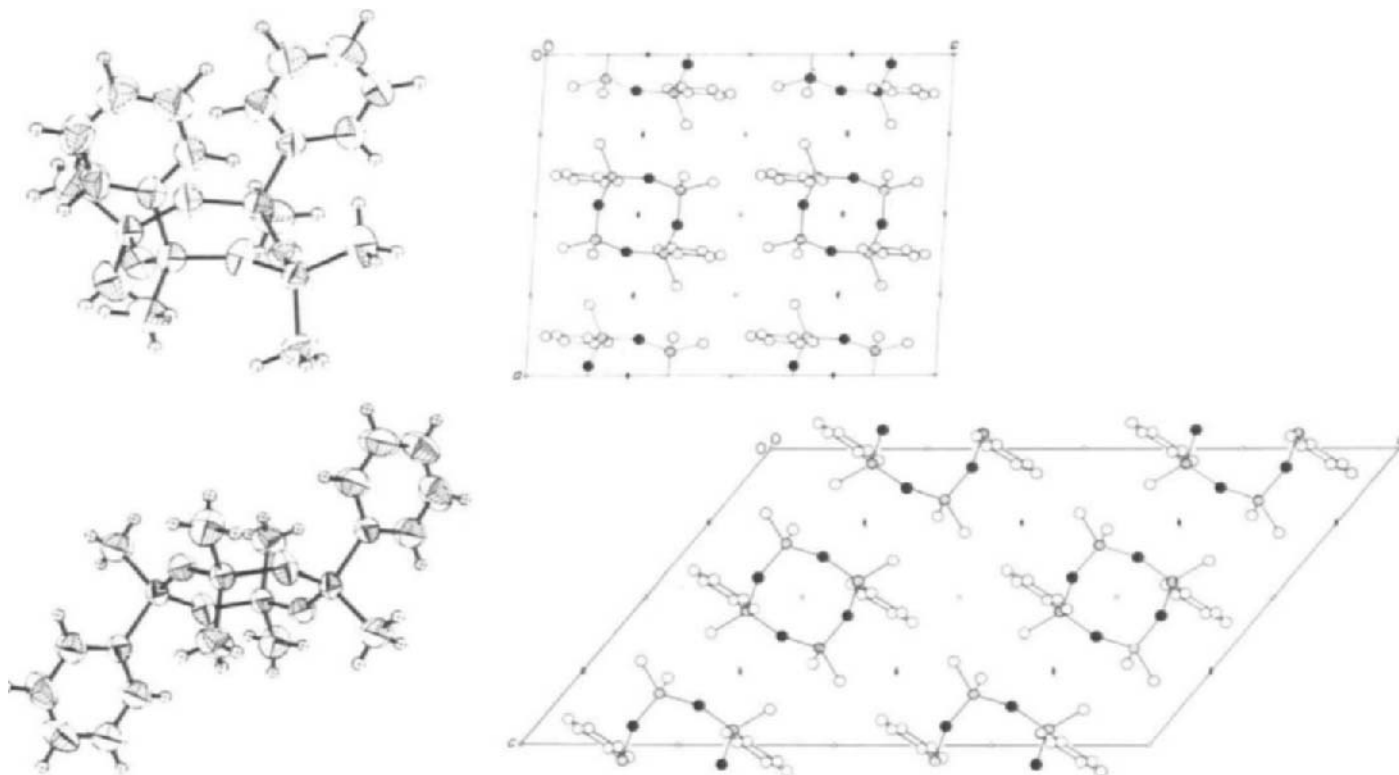


FIG. 2. Above: ORTEP plot showing configuration (right) and packing diagram (left) for *cis*-2,6-diphenylhexamethylcyclotetrasiloxane. Below: Similar diagrams for *trans*-2,6-diphenylhexamethylcyclotetrasiloxane. In the ORTEP plots, thermal ellipsoids are scaled to 50% probability, and hydrogen atoms are indicated by equally large spheres. The packing diagrams are both projections along the *b* axis of the crystals. The black, dotted, and open circles represent O, Si, and C, respectively. Reprinted with permission from M. Söderholm and D. Carlström, *Acta Chem. Scand. Ser. B* 31, 193 (1977).

Of more potential medicinal interest are those members of a class of compounds that are nontoxic, yet still possess potent activity. Of the silatranes, two nonaryl and nontoxic members have attracted considerable attention: chloromethylsilatrane ($R = ClCH_2-$), also referred to in the literature as *mival*, and ethoxysilatrane ($R = C_2H_5O-$), also called *migugen*.

The diverse biological effects of these two compounds have been investigated extensively by Voronkov and co-workers at the Irkutsk Institute of Organic Chemistry of the USSR. It was reported that these silatranes promote the healing of burns and wounds, growth of hair and fur, egg production in hens, growth of chicks (as well as of male rats and male lambs), and silkworm production (88-95). In addition, ethoxysilatrane (as well as other silatranes) is reported to have potent anticancer activity, especially in conjunction with other chemotherapeutic agents (7, 96). Table V surveys the toxicities and biological activities of some silatranes. Voronkov has reviewed the earlier work on silatranes (2, 4, 7, 8, 10, 97).

It is considered that the activity of these silatranes is due to stimulation of protein synthesis (especially collagen) within the cells. Indeed, studies

TABLE V
ACTIVITY OF SELECTED SILATRANES

Silatrane	LD ₅₀ (mg/kg)	Biological effects	References
Unsubstituted	100	—	10,86
Aryl			
Phenyl	0.33	Analeptic ^a	10
<i>p</i> -Chlorophenyl	1.7	Analeptic	10
<i>p</i> -Tolyl	0.20	Analeptic	10
3,5-Dimethyl-1-phenyl	14.7	—	10
Nonaryl			
Alkyl	3000	Antimicrobial, anticoagulant, growth stimulant (chicken)	10,89,91 94,98,101 102
Benzyl	1115	—	2
Chloromethyl	Nontoxic	Promoter of hair growth and wound healing, anticoagulant, antitumor, growth stimulant (chicken)	7,10,88 89,91,93 98,101
Ethoxy	3000	Anticoagulant, antitumor, silkworm stimulant	10,94,95 98,101
Fluoroalkyl	—	Sedative	103
Morpholinomethyl	—	Antitumor (mice)	104

^a Stimulates motor activity and respiration.

have shown that administration of methyl- and chloromethylsilatrane does promote protein and collagen production in chick embryos (98). It is also interesting that the natural silicon content of animals is highest in the connective tissue, lungs, skin, bones (especially the epiphysis, or growing end), and hair or feathers (99, 100).

IV

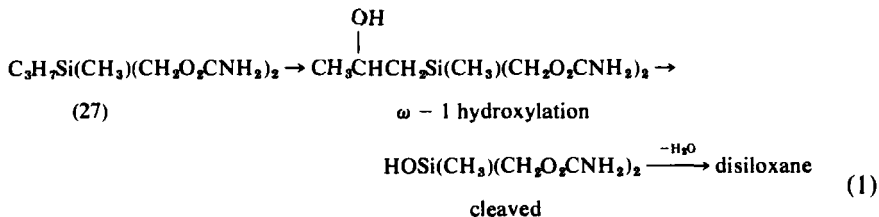
DETOXIFICATION AND ELIMINATION OF SILICON COMPOUNDS

Literature reports concerning the metabolism of organosilicon compounds are sparse. The information available indicates a rather normal detoxification pattern, as long as the chemical characteristics of silicon are taken into account.

Such volatile organosilicon compounds as trimethylsilanol are expelled via the respiratory tract as well as in the urine (4). Some ingested siloxanes, such as *n*-butylpentamethyldisiloxane (25), pass through the gastrointestinal tract unchanged and are eliminated in the feces (105). Some water-soluble organosilicon compounds, such as dimethylbis-(hydroxymethylcarbamoyl)silane (26), are absorbed after ingestion and are eliminated unchanged in the urine (32).

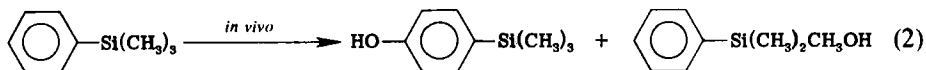


However, most organosilicon compounds are metabolized after ingestion or injection, and their metabolites are eliminated. For example, silameprobamate (27) undergoes $\omega - 1$ hydroxylation, following the same pattern as meprobamate itself. The difference in the metabolism of the two compounds is that the silicon compound also undergoes silicon-carbon cleavage to yield a silanol that can be isolated from the urine as a disiloxane (32); see Eq. (1).



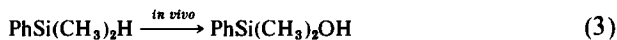
Phenylsilanes (PhSiR_3) undergo *in vivo* hydroxylation at the para position (106), as shown in Eq. (2). This is a common detoxification pathway

for aryl groups in nonsilicon compound as well. Of the compounds studied to date, silicon-phenyl cleavage has been insignificant. This lack of cleavage is surprising, considering the hydrolytic instability of the silicon-aryl bond when the aryl group contains an electron-withdrawing group such as OH.



Silicon-methyl groups also undergo hydroxylation *in vivo* (106). Again, such methyl-hydroxylation is also observed for carbon compounds. There is evidence that directly methyl transfer from the silicon (without prior oxidation) also occurs (107). In this respect, the silicon-methyl group behaves like other metal-methyl groups. Because of the ubiquity of silicon-methyl groups in compounds under investigation as potential drugs, further investigation into the fate of the silicon-methyl bond is warranted.

The silicon-hydride group is rapidly oxidized to a silanol group *in vivo*, according to one report (106). The silanol was isolated as the elimination product; see Eq. (3).



This instability of silicon hydrides is not surprising; in the laboratory these compounds are excellent reducing agents. However, the instability of the Si—H bond is disappointing because of the limitations it places on preparing silicon analogs of active carbon compounds. Most C—H bonds are stable *in vivo*, but a compound having a Si—H bond would be readily detoxified and eliminated.

V

SUMMARY

A variety of organosilicon compounds possess biological activity. The activities are probably not attributable to the silicon atom per se, but rather to the structure as a whole. Research in the area of organosilicon biological agents can be divided into two major sections: (1) substitution of a silicon atom onto or into a known active compound; and (2) investigation of the activities of organosilicon compounds without known carbon analogs. In general, work in the silicon-derivative area has indicated that the fundamental activity of the parent structure is retained, although usually to a lesser degree than is found with the parent structure.

To date, no dramatic enhancement or unique activities have been reported.

The area of active organosilicon compounds without carbon analogy appears to offer the greatest potential for future discovery. Unfortunately, this area of research is, to a large degree, governed by chance observations rather than by logical research plans. Consequently, it behooves all investigators in organosilicon chemistry to have their compounds tested whenever possible.

REFERENCES

1. R. J. Fessenden and J. S. Fessenden, *Adv. Drug Res.* **4**, 95 (1967).
2. M. G. Voronkov and E. Lukevics, *Usp. Khim.* **38**, 2173 (1969); *Russ. Chem. Rev.* **38**, 975 (1969); *Chem. Abstr.* **72**, 88,444 (1970).
3. L. R. Garson and L. K. Kirchner, *J. Pharm. Sci.* **60**, 1113 (1971).
4. M. G. Voronkov, *Int. Congr. Pure Appl. Chem.*, 24th **4**, 45 (1973); *Chem. Abstr.* **85**, 42,293 (1976).
5. M. G. Voronkov, *Vestn. Akad. Nauk SSSR* **21**, 564 (1972); *Chem. Abstr.* **78**, 54,133 (1973).
6. M. G. Voronkov, G. I. Zelvans, and E. Lukevics, "Silicon and Life." Zinatne, Riga, 1971; *Chem. Abstr.* **78**, 144,571 (1973).
7. M. G. Voronkov, *Chem. Br.* **9**, 411 (1973).
8. M. G. Voronkov, *Cesk. Farm.* **22**, 406 (1973); *Chem. Abstr.* **80**, 112,533 (1974).
9. M. J. Hunter and B. Aberg, *Acta Pharmacol. Toxicol., Suppl.* **36**, 9 (1975); *Chem. Abstr.* **83**, 2520 (1975).
10. M. G. Voronkov, *Annu. Rep. Med. Chem.* **10**, 265 (1975); *Chem. Abstr.* **84**, 83,881 (1976).
11. U. Wannagat, *Bild Wiss.* **14**, 130 (1977); *Chem. Abstr.* **88**, 114,963 (1978).
12. J. Thayer, *J. Chem. Educ.* **54**, 604 (1977).
13. K. Schwarz, *Proc. Natl. Acad. Sci. USA* **70**, 1608 (1973).
14. P. T. Henderson, E. J. Ariëns, B. W. J. Ellenbroek, and A. M. Simonis, *J. Pharm. Pharmacol.* **20**, 26 (1968).
15. I. Belsky, D. Gertner, and A. Zilkha, *J. Med. Chem.* **11**, 92 (1968).
16. S. Barcza, U.S. Patent 3,853,994 (1974); *Chem. Abstr.* **82**, 198,127 (1975).
17. R. Piekos, J. Teodorczyk, and W. Stozkowska, *Sci. Pharm.* **43**, 217 (1975).
18. R. J. Fessenden and R. Rittenhouse, *J. Med. Chem.* **11**, 1070 (1968).
19. M. Frankel, M. Broze, D. Gertner, and A. Zilkha, *J. Chem. Soc., C* **249** (1966); *Chem. Abstr.* **64**, 8227 (1966).
20. R. Tacke and U. Wannagat, *Monatsh. Chem.* **107**, 449 (1976).
21. R. Tacke and R. Niedner, *Z. Naturforsch. Teil B* **33**, 412 (1978).
22. R. J. Fessenden and M. D. Coon, *J. Med. Chem.* **8**, 604 (1965).
23. K. Sindelar, J. O. Jilek, V. Bartl, J. Metysova, B. Kakac, J. Holubek, E. Svatek, J. Pomykacek, and M. Protiva, *Collect. Czech. Chem. Commun.* **41**, 910 (1976).
24. J. Corey, J. P. Paton, and D. M. Rankin, *J. Organomet. Chem.* **139**, 1 (1977).
25. N. H. Andersen and N. M. Weinshenker, U.S. Patent 3,764,673 (1973); *Chem. Abstr.* **80**, 6947 (1974).
26. M. Hayashi, S. Kori, and T. Tanouchi, Japan Kokai 76 13,752; *Chem. Abstr.* **85**, 5272 (1976).

27. R. Piekos, A. Radecki, J. Lukasiak, K. Osmialowski, and R. Sujecki, *Rozpr. Wydz. Nauk Mat. Przyr. Gdansk. Tow. Nauk.* **3**, 71 (1972); *Chem. Abstr.* **80**, 47,612 (1974); **81**, 152,182 (1974); **85**, 20,769 (1976).
28. S. Barcza and C. W. Hoffman, *Tetrahedron* **31**, 2363 (1975).
29. C. G. Pitt, A. E. Friedman, D. Rector, and M. C. Wani, *Tetrahedron* **31**, 2369 (1975).
30. R. Piekos, K. Kobylczyk, and K. Osmialowski, *Rocz. Chem.* **49**, 273 (1975); *Chem. Abstr.* **83**, 97,183 (1975).
31. R. Piekos, K. Kobylczyk, and K. Osmialowski, *Sci. Pharm.* **45**, 234 (1977); *Chem. Abstr.* **89**, 43,554 (1978).
32. R. J. Fessenden and C. Ahlfors, *J. Med. Chem.* **10**, 810 (1967).
33. R. Tacke and U. Wannagat, *Monatsh. Chem.* **107**, 111 (1976).
34. G. Kuhr, H. Matties, H. Liebmann, and K. Ruehlmann, *Pharmazie* **31**, 849 (1976).
35. G. Kroening, E. Schultz, and W. D. Sprung, *Pharmazie* **30**, 765 (1975).
36. V. Lee, "Synthesis of (¹⁴C)Methylsilanes and Their Octanol-Water Partition Coefficient Determinations," M.S. thesis, San Jose State College, San Jose, Cal., 1967.
37. S. Barcza, U.S. Patent 3,764,597 (1973); *Chem. Abstr.* **79**, 146,644 (1973).
38. S. Barcza, U.S. Patent 3,692,798 (1972); *Chem. Abstr.* **78**, 43,692 (1973); U.S. Patent 3,787,437 (1974); *Chem. Abstr.* **80**, 82,971 (1974).
39. M. Kuehne, Ger. Offen. 2,507,929 (1975); *Chem. Abstr.* **84**, 31,236 (1976).
40. S. Barcza, U.S. Patent 3,780,175 (1973); *Chem. Abstr.* **80**, 60,027 (1974).
41. S. Barcza, U.S. Patent 3,585,228 (1971); *Chem. Abstr.* **75**, 49,312 (1971).
42. R. Piekos, J. Halkiewicz, and R. Sujecki, *Rocz. Chem.* **49**, 539 (1975); *Chem. Abstr.* **83**, 97,442 (1975).
43. R. Piekos and J. Teodorczyk, *Rocz. Chem.* **49**, 1603 (1975); *Chem. Abstr.* **84**, 59,628 (1976).
44. R. Piekos and M. Sandowski, *Rocz. Chem.* **50**, 363 (1976); *Chem. Abstr.* **85**, 78,182 (1976).
45. E. L. Pidemskii, A. A. Omorin, L. M. Obvintseva, and R. V. Alikina, USSR Patent 523,102 (1976); *Chem. Abstr.* **85**, 116,925 (1976).
46. L. E. Golubovskaya and K. K. Pivnitskii, *Khim.-Farm. Zh.* **10**, 52 (1976); *Chem. Abstr.* **85**, 33,260 (1976).
47. R. Piekos, J. Teodorczyk, and W. Stozkowska, *Sci. Pharm.* **44**, 13 (1976); *Chem. Abstr.* **85**, 37,143 (1976).
48. J. Lukasiak, Z. Jamrogiewicz, H. Lamparczyk, and R. Piekos, *Acta Pol. Pharm.* **32**, 429 (1975); *Chem. Abstr.* **85**, 5755 (1976).
49. Stanford Research Institute, Fr. Demande 2,241,320; *Chem. Abstr.* **83**, 179,410 (1975).
50. S. Barcza (to Sandoz Ltd.), Ger. Offen. 2,100,967; *Chem. Abstr.* **75**, 130,018 (1971).
51. A. T. McPhail and R. W. Miller, *J. Chem. Soc. Perkin Trans. 2*, p. 1180 (1975).
52. C. Eaborn, "Organosilicon Compounds," Academic Press, London, 1960.
53. E. Lukevics, V. P. Dremova, and S. N. Smirnova, *Latv. PSR Zinat. Akad. Vestis. Khim. Ser.* **4**, 454 (1976); *Chem. Abstr.* **86**, 5520 (1977).
54. R. Tacke and R. Niedner, *Z. Naturforsch. Teil B* **33**, 412 (1978).
55. E. Lukevics and M. G. Voronkov, *Dokl. Akad. Nauk SSSR* **216**, 103 (1974); *Chem. Abstr.* **81**, 8627 (1974).
56. S. Hillers, V. E. Golender, A. B. Rozenblit, R. Ya. Sturkovich, and E. Lukevics, *Khim.-Farm. Zh.* **10**, 29 (1976); *Chem. Abstr.* **85**, 72,829 (1976).
57. K. A. Andrianov, Yu. S. Nabokov, I. M. Prudnik, A. M. Kononov, and G. V. Kotrel'ov, *Khim.-Farm. Zh.* **10**, 46 (1976); *Chem. Abstr.* **86**, 16,731 (1977).
58. V. B. Kazimirovskaya, A. T. Platonova, V. M. D'yakov, V. P. Baryshok, and M. G.

- Voronkov, *Biol. Akt. Soedin. Elem. IV B Gruppy*, p. 99 (1977); *Chem. Abstr.* **89**, 100,082 (1978).
59. E. Lukevics, S. German, N. P. Erchak, and E. P. Popova, *Khim.-Farm. Zh.* **12**, 67 (1978); *Chem. Abstr.* **88**, 190,949 (1978).
60. A. Burger, ed., "Medicinal Chemistry," 2nd edn., Chapter 7, Wiley (Interscience), New York, 1960.
61. L. Parkanyi, L. Bihatsi, and P. Hencsei, *Cryst. Struct. Commun.* **7**, 435 (1978).
62. V. A. Pestunovich, S. N. Tandura, M. G. Voronkov, V. P. Baryshok, G. I. Zalcans, V. I. Glukhikh, G. Engelhardt, and M. Witanowski, *Spectrosc. Lett.* **11**, 339 (1978).
63. L. S. Goodman and A. Gilman, eds., "The Pharmacological Basis of Therapeutics," p. 241. Macmillan, New York, 1965.
64. R. Tacke and U. Wannagat, *Monatsh. Chem.* **107**, 439 (1976).
65. G. Friedrich, R. Bartsch, and K. Ruehlmann, *Pharmazie* **32**, 394 (1977).
66. R. Tacke and U. Wannagat, *Arch. Pharm. (Paris)* **310**, 714 (1977).
67. E. J. Hobbs, O. E. Fancher, and J. C. Calandra, *Toxicol. Appl. Pharmacol.* **21**, 45 (1972).
68. E. Bien and P. Buntrock, *Pharmazie* **29**, 530 (1974).
69. J. C. Calandra, M. L. Keplinger, E. J. Hobbs, and L. J. Tyler, *Polym. Prepr., Am. Chem. Soc. Div. Polym. Chem.* **17**, 12 (1976).
70. R. R. Le Vier and M. E. Jankowiak, *Toxicol. Appl. Pharmacol.* **21**, 80 (1972).
71. L. Nicander, *Acta Pharmacol. Toxicol., Suppl.* **36**, 40 (1975); *Chem. Abstr.* **83**, 72,432 (1975).
72. R. R. Le Vier, D. R. Bennett, and M. J. Hunter, *Acta Pharmacol. Toxicol., Suppl.* **36**, 68 (1975); *Chem. Abstr.* **83**, 72,433 (1975).
73. L. Albanus, N. E. Bjorklund, B. Gustafsson, and M. Jonsson, *Acta Pharmacol. Toxicol., Suppl.* **36**, 93 (1975); *Chem. Abstr.* **83**, 72,434 (1975).
74. R. R. Le Vier and M. E. Jankowiak, *Biol. Reprod.* **7**, 260 (1972).
75. R. Le Fevre, F. Coulston, and L. Golberg, *Toxicol. Appl. Pharmacol.* **21**, 29 (1972).
76. J. F. Hayden and S. A. Barlow, *Toxicol. Appl. Pharmacol.* **21**, 68 (1972).
77. J. F. Hyde and D. E. Speilvogel (to Dow Corning Corp.), Ger. Offen. 2,032,826; *Chem. Abstr.* **75**, 49,315 (1971).
78. D. R. Bennett and J. A. McHard (to Dow Corning Corp.), U.S. Patent 3,830,912; *Chem. Abstr.* **82**, 39,019 (1975).
79. D. R. Bennett and R. R. Le Vier (to Dow Corning Corp.), U.S. Patent 3,821,373; *Chem. Abstr.* **82**, 26,147 (1975).
80. D. R. Bennett and J. A. McHard (to Dow Corning Corp.), U.S. Patent 3,975,521; *Chem. Abstr.* **85**, 130,538 (1976).
81. D. R. Bennett, S. J. Gorzinski, and J. E. LeBeau, *Toxicol. Appl. Pharmacol.* **21**, 55 (1972).
82. M. Söderholm and D. Carlström, *Acta Chem. Scand. Ser. B* **31**, 193 (1977).
83. C. G. Schmitterlow and C. Sjogren, *Acta Pharmacol. Toxicol., Suppl.* **36**, 131 (1975).
84. E. A. Abbott and A. J. Isquith, Ger. Offen. 2,226,823 and 2,229,580; *Chem. Abstr.* **79**, 28,392, 39,346 (1973).
85. A. Nagata and J. Ayoda, Ger. Offen. 2,647,389; *Chem. Abstr.* **87**, 40,215 (1977).
86. M. G. Voronkov, A. T. Platonova, I. G. Kuznetsov, S. G. Shevchenko, E. A. Meierova, S. K. Suslova, I. S. Emel'yanov, V. M. D'yakov, and N. G. Ustinova, *Latv. PSR Zinat. Akad. Vestis, Kim. Ser.* p. 204 (1977); *Chem. Abstr.* **87**, 48,612 (1977).
87. M. Schwarcz, C. G. Beiter, S. Kaplin, O. Loeffler, M. Martino, and S. Damle, Ger. Offen. 2,009,964 (1970); *Chem. Abstr.* **73**, 120,748 (1970).

88. Irkutsk Institute of Organic Chemistry, Siberian Dept., Academy of Sciences, USSR, British Patent 1,465,455 (1977); *Chem. Abstr.* **87**, 73,369 (1977).
89. M. G. Voronkov, A. T. Platonova, V. M. D'yakov, K. M. Katrush, A. I. Kazakul, I. G. Kuznetsov, and L. A. Mansurova, USSR Patent 541,473 (1977); *Chem. Abstr.* **87**, 83,547 (1977).
90. G. A. Grigalinovich, Z. Atare, N. B. Milyakova, G. Zalcans, and E. Lukevics, *Biol. Akt. Soedin. Elem. IV B Gruppy* p. 113 (1977); *Chem. Abstr.* **89**, 100,938 (1978).
91. K. M. Katrush, M. G. Voronkov, and V. M. D'yakov, *Biol. Akt. Soedin. Elem. IV B Gruppy*, p. 162 (1977); *Chem. Abstr.* **89**, 58,833 (1978).
92. M. G. Voronkov, A. T. Platonova, L. A. Mansurova, I. G. Kuznetsov, G. Zalcans, and V. M. D'yakov, U.S. Patent 4,055,637 (1977); *Chem. Abstr.* **88**, 16,168 (1978).
93. M. G. Voronkov, A. T. Platonova, E. V. Bakhareva, I. G. Kuznetsov, V. M. D'yakov, G. Zalcans, I. I. Kolgunenko, and N. S. Samoshkina, Ger. Offen. 2,615,654 (1977); *Chem. Abstr.* **88**, 177,201 (1978).
94. M. G. Voronkov, I. V. Vititnev, V. F. Drozda, V. M. D'yakov, N. N. Sinitskii, N. G. Shkaruba, M. S. Sorokin, and V. P. Baryshok, *Dokl. Akad. Nauk SSSR* **239**, 238 (1978); *Chem. Abstr.* **89**, 39,717 (1978).
95. I. V. Vititnev, V. F. Drozda, N. G. Shkaruba, N. N. Sinitskii, and L. V. Orgil'yanova, *Biol. Akt. Soedin. Elem. IV B Gruppy* p. 170 (1977); *Chem. Abstr.* **89**, 106,384 (1978).
96. G. Zalcans, A. Lapsina, I. I. Solomennikova, A. Dauvarte, A. Zidermane, and E. Lukevics, *Biol. Akt. Soedin. Elem. IV B Gruppy* p. 28 (1977); *Chem. Abstr.* **89**, 109,694 (1978).
97. M. G. Voronkov, *Pure Appl. Chem.* **13**, 35 (1966); *Chem. Abstr.* **67**, 43,841 (1967).
98. B. Z. Simkhovich, E. Lukevics, G. Zalcans, T. V. Zamaraeva, and V. I. Mazurov, *Biokhimiya* **42**, 1128 (1977); *Chem. Abstr.* **87**, 79,039 (1977).
99. E. M. Carlisle, *Science* **178**, 619 (1972).
100. G. S. Smith and R. H. Robertson, *J. Anim. Sci.* **31**, 218 (1970).
101. S. G. Shevchenko, A. T. Platonova, V. V. Sadakh, and M. G. Voronkov, *Biol. Akt. Soedin. Elem. IVB Gruppy* p. 95 (1977); *Chem. Abstr.* **89**, 70,791 (1978).
102. H. Sakurei and A. Shirohata, Japan Kokai 78 31,689; *Chem. Abstr.* **89**, 43,759 (1978).
103. V. P. Baryshok, Y. M. D'yakov, M. G. Voronkov, S. S. Shevchenko, and I. G. Kuznetsov, *Biol. Akt. Soedin. Elem. IV B Gruppy* p. 14 (1977); *Chem. Abstr.* **89**, 109,691 (1978).
104. E. Lukevics, A. Lapsina, G. Zalcans, A. Dauvarte, and A. Zidermane, *Larv. PSR Zinat. Akad. Vestis, Kim. Ser.* p. 338 (1978); *Chem. Abstr.* **89**, 129,581 (1978).
105. A. N. Kazi-Girey, Jr., "An Examination of the Biochemical and Biological Properties of Butylpentamethyldisiloxane by Use of Radioactive Labeling," M.S. thesis, San Jose State College, San Jose, Cal., 1967.
106. R. J. Fessenden and R. A. Hartman, *J. Med. Chem.* **13**, 52 (1970).
107. G. S. Hughes, "A Study of the Metabolism of Tripropylsilane," M.S. thesis, University of Montana, Missoula, Montana, 1972.

This Page Intentionally Left Blank

Boron Heterocycles as Ligands in Transition-Metal Chemistry

WALTER SIEBERT

*Fachbereich Chemie der Philipps-Universität
Marburg, Federal Republic of Germany*

I. Introduction	301
A. Boron Heterocycles as Lewis Acids	302
B. Transition-Metal Complex Fragments as Lewis Bases	303
C. Considerations of Bonding in π -Complexes and Clusters	304
II. Mononuclear Complexes	307
A. Complexes Having Three-Electron Ligands	307
B. Complexes Having Four-Electron Ligands	309
C. Complexes Having Five-Electron Ligands	314
D. Complexes Having Six-Electron Ligands	320
III. Dinuclear Complexes	324
A. Carbon Monoxide as Bridging Ligand	324
B. Boron Heterocycles in Bridging Positions	325
IV. Trinuclear Complexes	333
A. Carbon Monoxide as Terminal Ligand	333
B. Tetra-decker Sandwich Complexes	335
V. Conclusion	337
References	337

I

INTRODUCTION

Since the discovery of bis(cyclopentadienyl)iron, carbocyclic π -complexes involving the aromatic ligands $C_8H_8^{2-}$, $C_7H_7^+$, C_6H_6 , $C_5H_5^-$, and $C_4H_4^{2-}$ have been intensively studied with respect to their structure, bonding, and reactivity. However, electron-rich heterocyclic systems have received far less attention. This article focuses on the ligand properties of Lewis acid boron heterocycles and reports on the newest developments in the expanding field of triple- and tetra-decker sandwich compounds. From structural and bonding considerations, metal complexes with electron-poor boron heterocycles link together the separately developed areas of classical hydrocarbon π -complexes (1,1a) and metallo-boron/metallocarborane cluster compounds (2). Boron-rich ligands with bridging hydrogen atom(s) will not be discussed here. Grimes (3) has reviewed metal sandwich complexes of cyclic planar ligands (e.g., $B_4H_8^{2-}$, $B_5H_{10}^-$, and $C_2B_3H_7^-$, the structural and electronic analogs of $C_4H_4^{2-}$ and $C_5H_5^-$) as well as pyramidal ligands containing boron. Organo-

boron transition-metal compounds including π -complexes have been described by Schmid (4). For a review on the borabenzene anion and its transition-metal complexes, see Allen and Palmer (8).

A. Boron Heterocycles as Lewis Acids

Replacement of carbon atoms by boron atoms in π -carbocyclic and heterocyclic systems leads to a wide variety of planar Lewis acid boron heterocycles (5, 6). The electron-deficient boron atoms generate unusual properties for some of these ligands, which, however, depend upon the exocyclic substituent at the boron as well as on the number and nature of the remaining ring atoms. The latter are responsible for the donor capacities of the ligands. Successive replacement of CH groups in the cyclopentadiene ring (1) with the borene group BH creates the seven cyclic species 2 through 8, having the B_nC_{5-n} skeleton with $n = 1-5$ (7). Of these boron compounds, only the borole (2) (8-10) and the 1,3-diborolene (3) (11) (one hydrogen atom added) have an independent existence. The 1,2-isomer 4, a cyclic π -allyl ligand, has not yet been prepared. Because of their high electron deficiency, species 5 through 8 cannot exist as planar rings, but adopt polyhedral structures. According to the $(2n + 2)$ electron rule (n = number of framework atoms) for cluster compounds (12-14), isomers 5 and 6 should have *closa* structures since the required 12 skeletal electrons are present. In the polyhedral electron-count theory, each vertex atom in an n -vertex *closa* system supplies three valence orbitals for cluster bonding. Because one electron of each vertex atom is used in bonding the external ligand (substituent), it is not included in the framework electron count. Thus, each :BH group donates two, and each :CH three electrons to occupy the $(n + 1)$ bonding molecular orbitals. A trigonal-bipyramidal structure is also expected for the yet unknown anions of 7 and 8, $(B_4CH_3)^-$ and $(B_5H_5)^{2-}$.

Further replacement of carbon by nitrogen and sulfur in 2 and 3 affords the heterocycles 9 through 16, of which all but species 10 are known.

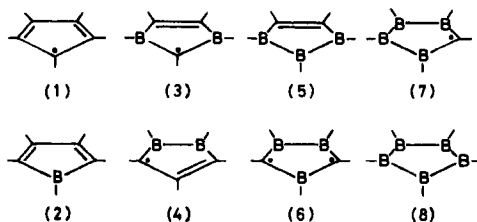


FIG. 1. Successive substitution of CH with BH groups in C_5H_5 .

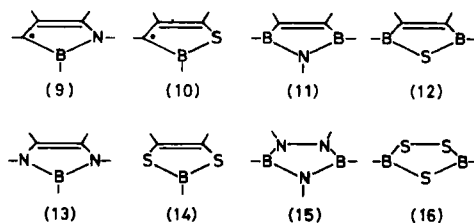


FIG. 2. Five-membered mono- and diboraheterocycles.

Six-membered Lewis acid ligands can be derived from benzene by substituting boron, nitrogen, and sulfur for carbon. Of the possible heterocycles, only a few are listed. The boracyclohexadiene (17) exists as a π^6 anion ($C_5H_5B-R^-$, borabenzene anion) prepared by two different methods (15, 16). The 1,4-diborine ring in 18 is a difunctional Lewis acid, of which derivatives with fluoro, alkoxyl, or ferrocenyl substituents at the boron have been reported (17, 18). According to electron-counting rules, derivatives with hydrogen at the boron are expected to rearrange to the known *nido*-tetracarbahehexaborane, a carborane with a pentagonal-pyramidal structure (19).

Formal replacement of two carbon atoms in 18 by nitrogen gives the 1,2-diaza-3,6-diborine system (19), which is isoelectronic with benzene (20). Among boron nitrogen compounds, the borazine derivatives 20 have been widely studied as ligands (21, 22). Tricarbonylmetal complexes of the six-electron ligand borthiine (21) have been reported (23). The smaller boron heterocycles 22 and 23 increase the range of potential ligands. Although the borirene ring of 24 is isoelectronic with the cyclopropenyl cation, of which several complexes are known, neither 24 nor any other complex of this species has been reported. The cation 24^+ is frequently observed in the mass spectra of 1,2,5-thiadiborolenes (12) (24).

B. Transition-Metal Complex Fragments as Lewis Bases

The aforementioned boron heterocycles act as strong electron acceptors toward transition-metal moieties if the other ligands present have

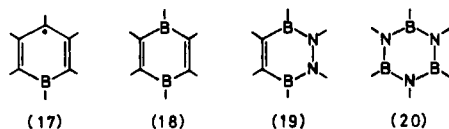


FIG. 3. Six-membered boron heterocycles.

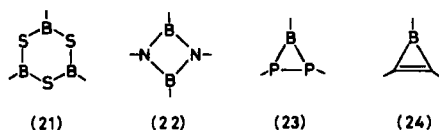


FIG. 4. Borthiine (21) and some small boron heterocycles.

fewer than six donor electrons. The heterocycles 13–16 and 19–21 are π^6 -ligands and therefore react preferentially with such d^8 -metal complex fragments as $\text{Cr}(\text{CO})_3$, $\text{Mn}(\eta^5\text{-C}_5\text{H}_5)$, or their homologs to form diamagnetic 18-valence-electron complexes. The five-electron ligands 9, 10, and 17 are one-electron acceptors, to complete the π^6 system. In a broader sense, they are to be compared with $\eta\text{-C}_5\text{H}_5$ and therefore should react with such d^7 fragments as $\text{Mn}(\text{CO})_3$ or $\text{Fe}(\eta\text{-C}_5\text{H}_5)$, yielding diamagnetic complexes, whereas paramagnetic species are obtained with d^n complex fragments when $n \neq 7$. The four-electron ligands 2, 11, 12, and 18 are expected to act as two-electron acceptors, thereby forming diamagnetic mono- and dinuclear complexes with d^8 and d^7 fragments. The latter should possess triple-decker structure. Among the boracycles (2–24), the 1,3-diborolene (3) is the only example of a three-electron acceptor. Other possible candidates would be the 1,2-diborolene (4) and ligands with a CB_3X skeleton ($\text{X} = \text{S}, \text{N-R}, \text{P-R}$).

Typical three-electron-donor transition-metal fragments (12c, 25) are the $(\eta^5\text{-C}_5\text{H}_5)\text{Ni}$ and the $(\text{CO})_3\text{Co}$ groups, which form mononuclear complexes with 3. However, 3 can also hold two metal moieties donating $(1 + 2)$, $(2 + 2)$, $(2 + 3)$, and $(3 + 3)$ electrons because slightly antibonding orbitals in the triple-decker complexes are then occupied. The planar ligands 5, 6, 7, and 8 with the formal acceptor capacities of 4, 5, and 6 electrons should only exist in dinuclear complexes when stabilized by a pair of $(2 + 2)$, $(2 + 3)$, and $(3 + 3)$ -electron-donor moieties (7).

C. Considerations of Bonding in π -Complexes and Clusters

Electron counts according to the 18-electron rule are restricted to mono- and dinuclear complexes if the latter have no μ^5 -ligands. For triple- and tetra-decker complexes the 18-electron rule has to be transformed into the 30- and 42-valence-electron rule by adding $d^6 + \pi^8$ (or σ^6) electrons once and twice.

Replacement of two carbon atoms in nickelocene by boron leads to complex 26 having the π^6/d^6 arrangement to which cluster formalism can be applied. The diamagnetic sandwich 26 is isoelectronic with ferrocene

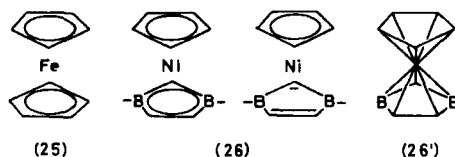


FIG. 5. Description of 1,3-diborolenylcyclopentadienylnickel (26) by the π^6/d^6 and cluster formalism.

(25). According to the π^6/d^6 formalism, 26 should contain d^6 nickel. However, such a high charge separation ($\pi^6/d^6/\pi^6$) is unrealistic. The probable $\pi^6/d^8/\pi^4$ electron configuration comes near to that calculated by the extended Hückel (EH) method (26).

As an alternative to the aromaticity formalism commonly used, compounds containing electron-deficient elements in addition to metal atoms can be regarded as clusters. The diamagnetic nickelocene analog 26 is built of a double-cone structure (26') that consists of two *nido* clusters. Each *nido* unit having $n = 6$ framework atoms needs, according to the electron rule, $2n + 4$ (i.e., 16) skeletal electrons to hold the C_3B_2Ni and the C_5Ni frameworks together. The electrons needed are supplied by C (3×3), B (2×2), and Ni (3) for the C_3B_2Ni skeleton and by C (3×5), Ni (1) for C_5Ni . Thus, four electrons of d^{10} nickel, as in the π^6/d^6 systematics, are counted for cluster bonding. The total number of electrons involved in the bonding between the eleven framework atoms can be listed as follows (27):

bonding electrons	$2 \times \sigma^{10} + 2 \times \pi^6 + d^6 = 38$
aromaticity formalism	$2 \times \pi^6 + d^6 = 18$
cluster formalism	$2 \times \sigma^{10} + 2 \times \pi^6 = 32$

In the π^6/d^6 formalism no σ electrons are counted whereas, in the cluster description, the d^6 electrons are omitted. Therefore, both bonding considerations are equivalent. In such paramagnetic sandwich complexes as $(C_5H_5)Ni(C_2B_2S)$ (28) ($2 \times \pi^6/d^7$; $C_2B_2S = 12$) and $(C_5H_5)_2Ni$ ($2 \times \pi^6/d^8$), the unpaired electrons occupy antibonding molecular orbitals (MOs), which results in a lengthening of the metal-ring distance. According to the cluster description, one or both *nido* structures would have 17 electrons; therefore, a small structural change is expected.

In clusters composed solely of main-group elements, the following electronic relationship between *closo*, *nido*, and *arachno* structures has been found (12, 29):



If two electrons are added to the $2n + 2$ count of a *closo* system, the cage opens to a *nido* structure, because a strong antibonding orbital is filled (a *nido* structure is derived from *closo*, where one vertex of the polyhedron is not occupied). However, this does not always apply for clusters with transition metals incorporated into the framework. Additional electrons in *closo* and *nido* species may occupy slightly antibonding orbitals, resulting only in distortion rather than opening of the cage (29b).

The aromaticity and cluster formalisms are also applicable for triple- and tetra-decker complexes with five-membered rings.

Metal complexes	Triple-decker sandwich	Tetra-decker sandwich
Bonding electrons	$3 \times \sigma^{10} + 3 \times \pi^6 + 2 \times d^6 = 60$	$4 \times \sigma^{10} + 4 \times \pi^6 + 3 \times d^6 = 82$
Aromaticity formalism	$3 \times \pi^6 + 2 \times d^6 = 30$	$4 \times \pi^6 + 3 \times d^6 = 42$
Cluster formalism	$3 \times \sigma^{10} + 3 \times \pi^6 = 48$	$4 \times \sigma^{10} + 4 \times \pi^6 = 64$

If ligands smaller or larger than the cyclopentadienyl ring are incorporated, the total number of bonding electrons used for the cluster description will vary, whereas the number for the aromaticity formalism is not changed.

Additional d electrons on the metals increase the number to be counted in the aromaticity formalism. As this can be applied by two metals ($d^6 \rightarrow d^8$), the family of triple-decker sandwich complexes should consist of members having 30, 31, 32, 33, and 34 valence electrons. Analogous to the 17-valence-electron ferricenium cation, obtained by oxidation of ferrocene, 29-valence-electron species ($\pi^6/d^5/\pi^6/d^6/\pi^6$) would be expected to be stable, and this has been confirmed by chemical and electrochemical studies (see Section III).

Hoffmann and co-workers (30) have carried out EH calculations for the first triple-decker sandwich, the 34-valence-electron ($3 \times \pi^6/2 \times d^8$)

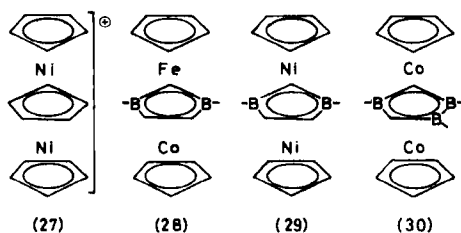


FIG. 6. Triple-decker sandwich complexes having 30–34 valence electrons. (Compound 27 has 34; 28 and 30, 30; and 29, 33 valence electrons.)

tricyclopentadienyldinickel cation (**27**) (31, 32). In the MO diagram for the diamagnetic **27**, the e_1' niveau is completely occupied, whereas in the 30-valence-electron species **28** and **30** it is empty. With the 1,3-diborolene **3** as bridging ligand, the complete family of triple-decker compounds with 30 to 34 valence electrons (34 valence electrons are present in **29**⁻) have been prepared (33, 34). Complex **30** and its 2,3-isomer (carbon atoms in adjacent positions) represent the first examples of a neutral triple-decker sandwich compound (35).

II

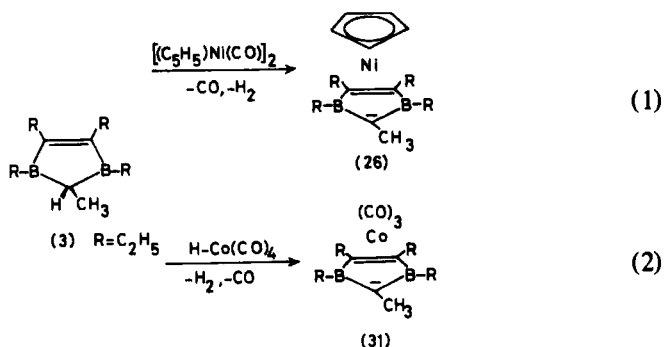
MONONUCLEAR COMPLEXES

A. Complexes Having Three-Electron Ligands

1. 1,3-Diborolene ($\eta^5\text{-C}_3\text{B}_2$)

Thermal reactions of 1,3,4,5-tetraethyl-2-methyl-1,3-diborolene (**3**) with nickelocene or cyclopentadienyl(carbonyl)nickel dimer in mesitylene yield the orange-red diamagnetic complex¹ **26** (64%), and the deep-green paramagnetic triple-decker sandwich **29** (20%). The sandwich structure was proposed on the basis of ¹H- and ¹¹B-NMR data and confirmed by an X-ray structure analysis (36, 37). In the nonplanar C_3B_2 ring, the unique carbon atom between the two boron atoms is above (+0.167 Å) the plane defined by the remaining ring atoms. The ring center-nickel distances are: $\text{C}_3\text{B}_2\text{—Ni}$ 1.656 and $\text{C}_5\text{—Ni}$ 1.715 Å. All metal-carbon distances are similar to those of ferrocene (2.063 ± 0.003 Å). Although **26** is isoelectronic with ferrocene, it is less reactive toward electrophilic substitution. The reduced electron density in the C_5H_5 ring is also evident from ¹H- and ¹³C-NMR data, which show a downfield shift relative to the NMR signals of ferrocene by 0.87 and 23.55 ppm, respectively. These findings are supported by EH calculations (26). In contrast to **26**, the yellow half-sandwich **31** (Scheme 1) is formed at room temperature from **3** and $[\text{Co}_2(\text{CO})_8]$ in low yield (increased to 16% by using $[\text{HCo}(\text{CO})_4]$ as the starting material) (38). The formation of several unidentified compounds, as well as $\text{Co}_4(\text{CO})_{12}$, and CO insertion into the 1,3-diborolene ring prevent higher yields (*vide infra*). Compound **31** shows $\nu(\text{CO})$ 2080(s)

¹ In most figures in this review, substituents R on the boron rings have been omitted for clarity. However, in the text, where specific derivatives are involved, ring substituents are indicated as follows: **26** (R = C_2H_5) and **31** (R = C_2H_5).



SCHEME 1. Synthesis of cyclopentadienyl-1,3-diborolenylnickel (26) and 1,3-diborolenyltricarbonylcobalt (31).

and 2030(vs) cm^{-1} and $\delta^{11}\text{B} = 30.8$ ppm. The upfield shift in the ^{11}B -NMR spectrum relative to the 1,3-diborolene 3 ($\delta = 68.6$ ppm) is 37.8 compared with 33.3 ppm for the sandwich complex 26.

2. 1-Oxa-2,6-diboracyclohexene ($\eta^3\text{-C}_3\text{B}_2\text{O}$)

Attempts to synthesize the electron-deficient sandwich 32, isoelectronic with bis(allyl)nickel, resulted in the formation of the unusual complex 33 (15%) (39). The X-ray structure analysis proved that each of the 1,3-diborolenyl ligands has incorporated one CO molecule and rearranged to an allylic system in which a diboryloxo unit bridges the allyl to afford a six-membered ring. The $\text{C}_3\text{B}_2\text{O}$ ring is not planar since the oxygen and boron atoms are bent away from the nickel (B and O deviate from the C_3 plane by 0.4 and 0.7 Å; Ni—C 2.07, Ni—B 2.55, and Ni—O 2.70 Å) (39, 40). ^1H - and ^{13}C -NMR data indicate that one substituent R in the molecule (3- or 5-position) is not an ethyl, but a vinyl, group. The insertion of CO into the free ligand 3 occurs at room temperature, yielding a ~1:3 mixture of the heterocycles 1,2,6-oxadiboracyclohexene ($\text{C}_3\text{B}_2\text{O}$) and 1,2,5-oxadiboracyclohexene ($\text{C}_2\text{B}_2\text{CO}$).² (See Fig. 7.)

3. 1-Borato-1,3-cycloheptadiene ($\eta^4\text{-C}_6\text{B}$)

For information on 1-borato-1,3-cycloheptadiene, see Section II,B,2.

² Both rings carry an exocyclic $=\text{C}(\text{H})\text{CH}_3$ group, as indicated by ^1H -NMR spectroscopy.

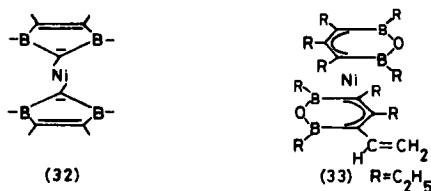


FIG. 7. The expected **32** and a reaction product (**33**) isolated from 1,3-diborolene (**3**) and $Ni(CO)_4$.

B. Complexes Having Four-Electron Ligands

1. Borole (η^5-C_4B)

Blue pentaphenylborole (**2**) reacts with $Fe_2(CO)_9$ or $Ni(CO)_4$, yielding the complexes **34** and **35**, respectively (10). Compound **34** was formed from 1-phenyl-4,5-dihydroborolepin and $Fe(CO)_5$ by ring contraction in boiling mesitylene. In these complexes, the four-electron ligands are pentahapto-bonded to the metal moieties. The IR spectra exhibit three strong CO absorptions for the tricarbonyliron complexes, viz., **34** ($R = C_6H_5$): 2056, 2001, and 1992 cm^{-1} (hexane); **34** ($R' = C_2H_5$): 2067, 2007, and 2000 cm^{-1} (hexane), and two for **35**: 2073 and 2031 cm^{-1} (hexane). The high-field ^{11}B -NMR signal of **35** (19.6 ppm) demonstrates the involvement of the boron atom in complex bonding. (See Fig. 8.)

2. Boracyclodienes (η^5-XC_4B , η^5-C_6B , η^4-C_6B)

Formal ring expansion of 1-boracyclopentadiene (borole) with $C(CH_3)_2$, $Si(CH_3)_2$, and $(CH_2)_2$ leads to six- and seven-membered boracycles. The ligands $X(CH=CH)_2B-C_6H_5$ [$X = C(CH_3)_2$, $Si(CH_3)_2$, or $(CH_2)_2$] have been obtained from the corresponding stannacyclohexadienes by treatment with $C_6H_5BCl_2$. They react photochemically with $Fe(CO)_5$ and $(\eta-C_5H_5)Co(CO)_2$, to yield $[X(CH=CH)_2B-C_6H_5]Fe(CO)_3$ (**36**) and $[(H_3C)_2C(CH=CH)_2B-C_6H_5]Co(\eta-C_5H_5)$ (**37**), respectively (41). The

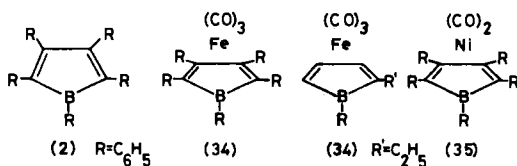


FIG. 8. Borole (**2**) and borole-carbonylmetal complexes.

constitution of these complexes was derived from IR, ^1H -, and ^{11}B -NMR spectroscopy. Again, the upfield shifts of 22–31 ppm in the ^{11}B -NMR spectrum upon complexation of the ligands indicate the participation of the boron atoms in complex bonding. An X-ray structural analysis of **36** [$\text{X} = \text{Si}(\text{CH}_3)_2$] proved that the $\text{Si}(\text{CH}_3)_2$ group is not in the BC_4 plane but is bent away from the Fe atom ($\text{C}-\text{Fe}$ 2.15–2.22, $\text{Si}-\text{Fe}$ 2.94, and $\text{B}-\text{Fe}$ 2.26 Å). Analogous to 1-phenyl-4,5-dihydroborepin-tricarbonyl-iron **36**, $\text{X} = (\text{CH}_2)_2$, tetracarbonyl metal complexes **38** ($\text{M} = \text{Cr}, \text{Mo}, \text{W}$) have been prepared photochemically from $\text{M}(\text{CO})_6$ or thermally from $[(\text{CH}_3\text{CN})_3\text{Cr}(\text{CO})_3]$ and $[(\text{H}_5\text{C}_5\text{N})_2\text{M}(\text{CO})_4]$ (**42**). The dihydroborepin-tetracarbonylmetal complexes exhibit a higher thermal stability (decomp. 140–180°C) than the corresponding 1,5-cyclooctadiene compounds. In the NMR spectra, the ^1H and ^{13}C signals of the olefinic carbon atoms and the ^{11}B signals ($\Delta\delta = 25\text{--}28$ ppm) are shifted to high field upon complexation.

Irradiation of $[(\eta\text{-C}_5\text{H}_5)\text{Mn}(\text{CO})_3]$ in the presence of 1-phenyl-4,5-dihydroborepin (**L**) yields the thermolabile compound $[(\eta\text{-C}_5\text{H}_5)\text{Mn}(\text{CO})\text{L}]$ (**42**).

During an attempt to synthesize a boracycloheptadienylrhodium complex from 1-phenyl-4,5-dihydroborepin, $\text{LiC}(\text{CH}_3)_3$, and $[\text{Rh}(1,5\text{-C}_8\text{H}_{12})\text{Cl}]_2$, the $\eta\text{-1,5-cyclooctadiene}$ (1-4- $\eta\text{-1-phenyl-1-borato-1,3-cycloheptadiene}$)rhodium **39** was obtained (**43**). Presumably, the unexpected formation of **39** (60%) occurs by addition of a rhodium-hydride compound (formed by elimination of isobutylene from a *t*-butylrhodium complex) to the 4,5-dihydroborepin. Its constitution is deduced from ^1H - and ^{11}B -NMR data. The bora-5,6,7-trihydroborepinyl acts as an allyl ligand and thus contributes three electrons to complex bonding. (See Fig. 9.)

3. 1,4-Diboracyclohexadienes ($\eta^6\text{-C}_4\text{B}_2$)

By cocondensation of boron monofluoride with alkynes, Timms (**17**) obtained 1,4-difluoro-1,4-diborines (1,4-difluoro-1,4-dibora-2,5-cyclohexadienes). With the 1,4-difluoro-2,3,5,6-tetramethyl-1,4-diborine (**18a**)

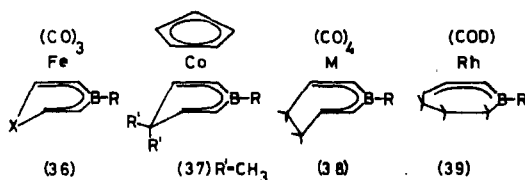


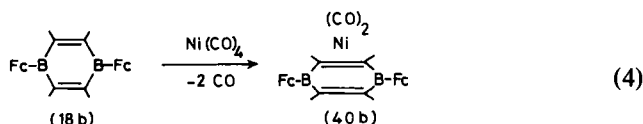
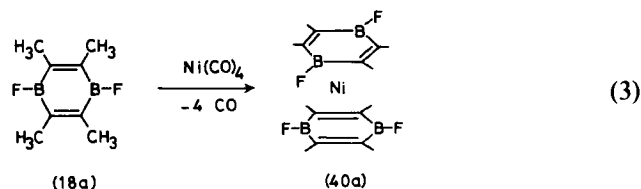
FIG. 9. Six- and seven-membered boracycle-metal complexes.

several complexes **[18a]·Fe(CO)₃**, **18a·Co(C₅H₅)**, **(18a)·Ni(CO)₂**, and **40a**] have been prepared and characterized by spectroscopic methods (44). X-Ray structure analysis of **18a** and **40a** showed that the ligand is also planar in the complex, having the four donor groups in tetrahedral positions. On complexation, the B—C bond is shortened from 1.56 to 1.53 Å, which is explained by a d-electron flow into (B—C) π orbitals (44, 45).

Herberich and Hessner (18) discovered a new route to 1,4-diboracyclohexadienes by treatment of 1,1,4,4-tetramethyl-1,4-distanna-2,5-cyclohexadiene with ferrocenyldibromoborane **Fc—BBr₂** [**Fc** = (C₅H₅)Fe(C₅H₄)]. The obtained compound (**18b**) undergoes controlled methanolysis, yielding **CH₃O—B(CH=CH)₂B—OCH₃** (**18c**), which was characterized as the nickel complex **[(CH₃O—B(CH=CH)₂B—OCH₃)₂Ni]** (**40c**). The methoxyl groups in **40c** can be replaced with methyl by using **Al₂(CH₃)₆**. Upon complexation of **18b** and **18c** with the metal, the ¹¹B-NMR signals (at 40.9 and 35 ppm) shift to 31 for **40b** and to 29.5 ppm for **40c**. ¹H-NMR data suggest a cyclic conjugation in the C₄B₂ ligand of **40b** and **40c**. (See Scheme 2.)

4. 1,2,5-Thiadiborolene (η^5 -C₂B₂S)

Several 3,4-diethyl-1,2,5-thiadiborolene derivatives (**12**; R = C₂H₅) obtained via redox reaction from (IBS)₃, BI₃, and 3-hexyne (24), have been studied with respect to their acceptor properties toward metal–ligand fragments. The synthesis of these complexes can be achieved thermally or photochemically (46, 47). The thermostable orange-red to deep-red tricarbonyliron complexes **41** [X = H, Cl, Br, I, CH₃, C₆H₅, SCH₃, OC₂H₅, N(CH₃)₂] are sensitive to moisture, with the exception of the organic derivatives. Presumably, the nucleophilic attack of H₂O occurs



SCHEME 2. Synthesis of 1,4-diboracyclohexadiene–metal complexes.

at the uncomplexed side of the C_2B_2S ring. The high reactivity of the iodo derivative allows controlled replacement of the iodine in the complex by H (with $LiBH_4$), by OC_2H_5 (with Et_2O , via ether cleavage) and by $N(CH_3)_2$ (with Me_2NH). Spectroscopic data indicate that the bonding situation between the ligand and the $Fe(CO)_3$ fragment is characteristically influenced by the Lewis acidity of the boryl group $B-X$. The ligand acts as a two-electron acceptor, a concept supported by Mössbauer, ^{11}B -NMR, and X-ray studies. The $\Delta\delta^{11}B$ values (15 to 53 ppm) increase with X in the following order: $N(CH_3)_2 < OC_2H_5 < C_6H_5 < SCH_3 < CH_3 < Cl < Br < I$. It is significant that reduction of the ligand **12** ($X = C_6H_5$) with potassium to the diamagnetic violet-red dianion results in an ^{11}B -NMR upfield shift of 17.5 ppm, similar to that observed on complexation with $Fe(CO)_3$ (**28**). In the IR spectrum, three CO bands are observed (with the exception of the dimethylamino derivative) [a_1 : 2034(s), e: 1966(vs) cm^{-1}]. The a_1 mode varies between 2075 ($X = Br$) and 2034 cm^{-1} , which reflects the decreasing acceptor properties of the ligand in **41**, X going from Br to $N(CH_3)_2$.

Krüger and co-workers (47) studied several thiadiborolene complexes by X-ray diffraction. A significant shrinking of the B—C bond length of the planar 2,5-bis(dimethylamino)-3,4-diethyl-1,2,5-thiadiborolene [B—C 1.59, B—S 1.84, C=C 1.36 Å] occurs on complexation with $Fe(CO)_3$, whereas the B—S and C—C bonds lengthen (B—C 1.54, B—S 1.88, C—C 1.45 Å). The excellent ligand properties of the thiadiborolene ring are best documented by the ability of benzothiadiborolene (**12**; $X = CH_3$, $RR = HC=CH-CH=CH$) to react with $Fe_2(CO)_9$, yielding the deep-red compound **42** (67%). Two electrons of the benzo system are used for η^5 -bonding, as suggested by ^{11}B - ($\delta = 26.4$ ppm) and ^{13}C -NMR (51) data, and proved by X-ray diffraction results (46). The distances in the benzo ring of **42** clearly demonstrate the fixation of the π^a -system as a cyclohexatriene having four long (1.42–1.45 Å) and two short (1.36, 1.34 Å) C—C bonds. The other relevant distances are: C—C 1.45, B—C 1.53, 1.52; B—S 1.87; C—Fe 2.22, 2.20; B—Fe 2.28; and S—Fe 2.34 Å. The short B—C bonds and the Mössbauer data are in agreement with the qualitative picture that the antiaromatic C_2B_2S ring accepts two electrons

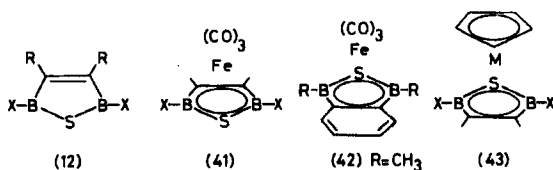


FIG. 10. 1,2,5-Thiadiborolene (**12**) and 1,2,5-thiadiborolene-metal complexes.

from the $\text{Fe}(\text{CO})_3$ fragment, forming a thiadiborolene dianion $[\text{C}_2\text{B}_2\text{S}^{2-}]$ isoelectronic with thiophene.

Cyclopentadienyl(1,2,5-thiadiborolene)cobalt (**43**; $\text{M} = \text{Co}$, $\text{X} = \text{CH}_3$) (**48**) and the paramagnetic nickel sandwich (**43**, $\text{M} = \text{Ni}$, $\text{X} = \text{CH}_3$) (**28**) have been obtained from the ligand **12**, $[(\text{C}_5\text{H}_5)\text{Co}(\text{CO})_2]$, and $[(\text{C}_5\text{H}_5)\text{Ni}(\text{CO})_2]$. As observed in the cyclopentadienyl-1,3-diborolenyl-nickel complex **26**, the electron density at the C_5H_5 ring is decreased in the cyclopentadienylthiadiborolenemetal sandwich complexes. An electrophilic attack of BX_3 , which, in the case of ferrocene, leads to the mono- and diborylation products $[\text{Fc}-\text{BX}_2, \text{Fc}(\text{BX}_2)_2]$ (**49**), does not occur at the C_5H_5 ligand, but at the thiadiborolene ring, resulting in replacement of a methyl group by halogen (**50**).

In contrast to compound **43** ($\text{M} = \text{Co}$), the 19-valence-electron sandwich **43** ($\text{M} = \text{Ni}$) is extremely air-sensitive. On heating to 120°C , ligand exchange occurs, yielding nickelocene and yellow-orange bis(thiadiborolene)nickel (**44**), which is also obtained from 1,2,5-thiadiborolene (**12**; $\text{X} = \text{CH}_3$) and $\text{Ni}(\text{CO})_4$ (**52**). In the first step, 1,2,5-thiadiborolene-dicarbonylnickel (**45**) is formed. For thiadiborolene nickel complexes, the expected tetrahedral arrangement of the electron-donating groups (S and $\text{C}=\text{C}$) was proved for the sandwich **44** by X-ray structural analysis ($\text{Ni}-\text{C}$ 2.12–21.5; $\text{Ni}-\text{B}$ 2.15–2.25; $\text{Ni}-\text{S}$ 2.30, 2.34 Å) (**52**). The parallel rings are rotated by $\sim 90^\circ$ in the crystal and in solution so that two different *B*-methyl groups are observed in the ^1H -NMR spectrum. However, in the ^{11}B -NMR spectrum, only a broad signal at 37 ppm appears. Molecular orbital calculations indicate a substantial barrier to internal rotation in thiadiborolene complexes (**53**). The tetrahedral position is 8.3 kcal/mol more stable than the planar arrangement of the four electron-donating groups in **45**, for which a "slipping" from η^5 - toward η^2 -coordination is predicted.

Like $\text{Ni}(\text{CO})_2$ and $\text{Fe}(\text{CO})_3$, the $\text{Cr}(\text{CO})_4$ fragment acts as a two-electron donor. Heating $\text{Cr}(\text{CO})_6$ and **12** yields the tetracarbonyl complex **46**, whereas photolysis produces the bis(thiadiborolene)dicarbonylchromium $[(\text{C}_2\text{B}_2\text{S})_2\text{Cr}(\text{CO})_2]$, in addition to **46** (**54**). The dicarbonyl compound is

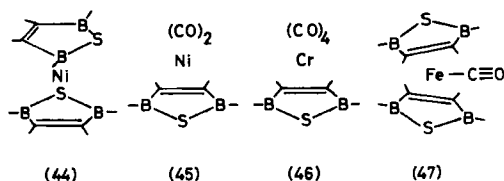


FIG. 11. Mono- and bis(thiadiborolene)metal complexes.

also obtained from $[(C_6H_6)Cr(CO)_3]$ and **12** ($X = CH_3$). From 1H -NMR and IR data, it was concluded that the CO groups are cis-arranged, each having a sulfur atom of ligand **12** in trans position. The red-violet bis(thiadiborolene)carbonyliron complex **47** has been obtained from **12** ($X = CH_3$) and $Fe(CO)_5$ in a photolytic reaction (39). An X-ray structural analysis (39, 40) revealed that the electron-donor groups build a square-pyramidal structure in which the two thiadiborolene rings are oriented trans to each other, and the CO is in apex position ($Fe-C$ 2.20–2.24; $Fe-B$ 2.30, 2.39; $Fe-S$ 2.33; $Fe-C\equiv O$ 1.79 Å). Attempts to eliminate the CO group from **47** to form the 16- and 18-electron sandwich complexes $[(C_2B_2S)_2Fe]$ and $[(C_2B_2S)_2Fe]^{2-}$ have failed. However, the isoelectronic anion **90** is obtained by "destacking" the triple-decker sandwich **84** with $C_5H_5^-$ (55). In an analogous reaction, $[(C_2B_2S)Mn(CO)_3]^-$ is formed from $[(CO)_3Mn(C_2B_2S)Fe(C_5H_5)]$ and $C_5H_5^-$ (56) (see Section IV,B).

5. 1,2,5-Azadiborolene ($\eta^5-C_2B_2N$)

The four-electron ligand **11** (57), obtained from **12** ($X = CH_3$) and $[(CH_3)_3Sn]_2NCH_3$, is a weak ligand in comparison with borole (**2**) and thiadiborolene (**12**). Due to the reduced donor and acceptor properties of **11**, complexes **48**, **49**, and **50** are only accessible, photochemically or thermally, in moderate yields. From the upfield ^{11}B -NMR shift ($\Delta\delta = 28$ –34 ppm), it is obvious that the 1,2,5-azadiborolene ligand is pentahapto-bonded to the metal (57). In the IR spectrum, the a_1 mode for the $Fe(CO)_3$ group in **48** is found at $\nu(CO)$ 2045 cm^{-1} , which indicates the weaker electron-acceptor properties of **11** in comparison with **12** ($a_1 = 2058$ cm^{-1} in **41**; $X = CH_3$). The complexes **48**–**50** exhibit lower thermal stability than the analogous thiadiborolene compounds. (See Fig. 12.)

C. Complexes Having Five-Electron Ligands

Borabenzene (η^6-C_5B)

Formal replacement of a CH group in benzene by boron should lead to borabenzene (borine, C_5H_5B), which is not known. Two synthetic ap-

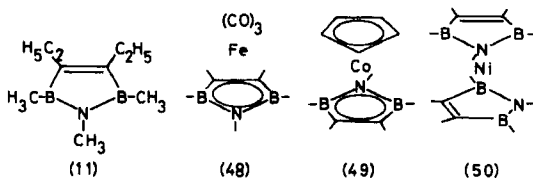


FIG. 12. 1,2,5-Azadiborolene (**11**) and 1,2,5-azadiborolene-metal complexes.

proaches to the borabenzene anion **17** have been reported. In 1970, Herberich and co-workers (15, 58a) discovered the ring expansion of cobaltocene with boron halides (e.g., CH_3BBr_2 , $\text{C}_6\text{H}_5\text{BCl}_2$, BCl_3 , $\text{C}_6\text{H}_5\text{BBr}_2$, BBr_3), yielding **51**, **52**, and **53**. The dark-red paramagnetic complexes **51** ($\text{R} = \text{C}_6\text{H}_5$, CH_3) are thermolabile and very air-sensitive, whereas the red paramagnetic compound **52** and yellow diamagnetic species **53** are thermo- and air-stable. The formation of these borinato-cobalt complexes proceeds by insertion of the borylene group $\text{R}-\text{B}:$ into the C_5H_5 ring, as in the reaction of cobaltocene with geminal dihalides H_2CX_2 . In the initial step, an *exo*-attack of RBX_2 on cobaltocene occurs, leading to $[(\text{C}_5\text{H}_5)_2\text{Co}]^+\text{X}^-$ and $(\text{C}_5\text{H}_5)\text{Co}(\text{C}_5\text{H}_5-\text{BR}(\text{X}))$. The latter is unstable and rearranges to **53**, which is reduced to the neutral complex **51** by cobaltocene. The second insertion of $\text{R}-\text{B}:$ into the C_5H_5 ring of **51** is much slower than the first, yielding bis(borinato)cobalt (**52**) [Eqs. (5)–(7)]. Both of the neutral complexes **51** and **52** are easily oxidized by FeCl_3 solution, affording the diamagnetic complexes **53** (58b, 59). Surprisingly, the oxidation product obtained from **52** [$\text{R} = \text{C}_6\text{H}_5$] is not the bis(borinato)cobalt cation, but the cyclopentadienylborinatocobalt cation **53**, isolated as the hexafluorophosphate in quantitative yield. This ring contraction is suppressed if such basic solvents as H_2O and CH_3OH are excluded. Oxidation of **52** with iodine or $[\text{Fe}(\text{C}_5\text{H}_5)_2]^+\text{PF}_6^-$ leads to $(\text{52})^+\text{I}_3^-$ and $(\text{52})^+\text{PF}_6^-$, respectively. The salts are extremely sensitive toward protonic solvents (59), forming **52** and **53**.

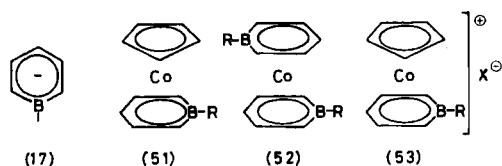
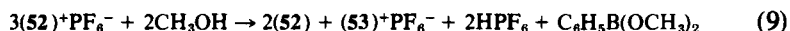
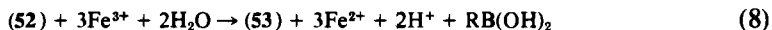
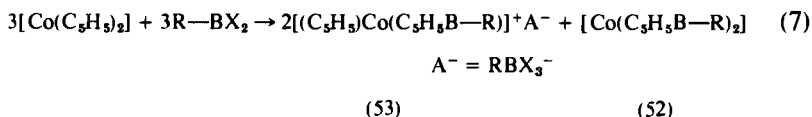
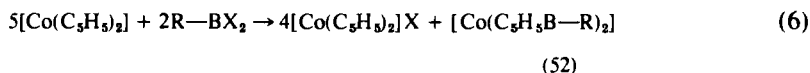
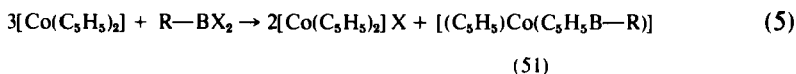


FIG. 13. Borabenzene anion (**17**) and borinatocobalt complexes (**51**–**53**).

It was concluded from ^1H - and ^{11}B -NMR data for the cationic borinato complexes and from the mass spectra of the neutral compounds that the borinato ligand is hexahapto-bonded. X-Ray diffraction analysis (60) of the bis(borinatocobalt) complexes (52, $\text{R} = \text{CH}_3$ and OCH_3) proved the proposed structures. In both centrosymmetric molecules, the nearly planar rings are parallel to each other. The $\text{Co}-\text{B}$ distances are 2.28 and 2.35 Å, and the $\text{Co}-\text{C}$ distances vary between 2.06 and 2.24 Å. This indicates that the cobalt atom is not symmetrically placed with respect to the borinato rings, but slightly slipped from the center of the rings toward the *para*-C atom (about 0.14 and 0.19 Å).

In an attempt to expand the *closo*-3-($\eta^5\text{-C}_5\text{H}_5$)-3-1,2- $\text{Co}(\eta^5\text{-C}_2\text{B}_9\text{H}_{11})$ to a 13-vertex metallocarborane, Hawthorne (58c) observed the insertion of $\text{C}_6\text{H}_5\text{-B}$ into the C_5H_5 ring, leading to the phenylborinato complex $\text{C}_6\text{H}_5\text{-(}\eta^6\text{-C}_5\text{H}_5\text{B)-3-1,2-Co}(\eta^5\text{-C}_2\text{B}_9\text{H}_{11})$ when the anion of the cobaltacarborane was reacted with phenylboron dichloride.

The second synthetic approach to the borinato (borabenzene anion) ligand was developed by Ashe and co-workers in 1971 (16, 61). The exchange reaction of 1,1-dialkylstannacyclohexa-2,5-diene with phenylboron dibromide yields the corresponding 1-boracyclohexadiene. On treatment with *t*-butyllithium, the borinato ligand is produced, which reacts with ferrous chloride to give red-orange bis(1-phenylborinato)iron (61), first reported by Herberich *et al.* (62) (*vide infra*). In analogous reactions, the methyl- and *t*-butylborinato iron complexes have been obtained.

Recently Herberich and co-workers (63, 64) described an elegant two-step synthetic route to borinato ligands by heating bis(borinato)cobalt complexes in acetonitrile with KCN or NaCN. The cyanide degradation of borinato complexes proceeds quantitatively to insoluble metal cyanide and borinato ligands.



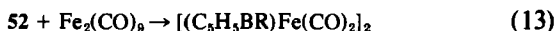
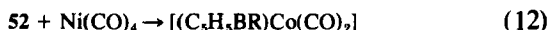
After filtration, the solutions were used directly for the synthesis (64) of diamagnetic $[\text{Ru}(\text{C}_5\text{H}_5\text{BR})_2]$, $[\text{Os}(\text{C}_5\text{H}_5\text{BR})_2]$, $[(1,5\text{-C}_6\text{H}_{12})\text{Rh}(\text{C}_5\text{H}_5\text{BR})]$, $[(\text{CH}_3)_3\text{Pt}(\text{C}_5\text{H}_5\text{BR})]$, and paramagnetic $[\text{Cr}(\text{C}_5\text{H}_5\text{BR})_2]$ (65) ($\text{R} = \text{C}_6\text{H}_5$, CH_3) as well as for the light-yellow thallium borinates $\text{Tl}[\text{C}_5\text{H}_5\text{BR}]$ ($\text{R} = \text{C}_6\text{H}_5$, CH_3). The latter are the first borabenzene derivatives of a main-group metal isolated in pure form (66). Their properties are similar to those of TlC_5H_5 .

In the paramagnetic electron-rich bis(borinato)cobalt complexes, the labilized metal-ligand interaction allows ligand exchange and transfer to other metals. The phenyl derivative of complex 52 reacts in boiling

toluene to give borinato-tricarbonylmanganese (67), whereas with $\text{Ni}(\text{CO})_4$ under similar conditions ligand exchange occurs to yield dicarbonyl(1-phenylborinato)cobalt (68). By treating **52** ($\text{R} = \text{CH}_3, \text{C}_6\text{H}_5$) with iron carbonyls, bis(borinato)diirontetracarbonyl complexes are obtained, for which a doubly CO-bridged cis-structure was proposed on the basis of IR data (62). The structures of the (1-phenylborinato)tricarbonylmanganese and di- μ -carbonyl-dicarbonylbis(1-methylborinato)diiron (**54**) have been determined by X-ray crystallographic methods (69). In both molecules the slightly acentric π -bonded borinato rings are almost planar (**54**: $\text{Fe}-\text{B}$ 2.30, $\text{Fe}-\text{C}$ 2.19–2.14 Å). Pyrolysis of **54** at 230°C affords the corresponding bisborinato-iron ($\text{C}_5\text{H}_5\text{BR}$)₂Fe (**55a**; $\text{R} = \text{C}_6\text{H}_5$) in good yield.



(52)



(54)

A third route to borinato complexes (**70**) involves thermal reaction of 4,4-dimethyl-1-phenyl-1-bora-2,5-cyclohexadiene with $\text{Mn}_2(\text{CO})_{10}$ and $\text{Re}_2(\text{CO})_{10}$, yielding **56** ($\text{M} = \text{Mn}, \text{Re}$). Upon heating the boracyclohexadiene complex **57**, bis(4-methyl-1-phenylborinato)iron (**55b**; $\text{R} = \text{H}$) is obtained by elimination of CH_3 , CO , and iron. In addition, higher methylated borinato complexes (e.g., **55c**, $\text{R} = \text{CH}_3$) have been isolated from the reaction mixture (**70**).

The synthesis of neutral borinato complexes of transition metals demonstrates the close structural and electronic relationship of this π^6 ligand to C_6H_6 and to C_5H_5^- , respectively. Herberich and co-workers (**71**) studied cationic and anionic species of the type $[\text{LM}(\text{C}_5\text{H}_5\text{B}-\text{C}_6\text{H}_5)]^+$ ($\text{L} = \text{Ligand}$), obtained by oxidation of neutral compounds or by reacting thallium phenylborinate with metal halide complexes. These cations are

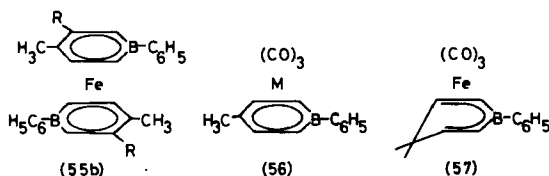
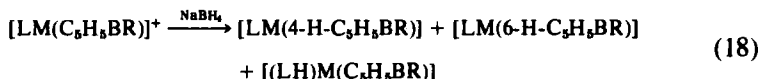
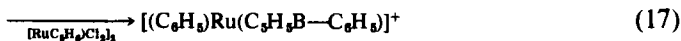
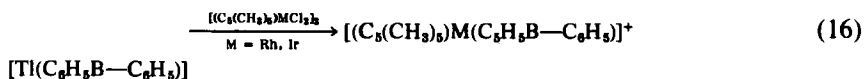
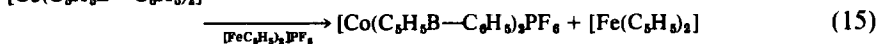
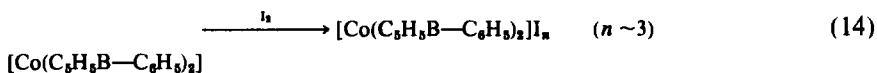


FIG. 14. Bis(borinato)iron (**55**) and borinato-tricarbonylmetal complexes (**56**) ($\text{M} = \text{Mn}$ or Re).

much more electrophilic than the corresponding cyclopentadienyl complexes $(LM(C_5H_5))^+$. With nucleophiles, three types of reaction are observed. Nucleophilic addition of pyridine at the boron atom of **51** yields **58**. The cyanide ion causes ring contraction of the cobalt complex, whereas the rhodium and iridium complexes $[(C_5(CH_3)_5)M(C_5H_5B-C_6H_5)]^+$ form stable donor-acceptor compounds (**59**). Sodium borohydride reacts with $[LM(C_5H_5BR)]^+$ in acetonitrile to yield three products ($R = C_6H_5$) by addition of H^- at the carbon atom. The addition of such nucleophiles as NH_3 , RNH_2 , R_2NH , OH^- , or CN^- to $[(C_5H_5)Co(C_5H_5BR)]^+$ ($R = C_6H_5$) results in quantitative ring contraction in the presence or absence of oxidizing reagents (**71a**).



ML	%	%	%
Co(C ₅ H ₅)	12	30	51
Co(C ₅ H ₅ BR)	30	38	—
Rh{C ₅ (CH ₃) ₅ }	20	21	60

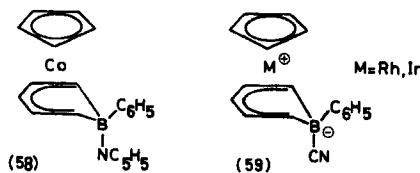
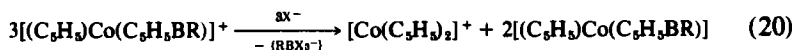
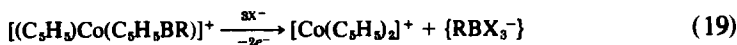
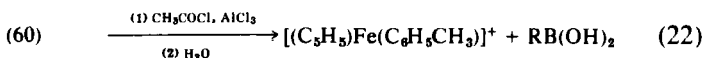
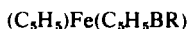
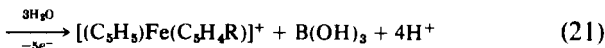


FIG. 15. Reaction products of borinato complexes with pyridine and cyanide.

This ring contraction by extrusion of the borylene group is the reverse of the insertion of $R-B:$ into the C_5H_5 ring of cobaltocene. The structures of these cationic species and their reaction products with nucleophiles have been elucidated by 1H - and ^{11}B -NMR and IR studies. In particular, the bonding situation at the boron was deduced by ^{11}B -NMR data, with shifts ranging from δ 24 to 17 for penta- and hexahapto complexes in which the boron atoms are involved in complex bonding. The pyridine addition products of type **58** exhibit ^{11}B shift values of δ -7 to -23 (upfield of external $Et_2O \cdot BF_3$), which proves the interaction of the pyridine with the boron atom.

Oxidation of the air-sensitive cyclopentadienyl(borinato)iron complexes (**60**; $R = CH_3, C_6H_5$) with silver salts or $(NH_4)_2Ce(NO_3)_6$ in methanol gives quantitative yields of monosubstituted ferricenium salts $[(C_5H_5)Fe(C_5H_4R)]^+$. This reaction is a new type of ring contraction in which the borinato ligand is converted into a monosubstituted cyclopentadienyl ligand by migration of R from the boron to the α -C atom. Similarly, bis(borinato)iron complexes are oxidized, yielding mono- and disubstituted cations $[(C_5H_5)Fe(C_5H_4R)]^+$ and $[Fe(C_5H_4R)_2]^+$, depending on the reaction conditions (71b).



Another interesting reaction has been observed in attempting a Friedel-Crafts acetylation of compound **60**. A unique ring-member substitution takes place, forming $[(C_5H_5)Fe(C_6H_5CH_3)]^+$ (**61**) and $RB(OH)_2$ after hydrolysis (71b). When applied to bis(borinato)iron, two products ($[(CH_3C_6H_5)Fe(C_5H_5BCH_3)]^+$ and/or the known (61) 2-acetyl derivative of $[Fe(C_5H_5BCH_3)_2]^+$) are obtained. For the 19-valence-electron cobaltocene, a polarographic half-wave potential of -1.88 V in acetonitrile was found (72). However, the anion is quite unstable at room temperature. Bis(borinato)cobalt (**52**; $R = CH_3, C_6H_5$) shows half-wave potentials at -0.018 and -1.245 V for the methyl and $+0.045$ and -1.105 V for the phenyl derivative of **52**. The anion **52**⁻ appears in the cyclic voltammogram as stable (73a). Again, this demonstrates that borinato ligands are stronger acceptors and weaker donors than the C_5H_5 ligand.

Cyclic voltammetry of (borinato)cyclopentadienyliron and of bis(borinato) complexes of iron, chromium, and vanadium revealed oxi-

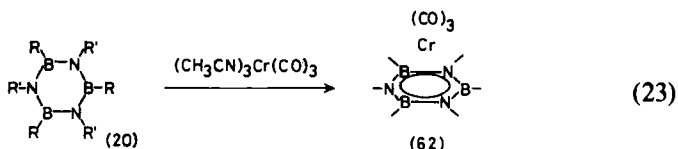
dation of the iron complexes with varying degrees of reversibility, depending on the solvent. Bis(borinato)iron is reduced in tetrahydrofuran (THF) to the corresponding anion, which is also obtained by reduction with K/Na alloy in THF. The chromium complexes reversibly give anions and cations, and the vanadium compound forms an anion. The potentials of all these electronic transitions are shifted to more positive values with respect to the isoelectronic metallocenes (73b).

Reduction of **52** with sodium amalgam produces $\text{Na}[\text{Co}(\text{C}_5\text{H}_5\text{BR})_2]$ compounds having 20 valence electrons. The phenyl derivative has a magnetic moment $\mu_{\text{eff}} = 2.97 \pm 0.1 \mu_{\text{B}}$ in THF solution. Metathesis with $[\text{P}(\text{C}_6\text{H}_5)_4]\text{Br}$ yields the stable salt $[\text{P}(\text{C}_6\text{H}_5)_4][\text{Co}(\text{C}_5\text{H}_5\text{BC}_6\text{H}_5)_2]$ with $\mu_{\text{eff}} = 2.89 \pm 0.05 \mu_{\text{B}}$. Reactions of the anions with nucleophiles afford products having one diene ligand (either 1-bora-2,5-cyclohexadiene or 1-bora-2,4-cyclohexadiene), which are also obtained by adding H^- to the corresponding cations $[\text{Co}(\text{C}_5\text{H}_5\text{BR})_2]^+$. Thermal decomposition of the anions in the presence of diene ligands leads to complexes of the type $(\text{cod})\text{Co}(\text{C}_5\text{H}_5\text{BC}_6\text{H}_5)$ ($\text{cod} = 1,5\text{-cyclooctadiene}$) and $(\text{nbd})\text{Co}(\text{C}_5\text{H}_5\text{BC}_6\text{H}_5)$ ($\text{nbd} = \text{norbornadiene}$) (**74**). INDO-SCF molecular orbital calculations for bis(borabenzene) metal complexes $\text{M}(\text{C}_5\text{H}_5\text{BR})_2$ ($\text{R} = \text{H}$; $\text{M} = \text{Cr, Mn, Fe, Co}$; $\text{R} = \text{CH}_3$; $\text{M} = \text{Fe, Co}$) have been reported (**75**). The results show that the borabenzene ligand is an intermediate between $\pi\text{-C}_5\text{H}_5$ and $\pi\text{-C}_6\text{H}_6$ in its bonding characteristics. For the bis(borinato)cobalt, the splitting of the formerly degenerate e_1 -level (d_{xz} , d_{yz}) is less than 3000 cm^{-1} , contrary to ESR interpretation (**76**).

D. Complexes Having Six-Electron Ligands

1. Borazine ($\eta^6\text{-B}_3\text{N}_3$)

Borazine ($\text{B}_3\text{N}_3\text{H}_6$) is isoelectronic and isostructural with benzene; it should thus function as an η^6 -ligand toward transition-metal complex fragments. However, no $[(\text{B}_3\text{N}_3\text{H}_6)\text{M}(\text{CO})_3]$ complex has been reported. Werner and co-workers (**21**) were the first to synthesize hexaalkylborazine-tricarbonylmetal compounds (**62**). Besides chromium (**62**; $\text{R} = \text{CH}_3$, C_2H_5 ; $\text{R}' = \text{CH}_3$, C_2H_5), molybdenum complexes have also been prepared and studied by nuclear magnetic resonance techniques (**21**, **22**). In the ^{11}B -NMR spectra a small upfield shift ($\Delta\delta = <10 \text{ ppm}$) occurs; this was observed by complexation of other π^6 -boron nitrogen heterocycles such as diazadiborines ($\text{C}_2\text{B}_2\text{N}_2$) and diazaboroline ($\text{C}_2\text{N}_2\text{B}$). Obviously, these small $\Delta\delta^{11}\text{B}$ values are a consequence of the π^6 system in the free ligand.



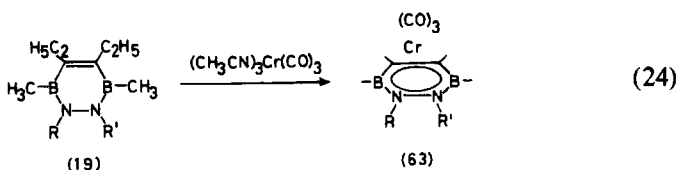
SCHEME 3. Synthesis of borazine-tricarbonylchromium complexes.

The electron density at the boron atoms in **20** seems to be less influenced by d^6 metal complex fragments than that in the π^4 systems 1,2,5-thiadiborolene ($\text{C}_2\text{B}_2\text{S}$) and 1,2,5-azadiborolene ($\text{C}_2\text{B}_2\text{N}$) by the $d^6\text{-Fe}(\text{CO})_3$ fragment.

An X-ray study of **62** ($\text{R} = \text{R}' = \text{C}_2\text{H}_5$) revealed that the borazine ring is slightly puckered (77) ($\text{Cr}-\text{B}$ 2.31(2), $\text{Cr}-\text{N}$ 2.22(2), $\text{B}-\text{N}$ 1.44(2) compared with 1.435(2) Å in free $\text{B}_3\text{N}_3\text{H}_6$). As the difference in the $\text{Cr}-\text{B}$ and $\text{Cr}-\text{N}$ distances is within the change in covalent radii, molecules of type **62** represent η^6 -complexes. Besides the π^6/d^6 -notation, cluster systematics apply to **62**, a compound that can be regarded as a seven-vertex *nido* structure with $(2n + 4) = 18$ framework electrons, supplied by $\text{B}(3 \times 2)$ and $\text{N}(3 \times 4)$.

2. 1,2-Diaza-3,6-diborine ($\eta^6\text{-C}_2\text{B}_2\text{N}_2$)

Between benzene and borazine, several isomeric boron-carbon-nitrogen heterocycles would be expected to exist as potential η^6 -ligands. The first example reported was the 1,2-diaza-3,6-diborine ring (**19**; $\text{R} = \text{R}' = \text{H}$ or CH_3 ; $\text{R} = \text{CH}_3$; $\text{R}' = \text{H}$) easily obtained from 1,2,5-thiadiborolenes (**12**) and hydrazines (**20**). Heating **19** with $[(\text{CH}_3\text{CN})_3\text{Cr}(\text{CO})_3]$ at 80°C (10 mm) affords orange-red diazadiborine-tricarbonylchromium complexes (**63**). The observed upfield shifts of 8–10 ppm are similar to those of borazine and diazaboroline complexes. In the IR spectrum, two bands [1955 and 1870 cm^{-1} for **63** ($\text{R} = \text{R}' = \text{H}$) in C_2Cl_4] appear, which indicates local C_{3v} symmetry for $\text{Cr}(\text{CO})_3$. X-Ray structural analysis, by Huttner (78), of **19** ($\text{R} = \text{R}' = \text{H}$) [$\text{B}-\text{N}$ 1.387(4), $\text{N}-\text{N}$ 1.391(3), $\text{B}-\text{C}$ 1.561(4), $\text{C}=\text{C}$ 1.371(4) Å] reveal that the $\text{B}-\text{N}$ distance is significantly shorter than in borazine [1.435(2) Å]. Upon complexation with $\text{Cr}(\text{CO})_3$, the $\text{N}-\text{N}$ and $\text{C}-\text{C}$ distances in **63** ($\text{R} = \text{R}' = \text{H}$) hardly change, whereas the $\text{B}-\text{N}$ bonds lengthen to 1.44(1) and 1.41(2) Å; the $\text{B}-\text{C}$ bonds shorten to 1.52(2) and 1.54(1) Å. Such shortening of $\text{B}-\text{C}$ bonds is typical for organoboron-transition-metal complexes. The metal ring-atom distances [$\text{Cr}-\text{N}$ 2.145(10), $\text{Cr}-\text{C}$ 2.30(1), $\text{Cr}-\text{B}$ 2.36(1)] vary with the



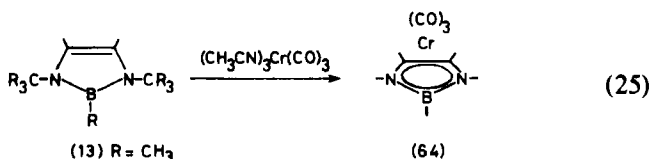
SCHEME 4. 1,2-Diaza-3,6-diborines (19) and tricarbylchromium complexes (63).

electron density at the atoms, as observed for other heteroaromatic complexes. In **63**, Cr—C is longer than in $[(\eta^6\text{-C}_6\text{H}_6)\text{Cr}(\text{CO})_3]$ (2.23 Å). The boron atoms are below the least-squares plane through the ring atoms by 0.08 and 0.1 Å, which indicates a bending of the $\text{C}_2\text{B}_2\text{N}_2$ ring along the B—B axis ($\angle \alpha = 12^\circ$).

As already outlined for other complexes, the bonding in **63** can be described by both the π^6/d^6 and the cluster systematics. The ligand offers its π^6 -system to the $\text{Cr}(\text{CO})_3$ fragment and accepts electron density from the filled d-orbitals. In the cluster description, compounds **63** have seven-vertex *nido* geometries with $2n + 4 = 18$ framework electrons, supplied by $\text{C}(2 \times 3)$, $\text{B}(2 \times 2)$, and $\text{N}(2 \times 4)$.

3. 1,3-Diaza-2-boroline ($\eta^5\text{-C}_2\text{N}_2\text{B}$)

Diazaborolines, isoelectronic with C_5H_5^- , have been obtained by dehydrogenation of diazaborolidines (79) and from α,β -diimines and halogenoboranes (80). From ^{11}B - and ^{14}N -NMR, UV, and PE studies, it was concluded that compounds of type **13** possess a π^6 -electron system and therefore should be able to complex the $\text{Cr}(\text{CO})_3$ fragment. This was proved by the formation (91%) of the yellow complex **64** (80a) (air-stable; decomp. above 170°C). As observed in borazine and diazadiborine complexes, only a small upfield shift (**13**, $\delta = 26.2$; **64**, $\delta = 18.3$ ppm) occurs in the ^{11}B -NMR spectrum. Its constitution has been derived from ^1H and ^{13}C -NMR, IR [$\nu(\text{CO})$ 1929 and 1813 cm^{-1}], and mass spectra data. (See Scheme 5.)



SCHEME 5. Synthesis of the 1,3-diaza-2-boroline-tricarbylchromium complex **64**.

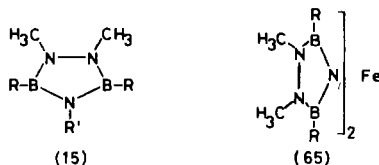


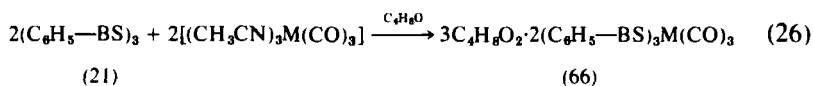
FIG. 16. 1,2,5-Triaza-3,5-diborolidine (15) and its iron complex (65).

4. 1,2,4-Triaza-3,5-diborolidine (B_2N_3)

The 1,2,4-triaza-3,5-diborolidine heterocyclic compound (15) is iso-electronic with $C_5H_5^-$ and 1,3-diaza-2-boroline (C_2N_2B) and therefore should function as a six-electron donor. However, attempts to synthesize η^5 -transition-metal complexes have failed (81). Metallation of 15 ($R' = H$; $R = CH_3$, C_6H_5) by alkyl lithium, gives the corresponding Li salts, which afford 65 (41%) on treatment with $FeCl_2$ (82). The tetramethyl derivative of 65 ($R = CH_3$) seems to be less stable in the solid state than in benzene solution. The ^{11}B -NMR signals of 65 ($R = CH_3$, $\delta = 28.5$; $R = C_6H_5$, $\delta = 26.8$ ppm) are only slightly shifted upfield by 2.9 and 2.1 ppm, respectively, relative to that of 15 (6). (See Fig. 16.)

5. Borthiine (B_3S_3)

In comparison with nitrogen, a sulfur atom is a "soft" electron donor, and therefore sulfur-containing ligands should readily form transition-metal complexes. However, early attempts by Nöth and Schuchardt (83, 85) and by Erl and Vahrenkamp (84) to complex boron sulfur compounds yielded only thermolabile products [e.g., $(RS)_3B \cdot Cr(CO)_3$]. This might be due either to weak acceptor properties or the "wrong" symmetry. In contrast, such cyclic boron sulfur ligands as 3,4-benzo-1,2,5-thiadiborolene (46) and 3,4-diethyl-1,2,5-thiadiborolene (47) proved to be good to excellent ligands, acting as four-electron donor-two-electron acceptors toward metal complex fragments. The six-membered-ring borthiine (21) reacts with $[(CH_3CN)_3M(CO)_3]$ ($M = Cr, Mo, W$) in dioxane solution to give the complexes 66 (23), in which the metal coordinates to the boron sulfur ring.



The complexes decompose slowly in C_6H_6 and CH_2Cl_2 solution, but are stable in dioxane. Attempts to remove the dioxane *in vacuo* resulted in

decomposition of **66**. This indicates that dioxane is chemically bound, most probably by coordination of the oxygen atom to the boron atoms. Thus, three dioxane molecules could bridge two $[(C_6H_5BS)_3M(CO)_3]$ molecules. The ^{11}B -NMR upfield shifts [**21**: $\delta = 62.7$; **66** ($M = Cr$): 30.5 ± 0.5 ppm] are in the range of C_2B_2S -metal complexes, which would indicate hexahapto bonding. However, coordination of dioxane to the boron atoms would result in a similar shift of the ^{11}B -NMR signal. Most probably, the B_3S_3 ring is no longer planar, having the sulfur coordinated to the $M(CO)_3$ fragment and the (sp^3) boron atoms to the oxygen atom of the solvent. The B_3S_3 ring in **66** may be regarded as an η^3 -trithia ligand.

III

DINUCLEAR COMPLEXES

A. Carbon Monoxide as Bridging Ligand

Several dinuclear complexes having π -ligands in terminal and CO in bridging positions have been reported since the first preparation of $[(C_5H_5)Fe(CO)_2]_2$. With boron heterocycles as five- and four-electron ligands, dimeric iron and cobalt complexes are to be expected. By reacting the bis(borinato)cobalt complexes (**52**; $R = CH_3$ or C_6H_5) with iron carbonyls at 70 – $120^\circ C$, the violet bis(borinato)diiron tetracarbonyl complexes **54** have been obtained (70–81%), for which a cis structure has been proposed on the basis of IR data (62) and established by X-ray structure analysis (69). Thermal decomposition of **54** at $230^\circ C$ yields bis(borinato)iron complexes (**55**).

Treating $[Co_2(CO)_8]$ with the four-electron donors thiadiborolene (**55**) and azadiborolene (**57**) yields dark red **67** and **68**. The IR data for **67** indicate a trans structure in the solid state [$\nu(CO) = 2025(s)$ and $1840(s)$ cm^{-1} , Nujol], whereas in *n*-hexane solution, four absorptions are found [$2028(vs)$, $1891(vs)$, $1852(s)$, and $1838(s)$ cm^{-1}], which reflect a cis structure. However, one of the bands ($\nu = 1891$ cm^{-1}) appears at an unex-

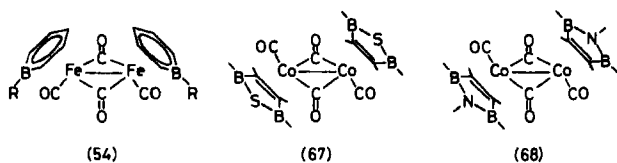


FIG. 17. Dinuclear complexes having borinato, thia-, and azadiborolene ligands.

pectedly low wavenumber. It is possible that this is caused by interaction of the sulfur atom with a terminal CO group. In contrast to **67**, the azadiborolene complex **68** shows only two CO bands [$\nu = 2004(s)$, $1826(s)$] in C_2Cl_4 solution. Most probably, the trans structure of **68** is caused by steric hindrance of the *N*-methyl group in the azadiborolene ring. A similar effect has been reported for $[(C_4H_4Me_2)Co(CO)_2]_2$ (trans), whereas $[(C_4H_6)Co(CO)_2]_2$ has a cis structure (86).

B. Boron Heterocycles in Bridging Positions

The most interesting feature of electron-poor boron heterocycles in complex chemistry is their use as bridging ligands in di- and trinuclear complexes. In 1972, the first, and at present the only, "triple-decker" sandwich having a $\mu-C_5H_5$ ligand, $[(C_5H_5)Ni(C_5H_5)Ni(C_5H_5)]^+$ (**27**), was reported (31, 32) and subsequently proved by X-ray structure analysis (87). Shortly thereafter, the synthesis of the first neutral triple-decker sandwich complexes—derivatives of $(C_5H_5)Co(C_2B_3H_5)Co(C_5H_5)$ (**30**)—was reported, with an X-ray structural study performed by Grimes and co-workers (35). Since 1976, systematic exploration of boron heterocycles as bridging ligands in dinuclear complexes has greatly extended our knowledge of this pattern of behavior, stimulated by Hoffmann's EH calculations (30) on Werner and Grimes's triple-decker sandwich complexes.

1. CO as Terminal Ligand

The tricarbonylmanganese fragment $(CO)_3Mn$ is a d^7 -electron species that supplies three orbitals and one electron for bonding to homo- and heterocycles (25). Thus, such two-electron acceptor ligands as borole (**2**), 1,2,5-thiadiborolene (**12**), and the hypothetical cyclopentadienyl cation $(C_5H_5^+)$ (**30**) should be capable of binding two $(CO)_3Mn$ fragments.

The first triple-decker complex of this type was obtained by Herberich and co-workers (88), when 1-phenyl-4,5-dihydroborepin and $Mn_2(CO)_{10}$ were heated for 70 hours in mesitylene. Chromatographic work-up gave the brown-red compound **69** (57%). From the IR pattern of the carbonyl groups [$\nu(CO) = 2022(vs)$, $1963(vs)$, $1952(vs)$ cm^{-1} in hexane], it was concluded that the borole, formed by ring contraction of the dihydroborepin, had replaced four CO ligands in $Mn_2(CO)_{10}$. The X-ray structure analysis established the triple-decker structure ($Mn-B = 2.24$ Å), having 30 valence electrons ($\sigma^6 d^6 \pi^6 d^6 \sigma^6$). Alternatively, **69** can be described as a metallocarbaborane cluster having a pentagonal-bipyramidal

framework. This is held together, according to the electron count for *closo* compounds (12), by $(2n + 2) = 16$ electrons, supplied by C (4×3), B (1×2), and $\text{Mn}(\text{CO})_3$ (2×1). The high-field ^{11}B -NMR signal at δ 17.6 ppm is typical for μ -ligands, in which the five-coordinated boron atoms are in bonding contact with two metal moieties.

As described earlier (Section II,B,4), the 1,2,5-thiadiborolene ring in **12** easily forms mononuclear complexes having *nido* structures. Analogous to **69**, the orange-red dinuclear compound **70** (21%) is obtained from **12** and $\text{Mn}_2(\text{CO})_{10}$ (89). Its constitution was deduced from IR [$\nu(\text{CO}) = 2021(\text{s})$, $1966(\text{s})$, $1956(\text{s}) \text{ cm}^{-1}$ in C_2Cl_4] and NMR data (^{11}B : 22.5 ppm; ^1H : a quartet signal) demonstrate the equivalence of the methylene protons of the ethyl group, and thus two equivalently bonded $\text{Mn}(\text{CO})_3$ groups in the triple-decker, which was proved by X-ray structure analysis [$\text{Mn} \cdots \text{Mn} = 3.51 \text{ \AA}$, one CO of $\text{Mn}(\text{CO})_3$ trans to sulfur (40)].

The formation of thiadiborolene triple-decker complexes depends on the Lewis acidity of the ring. In addition to **70** ($\text{X} = \text{CH}_3$), complexes with OC_2H_5 , SCH_3 , and C_6H_5 substituents at the boron atom have been prepared, whereas the dimethylamino derivative of **12** did not give any dinuclear complexes (90). A similar failure has been observed with the 1,2,5-azadiborolene heterocycle (57). Again, the bonding in these 30-valence-electron triple-decker compounds is described by either the π^6/d^6 or the cluster systematics, the latter requiring 16 framework electrons for the seven-atomic cage [$\text{C}(2 \times 3)$, $\text{B}(2 \times 2)$, $\text{S}(1 \times 4)$, $\text{Mn}(2 \times 1)$]. The C_3B_2 ligand **3a** can bind the $\text{Fe}(\text{CO})_3$ and the $\text{Mn}(\text{CO})_3$ moieties, yielding **71**, as indicated by mass spectra data (94). (See Fig. 18.)

2. CO and Cyclic Species as Terminal Ligands

A combination of a π -homocyclic or π -heterocyclic metal moiety, a carbonylmetal fragment $(\text{CO})_n\text{M}$, and an electron-poor boron heterocycle should lead to "unsymmetrical" triple-decker complexes. The first example (**72**) was reported by Grimes and co-workers (91), obtained from the reaction of $[(\text{CH}_3\text{---C})_2\text{B}_4\text{H}_4]_2\text{FeH}_2$ with $[(\text{C}_5\text{H}_5)\text{Co}(\text{CO})_2]$ under UV

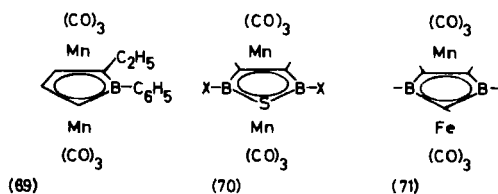


FIG. 18. Bis(tricarbonylmetal) triple-decker complexes.

light. The structure of red-brown compound **72** was proposed on the basis of ^1H - and ^{11}B -NMR and mass spectra data. However, an alternative isomer containing one metal in an equatorial location and the BH group in the apex position cannot be ruled out. Of course, the cluster description (16 framework electrons) applies for both the triple-decker and its (possible) isomer. The C_2B_3 ligand in **72** functions as an acceptor for four electrons, donated by the d^8 species $\text{Fe}(\text{CO})_3$ and $\text{Co}(\text{C}_5\text{H}_5)$.

Simultaneous reaction of 3,4-diethyl-2,5-dimethyl-1,2,5-thiadiborolene with $\text{Mn}_2(\text{CO})_{10}$ and $[(\text{C}_5\text{H}_5)\text{Fe}(\text{CO})]_2$ gives the green air-stable complex **73** (37%), which was characterized by ^{11}B - ($\delta = 18.0$ ppm) and ^1H -NMR, IR [2031(s), 1946(s), 1935(s) cm^{-1} , in C_2Cl_4], and mass spectra data (92). Treatment of **73** in benzene with AlCl_3 yields red-violet $[(\text{C}_6\text{H}_6)\text{Fe}\{(\text{EtC})_2(\text{CH}_3\text{B})_2\text{S}\}\text{Mn}(\text{CO})_3]^+\text{AlCl}_4^-$ (**85**). This triple-decker salt belongs to the diamagnetic 30-valence-electron species. It is the first dinuclear complex having a C_6H_6 ligand.

Heating of the paramagnetic triple-decker sandwich $[(\text{C}_5\text{H}_5)\text{Ni}\{(\text{EtC})_2(\text{EtB})_2\text{CMe}\}\text{Ni}(\text{C}_5\text{H}_5)]$ (**29**) with $\text{Mn}_2(\text{CO})_{10}$ in mesitylene forms paramagnetic blue-green **74** ($\text{M} = \text{Ni}$) (93). In contrast, the reaction of $[(\text{C}_5\text{H}_5)\text{Ni}\{(\text{EtC})_2(\text{EtB})_2\text{CMe}\}\text{Co}(\text{C}_5\text{H}_5)]$ (**80**) with $\text{Mn}_2(\text{CO})_{10}$ leads to diamagnetic **74** ($\text{M} = \text{Co}$) (94), which indicates a favorable formation of 30-over 31-valence-electron species. These exchange reactions of metal complex fragments are a new synthetic approach to triple-decker complexes.

Like $\text{Mn}(\text{CO})_3$, the $\text{Co}(\text{CO})_2$ group is a one-electron-donor moiety. However, attempts to prepare the bis(dicarbonylcobalt)- μ -thiadiborolene from tris(thiadiborolene)dicobalt (**84**) and $\text{Ni}(\text{CO})_4$ by ligand exchange failed. Only one thiadiborolene is substituted, resulting in the formation (69%) of the deep-red, unsymmetrical dinuclear complex **75** (55). The conformation of the two thiadiborolene rings is of particular interest with respect to that of tris(thiadiborolene)dicobalt (**84**), in which the bridging ring is rotated relative to the trans-oriented terminal rings by 90° (see the following section). The ^{11}B -NMR spectrum of **75** exhibits two signals ($\delta =$

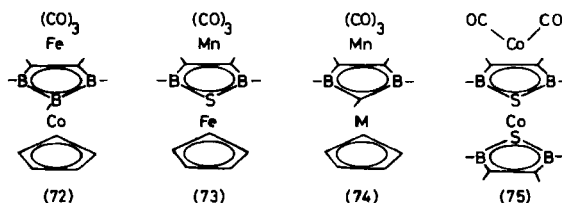


FIG. 19. Unsymmetrical triple-decker complexes with respect to terminal ligands and metals.

13.1 and 33.8 ppm) compared to $\delta = 15$ and 30 ppm (1:2 ratio) for the compound **84**. As usual, the highfield signal is assigned to the boron atoms in the bridging ligand. In the ^1H -NMR spectrum, two $\text{B}-\text{CH}_3$ signals in a 1:1 ratio are found; therefore, the two rings should be trans-oriented to each other as proposed for the anionic bis(thiadiborolene) cobalt (**90**). The interaction of the d^7 $\text{Co}(\text{CO})_2$ fragment with the sandwich (17 valence electrons) should be similar to that of $\text{Ni}(\text{CO})_2$ with 1,2,5-thiadiborolene, for which EH calculations predict a tetrahedral orientation of the electron-donor groups and a slipping of $\text{Ni}(\text{CO})_2$ from the center of the ring toward the $\text{C}=\text{C}$ group (**53**). To clarify this point, an X-ray structure analysis was carried out, which proved the conformation shown in **75** (**40**). The $\text{Co} \cdots \text{Co}$ distance (3.33 Å) is slightly longer than in **84** (3.30 Å). In the IR spectrum, $\nu(\text{CO})$ values 2035(s) and 1974(s) cm^{-1} are identical with those of $[(\text{C}_5\text{H}_5)\text{Co}(\text{CO})_2]$, but different from the values 2083(s) and 2038(s) of $[(\text{C}_2\text{B}_2\text{S})\text{Ni}(\text{CO})_2]$.

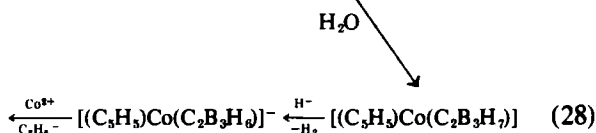
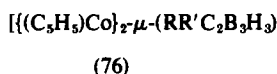
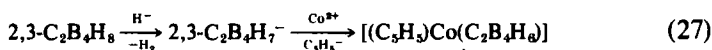
3. Triple-Decker Sandwich Complexes

According to the 30/34-valence-electron rule (**30**, **95**), the molecular architecture of triple-decker sandwich complexes allows for a variety of bridging ligands. In principle, homo- or heterocycles donating zero to eight electrons to two cyclopolyenyl- and/or heterocyclic metal complex fragments can be expected. Consider first the electron-rich carbocyclic ligands such as cyclooctatetraene and cyclopentadienyl. Skell *et al.* (**96**) reported that reduction of the yellow paramagnetic tris(cyclooctatetraene)dinitanium (**97**), which does not have an ideal triple-decker structure (**98**), yields diamagnetic $[(\text{C}_8\text{H}_8)_3\text{Ti}_2]^{2-}$, as predicted by theory (**30**). Surprisingly, only one C_8H_8 signal is observed in the ^1H -NMR spectrum of this 34-valence-electron species. Another $\mu\text{-C}_8\text{H}_8$ triple-decker complex was recently described by Moraczewski and Geiger (**99**). Electrochemical oxidation of $[(\eta\text{-C}_5\text{H}_5)\text{Co}(\mu\text{-C}_8\text{H}_8)\text{Co}(\eta\text{-C}_5\text{H}_5)]$, having 18 valence electrons around each metal, for a total of 36 electrons [a "near miss" to the triple-decker class (**30**)] generates the dication, which should have a triple-decker structure with a planar $\mu\text{-C}_8\text{H}_8$ ring (**99**).

No $\mu\text{-C}_7\text{H}_7^+$ and $\mu\text{-C}_6\text{H}_6$ dinuclear complex is as yet known. The only example of a $\mu\text{-C}_5\text{H}_5$ triple-decker is the cation $[(\eta^5\text{-C}_5\text{H}_5)\text{Ni}(\mu\text{-C}_5\text{H}_5)\text{Ni}(\eta^5\text{-C}_5\text{H}_5)]^+$ (**31**, **32**, **95**, **100**, **101**). Discovery of four-, three-, and two-electron μ -ligands has opened up this new field, as described later. A triple-decker complex having a one-electron [e.g., $\text{HC}(\text{BH})_4$] or the zero-electron ligand $[\text{B}_5\text{H}_5]$ has not yet been reported. Two $(\text{C}_5\text{H}_5)\text{Ni}$

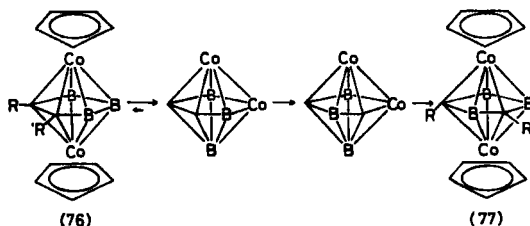
groups as three-electron donors are required for the Ni_2B_5 cluster $[(\eta^5\text{-C}_5\text{H}_5)\text{Ni}(\mu\text{-B}_5\text{H}_5)\text{Ni}(\eta^5\text{-C}_5\text{H}_5)]$ (7).

a. Complexes Having the Two-Electron μ -Ligands 2,3- C_2B_3 and 2,4- C_2B_3 . As outlined in Section I,A, the isomeric $\text{C}_2\text{B}_3\text{H}_5$ rings have no independent existence. However, Grimes and co-workers were able to construct triple-decker complexes with the hypothetical isomeric anions $\text{C}_2\text{B}_3\text{H}_5^{4-}$. The red complexes **76** ($\text{R} = \text{R}' = \text{H}$) and its derivatives have been prepared by the following reaction sequence [Eqs. (27, 28)] (35, 102, 103).



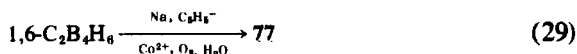
A small amount of the C, C' -1,3-propenylene-bridged derivative **76** ($\text{R} = \text{R}' = \text{CH}_2\text{-CH=CH}$) was obtained from the reaction of B_5H_8^- with Co^{2+} and C_5H_5^- in THF (104). The X-ray structural analysis ($\text{Co} \cdots \text{Co}$ 3.14 Å) proved the insertion of a cyclopentadienyl ring into the metalloboron cage.

The structural parameters of **76** ($\text{R} = \text{R}' = \text{H}$ and $\text{R} = \text{H}$, $\text{R}' = \text{CH}_3$) are nearly identical, the C_2B_3 rings being planar and symmetrically bonded to the $(\text{C}_5\text{H}_5)\text{Co}$ moieties [Co -ring plane 1.568(1) and 1.570(1) Å]. From ^1H - and ^{11}B -NMR and structural data, it was concluded that a strong (local) interaction is present between the metals and the $\text{C}=\text{C}$ bond as well as the central boron atom ($\delta^{11}\text{B}$: 53.3 ppm in the 5-position and 5.7 ppm in the 4,6-positions) (102). This is in contrast to the μ -2,4- C_2B_3 triple-decker complexes **77**, in which the electron density is more uniformly distributed over the three boron atoms ($\delta^{11}\text{B} = 21.2$ in the 5,6- and 11.9 ppm in the 3-position). The structures of green **77** are very similar to those of derivatives of **76** ($\text{Co} \cdots \text{Co}$ 3.14 Å); both types of triple-decker complexes are thermally and hydrolytically stable. However, the red compound **76** quantitatively isomerizes above 300°C to the green complex **77** having nonadjacent carbon atoms in the C_2B_3 ring (105). The rearrangement to the thermodynamically favored product occurs via two metallocarboranes having adjacent cobalt atoms in the $\text{C}_2\text{B}_3\text{Co}_2$ polyhedron. These were isolated when the reaction was carried out at lower temperatures (200–250°C). Possibly, the mechanism involves a cooperative rotation of Co_2B and CoB_2 triangular faces on the surface of the



SCHEME 6. Thermal rearrangement of 1,7,2,3-(η^5 -C₅H₅)Co(C₃B₂H₅)Co(η^5 -C₅H₅) (76) to the 1,7,2,4-isomer 77 via two metallocarboranes.

polyhedron. Compound 77 is also obtained from *closo*-1,6-C₂B₄H₆ in 4% yield (103) [cf. Eq. (29)]. (See Scheme 6.)



Sneddon *et al.* (106) described the reaction of cyclopentadiene, pentaborane(9), and 2-butyne with cobalt atoms, which yielded complex 76 (R = R' = CH₃, 1.3%), as well as two other metallocarboranes.

b. Complexes with the Three-Electron μ -Ligand 1,3-B₂C₃. As described in Section II,A,1, the difunctional Lewis acid 1,3-diborolene reacts with [(C₅H₅)Ni(CO)]₂ and [Co₂(CO)₈] to yield the mononuclear complexes 26 and 31 (Scheme 1), in which the η -ligand can act as three-electron acceptor. At 180–200°C, a simultaneous reaction of the 1,3-diborolene (3) with [(C₅H₅)Fe(CO)₂]₂ and [(C₅H₅)Co(CO)₂] as suppliers of (C₅H₅)Fe as a one- and (C₅H₅)Co as a two-electron donor moiety, affords the green compound 78 (R = C₂H₅, R' = CH₃; 10%). Its constitution is derived from ¹¹B- (δ = 19.6 ppm) and ¹H-NMR spectra studies; the latter exhibits two C₅H₅ signals in a 1:1 ratio (32). This unsymmetrical triple-decker sandwich is the first member of the μ -1,3-diborolenyl-bis(cyclopentadienylmetal) triple-decker family having 30–34 valence electrons. According to EH calculations (30), it should be possible to fill the slightly antibonding MOs (e_1' for [(C₅H₅)₃Ni₂]⁺) successively. As expected, the 31- and 33-valence-electron triple-decker complexes possess one unpaired electron, whereas the 32-valence-electron species have two.

The yellow-green Co₂ compound 79 (R = C₂H₅, R' = CH₃) has been obtained from 3 (Scheme 1) and [(C₅H₅)Co(CO)₂] in only 15% yield (34, 39) because of the formation of side products. (The released CO easily inserts into 3; see Section II,A,2.) However, blue-green 80 and deep-green 29 can be prepared almost quantitatively by "stacking" the diamagnetic nickelocene analog 26 with [(C₅H₅)Co(CO)₂] and [(C₅H₅)Ni(CO)]₂,

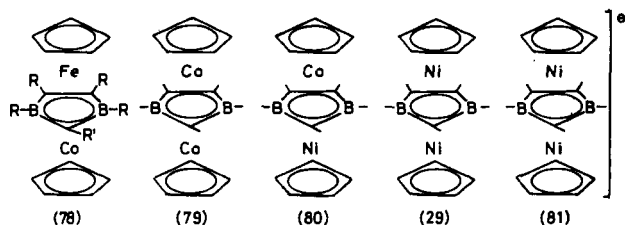
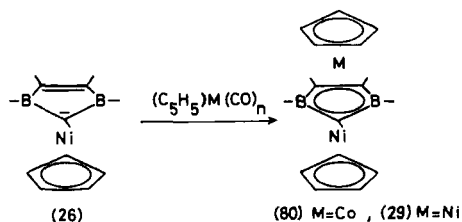


FIG. 20. Bis(η^5 -cyclopentadienylmetal)(μ -1,3-diborolene) triple-decker sandwich complexes (78—81).

respectively (34, 39). On reduction with potassium in tetrahydrofuran- d_8 , the deep-red diamagnetic complex **81** having 34 valence electrons is formed; this exhibits in its ^1H -NMR spectrum the expected singlet for the two C_5H_5 and a quartet for the methylene protons of the $\text{C}-\text{C}_2\text{H}_5$ groups. In comparison to **78** (δ 19.6), the ^{11}B -NMR signal is shifted upfield (δ 5.6), indicating the higher electron density at the boron atoms. A weaker metal-boron interaction would be expected in the 34- than in the 30-valence-electron complex because, in the former, the metal-metal distance should be near 3.55 Å, but in the latter, near 3.15 Å. Unfortunately, the poor quality of the crystalline material precluded X-ray structural studies of the neutral, the cationic, or the anionic species; this poor quality might be due to the four ethyl groups in the μ - C_3B_2 ring.

The neutral triple-decker sandwich complexes dissolve readily in hexane and can be recrystallized from $\text{Et}_2\text{O}/\text{CH}_3\text{CN}$. They sublime in melting-point tubes above 120°C and deliquesce between 220 and 270°C . On treatment with AgBF_4 , oxidation to the corresponding cationic triple-decker complexes occurs; these dissolve in CHCl_3 or CH_2Cl_2 , yielding olive-green 29^+ and 79^+ and deep-red solutions of 80^+ . Electrochemical investigations confirm the reversible uptake and release of electrons in these triple-decker sandwich complexes (107).

It is of interest that **78** and the isoelectronic cation 79^+ have the same



SCHEME 7. "Stacking" of the sandwich **26** with $(\text{C}_5\text{H}_5)\text{M}$ fragments.

^{11}B -NMR shift, δ 19.6. For the paramagnetic neutral and cationic dinuclear complexes, no ESR signals have been obtained. However, in the ^1H -NMR spectrum of the paramagnetic neutral compounds, typical paramagnetic shifts occur. As the 33-valence-electron triple-decker **29** is easily reduced to its diamagnetic anion, the contact shifts have been studied by successive reduction of **29** with potassium (39).

The bonding in **78** to **81** can be considered in terms of aromaticity and cluster formalisms. In each dinuclear compound, three π^6 -systems are held together by two metals with a total of 12–16 d-electrons. According to the cluster description, the seven-atomic *closo* systems $\text{C}_3\text{B}_2\text{MM}'$ require $(2n + 2) = 16$ skeletal electrons, supplied in **78** by C (3×3), B (2×2), Fe (1), and Co (2). Complex **81** has four electrons more than the required number for *closo* systems; consequently, instead of the $(2n + 2)$, the $(2n + 6)$ rule for *arachno* structures should apply. However, no opening of the cage, as observed upon reduction of polyhedral boranes and carbaboranes, is expected here, but rather a lengthening of the metal–ring distance as a consequence of successive filling of the weakly anti-bonding e'_1 level. This was first pointed out by Grimes (296) for **27**.

c. Complexes with the Four-Electron μ -Ligands C_4B and $\text{C}_2\text{B}_2\text{S}$. Within the series of isoelectronic 30-valence-electron triple-decker sandwich complexes $(\eta^5\text{-C}_5\text{H}_5)\text{M}(\mu\text{-R}_5\text{B}_n\text{C}_{5-n})\text{M}'(\eta^5\text{-C}_5\text{H}_5)$ (**7**), the borole complex **82** is located between the 1,3-diborolene complex **78** ($n = 2$) and the hypothetical $(\text{C}_5\text{H}_5)\text{Fe}(\text{C}_5\text{H}_5)\text{Mn}(\text{C}_5\text{H}_5)$ ($n = 0$).

Green complex **82** was obtained from 1-phenyl-3,4-dihydroborepin and $[(\text{C}_5\text{H}_5)\text{Fe}(\text{CO})_2]_2$. The X-ray structure analysis revealed that the metal–metal distance (3.27 Å) is longer than that (3.14 Å) in the two isomeric $[(\text{C}_5\text{H}_5)\text{Co}(\text{C}_2\text{B}_3\text{H}_5)\text{Co}(\text{C}_5\text{H}_5)]$ complexes.

Reaction of 1,2,5-thiadiborolene (**12**) with $[(\text{C}_5\text{H}_5)\text{Fe}(\text{CO})_2]_2$ in boiling mesitylene affords the green, diamagnetic complex **83** ($\text{R} = \text{C}_2\text{H}_5$) (11%). Its constitution was derived from ^{11}B - (δ 12.0) and ^1H -NMR spectroscopy and proved by an X-ray structure analysis (108). The central $\text{C}_2\text{B}_2\text{S}$ ring

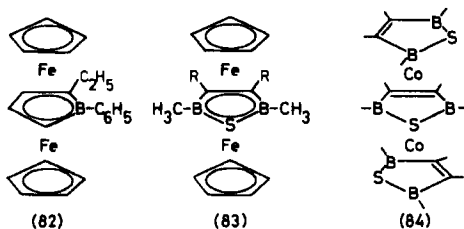


FIG. 21. Borole and thiadiborolene triple-decker sandwich complexes.

is planar, and the Fe...Fe distance [3.236(1) Å] is shorter than in **82**, which may reflect the favorable donor-acceptor properties of the C_2B_2S over the C_4B ligand. Bis(η -thiadiborolenecobalt) μ -thiadiborolene (**84**) is the first "homogeneous" triple-decker sandwich complex composed of three heterocyclic ligands and two metals. It is obtained by insertion of the ligand **12** (BCH_3) into the bridging position of **67**. An easier route to **84** is the direct reaction of **12** with $Co_2(CO)_8$, which applies also for the synthesis of the iodo (**84**, BI), the bromo (**84**, BBr), and the chloro derivative (**84**, BCl). The triple-decker structure follows from 1H - and ^{11}B -NMR data for **84** (BCH_3): ^{11}B (δ 15 and 30), 1:2 ratio for boron atoms in the bridging and terminal ligands, and an X-ray study thereof (40). Two molecules (enantiomers) are in the unit-cell, which differ in the orientation of the bridging ring relative to the trans-oriented terminal ligands, as shown in **84**. The metal-metal distance is 3.296(1) Å, and the metal-ring distance is slightly smaller for the bridging than for the terminal ligands. As with mononuclear complexes, the ligands are planar; however, the bond lengths indicate the differences in coordination: B—S = 1.894 Å in the bridging and 1.862 Å in the terminal ligand. Similarly, the C=C bond is lengthened in the central ring (1.458 vs. 1.425 Å); this is caused by coordination to both Co atoms. These structural data reflect the *closo* cluster with $(2n + 2) = 16$ framework electrons supplied by C (2×3), B (2×2), S (4), and Co (2×1). Each of the two *nido* clusters in **84** requires $(2n + 4) = 16$ skeletal electrons. A total of 48 framework electrons are counted in the cluster description, and 30 in the π^6/d^6 formalism.

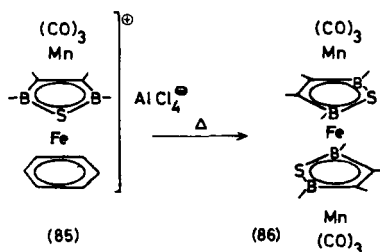
IV

TRINUCLEAR COMPLEXES

Since the first preparation of triple-decker complexes, the possibility of constructing oligo-decker and poly-decker species [quadruple-decker (95), "multiple-decked stacked compounds" (35)] has received attention. At this time, few published data are available.

A. Carbon Monoxide as Terminal Ligand

As described in Section III,B,2, the unsymmetrical triple-decker complex **73** reacts with $AlCl_3$ in benzene to afford the red-violet triple-decker salt **85** which, on heating to 140°C *in vacuo*, yields the orange-red trinuclear

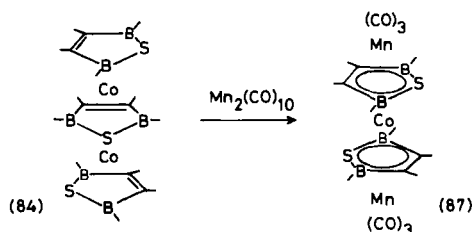


SCHEME 8. Thermolysis of the triple-decker salt **85**, yielding the tetra-decker complex **86**.

clear complex **86** in milligram amounts. The structure of this first tetra-decker compound was derived from the IR [$\nu(\text{CO}) = 2033, 1955, 1944 \text{ cm}^{-1}$] and field-desorption mass spectra data and proved by an X-ray diffraction study (92). The two independent molecules in the triclinic unit-cell are characterized by an inversion center (Fe); this is the first complex having two adjacent $\text{C}_2\text{B}_2\text{S}$ rings trans-arranged. Recently, a similar trans orientation for the two ligands in **90** (BCH_3) has been postulated on the basis of $^1\text{H-NMR}$ data (55), whereas in the isoelectronic nickel sandwich (**44**) and the triple-decker complex $(\text{C}_2\text{B}_2\text{S})_3\text{Co}_2$ (**84**) the electron-donating groups are in tetrahedral positions. If one regards **86** as being composed of two $[(\text{CO})_3\text{Mn}(\text{C}_2\text{B}_2\text{S})]^-$ half-sandwiches (18 valence electrons) and iron- d^6 , the trans orientation of the two π^6 -heterocycles is expected. As in the other thiadiborolene-tricarbonylmethyl complexes, one CO ligand of the $\text{Mn}(\text{CO})_3$ group is trans to the sulfur atom. The bond lengths of the bifacial coordinated $\text{C}_2\text{B}_2\text{S}$ rings are characteristically lengthened relative to those in mononuclear $\text{C}_2\text{B}_2\text{S}$ complexes [$\text{B-S } 1.928(7)$, $\text{B-C } 1.544(9)$, $\text{C-C } 1.477(9)$, $\text{Mn} \cdots \text{Fe } 3.408(1)$ and $3.391(1) \text{ \AA}$]. According to the π^6/d^{6-8} systematics, complex **86** represents the first member of the 42- to 48-valence-electron family ($2 \times \sigma^6 + 2 \times \pi^6 + 3 \times d^6$). The equivalent cluster description requires, for each of the two $\text{C}_2\text{B}_2\text{SFeMn}$ *closo* systems, 16 framework electrons, supplied by C (2×3), B (2×2), S (4), Fe (1), and Mn (1).

The next member of the hexacarbonyl-trinuclear complexes (43 electrons) was obtained in an attempt to exchange one $(\text{C}_2\text{B}_2\text{S})\text{Co}$ fragment in **84** for $\text{Mn}(\text{CO})_3$. Under the reaction conditions, the triple-decker product $(\text{C}_2\text{B}_2\text{S})\text{Co}(\text{C}_2\text{B}_2\text{S})\text{Mn}(\text{CO})_3$, formed in the first step, is "stacked" with $\text{Mn}(\text{CO})_3$ to the symmetrical tetra-decker complex (**87**).

The dark-green, paramagnetic complex exhibits an eight-line ESR spectrum due to the Co atom ($I = 7/2$). No coupling with Mn ($I = 5/2$) is observed, which indicates that the unpaired electron is in a cobalt orbital.

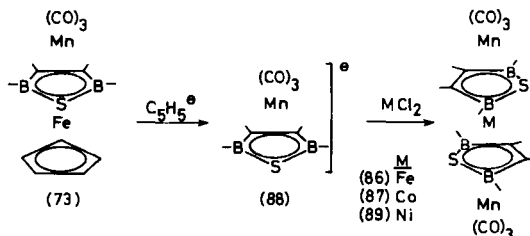


SCHEME 9. Replacement of one $(\text{C}_2\text{B}_2\text{S})\text{Co}$ fragment in **84** by two $\text{Mn}(\text{CO})_3$ groups.

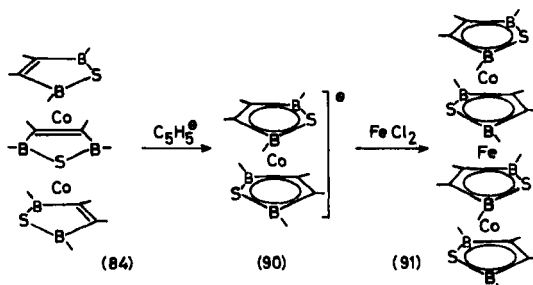
The $\nu(\text{CO})$ absorptions of **87** are identical to those of the corresponding iron complex (**92**). An independent route to these complexes was found, consisting of the following reaction sequence (Scheme 10). The unsymmetrical triple-decker **73** is attacked by C_5H_5^- , resulting in the formation of two mononuclear complexes, ferrocene and thiadiborolene-tricarbonylmanganese anion **88**, which could not be obtained from the reaction of 1,2,5-thiadiborolene **12** with $(\text{CO})_5\text{MnNa}$ (**90**). Anion **88** reacts with metal halides to yield the trinuclear species **86**, **87**, and **89**. IR and mass spectra data on the Ni complex **89** are in agreement with a tetra-decker structure.

B. Tetra-decker Sandwich Complexes

The triple-decker sandwich **73** is barely attacked by C_5H_5^- , yielding only minor quantities of ferrocene. However, **84**, having slightly longer metal-metal distances than **73**, reacts with cyclopentadienyl anion to yield **43** (BCH_3 , $\text{M} = \text{Co}$) and the sandwich anion **90**, which was isolated as its tetraphenylphosphonium salt. Treatment of **90** with FeCl_2 gave the dark-red crystalline trinuclear complex **91**, for which on the basis of analytical and spectroscopic data a tetra-decker sandwich structure was proposed (*55a*, *109*) and confirmed by an X-ray diffraction study (*110*).



SCHEME 10. Cleavage of **73** with C_5H_5^- to yield ferrocene and the anion **88**, which forms tetra-decker complexes with metal halides.



SCHEME 11. Reaction of the sandwich anion **90**, obtained by "destacking" of **84**, with FeCl_2 , to afford the tetra-decker sandwich **91**.

Tetra-decker sandwich complexes with terminal C_5H_5 rings have been reported by Grimes (111) and the author (109). The reaction of the anion $[(\text{C}_5\text{H}_5)\text{Co}(\text{Me}_2\text{C}_2\text{B}_3\text{H}_4)]^-$ with CoCl_2 yields the black compound **92**. Its structure is based on ^{11}B -NMR and mass spectra data. Confirmation by an X-ray diffraction study has not yet been possible (3, 111). Reduction of $[(\text{C}_5\text{H}_5)\text{Ni}(\text{Et}_4\text{C}_3\text{B}_2\text{Me})]$ with potassium gives a brown-red anion which, on treatment with NiCl_2 , yields deep-green **93** [27, 39]. The reactions of $[(\text{C}_5\text{H}_5)\text{Fe}(\text{C}_2\text{B}_2\text{S})]^-$ with MX_2 ($\text{M} = \text{Fe}, \text{Co}$) afford the tetra-decker sandwich complexes $[(\text{C}_5\text{H}_5)\text{Fe}(\text{C}_2\text{B}_2\text{S})]_2\text{M}$ with 42 and 43 valence electrons, respectively (112). Electron count according to cluster systematics divides these trinuclear compounds into two *nido* ($n = 6$) and two *closo* frameworks ($n = 7$), each requiring 16 electrons. Thus, a total of 64 skeletal electrons are counted in the cluster compared with 42 valence electrons for the first member of the corresponding tetra-decker sandwich families in the π^6/d^6 description.

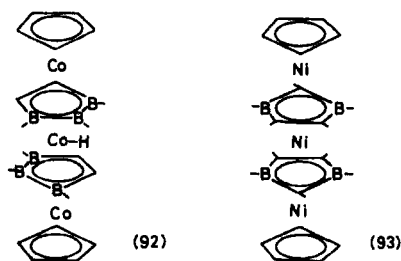


FIG. 22. Tetra-decker sandwich complexes having $\eta^5\text{-C}_5\text{H}_5$ ligands.

V

CONCLUSION

Among boron-containing ligands, the electron-poor heterocycles C_5B , C_4B , C_2B_2S , C_3B_2 , and C_2B_3 exhibit fascinating chemistry and link together the classical areas of π -complexes and polyhedral systems with such topics as metalloboranes and metallocarboranes. To demonstrate this relationship, the π^6/d^6 and the equivalent skeletal electron count have been frequently used in this article. In particular, ligands able to donate four or fewer electrons to metals and/or metal-complex fragments should allow further development of the field of oligo-decker compounds.

ACKNOWLEDGMENTS

I wish to thank my graduate and postdoctoral co-workers Gunter Augustin, Manfred Bochmann, Christian Böhle, Joseph Edwin, Mohyi El-Din M. El-Essawi, Roland Full, Klemens Kinberger, Holger Leichthammer, Thomas Renk, Wilfried Rothermel, Werner Ruf, Chitta Ranjan Saha, Hans Schmidt, and Gerhard Seibel for their individual contributions, indicated in the references. Generous support of our studies by the Deutsche Forschungsgemeinschaft and the Fonds der Chemischen Industrie is gratefully acknowledged.

REFERENCES

1. E. O. Fischer and H. Werner, "Metall- π -Komplexe mit di- und oligoolefinischen Liganden." Verlag Chemie, Weinheim, 1963.
- 1a. B. L. Shaw and N. I. Tucker, in "Comprehensive Inorganic Chemistry," Vol. 4, p. 781. Pergamon, Oxford, 1973.
2. R. N. Grimes, "Reactions of Metallocarboranes," in *Organometallic Reactions and Syntheses* (E. I. Becker and H. Tsutsui, eds.), Vol. 6. Plenum, New York, 1977; L. J. Todd, *Adv. Organomet. Chem.* **8**, 87 (1970); K. P. Callahan and M. F. Hawthorne, *ibid.*, **14**, 145 (1976).
3. R. N. Grimes, *Coord. Chem. Rev.* **28**, 47 (1979).
4. G. L. Schmid, "Houben/Weyl," Vol. XIII/3. Thieme, Stuttgart, 1979; *Angew. Chem.* **82**, 920 (1970).
5. K. Niedenzu and D. W. Dawson; M. F. Lappert; E. L. Muetterties, in "The Chemistry of Boron and Its Compounds." Wiley, New York, 1967.
6. H. Nöth, *Int. Symp. Inorg. Ring Systems*, 2nd., 1978; H. Nöth and B. Wrackmeyer, "Nuclear Magnetic Resonance Spectroscopy of Boron Compounds." Springer-Verlag, Berlin, and New York, 1978.
7. W. Siebert, *Nachr. Chem. Tech.* **25**, 597 (1977).
8. C. W. Allen and D. E. Palmer, *J. Chem. Ed.* **55**, 497 (1978).
9. (a) J. J. Eisch, N. K. Hota, and S. Kozima, *J. Am. Chem. Soc.* **91**, 4575 (1969); (b) J. J. Eisch, *Adv. Organomet. Chem.* **16**, 67 (1977).
10. G. E. Herberich, J. Hengesbach, U. Kölle, and W. Oschmann, *Angew. Chem.* **89**, 43 (1977); *Angew. Chem. Int. Ed. Engl.* **16**, 42 (1977).
11. P. Binger, *Angew. Chem.* **80**, 288 (1968); *Angew. Chem. Int. Ed. Engl.* **7**, 286 (1968).

12. (a) K. Wade, *Chem. Commun.* p. 792 (1971); (b) *Chem. Br.* 11, 177 (1975); (c) *Adv. Inorg. Chem. Radiochem.* 18, 1 (1976).
13. (a) R. W. Rudolph and W. R. Pretzer, *Inorg. Chem.* 11, 1974 (1972); (b) R. W. Rudolph, *Acc. Chem. Res.* 9, 446 (1976).
14. D. M. P. Mingos, *Nature (London)*, *Phys. Sci.*, 236, 99 (1972).
15. G. E. Herberich, G. Greiss, and H. F. Heil, *Angew. Chem.* 82, 838 (1970); *Angew. Chem. Int. Ed. Engl.* 9, 805 (1970).
16. A. J. Ashe, III and P. Shu, *J. Am. Chem. Soc.* 93, 1804 (1971).
17. P. L. Timms, *J. Am. Chem. Soc.* 90, 4585 (1968); *Adv. Inorg. Chem. Radiochem.* 14, 121 (1972); *Acc. Chem. Res.* 6, 118 (1973).
18. G. E. Herberich and B. Hessner, *J. Organomet. Chem.* 161, C36 (1978).
19. P. Binger, *Tetrahedron Lett.* p. 2675 (1966).
20. W. Siebert and R. Full, *Angew. Chem.* 88, 55 (1976); *Angew. Chem. Int. Ed. Engl.* 15, 45 (1976).
21. (a) R. Prinz and H. Werner, *Angew. Chem.* 79, 63 (1967); *Angew. Chem. Int. Ed. Engl.* 6, 91 (1967); (b) H. Werner, R. Prinz, and E. Deckelmann, *Chem. Ber.* 102, 95 (1969); (c) M. Scotti and H. Werner, *Helv. Chim. Acta* 57, 1234 (1974).
22. J. L. Adcock and J. J. Lagowski, *Inorg. Chem.* 12, 2533 (1973).
23. H. Nöth and U. Schuchardt, *J. Organomet. Chem.* 134, 297 (1977); U. Schuchardt, Ph.D. Dissertation, University of Munich, 1973.
24. W. Siebert, R. Full, J. Edwin, and K. Kinberger, *Chem. Ber.* 111, 823 (1978).
25. M. Elian, M. M. L. Chen, D. M. P. Mingos, and R. Hoffmann, *Inorg. Chem.* 15, 1148 (1976); M. Elian and R. Hoffmann, *Inorg. Chem.* 14, 1058 (1975).
26. P. Hofmann, to be published.
27. W. Siebert, *Eur. Inorg. Chem. Symp. 3rd*, 1978; *Autumn Meet. Chem. Soc. Warwick*, 1978.
28. M. El D. El-Essawi, Ph.D. Dissertation, University of Marburg, 1978.
29. (a) R. E. Williams, *Adv. Chem. Radiochem.* 18, 70 (1976); (b) R. N. Grimes, *N. Y. Acad. Sci.* 239, 187 (1974).
30. J. W. Lauher, M. Elian, R. H. Summerville, and R. Hoffmann, *J. Am. Chem. Soc.* 98, 3219 (1976).
31. H. Werner and A. Salzer, *Inorg. Met.-Org. Chem.* 2, 239 (1972).
32. A. Salzer and H. Werner, *Inorg. Met.-Org. Chem.* 2, 249 (1972).
33. W. Siebert and M. Bochmann, *Angew. Chem.* 89, 895 (1977); *Angew. Chem. Int. Ed. Engl.* 16, 857 (1977).
34. W. Siebert, J. Edwin, and M. Bochmann, *Angew. Chem.* 90, 917 (1978); *Angew. Chem. Int. Ed. Engl.* 17, 868 (1978).
35. D. C. Beer, V. R. Miller, L. G. Sneddon, R. N. Grimes, M. Mathew, and G. J. Palenik, *J. Am. Chem. Soc.* 95, 3046 (1973).
36. W. Siebert and M. Bochmann, *Angew. Chem.* 89, 483 (1977); *Angew. Chem. Int. Ed. Engl.* 16, 468 (1977).
37. W. Siebert, J. Edwin, M. Bochmann, C. Krüger, and Y.-H. Tsay, *Z. Naturforsch. Teil B* 33, 1410 (1978).
38. M. Bochmann, Master's Thesis, University of Marburg, 1977.
39. J. Edwin, Ph.D. Dissertation, University of Marburg, 1979.
40. C. Krüger and co-workers, unpublished results.
41. G. E. Herberich, E. Bauer, J. Hengesbach, U. Kölle, G. Huttner, and H. Lorenz, *Chem. Ber.* 110, 760 (1977).
42. U. Kölle, W.-D. H. Beiersdorf, and G. E. Herberich, *J. Organomet. Chem.* 152, 7 (1978).

43. G. E. Herberich, J. Hengesbach, and U. Kölle, *Chem. Ber.* **110**, 1171 (1977).
44. P. S. Maddres, A. Modinos, P. L. Timms, and P. Woodward, *J. Chem. Soc. Dalton Trans.* p. 1272 (1975).
45. J. A. K. Howard, I. W. Kerr, and P. Woodward, *J. Chem. Soc. Dalton Trans.* p. 2466 (1975).
46. W. Siebert, G. Augustin, R. Full, C. Krüger, and Y.-H. Tsay, *Angew. Chem.* **87**, 286 (1975); *Angew. Chem. Int. Ed. Engl.* **14**, 262 (1975).
47. W. Siebert, R. Full, J. Edwin, K. Kinberger, and C. Krüger, *J. Organomet. Chem.* **131**, 1 (1977).
48. R. Full, Ph.D. Dissertation, University of Würzburg, 1976.
49. T. Renk, W. Ruf, and W. Siebert, *J. Organomet. Chem.* **120**, 1 (1976).
50. W. Siebert and R. C. Saha, unpublished results, 1978.
51. G. Augustin, Ph.D. Dissertation, University of Würzburg, 1976.
52. W. Siebert, R. Full, C. Krüger, and Y.-H. Tsay, *Z. Naturforsch. Teil B* **33**, 203 (1976).
53. T. A. Albright and R. Hoffmann, *Chem. Ber.* **111**, 1578 (1978).
54. K. Kinberger and W. Siebert, *Chem. Ber.* **111**, 356 (1978).
55. (a) W. Rothermel, Ph.D. Dissertation, University of Marburg, 1979; (b) W. Siebert and W. Rothermel, *Angew. Chem.* **84**, 346 (1977); *Angew. Chem. Int. Ed. Engl.* **16**, 333 (1977).
56. C. Böhle, to be published.
57. H. Schmidt, Ph.D. Dissertation, University of Marburg, 1979.
58. (a) G. E. Herberich, G. Greiss, H. F. Heil, and J. Müller, *Chem. Commun.* p. 1328 (1971); (b) G. E. Herberich and G. Greiss, *Chem. Ber.* **105**, 3413 (1972); (c) R. N. Leyden and M. F. Hawthorne, *Inorg. Chem.* **14**, 2018 (1974).
59. G. E. Herberich and W. Pahlmann, *J. Organomet. Chem.* **97**, C51 (1975).
60. G. Huttner, B. Krieg, and W. Gartzke, *Chem. Ber.* **105**, 3424 (1972).
61. A. J. Ashe III, E. Meyers, P. Shu, T. von Lehmann, and J. Bustide, *J. Am. Chem. Soc.* **97**, 6865 (1975); A. J. Ashe III, W. Butler, and H. F. Sandford, *ibid.*, **101**, 7066 (1979).
62. G. E. Herberich, H. J. Becker, and G. Greiss, *Chem. Ber.* **107**, 3780 (1974).
63. G. E. Herberich and H. J. Becker, *Angew. Chem.* **87**, 196 (1975); *Angew. Chem. Int. Ed. Engl.* **14**, 184 (1975).
64. G. E. Herberich, H. J. Becker, K. Carsten, C. Engelke, and W. Koch, *Chem. Ber.* **109**, 2382 (1976).
65. G. E. Herberich and W. Koch, *Chem. Ber.* **110**, 816 (1977).
66. G. E. Herberich, H. J. Becker, and C. Engelke, *J. Organomet. Chem.* **133**, 265 (1978).
67. G. E. Herberich and H. J. Becker, *Angew. Chem.* **85**, 817 (1973); *Angew. Chem. Int. Ed. Engl.* **12**, 764 (1973).
68. G. E. Herberich and H. J. Becker, *Z. Naturforsch. Teil B* **29**, 439 (1974).
69. G. Huttner and W. Gartzke, *Chem. Ber.* **107**, 3786 (1974).
70. G. E. Herberich and E. Bauer, *Chem. Ber.* **110**, 1167 (1977).
71. (a) G. E. Herberich, C. Engelke, and W. Pahlmann, *Chem. Ber.* **112**, 607 (1979); (b) G. E. Herberich and K. Carsten, *J. Organomet. Chem.* **144**, C1 (1978).
72. W. E. Geiger, Jr., *J. Am. Chem. Soc.* **96**, 2632 (1974).
73. (a) U. Kölle, *J. Organomet. Chem.* **152**, 225 (1978); (b) U. Kölle, *J. Organomet. Chem.* **157**, 327 (1978).
74. G. E. Herberich, W. Koch, and H. Lueken, *J. Organomet. Chem.* **160**, 17 (1978).
75. D. W. Clack and K. D. Warren, *Inorg. Chem.* **18**, 513 (1979).
76. G. E. Herberich, T. Lund, and J. B. Raynor, *J. Chem. Soc. Dalton Trans.* p. 985 (1975).

77. G. Huttner and B. Krieg, *Angew. Chem.* **83**, 541 (1971); *Angew. Chem. Int. Ed. Engl.* **10**, 512 (1971); *Chem. Ber.* **105**, 3437 (1972).
78. W. Siebert, R. Full, H. Schmidt, J. von Seyerl, M. Halstenberg, and E. Huttner, *J. Organomet. Chem.* (in press).
79. J. S. Merriam and K. Niedenzu, *J. Organomet. Chem.* **51**, C1 (1973).
80. (a) L. Weber and G. Schmid, *Angew. Chem.* **86**, 519 (1974); *Angew. Chem. Int. Ed. Engl.* **13**, 467 (1974); (b) G. Schmid and J. Schulze, *Chem. Ber.* **110**, 2744 (1977).
81. R. Goetze, Ph.D. Dissertation, University of München, 1976.
82. H. Nöth and W. Regnet, *Z. Anorg. Chem.* **352**, 1 (1967).
83. H. Nöth and U. Schuchardt, *J. Organomet. Chem.* **24**, 435 (1970).
84. W. Erl and H. Vahrenkamp, *Chem. Ber.* **103**, 3563 (1970).
85. H. Nöth and U. Schuchardt, *Z. Anorg. Allg. Chem.* **418**, 97 (1975).
86. P. McArdle and A. R. Mannings, *J. Chem. Soc., A* p. 2123 (1970).
87. E. Dubler, M. Textor, H.-R. Oswald, and A. Salzer, *Angew. Chem.* **86**, 125 (1974); *Angew. Chem. Int. Ed. Engl.* **13**, 135 (1974).
88. G. E. Herberich, J. Hengesbach, U. Kölle, G. Huttner, and A. Frank, *Angew. Chem.* **88**, 450 (1976); *Angew. Chem. Int. Ed. Engl.* **15**, 433 (1976).
89. W. Siebert and K. Kinberger, *Angew. Chem.* **88**, 451 (1976); *Angew. Chem. Int. Ed. Engl.* **15**, 434 (1976).
90. C. Böhle, Master's Thesis, University of Marburg, 1977.
91. W. M. Maxwell, V. R. Miller, and R. N. Grimes, *Inorg. Chem.* **15**, 1343 (1976).
92. W. Siebert, C. Böhle, C. Krüger, and Y.-H. Tsay, *Angew. Chem.* **90**, 558 (1978); *Angew. Chem. Int. Ed. Engl.* **17**, 527 (1978).
93. G. Seibel, Master's Thesis, University of Marburg, 1979.
94. H. Leichthammer, Master's Thesis, University of Marburg, 1980.
95. H. Werner, *Angew. Chem.* **89**, 1 (1977); *Angew. Chem. Int. Ed. Engl.* **16**, 1 (1977).
96. S. P. Kolesnikov, J. E. Dobson, and P. E. Skell, *J. Am. Chem. Soc.* **100**, 999 (1978).
97. H. Breil and G. Wilke, *Angew. Chem.* **78**, 942 (1966); *Angew. Chem. Int. Ed. Engl.* **5**, 898 (1966).
98. H. Dierks and H. Dietrich, *Acta Crystallogr. Sect. B* **24**, 59 (1968).
99. J. Moraczewski and W. E. Geiger, Jr., *J. Am. Chem. Soc.* **100**, 7429 (1978).
100. A. Salzer and H. Werner, *Angew. Chem.* **84**, 949 (1972); *Angew. Chem. Int. Ed. Engl.* **11**, 930 (1972).
101. T. L. Court and H. Werner, *J. Organomet. Chem.* **65**, 245 (1974).
102. R. Weiss and R. N. Grimes, *J. Organomet. Chem.* **113**, 29 (1976).
103. R. N. Grimes, D. C. Beer, L. G. Sneddon, V. R. Miller, and R. Weiss, *Inorg. Chem.* **13**, 1138 (1974).
104. J. R. Pipal and R. N. Grimes, *Inorg. Chem.* **17**, 10 (1978).
105. V. R. Miller and R. N. Grimes, *J. Am. Chem. Soc.* **97**, 4213 (1975).
106. G. J. Zimmerman, R. Wilczynski, and L. G. Sneddon, *J. Organomet. Chem.* **154**, C29 (1978).
107. W. E. Geiger, Jr., and D. Brennan, personal communication.
108. W. Siebert, T. Renk, K. Kinberger, M. Bochmann, and C. Krüger, *Angew. Chem.* **88**, 850 (1976); *Angew. Chem. Int. Ed. Engl.* **15**, 779 (1976).
109. W. Siebert, *Autumn Meet. Chem. Soc. Warwick*, 1978.
110. W. Siebert, W. Rothermel, C. Böhle, C. Krüger, and D. J. Brauer, *Angew. Chem.* **91**, 1014 (1979).
111. R. N. Grimes, *Autumn Meet. Chem. Soc. Warwick*, 1978.
112. C. Böhle and W. Siebert, to be published.

Subject Index

A

- Absolute configuration, of chiral metal complexes, 193–195
- Acetonitrile ligand, deprotonation, 41
- Acetylenediolate, disodium salt, 5
- Alkylamines, pharmacological activity of silicon derivatives, 285–286
- Aluminoxanes, in Ziegler–Natta catalysis, 140–143
- Aminophosphines, optically active ligands, 160–161, 167, 176, 180–181, 187, 192–194
- Antihistamines, 286
 - silyl derivatives, 287
- Asymmetric synthesis, of chiral metal complexes, 186–188
- 1,2,5-Azadiborolene, 303, 314
 - metal complexes, 324–325

B

- Barbiturates, sedative activity and substituent chain length, 281
- Benzhydryl ethers, silylated, 286–287
- Bonding, in metal π -complexes of boron heterocycles, 304–307
 - electron-counting methods, 304–306
- Borabenzene anion, *see also* Borinato complexes, 303, 314–315
- Boracyclobutene metal complexes, 309–310
- Bora-5,6,7-trihydroborepinylrhodium complex, 310
- Borazine, 303
 - analogy with benzene, 320
 - Group VI tricarbonyl complexes, 320–321
- Borinato complexes, 315–320
 - analogy with benzene and cyclopentadienyl complexes, 317
- cobalt, 315
 - electron-transfer properties, 315, 317–320
 - via insertion into cyclopentadienyl ring, 315
 - ring-transfer reactions, 316–317

- reactions with nucleophiles, 318
 - ring contraction, 318–319
- Borole, 302
 - carbonyl complexes, 309
 - triple-decker manganese complex, 325–326
- Boron heterocycles, *see also* individual compounds
 - Lewis acidity, 302–303
 - as ligands, 301–340
 - five-electron donors, 314–320
 - four-electron donors, 309–314
 - six-electron donors, 320–324
 - three-electron donors, 307–309
 - metal complexes
 - bonding, 304–307
 - dinuclear, 324–333
 - mononuclear, 307–324
 - tetra-decker sandwiches, 335–336
 - trinuclear, 333–336
 - triple-decker sandwiches, 325–333
 - structures, 302–303
- Borathiine, 303–304
 - Group VI tricarbonyl complexes, 303, 323–324

C

- Calcium metabolism, effect of silicon, 276
- Carbamoylcarbonyl complexes
 - from amines and metal carbonyls, 23–33
 - cyclopentadienyls, 27–33
 - dimerization via hydrogen bonding, 28
 - Hofmann acid amide degradation, 24–27, 30
- Carbene complexes
 - analogy with olefins, 232–233
 - cluster formation with metal nucleophiles, 231–233
- Carbon monoxide, reaction with potassamide, 22–23
- Carbonyls, *see* Metal carbonyls
- Carbyne complexes
 - analogy with acetylenes, 231–233

- cluster formation with metal nucleophiles, 231–233
- Catalysis
 - by mixed-metal clusters, 207–208, 256–257
 - of olefin and diene polymerization
 - alkyllithium initiation, 55–97
 - Ziegler–Natta, 99–149
- Chirality, 152
 - and *R,S*-notation, 194–195
- Chiral metal complexes, *see also* individual metals, 151–205
 - absolute configuration, 193–195
 - notation, 194–195
 - X-ray determination, 193
 - chiroptical properties, 192–193
 - circular dichroism spectra, 171, 192–194
 - configurational stability, 168–169
 - diastereoisomeric enantiomers, 189–192
 - separation, 190–191
 - ligand transformation, 169–172
 - with inversion at metal, 170–172
 - with retention of metal configuration, 169–170
 - optical induction, 186–189
 - asymmetric synthesis, 186–188
 - epimerization equilibria, 188–189
 - optical purity, 166–168
 - optical resolution, 153–165
 - of diastereoisomers, 160–165
 - of enantiomers, 153–160
 - optical rotatory dispersion spectra, 192–194
 - separation of diastereoisomers, 165–166
 - square-pyramidal, metal-centered rearrangement, 177–180
 - stereochemistry of insertion reactions, 180–185
 - of carbon monoxide, 182–183
 - of sulfur dioxide, 180–182
 - tabulation, 196–200
- Chromium, *see also* Group VI metals
 - binuclear halo- and pseudohalo-decacarbonyls
 - anions, 13–14
 - neutral compounds, 16–17
 - chiral arene complexes, 196
 - optical resolution, 157–158
 - pentacarbonylhalides, 16–17
 - anion, 12–13
 - reaction with liquid ammonia, 32
 - reaction with Lewis bases, 17
 - pentacarbonylhydride, 5
 - Ziegler–Natta catalysts, 106
 - supported on silica, 119–121
 - tris(acetylacetonate), 125, 130
- Circular dichroism (CD), and chiral metal complexes, 171, 192–194
- Cluster complexes, heterometallic, *see* Mixed-metal clusters
- Cobalt complexes
 - carbamoyls, 25–27
 - chiral cyclopentadienyls, 185–186, 199
 - octacarbonyl, reactions
 - with ammonia, 21
 - with Lewis bases, 45–46
 - tricarbonyl trianion, 9
 - tricobaltnonacarbonyl cation derivatives, 265
- Cobalt, mixed-metal clusters, 210–212, 215–225
 - iron carbonylhydride
 - as norbornadiene dimerization catalyst, 256
 - stereochemical nonrigidity, 260–261
 - substitution, 250–251
 - ironruthenium carbonyl anions, 253
 - platinum carbonyls, 236–237
 - rhodium carbonyls, 223–225
 - adsorption onto alumina and silica, 257
 - as hydrogenation catalysts, 256
 - stereochemical nonrigidity, 259–260
 - synthesis, 238
 - ruthenium carbonylhydride, 221–222
 - stereochemical nonrigidity, 264
- Cone angle of ligands, and racemization of chiral complexes, 175–176
- Copolymerization of dienes and olefins, organolithium-catalyzed, 81–86
 - block copolymer formation, 85–86
 - coupling agents, 85–86
 - pure copolymer formation, 81–85
 - use of dilithio reagents, 82–85
- Copper, mixed-metal clusters, 220, 225, 239
- Cyclopropanes, synthesis via methylene shift reagents, 156–157
 - optical yield, 156–157

D

- Diastereoisomers
 - chromatographic separation, 165-166
 - determination by NMR, 152
 - optical resolution, 160-165
- 1,3-Diaza-2-boroline, 322
- 1,2-Diaza-3,6-diborine, 303, 321-322
- 1,4-Diborocyclohexadienes
 - from BF and alkynes, 310
 - complex formation, 310-311
- 1,3-Diborolene
 - complex formation, 307-308
 - reaction with nickel tetracarbonyl, 308-309
 - ring insertion of CO, 307
- Diene polymerization, catalyzed by organolithium reagents, 55-97
 - mechanism
 - in nonpolar solvents, 71-78
 - in presence of polar ligands, 65-71
- Dinitrogen complexes, chromium carbonyls, 12

E

- Electrochemical studies
 - borinatometal complexes, 319-320
 - triple-decker sandwich complexes, 328, 330-331
- Electronic spectra, of metal carbonyl clusters, 246
- Enantiomers, optical resolution, 153-160
- Epimerization, of chiral metal complexes, 168
 - cobalt, 185-186
 - equilibrium control by optically active ligands, 188
 - iron, 185
 - molybdenum, 177-178
- Ethylene
 - coordination, and reaction with ammonia, 29
 - oligomerization catalyzed by organolithium reagents, 62-65

G

- Group IVB halides, insertion into metal-metal bonds, 15, 17-18

Group VI metals

- binuclear decacarbonyl dianions, 6
 - insertion reactions, 15-18
 - iodine oxidation, 16
 - reaction with binuclear carbonyls, 15
 - structure, 7-9
- binuclear decacarbonylhydride anion, 6
 - reaction with sulfur ligands, 13-14
 - structure, 8
- chiral complexes, 162-163
- cyanocarbonyl anions, 12, 36-37
- hexacarbonyls
 - Lewis base derivatives, 10
 - reaction with ammonia, 19
 - reaction with bipyridyl ligands, 43
 - thiocarbonyl derivative, 18
- pentacarbonyl dianion, 5
 - infrared spectrum, 7
 - reaction with binuclear carbonyls, 15
 - reaction with Lewis bases, 10-12
 - reducing strength, 7, 10
- tetracarbonyl trianions, 5
- trinuclear carbonyl anions, 6

H

- High-pressure liquid chromatography, of carbonylhydride clusters, 248-249
- Hofmann acid amide degradation, of carbamoylcarbonyl compounds, 24-27, 30
- Hydrogenation, catalyzed by cobaltrhodium carbonyl cluster, 256

I

- Indium trihalides, insertion into metal-metal bonds, 18
- Infrared spectroscopy, of mixed-metal carbonyl clusters, 245-246
- Insertion,
 - of activated monomers during Ziegler-Natta polymerization, 101
 - of carbon monoxide,
 - into 1,3-diborolene ring, 307-309
 - into iron-carbon bonds, 182-183
 - of sulfur dioxide, into iron-carbon bonds, 156, 180-182
- Iridium, mixed-metal clusters, 220, 224-225, 239

Iron

- binuclear octacarbonyl dianion
 - insertion reaction with Group IIB metals, 15
 - reaction with tin(IV) compounds, 18
- carbamoyl cyclopentadienyl complexes, 28–29, 32
- carbonyls, reaction with ammonia, 20–21
- chiral cyclopentadienyl carbonyl phosphine complexes
 - carbonylation of alkyls, 182
 - circular dichroism, 171
 - decarbonylation of acyls, 182–183
 - diastereoisomeric enantiomers, 189–191
 - electrophilic cleavage of iron–ligand bonds, 183–185
 - epimerization and racemization, 177, 185
 - ligand transfer and configuration at iron, 170–172
 - optical resolution of alkyls, 156–157
 - sulfur dioxide insertion, 156, 180–182
- cyanocarbonyls, 38–41
 - alkylation, 41
 - allyls, 39
 - diene complexes, 39–41
- cyclopentadienyl cobalt and rhodium clusters, 258
 - Mössbauer spectra, 248
 - stereochemical nonrigidity, 248
- dicobaltnonacarbonylsulfide, 215
 - carbonyl substitution, 250–253
 - as donor ligand, 252–253
 - stereochemical nonrigidity, 258–259
 - synthesis, 228–229
- mixed-metal clusters, 210–220
- osmium and ruthenium carbonyl clusters, 215–216
 - analysis by mass spectrometry, 244
 - synthesis, 228
- osmium and ruthenium carbonylhydride clusters, 217–219
 - carbonylation, 255
 - carbonyl substitution, 208, 252
 - as catalysts for water–gas shift reaction, 256–257
 - deprotonation, 253
 - electronic spectra, 246

- hydrogenation, 255
- infrared spectra, 245–246
- mass spectra, 242–244
- reaction with alkynes, 255
- stereochemical nonrigidity, 261–264
- synthesis, 235–236, 241
- tricarbonyl cycloheptatrienide anion, 41–42
 - and cationic dienyliron compounds, 42
 - and chloroformic esters, 42
 - and Group IVB halides, 42
 - structure, 42
 - synthesis, 41

L

- Lewis acidity, of boron heterocycles, 302–303
- Lewis basicity, of transition-metal complex fragments, 303–304
- Lipid solubility of drugs, increase by silyl substituents, 282
- Liquid ammonia
 - physical properties, 4
 - reactions with metal carbonyls, 19–33
 - base reactions, 20–22
 - carbonyl substitution, 19–20
 - disproportionation, 20–22
 - as solvent
 - for metal carbonyl chemistry, 19–33
 - for organometallic reactions, 33–36

M

Manganese

- carbamoyl complexes, 30–31
- chiral cyclopentadienyl nitrosyl phosphine complexes
 - circular dichroism, 170–171
 - ligand transformations, 169–171
 - of optically active aminophosphines, 160–161, 176, 187
 - optical resolution, 154–155, 160–161
 - racemization of aroyls, 172–176
- chiral Schiff base complex, 163, 196
- cyanocarbonyl anions, 37
 - binuclear, 40
- decacarbonyl, reaction with liquid ammonia, 21–22

- hexacarbonyl cation derivatives, reaction with amines, 24–25
- pentacarbonylalkyl, stereospecific carbonylation, 153
- pentacarbonyl anion
 - oxidative elimination with iodine cyanide, 12
 - in redox condensation reactions, 234–235, 240
- Mass spectrometry, and mixed-metal clusters, 242–244
 - chemical ionization, 244
- Mechanism
 - of carbamoyl ligand formation, 25–26
 - of organolithium-initiated polymerization of dienes, 65–78
 - of olefins, 61–65
 - of racemization of chiral manganese complexes, 172–174
- Metal carbonyls, *see also* individual metals
 - chemistry in liquid ammonia, 1–53
 - alkali metal reduction, 4–7, 9
 - borohydride reduction, 6
 - reaction with bipyridine ligands, 42–46
 - reaction with solvent, 19–33
 - high-pressure synthesis, 3, 46–47
 - pyrolysis and cluster formation, 228–230
 - redox condensation with carbonyl anions, 233–236
- Metal carbonyl anions, *see also* individual metals
 - binuclear species
 - halide bridged, 13–14
 - heteronuclear, 9, 14–15
 - homonuclear, 6–12, 15, 18
 - hydrides, 5–6, 8–9, 14
 - insertion reactions, 15
 - cyanides, 12, 36–41
 - of Group VIB metals, 4–19
 - halides, 12–14, 16
 - reaction with metal halides, 236–237
- Mixed-metal clusters, *see also* individual metals, 207–273
 - carbonylation, 254–255
 - deprotonation of carbonylhydrides, 253
 - electronic spectra of carbonyls, 246
 - as heterogeneous catalyst precursors, 207–208, 257
 - to dispersed bimetallic species, 257
 - high-pressure liquid chromatography, 248–249
 - as homogeneous catalysts, 207–208
 - for hydrogenation, 256
 - for norbornadiene dimerization, 256
 - for water–gas shift reaction, 256–257
 - infrared spectroscopy, of carbonyls, 245–246
 - ligand substitution, 250–253
 - listing, 210–226, 268–269
 - mass spectra, 242–244
 - chemical ionization, 244
 - Mössbauer spectra, 247–248
 - NMR spectra of hydrides, 247
 - protonation of carbonyl anions, 253–254
 - reactions
 - with acetylenes, 255–256
 - of carbonylhydrides with hydrogen, 254
 - related linear polynuclear carbonyls, 265–267
 - stereochemical nonrigidity of carbonyls, 208, 257–269
 - NMR studies, 257–264
 - tetranuclear, 259–260
 - trinuclear, 258–259
 - synthesis, 209, 227–242
 - via addition to coordinatively unsaturated species, 230–233, 240–241
 - via addition to metal acetylides, 239
 - bridge-assisted reactions, 240
 - photolysis, 237–238
 - pyrolysis, 227–230
 - via reaction between carbonyl anions and metal halides, 236–238, 241
 - redox condensation, 233–236, 241
 - scrambling of carbonyl anion clusters, 238–239
 - strategy, 239–242
- Molecular orbital calculations,
 - on complexes of boron heterocycles, 305–307, 313, 320
 - on dinickeltricyclopentadienyl cation, 306–307
- Mössbauer spectra of iron complexes
 - mixed-metal clusters, 247–248
 - of 1,2,5-thiadiborolenes, 312
- Molybdenum, *see also* Group VI metals
 - carbamoyl complexes, 27–28
 - chiral cyclopentadienyl complexes

- absolute configuration, 193–194
asymmetric synthesis of aziridine derivatives, 187
of optically active aminophosphines, 167, 180–181, 194
optical purity, 167
optical resolution of Schiff base derivatives, 163–165
square-pyramidal, 177–181, 188–189
mixed-metal clusters, 210–211
tantalum halides, 210, 227–228
- N**
- Nickel**
addition reactions of zero-valent complexes
to metallocarbenes and -carbynes, 231–232
to unsaturated metal–metal bonds, 231–232
asymmetric synthesis of bis(π -pinenyl) complex, 187–188
mixed-metal clusters, 15, 211–213, 216–217, 220, 223–226
pentanuclear carbonyl anions, 15, 211–212, 233–234
phosphine complexes as Ziegler–Natta catalysts, 130
triple-decker cyclopentadienyl cation, 306–307, 325, 328
¹¹B-Nuclear magnetic resonance (NMR) studies, on complexes of boron heterocycles, 307–337
¹³C-NMR studies
of butadiene polymerization by complexed *n*-butyllithium catalyst, 67–71
degree of polymerization, 67–68
mechanism, 75–77
dynamic properties of mixed-metal clusters, 208, 257–264
homogeneous dicyclopentadienyltitanium Ziegler–Natta catalysts, 129–130
¹H-NMR studies, of chiral metal complexes
analysis of diastereoisomeric enantiomer mixtures, 191
determination of optical purity, 166–168
square-pyramidal molybdenum and tungsten complexes
inversion of configuration, 180
rate of epimerization, 178–179
- O**
- Olefin polymerization, catalysis
by organolithium reagents, 55–97
Ziegler–Natta, 99–149
Optical activity, of organo-transition-metal complexes, 151–205
Optical induction, 186–189
Optical purity, of chiral metal complexes, 166–168
Optical resolution, 153–165
of diastereoisomers, 160–165
of enantiomers, 153–160
Optical rotatory dispersion (ORD) spectra, of chiral metal complexes, 192–193
Optical yields, in synthesis of cyclopropanes, 156–157
Organolithium polymerization catalysts, 55–97
aggregation state, 71–72
effect of donor ligands, 59
and mechanism, 72–73
diene-olefin copolymerization, 78–79
solvent effects, 78–81
for dienes, 56–57, 65–78
mechanism, 65–78
and living polymers, 60
¹³C-NMR studies, 67
for olefins, 56–57, 60–65
kinetics for ethylene reaction, 62–65
mechanism, 60–65
with polar ligands, 65–71
bis(diphenylphosphino)ethane, 70–71
effect on polymer microstructure, 66, 69–71
effect of reaction conditions, 65–66
mechanism of action, 65–71
TMEDA, 66–69
use in polymer grafting, 86–89
use in preparation of telechelic polymers, 89–93
structure and reactivity, 59–60
telomerization of benzene and ethylene, 61
Organosilicon compounds, in biology, 275–330
amino derivatives, 285–286
benzhydryl ethers, 286–287
as derivatives of active carbon compounds, 276–287
activity comparison, 277

- detoxification, 294–295
as drug analogs, 281, 283
lipid solubility, 282–283
and metabolism, 294
natural occurrence, 275
partition coefficients, 282
pharmacological activity, 276–283
 effect of bulky trimethylsilyl group, 277
 effect of electronegativity, 277, 281
 and trimethylsiloxylation, 282–283
silatranes, 291, 293–294
silicon substitution of carbon or nitrogen, 277–280
siloxanes, 288–291
silyl groups as space fillers, 281–283
steroids, 283–285
without carbon analogs, 288–294
Organo-transition-metal complexes, optical activity, 151–205
Osmium
 dodecacarbonyl, activation toward substitution, 232
 tetracarbonyldihydride, reaction with platinum(0) complexes, 232
 trinuclear decacarbonyldihydride, addition to metal–metal double bond, 230–231
 mixed-metal clusters, 211–218, 220–223
 rhenium carbonylhydrides, 232, 234–235
1-Oxa-2,6-diboracyclohexene, nickel complex, 308–309

P

- Palladium
 mixed-metal clusters, 211, 220, 226
 zero-valent complexes, addition
 to metal carbenes and carbynes, 231–232
 to unsaturated metal–metal bonds, 231–232
Pharmacology, of silicon compounds, 276–281
Platinum
 mixed-metal clusters, 210–212, 214, 216–217, 220–226
 cobalt carbonyls, 236–237
 rhodium carbonyl anions, 238–239
 zero-valent complexes, addition, 231–233

- to metal carbenes and carbynes, 231–233
 to osmium carbonylhydride, 232
 to unsaturated metal–metal bonds, 231–233
Polymerization, of dienes and olefins
 via organolithium catalysts, 55–97
 via Ziegler–Natta catalysts, 99–149

R

- Racemization, of chiral metal complexes, 172–177
Redox condensation, in synthesis of clusters, 233–236, 241
Rhenium
 cyanocarbonyl anions, 37–38
 alkylation, 40–41
 binuclear, 40
 binuclear octacarbonyldihydride, addition to metal–metal double bond, 230–231, 241
 hexacarbonyl cation derivatives, carbamoyl formation with amines, 24–25
 mixed-metal clusters, 213–214, 232
 pentacarbonyl anion, in redox condensation reactions, 234–235
Rhodium
 chiral Schiff base complex, 200
 mixed-metal clusters, 215–216, 219–220, 223–225, 239
Ruthenium
 carbamoyl compounds, 29–30
 chiral arene complexes, 199
 circular dichroism, 193
 of optically active aminophosphine, 192–193
 mixed-metal clusters, 212, 214–222
 via pyrolysis reactions of dodecacarbonyl, 229–230

S

- Schiff bases, chiral metal complexes
 Group VI metal tricarbonyl phosphines, 162–163, 196
 manganese tricarbonylbromide, 163, 196
 molybdenum cyclopentadienyls, 164–165, 177–179, 195, 197
 of rhodium, 200

Sex hormones

- effect of polysiloxanes, 289
- silylation and activity, 283-285

Silatranes, in biology, 291-294

- activity, 291, 293-294
- stimulation of protein synthesis, 293-294

Silicates, as skeletal components, 275-276**Siloxanes**, in biology

- cis*-2,6-diphenylhexamethylcyclotetrasiloxane, 289

X-ray structure, 292

- estrogenic activity, 288-289, 291
- as holders of active groups, 291
- phenyl derivatives, 288-291
- structure and activity, 289-291
- ring conformation, 290

Sodium bis(trimethylsilyl)amide, reaction with metal carbonyl derivatives, 38-42

- deprotonation of coordinated ligands, 41-42

acetonitrile, 41

cycloheptatriene, 41-42

- synthesis of cyanide complexes, 38-41

Steroids, silylation, 283-285

- ring attachment, 284
- ring substitution and stereochemistry, 284-285
- and sex hormonal activity, 284-285

Sulfur dioxide

insertion

- into Group VI metal-metal bonds, 15
- into iron-carbon bonds, stereochemistry, 156, 180-182

- reduction to hydrosulfide ion, 16-17

T**Telechelic polymers**, 57-58

- carboxylated, 90
- synthesis via organolithium catalysts, 89-93
- thiolated, 90

Tetra-decker sandwich complexes

- bonding, 306, 334-336
- of 1,2,5-thiadiborolenes, 334-336

1,2,5-Thiadiborolenes, 311, 312

- boron-carbon bond length and complexation, 312
- metal complexes, 311-314

binuclear, 324-325

tetra-decker sandwiches, 334-336

triple-decker sandwiches, 326-327, 332-333

potassium reduction, 312

Titanium complexes

chiral dicyclopentadienyl derivatives, 196

optical resolution, 158-159

in Ziegler-Natta catalysis

and aluminosiloxanes, 140-143

dicyclopentadienyls, 124-129

formation of dimetalated species, 131

with magnesium compounds, 120-123

trihalide, 113-120

Transition-metal chemistry

of boron heterocycles, 301-340

of optically active complexes, 151-206

1,2,4-Triaza-3,5-diborolidine, 322-323

Trimethylamine oxide, use in substitution chemistry of carbonyl clusters, 232**Trimethylsiloxy group**, pharmacology, 282-283**Triple-decker sandwich complexes**, 306-307, 325-333

bonding, 306-307

containing C_6B_3 ring systems, 329-330

of cyclooctatetraene

cobalt cyclopentadienyl, 328

titanium, 328

of cyclopentadienyl nickel, 306-307, 325, 328

of 1,3-diborolenes, 306-307, 330-332

of 1,2,5-thiadiborolenes, 326-327, 332-333

Tungsten, *see also* Group VI metals

binuclear octacarbonyldihydride anion, 6

mixed-metal clusters, 211-212

pentacarbonylcarbene complexes, reaction with nucleophilic metal compounds, 231-232

U**Uranium**, allyl complex as Ziegler-Natta catalyst, 125, 130**V****Vanadium complexes**

- hexacarbonyl, reaction with liquid ammonia, 21

pentacarbonyl trianion, 9
tricarbonyl cyclopentadienyl anion, 9
in Ziegler-Natta catalysis, 125
 activity loss on reduction, 130
 and polymer stereoregulation, 108-109
 polymerization of higher α -olefins, 129

W

Walden cycle, and chiral manganese nitrosyl cyclopentadienyls, 174

Z

Ziegler-Natta catalysis, 99-149
 and gas-phase polymerization, 106-107
 homogeneous systems, 123-143
 cyclopentadienyl zirconium complexes, 132-135, 140
 dicyclopentadienyl titanium systems, 124-129, 135-139
 effect of water, 137-143
 side reactions, 131-137
 vanadium complexes, 125, 129-130
 magnesium-titanium catalysts, 120-123
 mechanism, 101, 103-104, 108-118
 chain propagation, 103-104
 chain termination, 103-105
 insertion of monomer into metal-carbon bonds, 101
 monomer adsorption, 101
 and stereoselectivity, 108-114
 and molecular weight of polymer products, 105
 decrease by hydrogenation, 103-105

 distribution and surface heterogeneity, 116-117
 origin of catalyst activity, 114-118
 formation of propagation centers, 117
 number of active sites, 114-115
 and solid-state structure of titanium trichloride, 114-116
 polymer stereoregulation, 99-101, 108-114
 and cis addition to double bond, 109, 111-112
 and chirality of active center, 111-112
 and chirality of growing chain, 109
 for dienes, 113-114
 and metal substitution, 109
 via titanium catalysts adsorbed onto magnesium compounds, 121
 by vanadium catalysts, 108-109
 process operation, 105-108
 second-generation catalysts, 102-105
 supported catalysts, 119-122
 tailoring of heterogeneous catalysts, 118-123
 aging, 118
 by milling, 115
 optimum catalyst components, 119
 use of single crystals, 119
Zirconium complexes, as Ziegler-Natta catalysts, 132-135
 dicyclopentadienyls, 132-135
 mechanism of action, 132-135
 structure of alkylaluminum adducts, 134-135
 tricyclopentadienyl aluminum adducts, 135-140

Cumulative List of Contributors

- Abel, E. W., 5, 1; 8, 117
 Aguilo, A., 5, 321
 Albano, V. G., 14, 285
 Armitage, D. A., 5, 1
 Atwell, W. H., 4, 1
 Behrens, H., 18, 1
 Bennett, M. A., 4, 353
 Birmingham, J., 2, 365
 Bogdanović, B., 17, 105
 Brook, A. G., 7, 95
 Brown, H. C., 11, 1
 Brown, T. L., 3, 365
 Bruce, M. I., 6, 273; 10, 273; 11, 447; 12, 379
 Brunner, H., 18, 151
 Cais, M., 8, 211
 Calderon, N., 17, 449
 Callahan, K. P., 14, 145
 Cartledge, F. K., 4, 1
 Chalk, A. J., 6, 119
 Chatt, J., 12, 1
 Chini, P., 14, 285
 Chiusoli, G. P., 17, 195
 Churchill, M. R., 5, 93
 Coates, G. E., 9, 195
 Collman, J. P., 7, 53
 Corey, J. Y., 13, 139
 Courtney, A., 16, 241
 Coutts, R. S. P., 9, 135
 Coyle, T. D., 10, 237
 Craig, P. J., 11, 331
 Cullen, W. R., 4, 145
 Cundy, C. S., 11, 253
 de Boer, E., 2, 115
 Dessy, R. E., 4, 267
 Dickson, R. S., 12, 323
 Eisch, J. J., 16, 67
 Emerson, G. F., 1, 1
 Ernst, C. R., 10, 79
 Evans, J., 16, 319
 Faller, J. W., 16, 211
 Fessenden, J. S., 18, 275
 Fessenden, R. J., 18, 275
 Fischer, E. O., 14, 1
 Forster, D., 17, 255
 Fraser, P. J., 12, 323
 Fritz, H. P., 1, 239
 Furukawa, J., 12, 83
 Fuson, R. C., 1, 221
 Geoffroy, G. L., 18, 207
 Gilman, H., 1, 89; 4, 1; 7, 1
 Gladfelter, W. L., 18, 207
 Green, M. L. H., 2, 325
 Griffith, W. P., 7, 211
 Grovenstein, Jr., E., 16, 167
 Gubin, S. P., 10, 347
 Gysling, H., 9, 361
 Haiduc, I., 15, 113
 Halasa, A. F., 18, 55
 Harrod, J. F., 6, 119
 Hartley, F. H., 15, 189
 Hawthorne, M. F., 14, 145
 Heck, R. F., 4, 243
 Heimbach, P., 8, 29
 Henry, P. M., 13, 363
 Hieber, W., 8, 1
 Hill, E. A., 16, 131
 Ibers, J. A., 14, 33
 Ittel, S. A., 14, 33
 James, B. R., 17, 319
 Jolly, P. W., 8, 29
 Jones, P. R., 15, 273
 Jukes, A. E., 12, 215
 Kaesz, H. D., 3, 1
 Kaminsky, W., 18, 99
 Katz, T. J., 16, 283
 Kawabata, N., 12, 83
 Kettle, S. F. A., 10, 199
 Kilner, M., 10, 115
 King, R. B., 2, 157
 Kingston, B. M., 11, 253
 Kitching, W., 4, 267
 Köster, R., 2, 257
 Kühlein, K., 7, 241
 Kuivila, H. G., 1, 47
 Kumada, M., 6, 19
 Lappert, M. F., 5, 225; 9, 397; 11, 253; 14, 345
 Lawrence, J. P., 17, 449
 Lednor, P. W., 14, 345
 Longoni, G., 14, 285
 Luijten, J. G. A., 3, 397
 Lupin, M. S., 8, 211
 McKillop, A., 11, 147

- Maddox, M. L., 3, 1
Maitlis, P. M., 4, 95
Mann, B. E., 12, 135
Manuel, T. A., 3, 181
Mason, R., 5, 93
Masters, C., 17, 61
Matsumura, Y., 14, 187
Mingos, D. M. P., 15, 1
Mochel, V. D., 18, 55
Moedritzer, K., 6, 171
Morgan, G. L., 9, 195
Mrowca, J. J., 7, 157
Nagy, P. L. I., 2, 325
Nakamura, A., 14, 245
Nesmeyanov, A. N., 10, 1
Neumann, W. P., 7, 241
Ofstead, E. A., 17, 449
Okawara, R., 5, 137; 14, 187
Oliver, J. P., 8, 167; 15, 235; 16, 111
Onak, T., 3, 263
Otsuka, S., 14, 245
Parshall, G. W., 7, 157
Paul, I., 10, 199
Petrosyan, V. S., 14, 63
Pettit, R., 1, 1
Poland, J. S., 9, 397
Popa, V., 15, 113
Pratt, J. M., 11, 331
Prokai, B., 5, 225
Pruett, R. L., 17, 1
Reetz, M. T., 16, 33
Reutov, O. A., 14, 63
Rijkens, F., 3, 397
Ritter, J. J., 10, 237
Rochow, E. G., 9, 1
Roper, W. R., 7, 53
Roundhill, D. M., 13, 273
Rubezhov, A. Z., 10, 347
Salerno, G., 17, 195
Schmidbaur, H., 9, 259; 14, 205
Schrauzer, G. N., 2, 1
Schulz, D. N., 18, 55
Schwebke, G. L., 1, 89
Seyferth, D., 14, 97
Siebert, W., 18, 301
Silverthorn, W. E., 13, 47
Sinn, H., 18, 99
Skinner, H. A., 2, 49
Slocum, D. W., 10, 79
Smith, J. D., 13, 453
Speier, J. L., 17, 407
Stafford, S. L., 3, 1
Stone, F. G. A., 1, 143
Su, A. C. L., 17, 269
Tamao, K., 6, 19
Tate, D. P., 18, 55
Taylor, E. C., 11, 147
Thayer, J. S., 5, 169; 13, 1
Timms, P. L., 15, 53
Todd, L. J., 8, 87
Treichel, P. M., 1, 143; 11, 21
Tsuji, J., 17, 141
Tsutsui, M., 9, 361; 16, 241
Turney, T. W., 15, 53
Tyfield, S. P., 8, 117
van der Kerk, G. J. M., 3, 397
Vezey, P. N., 15, 189
Wada, M., 5, 137
Walton, D. R. M., 13, 453
Wailles, P. C., 9, 135
Webster, D. E., 15, 147
West, R., 5, 169; 16, 1
Wiles, D. R., 11, 207
Wilke, G., 8, 29
Wojcicki, A., 11, 87; 12, 31
Yashina, N. S., 14, 63
Ziegler, K., 6, 1
Zuckerman, J. J., 9, 21

Cumulative List of Titles

Acetylene and Allene Complexes: Their Implication in Homogeneous Catalysis, 14, 245
 Activation of Alkanes by Transition Metal Compounds, 15, 147
 Alkali Metal Derivatives of Metal Carbonyls, 2, 157
 Alkyl and Aryl Derivatives of Transition Metals, 7, 157
 Alkylcobalt and Acylcobalt Tetracarbonyls, 4, 243
 Allyl Metal Complexes, 2, 235
 π -Allylnickel Intermediates in Organic Synthesis, 8, 29
 1,2-Anionic Rearrangement of Organosilicon and Germanium Compounds, 16, 1
 Applications of ^{119}mSn Mössbauer Spectroscopy to the Study of Organotin Compounds, 9, 21
 Arene Transition Metal Chemistry, 13, 47
 Aryl Migrations in Organometallic Compounds of the Alkali Metals, 16, 167
 Boranes in Organic Chemistry, 11, 1
 Boron Heterocycles as Ligands in Transition-Metal Chemistry, 18, 301
 Carbene and Carbyne Complexes, On the Way to, 14, 1
 Carboranes and Organoboranes, 3, 263
 Catalysis by Cobalt Carbonyls, 6, 119
 Catalytic Codimerization of Ethylene and Butadiene, 17, 269
 Catenated Organic Compounds of the Group IV Elements, 4, 1
 Chemistry of Carbon-Functional Alkylidyne-cobalt Nonacarbonyl Cluster Complexes, 14, 97
 Chiral Metal Atoms in Optically Active Organo-Transition-Metal Compounds, 18, 151
 ^{13}C NMR Chemical Shifts and Coupling Constants of Organometallic Compounds, 12, 135
 Compounds Derived from Alkynes and Carbonyl Complexes of Cobalt, 12, 323
 Conjugate Addition of Grignard Reagents to Aromatic Systems, 1, 221
 Coordination of Unsaturated Molecules to Transition Metals, 14, 33
 Cyclobutadiene Metal Complexes, 4, 95
 Cyclopentadienyl Metal Compounds, 2, 365
 Diene-Iron Carbonyl Complexes, 1, 1
 Dyotropic Rearrangements and Related σ - σ Exchange Processes, 16, 33
 Electronic Effects in Metallocenes and Certain Related Systems, 10, 79
 Electronic Structure of Alkali Metal Adducts of Aromatic Hydrocarbons, 2, 115
 Fast Exchange Reactions of Group I, II, and III Organometallic Compounds, 8, 167
 Fischer-Tropsch Reaction, 17, 61
 Fluorocarbon Derivatives of Metals, 1, 143
 Fluxional and Nonrigid Behavior of Transition Metal Organometallic π -Complexes, 16, 211
 Free Radicals in Organometallic Chemistry, 14, 345
 Heterocyclic Organoboranes, 2, 257
 α -Heterodiazalkanes and the Reactions of Diazoalkanes with Derivatives of Metals and Metalloids, 9, 397
 High Nuclearity Metal Carbonyl Clusters, 14, 285
 Homogeneous Catalysis of Hydrosilation by Transition Metals, 17, 407
 Hydroformylation, 17, 1
 Hydrogenation Reactions Catalyzed by Transition Metal Complexes, 17, 319
 Infrared Intensities of Metal Carbonyl Stretching Vibrations, 10, 199
 Infrared and Raman Studies of π -Complexes, 1, 239

- Insertion Reactions of Compounds of Metals and Metalloids, **5**, 225
- Insertion Reactions of Transition Metal–Carbon σ -Bonded Compounds. I. Carbon Monoxide Insertion, **11**, 87
- Insertion Reactions of Transition Metal–Carbon σ -Bonded Compounds. II. Sulfur Dioxide and Other Molecules, **12**, 31
- Isoelectronic Species in the Organophosphorus, Organosilicon, and Organoaluminum Series, **9**, 259
- Keto Derivatives of Group IV Organometalloids, **7**, 95
- Lewis Base–Metal Carbonyl Complexes, **3**, 181
- Ligand Substitution in Transition Metal π -Complexes, **10**, 347
- Literature of Organo-Transition Metal Chemistry 1950–1970, **10**, 273
- Literature of Organo-Transition Metal Chemistry 1971, **11**, 447
- Literature of Organo-Transition Metal Chemistry 1972, **12**, 379
- Mass Spectra of Metallocenes and Related Compounds, **8**, 211
- Mass Spectra of Organometallic Compounds, **6**, 273
- Mechanistic Pathways in the Catalytic Carbonylation of Methanol by Rhodium and Iridium Complexes, **17**, 255
- Metal Atom Synthesis of Organometallic Compounds, **15**, 53
- Metal Carbonyl Cations, **8**, 117
- Metal Carbonyl Chemistry in Liquid Ammonia, Four Decades of: Aspects and Prospects, **18**, 1
- Metal Carbonyls, Forty Years of Research, **8**, 1
- Metal Complexes of π -Ligands Containing Organosilicon Groups, **15**, 113
- Metal π -Complexes Formed by Seven- and Eight-Membered Carbocyclic Compounds, **4**, 353
- Metallocarboranes, Ten Years of, **14**, 145
- Methyltin Halides and Their Molecular Complexes, **14**, 63
- Mixed-Metal Clusters, **18**, 207
- Molecular Rearrangements in Polynuclear Transition Metal Complexes, **16**, 319
- Nitrogen Groups in Metal Carbonyl and Related Complexes, **10**, 115
- Nitrosyls, **7**, 211
- Nuclear Magnetic Resonance Spectra of Organometallic Compounds, **3**, 1
- Of Time and Carbon–Metal Bonds, **9**, 1
- Olefin Metathesis, **17**, 449
- Olefin Metathesis Reaction, **16**, 283
- Olefin Oxidation with Palladium Catalyst, **5**, 321
- Organic and Hydride Chemistry of Transition Metals, **12**, 1
- Organic Chemistry of Copper, **12**, 215
- Organic Chemistry of Lead, **7**, 241
- Organic Complexes of Lower-Valent Titanium, **9**, 135
- Organic Substituted Cyclosilanes, **1**, 89
- Organoantimony Chemistry, Recent Advances in, **14**, 187
- Organoarsenic Chemistry, **4**, 145
- Organoberyllium Compounds, **9**, 195
- Organolanthanides and Organoactinides, **9**, 361
- Organolithium Catalysis of Olefin and Diene Polymerization, **18**, 55
- Organomagnesium Rearrangements, **16**, 131
- Organometallic Aspects of Diboron Chemistry, **10**, 237
- Organometallic Benzheterocycles, **13**, 139
- Organometallic Chemistry: A Forty Years' Stroll, **6**, 1

- Organometallic Chemistry: A Historical Perspective, 13, 1
Organometallic Chemistry, My Way, 10, 1
Organometallic Chemistry of Nickel, 2, 1
Organometallic Chemistry of the Main Group Elements—A Guide to the Literature, 13, 453
Organometallic Chemistry, Some Personal Notes, 7, 1
Organometallic Complexes with Silicon–Transition Metal or Silicon–Carbon–Transition Metal Bonds, 11, 253
Organometallic Nitrogen Compounds of Germanium, Tin, and Lead, 3, 397
Organometallic Pseudohalides, 5, 169
Organometallic Radical Anions, 15, 273
Organometallic Reaction Mechanisms, 4, 267
Organometallic Reactions Involving Hydro-Nickel, -Palladium, and -Platinum Complexes, 13, 273
Organopolysilanes, 6, 19
Organosilicon Biological Research, Trends in, 18, 275
Organosulphur Compounds of Silicon, Germanium, Tin, and Lead, 5, 1
Organothallium Chemistry, Recent Advances, 11, 147
Organotin Hydrides, Reactions with Organic Compounds, 1, 47
Organozinc Compounds in Synthesis, 12, 83
Oxidative-Addition Reactions of d^8 Complexes, 7, 53
Palladium-Catalyzed Organic Reactions, 13, 363
Palladium-Catalyzed Reactions of Butadiene and Isoprene, 17, 141
Pentaalkyls and Alkylidene Trialkyls of the Group V Elements, 14, 205
Preparation and Reactions of Organocobalt(III) Complexes, 11, 331
Rearrangements of Organoaluminum Compounds and Their Group II Analogs, 16, 111
 α - π -Rearrangements of Organotransition Metal Compounds, 16, 241
Rearrangements of Unsaturated Organoboron and Organoaluminum Compounds, 16, 67
Recent Developments in Theoretical Organometallic Chemistry, 15, 1
Redistribution Equilibria of Organometallic Compounds, 6, 171
Radiochemistry of Organometallic Compounds, 11, 207
Selectivity Control in Nickel-Catalyzed Olefin Oligomerization, 17, 105
Strengths of Metal-to-Carbon Bonds, 2, 49
Structural Aspects of Organotin Chemistry, 5, 137
Structural Chemistry of Organo-Transition Metal Complexes, 5, 93
Structures of Main Group Organometallic Compounds Containing Electron-Deficient Bridge Bonds, 15, 235
Structures of Organolithium Compounds, 3, 365
Supported Transition Metal Complexes as Catalysts, 15, 189
Synthetic Applications of Organonickel Complexes in Organic Chemistry, 17, 195
Theoretical Organometallic Chemistry, Recent Developments, 15, 1
Transition Metal-Carborane Complexes, 8, 87
Transition Metal-Isocyanide Complexes, 11, 21
Ziegler-Natta Catalysis, 18, 99